

# Australian Rainfall & Runoff

Revision Projects

PROJECT 8

Use of Continuous Simulation  
Models for Design Flood Estimation

PROJECT 12

Selection of an Approach

STAGE 3 REPORT

P12/S3/008

DECEMBER 2015



Australian Government




ENGINEERS  
AUSTRALIA  
Water Engineering

**AUSTRALIAN RAINFALL AND RUNOFF  
REVISION PROJECT 8: USE OF CONTINUOUS SIMULATION FOR DESIGN FLOOD  
ESTIMATION  
REVISION PROJECT 12: SELECTION OF AN APPROACH 2015**

STAGE 3 REPORT

**DECEMBER 2015**

<b>Project</b> Project 8: Use of continuous for design flood estimation Project 12: Selection of an Approach 2015	<b>ARR Report Number</b> P12/S3/008
<b>Date</b> 4 December 2015	<b>ISBN</b> 978-085825-9690
<b>Contractor</b> Entura	<b>Contractor Reference Number</b> E303434/P508545
<b>Authors</b> Fiona Ling, Prafulla Pokhrel, William Cohen, Jayson Peterson, Sarah Blundy, Kim Robinson	<b>Verified by</b> 

## COPYRIGHT NOTICE



This document, Project 8: Use of continuous for design flood estimation and Project 12: Selection of an Approach 2015, is licensed under the [Creative Commons Attribution 4.0 Licence](#), unless otherwise indicated.

**Please give attribution to:** © Commonwealth of Australia (Geoscience Australia) 2015

We also request that you observe and retain any notices that may accompany this material as part of the attribution.

### **Notice Identifying Other Material and/or Rights in this Publication:**

The authors of this document have taken steps to both identify third-party material and secure permission for its reproduction and reuse. However, please note that where these third-party materials are not licensed under a Creative Commons licence, or similar terms of use, you should obtain permission from the rights holder to reuse their material beyond the ways you are permitted to use them under the 'fair dealing' provisions in the [Copyright Act 1968](#).

### **Further Information**

For further information about the copyright in this document, please contact:

Intellectual Property and Copyright Manager

Corporate Branch

Geoscience Australia

GPO Box 378

CANBERRA ACT 2601

Phone: +61 2 6249 9367 or email: [copyright@ga.gov.au](mailto:copyright@ga.gov.au)

## **DISCLAIMER**

The [Creative Commons Attribution 4.0 Licence](#) contains a Disclaimer of Warranties and Limitation of Liability.

## ACKNOWLEDGEMENTS

This project was made possible by funding from the Federal Government through the Department of Climate Change. This report and the associated project are the result of a significant amount of in kind hours provided by Engineers Australia Members.



ENGINEERS  
AUSTRALIA  
Water Engineering

### *Contractor Details*

Entura  
89 Cambridge Park Drive  
Cambridge 7170 TAS

Tel: (03) 6245 4500  
Email: [Fiona.ling@entura.com.au](mailto:Fiona.ling@entura.com.au)  
Web: [www.entura.com.au](http://www.entura.com.au)

 **entura** | The power of  
Hydro Tasmania natural thinking

## FOREWORD

Since its first publication in 1958, Australian Rainfall and Runoff (ARR) has remained one of the most influential and widely used guidelines published by Engineers Australia (EA). The current edition, published in 1987, retained the same level of national and international acclaim as its predecessors.

With nationwide applicability, balancing the varied climates of Australia, the information and the approaches presented in Australian Rainfall and Runoff are essential for policy decisions and projects involving:

- infrastructure such as roads, rail, airports, bridges, dams, stormwater and sewer systems;
- town planning;
- mining;
- developing flood management plans for urban and rural communities;
- flood warnings and flood emergency management;
- operation of regulated river systems; and
- prediction of extreme flood levels.

However, many of the practices recommended in the 1987 edition of ARR now are becoming outdated, and no longer represent the accepted views of professionals, both in terms of technique and approach to water management. This fact, coupled with greater understanding of climate and climatic influences makes the securing of current and complete rainfall and streamflow data and expansion of focus from flood events to the full spectrum of flows and rainfall events, crucial to maintaining an adequate knowledge of the processes that govern Australian rainfall and streamflow in the broadest sense, allowing better management, policy and planning decisions to be made.

One of the major responsibilities of the National Committee on Water Engineering of Engineers Australia is the periodic revision of ARR. A recent and significant development has been that the revision of ARR has been identified as a priority in the Council of Australian Governments endorsed National Adaptation Framework for Climate Change.

The update will be completed in three stages. Twenty one revision projects have been identified and will be undertaken with the aim of filling knowledge gaps. Of these 21 projects, ten projects commenced in Stage 1 and an additional 9 projects commenced in Stage 2. The remaining two projects will commence in Stage 3. The outcomes of the projects will assist the ARR Editorial Team with the compiling and writing of chapters in the revised ARR.

Steering and Technical Committees have been established to assist the ARR Editorial Team in guiding the projects to achieve desired outcomes. Funding for Stages 1 and 2 of the ARR revision projects has been provided by the Federal Department of Climate Change and Energy Efficiency. Funding for Stages 2 and 3 of Project 1 (Development of Intensity-Frequency-Duration information across Australia) has been provided by the Bureau of Meteorology.

*Project 8 – Continuous simulation models*

*The focal point of this project is the development of appropriate advice for the use of continuous simulation techniques as a technique for the development of point flow estimates with a given frequency or the development of a system performance estimate. While there have been a number of pilot studies that have developed alternative approaches (see, for example, Boughton et al., 1999; Droop and Boughton, 2003; Jung and Bae, 2005; and Newton and Walton 2000), a consistent and coherent approach has not resulted.*

*Project 12: Selection of an Approach*

*Estimation of the flood flow in the absence of at-site recorded data generally requires either a regional method (Project 5) or a rainfall based approach. Rainfall based approaches are based on using a catchment modelling system which may be conceptually complex or simple to predict the response of a catchment to a storm burst (or event) or to a sequence of storm events.*

*At the time of the publication of the current edition of the Australian Rainfall and Runoff, the recommended approach implicitly assumed that the frequency of the rainfall was translated into the desired frequency of flood flow through use of median valued of other input to the catchment modelling system. This implicit assumption has been tested in the period since publication of the current edition of Australian Rainfall and Runoff and a number of alternative approaches have been proposed as a means of circumventing the need for this implicit assumption. These methods include 'Monte Carlo' approaches and 'continuous simulation' approaches. The reliability of these approaches and their associated uncertainty in prediction need to be defined for different types of problems so that suitable guidance can be presented in the revision to Australian Rainfall and Runoff.*



**Mark Babister**  
Chair Technical Committee for  
ARR Research Projects



**Assoc Prof James Ball**  
ARR Editor

## ARR REVISION PROJECTS

The 21 ARR revision projects are listed below:

ARR Project No.	Project Title	Starting Stage
1	Development of intensity-frequency-duration information across Australia	1
2	Spatial patterns of rainfall	2
3	Temporal pattern of rainfall	2
4	Continuous rainfall sequences at a point	1
5	Regional flood methods	1
6	Loss models for catchment simulation	2
7	Baseflow for catchment simulation	1
<b>8</b>	<b>Use of continuous simulation for design flow determination</b>	<b>2</b>
9	Urban drainage system hydraulics	1
10	Appropriate safety criteria for people	1
11	Blockage of hydraulic structures	1
<b>12</b>	<b>Selection of an approach</b>	<b>3</b>
13	Rational Method developments	1
14	Large to extreme floods in urban areas	3
15	Two-dimensional (2D) modelling in urban areas.	1
16	Storm patterns for use in design events	2
17	Channel loss models	2
18	Interaction of coastal processes and severe weather events	1
19	Selection of climate change boundary conditions	3
20	Risk assessment and design life	2
21	IT Delivery and Communication Strategies	2

### ARR Technical Committee:

*Chair:* Mark Babister, WMAwater  
*Members:* Associate Professor James Ball, Editor ARR, UTS  
 Professor George Kuczera, University of Newcastle  
 Professor Martin Lambert, University of Adelaide  
 Dr Rory Nathan, Jacobs  
 Dr Bill Weeks  
 Associate Professor Ashish Sharma, UNSW  
 Dr Bryson Bates, CSIRO  
 Steve Finlay, Engineers Australia

### Related Appointments:

ARR Project Engineer: Monique Retallick, WMAwater  
 ARR Admin Support : Isabelle Testoni, WMAwater

## **PROJECT TEAM**

- Dr Fiona Ling, Entura #
- Dr Prafulla Pokhrel, Entura
- William Cohen, Entura
- Jayson Peterson, Entura
- Sarah Blundy, Entura
- Kim Robinson, Entura
- Mark Babister, WMA Water, TC manager



## EXECUTIVE SUMMARY

Estimation of flood flows in the absence of at-site recorded data generally requires either a regional method (Project 5) or a rainfall based approach. Rainfall based approaches are based on using a catchment modelling system which may be conceptually complex or simple to predict the response of a catchment to a storm burst (or event) or to a sequence of storm events. At the time of the publication of the current edition of Australian Rainfall and Runoff, the recommended Design Event approach implicitly assumed that the frequency of the rainfall was translated into the desired frequency of flood flow through use of median values of other inputs to the catchment modelling system. This implicit assumption has been tested in the period since publication of the current edition of Australian Rainfall and Runoff and a number of alternative approaches have been proposed as a means of circumventing the need for this implicit assumption. These methods include 'Monte Carlo' approaches and 'continuous simulation' approaches.

The reliability of the Monte Carlo, Design Event and continuous simulation approaches and their associated uncertainty in prediction needs to be defined for different types of problems so that suitable guidance can be presented in the revision to Australian Rainfall and Runoff. The purpose of this project is to investigate and compare the performance of the Monte Carlo, Design Event, and continuous simulation methods under a range of conditions.

The Design Event approach assumes a "probability-neutral" transformation from rainfall to runoff. This essentially means that a rainfall of a given AEP should always result in a flood of the same AEP. This is achieved by using representative values of model inputs and parameters. The Design Event approach is the most comprehensively used approach to estimate design floods in Australia. It is simple to implement and is not computationally intensive. It has been tailored to Australian conditions, and makes use of data that are readily available in Australia. The inputs used by the method are reasonably well defined, leading to good consistency between studies conducted using this approach. It has also been thoroughly tested in Australian catchments and the limitations of the method are well understood.

There are a number of limitations of the Design Event approach. There are many possible interactions between rainfall and catchment characteristics that cannot be properly characterised by the use of fixed representative values of the flood producing variables, especially when they are sensitive and show large variability. This possibly jeopardizes applicability of the probability neutral assumption in many catchments.

There is a strong consensus in the literature that the processes involved in generating the design flood are probabilistic in nature and are best represented under a joint probability framework. This essentially means that the model output, inputs, parameters and the model states should exist in the form of jointly distributed random variables. From this perspective, conditioning the model output on fixed (mean or median) values does not preserve the probability neutral transformation of rainfall to runoff and introduces biases in the estimate of design flood.

The Monte Carlo method has the advantage of removing the dependence on AEP-neutrality assumptions and provides a more rigorous approach to assigning probability distributions to random inputs rather than adopting mean or median values as 'representative'.

Another advantage of the Monte Carlo method is in representing the operation of infrastructure in models. Specific failure states such as spillway blockages or machine outages in a power station, or initial water levels in reservoirs can be represented through a distribution, just as any other model input. This is a more robust approach than assigning fixed values to these variables as would be the case when using the Design Event approach. Another strength of the Monte Carlo method is in its handling of uncertainty, and the ability to quantify uncertainty in individual model inputs.

One limitation of the Monte Carlo approach is that the determination of distributions for input parameters, and any relationship between input parameters can present difficulties when adopting the Monte Carlo method for flood estimation. Another difficulty associated with this approach is the separation of uncertainty from natural variability. Input observations and parameters, such as rainfall and streamflow records, initial loss values, the AEP of the PMP, are subject to varying degrees of uncertainty. This uncertainty is not always quantifiable, and therefore may be inadvertently captured as natural variability.

The main advantage of the continuous simulation approach is that it is not limited by the probability neutral assumption as it samples all the joint probability interactions among the flood producing variables through direct simulation. The main limitations of the continuous simulation approach include the availability of suitable data, lack of definition of the flood frequency curve for rare to extreme events, and that the ability of continuous simulation models to reproduce both flood peaks and other hydrograph characteristics adequately for design flood purposes has not been proven.

The reliability of the Monte Carlo, Design Event and continuous simulation approaches was investigated using ten test catchments located in different areas of Australia. The catchments were selected to cover a range of climatic conditions, catchment sizes and catchment characteristics. Monte Carlo and Design Event models were developed for each of the ten catchments, and calibrated using observed rainfall and flow data. Continuous simulation models were developed for five catchments and were calibrated using the same base data.

The results of the method testing showed that in general both the Monte Carlo and Design Event approaches performed well over the range of catchments tested, over a range of AEPs from 50% to 1%. The exception to this was that the Monte Carlo model did not perform well for Yates Flat Creek catchment in South West Western Australia, where the flow response to rainfall events varies widely. For this catchment, the initial loss – continuing loss model was considered to be inappropriate and SWMod, a variable loss model, was also trialled. This produced improved results. The advantage of the Monte Carlo method in this case is that it clearly shows the spread of peak flows that can result from a rainfall event of a given AEP, dependent on combinations of losses and temporal patterns. Whilst the results from the Design Event model were better for this catchment, the lack of information on the confidence in the results could lead to inappropriate use of the model.

Manton River and Mary River catchments were used to investigate the effect of record length on model performance. For both catchments, the observed flow record was split into two equal halves based on date. For both catchments, there were approximately twenty years of record in each period. The results from the two test catchments show that even when twenty years of data is available at a site, the model results can vary significantly based on the period of record used in analysis. This is particularly evident when one period is noticeably drier or wetter than the other. This highlights the need to investigate how representative the available flow data is in the context of any available long-term rainfall records. Both the Monte Carlo and Design Event approaches gave similar results.

To examine the applicability of the methods for ungauged catchments, parameters were transferred between models. This was to simulate the use of model parameters calibrated on a gauged catchment in a model of an ungauged catchment. The Florentine River and Tyenna River models were used to investigate this situation for two similar catchments. Both the Monte Carlo and Design Event approaches performed reasonably well over the full range of AEPs when Tyenna River models were run using the Florentine River model parameters. When the Florentine River models were run using the Tyenna River model parameters, the Monte Carlo method performed slightly better than the Design Event model which showed 43% higher flow, than the observed flood corresponding to 1 % AEP, compared to 36% for the Monte Carlo. The results illustrate that even when there is data available at a neighbouring gauged catchment, care must be taken in estimating floods for ungauged catchments, and the model inputs and parameters must be carefully considered.

When parameters were transferred between models from dissimilar catchments, the results of both the Monte Carlo and Design Event approaches were very poor. From these tests it is concluded that, as expected, only catchments with similar climatic conditions, catchment sizes and catchment characteristics should be considered for providing model parameters for ungauged catchments.

The performance of the Monte Carlo and Design Event models in replicating the flood frequency curve at three internal gauge sites within the Mary River catchment was investigated. The results showed that both the Monte Carlo and Design Event models performed poorly at the Kenilworth gauge site. Further investigation showed that this is likely due to underestimation of flows in the Kenilworth flow record. For the other two sites, both the Monte Carlo and Design Event models performed reasonably well, despite these sites being relatively high in the catchment.

The results of the method testing on continuous simulation models showed that calibrating the model to all available flow record resulted in the highest Nash Sutcliffe Efficiency (NSE) values and, in general, captured the shape of flood hydrograph. However, in all the catchments except one, the highest flow peaks were under estimated and the flood frequency curve calculated from simulated annual maximum series provided a very poor fit to the observed flood frequency curve. Calibrating the model to a subset of record produced results that were very similar to using the full record. Using half of the available record did not significantly degrade the performance of the model. Calibrating the model to larger events resulted in a reduction in NSE

values and larger volume biases, with only slight improvements in matching the observed flood frequency curves. Finally, calibrating the model to the observed flood frequency curve in general produced a very close fit to the flood frequency curve, but resulted in a poor representation of hydrograph behaviour and large volume biases.

Among the five catchments tested using the continuous simulation approach, only the simulated flow generated for Mary River was able to produce a reasonably good representation of the hydrograph behaviour as well as the flood quantiles consistently. This indicates that, given good quality data and model structure (well representing the processes occurring in the catchment), the continuous simulation method is capable of generating a reasonably good representation of flood quantiles and hydrograph behaviour. However, the study also points to the inability of the rainfall runoff models used to reproduce hydrograph behaviour consistently across catchments with widely varying characteristics.

From the testing it was concluded that whilst both the Monte Carlo and Design Event approaches generally performed well in producing a flood frequency curve when compared with observed floods, the advantage of the Monte Carlo method was in the quantification of uncertainty provided by the spread of results from individual model runs. The continuous simulation approach could provide a good representation of the flood frequency curve when calibrated to the observed frequency curve, but hydrograph behaviour was not well represented.

## TABLE OF CONTENTS

<b>1.</b>	<b>Introduction.....</b>	<b>1</b>
1.1.	Objectives.....	1
1.2.	Approach .....	1
1.3.	Report structure .....	2
<b>2.</b>	<b>Literature Review .....</b>	<b>4</b>
2.1.	Introduction.....	4
2.2.	Design Event approach .....	5
2.2.1.	Advantages of the Design Event approach .....	6
2.2.2.	Limitations of the Design Event approach.....	6
2.2.3.	Conclusion: Design Event approach .....	8
2.3.	Monte Carlo Simulation .....	8
2.3.1.	Description of the method .....	8
2.3.2.	Advantages.....	10
2.3.3.	Limitations .....	11
2.3.4.	Uncertainty estimation .....	13
2.3.5.	Implementation .....	13
2.4.	Continuous Simulation.....	13
2.4.1.	Description of the method .....	14
2.4.2.	Advantages.....	16
2.4.3.	Limitations .....	17
2.4.4.	Uncertainty estimation .....	17
2.5.	Alternative methods .....	18
2.5.1.	The US Bureau of Reclamation method of deriving hazard curve .....	18
2.5.2.	Revitalized-Flood Studies Report/Flood Estimation Handbook (Re- FSR/FEH) rainfall-runoff model approach .....	19
2.5.3.	Electricité de France: SCHADEX method .....	19
2.5.4.	Methods used in South Africa .....	19
2.5.5.	Applicability of international methods to Australian conditions .....	20
<b>3.</b>	<b>Test Catchments.....</b>	<b>21</b>
3.1.	Catchment selection and data .....	21
3.2.	Data.....	23

---

3.3.	Catchment descriptions .....	24
3.3.1.	Mary River .....	24
3.3.2.	Hann River .....	25
3.3.3.	Yates Flat Creek.....	25
3.3.4.	Manton River .....	26
3.3.5.	Sixth Creek.....	27
3.3.6.	Lerderderg Creek.....	28
3.3.7.	Florentine River .....	29
3.3.8.	Tyenna River .....	30
3.3.9.	Hobart Rivulet.....	31
3.3.10.	Orara River .....	32
<b>4.</b>	<b>Method overview.....</b>	<b>34</b>
4.1.	SWMod.....	34
4.2.	Water balance models .....	35
4.2.1.	AWBM .....	35
4.2.2.	SIMHYD .....	36
4.2.3.	GR4H .....	36
4.3.	Model structure.....	37
<b>5.</b>	<b>Monte Carlo and Design Event Model Calibration and Design Runs .....</b>	<b>38</b>
5.1.	Calibration of routing parameters.....	38
5.1.1.	Event selection .....	38
5.1.2.	Rainfall distribution .....	38
5.1.3.	Calibration .....	38
5.1.4.	Calibration of SWMod.....	39
5.2.	Monte Carlo model design runs .....	39
5.2.1.	Design inputs.....	39
5.2.2.	Design runs .....	40
5.3.	Design event model design runs.....	41
5.3.1.	Design inputs.....	41
5.3.2.	Design runs .....	42
5.4.	Runs for ungauged catchments .....	42
5.5.	Calibration to sub-set of data .....	43
<b>6.</b>	<b>Continuous Simulation Model Calibration .....</b>	<b>44</b>

---

6.1.	Scenario 1: Calibration to the whole record.....	44
6.2.	Scenario 2: Calibration to subset the of data.....	44
6.3.	Scenario 3: Calibration to large events .....	45
6.4.	Scenario 4: Calibration to the observed flood frequency curve.....	45
6.5.	Evaluation of the model output .....	46
<b>7.</b>	<b>Monte Carlo and Design Event Model Calibration Results .....</b>	<b>48</b>
7.1.	Event calibration .....	48
7.1.1.	Event calibration for SWMOD in Yates Flat Creek .....	48
7.2.	Calibration of losses .....	48
7.2.1.	Calibration of the initial soil storage parameters for SWMOD in Yates Flat Creek.....	49
7.3.	Calibration to sub-set of data .....	50
7.3.1.	Manton River .....	50
7.3.2.	Mary River .....	51
7.4.	Key issues .....	53
7.4.1.	Mary River .....	53
7.4.2.	Hann River .....	53
7.4.3.	Yates Flat Creek.....	53
7.4.4.	Manton River .....	53
7.4.5.	Sixth Creek.....	54
7.4.6.	Lerderderg River.....	54
7.4.7.	Florentine River .....	54
7.4.8.	Tyenna River .....	55
7.4.9.	Hobart Rivulet.....	55
7.4.10.	Orara River .....	55
<b>8.</b>	<b>Monte Carlo and Design Event Model Results .....</b>	<b>56</b>
8.1.	Full data set.....	56
8.1.1.	Mary River .....	56
8.1.2.	Hann River .....	57
8.1.3.	Yates Flat Creek.....	59
8.1.4.	Manton River .....	61
8.1.5.	Sixth Creek.....	62
8.1.6.	Lerderderg River.....	64

8.1.7.	Florentine River .....	65
8.1.8.	Tyenna River .....	67
8.1.9.	Hobart Rivulet.....	68
8.1.10.	Orara River .....	70
8.2.	Sub-set of data .....	72
8.2.1.	Manton River .....	72
8.2.2.	Mary River .....	74
8.3.	Results for ungauged catchments.....	76
8.4.	Internal gauge sites .....	82
<b>9.</b>	<b>Continuous Simulation Model Results .....</b>	<b>86</b>
9.1.	Scenario 1 .....	86
9.1.1.	Comparison of hydrograph behaviour .....	86
9.1.2.	Comparison of the event volumes.....	87
9.1.3.	Comparison of flood frequency curves.....	87
9.2.	Scenario 2 .....	93
9.2.1.	Comparison of hydrograph behaviour .....	94
9.2.2.	Comparison of event volumes .....	94
9.2.3.	Comparison of flood frequency curves.....	94
9.3.	Scenario 3 .....	99
9.3.1.	Comparison of hydrograph behaviour .....	100
9.3.2.	Comparison of event volumes .....	100
9.3.3.	Comparison of flood frequency curves.....	100
9.4.	Scenario 4 .....	105
9.4.1.	Comparison of hydrograph behaviour .....	105
9.4.2.	Comparison of event volumes .....	105
9.4.3.	Comparison of flood frequency curves.....	107
<b>10.</b>	<b>Discussion .....</b>	<b>112</b>
10.1.	Performance of the models over different catchments and AEPs.....	112
10.2.	Effect of record length on Monte Carlo and Design Event model performance .....	113
10.3.	Performance of the Monte Carlo and Design Event models on ungauged catchments .....	113
10.4.	Performance of the Monte Carlo and Design Event models at internal gauges.....	115



---

10.5.	Ability of Continuous Simulation models to reproduce hydrograph behaviour and match observed flood frequency curve .....	115
10.5.1.	Multi objective nature of the calibration problem .....	116
10.6.	Continuous Simulation model suitability for design flood estimation.....	117
<b>11.</b>	<b>Conclusions .....</b>	<b>118</b>
<b>12.</b>	<b>References .....</b>	<b>121</b>
<b>13.</b>	<b>Appendices .....</b>	<b>126</b>
<b>Appendix A</b>	<b>Catchment data.....</b>	<b>127</b>
<b>A.1</b>	<b>Temporal Patterns .....</b>	<b>130</b>
<b>Appendix B</b>	<b>Catchment models.....</b>	<b>145</b>
<b>Appendix C</b>	<b>Event calibration.....</b>	<b>156</b>
<b>Appendix D</b>	<b>Loss calibration .....</b>	<b>178</b>
<b>D.1</b>	<b>Mary River .....</b>	<b>178</b>
<b>D.2</b>	<b>Hann River .....</b>	<b>179</b>
<b>D.3</b>	<b>Yates Flat Creek.....</b>	<b>180</b>
<b>D.4</b>	<b>Manton River.....</b>	<b>181</b>
<b>D.5</b>	<b>Sixth Creek.....</b>	<b>182</b>
<b>D.6</b>	<b>Lerderderg River.....</b>	<b>183</b>
<b>D.7</b>	<b>Florentine River .....</b>	<b>184</b>
<b>D.8</b>	<b>Tyenna River .....</b>	<b>185</b>
<b>D.9</b>	<b>Hobart Rivulet.....</b>	<b>186</b>
<b>D.10</b>	<b>Orara River.....</b>	<b>187</b>
<b>Appendix E</b>	<b>Calibration to subset of data.....</b>	<b>188</b>
<b>Appendix F</b>	<b>Flood frequency curves .....</b>	<b>193</b>
<b>F.2</b>	<b>Hann River.....</b>	<b>193</b>
<b>F.3</b>	<b>Yates Flat Creek.....</b>	<b>194</b>
<b>F.4</b>	<b>Manton River .....</b>	<b>194</b>
<b>F.5</b>	<b>Sixth Creek.....</b>	<b>195</b>
<b>F.6</b>	<b>Lerderderg River .....</b>	<b>196</b>
<b>F.7</b>	<b>Florentine River.....</b>	<b>196</b>
<b>F.8</b>	<b>Tyenna River .....</b>	<b>197</b>
<b>F.9</b>	<b>Hobart Rivulet .....</b>	<b>198</b>
<b>F.10</b>	<b>Orara River .....</b>	<b>199</b>

---

<b>Appendix G</b>	<b>Additional model results .....</b>	<b>200</b>
<b>Appendix H</b>	<b>Continuous Simulation model structures .....</b>	<b>201</b>
<b>Appendix I</b>	<b>Data used for calibration.....</b>	<b>204</b>
<b>Appendix J</b>	<b>Results Scenario 1.....</b>	<b>211</b>
<b>Appendix K</b>	<b>Results : Scenario 2 .....</b>	<b>224</b>
<b>Appendix L</b>	<b>Results: Scenario 3 .....</b>	<b>237</b>
<b>Appendix M</b>	<b>Results Scenario 4.....</b>	<b>250</b>
<b>Appendix N</b>	<b>Rainfall data .....</b>	<b>263</b>
<b>Appendix O</b>	<b>Calibrated parameters.....</b>	<b>265</b>
<b>Appendix P</b>	<b>Events selected for volume comparison .....</b>	<b>269</b>
<b>Appendix Q</b>	<b>Temporal pattern selection and filtering for Design Event approach.....</b>	<b>281</b>

## Abbreviations

AEP	Annual Exceedance Probability
ARR	Australian Rainfall and Runoff
ARR87	Australian Rainfall and Runoff, 1987 edition
AVM	Average Variability Method
CL	Continuing Loss
CSS	Continuous Simulation System
DE	Design Event
FFA	Flood Frequency Analysis
FORGE	Focussed Regional Growth Estimation
IFD	Intensity-Frequency-Duration
IL	Initial Loss
MC	Monte Carlo
PMF	Probable Maximum Flood
PMP	Probable Maximum Precipitation

## Acknowledgements

The authors wish to acknowledge the assistance of the following people and agencies in supply and preparation of data/models for this project:

- Zuzanna Graszkiwicz and Peter Hill - Jacobs
- Brett Phillips - Cardno
- Peta Hansen - Government of South Australia Department of Environment, Water and Natural Resources
- Bryce Graham and Kirsten Adams - Tasmanian Department of Primary Industries, Parks, Water and Environment
- Greg Carson - Hydro Tasmania
- Lesley Rowland, Karin Xuereb - Bureau of Meteorology
- Lynda Bonar - Hobart City Council
- Leanne Pearce – Water Corporation
- Kai Kinkela, Water Corporation
- James Bennett – CSIRO Land and Water
- Thibault Mathevet - EDF
- Monique Retallick, Melanie Loveridge, Dan Morgan, Mark Babister, WMA Water
- The State of Queensland Department of Natural Resources and Mines
- State Government Victoria Department of Environment and Primary Industries
- Government of Western Australia Department of Water
- Jeffrey Watson, Department of Agriculture and Food, Western Australia
- Northern Territory Government Department of Land Resource Management

## 1. Introduction

Estimation of flood flows in the absence of at-site recorded data generally requires either a regional method (Project 5) or a rainfall based approach. Rainfall based approaches are based on using a catchment modelling system which may be conceptually complex or simple to predict the response of a catchment to a storm burst (or event) or to a sequence of storm events. At the time of the publication of the current edition of Australian Rainfall and Runoff, the recommended Design Event approach implicitly assumed that the frequency of the rainfall was translated into the desired frequency of flood flow through use of median values of other input to the catchment modelling system. This implicit assumption has been tested in the period since publication of the current edition of Australian Rainfall and Runoff and a number of alternative approaches have been proposed as a means of circumventing the need for this implicit assumption. These methods include 'Monte Carlo' approaches and 'continuous simulation' approaches.

### 1.1. Objectives

The reliability of the Monte Carlo, Design Event and Continuous Simulation approaches and their associated uncertainty in prediction need to be defined for different types of problems so that suitable guidance can be presented in the revision to Australian Rainfall and Runoff. The purpose of this project is to investigate and compare the performance of the Monte Carlo, Design Event and Continuous Simulation methods under a range of conditions. For the Monte Carlo and Design Event methods, the range of conditions includes:

- differing climatic conditions
- different size catchments
- rural and urban catchments
- gauged and ungauged catchments
- differing Annual Exceedance Probabilities (AEP)
- predictions at multiple points within catchments.

In this study the ability of Continuous Simulation models to reproduce design flood quantiles is investigated under four calibration scenarios including calibration of the model to:

- the whole record available
- a sub set of the record
- the larger events in the record and
- directly to the flood frequency curve fitted to the observed flow data (hereafter called observed flood frequency curve).

For each calibration, the ability to reproduce the hydrograph behaviour is also investigated.

### 1.2. Approach

In order to achieve the objectives of this project, data was collated from ten gauged catchments across Australian states and territories, representing a range of climatic conditions and catchment characteristics.

The tasks that were undertaken for testing of flood estimation methods were:

- i. Data acquisition
  - Collate continuous streamflow, rainfall, gauging and rating data for all catchments
  - Check all data for suitability for use in the project, including investigating inconsistencies and errors
- ii. Model development
  - Develop semi-distributed initial loss-continuing loss rainfall-runoff models for each catchment, with channel routing between sub-catchments
  - Develop continuous simulation models for a sub-set of five of the catchments, with channel routing between sub-catchments
- iii. Derive and collate all model inputs
  - Rainfall temporal patterns for Monte-Carlo methods
  - Distributions of losses
  - Design rainfalls for a range of durations and AEPs up to 1 in 100
  - Continuous rainfall and streamflow records for input to continuous simulation models
- iv. Performance of the Design Event and Monte Carlo methods at gauged and un-gauged locations
  - For gauged locations, the models were calibrated to recorded large flow events and the at-site frequency curve
  - To test the ability of the methods to perform on un-gauged basins the calibrated model parameters from one catchment were transposed to two other catchments; one with similar characteristics, and one with different characteristics
- v. Performance of the methods as a function of AEP
  - The results from the models calibrated using all available data were compared with at-site frequency curve
  - For selected sites, the models were re-calibrated using sub-sets of data and the results were then compared with the at-site frequency curve derived from the full data set
- vi. Ability to predict flood characteristics at multiple points within catchments.
  - A large catchment with observed rainfall and streamflow data available at the outlet as well as at interior sites was used for this test. The Design Event and Monte Carlo models were calibrated to the data available at the outlet of the catchment and the performance of the model was evaluated against the observed flood frequency curve at the interior site.
- vii. Performance of continuous simulation models using different calibration approaches.
  - For a sub-set of five of the selected catchments, continuous simulation models were calibrated to (1) the whole record, (2) a sub set of the record, (3) the larger events in the record and (4) directly to the flood frequency curve fitted to the observed flow data.
- viii. Analysis of results
- ix. Reporting

### **1.3. Report structure**

This report includes:

- a literature review on the alternative methods
- a description of the catchments used in the testing and the data available

- a description of the model development
- an outline of the calibration process and results
- presentation of results
- discussion of findings
- conclusions

## 2. Literature Review

### 2.1. Introduction

The design of major structures involving risk to life or property requires estimation of the risk posed by floods with very low probabilities of exceedance. In Australia estimation of such large magnitude floods is guided by the risk based approach recommended by Australian Rainfall and Runoff (ARR) guidelines (Engineers Australia, 1998).

In catchments with long series of measured flow data, at high temporal resolution, floods of large magnitude (up to 1% AEP) can be estimated using a flood frequency analysis (FFA) of the observed streamflow data. This involves fitting theoretical distributions to the maximum flood values (usually annual maximum or those determined through peak over threshold) observed in the historical record (Engineers Australia, 1998). It is generally accepted that the FFA is the best approach for estimation of design floods that are more frequent than the length of the observed flood data. However, the current reality is that in most catchments the flow data rarely extends over 50 years.

Estimation of rare to extreme floods using short records of flow data is problematic and prone to sampling problems, because the observed data may not sample the extreme events or capture the long term (decadal or more) climatic variability. Newton & Walton (2000) provide an example where use of a relatively short record of streamflow data, occurring over a period of relatively low flow, results in underestimation of large floods.

In catchments where the data period is short relative to the rarity of the design flood, design floods of very low frequency of occurrence can be estimated by augmenting the observed data by additional information derived from other sources, such as paleo-flood investigations (J. England, 2011), or through rainfall based approaches (Engineers Australia, 1998) or regional methods. The rainfall based approaches mainly transform the probabilistic inputs of rainfall to probabilistic outputs of streamflow, using statistical (Naghattini et al. 1996), empirical or conceptual rainfall-runoff models (Engineers Australia, 1998).

In Australia, the current recommended rainfall based approach for estimating large to extreme floods, recommended by the Australian Rainfall-runoff (ARR) guidelines is the Design Event (DE) approach (Engineers Australia, 1998). The method has been comprehensively used for design flood estimation in Australia, however its implementation has raised a number of practical and theoretical questions. Two other approaches to design flood estimation, Monte Carlo based and Continuous Simulation, have the potential of overcoming some of the limitations posed by the DE approach.

This section contains a review of proposed methods for flood estimation in Australia. Specifically, the proposed Monte Carlo and Continuous Simulation methods are compared with the currently used DE approach, and a brief summary of alternative methods used internationally is provided. A brief description of each method is given, along with advantages and limitations of each.

## 2.2. Design Event approach

Rainfall based design flood estimation methods typically transfer probabilistic inputs of rainfall of a given Annual Exceedance Probabilities (AEP) to design flood outputs. The Design Event (DE) approach recommended by ARR assumes a “probability-neutral” transformation from rainfall to runoff. This essentially means that a rainfall of a given AEP should always result in the flood of the same AEP.

The DE method starts by estimating the depth of rainfall corresponding to a given AEP for a range of durations using Intensity-Frequency-Duration curves (IFD). The design rainfall depth for the AEP of interest and a range of rainfall burst durations and fixed representative temporal and spatial storm patterns are driven through a conceptual loss model to generate precipitation excess hyetographs.

The fixed temporal patterns are either derived using the average variability method (Pilgrim and French 1969) or sourced from the Probable Maximum Flood method (for example Bureau of Meteorology 1994) depending on AEP of interest. Generally, uniform spatial patterns are applied for the estimation of large floods and spatial patterns sourced from the PMP methods are used for estimation of extreme floods. The spatial patterns are assumed to have less influence (compared to temporal patterns) on the size and shape of the resulting design flood hydrographs (Engineers Australia, 1998).

Various types of models ranging from a simple loss model to complex conceptual rainfall-runoff models can be used to derive the precipitation excess hyetograph (Hoang et al. 1999). In Australia the most comprehensively used loss model (for design flood estimation) is the Initial Loss Continuing Loss (IL-CL) model (Hoang et al. 1999; Hill & Mein 1996; Nathan et al. 2003; Rahman et al. 2002). The IL-CL model is an event based model in which loss parameters are used to represent processes contributing to losses such as interception, infiltration, soil storage evapotranspiration, and initial moisture content (or catchment wetness) of the catchment (Kuczera, et al. 2006a; Nathan et al. 2002). Generally, the initial catchment wetness (antecedent conditions) is accounted for by an initial loss (IL) parameter, while other processes contributing to losses are lumped together and represented by a continuous loss (CL) parameter.

The precipitation excess simulated by the loss model is then routed through the catchment to generate the design flood hydrograph. The hydrograph corresponding to the burst duration that results in the highest peak (critical duration) is taken as the design flood hydrograph and the peak is taken as the design flood of AEP equal to the rainfall AEP.

In the DE approach, the only probabilistic variable is the rainfall intensity, while the other inputs (losses, temporal pattern, spatial pattern, storm duration) are represented by median or average values (Kuczera et al. 2003; Mirfenderesk et al. 2005; Nathan et al. 2002; Nathan et al. 2003; Rahman et al. 1998; Rahman et al. 2002).



## **2.2.1. Advantages of the Design Event approach**

The DE approach is the most comprehensively used approach to estimate design floods in Australia. It is simple to implement and is not computationally intensive. Importantly, it has been tailored for Australian conditions, and makes use of data (for example IFD curves, spatial and temporal patterns for extreme floods) that are readily available in Australia. The inputs used by the method are reasonably well defined, leading to consistency between the studies conducted using this approach. It has also been thoroughly tested in Australian catchments and the limitations of the method are well understood (Engineers Australia, 1998; Hill & Mein, 1996; Rigby & Bannigan, 1996; Walsh, Pilgrim, & Cordery, 1991).

## **2.2.2. Limitations of the Design Event approach**

The probability neutrality assumption in the DE approach is maintained by selecting representative (usually average) temporal patterns, spatial patterns and fixed values (median/average) of parameters. The success of the DE approach lies in how strongly the fixed values of the flood producing variable are able to preserve the 'probability neutrality' assumption.

Kuczera et al. (2006a) analyzed the conditions under which the selection of average values for initial catchment conditions (specifically initial loss) and a given storm temporal pattern could preserve the probability neutrality assumption. Using the joint probability description of the rainfall-runoff process they showed that the use of fixed average values can only be justified (to preserve 'probability neutrality') if the flood response of a catchment was linear.

### **2.2.2.1. Non-linearity of the catchment and natural variability of hydrologic variables**

The partitioning of the rainfall into surface runoff, sub-surface flow, and losses is governed by complex physical processes and interactions between various components (including climate, vegetation and soil) in the system. This results in a rainfall-runoff relationship that is non-linear and dynamic; changing and evolving with catchment characteristics, antecedent conditions and rainfall characteristics. In addition, the flood producing variables (initial loss parameters, the temporal patterns and spatial patterns and spatial patterns) exhibit a large variability over time and over catchments (Walsh et al. 1991; Mirfenderesk et al. 2005; Rahman et al. 2002). This means that a flood of a given AEP could be produced by a number of storms of varying AEPs, depending upon whether the catchment is wet or dry (antecedent catchment condition) at the start of the storm (Weinmann et al. 2002). The nonlinear hydrologic behavior of the catchment seriously undermines the probability neutral assumption. Importantly, the use of fixed representative values for estimation of the design flood does not capture the natural variability and the interactions between the flood producing variables to preserve the probability neutral assumption (Weinmann et al., 2002).

Nathan et al. (2003) showed that the bias introduced by use of a fixed initial loss parameter could be as high as 30% for more frequent floods, but lower for extreme floods as the influence of the catchment characteristics becomes less dominant compared to rainfall characteristics with increasing magnitude of storm.

Walsh et al. (1991) observed considerable variability in the calibrated values of the initial loss parameter over catchments and over the range of rainfall AEPs and suggested that the parameters/variables used in the estimation of the design flood should be treated as random variables. Weinmann et al. (2002) compared the flood peaks generated using the 'typical' temporal pattern (based on the average variability of the storms) and randomly sampled pattern and reported that the former resulted in an underestimation of peak by 15-20%. In fact, ARR guidelines acknowledges the limitation of using fixed temporal pattern and recommends use of their use only 'in the absence of more sophisticated procedures'.

#### **2.2.2.2. Critical durations**

The approach of using critical durations to derive the design flood estimate has also been questioned. The duration at which the flood attains its highest peak is governed by interplay between the catchment and rainfall characteristics (Weinmann et al. 2002). Therefore the design flood peak values conditioned on the critical duration storm ignores other possible combinations of intensity and duration that contribute to the total probability of the flood (Kuczera et al. 2006a). Furthermore, Weinmann et al. (2002) highlighted the problem of using the critical duration by comparing the process of deriving the flood frequency curve using observed values to that derived using the DE approach. They found that the flood magnitude generated from observed annual series considers floods produced from storms of all durations and corresponds to the marginal distribution of the flood magnitude (i.e. integrated over all possible values of rainfall durations). The flood magnitude estimated using the DE approach is conditioned on critical duration of the storm and represents the conditional distribution of the flood magnitude.

#### **2.2.2.3. Inconsistencies due to use of complete storm and storm bursts**

The rainfall intensities and the temporal patterns used in the DE approach are derived based on the storm burst while the losses are derived from complete storms. Therefore the estimated initial loss takes into account the pre-burst rainfall, not included in the design rainfall intensity and temporal pattern, leading to underestimation of loss and over estimation of peak design flood (Hill & Mein 1996; Kuczera, et al. 2006a). This seems to be more severe for 'early peaking' temporal patterns (Hill & Mein, 1996). On the other side, Rigby & Bannigan (1996) reported that failure to account for pre-burst rainfall on smaller catchments with large natural or man-made storages leads to under estimation of the catchment wetness and the underestimation of the design flood. A larger amount of the design rainfall is required to compensate for the drier storages in the absence of pre-burst rainfall. They suggested using a pre-burst temporal pattern to account for this. It is apparent that the two sources of errors have opposite effects, but it is not clear how much these two compensate for each other.

#### **2.2.2.4. System state**

When dealing with catchment infrastructure (such as power stations) and reservoirs, it is necessary to capture appropriate values for the model parameters that represent system state values (e.g. initial storage level, number of machines available). A single value for these parameters is not likely to be fully representative of the probable state. Very different peak

discharges from a storage may be result from different reservoir starting levels (e.g. full supply level vs another selected value).

### **2.2.3. Conclusion: Design Event approach**

It is well understood that there are many possible interactions between rainfall and catchment characteristics which cannot be properly characterised by the use of fixed representative values of the flood producing variables, especially when they are sensitive and show large variability. This possibly jeopardizes applicability of the probability neutral assumption in many catchments. There is a strong consensus in the literature that the processes involved in generating a design flood are probabilistic in nature and are best represented under a joint probability framework (Engineers Australia 1998, Kuczera et al. 2006a; Mirfenderesk et al. 2005; Nathan et al. 2003; Rahman et al. 2002b). This essentially means that the model output (design flood), inputs (rainfall duration, losses, intensity, spatial and temporal patterns), parameters and the model states should exist in the form of jointly distributed random variables. From this perspective, conditioning the model output on fixed (mean or median) values does not preserve the probability neutral transformation of rainfall to runoff and introduces biases (Nathan et al. 2003; Weinmann et al. 2002; Hill & Mein 1996) in the estimate of design flood (Kuczera et al. 2006a; Mirfenderesk et al. 2005; Nathan et al. 2003; Rahman et al. 2002b).

## **2.3. Monte Carlo Simulation**

Considerable attention has been given to applying Monte Carlo methods, also referred to as joint probability methods, to flood models over the last two decades in Australia (Rahman et al. 2002a; Mirfenderesk et al. 2005; Charalambous et al. 2013). A common argument in favor of this approach over the Design Event (DE) approach is that sampling from a distribution of values for model inputs is more representative of the physical system being modeled (Weinmann et al. 2002; Kuczera, et al. 2006a).

The Monte Carlo Simulation method for flood analysis outlined by Engineers Australia (2013) offers a significantly different approach to determining flood magnitudes and probabilities than the DE approach outlined in Section 2.2. This method is also event based, and can be regarded as an extension of the DE approach with more rigorous treatment of parameter variability (Weinmann et al., 2002). The advantages of the Monte Carlo method are best exploited when the catchment being modeled is thought to have a non-linear response to input rainfall (Nathan & Weinmann 2013). In catchments where this is not the case (i.e. catchments with a linear response), the application of the Monte Carlo method may not be warranted.

### **2.3.1. Description of the method**

The first step when implementing the method is the selection of an appropriate flood simulation model, as would be used in the DE approach. Due consideration should be given to model execution speed, as many thousands of model executions are required for the Monte Carlo method.

The model inputs need to be reviewed to understand which are most sensitive to determining

peak outflow for a given model run. Consideration can be given to treating parameters that are less sensitive as constants. Initial loss is commonly assigned a distribution, which captures the variability in antecedent catchment conditions, while continuing loss is commonly treated as a constant (Mirfenderesk et al. 2005; Charalambous et al. 2013; Rahman et al. 2002a). Temporal patterns are universally adopted as a variable input, presumed to be a uniform distribution of nominal data. Spatial patterns are typically treated as constant for rainfalls of a given AEP (e.g. Mirfenderesk et al. (2005)). There is scope in the Monte Carlo method, specifically in the URBS implementation, for treating spatial patterns as a non-uniform distribution, assuming that systematic spatial patterns can be detected (Rahman et al. 2002a).

Once sensitive model parameters have been identified, appropriate and representative distributions need to be determined for each parameter. These distributions may be parameterized or empirical. During the stochastic analysis, each model run will have its input parameters selected from its distribution.

It is possible that a correlation exists between two input variables. If this is the case, the independent variable needs to be identified and the relationship between the two needs to be defined. From this, the stochastic sampling step (defined below) can generate random variables based on this relationship.

The next step is running the rainfall-runoff model with stochastic sampling of input variables. This typically involves thousands of model executions. For each execution, the model input parameters will be randomly selected based on their distributions. If there is a correlation between two parameters, the independent parameter will be assigned a value randomly selected from its distribution. The dependent parameter will then be assigned a value based on the independent parameter's value and the relationship between the two. This stage will produce many outputs, principally a flood peak for each run. Discharge hydrographs are also a valuable output from this stage of the analysis.

The model is executed a pre-determined number of times; for the direct sampling approach (see Section 2.3.1.1), this number is typically 10 to 100 times the inverse of the largest AEP (R. Nathan & Weinmann, 2013) (ie if results are required up to an AEP of 0.1%, then 10,000 – 100,000 model executions will be required). For each model run, values are selected for its parameters from the distributions assigned in the previous step. Once the model runs have completed, a distribution is fitted to the results; this forms the flood frequency analysis component of the study.

#### **2.3.1.1. Determining distributions for input parameters**

A major consideration when adopting the Monte Carlo method is the determination of distributions for the model input parameters. As an event approach, input parameters identifying antecedent conditions (such as initial loss in an IL-CL model) need to be determined separately to the events being modelled: distributions for these parameters must be determined separately (Kuczera et al. 2006a).

### 2.3.1.2. Variations of the method

Engineers Australia (2013) describe two broad approaches to the Monte Carlo sampling. The first is 'direct sampling', which extracts values directly from the distributions of each variable. This approach is suited when model execution time is low and exceedance probabilities are relatively high, for example 0.1% AEP or more frequent. A guide of 10 to 100 times the inverse of the probability of exceedance is a guide to the number of required runs, for example to determine the 0.1% AEP flood, 10,000 to 100,000 model executions will be required.

The second approach is stratified sampling: this allows the user to sample around probabilities of interest, and is ideally suited when looking to determine the magnitude of rare to extreme events or when faced with a lengthy model execution time. The rainfall frequency curve is divided into intervals. These intervals are sampled from evenly during stochastic sampling. Intervals are defined around the AEPs of interest.

The method described by Engineers Australia (2013) adopts flood depths from a range of fixed storm burst durations, as is used in the DE approach. The Monte Carlo method offers an improvement over this approach by determining a distribution of storm durations. Hoang et al. (1999) introduce a method of achieving this through identifying 'complete storms' and 'storm cores'. Though these are given more mathematical definitions, a broad definition of a complete storm is "a period of significant rain preceded and followed by an arbitrary selected period of 'dry hours'" (Charalambous et al. 2013, p. 4103). A storm core is defined by Hoang et al. (1999, p. 380) as "the most intense rainfall burst within a complete storm"; they suggest that fitting distributions to storm cores is a promising approach. Charalambous et al. (2013) applied this method to a large catchment (1,000 km<sup>2</sup>) in North Queensland by determining distributions of initial loss prior to any storm runoff, i.e. using a distribution of initial loss based on a complete storm ( $IL_S$ ). A mapping from  $IL_S$  and storm core duration ( $d_C$ ) to initial loss prior to a storm core ( $IL_C$ ) was determined, and this value was used as a model run parameter.

### 2.3.1.3. Seasonal indexing

To refine the Monte Carlo analysis, data may be divided into seasons: instead of deriving single distributions for each parameter, seasonal distributions may be used. This is applicable when parameter values (such as losses and rainfall) are distinctly different in each season (Nathan et al., 2003).

## 2.3.2. Advantages

The Monte Carlo method addresses many issues present in the DE approach, identified in Section 2.2.2. The more rigorous approach to assigning probability distributions to random inputs rather than adopting mean or median values as 'representative' is a major argument in favour of a Monte Carlo method (Kuczera et al. 2006a). The removal of the dependence on the AEP-neutrality assumption is an important improvement, particularly so for rarer and extreme events (Rory Nathan et al., 2003).

The ability for the Monte Carlo method to relax critical duration, ie to assign a distribution to

storm duration as an input, allows this method to remove or reduce bias introduced by using fixed durations in the DE approach (Rory Nathan et al., 2003).

Although Monte Carlo methods typically use many thousands of model executions, and can potentially require significant processing time, adopting a stratified sampling approach can limit model run time by focusing the analysis on the area of interest (R. Nathan & Weinmann, 2013). This is an advantage of the stratified Monte Carlo method over the direct sampling method and the Continuous Simulation method. Both of these methods are computationally inefficient if an understanding of extreme events is desired (R. Nathan & Weinmann, 2013).

When modeling infrastructure is a requirement (as discussed in Section 2.2.2.4), as is common with studies examining extreme events, it is possible to represent the probability of system failure (such as spillway blockages or machine outages in a power station) through a distribution, just as any other model input. Appropriate and representative drawdown levels on reservoirs may also be assigned distributions (Rory Nathan et al., 2003). These may be dependent on the extremity of the rainfall: this relationship can be represented through parameter correlation, as discussed in Section 2.3.1. This is thought to be a much more robust approach than assigning of fixed values to these variables as would be the case in the DE approach.

Engineers Australia (2013) give the following advantages of the Monte Carlo approach:

- The ability to concurrently determine flood characteristics at multiple points within a system/catchment
- The ability to sample the range of storm durations, as opposed to using fixed durations
- The stochastic sampling of variable values overcomes the limitation of fixing values. For example, antecedent catchment conditions can be captured through a distribution of loss values rather than relying on fixed values.
- The probability of a given peak discharge (or other measure of runoff intensity) is not linked to the probability of a given rainfall input (ie the method relaxes probability neutrality)

Another strength of the Monte Carlo method is its handling of uncertainty (see Section 2.3.4).

### **2.3.3. Limitations**

The run time of the Monte Carlo Simulation approach will be much greater than with the DE approach. This is due to the many thousands of model runs that are required to complete the analysis. As such, large, complex models with long run times might not be suitable for this approach (Engineers Australia 2013 p 17).

The determination of distributions for input parameters can present difficulties when adopting the Monte Carlo method for flood estimation (Kuczera et al. 2006a). Determining parameter sensitivity, and therefore which parameters to use as variable inputs and which parameters to assign constant values, can also be a complex task. A related area of complexity is identifying relationships between parameters and the nature of these relationships (e.g. linear or otherwise) (R. Nathan & Weinmann, 2013). Another difficulty associated with this approach is the

separation of uncertainty from natural variability (R. Nathan & Weinmann, 2013). Input observations and parameters, such as rainfall and streamflow records, initial loss values, the AEP of the PMP, are subject to varying degrees of uncertainty. This uncertainty is not always quantifiable, and therefore may be inadvertently captured as natural variability.

### **2.3.4. Uncertainty estimation**

The Monte Carlo Simulation method inherently handles uncertainty estimation through its stochastic modeling approach. The technique outlines a method for quantifying uncertainty through separation of uncertainty in model parameters from natural variability in each parameter; this is the first step in developing confidence intervals (Nathan and Weinmann 2013).

### **2.3.5. Implementation**

Suggested implementations of this method include spreadsheets and customized computer programs or batch files Nathan and Weinmann (2013). Some desirable features of a development environment (such as a spreadsheet or programming language) for this method include:

- A library of suitable statistical distributions
- An effective and unpredictable pseudo-random number generator
- A good user interface
- A sophisticated plotting environment
- Good interfacing with the rainfall-runoff modeling environment

Some examples are Excel and the R programming language. The RORB modeling environment also includes Monte Carlo Simulation capability. The URBS model has also been used to undertake Monte Carlo Simulation (Rahman et al. 2002a).

## **2.4. Continuous Simulation**

The last few decades have seen considerable advances in computational power. This has allowed implementation of models that are more complex and that provide greater (and more elaborate) representation of the physical processes occurring in a catchment (Boughton & Droop, 2003). This has led to development of large numbers of physically based and conceptual rainfall-runoff models from the Stanford Watershed model (Linsley and Crawford 1960) to physically based models such as Systeme Hydrologique Europeen Model (SHE; Abbott et al. 1986). Traditionally, rainfall based methods of estimating the design flood have predominately been event based, while Continuous Simulation has been applied for flood forecasting and yield modelling. However, development of tools and methods that allow generation of long periods of synthetic rainfall data has led to increased interest in using Continuous Simulation for design flood estimation and the concept of using models traditionally developed for flood forecasting in the estimation of design floods (W. Boughton & Droop, 2003).

The Continuous Simulation method of estimating the design flood is, in principle, similar to the event based Monte-Carlo approach discussed in Section 3. Both methods seek to adequately simulate the interactions between flood producing (rainfall and catchment characteristics) variables (Kuczera et al. 2006a). Conceptually, the differences between the two methods arise in how wet and dry periods are sampled and incorporated into the process of estimating the design flood.



The event based Monte-Carlo method uses rainfall-runoff models to simulate the interactions occurring during the storm (wet period) event. It implicitly considers the influence of the dry periods by sampling the catchment-rainfall interactions (antecedent conditions, temporal patterns, storm durations) from exogenously derived distributions (Kuczera et al. 2006a).

The Continuous Simulation method, on the other hand, accounts for these interactions (occurring over a long period of drought and storm) through direct simulation of the processes occurring in the catchment (Kuczera et al. 2006a; Boughton et al. 1999; Cameron et al. 1999).

### **2.4.1. Description of the method**

The Continuous Simulation method of estimating a design flood involves running a conceptual rainfall-runoff model for a long period of time such that all important interactions (covering the dry and wet periods) between the storm (intensity, duration, temporal pattern) and the catchment characteristics are adequately sampled to derive the flood frequency distribution. In general, pluviograph data of hourly resolution (or less) is used to drive the rainfall-runoff models. In most cases the pluvio data rarely exceeds 50 years, therefore the rainfall data needs to be extended by using stochastic rainfall data generators. The rainfall-runoff model is calibrated using flow data and the calibrated model is then used to generate a long series of simulated flow. Finally the simulated flow is then used to derive the annual maximum series and estimate the derived flood frequency curve. Important components of Continuous Simulation approach are further discussed below.

#### **2.4.1.1. Rainfall-runoff model**

Types of rainfall-runoff models used to simulate the flow can be varied and depend upon the complexity required to provide unbiased simulation of the hydrologic process in the catchment. For example, Boughton et al. (1999) and Droop & Boughton (2002) used a simple lumped Australian Water Balance Model (AWBM) to simulate a long series of precipitation excess, for small to mid-sized catchments, which were then routed using hourly hydrograph generation model. Haberlandt & Radtke (2013) used HEC-HMS (Feldman 2000), a semi distributed rainfall-runoff model, in three medium sized catchments in Germany. Cameron et al. (1999) applied a semi-distributed conceptual rainfall-runoff model known as TOPMODEL (Beven, 1987) for design flood estimation in small sized catchments in the UK. For large catchments with large spatial heterogeneity, England (2006) recommends using a physically based distributed model to fully characterize the spatial distribution of the process occurring in the catchment.

In general, there are no strict guidelines on use of rainfall-runoff modelling for Continuous Simulation (W. Boughton & Droop, 2003), however two factors that should be considered in selecting the model are: the ability of the model to represent the physical processes occurring in the catchment (model complexity), and the amount of data and computational resources available to properly describe and calibrate the model (model parsimony).

#### **2.4.1.2. Stochastic rainfall data generation**

The effectiveness of the Continuous Simulation method depends upon the availability of a sufficiently long rainfall dataset to provide adequate information on extreme storm (and drought)

events. In reality however, the pluviograph data rarely extends over 50 years, and the inference of floods greater than 2% AEP is difficult (W. C. Boughton et al., 1999).

In such cases stochastic rainfall generation has been used to provide a long time series of the synthetic rainfall dataset (W. C. Boughton et al., 1999; Cameron et al., 1999; Droop & Boughton, 2002; Haberlandt & Radtke, 2013). The synthetic dataset thus generated is designed to be statistically indistinguishable from observed rainfall data (Kuczera et al. 2006).

There are well established methods to generate stochastic data at a coarse scale. However, generating fine resolution synthetic data that can reproduce the statistics of the observed rainfall series at various temporal scales (annual, monthly, daily and hourly) is challenging (Srikanthan & McMahon 2001; Boughton & Droop 2003; Kuczera et al. 2006a). Therefore, a commonly used approach is to generate the synthetic rainfall data at a daily time step first, and then disaggregate to a sub-daily time step by conditioning the coarser resolution data on sub-daily rainfall statistics. Boughton et al. (1999) used the transition probability matrix (TPM) model to generate thousands of years of daily rainfall data and then disaggregated the daily data to an hourly time-step using the sub-daily rainfall statistics derived from IFD curves (Nathan and Weinmann 2013) and temporal patterns. Kuczera et al. (2006) tested the ability of a rainfall generating model (modified version of Disaggregated Rectangular Impulse Point [DRIP] rainfall model) to reproduce observed rainfall statistics at different levels of aggregation (hourly to yearly) and found that the model was able to reproduce the observed rainfall statistics satisfactorily for the large storms.

Commenting on the effectiveness of the rainfall generating models, Kuczera et al. (2006) mention that “stochastic rainfall models suggests they are capable of satisfactorily reproducing what appear to be important rainfall characteristics and are on the verge of practical application”.

#### **2.4.1.3. Model calibration (Rainfall – runoff and rainfall generation models)**

Implementation of Continuous Simulation, and the use of synthetic data, is complicated by the need to calibrate both the rainfall model and the rainfall-runoff model using the observed dataset. Effective calibration depends upon the calibration method applied, the length and the quality of data used for calibration. Gupta & Sorooshian (1985) report that the benefit of using additional data (with similar information content) diminishes with the reciprocal of the square root of the number of data points used in the calibration. Therefore, while the length of data is an important factor, the data series should also contain sufficient number of ‘unusual events’ (or extreme events) to enable estimation of the parameter values (Singh and Bárdossy 2012).

The rainfall generation model is generally calibrated to storm events, as in alternating-renewal models like DRIP or to aggregation statistics (like mean, skewness, coefficient of variation, auto correlations etc.) at various time scales (Kuczera et al. 2006a). While the rainfall runoff models are calibrated to observed flow data, flow statistics (W. C. Boughton et al., 1999) and in some cases flood frequency curve (Cameron et al., 1999).

Lack of observed data is a major problem for calibration of rainfall generation models or rainfall-runoff models. In the case of rainfall generation model, a short rainfall dataset is unlikely to

include extreme rainfall events caused by various rain producing mechanisms (for example cyclones vs. thunderstorm) and sample the full range of natural variability.

#### **2.4.1.4. Applications of the Continuous Simulation approach to design flood estimation**

With improvements of methods and computational efficiency in generating stochastic rainfall data, there has been increased interest in developing, testing and applying Continuous Simulation methods to design flood estimation.

Boughton et al. (1999) developed a Continuous Simulation System (CSS) for estimation of design floods, and applied this to a number of catchments of mid to small sizes in Victoria. The CSS comprised of a stochastic rainfall generator, an AWBM water balance model and a hydrograph model. The 2000 years of synthetic rainfall daily rainfall was generated by a transition probability matrix model, using the FORGE estimates of daily rainfall data and disaggregated to hourly data. A multi objective calibration strategy was used to calibrate the rainfall-runoff model against the monthly runoff volume and maximum values of daily flow. To reduce the computational time, the model was run at daily time step during the long periods of droughts and hourly time step during the storm event. They estimated design flood values up to 0.05% AEP and showed that the derived frequency curve calculated by the method was able to properly match the observed flood frequency curve for more frequent floods ( to AEP 5%).

Newton & Walton (2000) further applied the CSS in a large (13,000 km<sup>2</sup>), semi-arid catchment in Western Australia. They compared the design estimates produced by the CSS to the observed flood frequency curve and found that the design flood estimates overestimated the observed flood frequency curve for more frequent floods. They speculate that the discrepancy between the observed flood frequency curve and the CSS result might be due to sampling problems; the observed flood frequency curve was estimated based on a shorter period (31 years) of data, while the rainfall generation model was calibrated to a longer (93 years) data series. The observed streamflow data covered a relatively dry period and did not represent the total climatic variability over a longer period.

There have been other applications of Continuous Simulation approaches for estimation of the derived flood frequency curve, for example Haberlandt & Radtke (2013), Cameron et al. (1999) and Droop & Boughton (2002), to catchments of various sizes and characteristics. In all cases stochastic rainfall generators were used to extend the rainfall data. Although different models (rainfall generator and the rainfall-runoff models) were used, all report that the derived distribution curve produced by the method was able to provide satisfactory match to the observed flood frequency curves for large floods. However, in all cases described, the ability of the model to properly reproduce the extreme flood event has not been done, due to lack of extreme data.

#### **2.4.2. Advantages**

As with the event based Monte Carlo method, the Continuous Simulation approach is not limited by the probability neutral assumption. It is the most rigorous among the three methods described and samples all the joint probability interactions (including that observed over a long

period of drought) among the flood producing variables through direct simulation. This offers an advantage over the event based Monte Carlo method, which requires specification of the distribution for antecedent conditions and the model parameters, including the initial levels of the reservoirs and storages, through pre-specified distributions (Kuczera et al. 2006a). In practice, specification of the distribution of the sensitive flood producing variables (especially parameters) is difficult because the model parameters are conceptual representations of components of the hydrologic process that cannot be directly measured (H. V. Gupta, Sorooshian, & Yapo, 1998).

### **2.4.3. Limitations**

Effectiveness of Continuous Simulation models relies upon the length of the rainfall data (to drive the model) and the observed streamflow data (for calibration and validation). In many cases generation of stochastic rainfall data with a distribution that is close to the observed distribution is challenging. It is especially difficult to reproduce rainfall statistics (more importantly the extremes) at all-time scales (Boughton et al. 1999; Kuczera et al. 2006a).

In Australia, a large amount of effort has been spent on developing the data (for example IFD, temporal patterns etc.) for use in the event based approach. The event based Monte Carlo method has been adapted to take full advantage of this (R. Nathan & Weinmann, 2013). In the case of Continuous Simulation approaches, some components of this can be directly used (for example the use of temporal patterns and FORGE data to generate the stochastic data; Boughton et al. (1999)), but considerable confusion still exists on implementation of the approach to Australian conditions; for example which rainfall-runoff model to use and which stochastic rainfall generator to use. In addition, even with improved methods of data generation, there will still be very few points to define the top end of the frequency curve (unless the stochastically generated rainfall data are conditioned on the PMP values).

Finally, the ability of Continuous Simulation models to reproduce both flood peaks and other hydrograph characteristics adequately for design flood purposes has not been proven.

### **2.4.4. Uncertainty estimation**

Estimation of the design flood using Continuous Simulation is subject to uncertainty due to errors in data (used to drive the model and for calibration of rainfall and the rainfall-runoff model), parameters (both models), model structures (both models) and the methods used to derive the flood frequency curves. The uncertainty in the estimate of the design flood increases with the increase in the magnitude of the flood (Nathan and Weinmann 2013).

While, there are a large number of studies attempting to quantify 'lumped' hydrological and meteorological uncertainties in rainfall-runoff models (Kuczera et al. 2006b; Montanari & Brath 2004; Montanari & Grossi 2008), their application to quantifying uncertainty in design floods of very low frequency of occurrence is very limited. This can be due to the difficulty in specifying residual error distributions that adequately account for the errors at such low frequency of occurrence. Similarly, adaptation of the Monte-Carlo based uncertainty estimation methods to Continuous Simulation, as that recommended by Nathan and Weinmann (2013) is challenging due to the need for specifying the distribution of all the sensitive (and varying) parameters and

the inputs of the continuous rainfall-runoff model.

While the use of realizations of stochastically generated rainfall data can provide some estimate of the inherent uncertainty in deriving these inputs, this does not adequately account for other sources of error. Indeed, Haberlandt & Radtke (2013) note that uncertainty in specification of the parameters of the rainfall generation model and the hydrologic models are greater than spread displayed the different realizations of stochastically generated time series.

A particular example of an attempt to quantify the uncertainty in design flood estimation using the Continuous Simulation method is provided by Cameron et al. (1999). They used the Generalized Likelihood Uncertainty Estimation method (GLUE) to quantify the uncertainty in simulated hydrographs and the derived flood frequency curve. A feature of GLUE is that it does not require specification of the residual error structure, but weights the model output using a subjectively derived likelihood measure (not based on formal maximum likelihood theory, which requires specification of error distribution). The parameters are assumed to vary uniformly over the fixed parameter ranges. The parameter sets which are deemed acceptable or 'behavioural', as measured by the derived likelihood measure, are propagated to define uncertainty in the model output. To derive a consistent sets of parameters that provide good representation of uncertainty in both the simulated hydrographs and the derived flood frequency curve, Cameron et al. (1999) assessed the likelihoods sequentially, such that they produced 'behavioural' sets of parameters with respect to the hydrographs and the flood frequency curves.

## **2.5. Alternative methods**

Examples of some alternative methods of flood estimation used internationally are described in the following sections. This is a small sample of the many methods used.

### **2.5.1. The US Bureau of Reclamation method of deriving hazard curve**

The US approach for design flood estimation traditionally has been flood frequency analysis using streamflow data for small hydraulic structures with lower acceptable risk (for example with acceptable flood risk of less than 0.2% AEP). However, critical infrastructure, such as dams or nuclear facilities, with a high hazard category are designed based on the Probable Maximum Flood (PMF). The methods of estimating the PMF are deterministic and have not changed in over 30 years (J. England, 2011). However, in recent years there has been increased interest in using risk based approaches for the design of critical infrastructure. Consequently the US Bureau of Reclamation (BR-US), recommends using a 'hydrologic hazard curve', which requires plotting the estimates of flood peaks and volume against their AEPs (J. England, 2011).

The BR-US recommends using a number of methods to derive the hydrologic hazard curve including the use of paleo-flood information to extrapolate the flood frequency to less frequent floods (streamflow based approach), the Gradient of extreme values (GRADEX) method (Naghetini et al. 1996), Australian Rainfall and Runoff (Nathan and Weinmann, 1999), use of Stochastic Event Flood Model (SEFM; Bullard et al. 2007) and use of stochastic physically based distributed rainfall-runoff model.

The GRADEX is a statistical rainfall based approach that seeks to estimate the upper tail of the flood volume distribution based on the statistical relation with the upper tail of the rainfall volume distribution. The SEFM is a stochastic event-based flood frequency model that is conceptually similar to the Monte-Carlo event based model discussed in Section 3. The difference arises in the choice of model used and the rainfall characteristics derived for simulation. The use of a physically-based distributed model (known as TREX) allows a detailed description of the watershed characteristics, based on the spatio-temporal information obtained from digital elevation models, soil survey datasets, weather radar observation data and stochastically generated rainfall intensities (J. England, 2011).

### **2.5.2. Revitalized-Flood Studies Report/Flood Estimation Handbook (Re-FSR/FEH) rainfall-runoff model approach**

The UK method of design flood estimation is based on a statistical approach using the observed flow data for more frequent floods and the use of a rainfall based approach for AEPs up to 0.05%. The flood estimation handbook (FEH) in the UK recommends using the Re-FSR/FEH rainfall-runoff model to estimation of the design flood peaks and hydrographs (Kjeldsen, 2007). Conceptually, the method is similar to the Design Event (DE) approach used in Australia. It uses the values of rainfall depth inputs derived from a depth-frequency-duration model, and a design storm duration (critical duration) calculated based on an empirical relationship using the time to peak and the wetness of the catchment, and a fixed single peaked symmetrical temporal pattern to derive the rainfall hyetograph. The rainfall hyetograph is passed through a loss model and a routing model to derive the flood hydrograph. The loss model used is the uniform probability distributed model (PDM; Kjeldsen 2007). The fixed parameter values for the loss model and the routing model are estimated either using regionalised values or by calibrating to flood events. The FEH acknowledges the limitations of the method and research efforts are underway to implement the Continuous Simulation method for the estimation of the design flood in the UK (Calver et al. 2005).

### **2.5.3. Electricité de France: SCHADEX method**

The SCHADEX Method is utilized by Electricité de France (EDF) in France for the design of dams and spillways (Paquet, Garavaglia, Garcon, & Gailhard, 2013). The SCHADEX is a hybrid event-based/Continuous Simulation (semi-continuous) approach that involves running a Continuous Simulation for a long period of time to generate adequate samples of the modeled soil moisture state. Then for each modeled state, distributions of flood volumes are generated by randomly sampling synthetic rainfall patterns from a large number of stochastically generated rainfall events. The rainfall-runoff modeling and the generation of precipitation are undertaken for fixed durations (for example daily). Then the peak-to-volume ratios for that duration, inferred from historical streamflow series, are used to convert the distribution of the volumes to peaks.

### **2.5.4. Methods used in South Africa**

Smithers (2012) provides a summary of flood estimation methods used around the world with a focus on their applicability in South Africa. A taxonomy of methods is provided, generally breaking methods down into two categories: analysis of streamflow and rainfall based methods.

Smithers (2012) summarizes that regional methods are generally sound and supported by many researchers. In particular, he finds that the index flood based method (Hosking and Wallis 1993; 1997) using L-moments is a robust procedure. The Regional Estimation of Extreme Flood Peaks by Selective Statistical Analyses (REFSSA) developed in 2010, is suitable for estimating extreme flood peaks from regional peak data for AEPs of 0.01% to 0.01% and catchment areas between 100 km<sup>2</sup> and 7,000 km<sup>2</sup> within certain catchment-based hydrological regions. Smithers also references Bobee and Rasmussen (1995), whose research has focused on determining hydrologically homogenous regions, given that geographical proximity is not necessarily a good indicator of hydrologic similarity. The run-hydrograph method is a regional method of flood estimation based on historical data, though it is generally not recommended. It has been further developed into the Joint Peak Volume (JPV) method, which is thought to give improved results. The Rational Method, Unit Hydrograph Method, and SCS are rainfall-based DE models used in South Africa (Smithers 2012). Smithers highlights similar deficiencies in these approaches to Kuczera (2003). Smithers provides wide ranging recommendations for future developments of flood estimation in South Africa, including:

- Investigation and development of Continuous Simulation methods of flood estimation,
- Investigation and development of Joint Probability methods of flood estimation,
- The development of a statistical regional approach to flood frequency estimation,
- An investigation into the methods of calculating Areal Reduction Factors (ARFs),
- Further development of existing rainfall based DE methods such as unit hydrograph, SCS, and a probabilistic rational method.

### **2.5.5. Applicability of international methods to Australian conditions**

In general the alternative methods discussed above are, in principle, similar and do not offer significant advantages to the three methods discussed in this report. Their use is complicated by the requirement to derive parameters and input datasets to suit Australian conditions. For many of the methods discussed, it would be a huge undertaking without any substantial benefit. For example, use of physically based models (e.g. TREX), while useful in large catchments, requires specification of a large number of spatially distributed parameters and rainfall fields.

The Re-FSR/FEH event approach is similar to the DE approach, but uses very simplistic rainfall patterns (symmetric and single peaked) and is not suitable to Australian conditions, where the storms are usually non-symmetrical and multi peaked. Statistical approaches like GRADEX are simplistic and do not offer significant advantage over the event based Monte Carlo or the Continuous Simulation approaches. The hybrid continuous-event based approach (SCADEX) is rigorous and adequately accounts for the joint probability interactions between the rainfall and catchment characteristics. Although theoretically appealing, it offers no obvious advantage over the two methods (Continuous Simulation and event based Monte Carlo) and its implementation to Australian condition could take significant investment and research (for example, to develop datasets). There is a wide support for the Monte Carlo and Continuous Simulations methods worldwide (Smithers 2012).

### 3. Test Catchments

#### 3.1. Catchment selection and data

To test the methods, catchments were selected to cover a range of geographic locations, climatic conditions, catchment characteristics and catchment sizes (areas) across Australia. A list of the catchments selected for use in the study is shown in Table 3-1 and these are mapped in Figure 3-1 and Figure 3-2. A list of the rainfall sites used in calibration of the models is shown in Appendix A.

The criteria for catchment selection were:

- At least 20 years of continuous records
- Pluviograph within or close to the catchment, with co-incident record to the flow record
- Data readily available and reliable. Catchments used for other ARR projects were selected where possible, as the data for these sites had already been checked and found to be reliable for analysis. Other catchments were selected as the project team had familiarity with the catchments and the quality of the data available.

Table 3-1 Catchments selected for testing

State	Station ID	River Name	Station Name	Data Custodian	Catchment Area (km <sup>2</sup> )	Start	End
QLD	138111A	Mary River	Moy Pocket	DNRM	820	1964	2004
WA	802213	Hann River	Phillips Range	WADW	5070	1967	2008
WA	603190	Yates Flat Creek	Woonanup	WADW	56	1963	2008
NT	G8170075	Manton River	upstream Manton Dam	DLRM	28	1965	2007
SA	A5040523	Sixth Creek	Castambul	DEWNR	44	1979	2008
VIC	231213	Lerderderg River	Sardine Ck-O'Brien	DEPI	153	1959	2005
TAS	304040	Florentine River	upstream Derwent Junction	HT	436	1951	2008
TAS	499	Tyenna River	at Newbury	HT	198	1965	1997
TAS	353	Hobart Rivulet	at Gore St	HCC	16	1985	2014
NSW	204025	Orara River	Orara River at Kurangai	NOW	134	1969	2012

DNRM - State of Queensland Department of Natural Resources and Mines

WADW - Government of Western Australia Department of Water

DLRM - Northern Territory Government Department of Land Resource Management

DEWNR - Government of South Australia Department of Environment, Water and Natural Resources

DEPI - State Government Victoria Department of Environment and Primary Industries

HT – Hydro Tasmania

HCC – Hobart City Council

NOW – NSW Office of Water



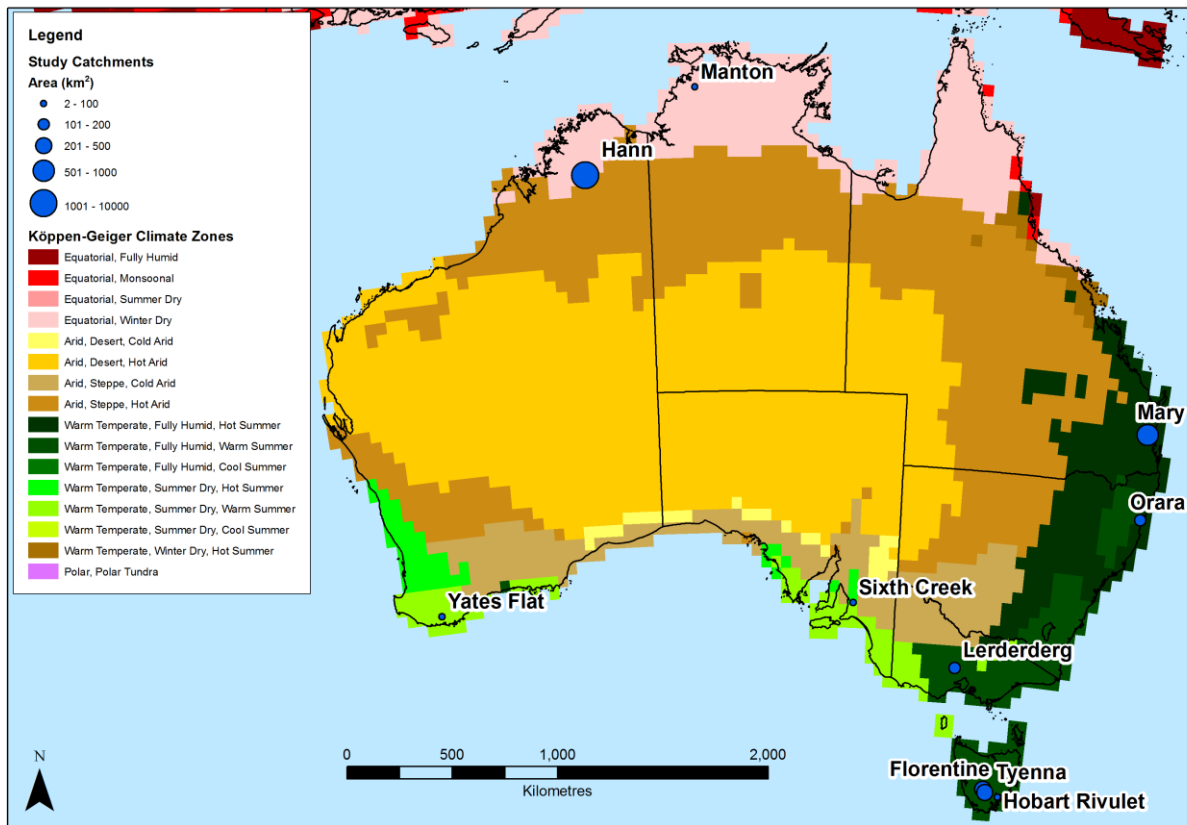


Figure 3-1 Test catchments shown with Köppen-Geiger climate zones (Institute for Veterinary Public Health, 2010)

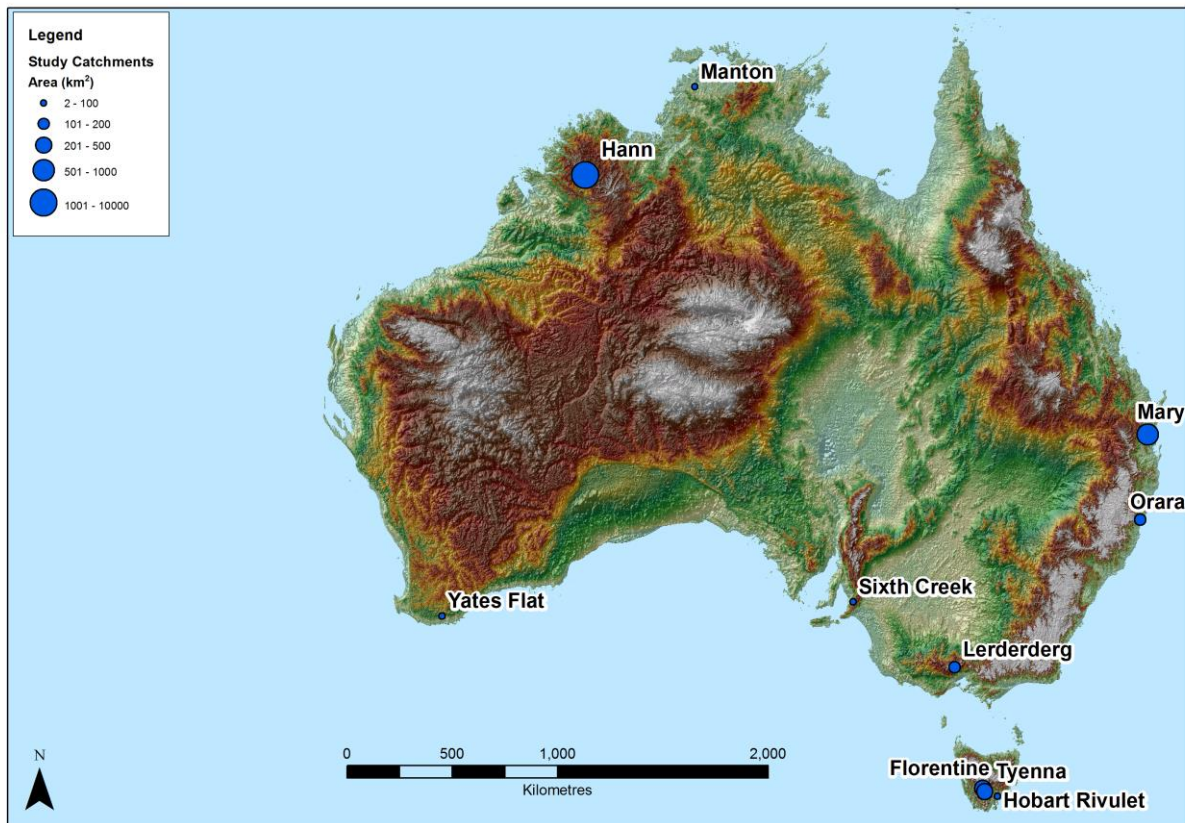


Figure 3-2 Test catchments

### 3.2. Data

The sources of data used in the analysis are shown in Table 3-1. The following steps were used to check the quality and reliability of the data:

- Quality codes were examined and periods of missing or low quality data were excluded from the analysis
- The full timeseries of flow and rainfall records were plotted for each site, both as hydrographs and hyetographs, and cumulatively
- Flow and rainfall volumes over defined periods were compared
- Flow and rainfalls were plotted for a number of large flow events
- The rating curve and associated gaugings were investigated for sites where the rating curve had not been previously investigated for other projects. In particular, high flow gaugings and rating curve extrapolation were examined.
- For catchments with more than one flow site, consistency between sites was investigated by comparing volume and timing of events.
- For continuous simulation method relatively continuous rainfall and streamflow data from the gauges from within or closest to the catchments were used to drive the model. The missing rainfall data in any of these stations were augmented by using the neighbouring stations. The rainfall and streamflow data used for continuous simulation is shown in Appendix I.

- The daily Potential Evapotranspiration (PET, Appendix I), derived using the FAO Penman-Monteith formula, was obtained from the SILO data drill website (<http://www.longpaddock.qld.gov.au/silo>). The data was converted to hourly by uniformly distributing it over the 24 hour period.

### 3.3. Catchment descriptions

#### 3.3.1. Mary River

The Mary River catchment (Figure 3-3) is located in South East Queensland and has a total catchment area of 820 km<sup>2</sup> at the Moy Pocket gauge. In 1989 the Baroon Pocket Dam was completed upstream of the Moy Pocket gauge. The catchment area to the Dam is 72 km<sup>2</sup> or 8.8% of the catchment contributing to Moy Pocket. For large events, the dam was found to have little influence on the flood hydrograph. The climate of the Mary River catchment is predominantly moist sub-tropical, with the majority of rainfall falling between November and April (Pointen and Collins, 2000). The Mary River catchment has been selected for assessing the performance of the models at internal gauge sites within the catchment as there are three gauges within the catchment upstream of Moy Pocket.

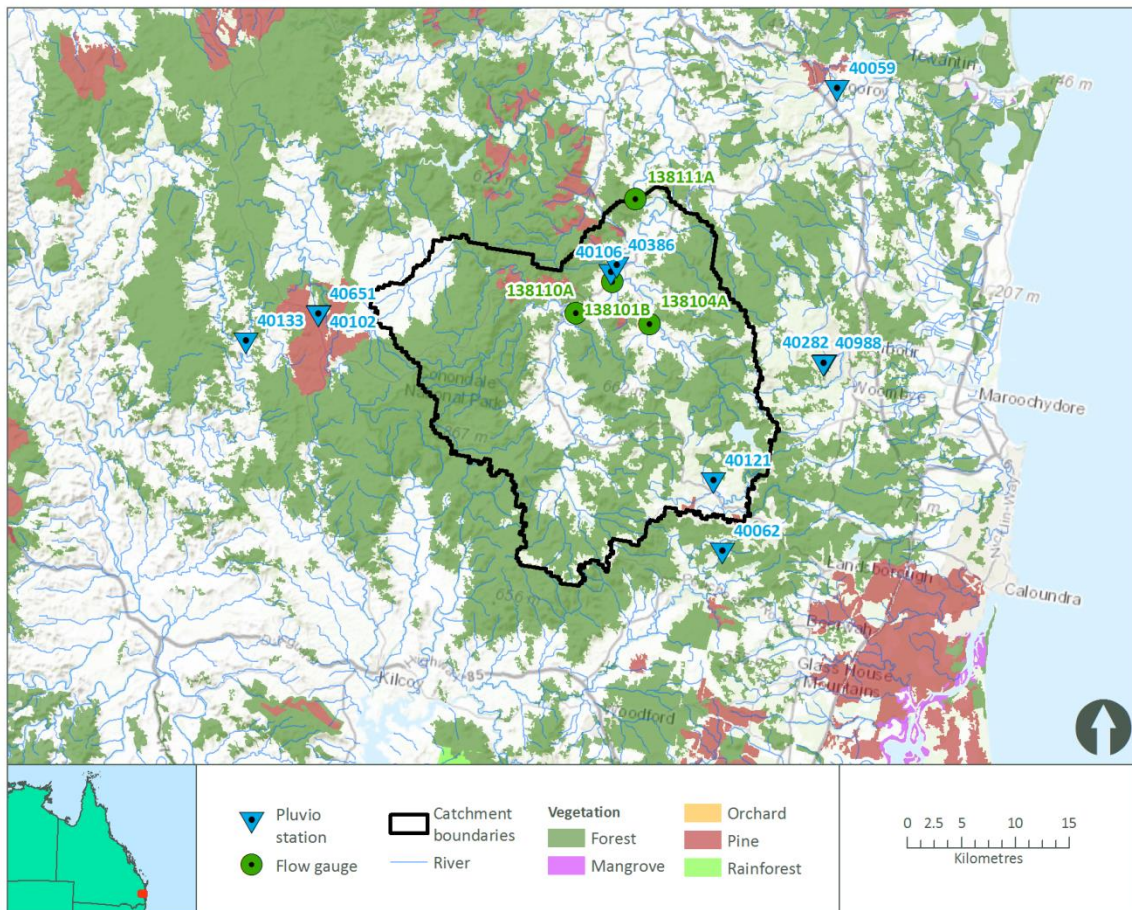


Figure 3-3 Mary River catchment

### 3.3.2. Hann River

The Hann River catchment (Figure 3-4) is located in the Kimberly region of north Western Australia, and has a catchment area of 5070 km<sup>2</sup> at the Phillips Range gauge. The Hann River is a tributary of the Fitzroy River. The Kimberly Region has a tropical monsoon climate, with around 90% of annual rainfall occurring over the November to April wet season, when cyclones are common. During this season conditions are hot and humid, and the weather system is generally characterized by low pressure systems and unstable air. Heavy and sustained rainfall can occur over the wet season and it is common for a single event to deliver a significant amount of an area's annual rainfall. During the dry season from May to October, the region is influenced by high pressure systems and a predominantly south easterly airflow (Government of Western Australia, Kimberly Development Commission, 2014).

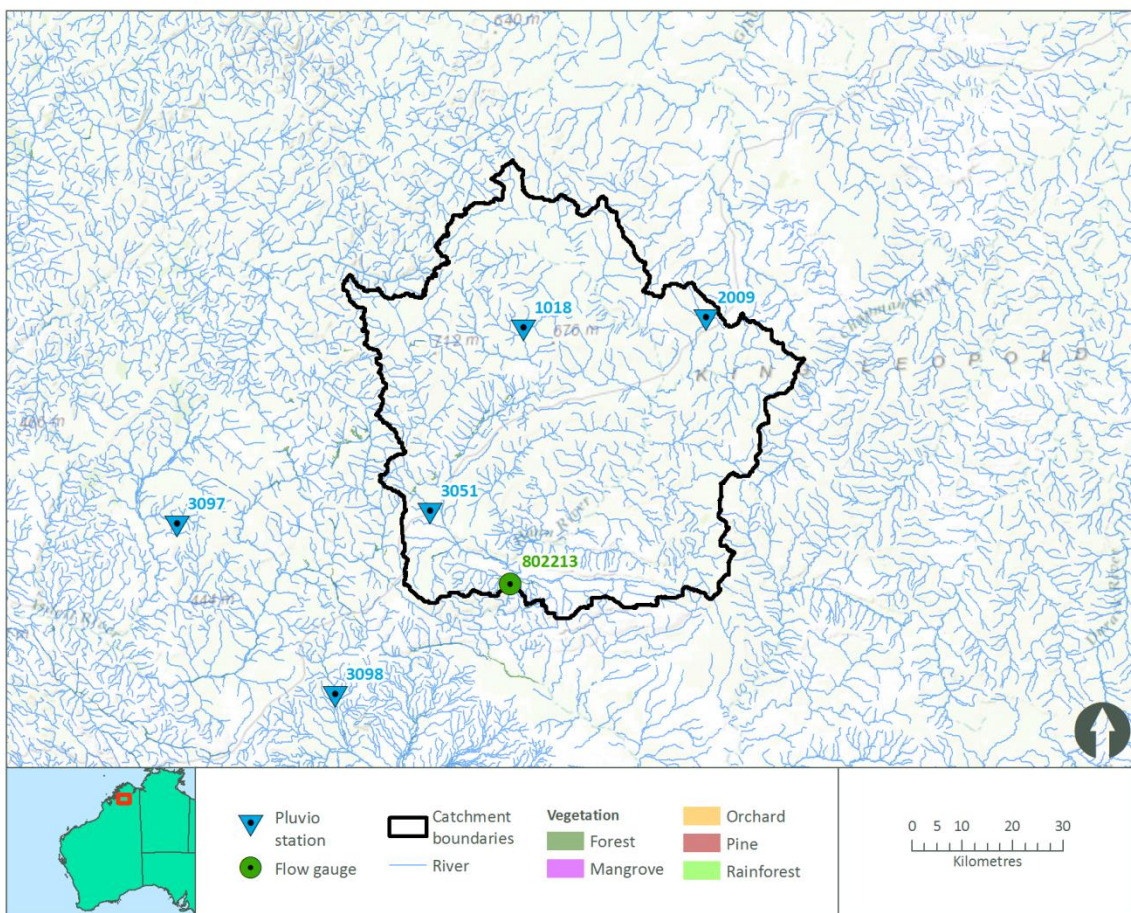


Figure 3-4 Hann River catchment

### 3.3.3. Yates Flat Creek

The Yates Flat Creek catchment (Figure 3-5) is located in the South-West region of Western Australia, and has a catchment area of 56 km<sup>2</sup> at the Woonoonup gauge. It is located in a region of Mediterranean climate with dry, warm summers and mild, wet winters (Garden, 1977).

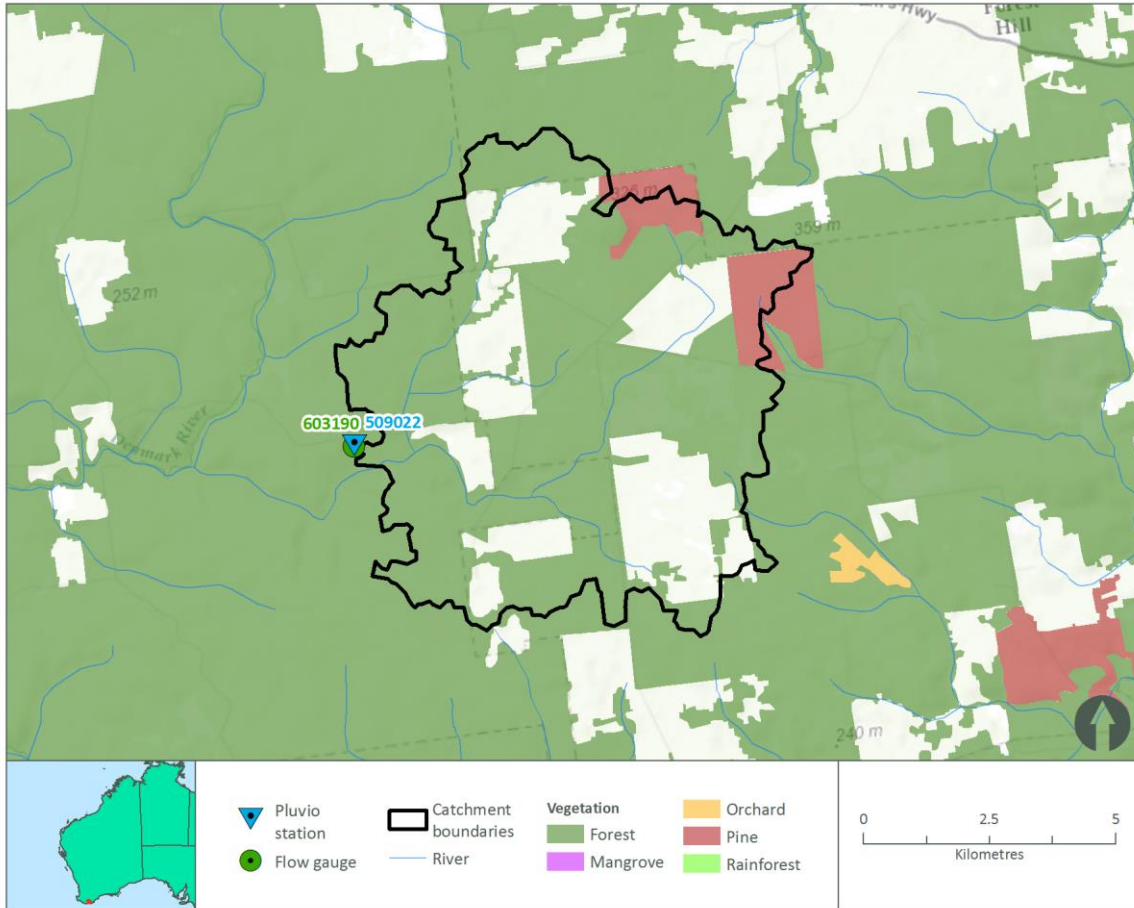


Figure 3-5 Yates Flat Creek catchment

### 3.3.4. Manton River

The Manton River catchment (Figure 3-6) is located in the north of the Northern Territory, and has a catchment area of 28 km<sup>2</sup> at the gauge upstream of Manton Dam. The climate is monsoonal, with a summer wet season between December and March and a winter dry season. During the wet season, high intensity rainfall events and thunderstorms are common. The wet season is associated with tropical cyclones and monsoon rains.

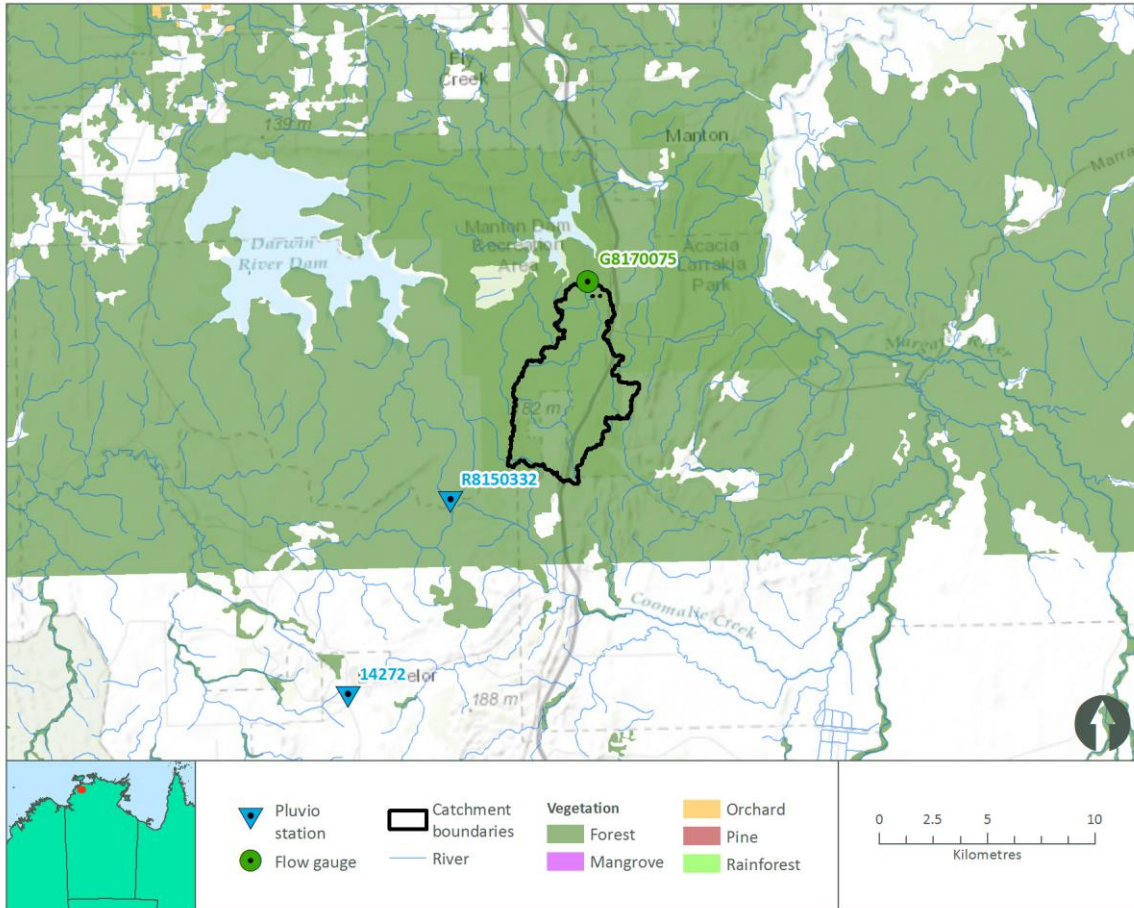


Figure 3-6 Manton River catchment

### 3.3.5. Sixth Creek

The Sixth Creek catchment (Figure 3-7) is located in the Adelaide Hills area, east of Adelaide in South Australia, and has a catchment area of 44 km<sup>2</sup> at the Castambul gauge. It is in a warm temperate climate zone, with warm and dry summers. Most of the rain in the area falls during the winter months when the sub-tropical high-pressure belt is displaced to the north, permitting lower-pressure systems to extend further to the north, and allowing strong cold-frontal activity to penetrate across the area (Government of South Australia, 2012)

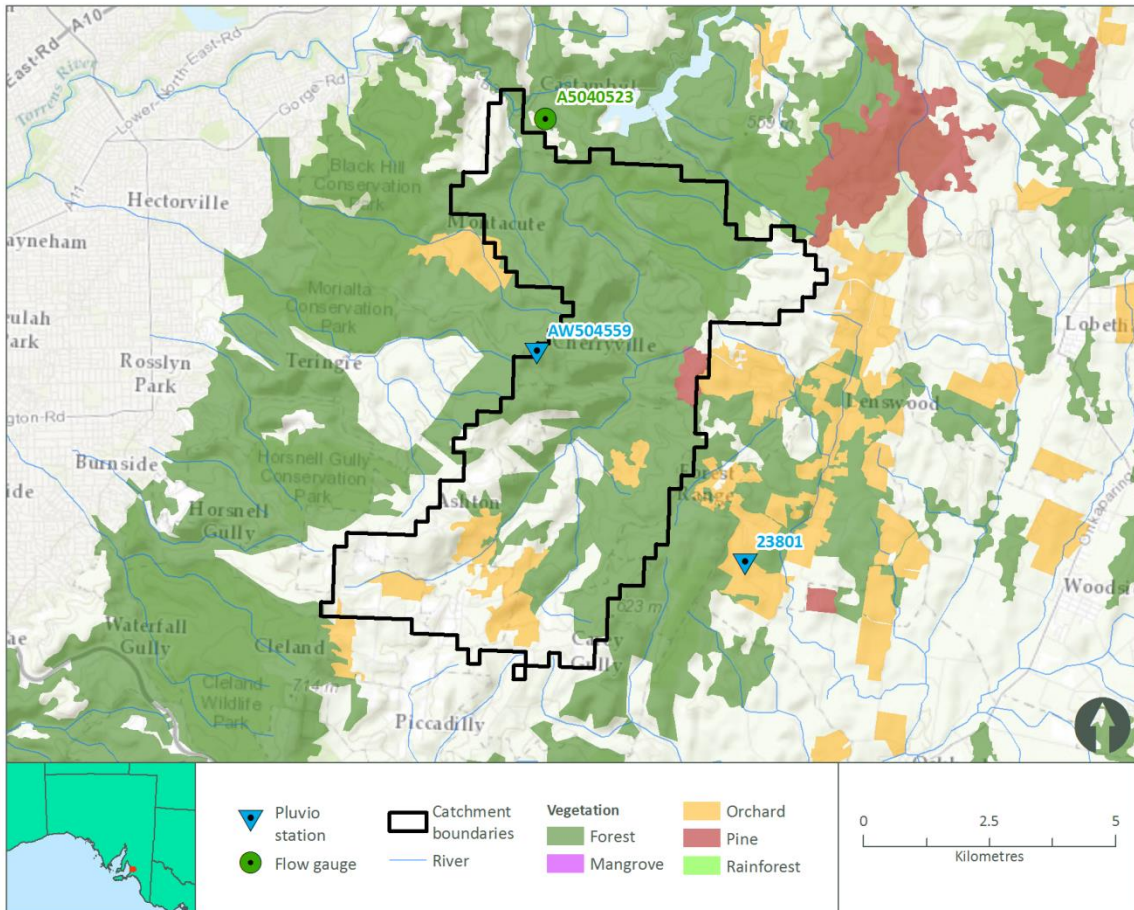


Figure 3-7 Sixth Creek catchment

### 3.3.6. Lerderderg Creek

The Lerderderg Creek catchment (Figure 3-8) is part of the Werribee River Basin, west of Melbourne in Victoria. It has a catchment area of 153 km<sup>2</sup> at the Sardine Creek O’Brian Crossing gauge. It is located within a temperate climate region. Land use in the catchment is mainly forestry (approximately 75%) along with conservation and the natural environment (22%) (Bureau of Meteorology, 2014).

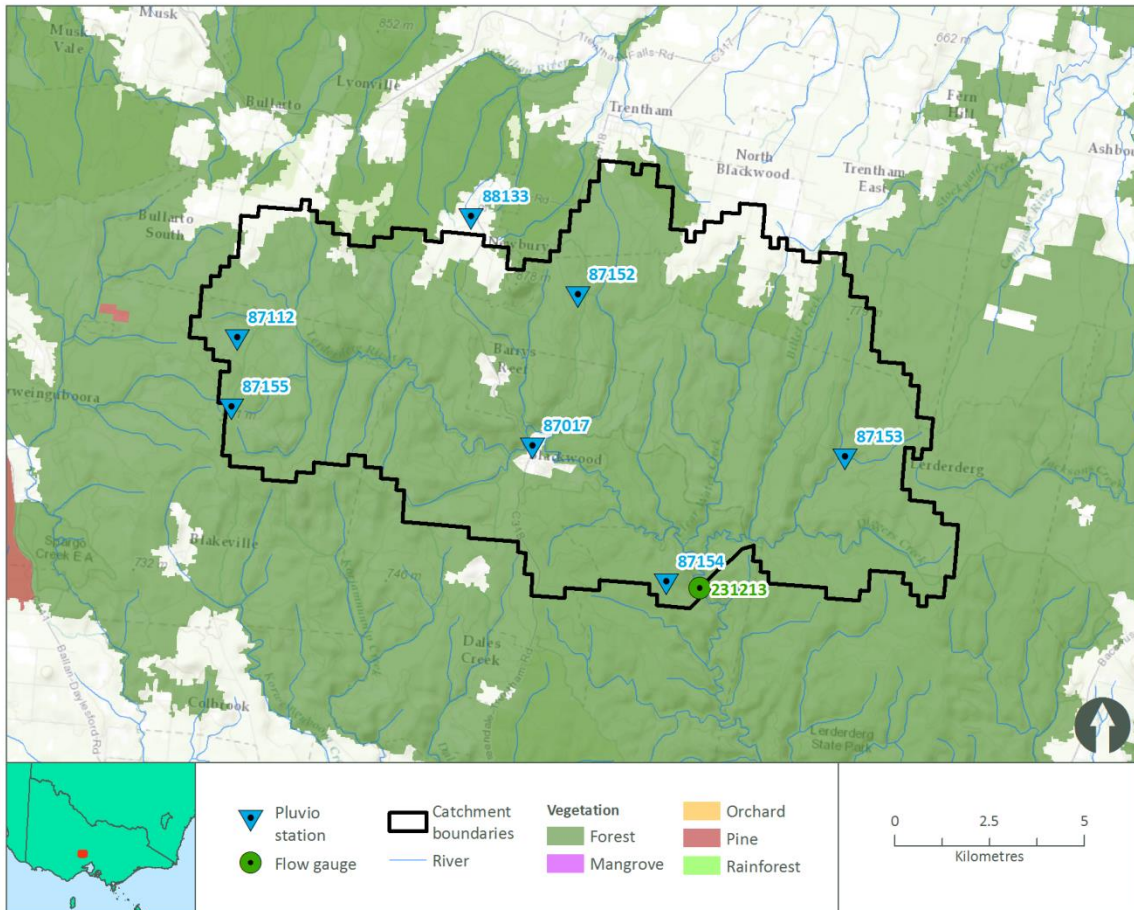


Figure 3-8 Lerderderg River catchment

### 3.3.7. Florentine River

The Florentine River catchment (Figure 3-9) is part of the Derwent River Basin, located to the west of Hobart in Tasmania. It has a catchment area of 436 km<sup>2</sup> at the gauge upstream of Derwent River junction. The catchment is located within a temperate climate region. The largest rainfalls generally occur between June and September.



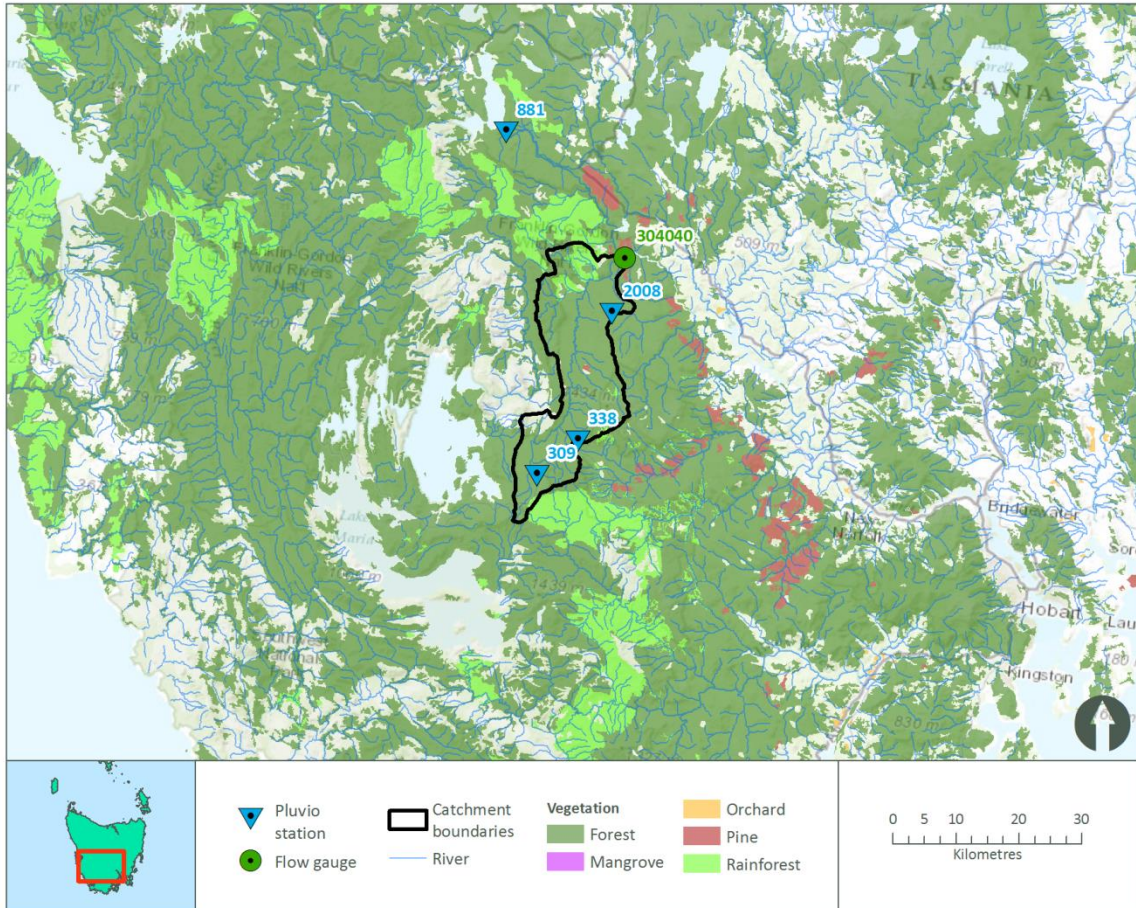


Figure 3-9 Florentine River catchment

### 3.3.8. Tyenna River

The Tyenna River catchment (Figure 3-10) is part of the Derwent River Basin, located to the west of Hobart in Tasmania. It has a catchment area of 198 km<sup>2</sup> at the Newbury gauge. The catchment is located within a temperate climate region. The largest rainfalls generally occur between June and September. The Tyenna catchment was selected for this study as a catchment with similar characteristics to the Florentine River catchment, for the paired catchment experiment.

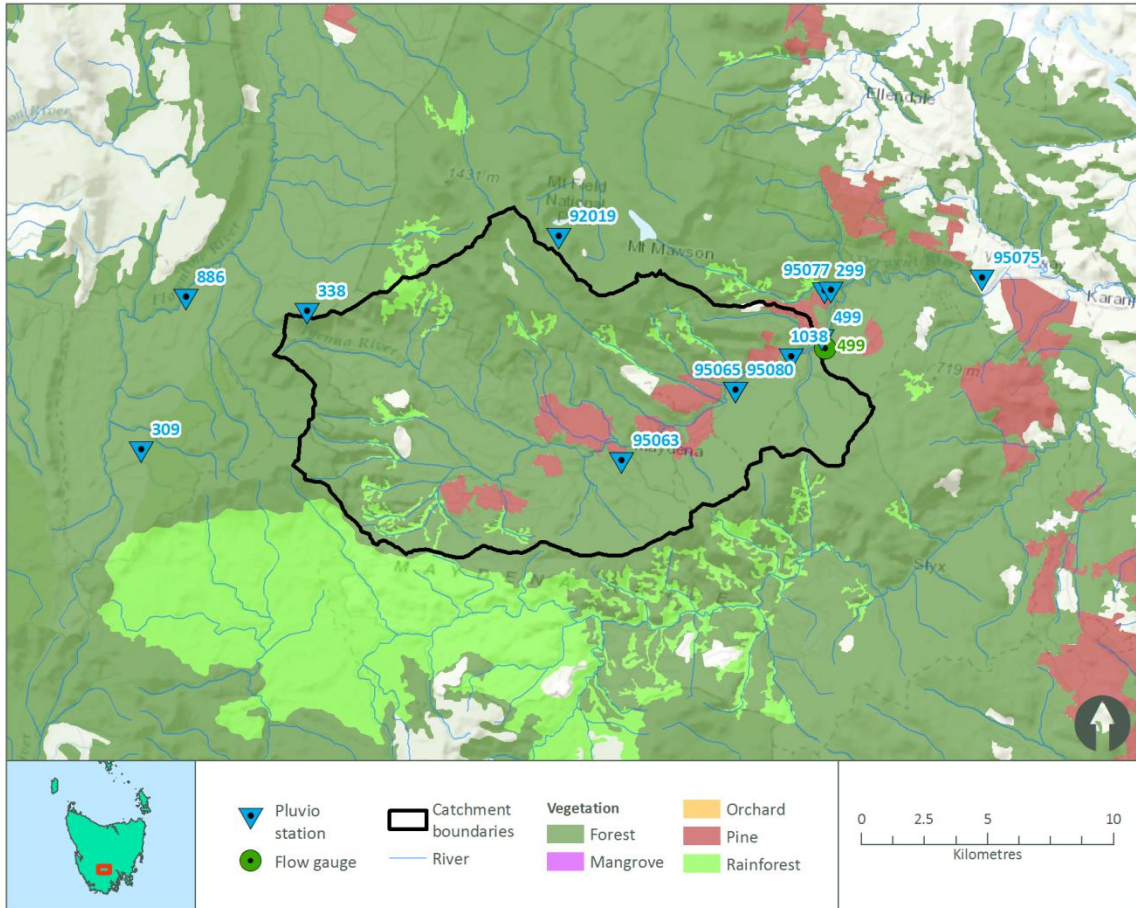


Figure 3-10 Tyenna River catchment

### 3.3.9. Hobart Rivulet

The upper portion of the Hobart Rivulet Catchment (Figure 3-11) is located on Mount Wellington. The rivulet flows through the suburbs of Hobart before running into a channel under the city of Hobart. The catchment area to the Gore Street gauge is 16km<sup>2</sup>. The upper part of the catchment is heavily forested, whilst the lower portion is urbanised. There are some periods of missing data at the Gore Street gauge from 1998 – 2006.

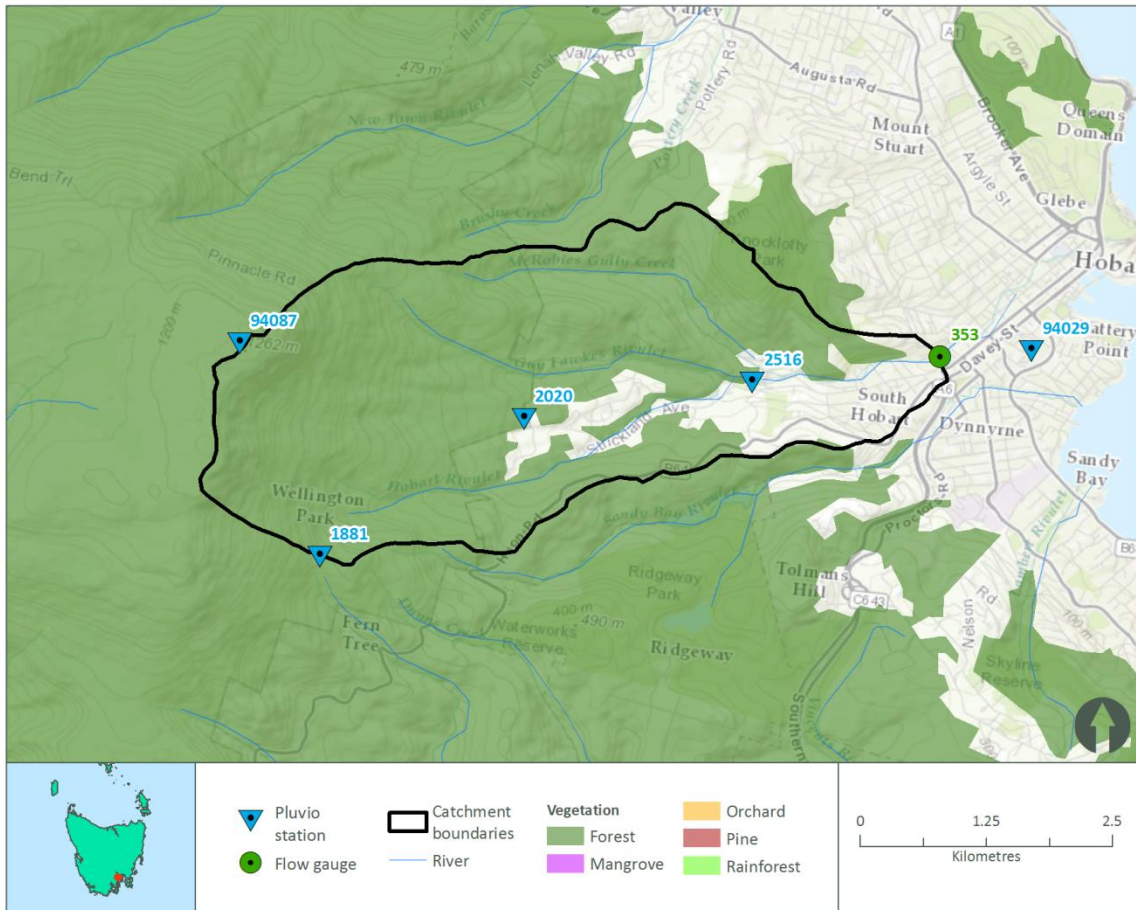


Figure 3-11: Hobart Rivulet catchment

### 3.3.10. Orara River

The Orara River Valley is located north-west of Coffs Harbour on the mid north coast of New South Wales. The Orara River is part of the greater Clarence River system, which is the largest coastal river system in New South Wales. The Orara River flows through Karangi, Coramba and Nana Glen, and flows into the Clarence River east of Copmanhurst (Coffs Harbour City Council, 2013).

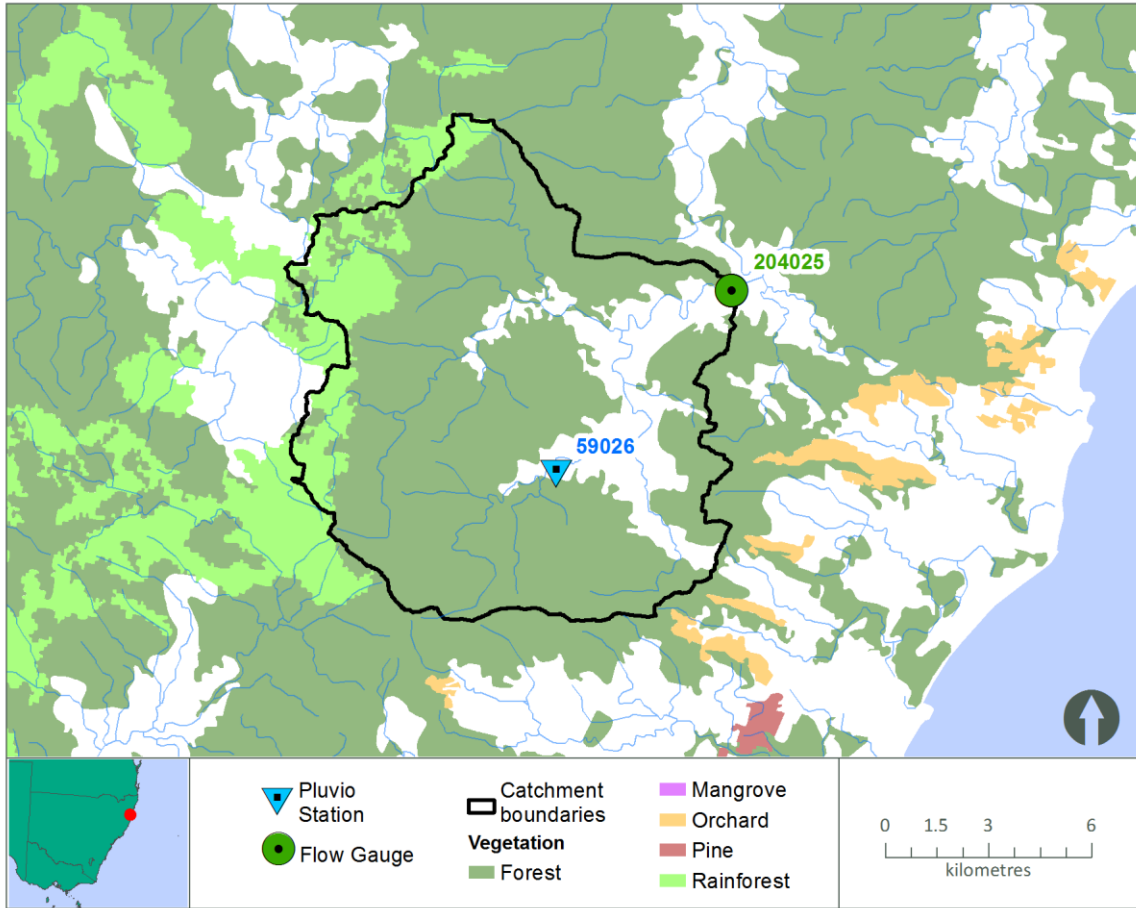


Figure 3-12: Orara River catchment

## 4. Method overview

The method for developing, calibrating, and running the models included the following steps:

- Delineation of sub-catchments and development of streamflow routing network
- Calibration of routing parameters through calibration to selected large flow events for Monte Carlo and Design Event models
- Calibration of model losses by fitting the modelled flood frequency curve to flood frequency curve fitted to observed flow data for Monte Carlo and Design Event models
- Calibration of Continuous Simulation model parameters for each of the four calibration tests described in Section 1.2.
- Collation and derivation of design model inputs
- Design model runs

The Monte Carlo and Design Event models were run based on annual data. The loss model used for Monte Carlo and Design Event models was initial loss with a constant continuing loss with the exception of Yeates Creek catchment where SWMod (Water and Rivers Commission, 2003) was also trialled.

### 4.1. SWMod

Soil Water balance MODel (SWMOD) is a type of probability distributed model that allows for the spatial variability in runoff generation process over the catchment. The model explicitly represents the saturation – excess mechanism and was designed to suit the conditions that occur in Western Australia. The spatial variability of the hydrologic process is represented by the distribution of the soil water retaining capacity (or hereafter called infiltration capacity) in the catchment (or sub-catchment). The distribution of the soil infiltration capacity in the catchment is assumed to be described by equation 4.1.

$$C_f = C_{max} - (C_{max} - C_{min}) * (1-F)^{1/B} \quad (4.1)$$

Where,  $C_f$  is the infiltration capacity at fraction  $F$  of the sub-catchment,  $F$  is the saturation fraction of the sub-catchment,  $B$  is the shape parameter,  $C_{max}$  is the maximum infiltration capacity, and  $C_{min}$  is the minimum infiltration capacity. The values of  $C_{max}$  and  $C_{min}$  are calculated as the factor of soil depth (depth to A soil horizon) and porosity and can be directly inferred from the soil maps.

For practical implementation of SWMOD the values of  $C_{max}$ ,  $C_{min}$  and the parameter  $B$  have previously been derived for five dominant landforms (Water and Rivers Commission, 2003) that are typically observed in Western Australia. The distribution of these landforms can be obtained from Department of Conservation and Land Management (CALM) system 6 Soil-Landscape map (Department of Agriculture and Food, Western Australia) for Western Australia. The values of the maximum, minimum infiltration capacity and the exponent ( $B$ ) are given in Table 4-1.

The rainfall over the catchment first infiltrates the soil layer and precipitation exceeding the soil infiltration capacity constitutes precipitation excess which is routed to generate the runoff. The

model can be calibrated to match the flood event by varying the values of initial soil water storage (hereafter called  $C_i$ ) of the catchment (Water and Rivers Commission, 2003). The distribution of the five landforms in Yates Flat Creek is shown in Figure B 13.10 (Appendix B) The CALM system 6 soil maps were not available for Yates Flat Creek (personal communication Leanne Pearce) therefore Soil - Landscape mapping data (Department of Agriculture and Food, Western Australia) were used to derive the distribution of the landforms in Yates Flats Creek. Distributions of the landforms were derived by matching the description of the landform and soil properties defined in soil – landscape mapping data with the soil properties of the 5 landform types.

**Table 4-1: Landform Soil Water Characteristics**

Landform	Minimum Soil depth (mm)	Maximum Soil depth (mm)	Porosity (W)	Cmin (mm)	Cmax (mm)	B
Dwellingup	400	6000	0.24	96	1440	2.25
Yarragil	500	5000	0.32	160	1600	2
Pindalup	250	4000	0.35	87.5	1400	2
Swamp	300	400	0.41	123	164	1
Murray	25	3000	0.34	8.5	1020	2

## 4.2. Water balance models

To reduce the sensitivity of the study outcome to the choice of the water balance model, three separate soil moisture accounting models were tested in each of the four catchments. The three models were the Australian Water Balance Model (AWBM, Boughton & Droop, 2003), SIMHYD (Chiew et al. 2002) and GR4H (Mathevet, 2005). All three models have been widely tested in the Australian conditions (Bennett et al., 2014, Boughton & Droop, 2003, Chiew et al. 2002). A brief description of each model is provided below.

### 4.2.1. AWBM

AWBM (Boughton & Droop, 2003) is a water balance model that has been widely applied in Australia. The model uses rainfall and potential evapotranspiration as input to produce precipitation excess that is then routed to produce streamflow at every time step. In the current study, the model is run at an hourly time step.

The model is composed of three surface stores to simulate partial areas of runoff and a ground water store to simulate the baseflow. The runoff is generated as an excess from the surface stores and a baseflow index parameter is used to partition ground water recharge from the surface flow. The model is very parsimonious with only three parameters to be calibrated. The structure of the model is included in Figure H. 1, Appendix H.

**Table 4-2: Parameters of the AWBM model**

Parameter name	Description	Range
Capave	Average capacity of the variable surface stores (mm)	10 - 1500
BFI	Baseflow index	0.01 – 0.99
K	Baseflow recession constant	0.01 – 0.99

#### 4.2.2. SIMHYD

SIMHYD (Chiew, et al. 2002), is a water balance model with three state variables and seven parameters. The model allows for interception of rainfall, through an interception store, runoff occurs through infiltration access as well as saturation access mechanism. The ground water store allows for baseflow through a linear recession parameter. The structure of the model is given in Figure H. 1, Appendix H.

**Table 4-3: Parameters of the SIMHYD models**

Parameter name	Description	Range
INSC	Interception store capacity (mm)	0 - 5
COEFF	Maximum infiltration loss (mm)	0 - 400
SQ	Exponent controlling the Infiltration loss	0 - 10
SMSC	Soil moisture store capacity (mm)	1 - 500
SUB	Constant of proportionality in interflow equation	0 - 1
CRAK	constant of proportionality in groundwater recharge equation	0 - 1
K	Baseflow linear recession parameter	0 - 1

#### 4.2.3. GR4H

GR4H (Mathevet, 2005) is an hourly rainfall runoff model, with two storages and four parameters. The model consists of a production function and a routing function based on the unit hydrograph. The model was developed based on an empirical approach and does not have prior physical underpinning (Andreassian et al., 2006). The structure of the model is given in Appendix H, Figure H. 3.

**Table 4-4: Parameters of the GR4H model**

Parameter name	Description	Range
X1	Capacity of the soil moisture store (mm).	1 – 8.5
X2	Groundwater exchange coefficient (mm).	-2.5 – 2.5
X3	capacity of the routing store (mm).	1 - 6
X4	Time base of the unit hydrograph in days.	-0.9 - 3

### 4.3. Model structure

Rainfall-runoff routing models were set up for each catchment. The models were set up as semi-distributed models with 10 to 15 sub-areas for each catchment, depending on the stream network and catchment size. Catchments and sub-areas were delineated via a semi-automated method using the Bureau of Meteorology's Australian Hydrological Geospatial Fabric, Version 2 (Geofabric, Bureau of Meteorology, 2014), with general rules as follows:

- Catchment outlet at target flow gauging site
- No sub-area greater than 10 percent of total catchment area
- Sub-areas of consistent sizes
- Breaks between sub-areas at any flow gauging site
- Breaks between sub-areas at junctions of major tributaries

The outlet sub-area was manually identified from the Geofabric (ie the catchment containing the flow gauge) along with any other sub-area of significance (ie at the locations of internal gauges, or major confluences). A minimum size threshold for sub-areas was determined and an algorithm was applied that aggregated Geofabric sub-areas to combine above the set threshold. Manual edits were applied if necessary to ensure sub-area outlets aligned with flow gauge locations. Checks were performed to ensure catchment areas approximated the catchment areas defined in flow gauge metadata. This method performed well for larger catchments. For the smaller catchments, more manual intervention was required.

The Geofabric river network was used as the basis for developing the streamflow network in the models. Channel routing distances were derived from this layer.

A node-link network model was coded in WISKI Modelling (Kisters, 2005). Each sub-area was coded as a lumped conceptual initial loss - constant continuing loss model for the Monte Carlo and Design Event model testing, and a water balance model (AWBM, SIMHYD and GR4H) for the continuous simulation model testing.

Non-linear channel routing was included in the model links to represent routing of the runoff produced from each sub-area through the river system. The routing equation used was based on a power function storage relationship.

$$S = K.Q^n$$

K is a dimensional empirical coefficient, the reach lag (time):

$$K = \alpha L_i$$

$\alpha$  = Channel Lag Parameter

n = Non-linearity Parameter

$L_i$  = Channel length for channel reach i (km)

Q = Outflow from channel reach ( $m^3/s$ )

Figures showing sub-areas and the node-link network used in each model are shown in Appendix B.



## **5. Monte Carlo and Design Event Model Calibration and Design Runs**

### **5.1. Calibration of routing parameters**

The routing parameters were calibrated by fitting the model output to selected events from the streamflow gauge record.

#### **5.1.1. Event selection**

For each catchment, events were selected for calibration based on the following method:

- The events resulting in the ten highest peak flows at the streamflow gauge site were extracted
- For each of these events, the corresponding rainfalls were extracted
- Where no rainfall was available, events were excluded
- The flow hydrographs and rainfall hyetographs for each event were examined to check that the runoff response looked appropriate. Any events where there appeared to be issues with the data were excluded
- From the remaining events, between five and eight events with the highest peaks were then used for event calibration. If there were less than five events remaining, additional events were selected based on the process given.

#### **5.1.2. Rainfall distribution**

For each event, rainfall was distributed over each sub-area using inverse distance weighting of the rainfall at gauges in and surrounding the catchment. To distribute the rainfall, in each time step a weighting was computed for each identified rain-gauge in or near the catchment that has data available. Up to four raingauges were used to calculate sub-area rainfall, including each gauge nearest to the sub-area centroid in each geographical quadrant (ie North-East, North-West, South-East, South-West). The weighting for each rainfall site is computed as the inverse of the squared distance between the centroid of the sub-area and the rainfall gauge. Total rainfall for the sub-area in each time step is the sum of all weighted rainfalls, normalised by the total rainfall from all the gauges in that time step. For catchments or events which only had one rainauge available, no weighting or spatial distribution of rainfall was applied.

#### **5.1.3. Calibration**

The calibration for the initial loss – constant continuing loss models was undertaken using the steps described below.

##### **5.1.3.1. Event calibration**

The model was run for each selected event and the modelled and observed streamflow were plotted. Statistics used to fit each event were:

- Difference between average flow over the events
- R squared

- Difference between observed and modelled peak

The routing parameters  $\alpha$  and  $n$ , baseflow, and initial loss (median value or fixed loss, depending on method) and continuing loss were selected to best fit each individual event based on the statistics and visual fit. One value of each of  $\alpha$  and  $n$  was then selected that would provide an acceptable fit across all events. A suitable baseflow was identified for use in design runs based on the best fit to all events.

#### **5.1.3.2. Calibration of losses**

The IL and CL were calibrated by fitting modelled design floods to the observed flood frequency curve, as described below.

- The flood frequency curve was fitted to the observed streamflow data using FLIKE software (University of Newcastle, 2013). For each site, a range of distributions were investigated and fitted using both Bayesian method and L2-moments. The distribution that best fitted the observed data was selected.
- Design floods for AEPs from 50% to 1% were generated by running the flood model with design inputs (detailed in Sections 5.2 and 5.3).
- Initial and continuing loss values were varied until the observed and modelled flood frequency curves were as closely matched as possible, with emphasis on fitting the 2% and 1% AEP floods. The IL and CL values were selected from within the range of values fitted in the event calibration.

#### **5.1.4. Calibration of SWMod**

The SWMOD calibration on Yates Flat Creek was performed in two stages (similar to IL-CL loss models). In the first stage the routing parameter was calibrated against six flood events (Table C. 7, Appendix C). The initial soil water storage parameters ( $C_i$ ) corresponding to the four landforms (available in Yates Flat Creek) were also adjusted to provide a closer match to the event hydrograph.

In the second phase the routing parameter was held fixed and the  $C_i$  parameters corresponding to the four landforms were calibrated against the observed flood frequency curve. A total of 10 temporal patterns were used to drive the SWMOD model, thus generating 10 realizations of the derived flood frequency curves. The median of these 10 realizations were used to match the observed flood frequency curve.

### **5.2. Monte Carlo model design runs**

#### **5.2.1. Design inputs**

##### **5.2.1.1. Design rainfalls**

2013 IFD point rainfalls were extracted for each catchment centroid from the Bureau of Meteorology's website (Bureau of Meteorology, 2013). Areal reduction factors were applied using the equations given in Australian Rainfall and Runoff (2013) for each state. Design rainfalls for

each catchment are shown in Appendix A.

Temporal patterns were extracted from the nearest representative pluviograph site for each catchment. 30 patterns were selected for each duration and AEP. Temporal patterns for each site are shown in Appendix A.

A uniform rainfall spatial pattern was used, consistent with advice in ARR for large floods up to 1% AEP (ARR Book VI, Table 8, The Institution of Engineers Australia, 1999).

#### 5.2.1.2. Losses

A distribution was applied to initial losses in the analysis. This distribution was taken from Nathan et al (2003) and Laurenson et al (2009). The upper values of this distribution were adjusted so a random sampling regime returned an average value of 1.

**Table 5-1: Distribution of initial losses**

Percentile	Proportion of Median	Adopted Distribution
0%	3.27	2.10
10%	2.19	1.75
20%	1.74	1.55
30%	1.45	1.35
40%	1.17	1.16
50%	1.00	1.00
60%	0.82	0.82
70%	0.65	0.65
80%	0.45	0.45
90%	0.27	0.27
100%	0.07	0.07
0%	3.27	2.10
10%	2.19	1.75

The continuing loss was kept constant for all design runs.

#### 5.2.2. Design runs

The catchment model was run for durations of between 1 and 96 hours, with the range of durations used dependent on the individual catchment. For each duration the model was run 5,000 times. Model parameters were sampled stochastically for each run in the sequence. The Total Probability Theorem (Nathan et.al. 2002, 2003) was applied to the results for each duration and AEP to derive the modelled flood frequency curve.

### 5.2.2.1. Rainfall

For each duration the rainfall frequency curve was split into 50 intervals of a constant magnitude on a standard normal distribution. Within each interval 100 rainfall depths were randomly sampled on a standard normal distribution. This resulted in 5,000 runs being generated for each rainfall duration.

### 5.2.2.2. Losses

For each run a factor was stochastically sampled from the initial loss distribution described in Section 5.2.1.2 and applied to the calibrated initial loss. A constant continuing loss was used.

### 5.2.2.3. Temporal Patterns

For each run the temporal pattern was stochastically sampled from the available set based on duration and rainfall AEP (Section 5.2.2.3).

## 5.3. Design event model design runs

### 5.3.1. Design inputs

The same design rainfalls were used as for the Monte Carlo method.

The advice on use of the 2013 IFD rainfalls given by BoM states that “.....careful consideration should be given before using the 2013 IFD design rainfalls with the Average Variability Method (AVM) temporal patterns.....from ARR87.” The AVM temporal patterns from ARR87 Volume 2 (The Institution of Engineers Australia, 1987) were plotted with the temporal patterns extracted from the pluviographs for each catchment and for each duration to investigate whether these were reasonable. However it was later concluded that, the AVM patterns would not be appropriate for the use in this study and alternative temporal patterns were more suitable in the testing of the Design event models. Therefore, the Design event approach implemented for this project used the 10 temporal patterns for each catchment, which were provided for this purpose from the ARR Revision project.

These patterns were sampled from a database of approximately 140,000 events within Australia. For each catchment the patterns were sampled from gauges located within the sampling regions shown in **Error! Reference source not found. (Error! Reference source not found.** and REF\_Ref434414828 \h \\* MERGEFORMAT **Error! Reference source not found.**). For each catchment and duration 300 burst patterns (30 for each catchment) corresponding to AEPs rarer than 3.2%, and more frequent than 14.4%, and durations ranging from 1 hour to 72 hours were provided. These burst patterns were further analysed to censor out the patterns that contain embedded storms. For use in the design event approach, 10 patterns free from embedded storms were selected for each catchment and duration. In sampling these 10 patterns (for each catchment and duration) first priority was given to select patterns with no embedded storms, followed by the rarity of the storm.

In most catchments it was not possible to obtain 10 patterns corresponding to storms rarer than 3.2% AEP for all durations, and patterns corresponding to more frequent storm were included. In Mary River and Florentine River catchments, further filtering (see **Error! Reference source not found.** for details) was applied to sample 10 temporal patterns for some longer duration storm patterns.

For each catchments and duration, these 10 temporal patterns were used to drive the IL-CL model, thus generating 10 realizations of the derived flood frequency curves. The median of these 10 realizations were used to match the observed flood frequency curve.

A uniform rainfall spatial pattern was used, consistent with advice in ARR for large floods up to 1% AEP (ARR Book VI, Table 8, The Institution of Engineers Australia, 1999). The initial loss and continuing loss were held constant for the design runs at the values determined in calibration.

### 5.3.2. Design runs

The catchment model was run for durations of between 1 and 72 hours, with the range of durations used dependent on the individual catchment. The maximum peak flow produced at the critical duration was plotted at each AEP, resulting in the modelled frequency curve.

## 5.4. Runs for ungauged catchments

Where a catchment is ungauged, common practice is to use model parameters from another catchment model that have been calibrated to a gauge site (donor catchment). The donor catchment will ideally have similar characteristics as the catchment of interest, such as catchment area, vegetation, terrain and climate. To investigate the performance of the models in this situation, a number of trials were run. The aim was to investigate model performance when parameters were transferred between similar catchments, and also between catchments which would be considered unsuitable for transferring parameters.

The following catchments were selected for this test:

- Florentine River and Tyenna River. These catchments are adjoining, and are both within the Derwent River Basin. The catchments are similar in terms of terrain, soil types and vegetation, and are subject to the same climate. The areas of the Florentine River and Tyenna River catchments are 436 km<sup>2</sup> and 198 km<sup>2</sup> respectively.
- Hann River and Manton River. These catchments are both in the north of Australia in a similar climate zone, however their catchment areas are vastly different. Hann River catchment has a catchment area of 5070km<sup>2</sup> compared with Manton River catchment area of 28km<sup>2</sup>.
- Hann River and Mary River. These catchments are in different climate zones. Mary River catchment has an area of 820km<sup>2</sup>.
- Tyenna River and Hann River. These catchments are in different climate zones, have different catchment areas and catchment characteristics.

## **5.5. Calibration to sub-set of data**

To examine the impact of shorter record lengths on design flood estimates, the models were calibrated to a sub-set of data for two catchments, Manton River and Mary River. In each case, the flow record was halved, and the calibration process was repeated using each half of the record only.

## 6. Continuous Simulation Model Calibration

Each catchment model was calibrated to the observed flow available at the outlet of the catchment. The parameters of each model were calibrated using a global optimization algorithm called shuffled complex evolution (SCE, Duan et al., 1992). For each model, the soil moisture accounting parameters (Table 4-2, Table 4-3 and Table 4-4) and the channel lag parameter (equation 1) were calibrated, while the non-linearity parameter (n) was kept fixed at a value of 0.8. Fixing the non-linearity parameter was considered reasonable as it shows a high degree of parameter interdependence (see equation 1 and 2) with the channel lag parameter. In each model an additional parameter, rainfall multiplier, was also introduced to adjust for any discrepancy in the volume between the flow and the rainfall.

The catchments model was tested on four calibration scenarios. All four calibrations scenarios were applied to Manton, Sixth Creek, Mary and Florentine catchments. Yates Flat Creek was included at a later stage, due to its unusual input-output behaviour, and the fact that it performed very poorly when tested using the event based Monte Carlo method in project 12. In Yates Flat Creek only two scenarios, believed to be the best strategies to reproduce the hydrograph behaviour (Scenario 1, Section 6.1) and the observed flood frequency curves (Scenario 4, Section 6.4) were tested.

In total 56 number of calibration runs were conducted. For each calibration the number of complexes (used for the SCE), equalled the dimension of the problem (N). The simplex sizes were taken as N + 1 and the population sizes were taken N(2N+1) (Duan et al., 1992). Prior to each model run a warm up period (shown by dashed light blue line in Figure I. 1 to Figure I. 5 in 0) of one year was allowed to reduce errors due to improper initialization of the model states.

### 6.1. Scenario 1: Calibration to the whole record

This scenario tested the ability of the model to reproduce the hydrograph behaviour and the observed flood frequency curve, when the model is calibrated to all the data available in the catchment. The models were calibrated by minimizing the normalised squared error (NORMSE) shown in 3. The NORMSE is generally more sensitive to large flow magnitudes and was considered appropriate objective function to use, when reproducing large flows were of interest.

$$\text{Normalised Squared Error} = \frac{\sum(Q_{obs} - Q_{sim})^2}{\sum(Q_{obs} - \overline{Q_{obs}})^2} \quad (3)$$

Where,  $Q_{obs}$  is the observed flow,  $Q_{sim}$  is the simulated flow and  $\overline{Q_{obs}}$  is the mean of the observed flow.

### 6.2. Scenario 2: Calibration to subset the of data

This scenario tested the ability of the model to reproduce the hydrograph behaviour and the observed flood frequency curve, when only a subset of the data was available in the catchment. For each catchment, the total data available was split into two and the model was calibrated for

the first period (data period within light blue and light green dashed lines in Figure I. 1 to Figure I. 5 in (Appendix I)).

### 6.3. Scenario 3: Calibration to large events

This scenario tested the ability of the model to reproduce the observed flood frequency curve and hydrograph behaviour when calibrated to a number of large events in the data. To identify large events a threshold value was determined. The model was calibrated to flow values larger than the threshold value for each catchment. In most cases the threshold value was taken as flood magnitude corresponding to 1:1.1 AEP of the observed flood frequency curve (Table 6-1). For Manton River this resulted in less than 1% of the total data points available for calibration, therefore the threshold was reduced to AEP 1:1:01.

**Table 6-1: The values used for the threshold limit**

Catchment	Threshold value (m <sup>3</sup> /s)	% data included in calibration	Corresponding AEP
Manton River	6.0	1.5	1:1.01
Sixth Creek	3.4	1.0	1:1.1
Mary River	66.5	1.8	1:1.1
Florentine River	44.7	1.8	1:1.1

### 6.4. Scenario 4: Calibration to the observed flood frequency curve

This scenario tested the ability of the model to reproduce the observed flood frequency curve, and the hydrograph behaviour when calibrating directly to the observed flood frequency curve. This calibration differs from the other scenarios in that the calibration to the observed flood frequency curve does not preserve the timing in of the observed hydrograph.

The following steps were used for calibration to the observed flood frequency curve:

- For each function evaluation, the model was run and annual maximum series ( $y_{sim} = f(M, I, \theta_m)$ ) was extracted from the simulated time series. Where  $M$  represents the rainfall runoff model,  $I$  represents the input data (rainfall and potential evapotranspiration) and  $\theta_m$  represents the parameters of the rainfall runoff model.
- A flood frequency distribution was fitted to  $y_{sim}$ , resulting in parameter set  $\theta_s$  (parameters of the fitted distribution).
- The parameters of the fitted simulated flood frequency distribution were then used to calculate the predictive density [ $p(y_{obs} | \theta_s, y_{sim})$ ] of the observed annual maximum series given fitted parameters  $\theta_s$ . The negative log of the predictive density (hereafter called likelihood function;  $L(\theta_s) = -\log(p(y_{obs} | \theta_s, y_{sim}))$ ) was then minimized.
- In Mary River and Manton River GEV distribution function was fitted to the annual maximum series and negative log likelihood was calculated as shown in equation 4 and 5 and in Sixth Creek, Florentine River and Yates Flat Creek log normal distribution was used and the negative likelihood function is given in 6.



for  $k_s \neq 0$

$$L(\theta_s = \mu_s, \alpha_s, k_s) = \text{nlog}(\alpha_s) - \sum_{i=1}^n \left[ \left( -\frac{1}{k_s} - 1 \right) \log \left( 1 + k_s \left( \frac{y_{obs} - \mu_s}{\alpha_s} \right) \right) - \left( 1 + k_s \left( \frac{y_{obs} - \mu_s}{\alpha_s} \right) \right)^{\frac{-1}{k_s}} \right] \quad (4)$$

for  $k_s = 0$

$$L(\theta_s = \mu_s, \alpha_s) = \text{nlog}(\alpha_s) - \sum_{i=1}^n \left[ -\left( \frac{y_{obs} - \mu_s}{\alpha_s} \right) - \exp \left( \frac{y_{obs} - \mu_s}{\alpha_s} \right) \right] \quad (5)$$

$$L(\theta_s = \mu_s, \sigma_s) = \frac{n}{2} \log(2\pi\sigma) + \sum_{i=1}^n \log(y_{obs}) + \frac{1}{2\sigma^2} \sum_{i=1}^n (\log(y_{obs}) - \mu_s)^2 \quad (6)$$

Where, n is the total number of annual maximum peaks,  $\mu_s, \alpha_s, k_s, \sigma_s$  are the parameters of the distribution.

The adopted method is similar to that used by (Cameron et al., 1999). The advantage of this procedure over mean squared error (MSE) or mean absolute difference (MAE) of the peaks is that this provides equal weighing to all the events, while MAE or MSE weigh larger events more heavily and thus reduces the importance of smaller events to the identification of model parameters. Finally, the likelihood based objective function given above can easily be normalised and be used along with normalised squared error (equation 3) in a constrained calibration approach.

## 6.5. Evaluation of the model output

The ability of the calibrated models to reproduce the observed flood frequency curve and the hydrograph behaviour was evaluated using a series of plots and statistical metrics. In particular, hydrographs, flow duration and scatter plots were generated for each calibration. The model to data fit was evaluated using Nash Sutcliff Efficiency (NSE = 1-NORMSE), and the ability of the model to reproduce the flow volume over the longer period was measured using volume bias (equation 6). In addition, ten largest flood events at each catchment were assessed for their ability to represent flood volumes.

$$vol\ bias = \left( 1 - \frac{\overline{Q_{sim}}}{Q_{obs}} \right) \times 100 \quad (6)$$

For each catchment, annual maximum series (hereafter called observed annual maximum) were extracted from the observed dataset and observed flood frequency curves were fitted using L - moments. For each calibrated model run, the annual maximum flow values (hereafter called simulated annual maximum) were extracted and the flood frequency (hereafter called simulated flood frequency) were fitted using L - moments. The simulated flood frequency plots were generated and compared with the observed flood frequency plots. The types of distribution fitted to the observed values are given in Table 6-2. In this case the flood frequency curves were selected based on the best fit to the entire annual series.

**Table 6-2: Flood frequency fitting for each catchment**

<b>Catchment</b>	<b>Distribution (Probability model)</b>
Manton River	GEV
Sixth Creek	Log Normal
Mary River	GEV
Florentine River	Log Normal
Yates Flat Creek	Log Normal

## 7. Monte Carlo and Design Event Model Calibration Results

### 7.1. Event calibration

The results of the event calibrations for each catchment are shown in Appendix C. In all cases, an n parameter of 0.8 was used. A summary of the calibrated model parameters is shown in Table 7-1.

**Table 7-1: Event calibration parameters**

Catchment	Alpha	Initial Loss (mm)		Continuing loss (mm/hr)	
		Low	High	Low	High
Mary River	1.0	0	60	0.0	6.0
Hann River	0.8	0	30	0.0	16.0
Yates Flat Creek	1.8	10	35	0.0	11.0
Manton River	1.2	0	10	3.0	12.0
Sixth Creek	0.8	0	22	2.0	8.0
Lerderderg River	1.2	0	27	0.0	3.0
Florentine River	2.5	0	15	0.8	1.9
Tyenna River	1.6	0	4	0.8	2.5
Hobart Rivulet	1.3	0	8	0.9	7.0
Orara River	1.75	0	22	0	12

#### 7.1.1. Event calibration for SWMOD in Yates Flat Creek

The results of the SWMOD calibration in Yates Flats Creek are shown in Appendix C. Among the six events selected for calibration, the model provided a very close match to five events (Figure C3.2 Appendix C), whilst performing very poorly in one event (event number 4, Figure C3.2 in Appendix C). The value of the routing parameter Alpha obtained from the calibration to the five events was 1.75.

### 7.2. Calibration of losses

The flood frequency curves found to give the best fit to the observed data are shown in Table 7-2. A range of distributions and fitting methods were found to give the best fit to the data. The results from FLIKE for each catchment are shown in Appendix F. In selecting the distribution to use, more weight was given to the distribution that gave a better fit to the less frequent events.

**Table 7-2: Flood frequency fitting for each catchment**

Catchment	Distribution (Probability model)	Fitting (Inference) method
Mary River	Generalised Extreme Value	L2-moments
Hann River	Log Pearson III	Bayesian
Yates Flat Creek	Generalised Pareto	Bayesian
Manton River	Generalised Pareto	Bayesian
Sixth Creek	Log Normal	Bayesian
Lerderderg River	Generalised Pareto	Bayesian
Florentine River	Log Normal	Bayesian
Tyenna River	Generalised Extreme Value	L2-moments
Hobart Rivulet	Generalised Extreme Value	Bayesian
Orara River	Log Pearson III	Bayesian

The calibrated loss values for each catchment are shown in **Table 7-3**.

**Table 7-3: Calibrated initial and continuing losses for each catchment**

Catchment	Monte Carlo		Design Event	
	Median IL (mm)	CL (mm/hr)	IL (mm)	CL (mm/hr)
Mary River	10	0.0	0.0	0.0
Hann River	10	4.0	10	4.2
Yates Flat Creek	10	8.0	4	5.5
Manton River	3	12.0	15	5.0
Sixth Creek	10	5.5	4	5.0
Lerderderg River	10	2.5	3	1.75
Florentine River	15	0.6	10	1.6
Tyenna River	25	1.4	15	1.35
Hobart Rivulet	5	2.5	8.0	2.0
Orara River	1.5	0.8	0.0	0.0

The fitted flood frequency curves for Design Event and Monte Carlo model runs are shown in Section 8. Additional plots of Monte Carlo runs, with observed annual maximum series are also shown in Appendix D.

### 7.2.1. Calibration of the initial soil storage parameters for SWMOD in Yates Flat Creek

The final values of the  $C_i$  parameters corresponding to the four landforms found in Yates Flat Creek are shown in Table 7-4.

**Table 7-4 : Calibrated values of the SWMOD parameters**

Landforms	Ci (mm)
Dwellingup	315
Yarragil	300
Pindalup	226
Murray	87

### 7.3. Calibration to sub-set of data

#### 7.3.1. Manton River

The Manton River record was split into two separate periods from 1965 – 1985 and 1990 – 2012 (Figure 7-1). Period 1 was noticeably drier than Period 2 with few large flood events.

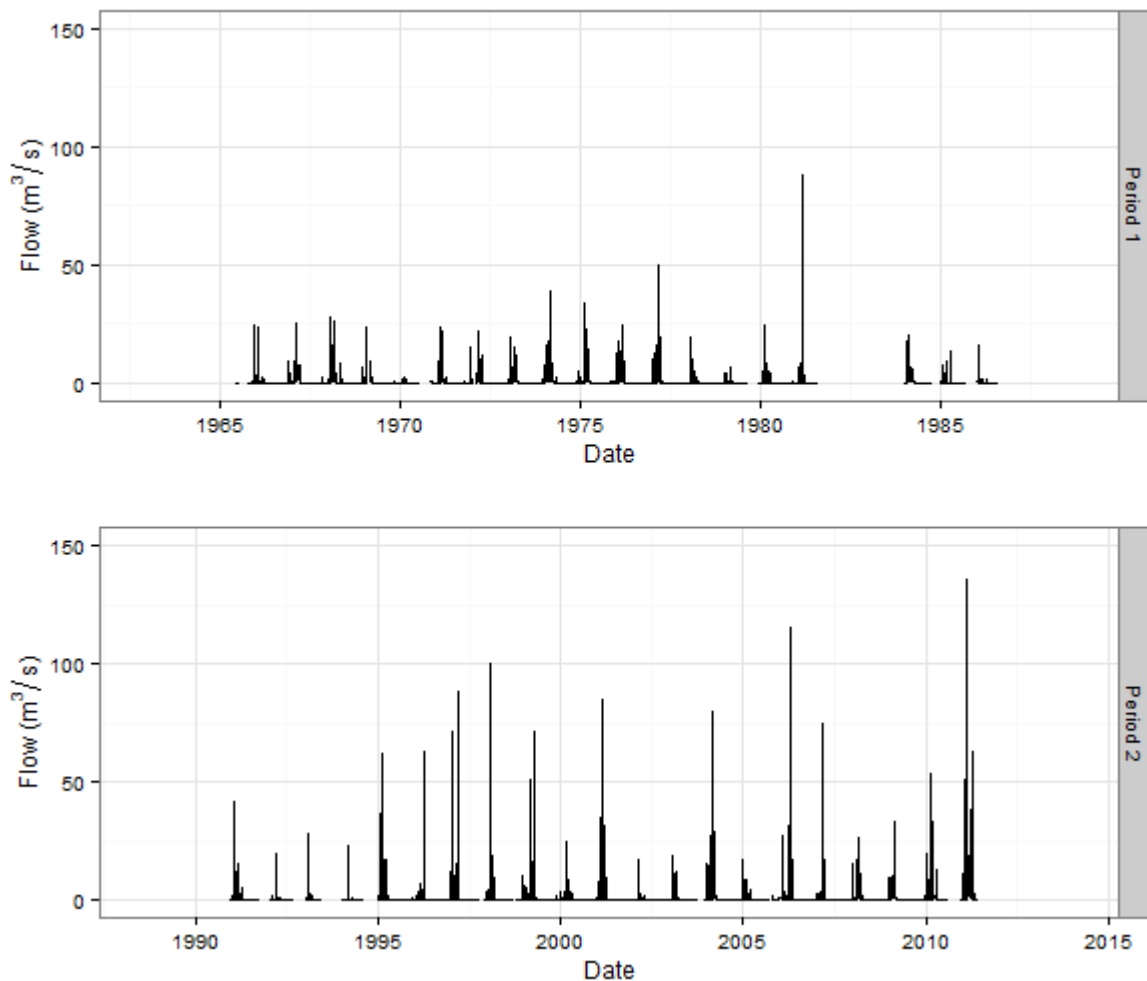


Figure 7-1: Manton River record sub-sets

The five largest flood events used in calibration of the Manton River model for the full data set were all in the second period of record, therefore the event calibration for Period 2 was unchanged from the full record event calibration. The event calibration results for Period 1 are shown in Appendix E.

Frequency curves were derived for Period 1 and Period 2 flows for calibration of the losses for both the Monte Carlo and Design Event models. As Period 1 was a much drier period, with lower flood peaks, the flood frequency curve for this period was lower than for the full record or Period 2.

**Table 7-5: Monte Carlo model parameters**

Parameter	Period of record		
	Full	Period 1	Period 2
Alpha	1.2	1.2	1.2
IL	3	40.0	3.0
CL	12.0	16.0	10.0

**Table 7-6: Design Event model parameters**

Parameter	Period of record		
	Full	Period 1	Period 2
Alpha	1.2	1.2	1.2
IL	15	19.0	6.5
CL	5	11.5	5.5

### 7.3.2. Mary River

The Mary River record was split into two separate periods from 1965 – 1987 and 1988 – 2013 (Figure 7-2).

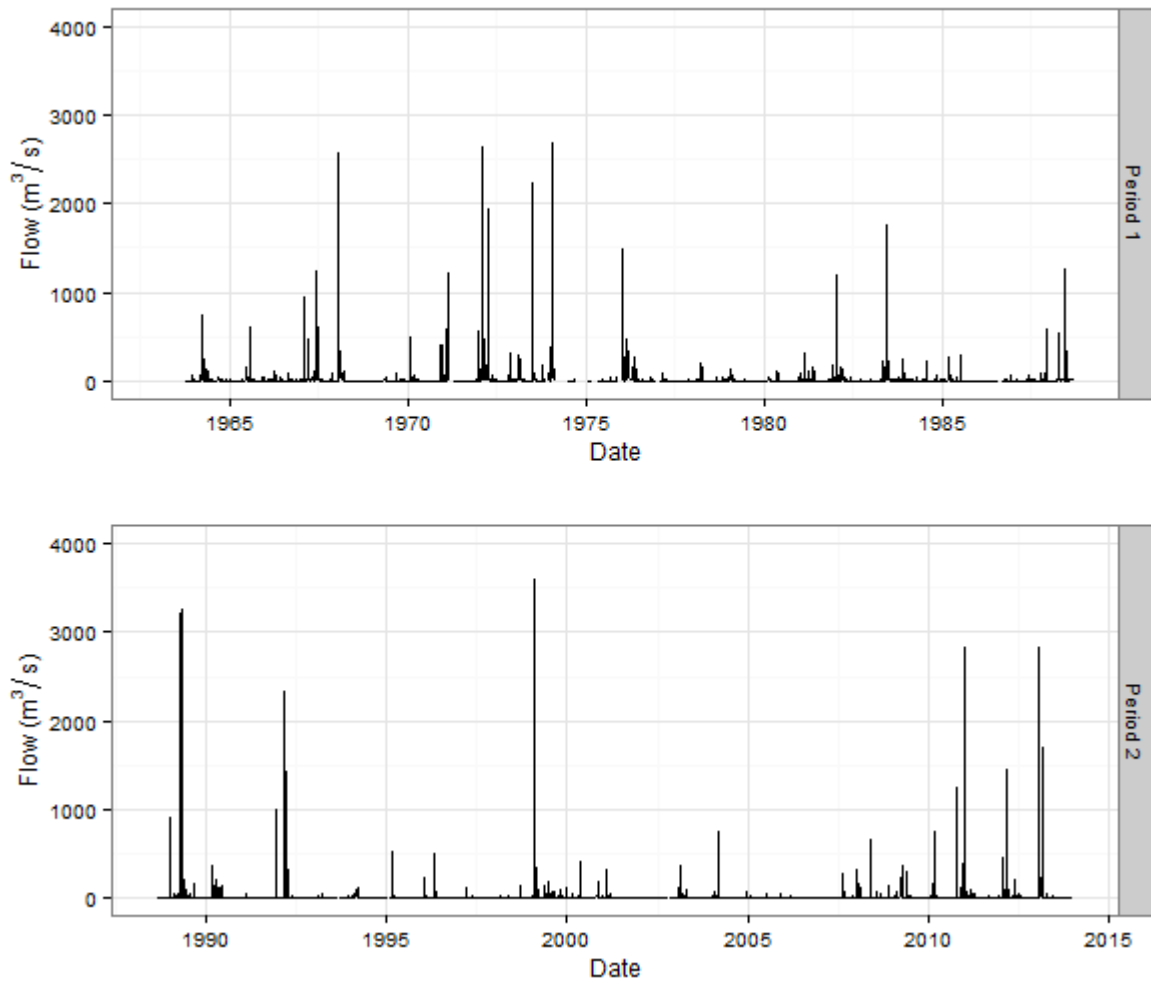


Figure 7-2: Mary River record sub-sets

The flood events used in calibration of the Mary River model for the full data set were spread throughout both Periods 1 and 2. Additional events were selected for each period for event calibration. The event calibration results are shown in Appendix E.

Frequency curves were derived for Period 1 and Period 2 flows for calibration of the losses for both the Monte Carlo and Design Event models.

**Table 7-7: Monte Carlo model parameters**

Parameter	Period of record		
	Full	Period 1	Period 2
Alpha	1.0	1.2	0.8
IL	0.0	0.0	40.0
CL	0.0	0.0	0.0

**Table 7-8: Design Event model parameters**

Parameter	Period of record		
	Full	Period 1	Period 2
Alpha	1.0	1.2	0.8
IL	10	19.0	11.5
CL	0	1.0	1.0

## 7.4. Key issues

A number of issues were encountered in the event calibration for each catchment model.

### 7.4.1. Mary River

There is a dam in the upper catchment of the Mary River catchment, Baroon Pocket Dam. This was constructed in 1989. The affected catchment area is less than 10% of the total catchment to the Moy Pocket gauge. Other gauges in the Mary River catchment are unaffected. The flow and rainfall records at Moy Pocket gauge were examined to investigate any impacts of this dam on the flood response in terms of flood peaks, volumes and shape. No noticeable change in flood response was detected, therefore the reservoir operation was not modelled in detail.

### 7.4.2. Hann River

In the Hann River model, the calibrated value of the routing parameter was low, particularly for a large catchment. The baseflow for this catchment was consistently above 100m<sup>3</sup>/s for the events investigated, so it is possible that this contributes to the relative lack of attenuation of flood events.

### 7.4.3. Yates Flat Creek

When the initial loss-continuing loss model was run in Yates Flat Creek catchment there was a wide range of flow responses to large rainfall events, depending on season and the antecedent rainfall. Fitting to the observed frequency curve was difficult. The Bureau of Meteorology design rainfall inputs were compared to design rainfalls derived from the closest pluviograph to the catchment, and a good agreement was found. A range of temporal patterns was trialled for the Design Event model. The calibration using SWMOD was found to be more successful, reflecting the fact that the catchment response cannot be characterised with a constant continuing loss. The results are further discussed in Section 10.

### 7.4.4. Manton River

The data at the rainfall gauge closest to the Manton River catchment (Darwin River At West Track) was at an hourly time step, therefore the data from Batchelor Airport gauge was used to derive a sub-hourly rainfall pattern for calibration, and was used to derive temporal patterns for use in the Monte Carlo model.



### **7.4.5. Sixth Creek**

There was a wide variation in the calibrated value of the routing parameter, Alpha, in the Sixth Creek model between events, with a range of 0.25 to 1.0. Alpha was calibrated to 0.8 for three of the six events, and this value was selected for use in the model runs. The calibration of losses using this value of Alpha resulted in a good agreement between modelled and observed flood frequency curves.

### **7.4.6. Lerderberg River**

For two of the events (1 and 7) used in calibration, it was not possible to accurately model the hydrograph shape as the rainfall available at the gauges did not appear to match the shape of the hydrograph. A reasonable fit to the peak flow and volume was still obtained for these events. The frequency distributions fitted using FLIKE did not give a good fit to the observed values. The Generalised Pareto distribution was selected as the best fit from those investigated.

### **7.4.7. Florentine River**

During the event calibration for the Florentine River model, it was found that it was not possible to replicate the shape of some of the event hydrographs with a single set of routing and loss parameters over the model. The hydrographs were characterised by a double peak 24 hours apart, which resulted from a single rainfall burst. Three catchment characteristics were considered as possible causes for this:

1. As the flow gauge site is located close to Lake Catagunya, tailwater influences were investigated. However the peak levels/spill at the lake did not coincide with either of the two peaks for the reviewed events.
2. The Junee cave system underlies a portion of the lower catchment, and there may be water stored and released from this system, or it may be providing a faster flow path causing the initial peak.
3. The surface topography shows that the river in the upper catchment is long, flat and meandering. It reaches a point lower in the catchment where the river straightens and steepens through to the gauge location.

A good flow record is available at an internal gauge within the catchment at Eleven Rd Bridge. No double peak is evident in the flows at Eleven Rd Bridge, suggesting that the steepness of the lower catchment is the main influence the shape of the hydrograph. Two model calibrations were undertaken. The first calibration used one parameter set over the entire catchment, whilst the second calibration used a parameter set for each of the upper and lower catchments, using the flow records at both Eleven Rd Bridge and u/s Derwent gauges.

There is evidence of snow influence on the rainfall gauges around the catchment, particularly for the gauges located at higher elevations. It was found that the Tim Shea rainfall gauge records no rainfall once the air temperature drops below zero degrees, and two days later a rainfall pulse can be seen at each gauge with no corresponding flow response in the catchment. It is assumed that this small recorded pulse represents the period where the snow pack on the

gauge melts into the gauge. As the gauges are located at elevations higher than the majority of the catchment it is also assumed that the snow impact recorded by these gauges is higher than for the whole catchment. Some allowances for this have been made during event calibration of the model, usually by selecting lower elevation rainfall gauges during periods of snowfall.

Difficulties were encountered fitting the Florentine River model to the observed flood frequency curve. An investigation found that the design rainfall values differed from Bureau of Meteorology differed from those derived from rainfall data at Florentine Crossing and Salvation Creek gauges, overestimating the rainfall by up to 15%. Two model runs were undertaken using the Bureau of Meteorology IFDs and IFDs derived from a representative pluviograph site for the Florentine River catchment rainfall. The results of the Monte Carlo model run using Bureau of Meteorology IFDs are reported. The results using the at-site IFDs are shown in Appendix G.

#### **7.4.8. Tyenna River**

A similar double peak response as was seen in the Florentine River catchment was evident in the Tyenna River events, although this was less pronounced. Two sets of parameters were again trialled for this catchment. The results using a single parameter set are reported.

As for the Florentine River catchment, design rainfalls derived from at-site rainfalls were significantly below the Bureau of Meteorology IFDs, with difference of 15% to 24%. The slope of the two design IFD plots were very similar. The model was run using the BoM IFDs.

#### **7.4.9. Hobart Rivulet**

All five events used in calibration of the Hobart Rivulet model occurred after 2009. A large event that occurred in 2007 could not be calibrated and was discarded. Among the five events calibrated, two event calibrations resulted in Alpha values of 2.5 and 3.5, whilst the remaining three events had lower values of 1.25. The two events with higher Alpha values were of smaller magnitudes, therefore the Alpha value of 1.25 was adopted.

#### **7.4.10. Orara River**

Five events were selected for event calibration. As far as practicable the five largest floods were selected but in cases where the rainfall data was missing the next highest flood event was selected. In general the IL-CL model provided a good match to the observed event hydrographs, in the five events selected. An Alpha value of 1.75 was consistent over the four events and was applied for loss calibration.

## 8. Monte Carlo and Design Event Model Results

The results from both the Monte Carlo and Design Event model runs are presented in the following sections. The spread of results from the Monte Carlo model run at the duration that results in the highest peak flow are shown, along with the 5 and 95 percentiles. The 90 percent confidence interval is shown for the flood frequency curve fitted to observed values. The Design Event runs with 10 different temporal patterns are indicated as the grey dots in the figures, while the median of the 10 individual runs is shown as the line.

### 8.1. Full data set

#### 8.1.1. Mary River

Table 8-1: Mary River model results

Annual Exceedance Probability	Frequency curve fitted to observed values (m <sup>3</sup> /s)	Monte Carlo (m <sup>3</sup> /s)	Monte Carlo % difference	Design Event (m <sup>3</sup> /s)	Design Event % difference	Critical Duration (hours)
20%	1658	1904	15%	1771	7%	18
10%	2369	2483	5%	2239	-6%	18
5%	3029	3101	2%	2728	-10%	18
2%	3852	4072	6%	3430	-11%	36
1%	4446	4869	10%	4062	-9%	36

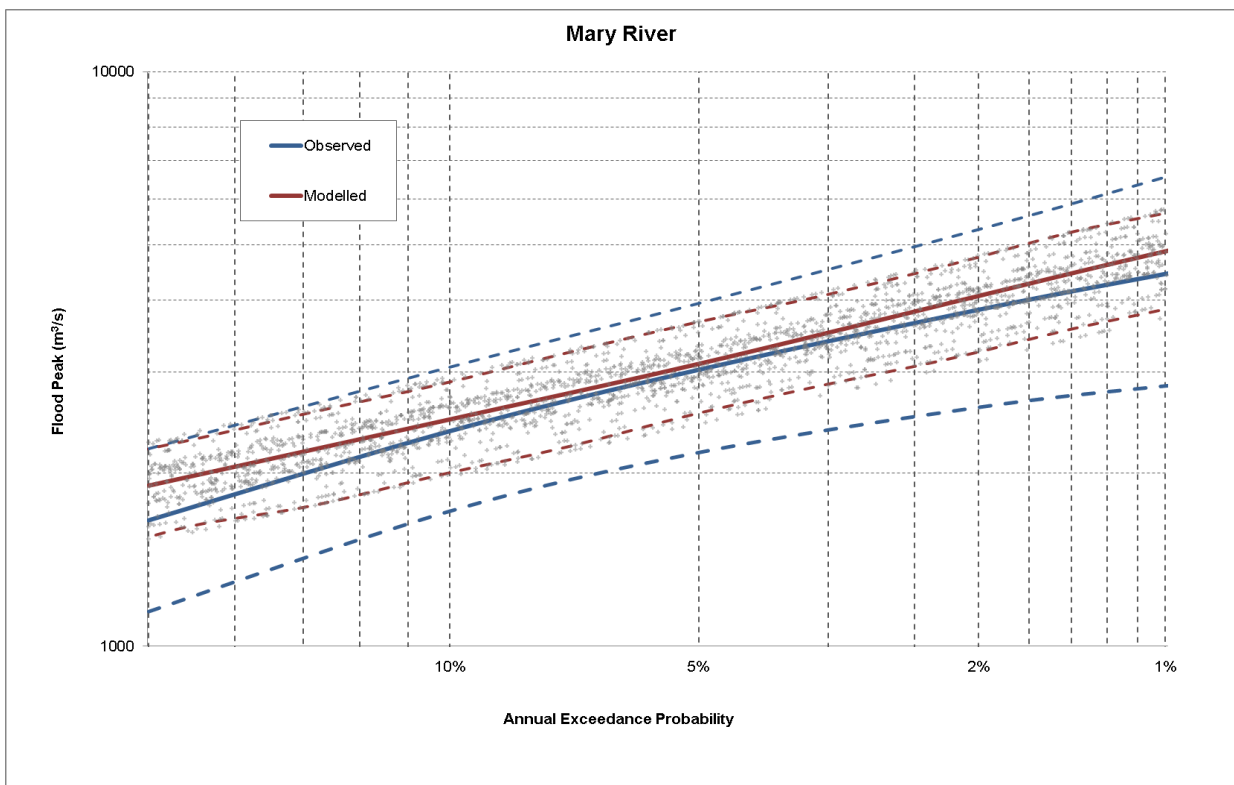


Figure 8-1: Monte Carlo model results – Mary River

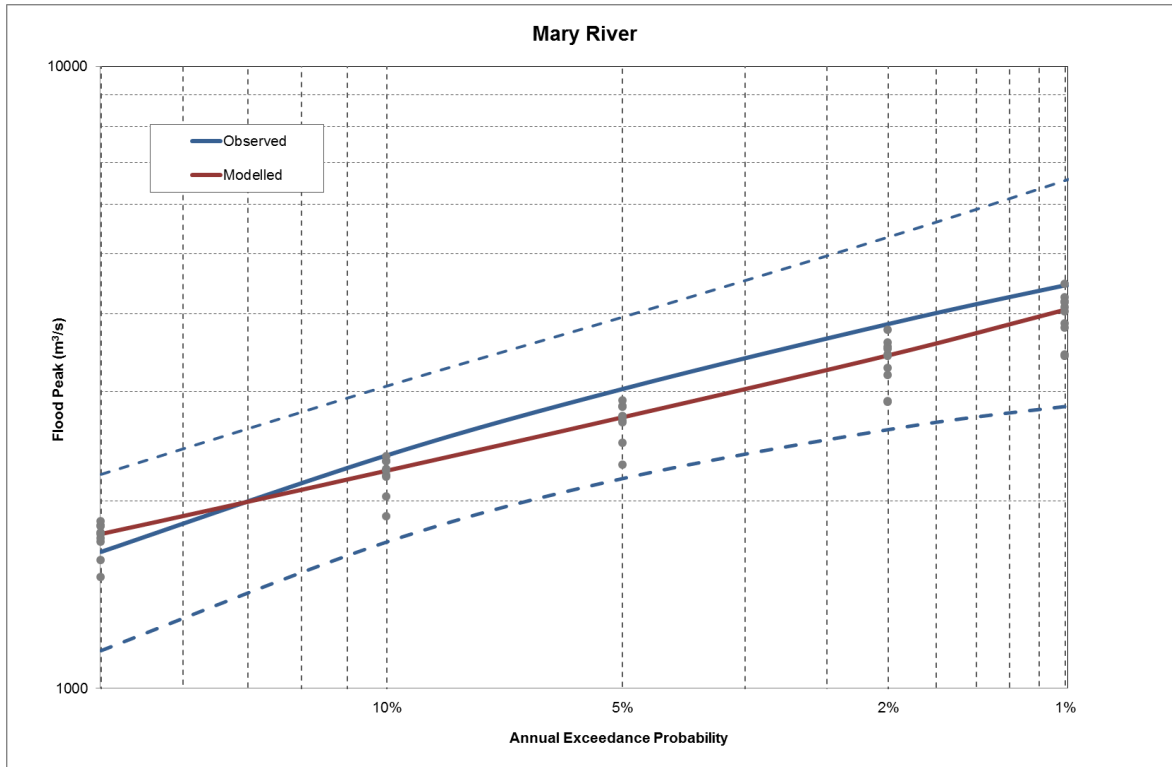


Figure 8-2: Design Event model results – Mary River

### 8.1.2. Hann River

Table 8-2: Hann River model results

Annual Exceedance Probability	Frequency curve fitted to observed values (m <sup>3</sup> /s)	Monte Carlo (m <sup>3</sup> /s)	Monte Carlo % difference	Design Event (m <sup>3</sup> /s)	Design Event % Difference	Critical Duration (hours)
20%	1807	1792	-1%	1619	-10%	72
10%	2660	2502	-6%	2518	-5%	72
5%	3489	3475	0%	3494	0%	72
2%	4515	4793	6%	4801	6%	72
1%	5225	5969	14%	5894	13%	72

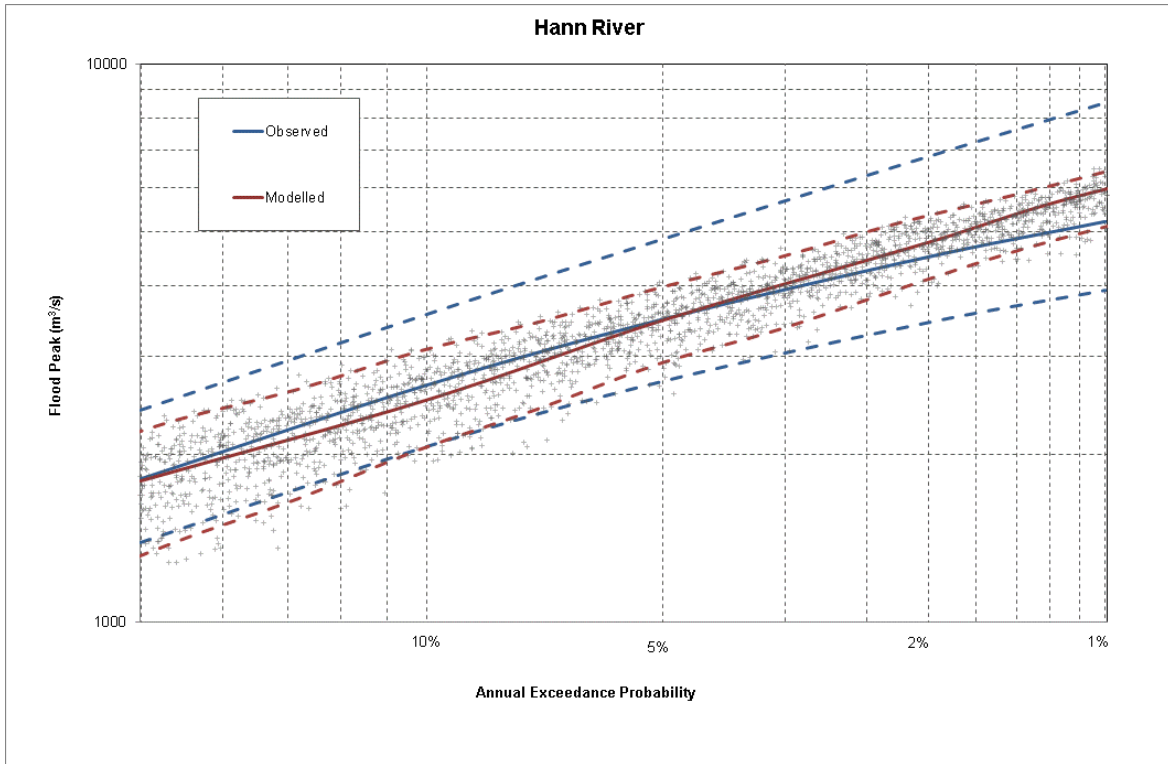


Figure 8-3: Monte Carlo model results – Hann River

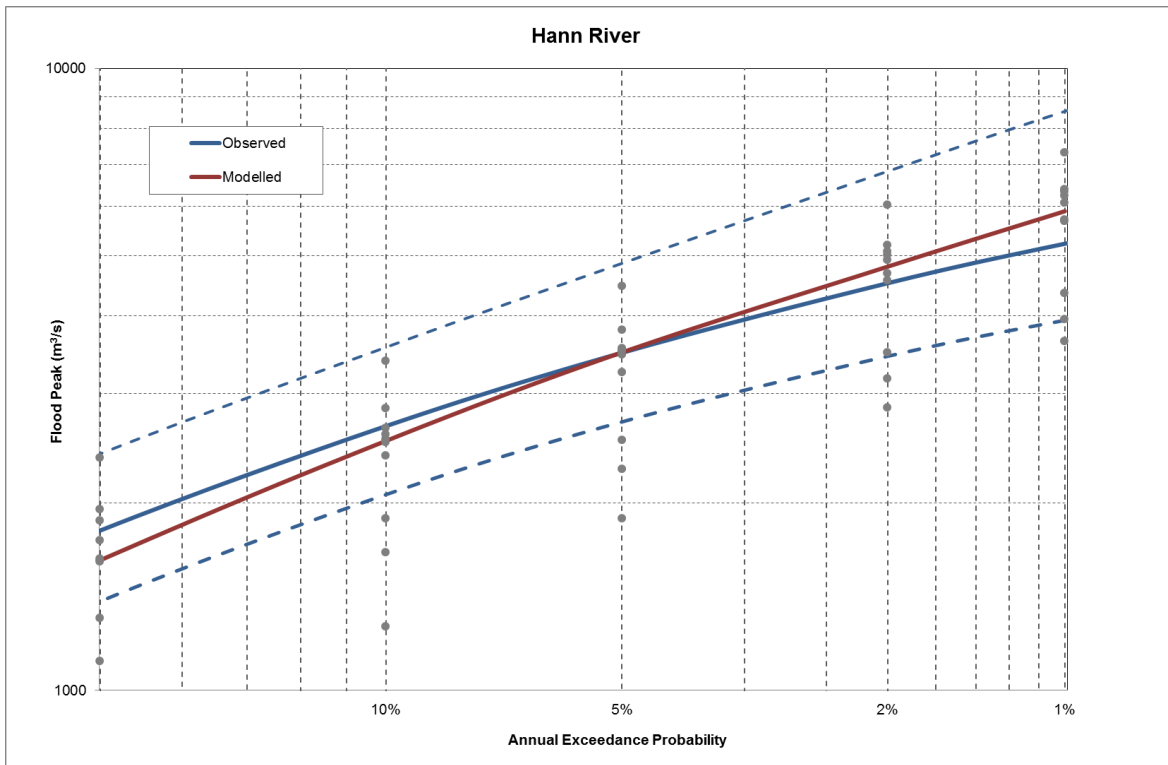


Figure 8-4: Design Event model results – Hann River

### 8.1.3. Yates Flat Creek

Table 8-3: Yates Flat Creek model results

Annual Exceedance Probability	Frequency curve fitted to observed values (m <sup>3</sup> /s)	Monte Carlo (m <sup>3</sup> /s)	Monte Carlo % difference	Design Event (m <sup>3</sup> /s)	Design Event % Difference	Critical Duration (hours)
20%	14	5	-63%	11	-24%	3
10%	20	11	-45%	18	-12%	3
5%	25	18	-26%	25	-1%	6
2%	31	30	-2%	38	24%	6
1%	35	43	22%	51	45%	6

Table 8-4 : SWMOD

Annual Exceedance Probability	Frequency curve fitted to observed values (m <sup>3</sup> /s)	SWMOD (m <sup>3</sup> /s)	SWMOD % Difference	Critical Duration (hours)
20%	14	15	8%	18
10%	20	19	-1%	18
5%	25	24	-2%	18
2%	31	32	4%	18
1%	35	39	12%	18

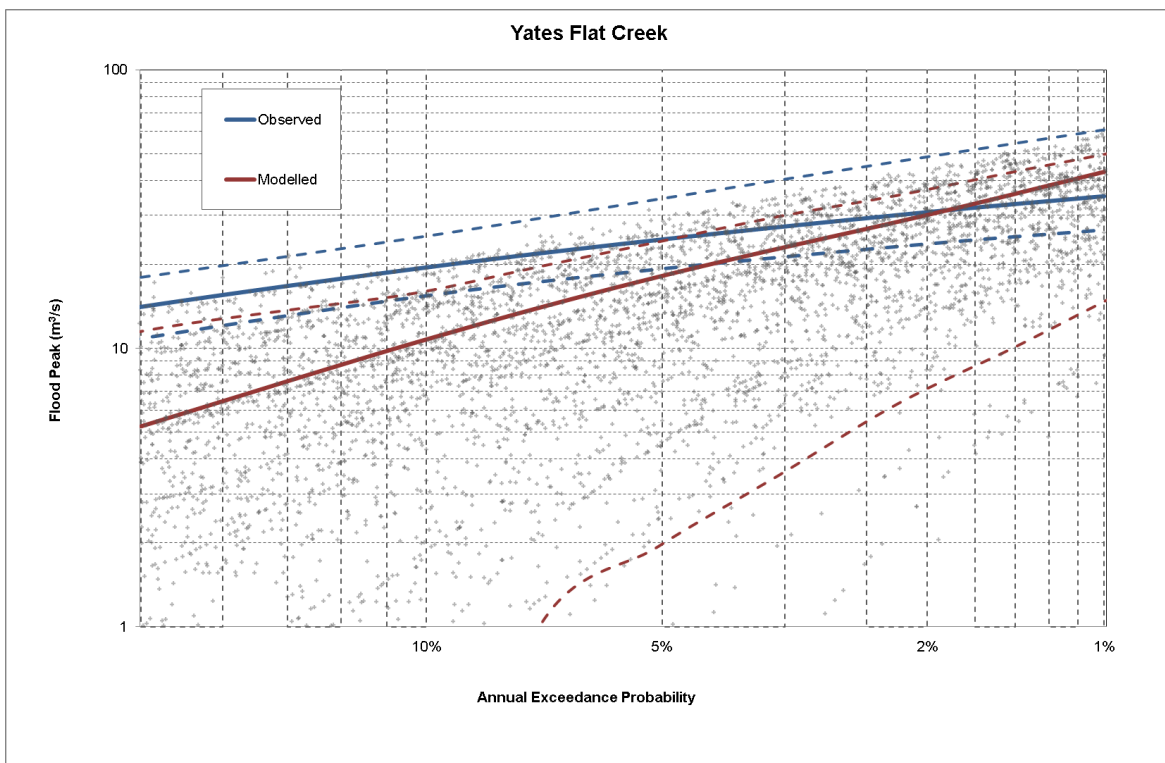


Figure 8-5: Monte Carlo model results – Yates Flat Creek

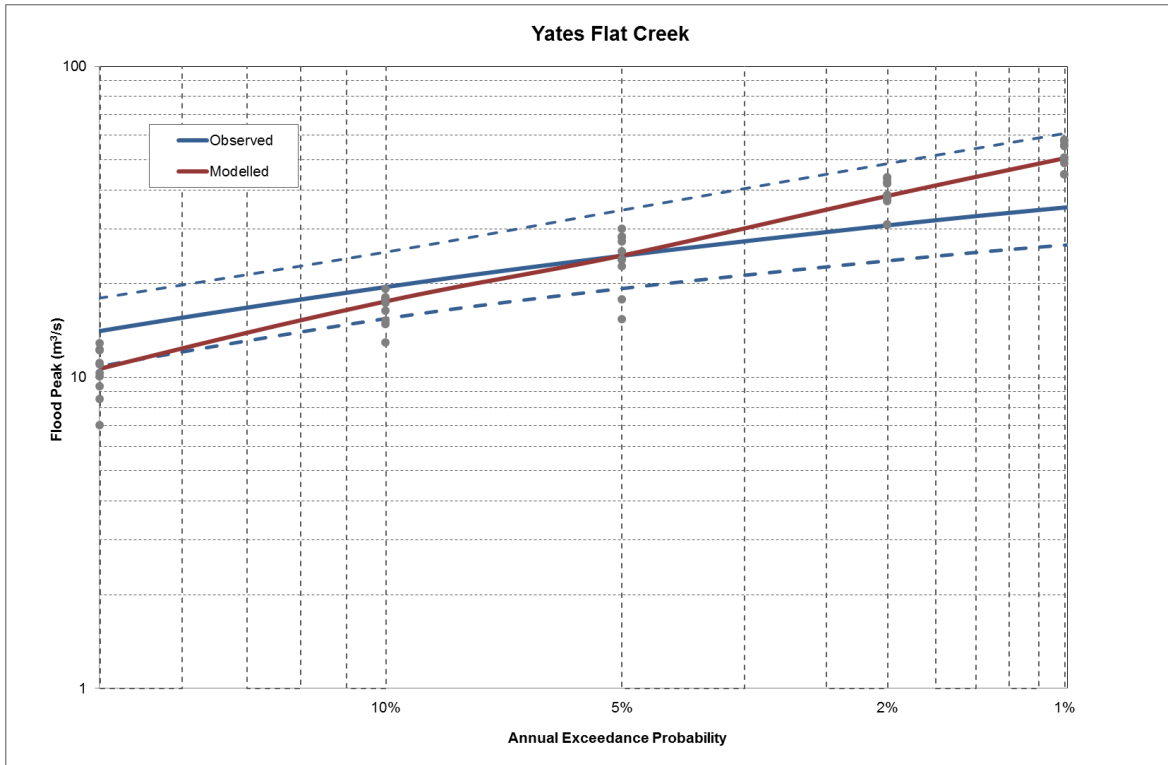


Figure 8-6: Design Event model results – Yates Flat Creek

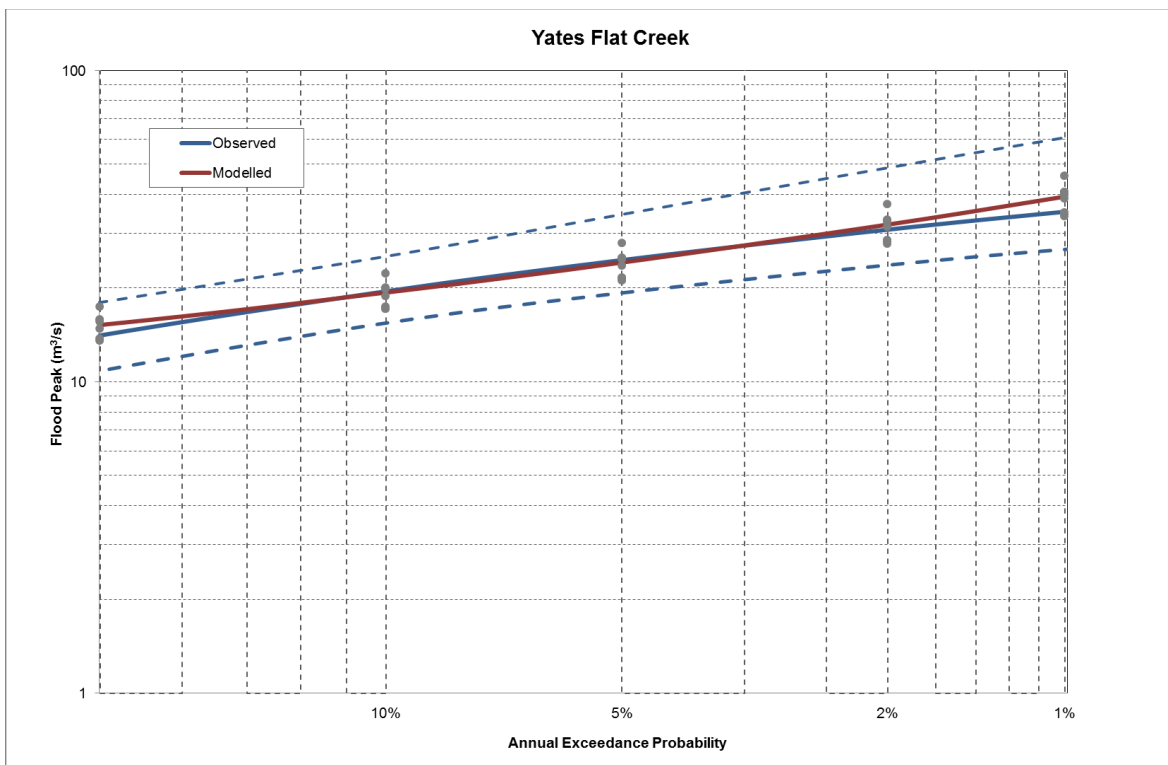


Figure 8-7: SWMOD initial soil water storage calibration results – Yates Flat Creek (grey dots show the 10 realizations of the modelled flood using 10 different temporal patterns)

### 8.1.4. Manton River

Table 8-5: Manton River model results

Annual Exceedance Probability	Frequency curve fitted to observed values (m <sup>3</sup> /s)	Monte Carlo (m <sup>3</sup> /s)	Monte Carlo % difference	Design Event (m <sup>3</sup> /s)	Design Event % Difference	Critical Duration (hours)
20%	73	74	1%	71	-3%	4.5
10%	97	95	-2%	93	-4%	4.5
5%	117	114	-2%	113	-4%	4.5
2%	139	140	1%	142	2%	4.5
1%	152	162	6%	162	6%	4.5

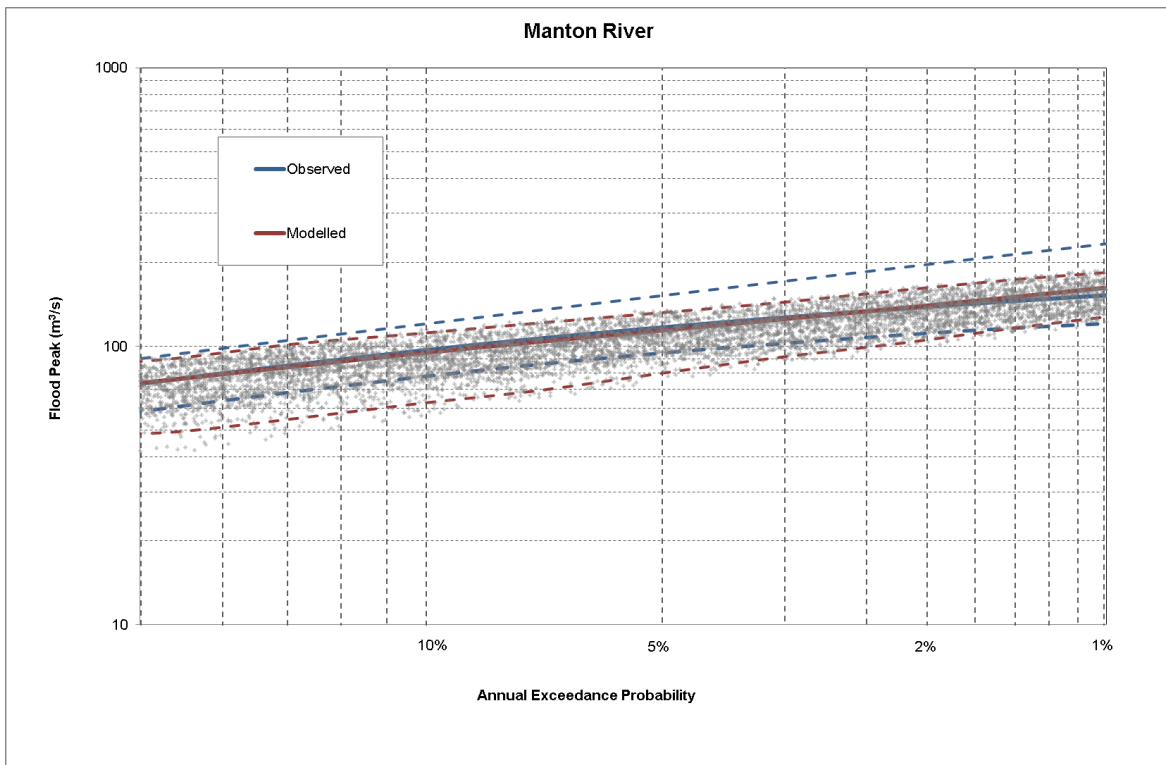


Figure 8-8: Monte Carlo model results – Manton River



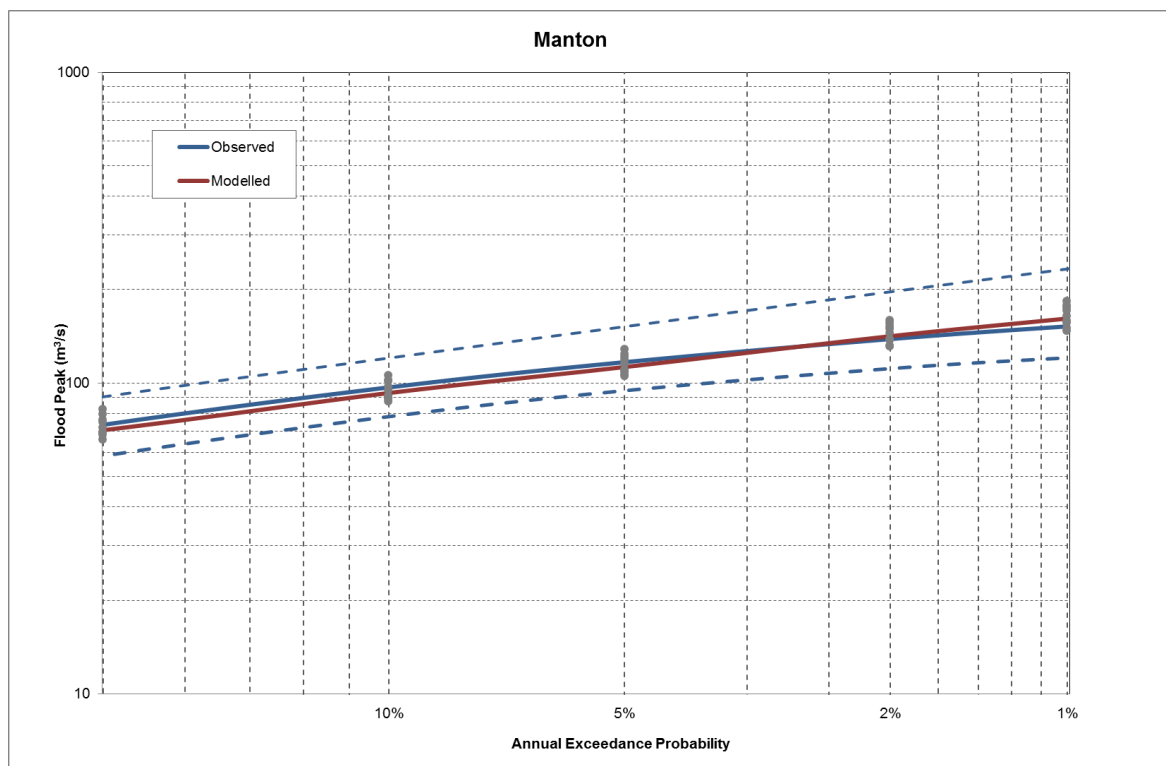


Figure 8-9: Design Event model results – Manton River

### 8.1.5. Sixth Creek

Table 8-6: Sixth Creek model results

Annual Exceedance Probability	Frequency curve fitted to observed values (m <sup>3</sup> /s)	Monte Carlo (m <sup>3</sup> /s)	Monte Carlo % difference	Design Event (m <sup>3</sup> /s)	Design Event % Difference	Critical Duration (hours)
20%	24	23	-2%	23	-4%	3
10%	35	36	0%	35	1%	4.5
5%	49	49	0%	50	2%	4.5
2%	71	68	-5%	73	3%	4.5
1%	91	90	-1%	94	3%	4.5

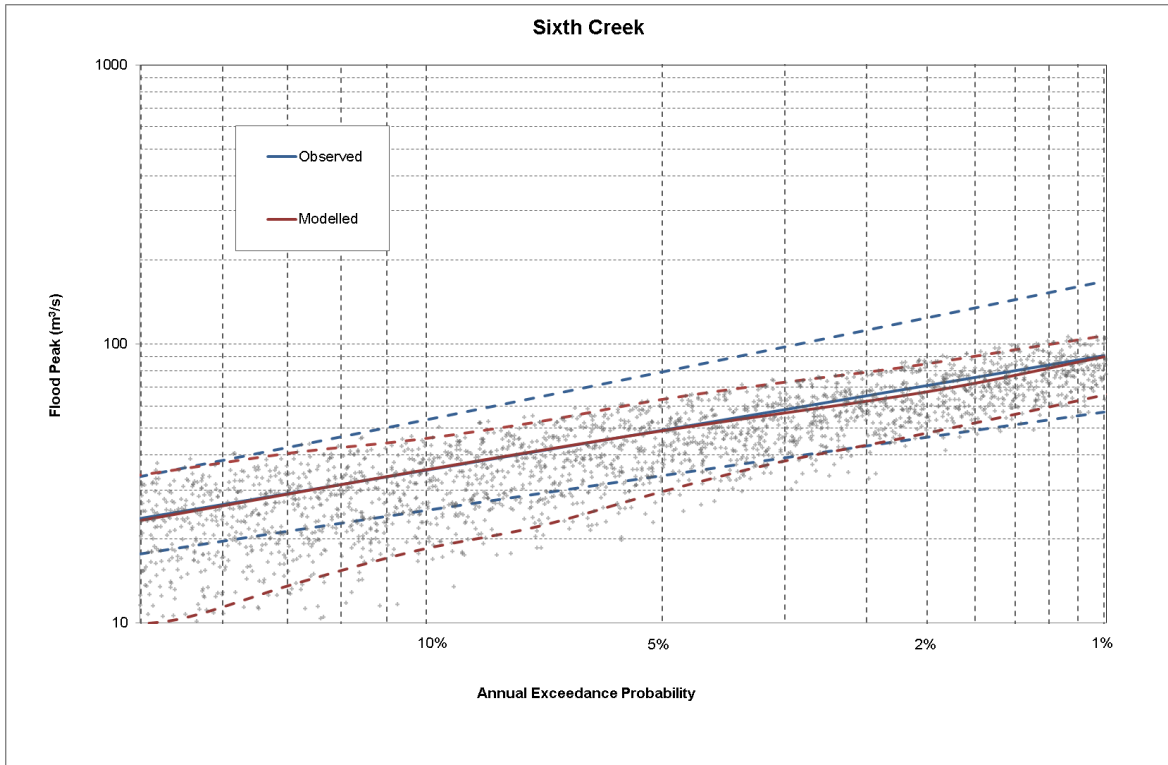


Figure 8-10: Monte Carlo model results – Sixth Creek

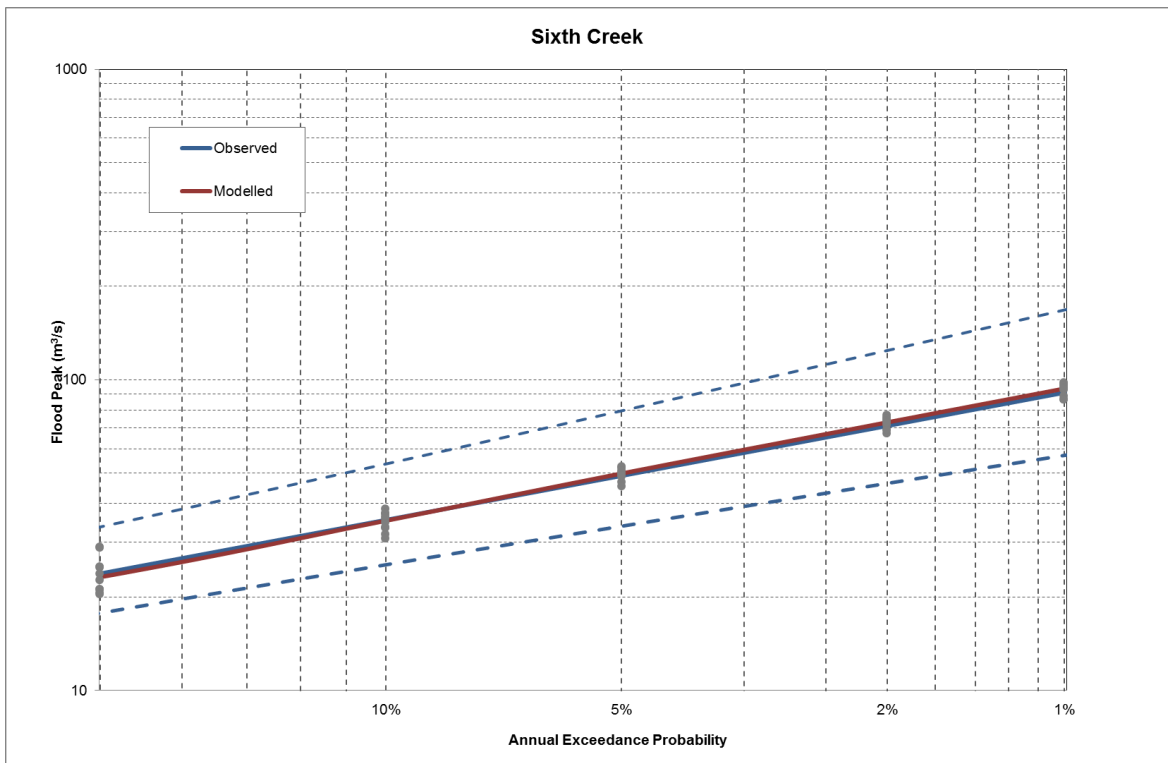


Figure 8-11: Design Event model results – Sixth Creek

### 8.1.6. Lerderderg River

Table 8-7: Lerderderg River model results

Annual Exceedance Probability	Frequency curve fitted to observed values (m <sup>3</sup> /s)	Monte Carlo (m <sup>3</sup> /s)	Monte Carlo % difference	Design Event (m <sup>3</sup> /s)	Design Event % Difference	Critical Duration (hours)
20%	87	67	-30%	85	-3%	12
10%	119	100	-20%	114	-5%	12
5%	149	133	-12%	147	-1%	12
2%	183	185	1%	196	7%	12
1%	207	229	10%	237	15%	12

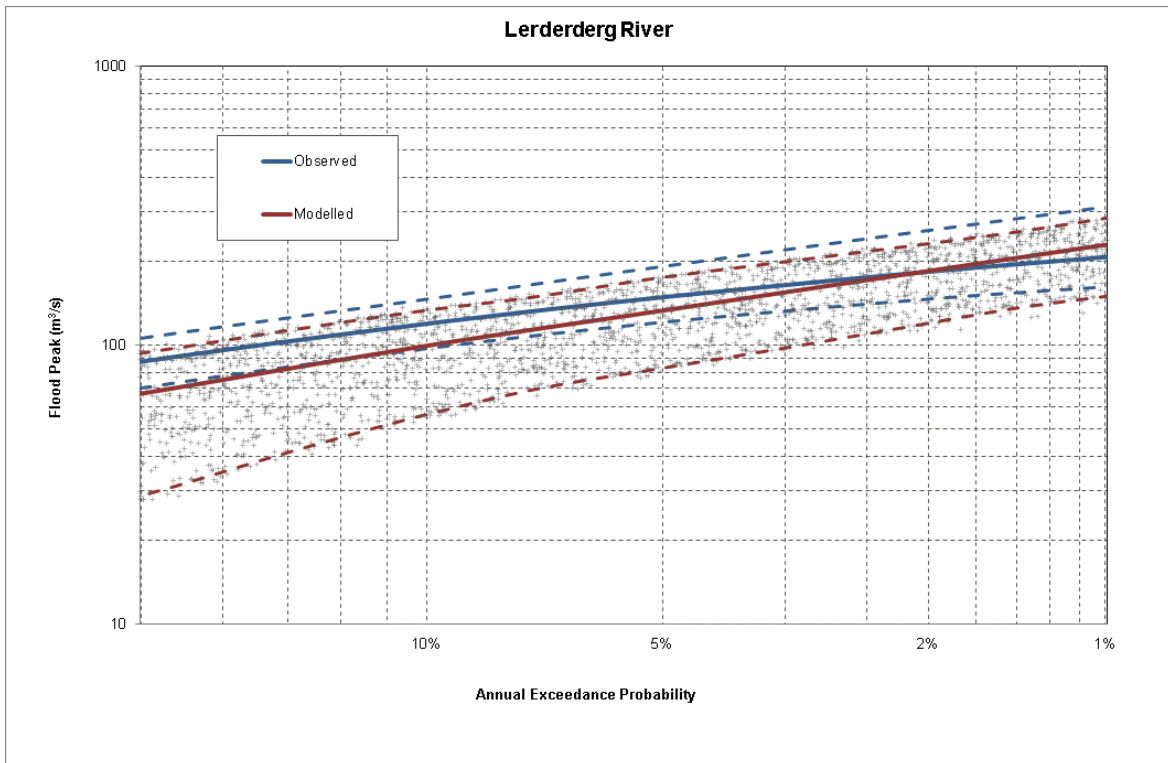


Figure 8-12: Monte Carlo model results – Lerderderg River

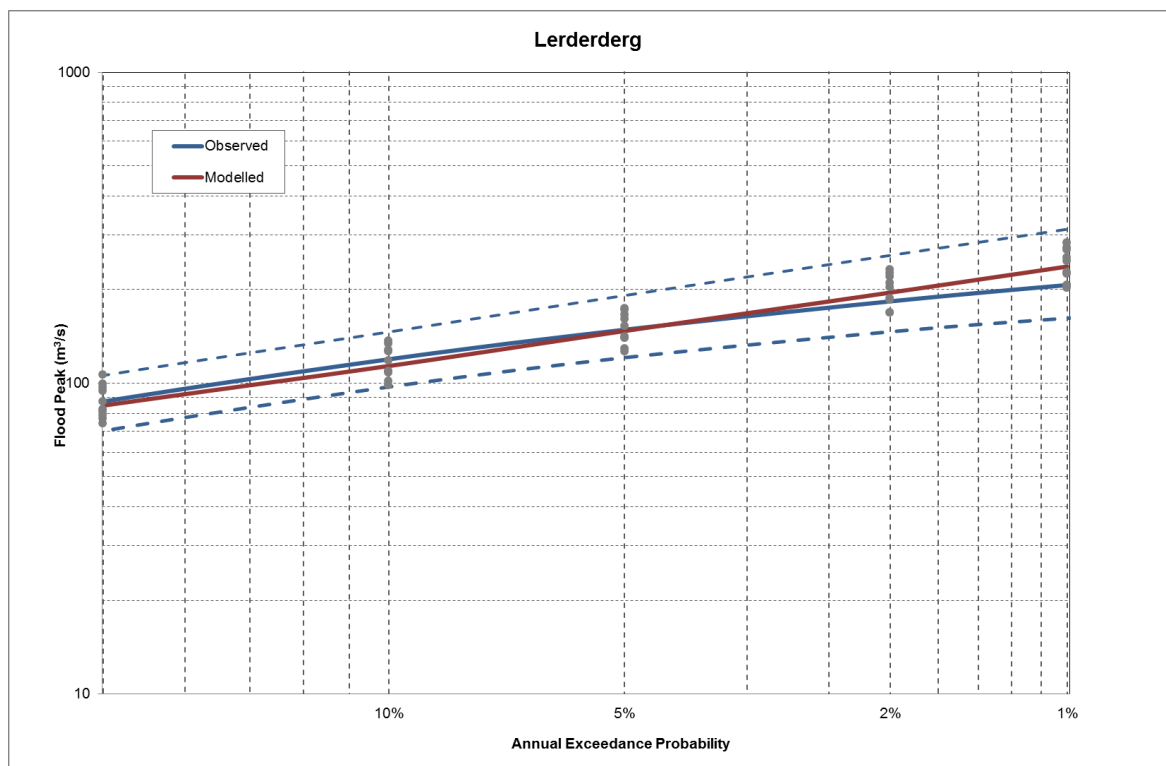


Figure 8-13: Design Event model results – Lerderderg River

### 8.1.7. Florentine River

The results shown in Table 8-8 and Figure 8-14 are for the runs with the Bureau of Meteorology IFDs, and a single set of model parameters. The model results using the IFDs derived from the catchment rainfall gauges are shown in Appendix G.

Table 8-8: Florentine River model results

Annual Exceedance Probability	Frequency curve fitted to observed values (m³/s)	Monte Carlo (m³/s)	Monte Carlo % difference	Design Event (m³/s)	Design Event % Difference	Critical Duration (hours)
20%	104	80	-24%	98	-6%	72
10%	127	103	-18%	123	-3%	72
5%	149	130	-13%	149	0%	72
2%	178	172	-4%	191	7%	72
1%	201	206	3%	223	11%	72

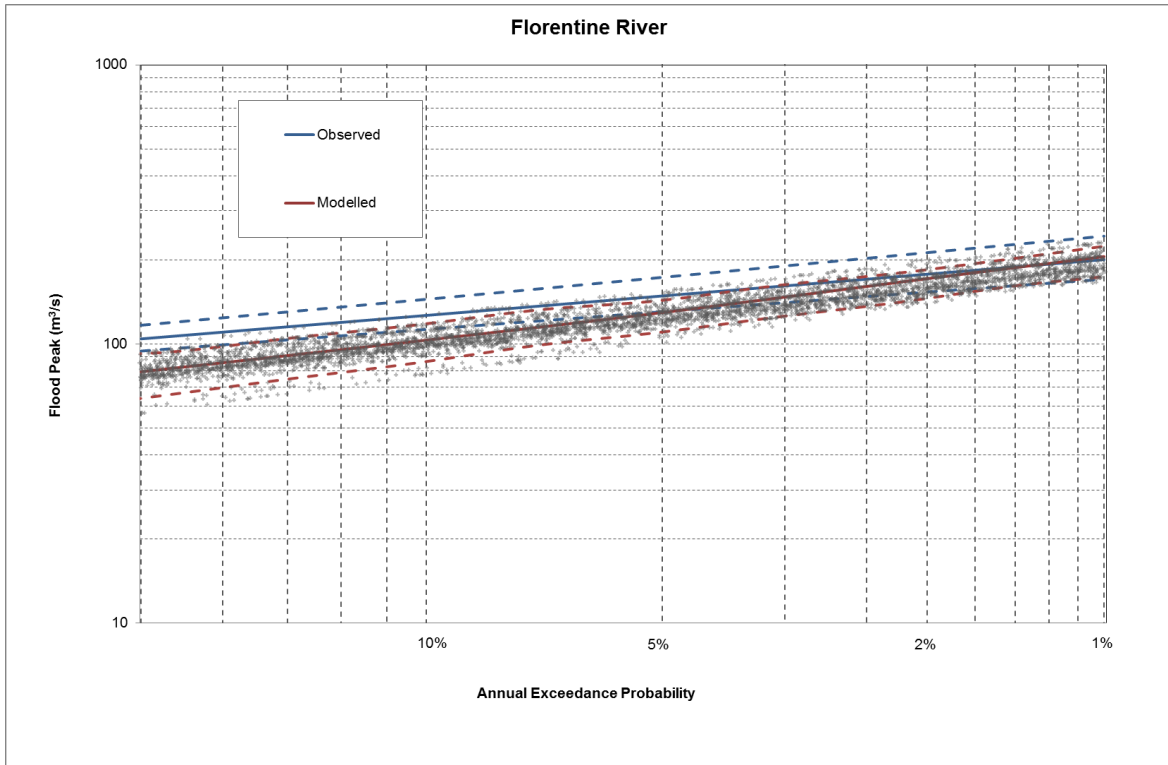


Figure 8-14: Monte Carlo model results – Florentine River

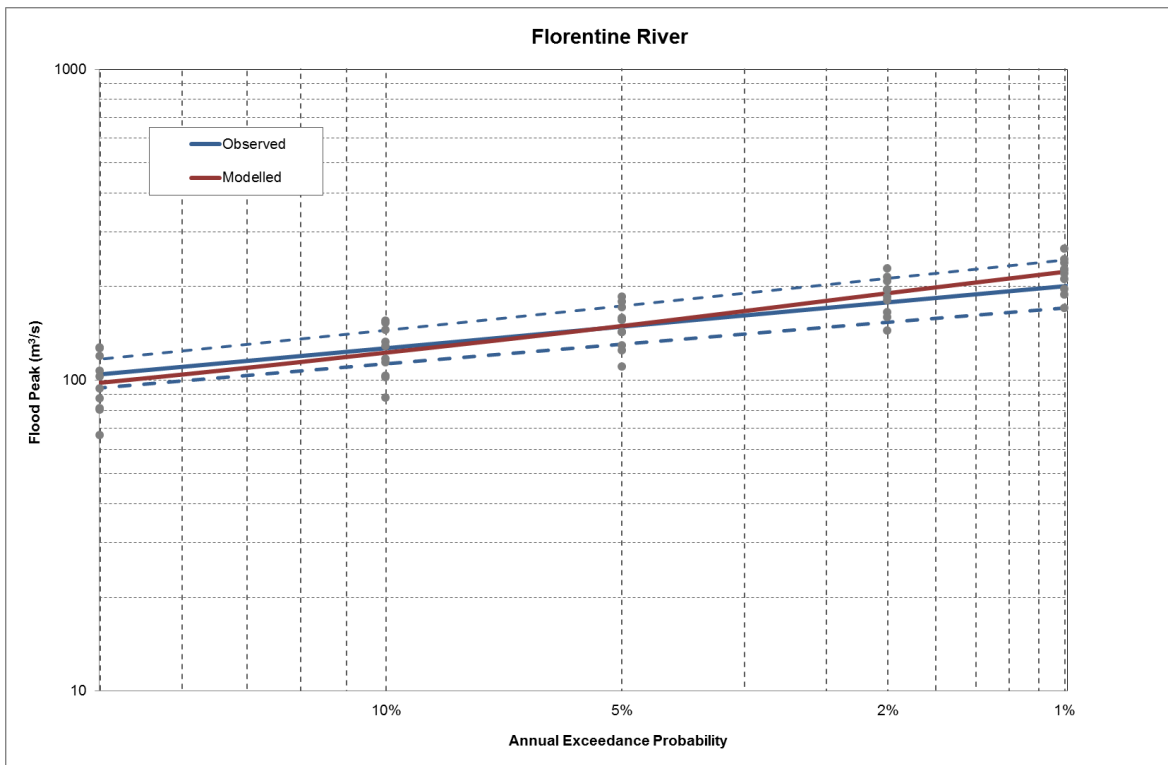


Figure 8-15: Design Event model results – Florentine River

### 8.1.8. Tyenna River

Table 8-9: Tyenna River model results

Annual Exceedance Probability	Frequency curve fitted to observed values (m <sup>3</sup> /s)	Monte Carlo (m <sup>3</sup> /s)	Monte Carlo % difference	Design Event (m <sup>3</sup> /s)	Design Event % Difference	Critical Duration (hours)
20%	74	70	-5%	72	-2%	36
10%	98	97	0%	96	-2%	24
5%	124	125	1%	122	-1%	24
2%	165	167	1%	157	-5%	24
1%	201	201	0%	185	-8%	24

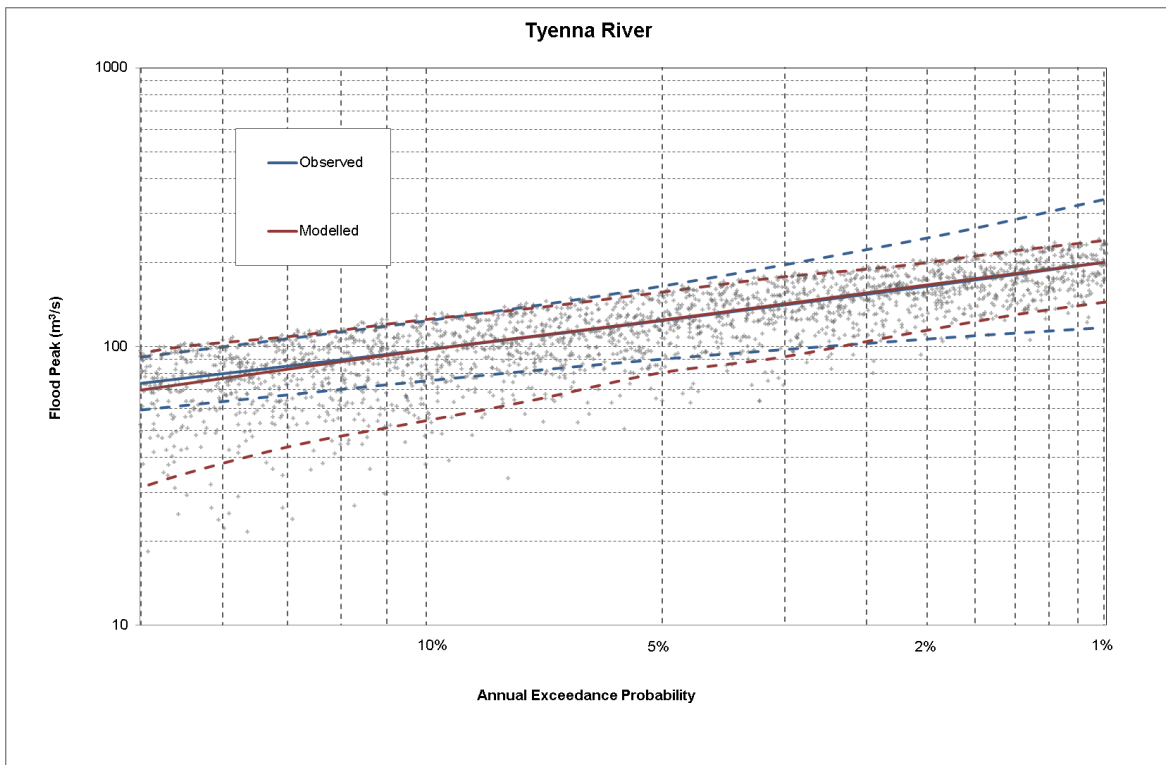


Figure 8-16: Monte Carlo model results - Tyenna River

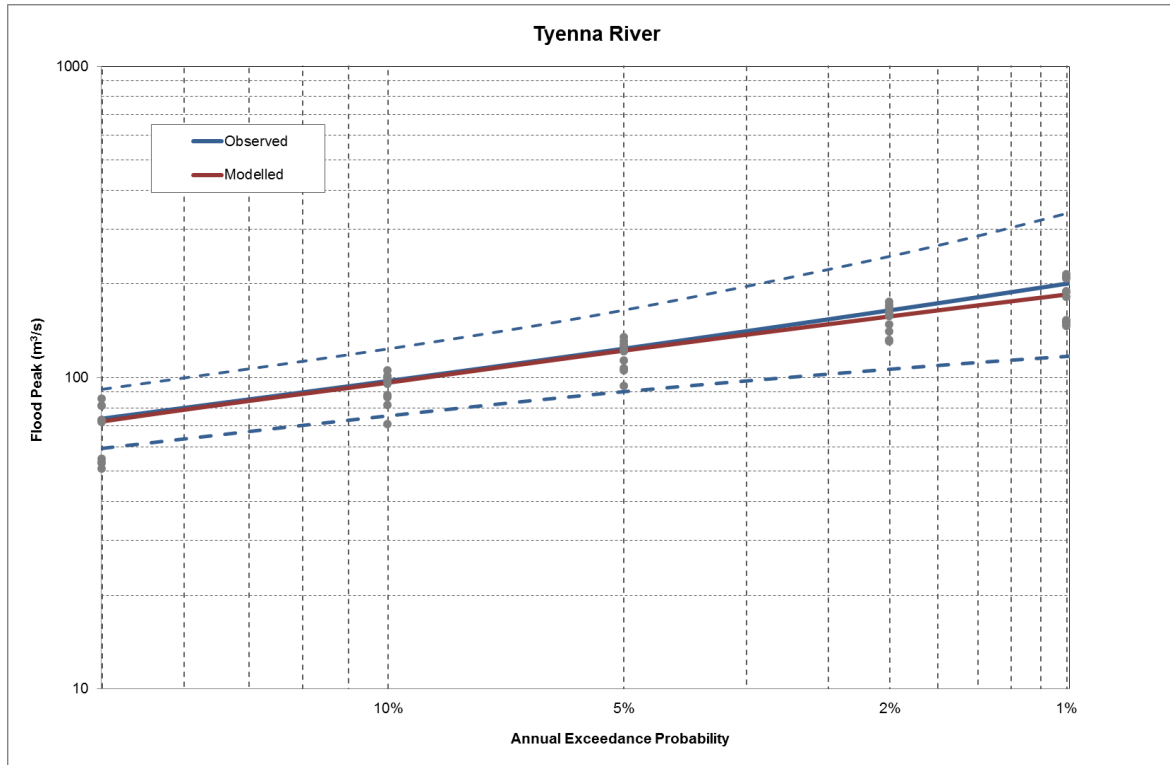


Figure 8-17: Design Event model results – Tyenna River

### 8.1.9. Hobart Rivulet

Table 8-10: Hobart Rivulet model results

Annual Exceedance Probability	Frequency curve fitted to observed values (m <sup>3</sup> /s)	Monte Carlo (m <sup>3</sup> /s)	Monte Carlo % difference	Design Event (m <sup>3</sup> /s)	Design Event % Difference	Critical Duration (hours)
20%	21	19	-9%	19	-10%	6
10%	26	26	1%	25	-3%	6
5%	30	32	7%	31	4%	6
2%	36	42	16%	39	8%	6
1%	40	49	23%	45	12%	6

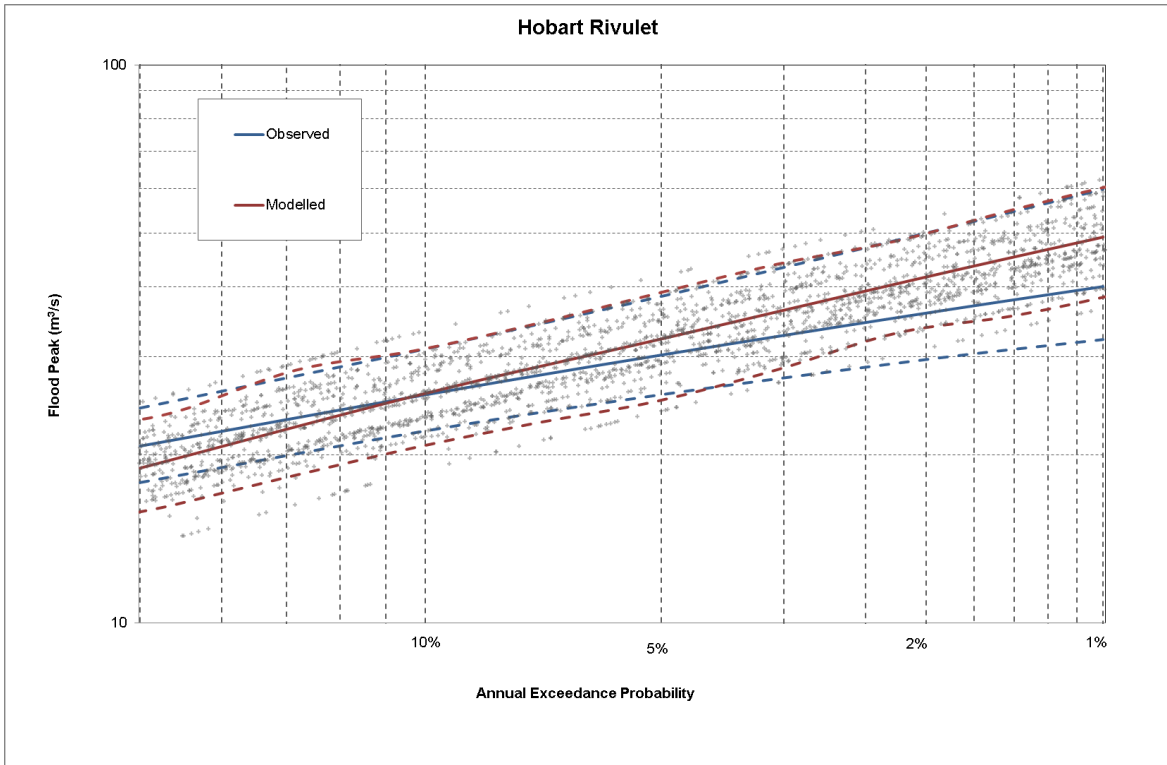


Figure 8-18: Monte Carlo model results – Hobart Rivulet

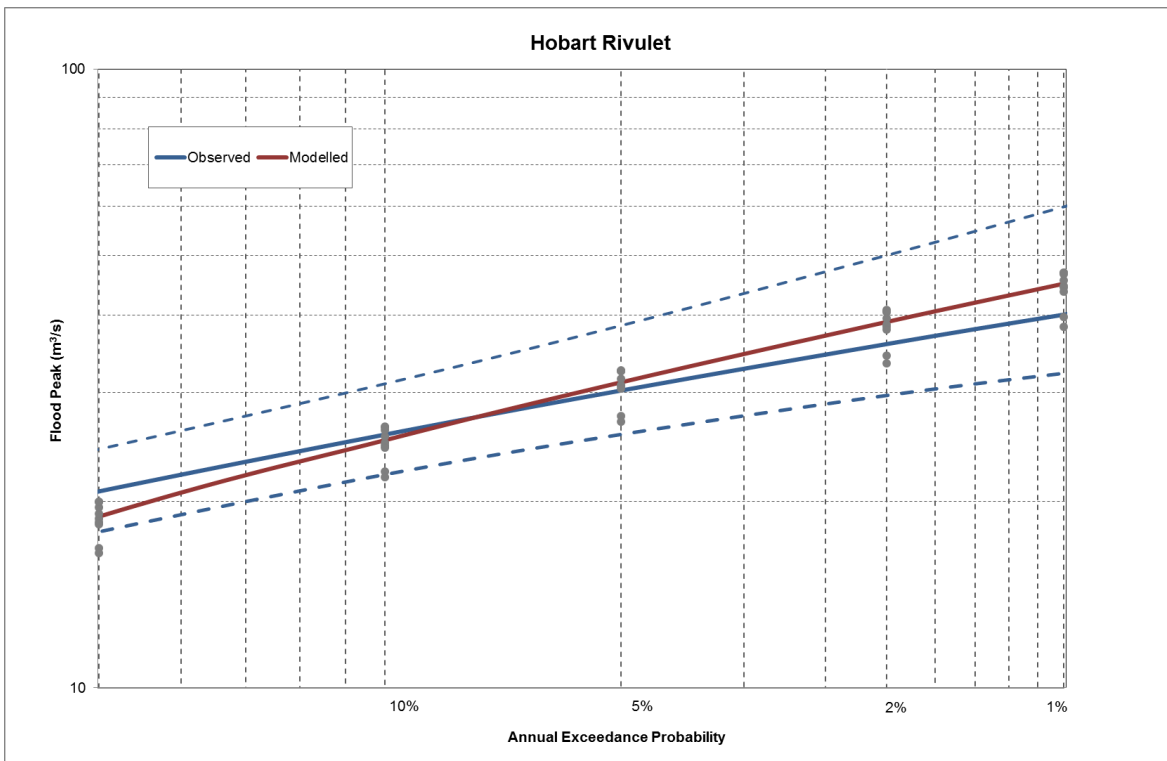


Figure 8-19: Design Event model results – Hobart Rivulet



### 8.1.10. Orara River

Table 8-11 : Orara River model results

Annual Exceedance Probability	Frequency curve fitted to observed values (m <sup>3</sup> /s)	Monte Carlo (m <sup>3</sup> /s)	Monte Carlo % difference	Design Event (m <sup>3</sup> /s)	Design Event % Difference	Critical Duration (hours)
20%	414	418	1%	425	3%	18
10%	517	529	-7%	532	3%	18
5%	718	652	-9%	649	-10%	12
2%	895	823	-8%	820	-8%	12
1%	1016	981	-3%	966	-5%	12

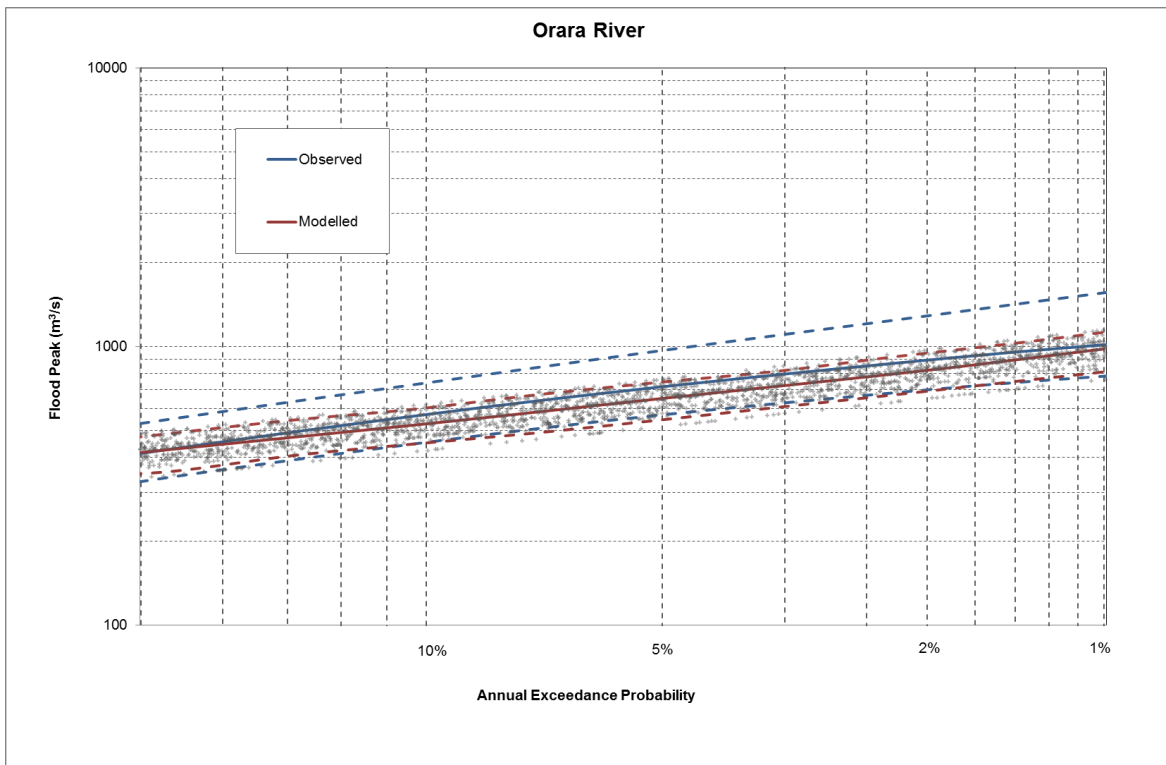


Figure 8-20 : Monte Carlo model results – Orara River

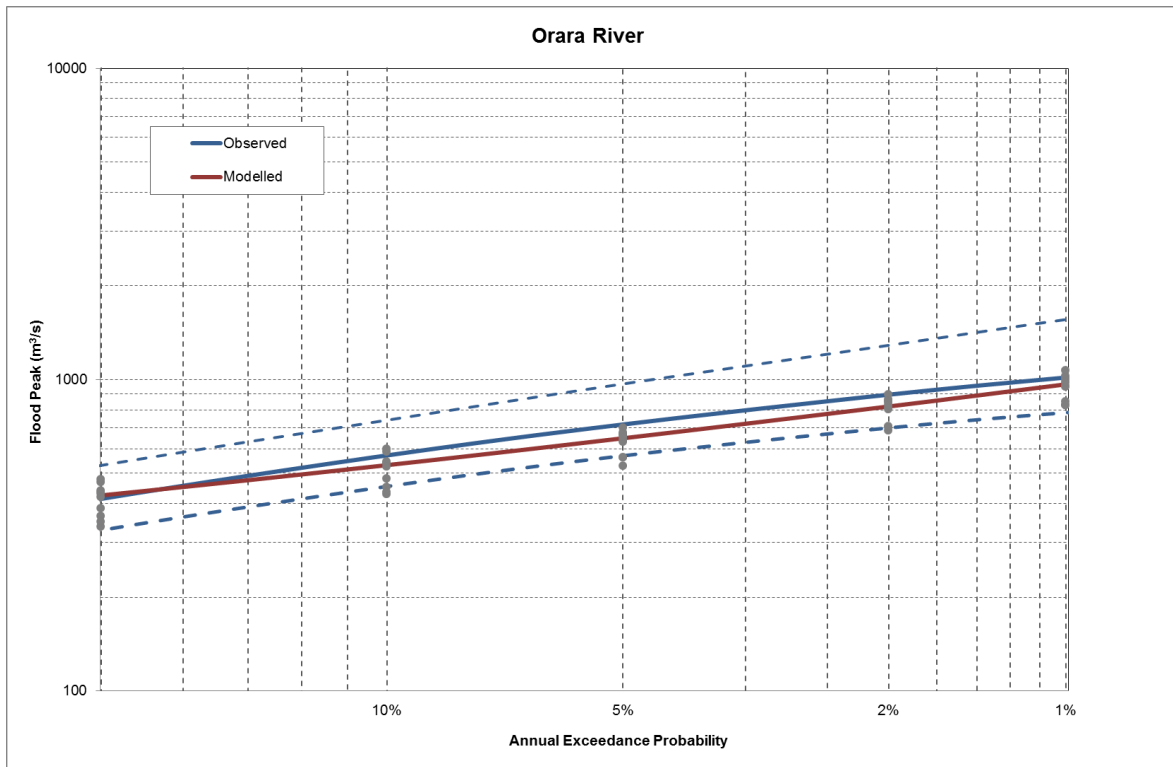


Figure 8-21: Design Event model results – Orara River

## 8.2. Sub-set of data

The results of running the Manton River and Mary River models using sub-sets of data are shown in the following sections.

### 8.2.1. Manton River

**Table 8-12: Results of Monte Carlo method**

Annual Exceedance Probability	Frequency curve fitted to observed values (m <sup>3</sup> /s)	% difference Full record	% difference Period 1	% difference Period 2
20%	73	1%	-49%	8%
10%	97	-2%	-43%	3%
5%	117	-2%	-38%	4%
2%	139	1%	-29%	6%
1%	152	6%	-21%	12%

**Table 8-13: Results of Design Event method**

Annual Exceedance Probability	Frequency curve fitted to observed values (m <sup>3</sup> /s)	% difference Full record	% difference Period 1	% difference Period 2
20%	73	-3%	-40%	11%
10%	97	-4%	-40%	3%
5%	117	-4%	-36%	2%
2%	139	2%	-31%	6%
1%	152	6%	-25%	11%

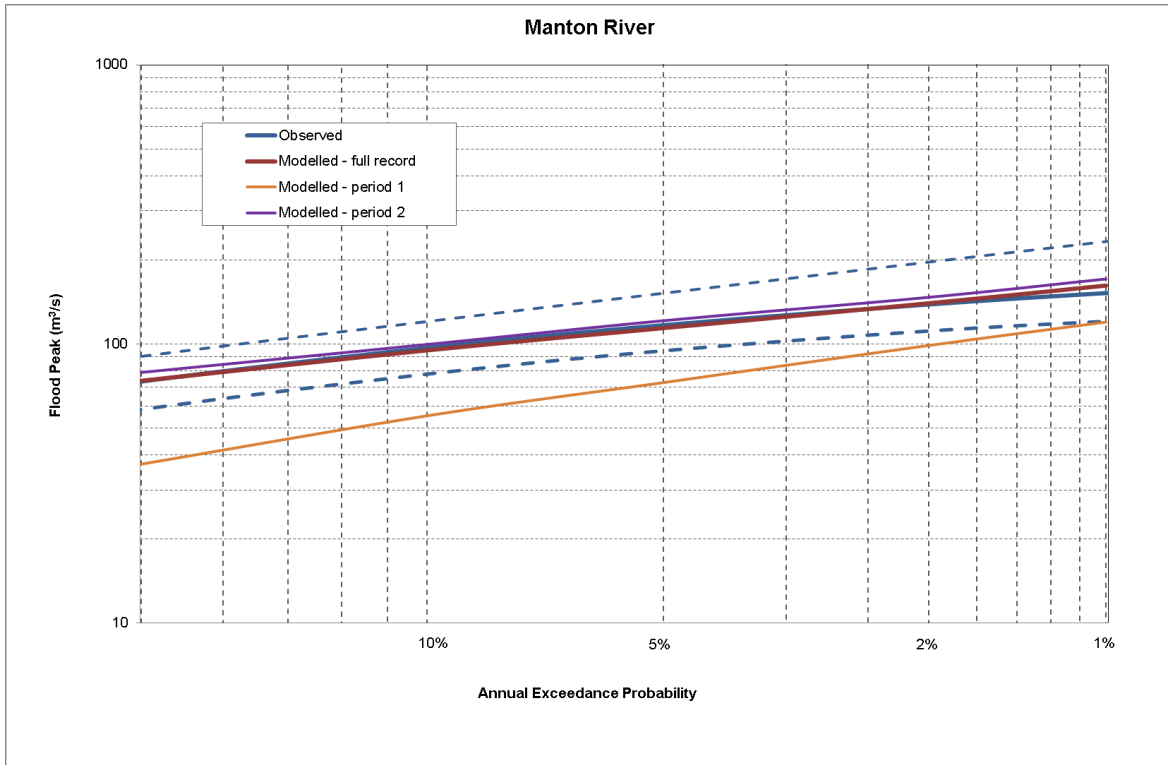


Figure 8-22: Monte Carlo model results for sub-sets of data for Manton River

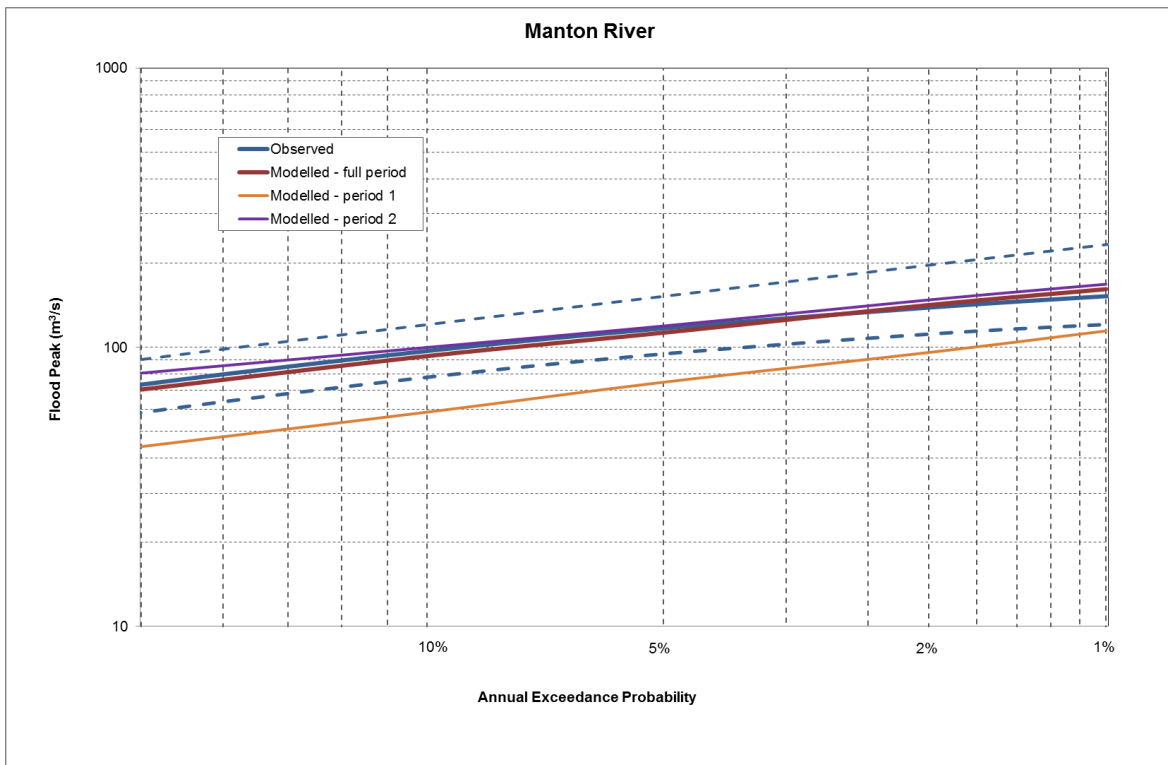


Figure 8-23: Design Event model results for sub-sets of data for Manton River

## 8.2.2. Mary River

**Table 8-14: Results of Monte Carlo method**

Annual Exceedance Probability	Frequency curve fitted to observed values (m <sup>3</sup> /s)	% difference Full record	% difference Period 1	% difference Period 2
20%	1658	15%	-9%	23%
10%	2369	5%	-15%	13%
5%	3029	2%	-14%	12%
2%	3852	6%	-10%	15%
1%	4446	10%	-5%	21%

**Table 8-15: Results of Design Event method**

Annual Exceedance Probability	Frequency curve fitted to observed values (m <sup>3</sup> /s)	% difference Full record	% difference Period 1	% difference Period 2
20%	1658	7%	-1%	-13%
10%	2369	-6%	-12%	0%
5%	3029	-10%	-15%	4%
2%	3852	-11%	-15%	2%
1%	4446	-9%	-13%	0%

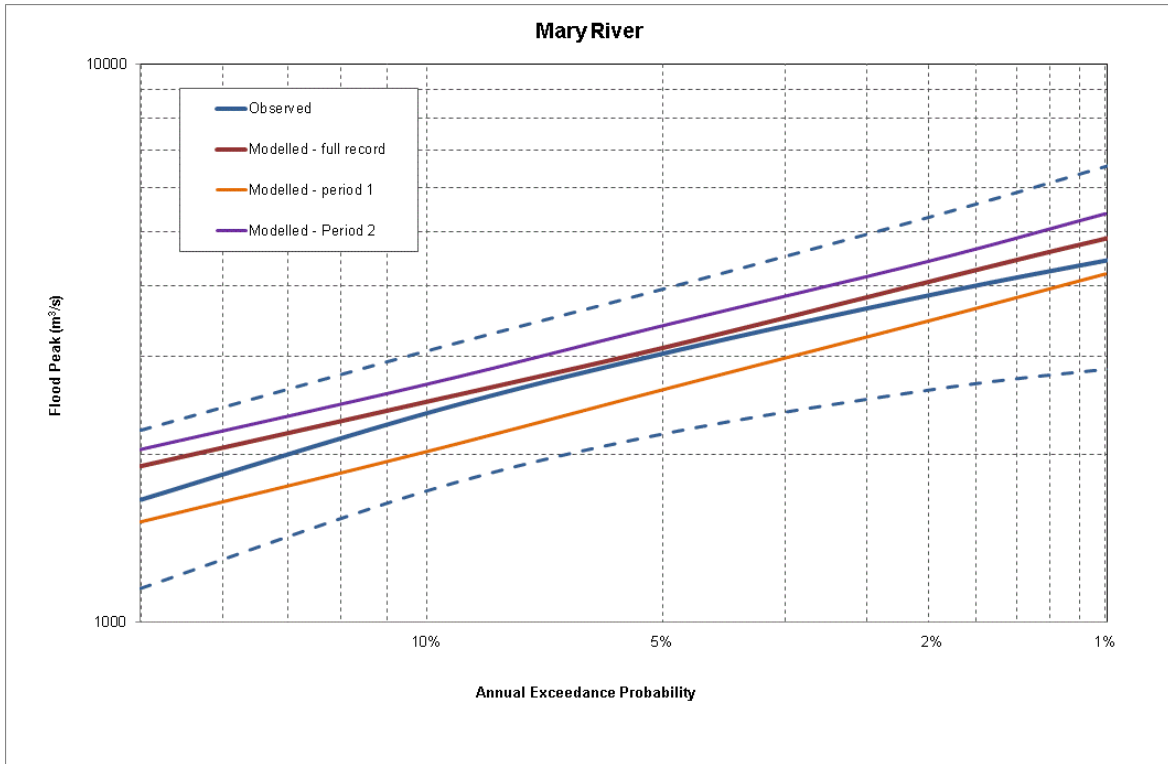


Figure 8-24: Monte Carlo model results for sub-sets of data for Mary River

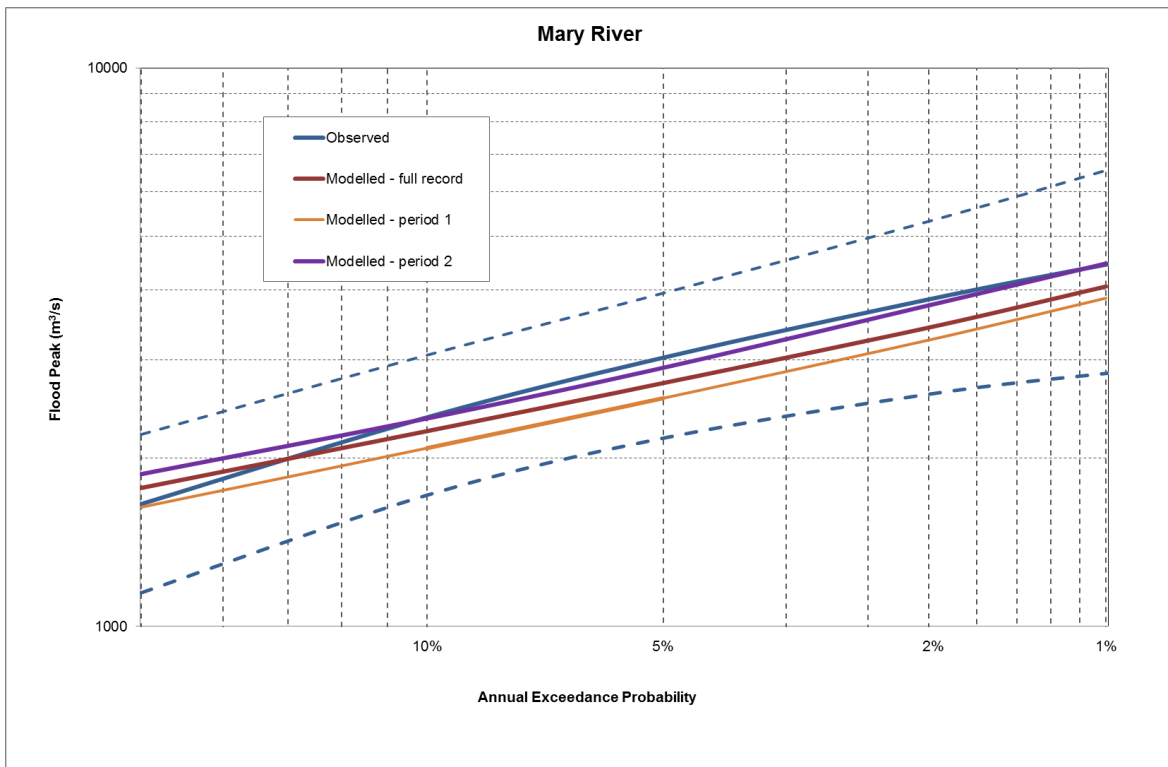


Figure 8-25: Design Event model results for sub-sets of data for Mary River

### 8.3. Results for ungauged catchments

The following tables and figures show the results of running models using parameters from another catchment model.

**Table 8-16: Tyenna River model run using parameters from Florentine River model**

Annual Exceedance Probability	Frequency curve fitted to observed values (m <sup>3</sup> /s)	Monte Carlo (m <sup>3</sup> /s)	Monte Carlo % difference	Design Event (m <sup>3</sup> /s)	Design Event % Difference
20%	74	70	-5%	70	-5%
10%	98	88	-10%	90	-8%
5%	124	109	-12%	111	-11%
2%	165	137	-17%	140	-15%
1%	201	162	-19%	164	-18%

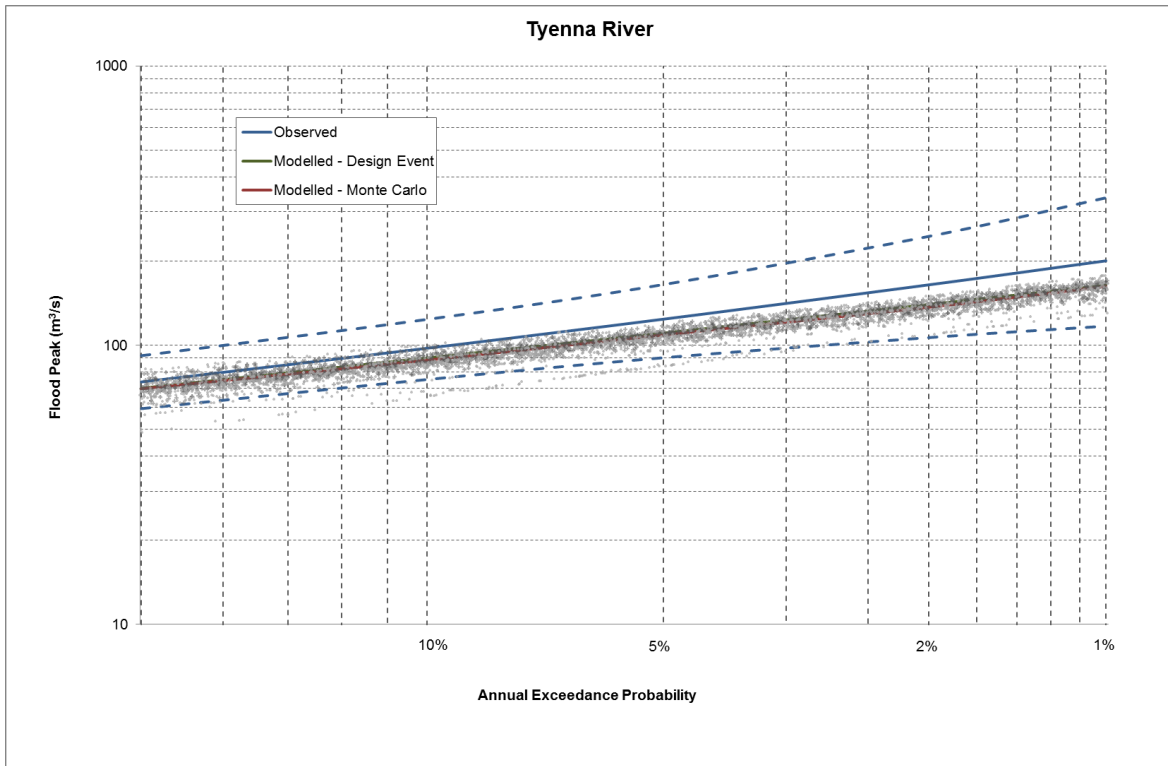


**Figure 8-26:** Tyenna River model run using parameters from Florentine River

**Table 8-17: Florentine River model run using parameters from Tyenna River model**

Annual Exceedance Probability	Frequency curve fitted to observed values (m <sup>3</sup> /s)	Monte Carlo (m <sup>3</sup> /s)	Monte Carlo % difference	Design Event (m <sup>3</sup> /s)	Design Event % Difference
20%	104	91	-13%	107	2%
10%	127	129	1%	138	9%
5%	149	169	13%	179	21%
2%	178	225	26%	239	34%
1%	201	272	36%	287	43%

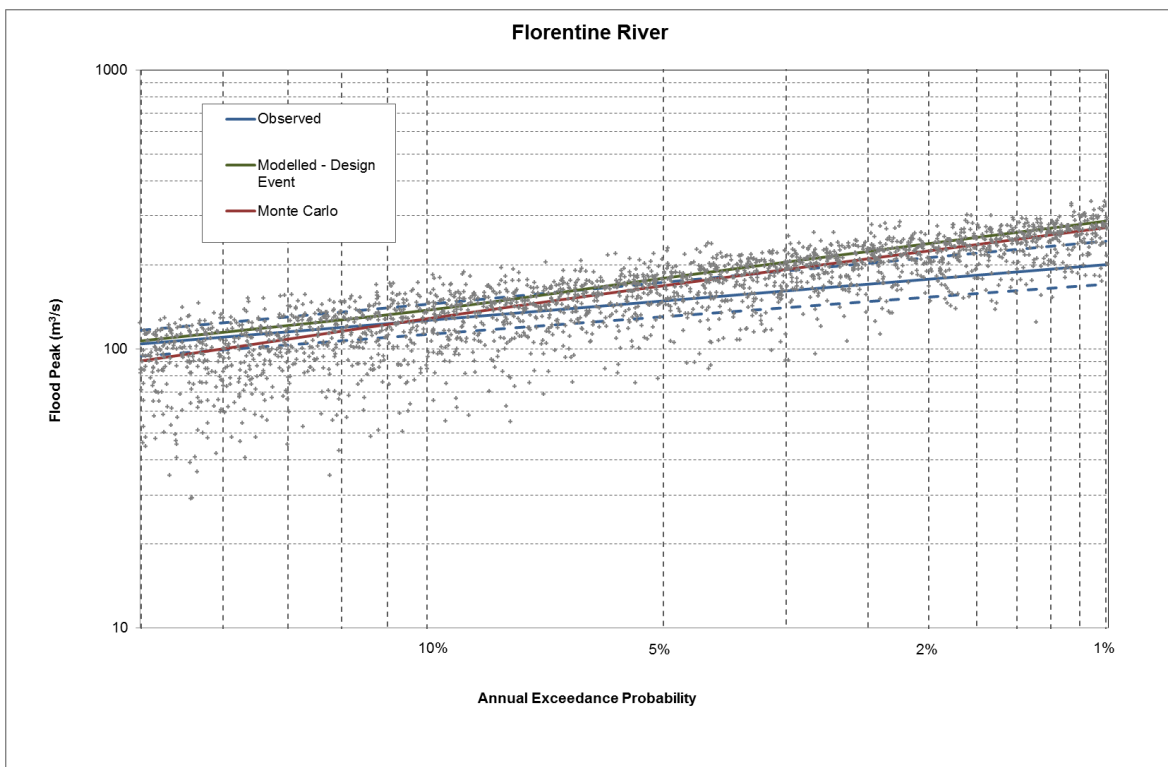


**Figure 8-27: Florentine River model run using parameters from Tyenna River model**



**Table 8-18: Tyenna River model run using parameters from Hann River model**

Annual Exceedance Probability	Frequency curve fitted to observed values (m <sup>3</sup> /s)	Monte Carlo (m <sup>3</sup> /s)	Monte Carlo % difference	Design Event (m <sup>3</sup> /s)	Design Event % Difference
20%	74	37	-50%	26	-65%
10%	98	63	-35%	49	-50%
5%	124	91	-27%	76	-39%
2%	165	134	-19%	122	-26%
1%	201	177	-12%	155	-23%

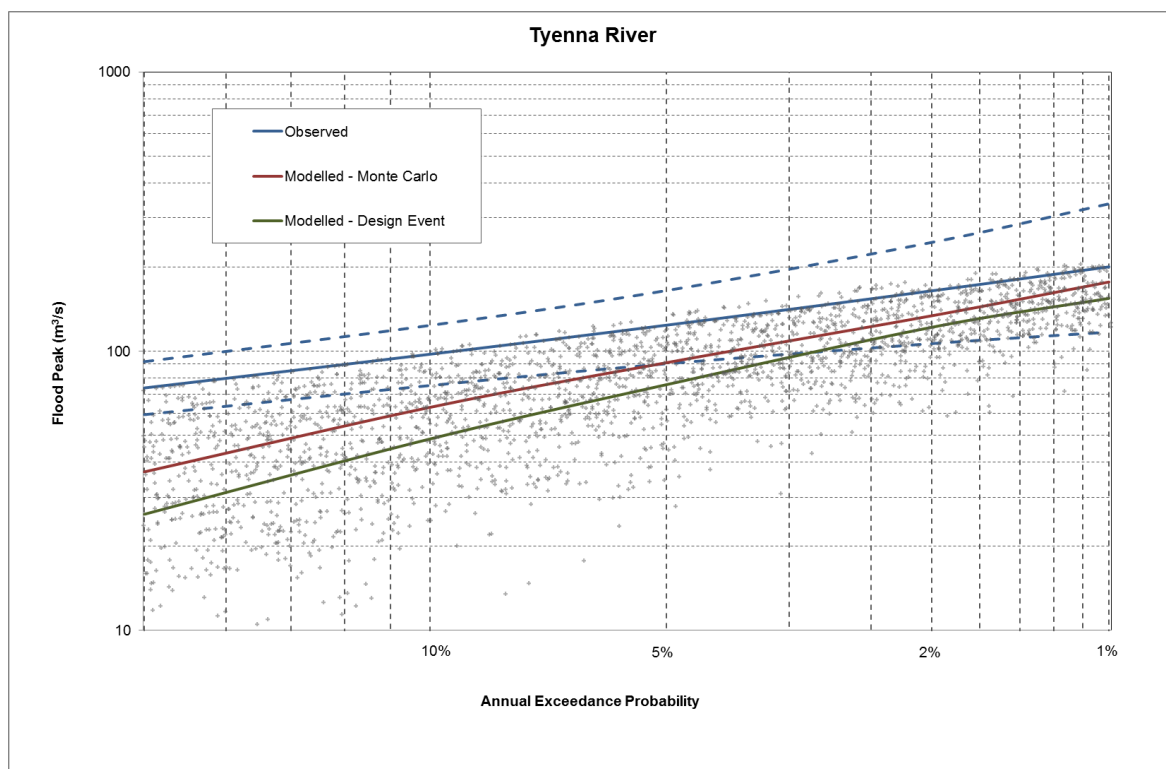


Figure 8-28: Tyenna River model run using parameters from Hann River model.

**Table 8-19: Hann River model run using parameters from Manton River model**

Annual Exceedance Probability	Frequency curve fitted to observed values (m <sup>3</sup> /s)	Monte Carlo (m <sup>3</sup> /s)	Monte Carlo % difference	Design Event (m <sup>3</sup> /s)	Design Event % Difference
20%	1807	375	-79%	884	-51%
10%	2660	567	-79%	1450	-45%
5%	3489	792	-77%	2110	-40%
2%	4515	1259	-72%	3023	-33%
1%	5225	1687	-68%	3875	-26%

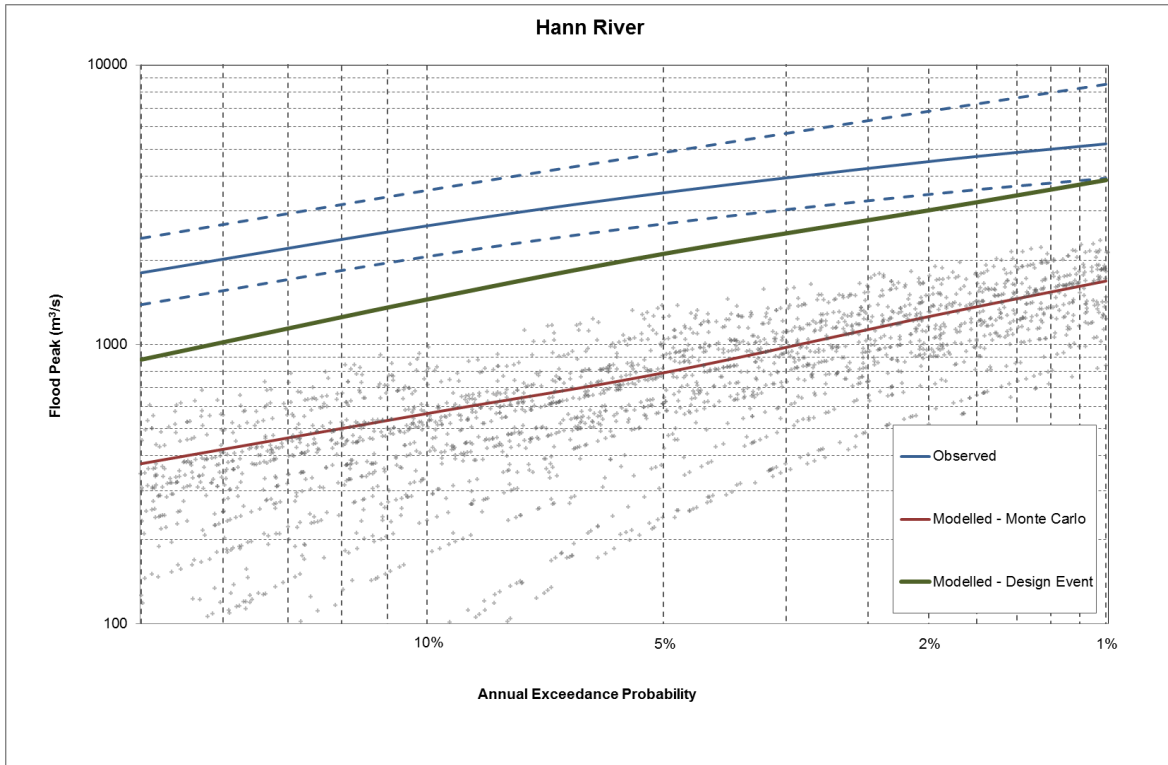


Figure 8-29: Hann River model run using parameters from Manton River model

**Table 8-20: Manton River model run using parameters from Hann River model**

Annual Exceedance Probability	Frequency curve fitted to observed values (m <sup>3</sup> /s)	Monte Carlo (m <sup>3</sup> /s)	Monte Carlo % difference	Design Event (m <sup>3</sup> /s)	Design Event % Difference
20%	73	142	93%	133	82%
10%	97	173	79%	163	68%
5%	117	205	75%	193	65%
2%	139	248	79%	227	64%
1%	152	282	85%	256	69%

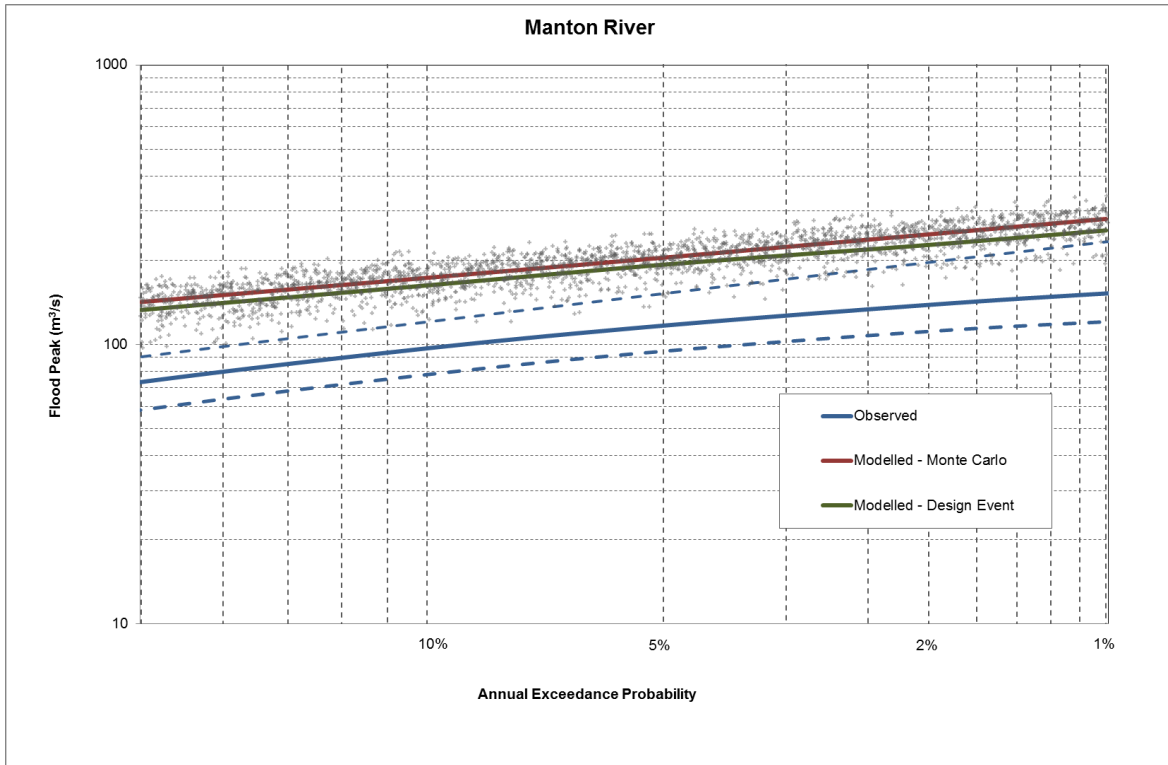


Figure 8-30: Manton River model run using parameters from Hann River model

Table 8-21: Hann River model run using parameters from Mary River model

Annual Exceedance Probability	Frequency curve fitted to observed values (m³/s)	Monte Carlo (m³/s)	Monte Carlo % difference	Design Event (m³/s)	Design Event % Difference
20%	1807	4089	126%	4113	128%
10%	2660	5213	96%	5110	92%
5%	3489	6311	81%	6132	76%
2%	4515	7886	75%	7541	67%
1%	5225	9140	75%	8668	66%

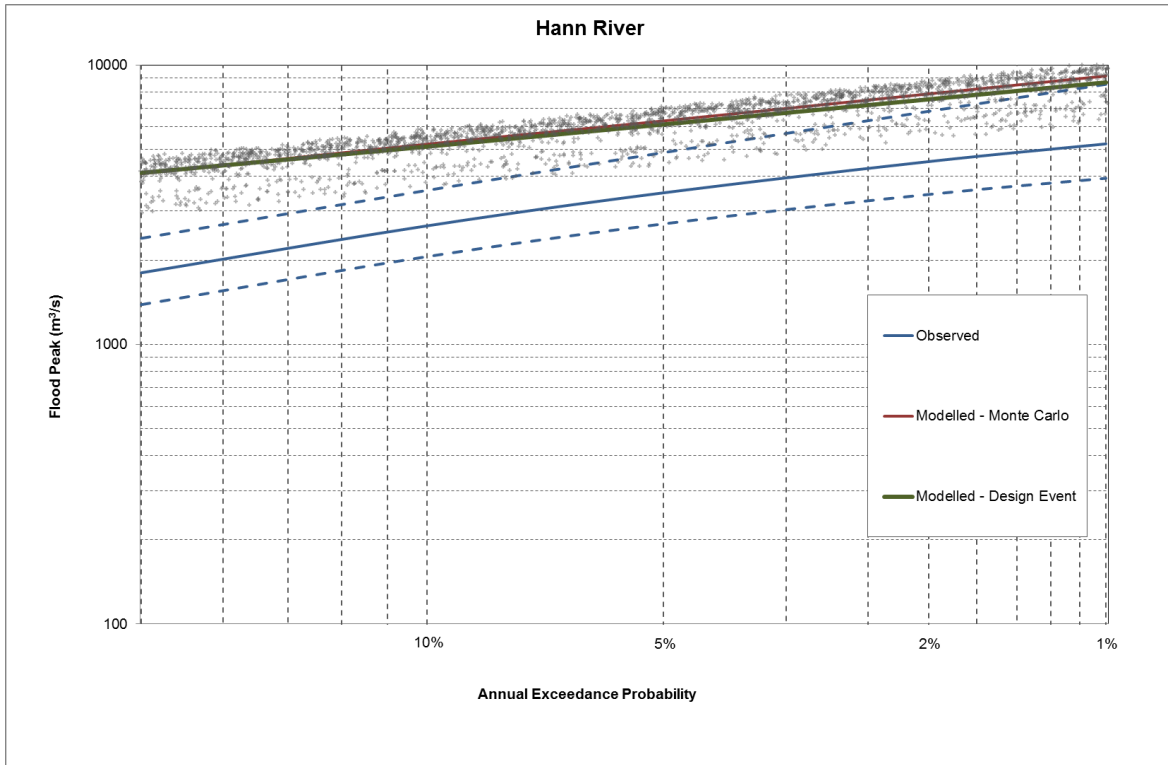


Figure 8-31: Hann River model run using parameters from Mary River model

Table 8-22: Mary River model run using parameters from Hann River model

Annual Exceedance Probability	Frequency curve fitted to observed values (m <sup>3</sup> /s)	Monte Carlo (m <sup>3</sup> /s)	Monte Carlo % difference	Design Event (m <sup>3</sup> /s)	Design Event % difference
20%	1658	1284	-23%	1018	-39%
10%	2369	1916	-19%	1496	-37%
5%	3029	2579	-15%	1997	-34%
2%	3852	3622	-6%	2834	-26%
1%	4446	4552	2%	3560	-20%

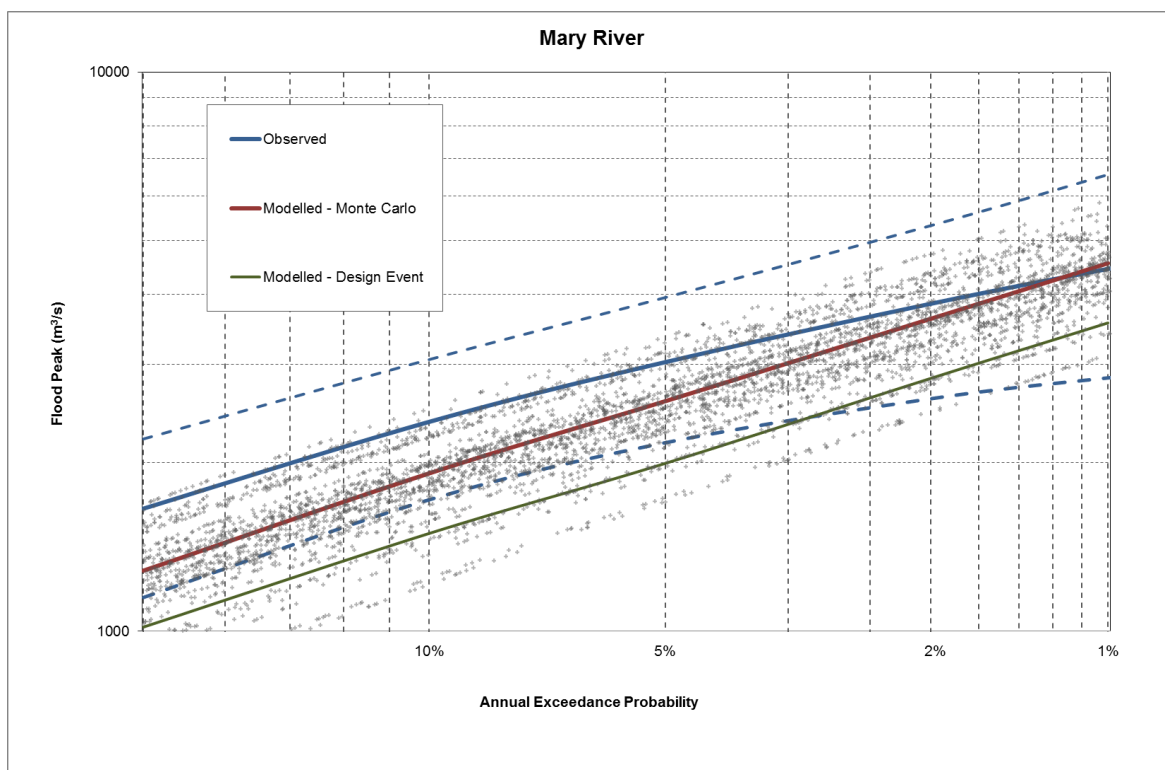


Figure 8-32: Mary River model run using parameters from Hann River model

#### 8.4. Internal gauge sites

The Mary River catchment was used to investigate the model performance at internal gauge sites. There were three internal streamflow gauges within the Mary River catchment. The results from the model were extracted at these gauge sites to investigate estimation of the flood frequency curve at internal gauges in the catchment, when the model has been calibrated to a downstream site.

The catchment areas and record lengths of the Mary River catchment gauges are shown in **Table 8-23**. All gauges have at least 40 years of records over differing periods.

**Table 8-23: Mary River catchment gauge sites**

Gauge Site	Catchment area (km <sup>2</sup> )	Start date	End date
Moy Pocket	820	1964	2014
Kenilworth	720	1921	1972
Bellbird Creek	486	1960	2004
Obi-Obi Creek at Kidaman	174	1921	1963

The results are shown in Table 8-24 to Table 8-26 and Figure 8-33 to Figure 8-35.

**Table 8-24: Kenilworth gauge site results**

Annual Exceedance Probability	Frequency curve fitted to observed values (m <sup>3</sup> /s)	Monte Carlo (m <sup>3</sup> /s)	Monte Carlo % difference	Design Event (m <sup>3</sup> /s)	Design Event % Difference
20%	1307	1872	43%	1679	28%
10%	1608	2452	52%	2110	31%
5%	1872	3060	63%	2594	39%
2%	2183	3952	81%	3333	53%
1%	2394	4784	100%	3936	64%

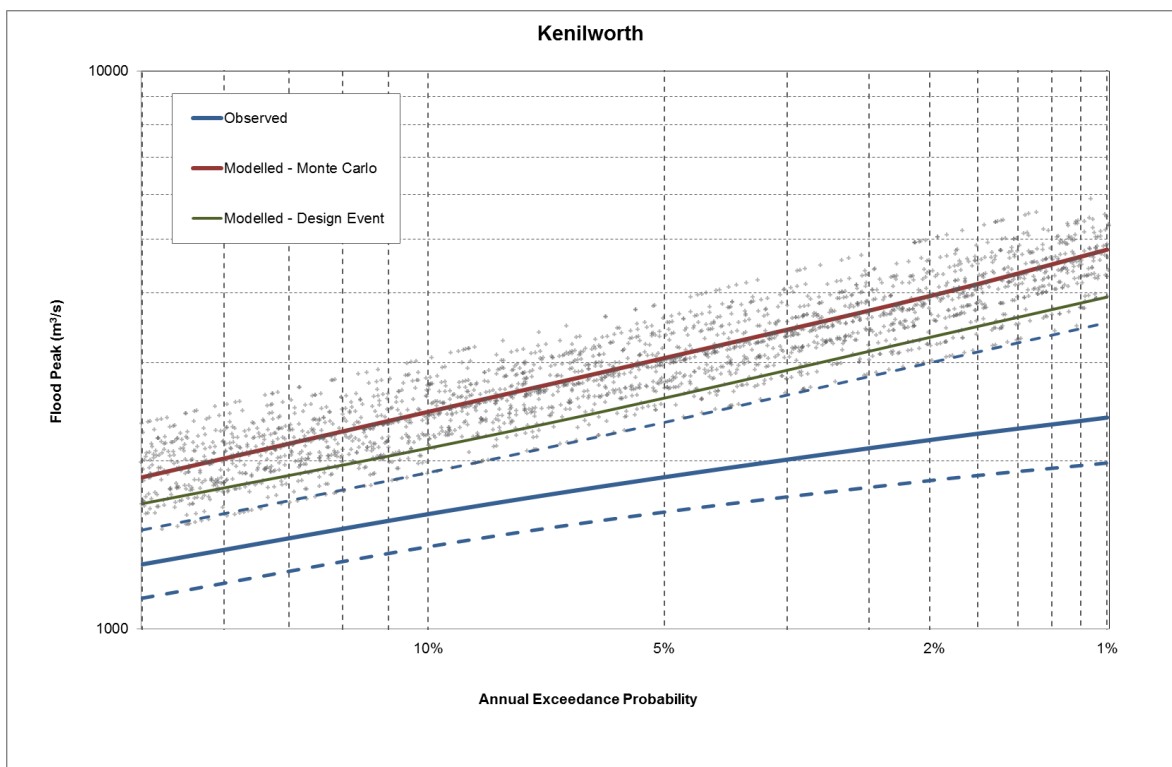


Figure 8-33: Kenilworth gauge site results

**Table 8-25: Bellbird Creek gauge site results**

Annual Exceedance Probability	Frequency curve fitted to observed values (m <sup>3</sup> /s)	Monte Carlo (m <sup>3</sup> /s)	Monte Carlo % difference	Design Event (m <sup>3</sup> /s)	Design Event % Difference
20%	1076	1317	22%	1183	10%
10%	1673	1708	2%	1485	-11%
5%	2309	2136	-8%	1817	-21%
2%	3180	2773	-13%	2313	-27%
1%	3843	3368	-12%	2731	-29%

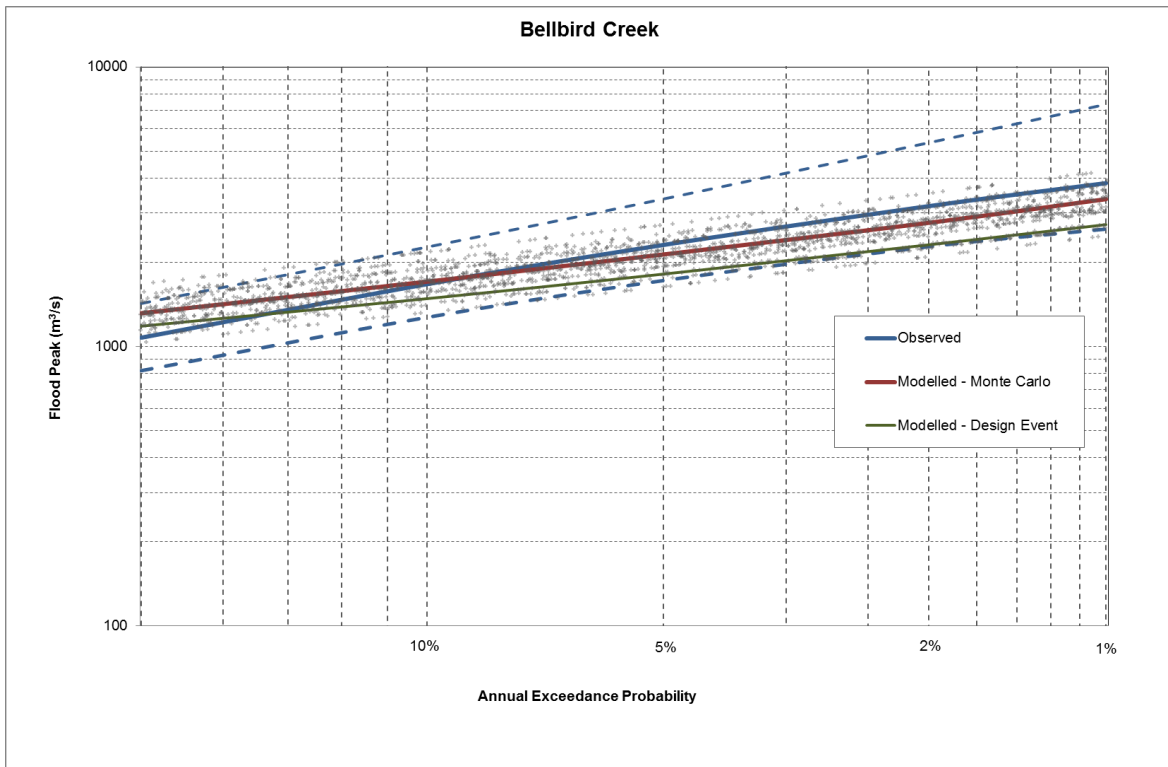


Figure 8-34: Bellbird Creek gauge site results

Table 8-26: Obi-Obi Creek at Kidaman gauge site results

Annual Exceedance Probability	Frequency curve fitted to observed values (m <sup>3</sup> /s)	Monte Carlo (m <sup>3</sup> /s)	Monte Carlo % difference	Design Event (m <sup>3</sup> /s)	Design Event % Difference
20%	616	541	-12%	485	-21%
10%	768	699	-9%	607	-21%
5%	895	872	-3%	733	-18%
2%	1033	1134	10%	929	-10%
1%	1119	1338	20%	1096	-2%

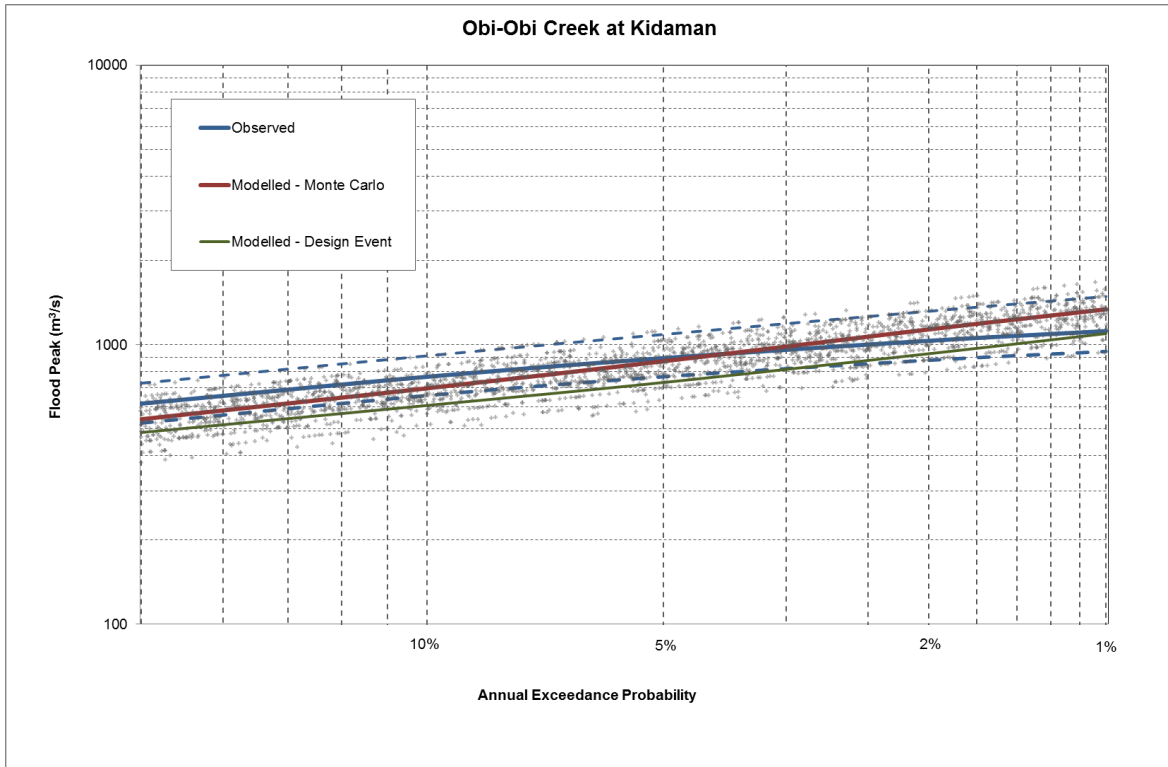


Figure 8-35: Obi-Obi Creek at Kidaman gauge site results



## 9. Continuous Simulation Model Results

The calibrations were generally terminated at pre-defined number of SCE generations (or iterations). For scenarios 1, 2 and 3 this varied from 100 to 150. The calibration was deemed to have converged to a global optimum when the objective function value did not improve over the last 10 generations. The calibration to the observed flood frequency curve (scenario 4) converged much faster, resulting in stable values of the objective function in less than 100 iterations. In general, calibration to scenario 4 required about 3,000 function evaluations to converge, compared to more than 9,000 to 15,000 function evaluations for others.

In general the time required for calibrations ranged from 30 hours (for calibration in Manton River) to 202 hours (for Mary River) for scenarios 1 and 3. Scenario 2 took about the half of that required for scenarios 1 and 3.

### 9.1. Scenario 1

The NSE and the volume biases calculated for each catchment and model under scenario 1 is shown in Table 9-1. The model to data fit as measured by NSE is higher than 0.6 in all the catchments. The NSE is highest in Mary River catchment with 0.82 and lowest in Manton. Among the four models tested GR4H, shows the highest NSE values in all the catchments and lowest volume bias in Manton River, Sixth Creek and in Florentine.

**Table 9-1: NSE values calculated for Scenario 1**

Model	Measure	Catchments				
		Manton River	Sixth Creek	Mary River	Florentine River	Yates Flat River
AWBM	NSE	0.62	0.66	0.80	0.73	0.73
SIMHYD	NSE	0.62	0.60	0.80	0.74	0.67
GR4H	NSE	0.68	0.74	0.82	0.73	0.77
AWBM	Volume bias (%)	12	24	11	27	-21
SIMHYD	Volume bias (%)	17.0	15.5	9.5	30.0	-13
GR4H	Volume bias (%)	-3.5	5.0	-14.3	-7.5	-33

#### 9.1.1. Comparison of hydrograph behaviour

While NSE values greater than 0.6 are generally considered “acceptable” in hydrological literature, the comparison of hydrographs and flow duration curves (Appendix J, Figure J. 1 to Figure J. 24) and scatter plots (Figure 9-1) in all catchments except Mary River, shows that all the model simulations underestimate the peaks. Similarly, as expected (possibly due to the use of objective function that is more sensitive to the high flow magnitudes), the simulated hydrographs also provide poor representation of the low flows. Among the three models GR4H provides a better representation of low flows, high flows as well as the observed flow volume in

all the catchments. Similarly, the scatter around the 1:1 line (Figure 9-1), is not completely random and suggests presence of systematic error, possibly due to error in timing in all the models.

### 9.1.2. Comparison of the event volumes

The ability of the calibrated model to reproduce large flood event volumes were, analysed for 10 largest flood events (Table P. 1, Appendix P) extracted from the annual maximum series. The differences in flood volumes of these 10 events are shown in Table 9-2.

In general, the table shows that the calibrated models do not seem to be able to reproduce the observed flood volumes for many cases. The % difference (positive corresponds to underestimation of the volume by the model) between the observed and simulated is greater than 50%, in 24 out of the total of 150 (from 3 models 10 events and 5 catchments) of the events simulated.

The number of events showing volume differences more than 25 % is highest in Yates Flat Creek. The number of events showing volume difference greater than 25% is least in Mary (21 out of 30 events). While all the three models do not consistently preserve the event volumes, GR4H provides the best overall performance among the three.

**Table 9-2: Volume differences (%) calculated for 10 largest events** [colour codes: red for volume bias greater than 50%, orange for values between 50% and 25 %, and green for values equal to and less than 25 %, AW = AWBM, SI = SIMHYD, GR = GR4H]

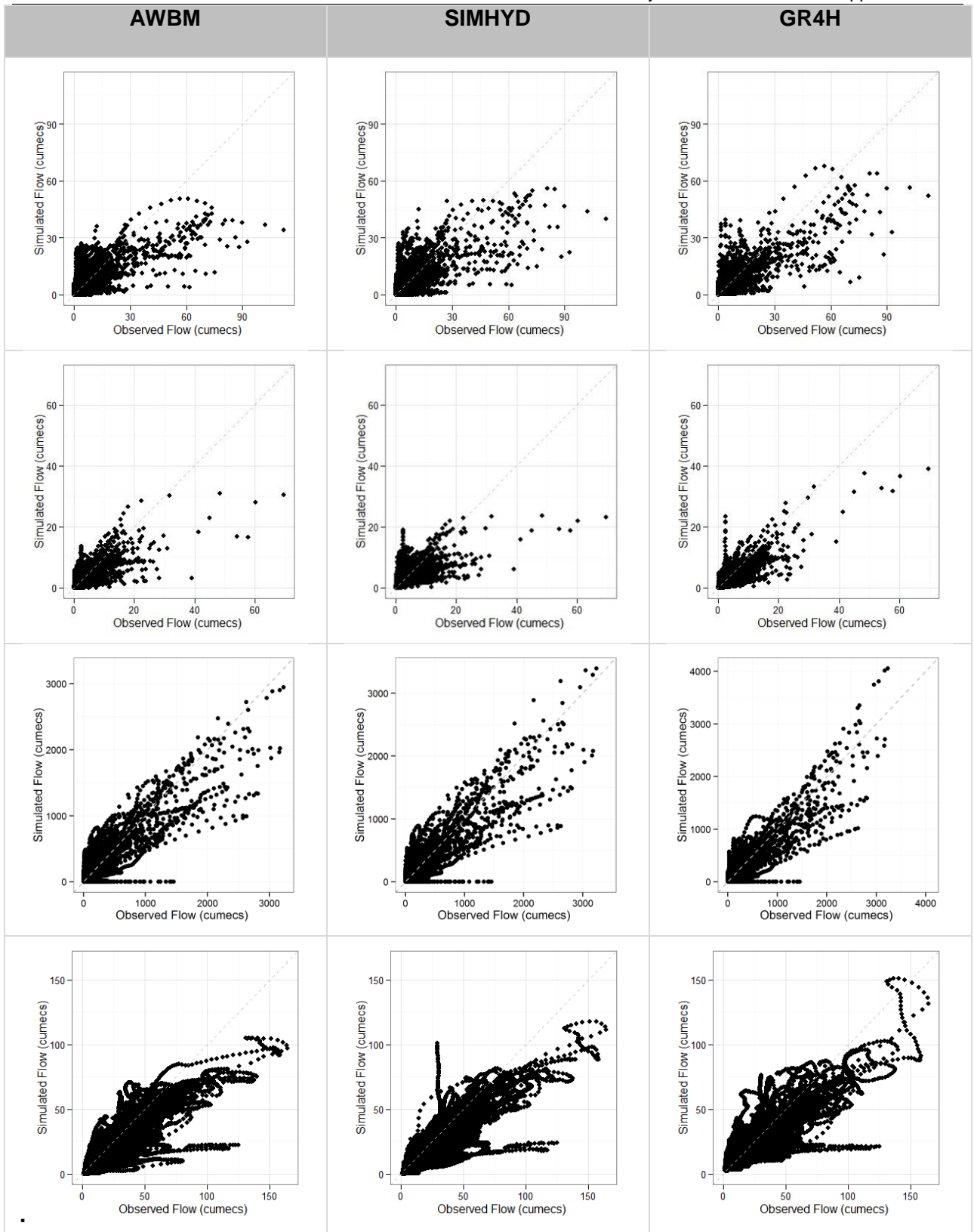
Events	Manton			Sixth creek			Mary			Florentine			Yates Flats		
	AW	SI	GR	AW	SI	GR	AW	SI	GR	AW	SI	GR	AW	SI	GR
1	13	25	18	-21	-10	-14	60	64	64	72	72	71	21	26	15
2	71	70	38	64	33	7	-6	-9	-8	22	29	20	66	50	31
3	4	-11	13	8	30	5	4	-1	-1	29	25	33	15	44	29
4	29	40	11	48	52	51	10	15	16	-5	18	-8	49	46	30
5	-4	11	16	32	36	24	-4	-9	3	20	20	24	24	7	41
6	5	-6	8	68	78	69	36	45	48	33	31	34	50	64	44
7	55	54	60	25	32	26	-6	-10	-3	29	27	27	16	42	18
8	36	31	41	5	22	20	12	11	8	11	7	13	29	54	41
9	25	33	23	26	12	39	12	21	11	21	20	20	-9	-26	-29
10	18	30	34	36	50	35	41	39	39	26	23	26	-84	-116	-39

### 9.1.3. Comparison of flood frequency curves

The comparison of the observed and fitted flood frequency curves for scenario 1 (Figure 9-2 to Figure 9-6 and Table 9-3) shows that, except in Mary River, the simulated flood frequency curves generally provide a poor fit to the observed flood frequency curve.

**Table 9-3: % Difference (observed – simulated) in flood quantiles for scenario 1** [colour codes: red for values greater than 30%, orange for values between 30% and 10 %, and green for values equal to and less than 10 %]

Catchment	Model	Annual Exceedance Probability					
		1%	2%	5%	10%	20%	50%
Manton	AWBM	62	62	62	62	61	60
	SIMHYD	50	52	54	56	58	59
	GR4H	31	35	40	43	45	44
Sixth Creek	AWBM	57	56	54	53	51	48
	SIMHYD	59	59	58	57	57	55
	GR4H	25	28	32	36	40	47
Mary	AWBM	23	23	22	22	21	16
	SIMHYD	11	13	17	19	21	21
	GR4H	1	4	8	11	12	12
Florentine	AWBM	48	46	42	38	34	24
	SIMHYD	37	35	33	31	29	23
	GR4H	27	26	25	23	21	17
Yates Flat	AWBM	48	49	50	50	48	39
	SIMHYD	36	44	51	56	58	57
	GR4H	16	25	34	39	42	39



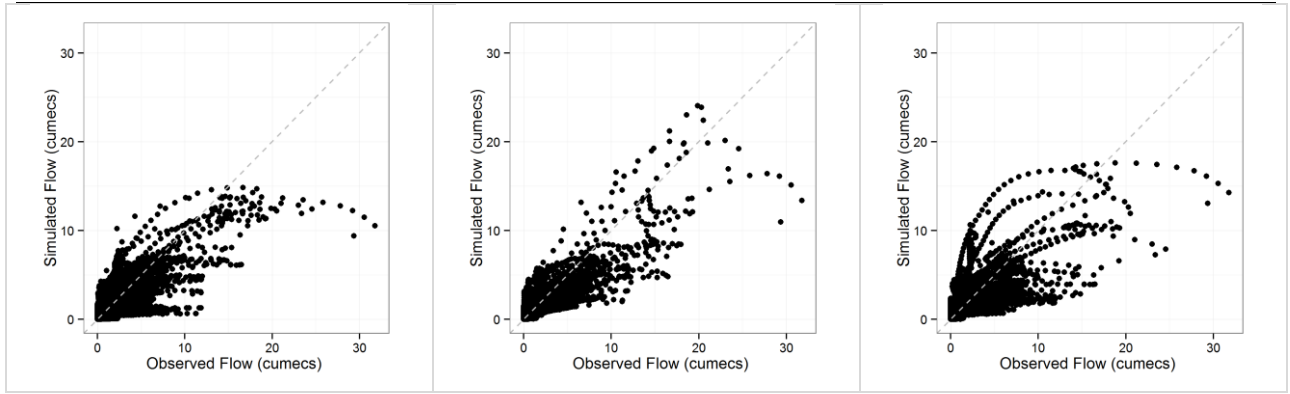


Figure 9-1 : Comparison of the observed and simulated flows [Rows: 1. Manton River, 2. Sixth Creek, 3. Mary River, 4. Florentine River, 5 Yates Flat Creek]

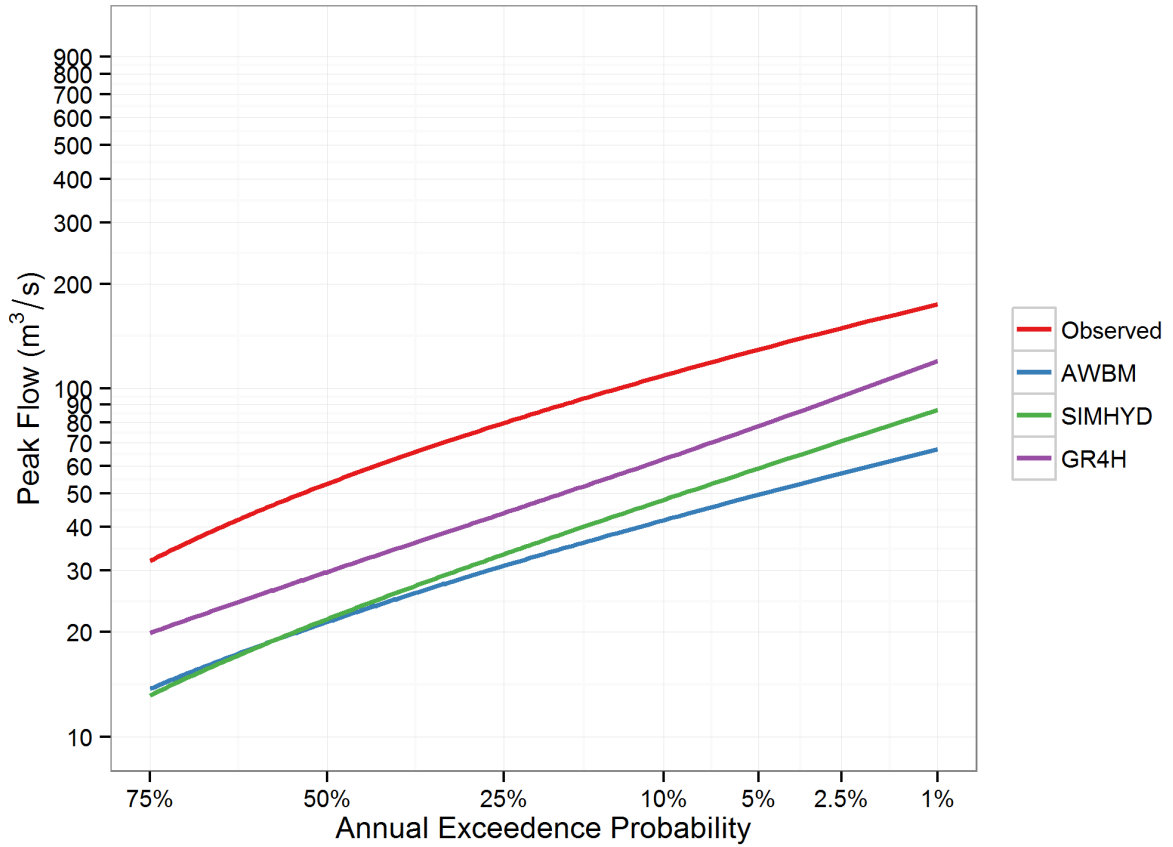


Figure 9-2: Comparison of the flood frequency curves in Manton River [distribution – GEV]

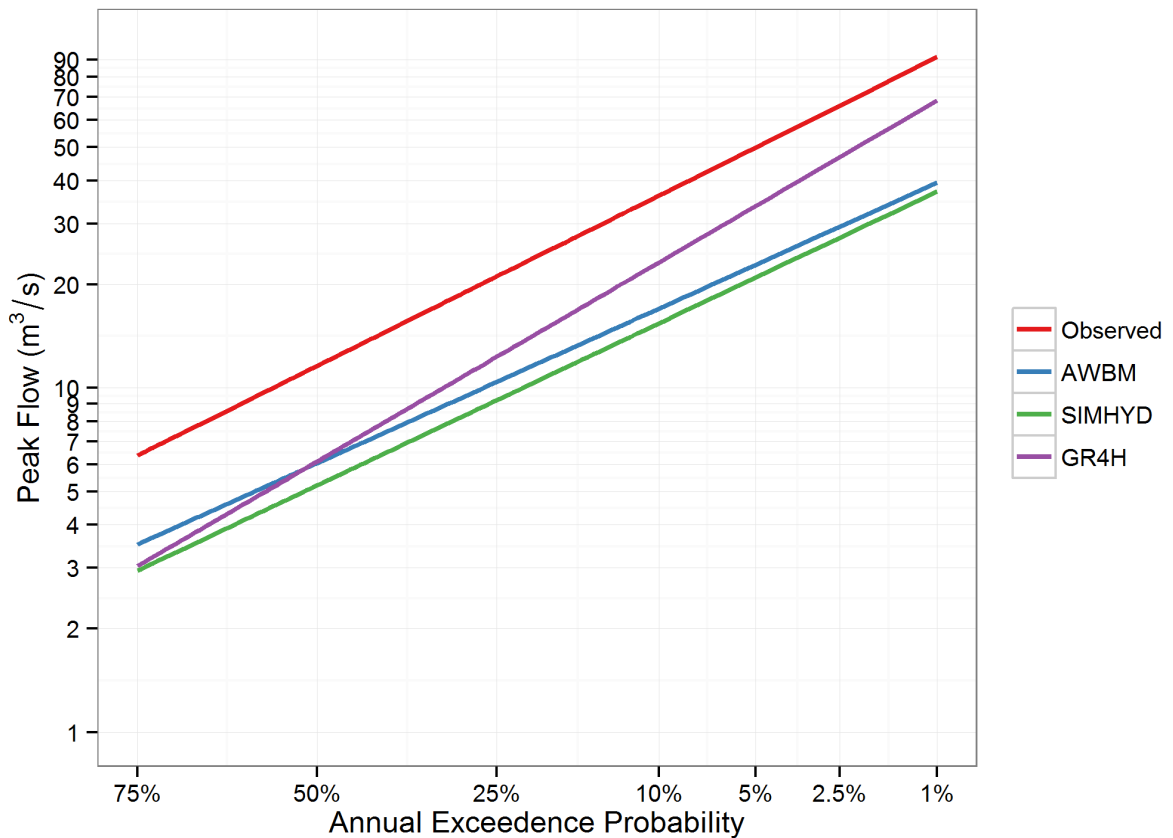


Figure 9-3: Comparison of the flood frequency curves in Sixth Creek [Log normal]

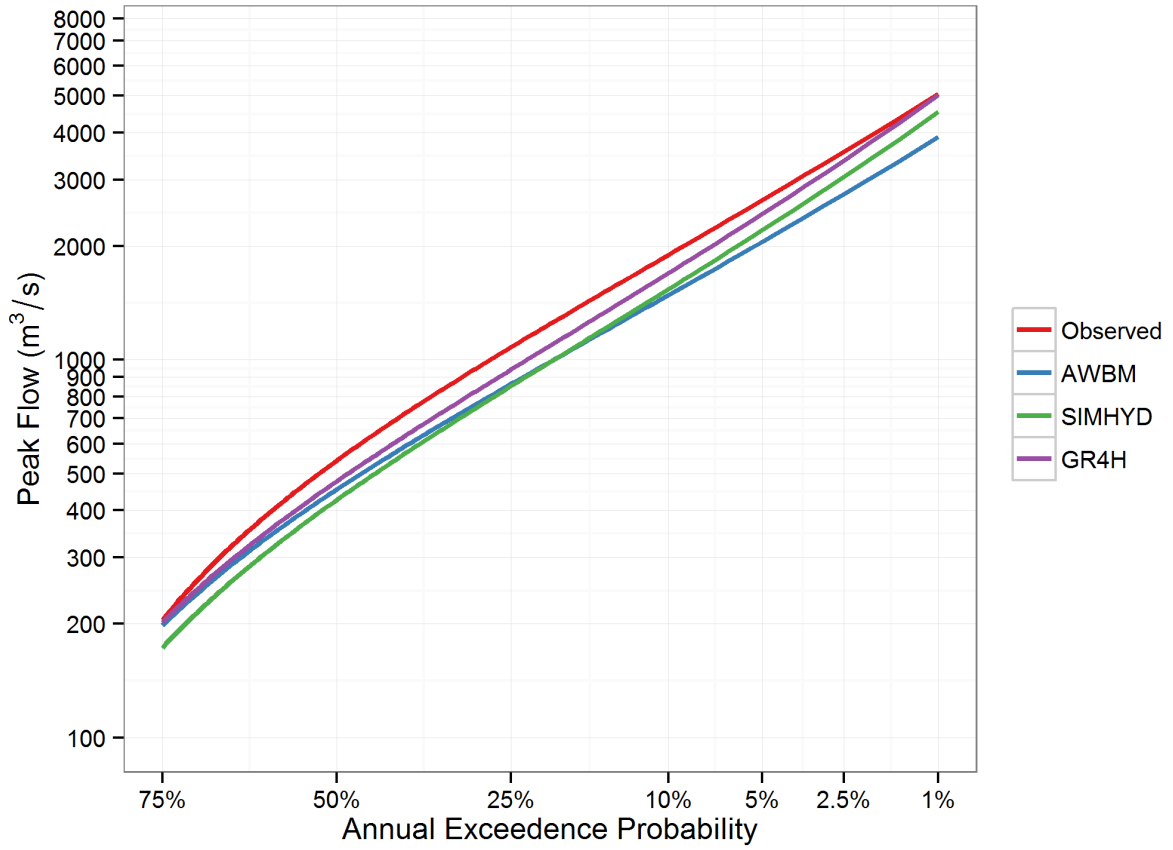


Figure 9-4: Comparison of the flood frequency curves in Mary River [distribution – GEV]

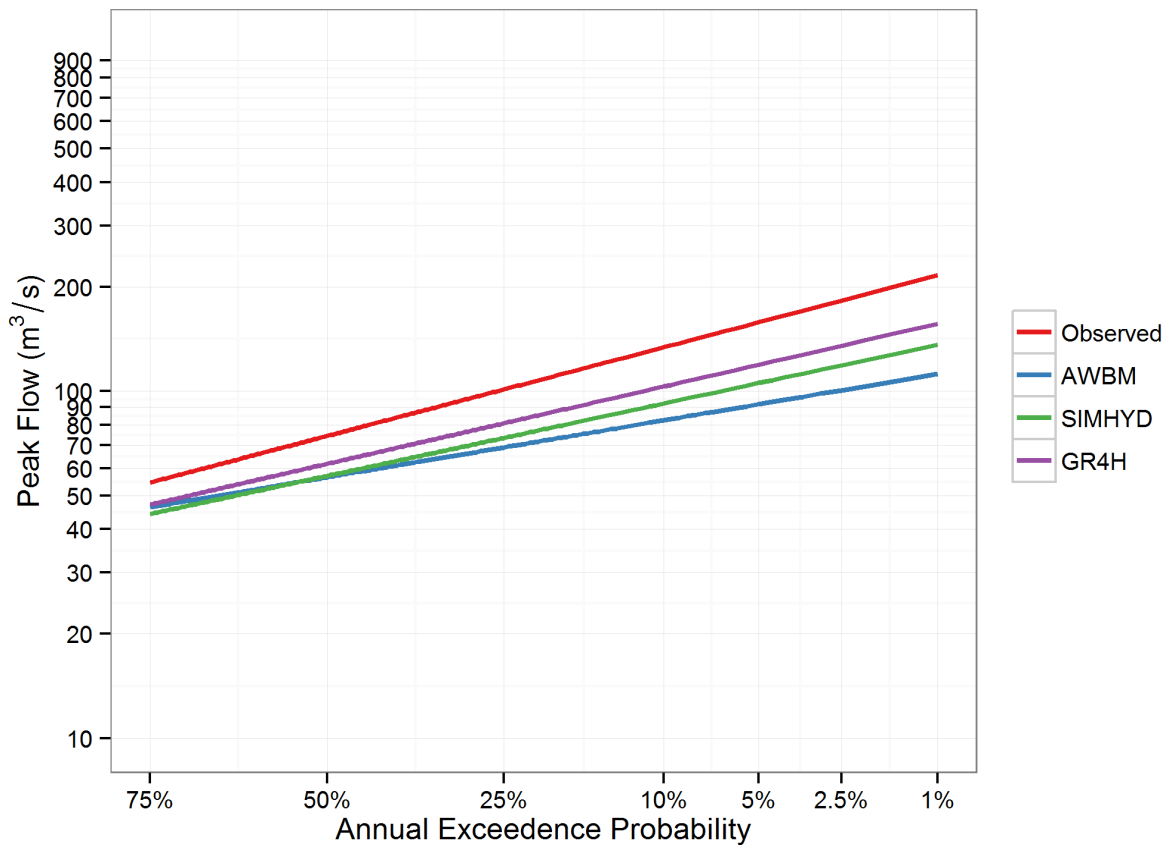


Figure 9-5: Comparison of flood frequency curves in Florentine River [Log normal]

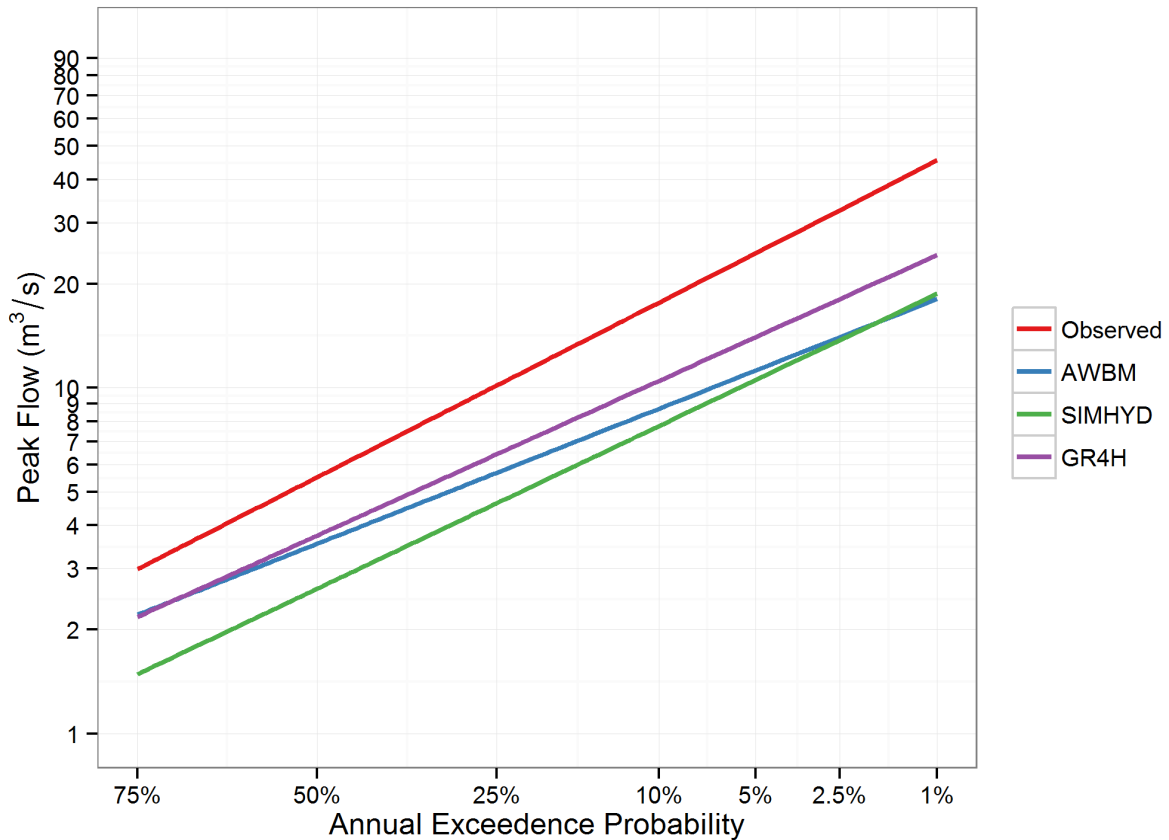


Figure 9-6: Comparison of the flood frequency curves in Yates Flat Creek [distribution – Log normal]

## 9.2. Scenario 2

The NSE and the volume biases calculated for each catchment and model under Scenario 2 is shown in Table 9-4 . In this case the model was calibrated to half of the available data and the parameters obtained from the calibration were used to simulate the flow for the whole period. The NSE values and the volume biases were calculated using the simulated flow for the whole period.

In general, calibrations of the model to shorter time period do not seem to have a large impact in terms of NSE or the volume bias. In most cases the length of data is still significant enough for the identification of the parameters.

**Table 9-4: NSE and volume bias values calculated for Scenario 2**

Model	Measure	Catchments			
		Manton River	Sixth Creek	Mary	Florentine
AWBM	NSE	0.61	0.66	0.80	0.72
SIMHYD	NSE	0.61	0.60	0.80	0.73
GR4H	NSE	0.67	0.74	0.82	0.72
AWBM	Volume bias (%)	19.0	23.0	7.2	20.0
SIMHYD	Volume bias (%)	23.0	7.2	12.7	30.0
GR4H	Volume bias (%)	13.0	-5.0	-14.0	-7.5



### 9.2.1. Comparison of hydrograph behaviour

In general, the hydrographs and flow duration curves (Figure K. 1 to Figure K. 24) and the scatter plots (Figure 9-7) are similar to Scenario 1. The hydrographs and the flow duration curves of the simulated flow generated using Scenario 2 does not show large and consistent changes in behaviour/pattern compared to Scenario 1.

### 9.2.2. Comparison of event volumes

The event volume differences (Table 9-5) for the ten largest events were similar to that generated using the model calibrated using all available record (Scenario 1).

**Table 9-5: Volume differences (%) calculated for 10 largest events** [colour codes: red for volume bias greater than 50%, orange for values between 50% and 25 %, and green for values equal to and less than 25 %, AW = AWBM, SI = SIMHYD, GR = GR4H]

Events	Manton			Sixth Creek			Mary			Florentine		
	AWB	SIM	GR4	AWB	SIM	GR4	AWB	SIM	GR4	AWB	SIM	GR4
1	17	30	28	-36	-3	-21	58	59	64	72	72	71
2	70	68	46	61	21	-2	-9	-9	-8	27	19	22
3	1	-2	22	1	22	-3	2	1	0	36	24	34
4	36	41	23	42	58	47	6	21	15	6	-11	-5
5	-7	28	25	25	44	20	-6	-9	3	27	14	25
6	4	9	19	66	75	67	34	37	46	38	30	36
7	55	63	65	18	30	21	-9	-10	-2	36	24	29
8	35	46	47	-5	42	16	10	11	8	17	6	14
9	32	39	31	20	28	37	9	18	11	27	17	21
10	15	42	41	34	48	29	39	39	40	33	22	28

### 9.2.3. Comparison of flood frequency curves

In this case, the observed flood frequency curves were calculated using the data available for the whole period however the simulated flood frequency curves were calculated using the shorter length of the data. The comparison of the observed and fitted flood frequency curves for Scenario 2 (Figure 9-8 to Figure 9-11), do not show consistent degradation or improvements in reproducing the observed flood frequency curve compared to Scenario 1. As in Scenario 1, except for Mary River, the simulated flood frequency curves provide a poor fit to the observed flood frequency curve.

**Table 9-6 : % Difference (observed – simulated) in flood quantiles for scenario 2** [colour codes: red for values greater than 30%, orange for values between 30% and 10 %, and green for values equal to and less than 10 %]

Catchment	Models	Annual Exceedance Probability					
		1%	2%	5%	10%	20%	50%
Manton	AWBM	62	62	62	61	61	61
	SIMHYD	44	50	57	61	64	67
	GR4H	35	38	43	45	48	49
Sixth Creek	AWBM	59	58	56	55	53	49
	SIMHYD	72	71	69	67	65	60
	GR4H	16	20	26	30	35	44
Mary	AWBM	14	9	2	-4	-10	-23
	SIMHYD	9	5	-1	-6	-11	-19
	GR4H	-9	-10	-12	-13	-16	-23
Florentine	AWBM	58	55	52	48	44	35
	SIMHYD	46	44	40	37	33	23
	GR4H	42	40	38	35	32	26

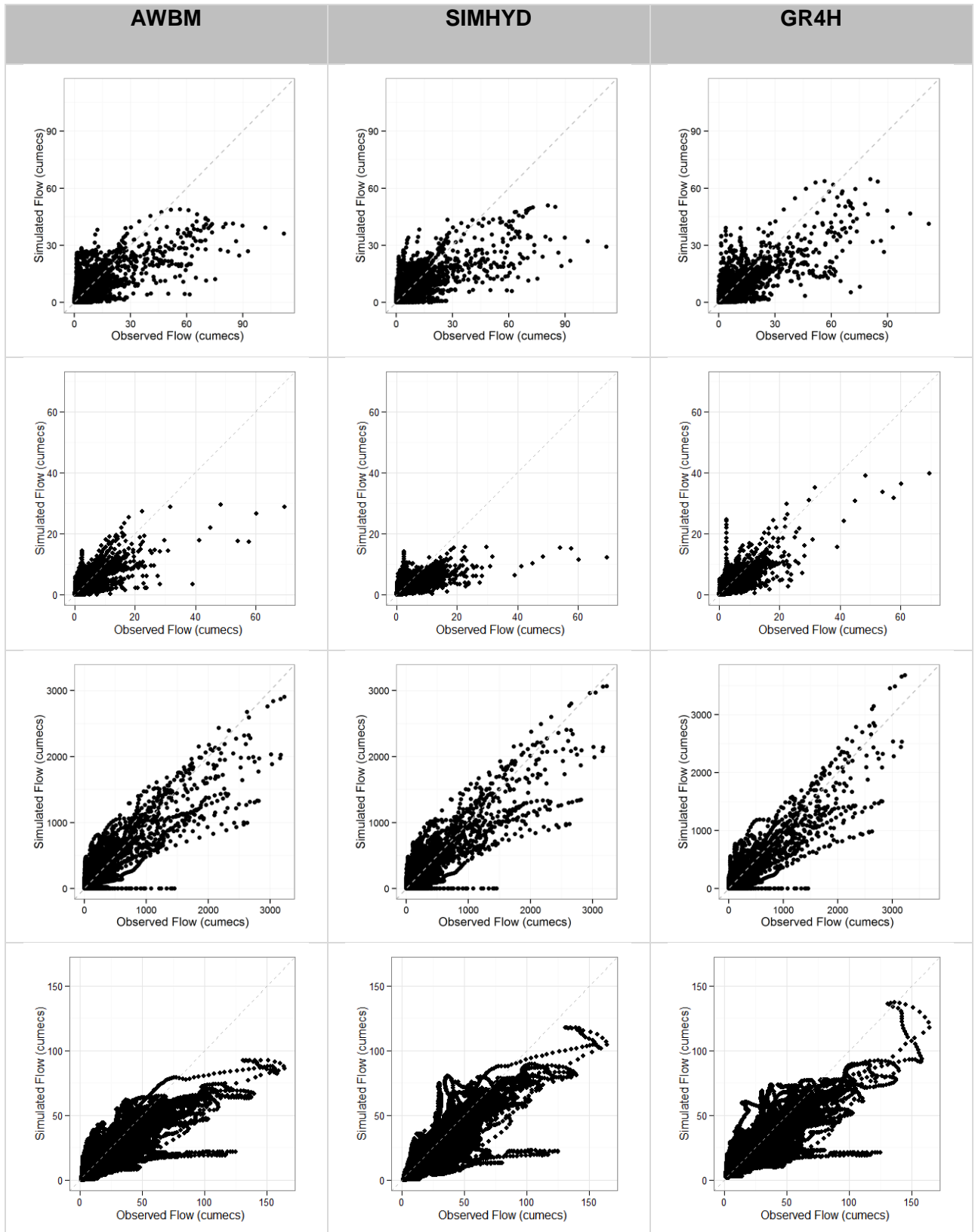


Figure 9-7 : Comparison of the observed and simulated flows [Rows: 1. Manton River, 2. Sixth Creek, 3. Mary River, 4. Florentine River]

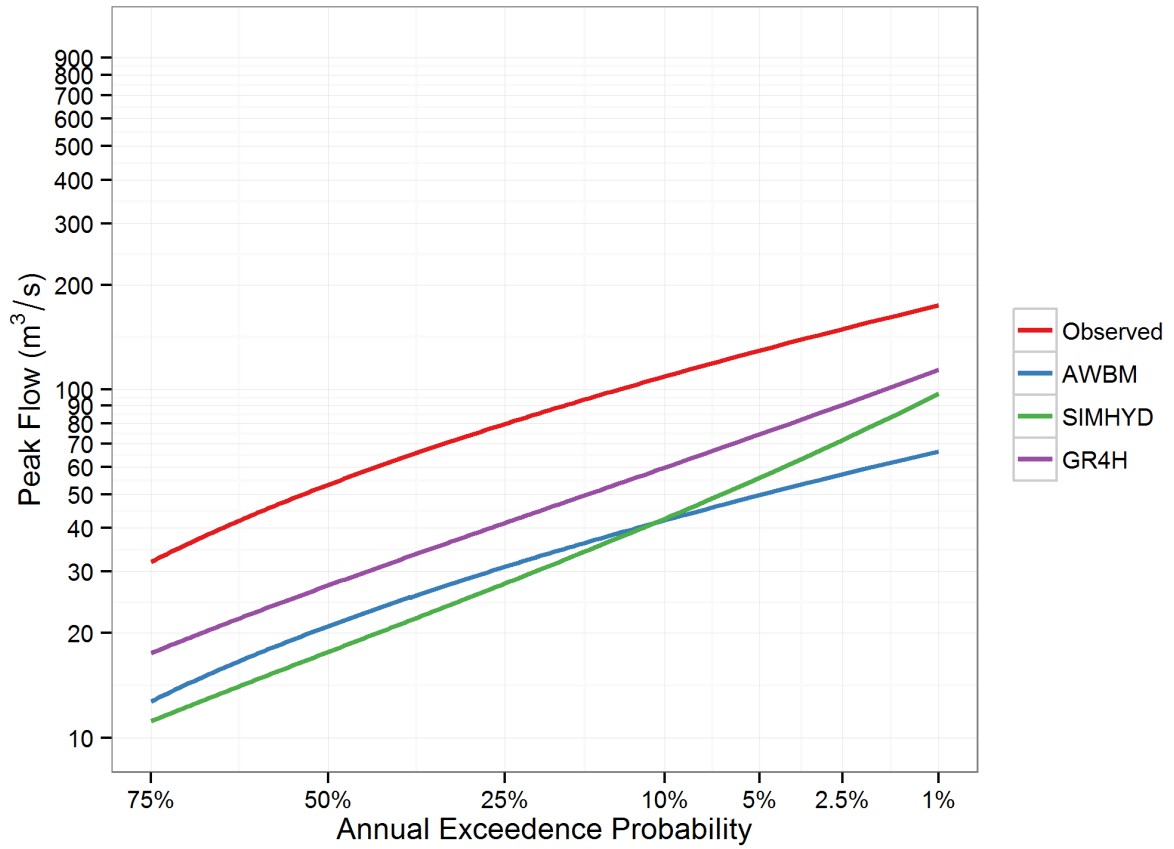


Figure 9-8 : Comparison of the flood frequency curves in Manton River [distribution – GEV]

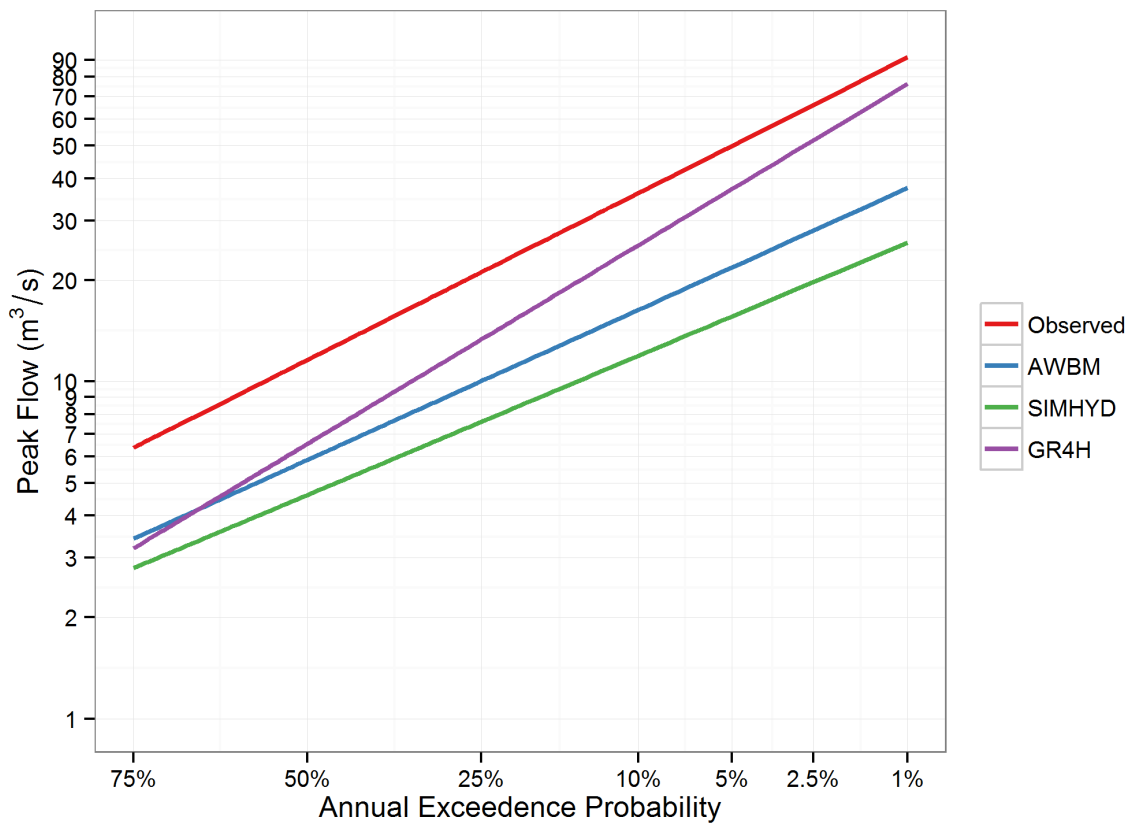


Figure 9-9: Comparison of the flood frequency curves in Sixth Creek [Log normal]

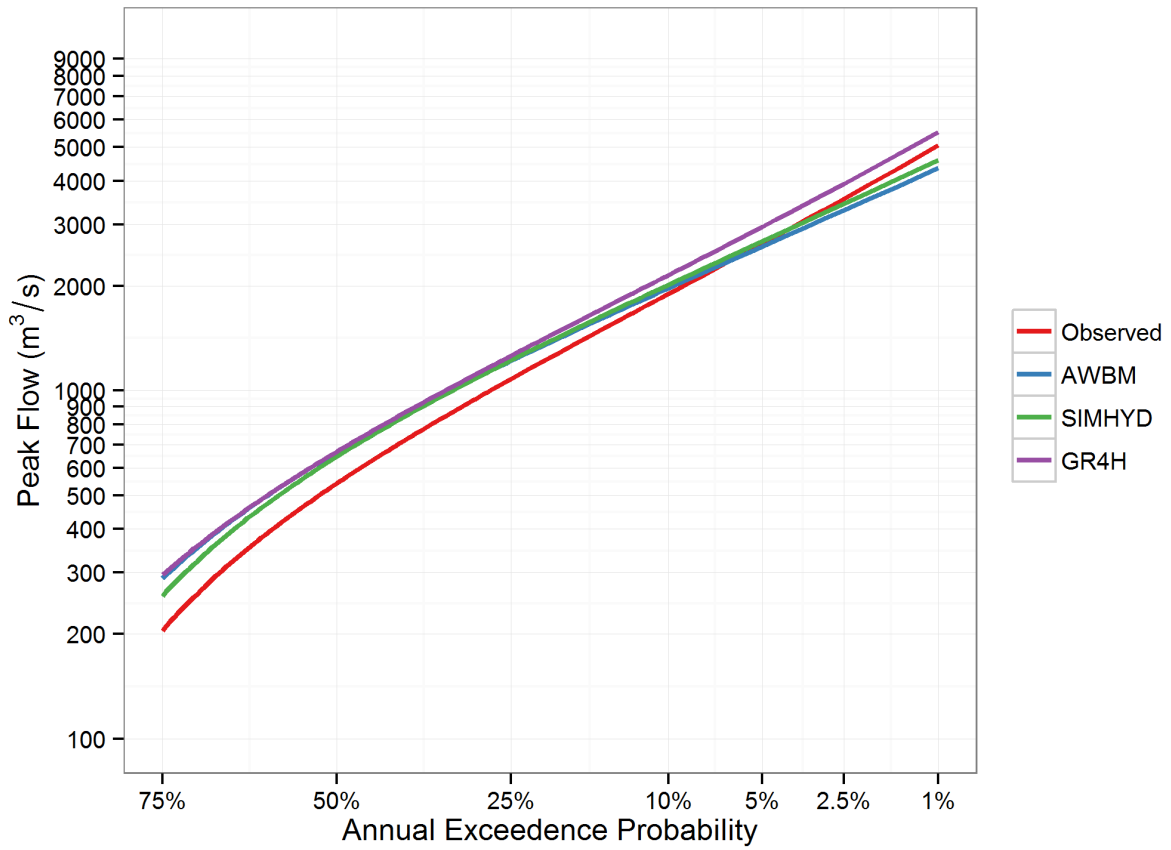


Figure 9-10 : Comparison of the flood frequency curves in Mary River [distribution – GEV]

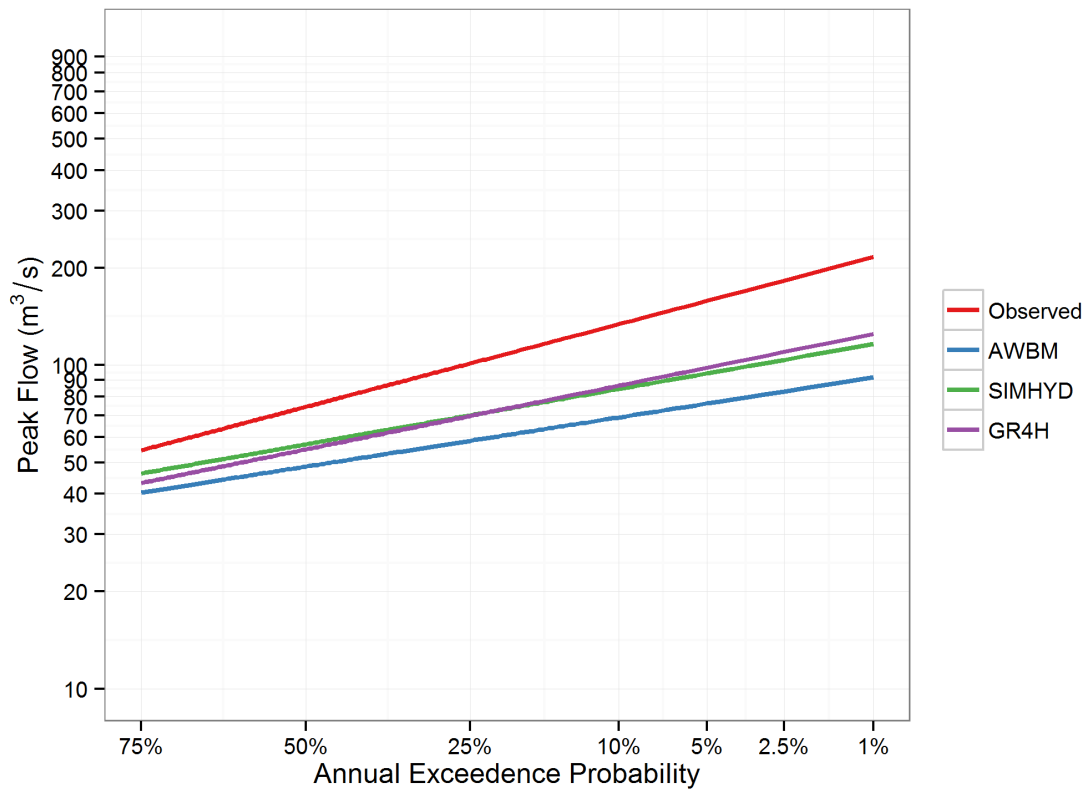


Figure 9-11: Comparison of the flood frequency curves in Florentine River [Log normal]

### 9.3. Scenario 3

The NSE and the volume biases calculated for each catchment and model under Scenario 3 are shown in Table 9-7. For Scenario 3, the models were calibrated for large floods exceeding a targeted threshold (Table 6-1).

**Table 9-7: NSE and volume bias values calculated for scenario 3**

Model	Measure	Catchments			
		Manton River	Sixth Creek	Mary	Florentine
AWBM	NSE	0.38	0.32	0.8	0.64
SIMHYD	NSE	0.41	0.34	0.79	0.7
GR4H	NSE	0.50	0.58	0.82	-
AWBM	Volume bias (%)	71	-67	2.7	19.5
SIMHYD	Volume bias (%)	33	60	-2.3	32
GR4H	Volume bias (%)	-70	-60	-27	-

In general, except for Mary River, the NSE shows significant reduction in values, with the reduction of the NSE values particularly large for AWBM and SIMHYD models in Manton River and Sixth Creek. In addition, calibration to events also results in large volume biases, in Sixth Creek and Manton River, where the volume bias is as high as 71%. In Mary River, the calibration to large flood values still results in high NSE values and generally low volume bias. Although GR4H results in highest NSE values among the three models, it also results in high volume biases.

In Florentine, the calibration of the GR4H model resulted in an unusual hydrograph behaviour (Figure 9-12 and Figure L. 19). This was due to the fact that the ground water exchange parameter X2 used in the GR4H model allows a large volume of moisture to be imported to match the very high observed flow values. The use of the ground water exchange parameter in GR4H allows it to simulate highly nonlinear characteristics of the catchments (Bennett et al., 2014), however in doing so it does not necessarily preserve the water balance within the catchment.

The range of flows in Florentine is small and the flow is relatively uniform (Figure I. 5 and also see the slope of FDC in log scale; Figure K. 24) and the imposed threshold corresponding to AEP 1:1 flood (~ 45 m<sup>3</sup>/s) is high (almost 1/3.5 of the highest peak). Therefore in trying to match the flows greater than the threshold the model imports large volume of water (through X2), and because the calibration is not constrained by the requirement of fitting the low flows and maintaining the overall volume bias it provides good fit to data greater than 45 and ignoring flows below it. This results in unusually high baseflow behaviour in the Florentine River.

AWBM and SIMHYD tend to preserve the water balance and provide a much better representation of the baseflow flow compared to GR4H for Scenario 3 in Florentine. It seems using the whole event (as opposed to the flow values above a threshold) would have avoided this problem. However in the context of the current study, where the focus is to produce a better fit to the high flows, use of the whole event would not have improved the chances of providing

the a better fit to the flood peaks.

### 9.3.1. Comparison of hydrograph behaviour

Despite calibration of the models to large flood values, the comparison of hydrographs and flow duration curves (Figure L. 2 to Figure L. 25 in Appendix L) and scatter plots (Figure 9-12) in all catchments except Mary River, shows that all the model simulations still underestimate the peaks. In addition, the scatter around the 1:1-line (Figure 9-12) is not random and indicates the presence of systematic errors possibly indicating large errors in timing, which are more evident in Sixth Creek, Manton River and Florentine River.

### 9.3.2. Comparison of event volumes

Interestingly, while the overall volume bias in three catchments considerably degrade by calibrating to large events, the volume differences between the observed and simulated flood events actually decrease in all the catchments. Largest improvements were seen Manton River and Sixth Creek.

Calibrations to large flood events improve the hydrograph representation over large flood events while degrading the performance at other times. This results in better representation of the volumes during the large events, but larger overall volume bias.

**Table 9-8 : Volume differences (%) calculated for 10 largest events** [colour codes: red for volume bias greater than 50%, orange for values between 50% and 25 %, and green for values equal to and less than 25 %, AWB = AWBM, SIM = SIMHYD, GR4 = GR4H]

Events	Manton			Sixth Creek			Mary			Florentine		
	AWB	SIM	GR4	AWB	SIM	GR4	AWB	SIM	GR4	AWB	SIM	GR4
1	-45	-7	-15	-64	-59	-59	58	62	63	72	72	-
2	-19	5	7	4	-15	-23	-6	-15	-9	15	15	-
3	-23	-29	-17	-15	-18	-24	0	-7	-7	16	17	-
4	-5	-11	8	28	27	30	6	10	14	-25	-15	-
5	-31	-28	-16	9	12	0	-6	-14	0	8	8	-
6	-19	-4	-8	46	62	55	32	40	44	27	27	-
7	31	39	37	-9	5	-4	-10	-16	-8	18	17	-
8	17	17	23	-4	-41	-7	11	5	6	1	0	-
9	11	16	18	-21	-12	8	9	14	9	12	12	-
10	-3	-2	11	9	17	11	39	36	36	17	16	-

### 9.3.3. Comparison of flood frequency curves

Simulated flood frequency curves (Figure 9-13 to Figure 9-16 and Table 9-9) generated for Scenario 3, provide a relatively closer representation of the observed flood frequency curves compared to Scenarios 1 and 2 in Sixth Creek (for GR4H model) and Florentine River (for SIMHYD model). However, the difference between the observed and simulated flood frequency curves in Manton River, Sixth Creek and Florentine is still very large.

**Table 9-9: % Difference (observed – simulated) in flood quantiles for scenario 3** [colour codes: red for values greater than 30%, orange for values between 30% and 10 %, and green for values equal to and less than 10 %]

Catchment	Models	Annual Exceedance Probability					
		1%	2%	5%	10%	20%	50%
Manton	AWBM	55	54	53	51	49	42
	SIMHYD	52	50	48	46	44	38
	GR4H	41	40	38	37	35	31
Sixth Creek	AWBM	52	50	45	41	36	24
	SIMHYD	68	65	61	56	49	33
	GR4H	18	19	22	23	26	30
Mary	AWBM	21	21	21	20	19	14
	SIMHYD	11	13	17	19	20	18
	GR4H	4	8	13	15	17	16
Florentine	AWBM	34	31	26	22	16	3
	SIMHYD	14	13	11	9	7	3
	GR4H	39	36	30	25	19	4



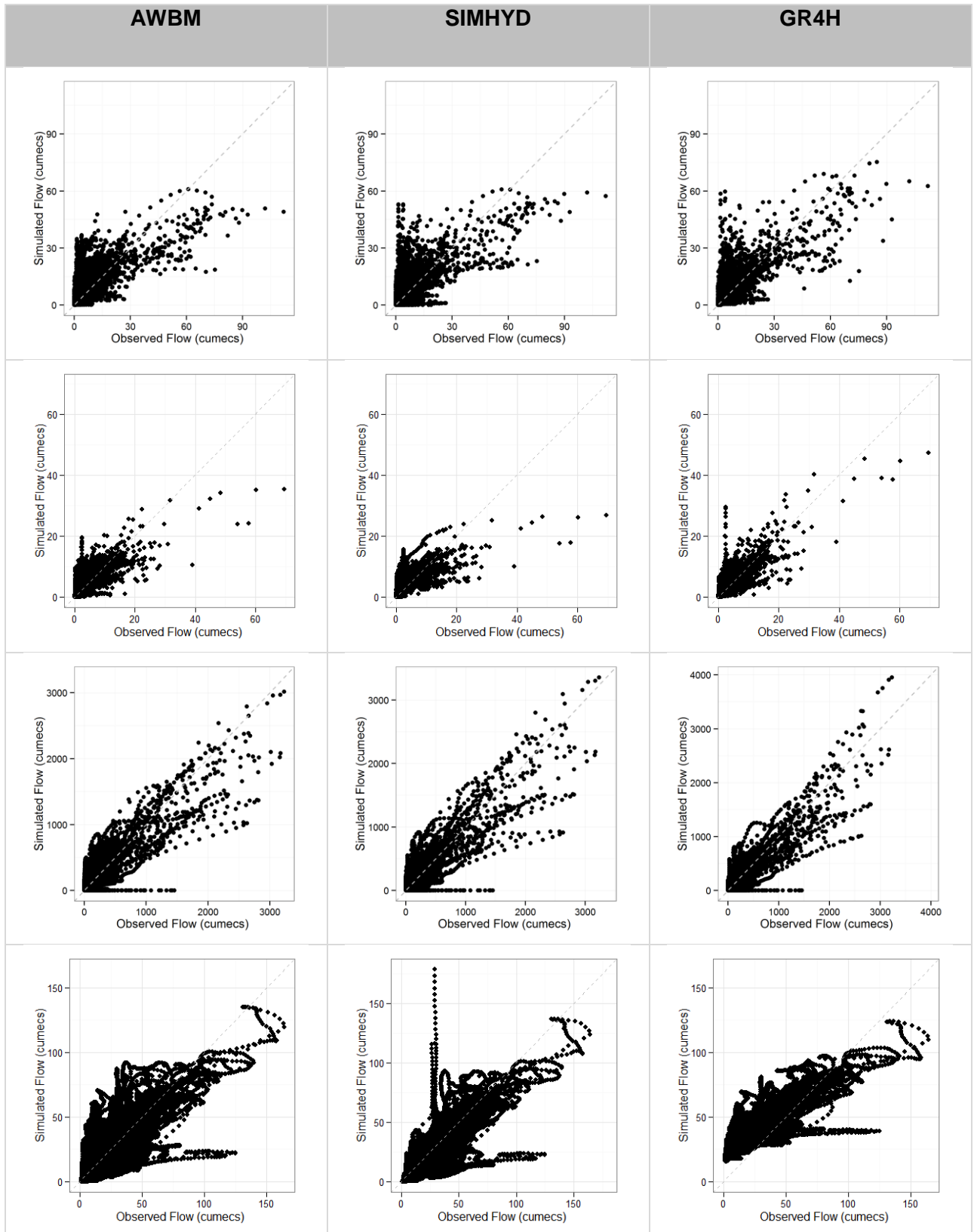


Figure 9-12 :Comparison of the observed and simulated flows [Rows: 1. Manton River, 2. Sixth Creek, 3. Mary River, 4. Florentine River]

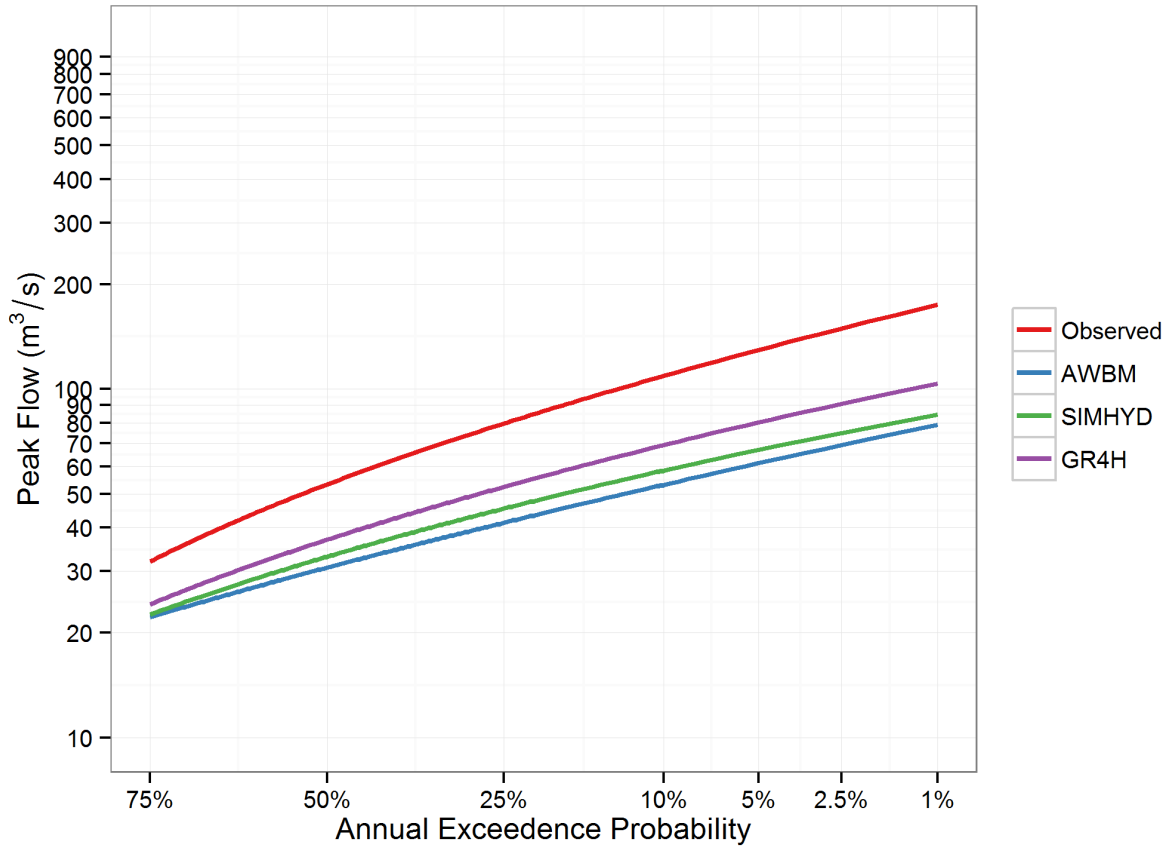


Figure 9-13: Comparison of the flood frequency curves in Manton River [GEV]

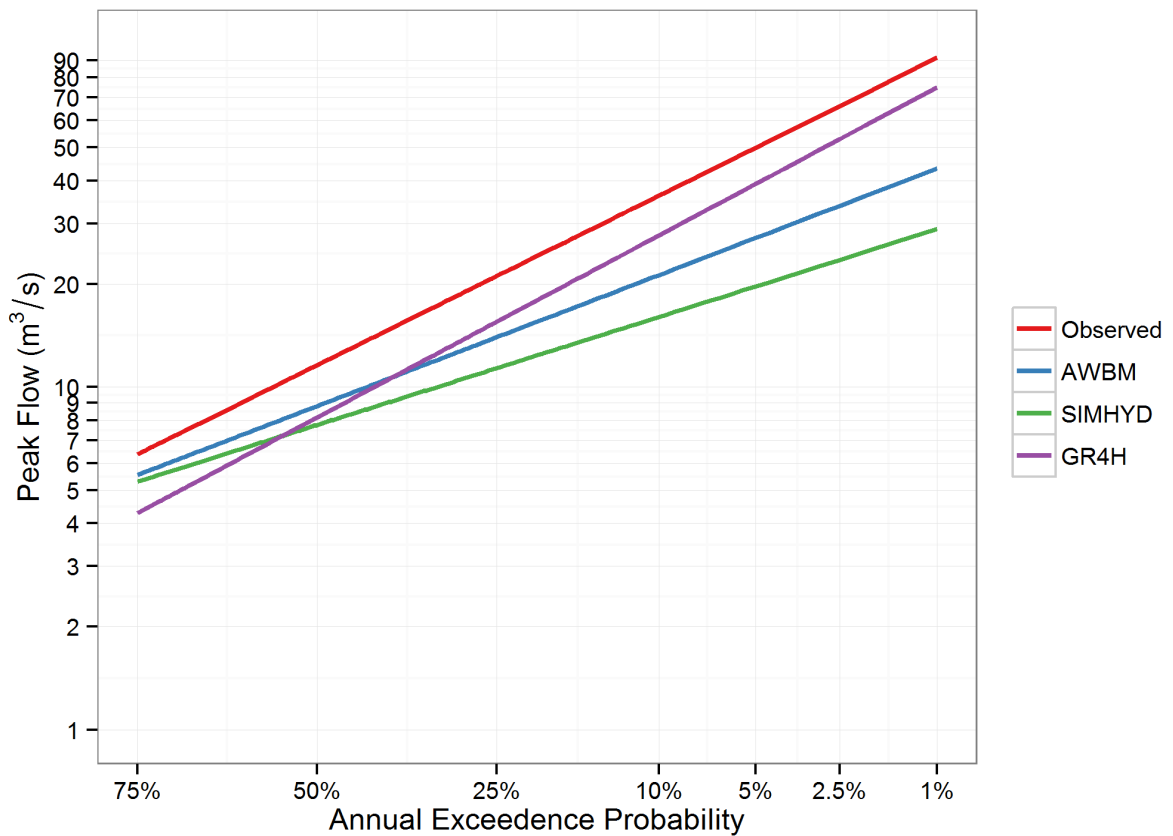


Figure 9-14: Comparison of the flood frequency curves in Sixth Creek [distribution – Log normal]

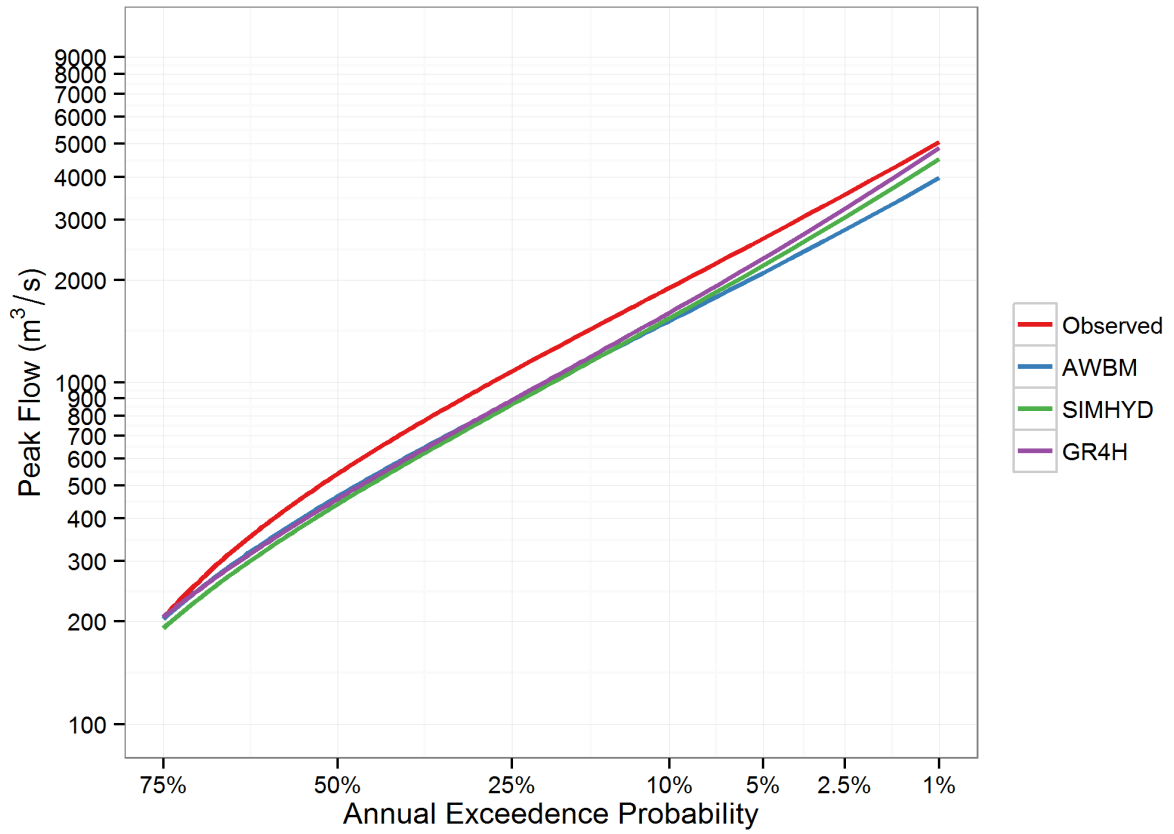


Figure 9-15: Comparison of the flood frequency curves in Mary River [distribution – GEV]

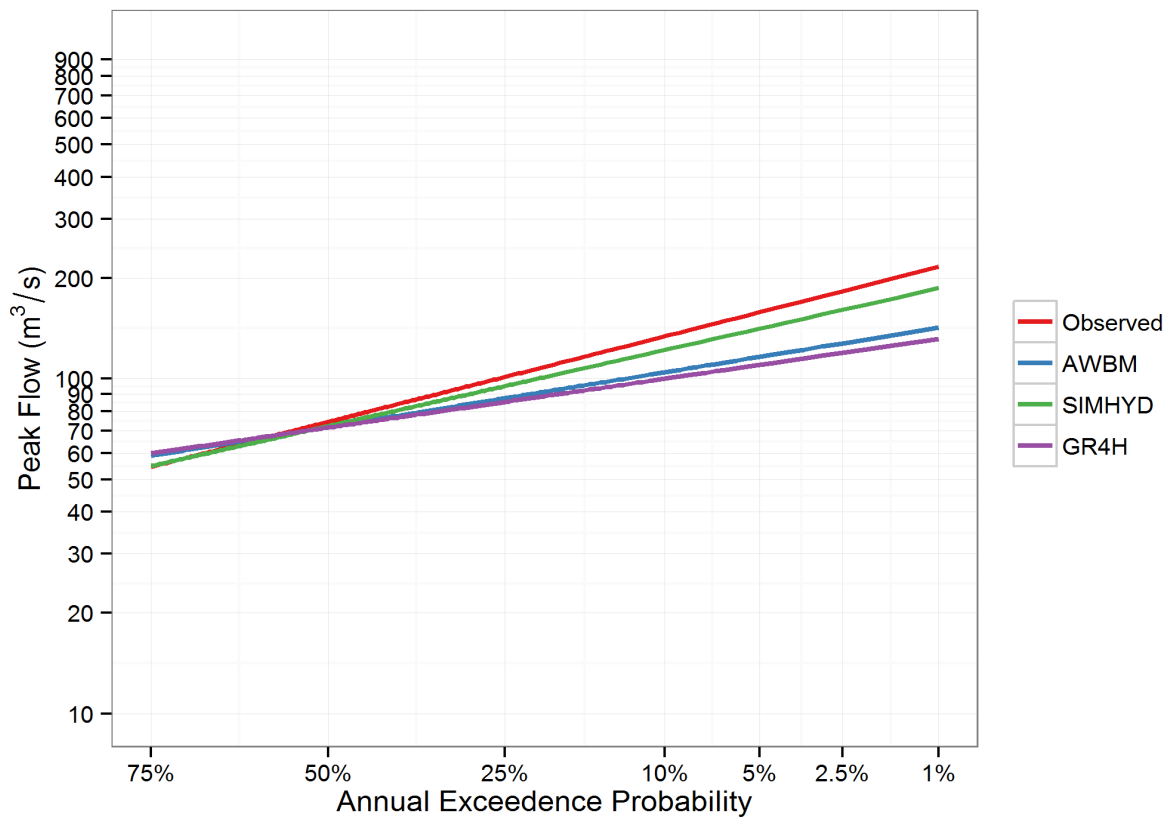


Figure 9-16: Comparison of the flood frequency curves in Florentine River [distribution – Log normal]

## 9.4. Scenario 4

The NSE and the volume biases calculated for each catchment and model under Scenario 4 are shown in Table 9-10. In general, calibration of the models against the flood frequency curves resulted in poor NSE values and high volume biases in all catchments except Mary River. In Mary River, NSE values were 0.7, 0.66 and 0.75 for AWBM, SIMHYD and GR4H model respectively.

**Table 9-10: NSE and volume bias values calculated for Scenario 4**

Model	Measure	Catchments				
		Manton River	Sixth Creek	Mary	Florentine	Yates Flats
AWBM	NSE	-0.02	0.1	0.70	0.17	0.38
SIMHYD	NSE	-0.30	-0.22	0.66	0.3	0.41
GR4H	NSE	0.17	0.1	0.75	0.5	-0.1
AWBM	Volume bias (%)	-29	-8	8	68	-2.5
SIMHYD	Volume bias (%)	-22	-45	-21	52	-53
GR4H	Volume bias (%)	-58	-93	-65	26	-43

### 9.4.1. Comparison of hydrograph behaviour

While the simulated hydrographs and flow duration curves in all the catchments (Figure N. 1 to Figure N. 24) seem to be able to reproduce the large floods, they do so at the expense of timing. This is clearly evident in the scatter plot shown in Figure 9-17 for Manton River, Sixth Creek and Florentine.

### 9.4.2. Comparison of event volumes

The differences in volumes between the observed and simulated flows are given in Table 9-11. In Florentine River, Sixth Creek and Yates Flat Creek, calibration to flood frequency curves resulted in increases in the volume bias for most model simulations. The volume bias is as high as -556% for GR4H model in Yates Flat Creek. In Florentine River, the volume difference is greater than 25% in all 10 events.

In Mary River, calibration to the flood frequency curve results in increased volume differences for GR4H and SIMHYD. However, calibration of AWBM model in Mary River results in differences in event volumes that are less than 25% for 8 out of the 10 events.

**Table 9-11: Volume differences (%) calculated for 10 largest events** [colour codes: red for volume bias greater than 50%, orange for values between 50% and 25 %, and green for values equal to and less than 25 %, AWB = AWBM, SIM = SIMHYD, GR4 = GR4H]

Events	Manton			Sixth Creek			Mary			Florentine			Yates Flats		
	AWB	SIM	GR4	AWB	SIM	GR4	AWB	SIM	GR4	AWB	SIM	GR4	AWB	SIM	GR4
1	7	-11	-20	-67	-119	-93	61	54	40	82	82	81	21	-8	-20
2	1	15	1	38	-27	-112	-11	-24	-55	40	53	43	37	25	-43
3	-60	-34	-27	-52	-40	-90	-18	-39	-48	37	32	43	65	11	15
4	2	-5	-13	23	-3	17	12	2	-36	71	45	17	-3	-7	60
5	-74	-16	-17	-8	-45	-21	-17	-42	-45	35	41	42	5	-21	38
6	-48	3	-15	57	53	43	24	18	21	47	54	51	74	56	18
7	22	42	40	1	-24	-27	-24	-45	-52	37	38	42	50	16	-45
8	-8	22	19	-116	-102	-25	14	2	-32	23	31	31	30	31	37
9	11	19	5	-49	-72	16	-1	-20	-46	35	43	40	-91	-101	-44
10	-37	3	6	-23	1	-40	30	19	3	37	37	43	-68	-218	-556

### 9.4.3. Comparison of flood frequency curves

The simulated flood frequency curves (Figure 9-18 to Figure 9-22) provide a close match to the observed in all catchments. The percentage differences between the simulated and observed flood frequency curves are generally small, except for Mary River, which shows 29% difference between the flood events corresponding to AEP 1% for GR4H model.

Calibration to Scenario 4 in Mary River initially resulted in a poor fit to the observed flood frequency curve as large number of parameter samples were unable to provide a good fit to the simulated flood frequency curve and resulted in unfeasible GEV parameter sets. It was found that censoring of the low flow values could improve the overall fit to the observed flood frequency curve. To this end, annual maximum flood values below a threshold were fitted separately and its likelihood values added to the likelihood value for the rest of the curve. This improved the fit to the observed flood frequency curve and convergence of the calibration algorithm considerably.

**Table 9-12 : Difference (observed – simulated) in flood quantiles for scenario 4 [colour codes: red for values greater than 30, orange for values between 30 and 10 , and green for values equal to and less than 10 ]**

Catchment	Models	Annual Exceedance Probability					
		1%	2%	5%	10%	20%	50%
Manton	AWBM	16%	15%	14%	13%	11%	8%
	SIMHYD	-12%	-8%	-4%	-1%	2%	3%
	GR4H	3%	4%	5%	5%	6%	4%
Sixth Creek	AWBM	7%	6%	5%	4%	3%	0%
	SIMHYD	6%	6%	5%	4%	3%	0%
	GR4H	7%	7%	5%	4%	3%	0%
Mary	AWBM	-13%	-9%	-5%	-2%	1%	2%
	SIMHYD	-25%	-18%	-10%	-5%	0%	5%
	GR4H	-29%	-21%	-11%	-5%	-1%	1%
Florentine	AWBM	5%	4%	4%	3%	2%	0%
	SIMHYD	5%	5%	4%	3%	2%	0%
	GR4H	6%	5%	4%	3%	2%	-1%
Yates Flat	AWBM	6%	6%	5%	4%	3%	1%
	SIMHYD	5%	5%	4%	4%	3%	2%
	GR4H	5%	5%	4%	4%	3%	1%

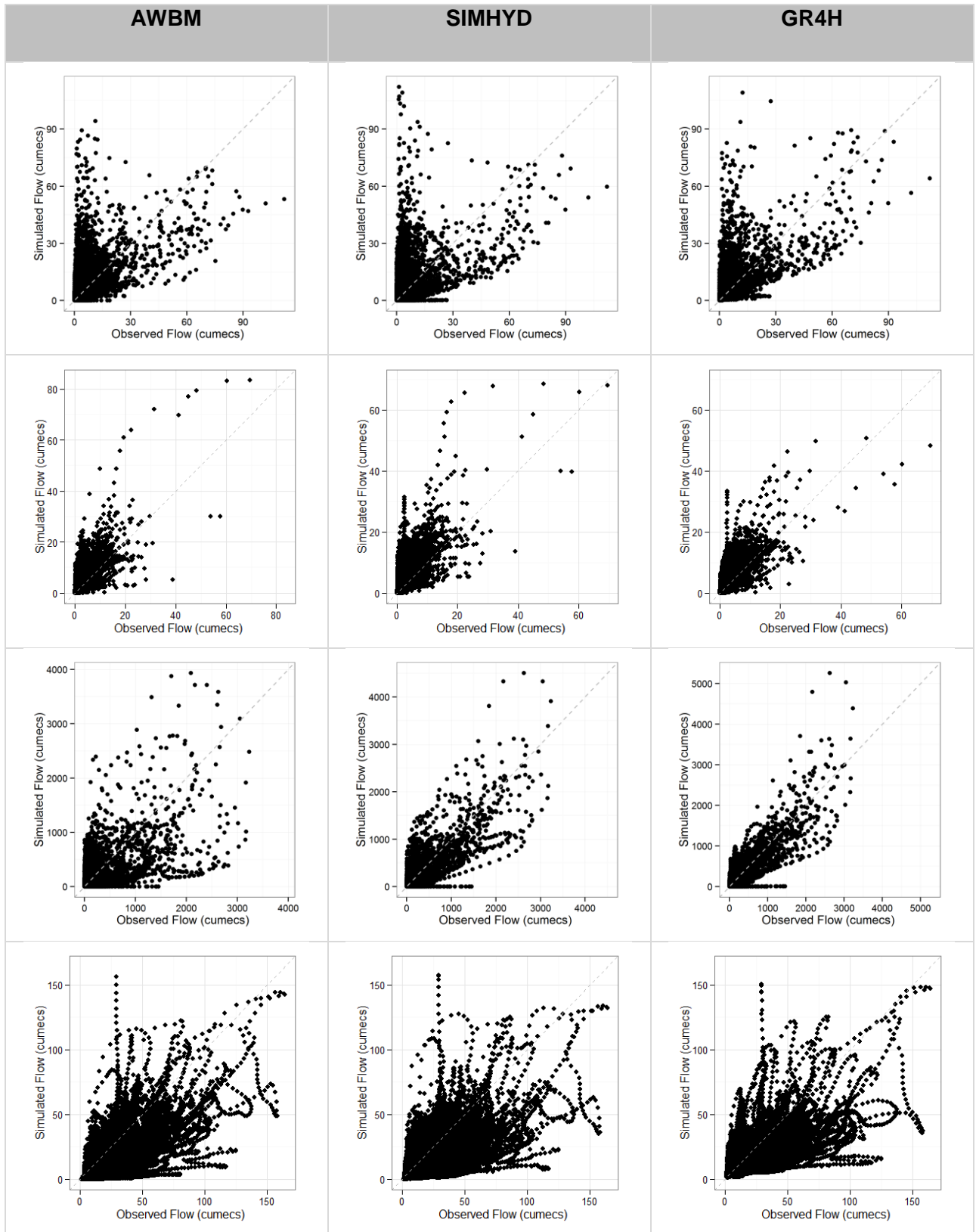


Figure 9-17: Comparison of the observed and simulated flows [Rows: 1. Manton River, 2. Sixth Creek, 3. Mary River, 4. Florentine River]

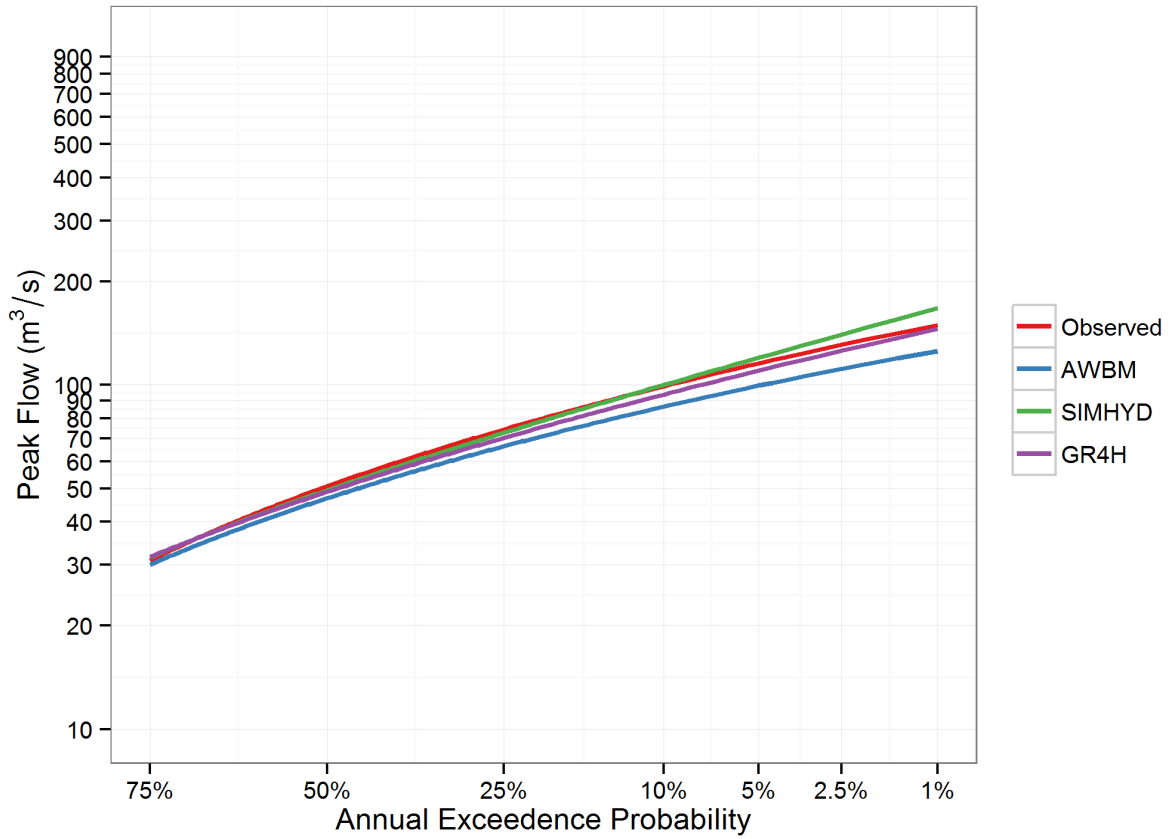


Figure 9-18: Comparison of the flood frequency curves in Manton River [distribution – GEV]

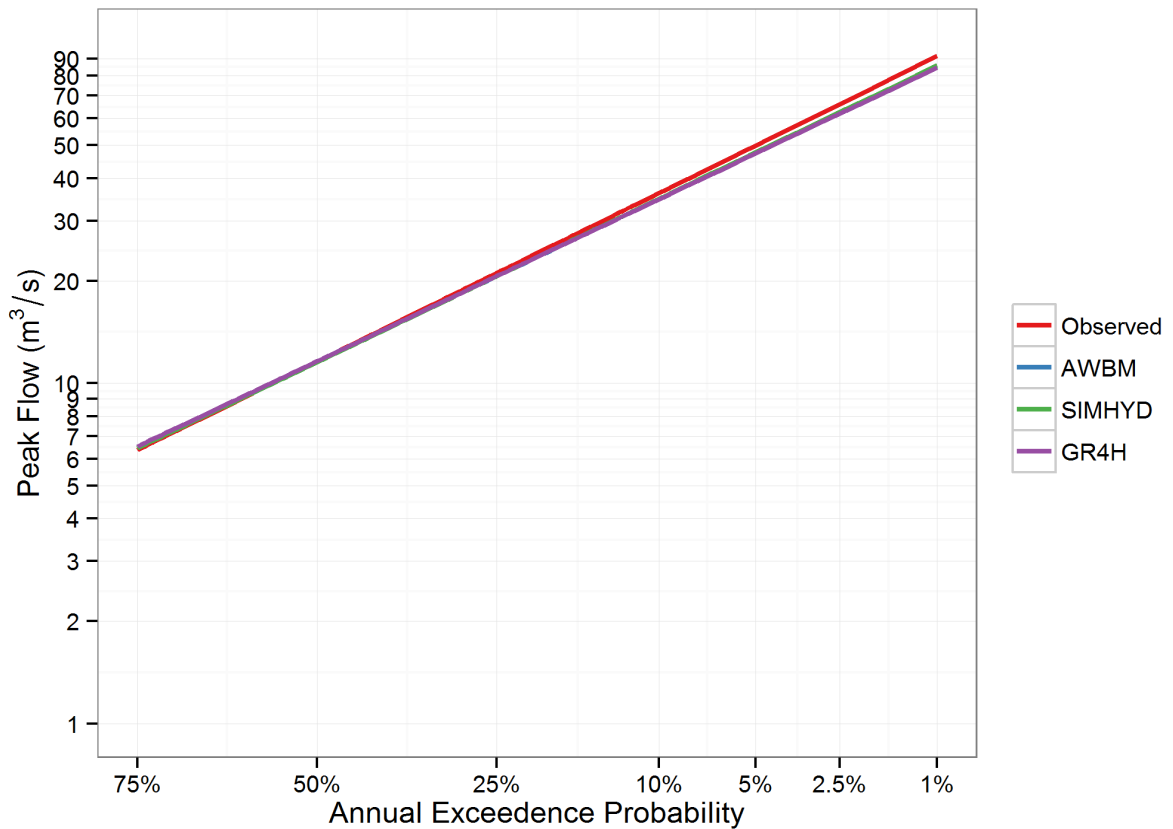


Figure 9-19: Comparison of the flood frequency curves in Sixth Creek River [distribution – Log normal]



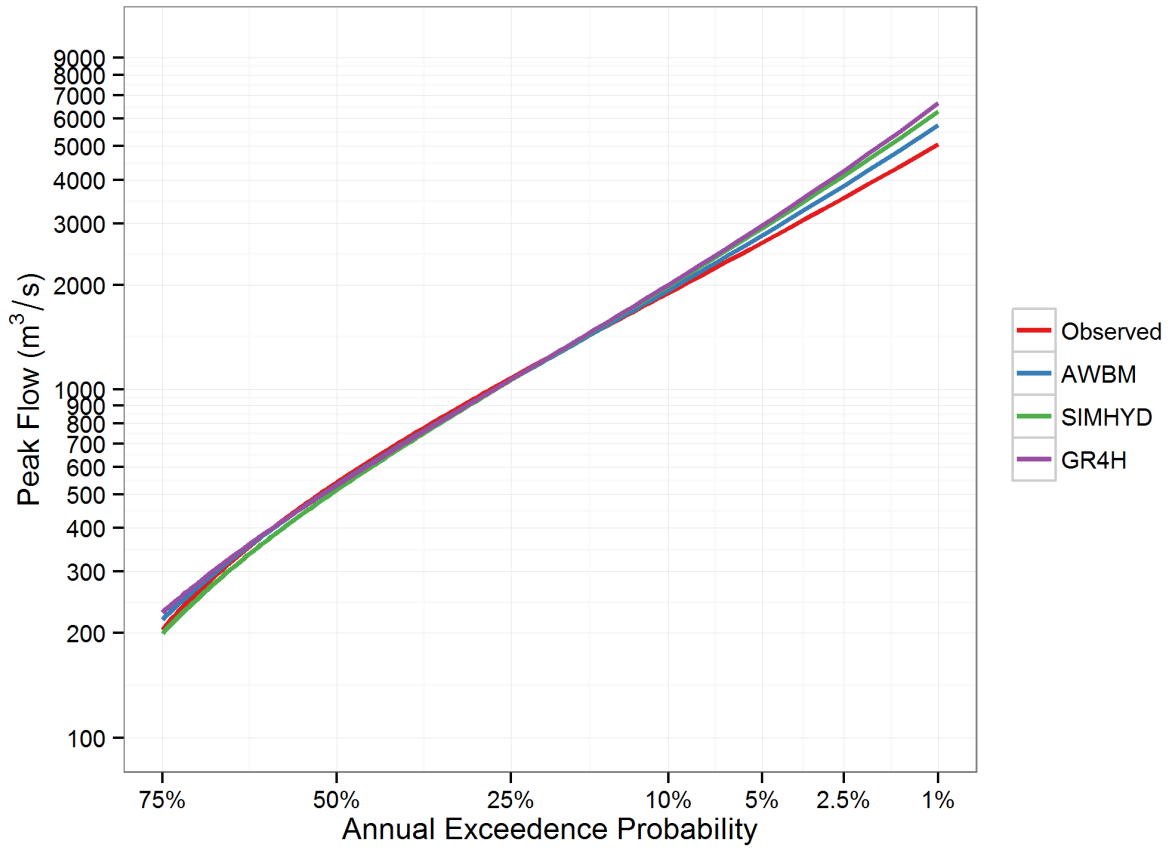


Figure 9-20: Comparison of the flood frequency curves in Mary River [distribution – GEV]

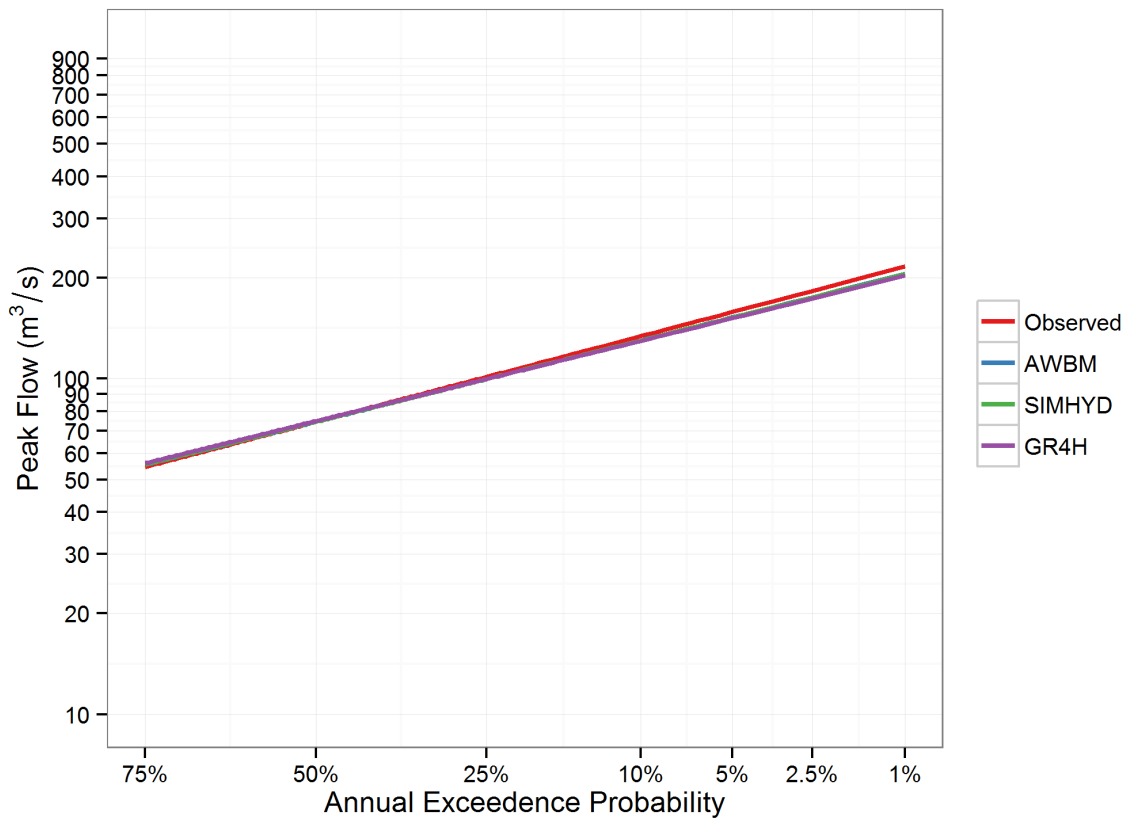


Figure 9-21: Comparison of the flood frequency curves in Florentine River [Log normal]

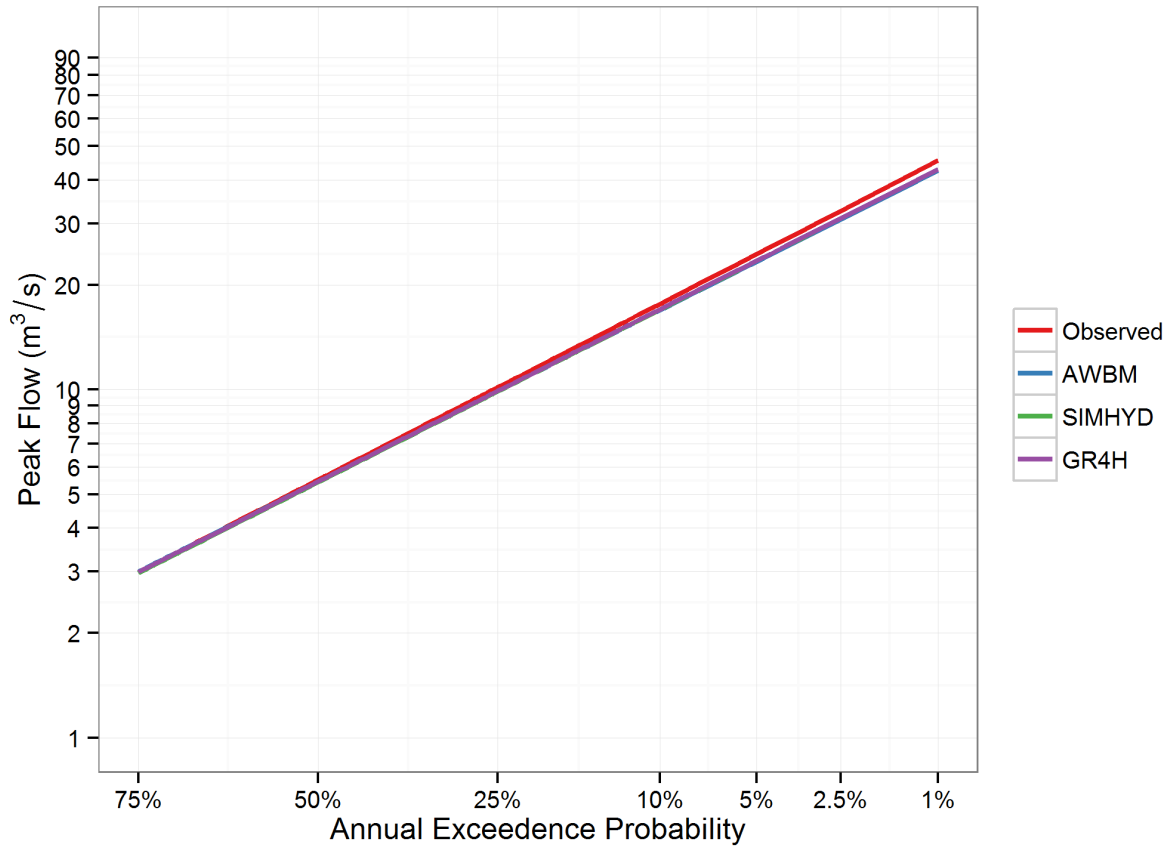


Figure 9-22: Comparison of the flood frequency curves in Yates Flat Creek [Log normal]

## 10. Discussion

### 10.1. Performance of the models over different catchments and AEPs

The results showed that both the Monte Carlo and Design Event models performed well for the majority of the test catchments in replicating the frequency curve fitted to observed data. These catchments covered a range of catchment sizes from 16km<sup>2</sup> for Hobart Rivulet to 5070km<sup>2</sup> for Hann River. The catchments were within a range of different climatic zones and had varying vegetation cover, catchment slopes and soil types. Hobart Rivulet is a partially urbanised catchment, whereas all other catchments are largely rural or forested. Based on the test results, both methods appear to be appropriate over a wide range of catchment sizes, catchment conditions and climate zones.

The advantage of the Monte Carlo approach over the Design Event approach was in providing information on the uncertainty in model results. The spread of results from the Monte Carlo modelling shows that in the relatively smaller and drier catchments of Lerderderg River, Sixth Creek and Yates Flat Creek, the combination of initial loss and temporal patterns results in a wide range of possible flood peaks for a given rainfall probability for more frequent events. This reflects that the initial loss can be a large proportion of the event rainfall.

The exception to the generally good model performance was the Monte Carlo model for the Yates Flat Creek catchment. The slope of the observed frequency curve was not well replicated and there was a very wide spread of results from the model runs. The Bureau of Meteorology IFD design rainfalls were reviewed and compared to IFDs derived from a nearby gauge site, and a close agreement was found. Examination of the flow and rainfall record at Yates Flat Creek showed that there is a very variable flow response to rainfall in the catchment, depending on the catchment wetness at the time of the rainfall event. Theoretically, the Monte Carlo method should allow for this through sampling from the initial loss distribution. For this catchment, it is possible that undertaking a seasonal Monte Carlo approach would provide a better fit to the observed values, considering the seasonal variation in catchment wetness. The wide range of flood response may indicate that a constant loss model is not appropriate for this catchment (Australian Rainfall and Runoff, 2013a), or that the distribution of initial losses used is not appropriate. The Design Event approach performed better at this site in terms of matching the observed frequency curve. The range of results available from the Monte Carlo runs provides valuable information for this catchment on how the combination of losses, temporal patterns and design rainfalls can give a widely varying estimate of the flood response.

SWMod was used as an alternative loss model for Yates Flat Creek Catchment and the results fitted the observed frequency curve very well. This showed that accounting for the change in losses as the catchment becomes more saturated produced better results for this particular catchment.

Both the Monte Carlo and Design Event models generally perform well over the range of AEPs from 50% to 1% investigated for this project. In calibrating the models, emphasis was placed on fitting the less frequent events whilst aiming to also replicate the slope of the observed flood frequency curve. For Yates Flat Creek and Hobart Rivulet catchments, it was difficult to obtain a

good fit over the full range of AEPs investigated. The simple rainfall-runoff model used for the Hobart Rivulet catchment may not provide enough detail of flow pathways in the urban portion of the catchment, particularly for more frequent events.

## **10.2. Effect of record length on Monte Carlo and Design Event model performance**

Manton River and Mary River catchments were used to investigate the effect of record length on model performance. For both catchments, the observed flow record was split into two equal halves based on date. For both catchments, there were approximately twenty years of record in each period.

For Manton River, Period 1 was significantly drier than Period 2. All the flood events used for the original Manton River model calibration were contained within Period 2. The routing parameters remained the same for all periods, but the calibrated losses were higher for Period 1. A poor agreement with the flood frequency curve fitted to the full record was found when the parameters calibrated to Period 1 were used in the modelling (Figure 8-22 and Figure 8-23). At 20% AEP, the difference between the observed and modelled flows was 40% for the Design Event model and 49% for the Monte Carlo model. When the parameters calibrated using data from Period 2 were used in the model, the results of both methods showed reasonable agreement with the flood frequency curve.

For Mary River, there were large flood events in both periods of record, with the two largest events being in Period 2. For this catchment, it was found that it was necessary to vary the routing parameter alpha to obtain a good fit to the events and frequency curves derived from the shorter data sets. For all periods, the continuing and initial losses were zero. The results from the model runs using the parameters calibrated to the shorter data sets showed that the Period 2 parameters gave a higher estimate of the flood frequency curve and the Period 1 parameters gave a lower estimate (Figure 8-24 and Figure 8-25). This is consistent with the higher flood events being contained in Period 2.

The results from the two test catchments show that even when twenty years of data is available at a site, the model results can vary significantly based on the period of record used in analysis. This is particularly evident when one period is noticeably drier or wetter than the other. This highlights the need to investigate how representative the available flow data is in the context of any available long-term rainfall records. Both the Monte Carlo and Design Event models showed similar results.

## **10.3. Performance of the Monte Carlo and Design Event models on ungauged catchments**

To test the performance of the models on ungauged catchments, the following catchments were used:

- Florentine River and Tyenna River. These are adjoining catchments with very similar catchment characteristics and the same climatic influences. The catchment area of the

Florentine River catchment is 436 km<sup>2</sup> and the Tyenna River catchment area is 198km<sup>2</sup>.

- Hann River and Manton River. These catchments are both in the north of Australia in a similar climate zone, however their catchment areas are vastly different. Hann River catchment has a catchment area of 5070km<sup>2</sup> compared with Manton River catchment area of 28km<sup>2</sup>.
- Hann River and Mary River. These catchments are in different climate zones. Mary River catchment has an area of 820km<sup>2</sup>.
- Florentine River and Hann River. These catchments are in different climate zones, have different catchment areas and catchment characteristics.

As neighbouring catchments, the Florentine River and Tyenna River catchments are very similar in terms of characteristics, flow response to rainfall, event hydrograph shapes, and climatic zone. The catchment area of the Florentine River model is 2.2 times that of the Tyenna River. It would be expected that the calibrated model parameters would be similar for these models, however this was not the case. The routing parameter, Alpha, was 1.6 in the Tyenna River models and 2.5 in the Florentine River models. The loss parameters also varied between the catchment models for both the Monte Carlo and Design Event calibrations. There are likely to be a number of combinations of routing and loss parameters that will produce acceptable model outputs. When the Tyenna River models were run using the Florentine River model parameters, the results of both the Monte Carlo and Design Event models were within 20% of the observed values over the full range of AEPs. However, when the Florentine River models were run using the Tyenna River model parameters, the Monte Carlo method performed slightly better than the Design Event model which showed 43% higher flow compared to 36% for the Monte Carlo. The results illustrate that even when there is a neighbouring gauged catchment, care must be taken in estimating floods for ungauged catchments.

As expected, the results show a poor agreement with the observed flood frequency curve when two catchments are used with differing catchment areas, climatic influences or catchment characteristics. The Tyenna River and Hann River catchments are in very different climate zones, and are dissimilar in terms of catchment characteristics. The results from transposing the parameters between the two catchments are very poor.

The Hann River and Manton River catchments are similar in terms of climate, however the catchment area of the Hann River is more than 150 times that of the Manton River. The results from transposing the parameters between these catchment models are very poor. The considerable differences in routing lengths and catchment conditions result in differences in calibrated model routing parameter and loss values that do not translate between the different models. The Mary River catchment area is 16 percent of the catchment area of Hann, and is in a different climate zone. The results from transposing the parameters between these two models results in smaller differences between the observed and modelled flood frequency curve in Mary, compared to Hann. This indicates that the Mary River model is less sensitive to changes in model parameters.

It is noted that the routing parameter values are closer between the Mary River and Hann River models (1.0 and 0.8 respectively), than the Manton River and Hann River models (1.2 and 0.8

respectively). The continuing loss in the Manton River model is three times that in the Hann River model for the Monte Carlo model. The combination of the increased routing parameter and higher continuing loss results in a very large underestimation of flood peaks from the Hann River model when Manton River model parameters are used.

The results illustrate that care must be taken in selecting a gauged catchment to use as a surrogate for an ungauged catchment, even when it would be expected that the two catchments are similar.

#### **10.4. Performance of the Monte Carlo and Design Event models at internal gauges**

The performance of the models in replicating the flood frequency curve at internal gauge sites within the Mary River catchment was investigated. The results showed that both the Monte Carlo and Design Event models performed poorly at the Kenilworth gauge site. The poor result at Kenilworth gauge was not expected as this gauge is on the main stream of the Mary River and is the closest gauge to the Moy Pocket gauge which was used to calibrate the model. An examination of the annual flood series for the period of overlapping record at Moy Pocket and Kenilworth from 1964 – 1971 showed a strong relationship between the two series, however the flows at Kenilworth were lower than would be expected given the relative catchment areas and rainfall patterns to the two gauges. The flows at the two gauges matched well at lower flows. It is possible that the rating curve at Kenilworth is uncertain for higher flows. This was not investigated further for this project.

Both the Monte Carlo and Design Event models performed reasonably well at the Obi-Obi Creek at Kidaman and Bellbird Creek sites, despite these sites being relatively high in the catchment. Overall Monte Carlo model resulted in higher flow values than Design Event for all the internal gauges; this is however due to the fact that the modelled flood frequency curve at the outlet of catchment is higher when using the Monte Carlo method compared to the Design Event.

#### **10.5. Ability of Continuous Simulation models to reproduce hydrograph behaviour and match observed flood frequency curve**

Among the four catchments tested, calibration on Mary River resulted in a reasonably good representation of the hydrograph behaviour as well as the observed flood frequency curve consistently. This certainly points to the fact that given good quality data and model structure (representing the processes occurring in the catchment), the continuous simulation method is capable of generating a reasonably good representation of flood frequency and the hydrograph behaviour. In other catchments, while calibration of model parameters to the observed flood frequency curve did produce a good fit to the observed flood frequency curve, this came at the expense of hydrograph “timing” and event volumes.

This point is further illustrated in Figure P. 1 to Figure P. 16, which show the comparison of event hydrographs for the largest flood event in the record (for calibration scenarios 1, 3 and 4 for AWBM and GR4H). Calibration to Scenario 1 (Figure P. 1 to Figure P. 3 and Figure P. 9 to Figure P. 11) captured the timing of the peak, but underestimated the peak magnitude in 4 out

of the 5 catchments. Scenario 3 (Figure P. 4,

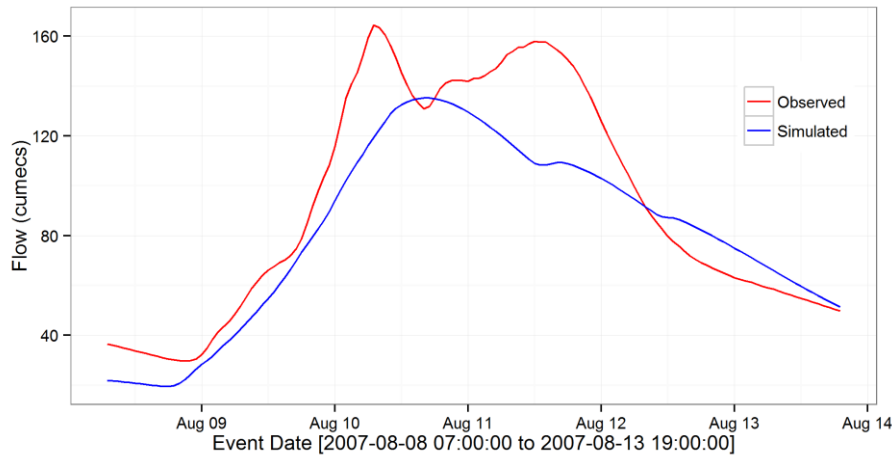


Figure P. 5 and Figure P. 12, Figure P. 13) resulted in slight improvement in terms of reproducing the peak magnitude and event volume. Calibration to Scenario 4 (Figure P. 6, Figure P. 8, Figure P. 14) resulted in improvement in matching the peak magnitude, but poor hydrograph timing.

Calibration results from Scenario 4 shows that that it is relatively easy to match the observed flood frequency curve, given the complexity of the models and relatively simple target to calibrate against. After all it is possible to generate floods of large magnitudes through many different configurations of model parameter when timing, volume and order of occurrence of the peak events were to be completely ignored. However, for a continuous simulation model to be used confidently for design flood analysis, it should be able to provide a good representation of the observed flood frequency curve as well as overall general hydrograph behaviour, including timing, shape and volume.

### 10.5.1. Multi objective nature of the calibration problem

The current study clearly illustrates the multi-objective (Gupta et al. 1998) nature of the calibration problem, and shows that it is not possible, in many cases, to obtain very good fit to both flood frequency curves and the hydrograph behaviour. Furthermore, the calibrated parameters show large differences in values (Figure O. 1 to Figure O. 3 in Appendix O) for Scenarios 1 and 4 representing a trade-off between reproducing the overall hydrograph behaviour and best representation of the flood frequency curve.

This seems to suggest that a compromise solution between the parameters obtained from Scenarios 1 and 4 would provide a more balanced match to the hydrograph behaviour and the observed frequency curve. This could be implemented, either through a multicriteria optimization (Gupta et al. 1998) or a penalized/constrained minimization.

However, regardless of the calibration strategy used, the major problem resulting in the poor overall performance of the model in these catchments seem to be the inability of the models to adequately represent the hydrological processes occurring in these catchments for flood estimation.

## **10.6. Continuous Simulation model suitability for design flood estimation**

This study implicitly assumes that a common model structure is applicable to all catchments, and that catchment specific model behaviour could be obtained through parameter calibration. In this regard generic model structures (AWBM, GR4H and SIMHYD) were all applied to catchments of very different climatic and catchment behaviours. The results of the study seem to indicate that rainfall runoff models adopted in this study were not adequate to represent the widely varying climatic and catchment characteristics displayed in all the catchments, and the impact of these on flood estimates. For example Figure P.17 shows a common problem displayed by all the models, which was the inability of the model to represent multi-peaked flood response in Florentine catchment.

Detailed model diagnosis and subsequent model improvements following the calibration, as recommended by (Martinez and Gupta 2010, Gupta et al. 2008), might further improve the result in some catchments, however these were beyond the scope of the current study and were not conducted.



## 11. Conclusions

The Monte Carlo, Design Event and Continuous Simulation approaches were compared and tested in this project.

The main advantages of the Design Event approach identified were:

- It is simple to implement and is not computationally intensive.
- It has been tailored to Australian conditions, and makes use of data that are readily available in Australia.
- The inputs used by the method are reasonably well defined, leading to good consistency between studies conducted using this approach.
- It has also been thoroughly tested in Australian catchments and the limitations of the method are well understood.

Limitations of the Design Event approach include:

- The use of fixed representative values of the flood producing variables cannot properly characterize interactions between rainfall and catchment characteristics
- Conditioning the model output on fixed (mean or median) values does not necessarily preserve the probability neutral transformation of rainfall to runoff and can introduce biases in the design flood estimate.

The main advantages of the Monte Carlo approach were seen as:

It removes the dependence on AEP-neutrality assumptions

- A more rigorous approach is taken to assigning probability distributions to random inputs rather than adopting mean or median values. Bias introduced by fixed durations of rainfalls is reduced in this method by sampling from a range of durations.
- Infrastructure operation can be represented through a distribution
- Uncertainty in individual model inputs and model results can be quantified.

The main limitation of the Monte Carlo approach is in the specification of the distribution for antecedent conditions and the model parameters, including the initial levels of the reservoirs and storages, through pre-specified distributions (Kuczera et al. 2006a). In practice, specification of the distribution of the sensitive flood producing variables (especially parameters) is difficult because the model parameters are conceptual representations of components of the hydrologic process that cannot be directly measured (H. V. Gupta et al., 1998).

The main advantage of the Continuous Simulation approach is that it is not limited by the probability neutral assumption as it samples all the joint probability interactions among the flood producing variables through direct simulation. The main limitations of the Continuous Simulation approach are:

- Effectiveness of Continuous Simulation models relies upon the length of the rainfall data and the observed streamflow data. In many cases generation of stochastic rainfall data with a distribution that is close to the observed distribution is challenging. It is especially difficult to reproduce rainfall statistics (more importantly the extremes) at all-time scales.

- Even with improved methods of data generation, there will still be very few points to define the top end of the frequency curve (unless the stochastically generated rainfall data are conditioned on the PMP values).
- The ability of continuous simulation models to reproduce both flood peaks and other hydrograph characteristics adequately for design flood purposes has not been proven.

The results of the method testing showed that, in general, an initial loss-continuing loss model run using both the Monte Carlo and Design Event approaches performed well over the range of catchments tested, over a range of AEPs from 50% to 1%. The exception to this was that the Monte Carlo model did not perform well for Yates Flat Creek catchment in South West Western Australia, where the flow response to rainfall events varies widely. SWMOD was used as an alternative loss model for Yates Flat Creek, and it was found that use of this model improved the results significantly over the initial loss-continuing loss model.

Manton River and Mary River catchments were used to investigate the effect of record length on model performance. The results from the two test catchments show that even when twenty years of data is available at a site, the model results can vary significantly based on the period of record used in analysis. This is particularly evident when one period is noticeably drier or wetter than the other. This highlights the need to investigate how representative the available flow data is in the context of any available long-term rainfall records. Both the Monte Carlo and Design Event approaches gave similar results.

To examine the applicability of the methods for ungauged catchments, parameters were transferred between models. The Florentine River and Tyenna River models were used to investigate this situation for two similar catchments. Both the Monte Carlo and Design Event approaches performed well over the full range of AEPs when Tyenna River models were run using the Florentine River model parameters. However, when the Florentine River models were run using the Tyenna River model parameters, the Monte Carlo method performed slightly better than the Design Event model which showed 43% higher flow compared to 36% for the Monte Carlo. The results illustrate that even when there is a neighbouring gauged catchment, care must be taken in estimating floods for ungauged catchments, and the inputs and parameters must be carefully considered.

When parameters were transferred between models from dissimilar catchments, the results of both the Monte Carlo and Design Event approaches were very poor. From these tests it is concluded that only catchments with similar climatic conditions, catchment sizes and catchment characteristics should be considered for providing model parameters for ungauged catchments.

The performance of the models in replicating the flood frequency curve at three internal gauge sites within the Mary River catchment was investigated. The results showed that both the Monte Carlo and Design Event models performed poorly at the Kenilworth gauge site. Further investigation showed that this is likely due to underestimation of flows in the Kenilworth flow record. For the other two sites, both the Monte Carlo and Design Event models performed reasonably well, despite these sites being relatively high in the catchment.

The results of the method testing on Continuous Simulation models showed that calibrating the model to all available flow record resulted in the highest NSE values and in general captured the shape of hydrograph. However, in all the catchments except one, the highest flow peaks were under estimated and the simulated flood frequency curve calculated from simulated annual maximum series provided a very poor fit to the observed flood frequency curve. Calibrating the model to a subset of record produced results that were very similar to using the full record. Using half of the available record did not significantly degrade the performance of the model. Calibrating the model to larger events resulted in a reduction in NSE values and larger volume biases, with only slight improvements in matching the observed flood frequency curves. Finally, calibrating the model to the observed flood frequency curve in general produced a very close fit to the flood frequency curve, but poor representation of hydrograph behaviour and large volume biases.

Among the five catchments tested using the Continuous Simulation approach, only the simulated flow generated for Mary River was able to produce a reasonably good representation of the hydrograph behaviour as well as the flood quantiles consistently. This indicates that, given good quality data and model structure (representing the processes occurring in the catchment), the continuous simulation method is capable of generating a reasonably good representation of flood quantiles and hydrograph behaviour. However, the study also points to the inability of rainfall runoff models to reproduce flood hydrograph behaviour consistently across catchments with widely varying characteristics.

From the testing it was concluded that whilst both the Monte Carlo and Design Event approaches generally performed well in producing a flood frequency curve for AEPs in the range of 50% to 1%, the advantage of the Monte Carlo method was in the quantification of uncertainty provided by the spread of results from individual model runs. The Continuous Simulation approach could provide a good representation of the flood frequency curve when calibrated to the observed frequency curve, however hydrograph behaviour was not well represented. Calibration of Continuous Simulation models to hydrograph characteristics resulted in a poor estimation of flood quantiles across the full range of AEPs up to 1%.

## 12. References

- Abbott, M.B., Bathurst, J.C., Cunge, J.A., O'Connell, P.E., Rasmussen, J., 1986. An introduction to the European hydrological system— Systeme Hydrologique Europeen, SHE, 1: history and philosophy of a physically-based, distributed modelling system. *Journal of Hydrology*, 87(1-2), pp.45–59.
- Andreassian, V., Bergström, S., Chahinian, N., DUAN, Q., GUSEV, Y. M., LITTLEWOOD, I., ... XIE, Z. (2006). Catalogue of the models used in MOPEX 2004 / 2005. In *Large Sample Basin Experiments for Hydrological Model Parameterization: Results of the Model Parameter Experiment–MOPEX* (pp. 41–94). IAHS Publ. 307.
- Australian Rainfall and Runoff , 2013: *Project 2 - Spatial Patterns Of Design Rainfall. Collation And Review Of Areal Reduction Factors From Applications Of The Crc-Forge Method In Australia*. Final Report, P2/S2/012
- Australian Rainfall and Runoff , 2013a: *Project 6 – Loss Models for Catchment Simulation – Rural Catchments*. Stage 2 Report, P6/S2/016A
- Bennett, J. C., Robertson, D. E., Lal, D., Wang, Q. J., Enever, D., Hapuarachchi, P., & Tuteja, N. K. (2014). A System for Continuous Hydrological Ensemble Forecasting ( SCHEF ) to lead times of 9 days. *JOURNAL OF HYDROLOGY*. doi:10.1016/j.jhydrol.2014.08.010
- Beven, K., 1987. Towards the use of catchment geomorphology in flood frequency predictions. *Earth Surface Processes and Landforms*, 12(1), pp.69–82. Available at: <http://doi.wiley.com/10.1002/esp.3290120109>.
- Boughton, W. & Droop, O., 2003. Continuous simulation for design flood estimation—a review. *Environmental Modelling & Software*, 18(4), pp.309–318. Available at: <http://linkinghub.elsevier.com/retrieve/pii/S1364815203000045> [Accessed October 3, 2013].
- Boughton, W.C., Muncaster, SH, Srikanthan, R, Weinmann, PE, and Mein, RG, 1999. Continuous simulation for design flood estimation - a workable approach. In *WATER99 Joint Congress*. Brisbane, ACT, pp. 6–11.
- Bullard, K.L., Schaeffer, M.G., Barker, B.A., Sutley, D. and Levenson, V., 2007. The Stochastic Event Flood Model Applied to Minidoka Dam on the Snake River, Idaho. *World Environmental and Water Resources Congress 2007*, pp.1–11. Available at: <http://ascelibrary.org/doi/abs/10.1061/40927%28243%29425>.
- Bureau of Meteorology, 2014, Hydrologic Reference Stations - Feature Stations, <http://www.bom.gov.au/water/hrs/feature.shtml>, viewed on 24/09/2014
- Bureau of Meteorology (BoM), 2014, Australian Hydrological Geospatial Fabric (Geofabric) GIS Layers Version 2 <http://www.bom.gov.au/water/geofabric/>, Accessed 24 June 2014
- Bureau of Meteorology, 1994. *The estimation of probable maximum precipitation in Australia: Generalised Short Duration Method*.
- Calver, A.; Crooks, S; Jones, D.; Kay, A.; Kjeldsen, T; Reynard, N., 2005. *National river catchment flood frequency method using Continuous Simulation*, London.
- Cameron, D.S, Beven, K.J, Tawn, J, Blazkova, S. and Naden, P., 1999. Flood frequency estimation by Continuous Simulation for a gauged upland catchment (with uncertainty). *Journal*

---

of *Hydrology*, 219(3-4), pp.169–187. Available at:  
<http://linkinghub.elsevier.com/retrieve/pii/S0022169499000578>.

Charalambous, J., Rahman, A. & Carroll, D., 2013. Application of Monte Carlo Simulation Technique to Design Flood Estimation: A Case Study for North Johnstone River in Queensland, Australia. *Water Resources Management*, 27(11), pp.4099–4111. Available at:  
<http://link.springer.com/10.1007/s11269-013-0398-9> [Accessed October 7, 2013].

Chiew, F.H.S., Peel, M.C., Western, A. W. (2002). Application and testing of the simple rainfall-runoff model SIMHYD. In V. P. Singh & D. K. Frevert (Eds.), *Math. Models of Small Watershed Hydrol. & Applications* (pp. 335–367). Colorado: Water Resour. Pub.

Coffs Harbour City Council 2013, *Draft Orara River Rehabilitation Strategy 2013–2022*, CHCC, Coffs Harbour, NSW.

Costa, J. P. da, Rankings and Preferences: New Results in Weighted Correlation and Weighted Principal Component Analysis with Applications, SpringerBriefs in Statistics, Springer, ISBN 3662483440, 9783662483442, 2015

Droop, O.P. & Boughton, W.C., 2002. *Integration of WBNM into A Continuous Simulation System for Design Flood Estimation*, Brisbane.

Duan, Q., Sorooshian, S., & Gupta, V. (1992). Effective and Efficient Global Optimization for Conceptual Rainfall-Runoff Models. *Water Resources Research*, 28(4), 1015–1031.

Engineers Australia, 1998. *Australian Rainfall and Runoff*, Barton, ACT.

England, J., 2011. Flood frequency and design flood estimation procedures in the United States: Progress and Challenges. *Australian Journal of Water Resources*, 15(1), pp.33–45.

England, J.F., 2006. Frequency Analysis And Two-Dimensional Simulations Of Extreme Floods On A Large Watershed. Colorado State University.

Garden, D. S. (1977). *Albany: a panorama of the Sound from 1827*. West Melbourne, Vic.: Thomas Nelson (Australia).

Government of South Australia, 2012, Climate and Weather Atlas of South Australia, <http://www.atlas.sa.gov.au/resources/atlas-of-south-australia-1986/environment-resources/climate-and-weather>, viewed 23/09/2014

Government of Western Australia, Kimberly Development Commission, 2014 <http://kdc.wa.gov.au/the-kimberly/climate/>. Viewed on 23/09/2014

Gupta, H.V., Sorooshian, S. & Yapo, P.O., 1998. Toward improved calibration of hydrologic models: Multiple and noncommensurable measures of information. *Water Resources Research*, 34(4), pp.751–763.

Gupta, V.K. & Sorooshian, S., 1985. The relationship between data and the precision of parameter estimates of hydrologic models. *Journal of Hydrology*, 81, pp.57–77.

Haberlandt, U. & Radtke, I., 2013. Derived flood frequency analysis using different model calibration strategies based on various types of rainfall–runoff data – a comparison. *Hydrology and Earth System Sciences Discussions*, 10(8), pp.10379–10417. Available at:  
<http://www.hydrol-earth-syst-sci-discuss.net/10/10379/2013/> [Accessed October 13, 2013].

- Hill, P. & Mein, R.G., 1996. Incompatibilities between storm temporal patterns and losses for design flood estimation. In *23rd Hydrology and Water Resources Symposium*. Hobart, pp. 445–451.
- Hoang, T.M.T. et al., 1999. Joint Probability Description of Design Rainfalls. In *Water 99 Joint Congress*. Brisbane, pp. 6–11.
- Institute for Veterinary Public Health, 2010. *World Maps of the Koppen-Geiger Climate Classification, Koppen-Geiger Observed Climate zones 1976-2000*, <http://koeppen-geiger.vu-wien.ac.at/shifts.htm>, accessed 10 June 2014
- Kisters, 2005. WISKI Modelling version 4.2.0.8. <http://kisters.com.au/wiski-modules.html>
- Kjeldsen, T.R., 2007. *The revitalised FSR / FEH rainfall-runoff method*,
- Klemeš, V., 1986. Operational testing of hydrological simulation models. *Hydrological Sciences Journal*, 31(1), pp.13–24. Available at: <http://www.tandfonline.com/doi/abs/10.1080/02626668609491024> [Accessed October 13, 2013].
- Kuczera, G., Lambert, M., Heneker, T., Jennings, S., Frost, A. and Coombes, P., 2006a. Joint probability and design storms at the crossroads. In *28th International Hydrology and Water Resources Symposium*. Wollongong, pp. 10–14.
- Kuczera, G., Kavetski D., Franks, S. and Thyer, M., 2006b. Towards a Bayesian total error analysis of conceptual rainfall-runoff models: Characterising model error using storm-dependent parameters. *Journal of Hydrology*, 331(1-2), pp.161–177.
- Linsley, R.K., Crawford, N.H., 1960. Computation of a synthetic streamflow record on a digital computer. In *Int. Assoc. Sci. Hydrol.* pp. 526–538.
- Martinez, G. F., & Gupta, H. V. (2010). Toward improved identification of hydrological models : A diagnostic evaluation of the “ abcd ” monthly water balance model for the conterminous United States. *Water Resources Research*, 46, 1–21. doi:10.1029/2009WR008294
- Mathevet, T. (2005). *Which rainfall–runoff model at the hourly time-step? Empirical development and intercomparison of rainfall–runoff models on a large sample of watersheds*. ENGREF, Paris, FRANCE
- Mirfenderesk, H., Chong, D., Carroll E., Rahman, M., Kabir, M., Doorn, R.V. and Vis, S., 2005. Comparison between Design Event and Joint Probability Hydrological Modelling. , pp.1–9.
- Montanari, A. & Brath, A., 2004. A stochastic approach for assessing the uncertainty of rainfall-runoff simulations. *Water Resources Research*, 40(1).
- Montanari, A. & Grossi, G., 2008. Estimating the uncertainty of hydrological forecasts: A statistical approach. *Water Resources Research*, 44(12).
- Naghetini, M., Potter, K.W. & Illangasekare, T., 1996. Estimating the upper tail of flood-peak frequency distributions using hydrometeorological information. *Water Resources Research*, 32(6), pp.1729–1740. Available at: <http://doi.wiley.com/10.1029/96WR00200>.
- Nathan, R., Weinmann, E., Hill, P. , 2003: *Use of Monte Carlo Simulation to Estimate the Expected Probability of Large to Extreme Floods*, Pro. 28<sup>th</sup> Int. Hydrology and Water Resources Symposium, Wollongong, pp 1.105-1.112

- Nathan, R. & Weinmann, E., 2013. *Australian Rainfall & Runoff, Discussion Paper: Monte Carlo Simulation Techniques*, Barton, ACT.
- Nathan, R., Weinmann, E. & Hill, P., 2003. Use of Monte Carlo Simulation to Estimate the Expected Probability of Large to Extreme Floods. In *28th International Hydrology and Water Resources Symposium*. Wollongong, NSW: The Institution of Engineers, Australia, pp. 105 – 112.
- Nathan, R.J., Weinmann, P.E. & Hill, P.I., 2002. Use of a Monte Carlo Framework to Characterise Hydrologic Risk. In *ANCOLD Conference on Dams*. pp. 53–62.
- Nathan, R.J.; Weinmann, P.E., 1999. Estimation of Large to Extreme Floods. In *Australian Rainfall and Runoff, A guide to Flood Estimation, Book VI*. Institution of Engineers Australia.
- Newton, D. & Walton, R., 2000. Continuous Simulation for Design Flood Estimation in the Moore River Catchment, Western Australia. In *Hydro 2000 Hydrology and Water Resources Symposium*. Canberra, ACT, pp. 475–480.
- Paquet, E., Garavaglia, F., Garcon, R. and Gailhard, J., 2013. The Schadex Method - A Semi-Continuous Rainfall Runoff Simulation for Extreme Flood Estimation. *Journal of Hydrology*, 495, pp.23–37.
- Pilgrim, D.H, Cordery, I. and French, R., 1969. Temporal patterns of design rainfall for Sydney. *Civil Engng. Trans., I.E. Aust*, CE11(1), pp.9–14.
- Pointen, S.M. and A.W.Collins, 2000. Mary River Catchment Resource Atlas. Queensland Government, Department of Natural Resources, DNRQ00114
- Rahman, A., Carroll, D. & Weinmann, E., 2002a. Integration Of Monte Carlo Simulation Technique With URBS Model For Design Flood Estimation. In *Hydrology and Water Resources Symposium*.
- Rahman, A., Weinmann, E. & Mein, R.G., 2002b. The Use of Probability-distributed Initial Losses in Design Flood Estimation. *Australian Journal of Water Resources*, 6(1), pp.17–29.
- Rigby, E.H. & Bannigan, D.J., 1996. The Embedded Design Storm Concept · A Critical Review. In *23rd Hydrology and Water Resources Symposium*. Hobart, pp. 453–459.
- SEQ Water, 2013, Baroon Pocket Dam <http://www.seqwater.com.au/water-supply/dam-operations/baroon-pocket-dam>
- Singh, S. K. and Bárdossy, A., 2012. Calibration of hydrological models on hydrologically unusual events. *Advances in Water Resources*, 38, pp.81–91.
- Srikanthan, R. & McMahon, T. a., 2001. Stochastic generation of annual, monthly and daily climate data: A review. *Hydrology and Earth System Sciences*, 5(4), pp.653–670. Available at: <http://www.hydrol-earth-syst-sci.net/5/653/2001/>.
- The Institution of Engineers Australia, 1987: *Australian Rainfall and Runoff, A Guide to Flood Estimation*, Volume 2. Ed. R.P.Canterford. Canberra, Australia.
- University of Newcastle, 2013: FLIKE Flood Frequency Analysis, Beta Version 5. September 2013.

Walsh, M.A., Pilgrim, D.H. & Cordery, I., 1991. Initial Losses for Design Flood Estimation in New South Wales. In *Hydrology and Water Resources Symposium*. pp. 283–288.

Water and Rivers Commission, 2003. SWMOD Version 2 A Rainfall Loss Model for Calculating Rainfall Excess, User Manual (Version 2.11)

Weinmann, P.E., Rahman, A., Hoang, T.M.T., Laurenson, E.M. and Nathan, R.J., 2002. Monte Carlo Simulation of Flood Frequency Curves from Rainfall – The Way Ahead. *Australian Journal of Water Resources*, 6(1), pp.71–79.



## **13. Appendices**

## Appendix A Catchment data

Table A.1: Pluviograph data

State	Catchment	Station ID	Station Name	Data Source*	Time step	Start	End
QLD	Mary	40059	Cooroy Composite	BOM	6 min	01/11/1971	01/03/2012
QLD	Mary	40062	Crohamhurst	BOM	6 min	01/02/1960	01/02/2001
QLD	Mary	40102	Jimna Composite	BOM	6 min	01/02/1972	01/02/2000
QLD	Mary	40106	Kenilworth Township	BOM	6 min	01/07/1981	01/04/2010
QLD	Mary	40121	Maleny Tamarind St	BOM	6 min	01/08/2002	01/05/2014
QLD	Mary	40133	Monsildale	BOM	6 min	01/08/1963	01/02/1978
QLD	Mary	40282	Nambour Dpi	BOM	6 min	01/01/1954	01/12/2008
QLD	Mary	40386	Kenilworth Bridge	BOM	6 min	01/06/1963	01/08/1981
QLD	Mary	40651	Jimna Forestry	BOM	6 min	01/04/2001	01/02/2014
QLD	Mary	40988	Nambour Daff - Hillside	BOM	6 min	01/12/2007	01/02/2014
WA	Hann	1018	Mount Elizabeth	BOM	6 min	01/11/1993	01/03/2013
WA	Hann	2009	Gibb River	BOM	6 min	01/02/1963	01/05/2012
WA	Hann	3051	Mount Barnett	BOM	6 min	01/09/1983	01/05/2012
WA	Hann	3097	Beverley Springs Airstrip	BOM	6 min	01/10/1999	01/10/2002
WA	Hann	3098	Mount House Airstrip	BOM	6 min	01/09/2002	01/11/2008
WA	Yates	509022	Woonanup	DOW	6 min	25/05/1972	11/06/2012
NT	Manton	14272	Batchelor Airport	BOM	6 min	01/03/2001	01/03/2013
NT	Manton	R8150332	Darwin R At West Track	DLRM	Hourly	18/01/1963	10/02/2011
SA	Sixth Creek	AW504559	Cherryville		6 min	20/07/1983	22/08/2011

SA	Sixth Creek	23801	Lenswood Research Centre	BOM	6 min	01/10/1972	01/08/2011
VIC	Lerderderg	87017	Blackwood	BOM	6 min	01/02/1974	01/07/2011
VIC	Lerderderg	87112	Blakeville (Bullarto Camp)	BOM	6 min	01/11/1965	01/06/1970
VIC	Lerderderg	87155	Lerderderg No 1 Recorder	BOM	6 min	01/02/1974	01/03/1981
VIC	Lerderderg	87154	Lerderderg No2 Recorder	BOM	6 min	01/05/1973	01/03/1981
VIC	Lerderderg	87153	Lerderderg No3 Recorder	BOM	6 min	01/05/1973	01/03/1981
VIC	Lerderderg	87152	Lerderderg No4 Recorder	BOM	6 min	01/11/1973	01/02/1981
VIC	Lerderderg	88133	Newbury	BOM	6 min	01/08/1968	01/02/1997
TAS	Florentine	2008	Misery Plateau	HT	5 min	09/05/1997	13/10/2014
TAS	Florentine	881	Butlers Gorge	HT	5 min	13/05/1992	23/06/2012
TAS	Florentine /Tyenna	886	Florentine Crossing	HT	6 min	17/06/1960	03/01/1989
TAS	Tyenna	1038	Tyenna at Sharpes Siding	HT	6 min	29/06/1982	29/12/1988
TAS	Tyenna	92019	Mt Mawson	BOM	6 min	01/05/2007	14/01/2012
TAS	Tyenna	95063	Maydena PO	BOM	Daily	01/10/1992	23/09/2014
TAS	Tyenna	95065	Tyenna (Marriotts Falls Rd)	BOM	Daily	01/04/1994	31/10/2006
TAS	Tyenna	95075	Westerway	BOM	Daily	01/06/2002	31/08/2014
TAS	Tyenna	95077	National Park	BOM	Daily	26/02/2004	31/08/2014
TAS	Tyenna	95080	Tyenna (Tyenna Road)	BOM	Daily	01/11/2006	30/06/2014
TAS	Tyenna	299	Tyenna Pluvio - National Park	HT	5 min	21/02/1989	15/12/2011
TAS	Florentine/ Tyenna	309	Salvation Creek	HT	5 min	17/08/1989	30/09/2014
TAS	Tyenna	338	Mt Tim Shea	HT	5 min	08/08/1990	18/09/2014
TAS	Tyenna	499	Tyenna At Newbery	DPIPWE	5 min	23/04/2010	28/09/2014

TAS	Hobart	94029	Ellerslie Rd	BOM	30 min	20/10/1994	09/02/2012
TAS	Hobart	94087	Mt Wellington	BOM	30 min	05/07/1990	09/02/2012
TAS	Hobart	2020	Myrtle Gully	HCC	30 min	03/01/1995	06/10/2014
TAS	Hobart	2516	Cascade Gardens	HCC	Event	26/06/2006	06/10/2014
TAS	Hobart	1881	Springs	HCC	Event	01/10/1993	06/10/2014
NSW	Orara	59026	Upper Orara (Aurania)	BOM	Hourly	01/04/1970	01/02/2010

\*BOM – Bureau of Meteorology

HCC – Hobart City Council

DPIPWE – Department of Primary Industries Water and Environment

HT – Hydro Tasmania

DLRM – Department of Land and Resource Management

DOW - Department of Water

## A.1 Temporal Patterns

### A.1.1 Mary River

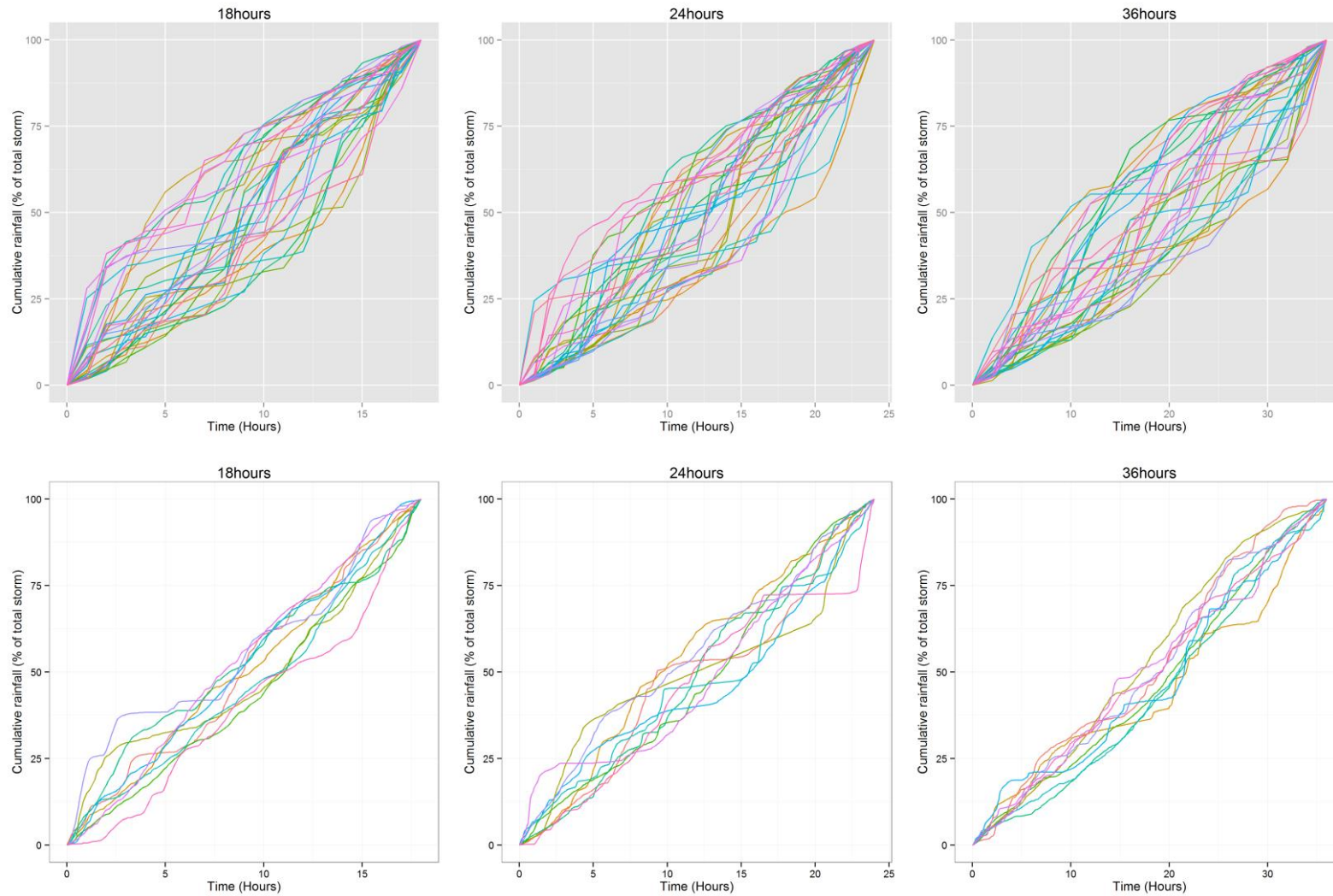


Figure A.1: Temporal patterns used in Mary River models for the Monte Carlo (top row) and Design events (bottom row) runs

A1.1.2 Hann River

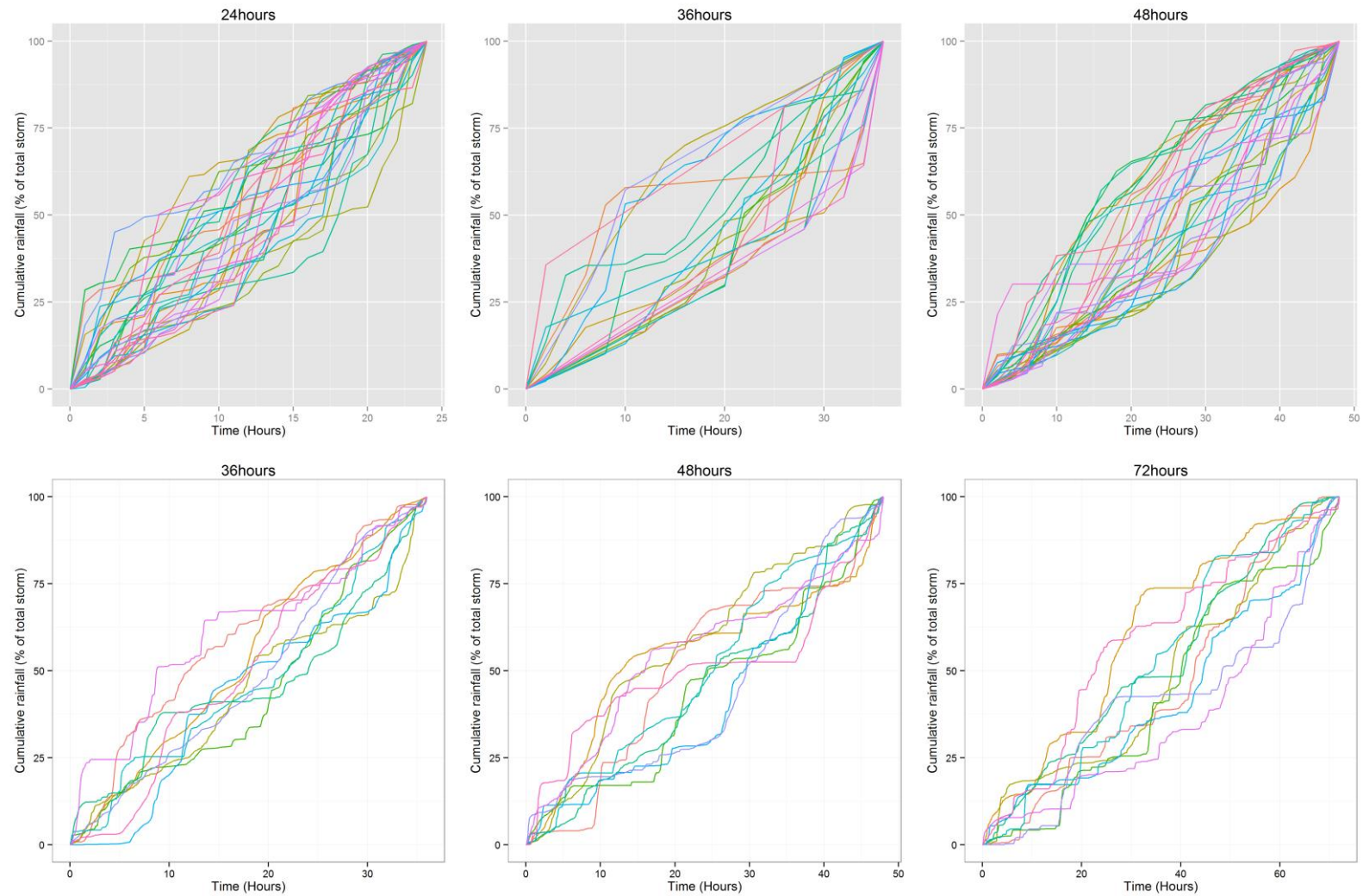


Figure A.2: Temporal patterns used in Hann River models for Monte Carlo (top row) and Design events (bottom row) runs

### A1.1.3 Yates Flat Creek

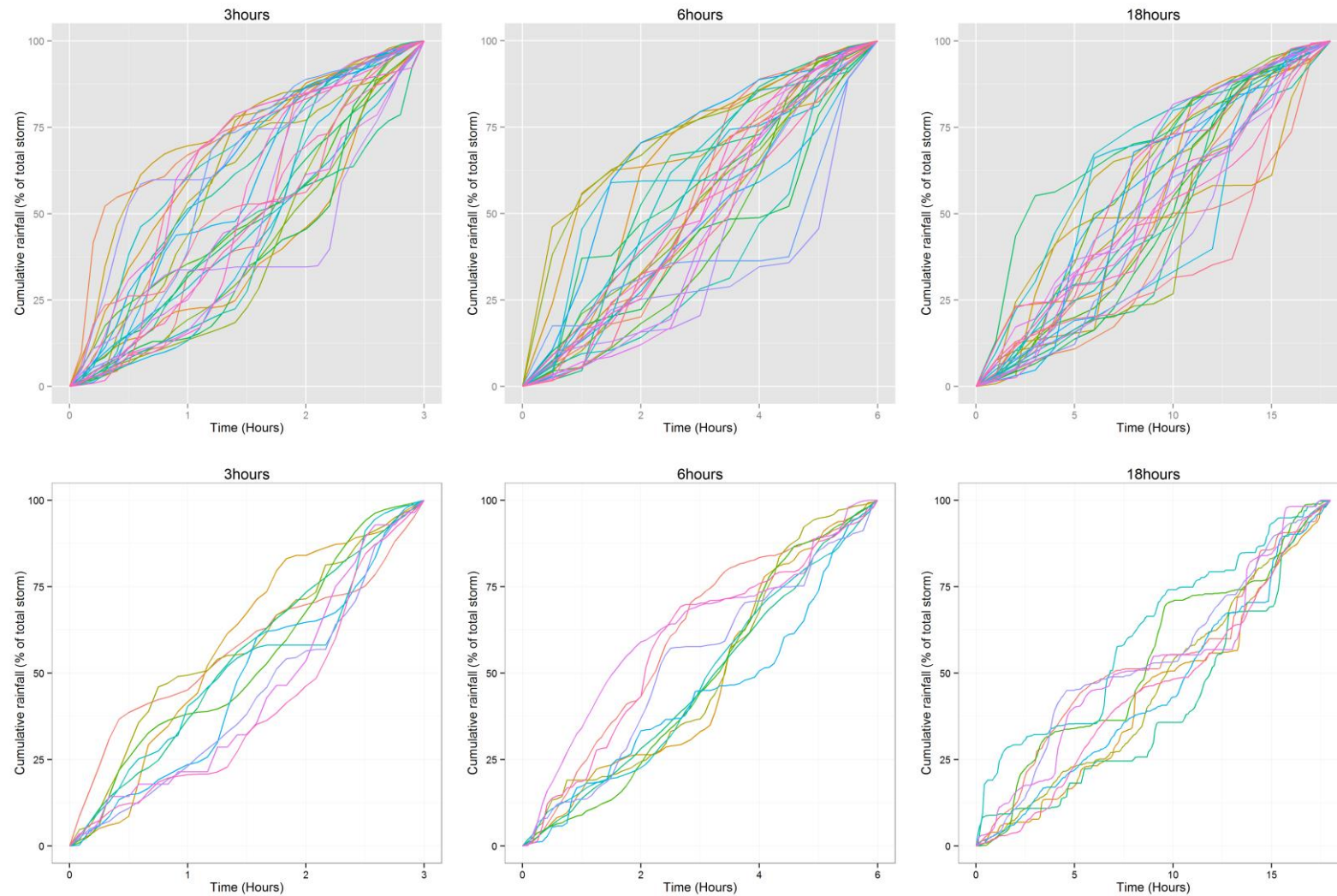


Figure A.3: Temporal patterns used in Yates Flat Creek models for Monte Carlo (top row) and Design events (bottom row) runs

A1.1.4 Manton River

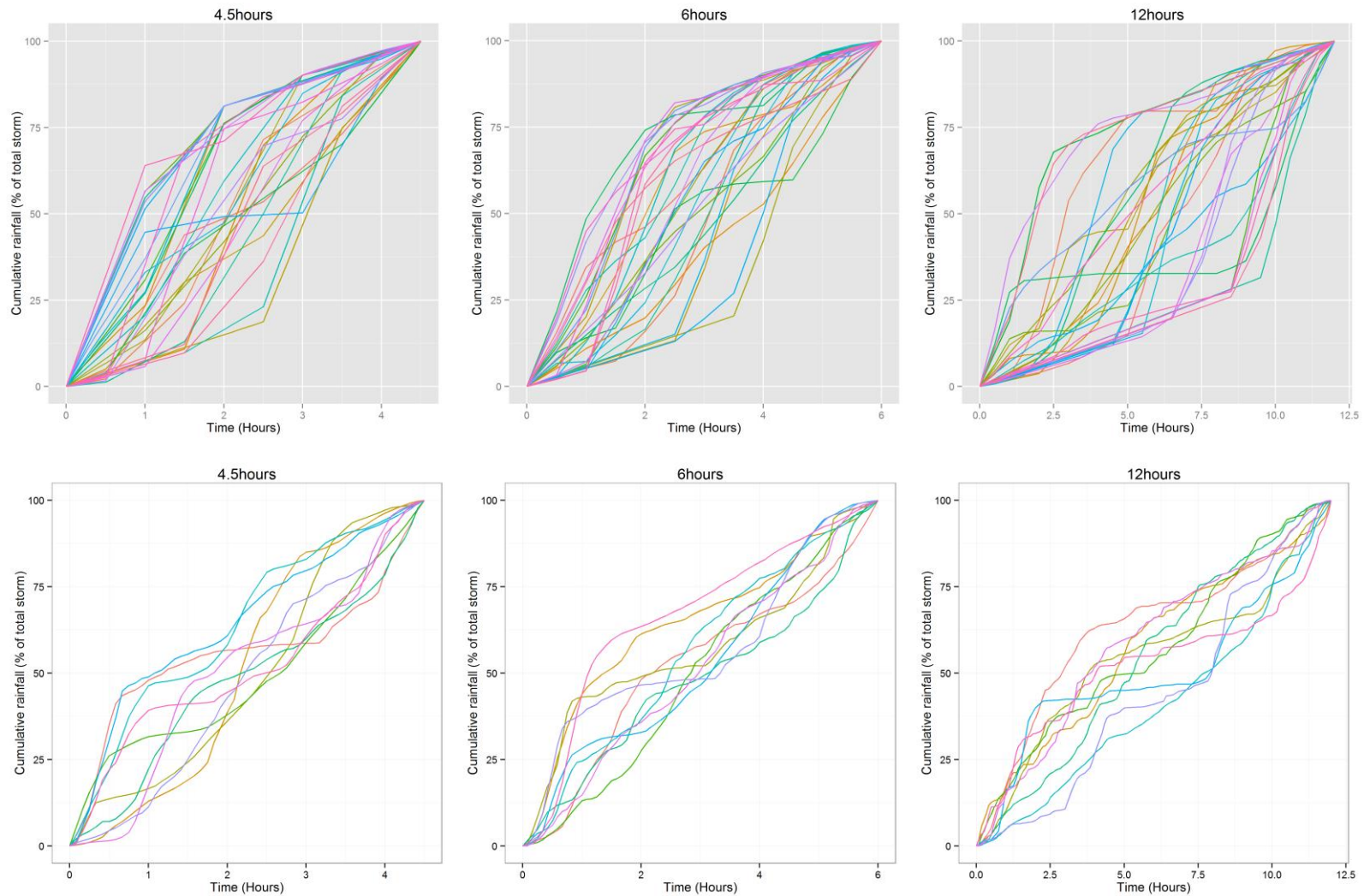


Figure A.4: Temporal patterns used in Manton River models for Monte Carlo (top row) and Design events (bottom row) runs



A1.1.5 Sixth Creek

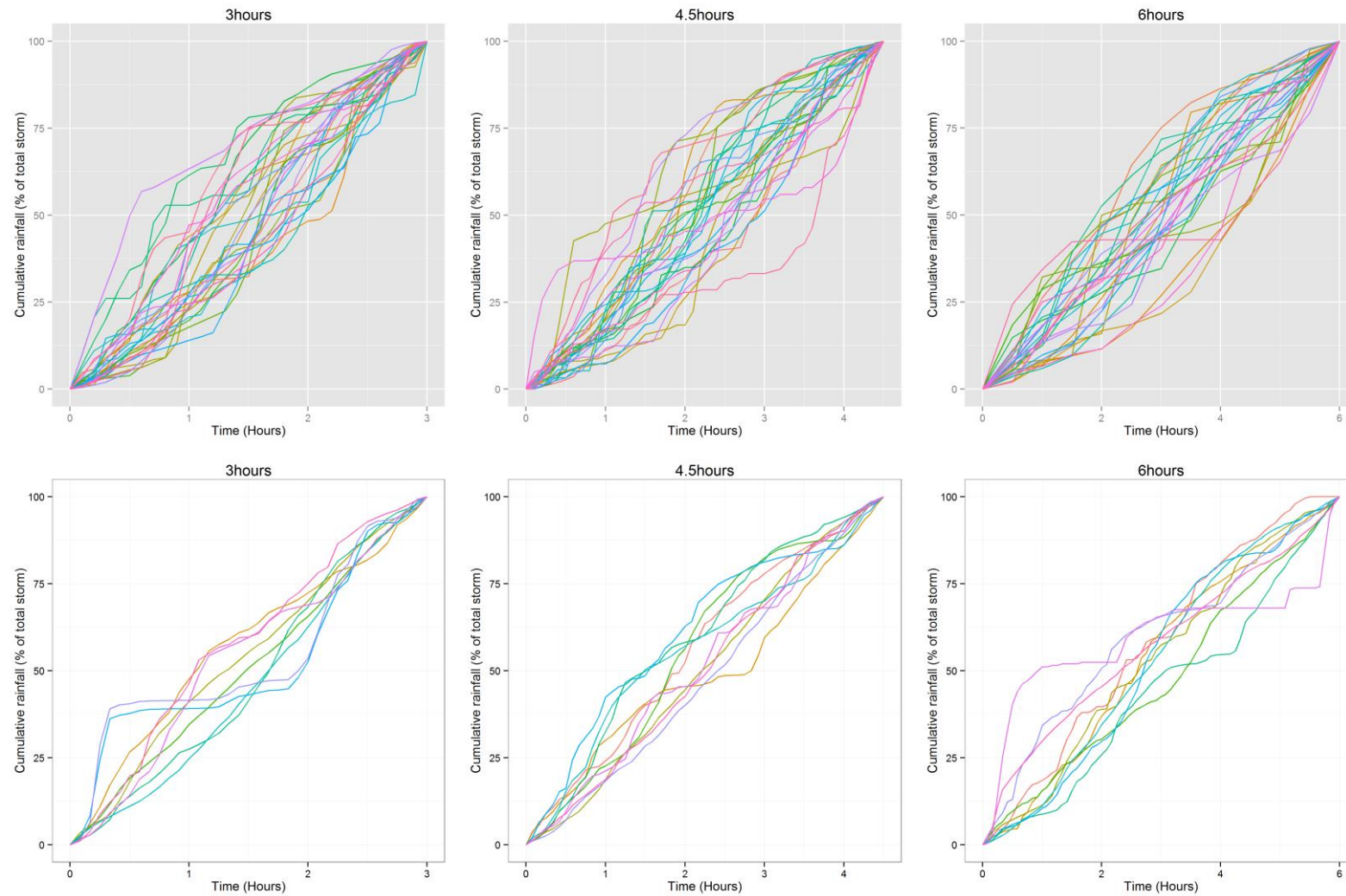


Figure A.5: Temporal Patterns used in Sixth Creek models for Monte Carlo (top row) and Design events (bottom row) runs

### A1.1.6 Lerderderg River

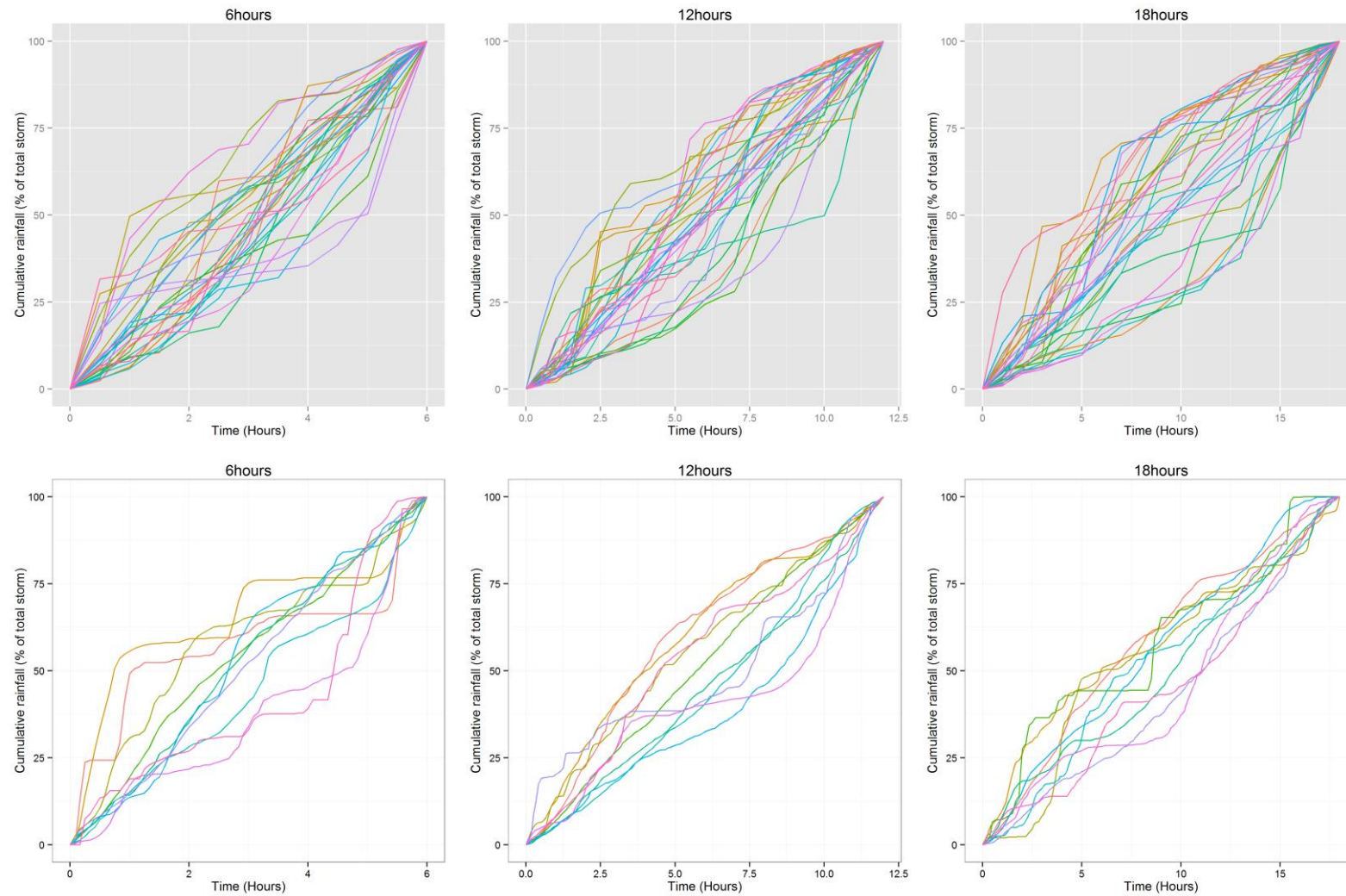


Figure A.6: Temporal Patterns used in Lerderderg River models for Monte Carlo (top row) and Design events (bottom row) runs

A1.1.7 Florentine

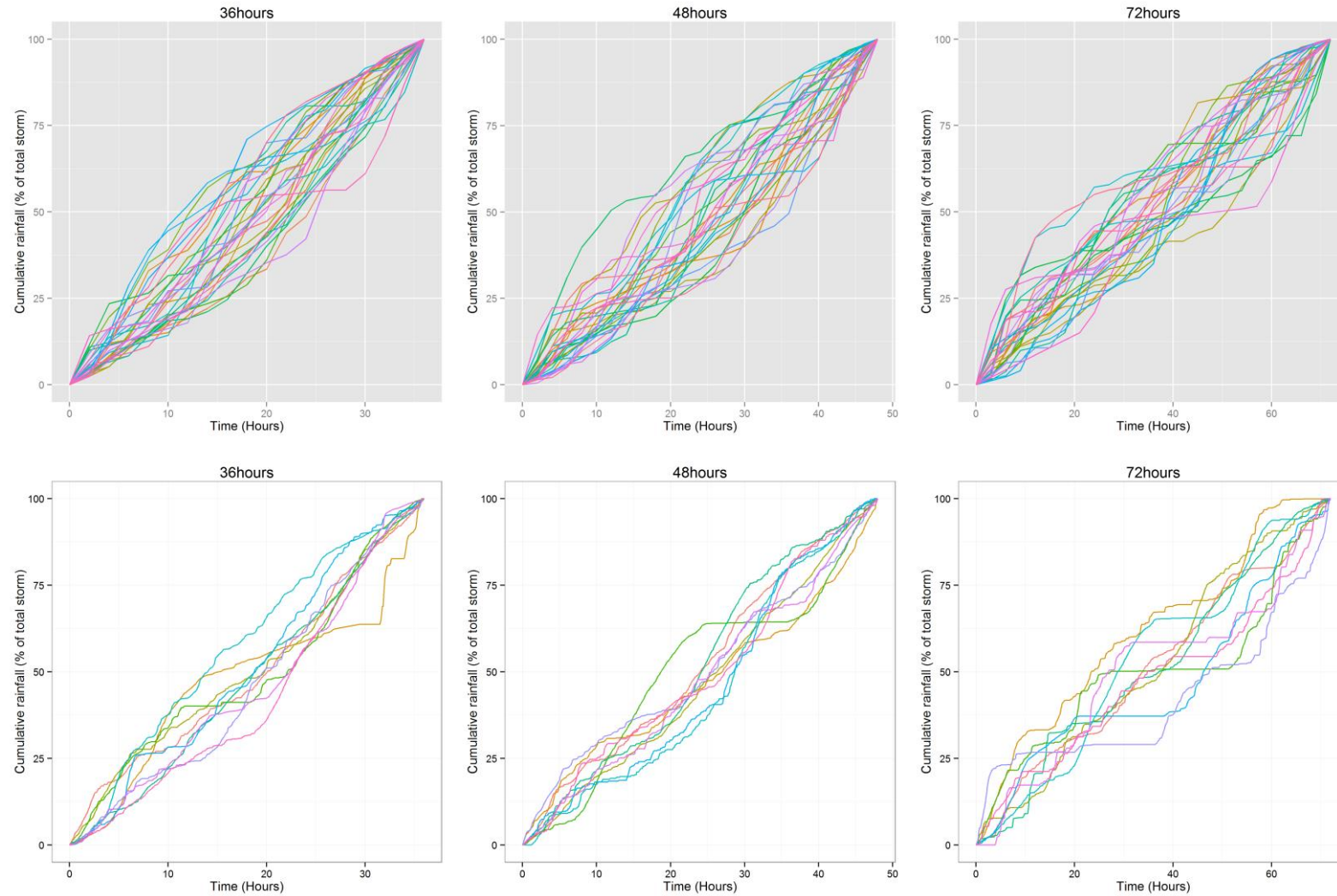


Figure A.7: Temporal Patterns used in Florentine River models for Monte Carlo (top row) and Design events (bottom row) runs

### A1.1.8 Tyenna River

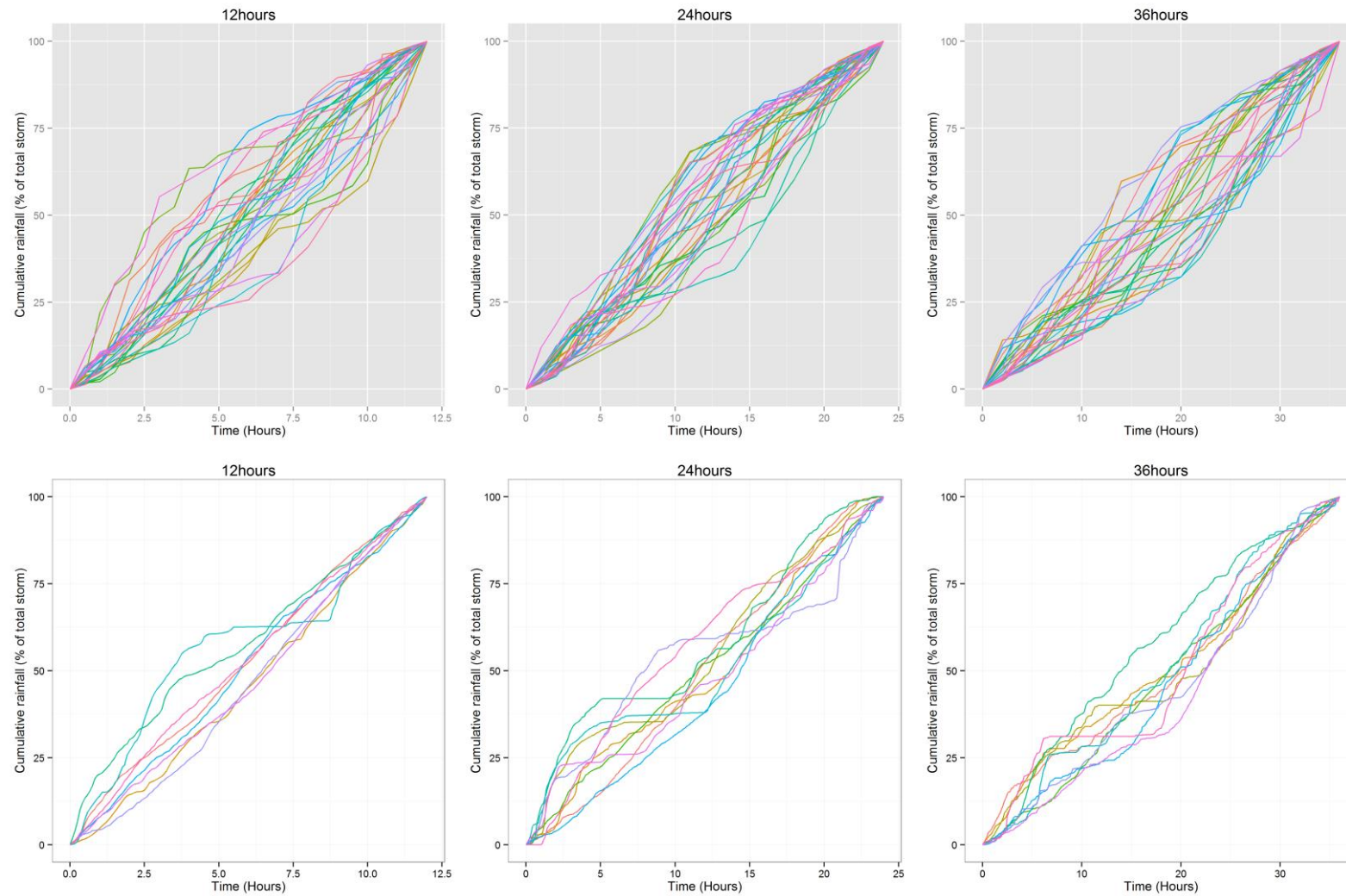


Figure A.8: Temporal Patterns used in Tyenna River models for Monte Carlo (top row) and Design events (bottom row) runs

A1.1.9 Hobart Rivulet

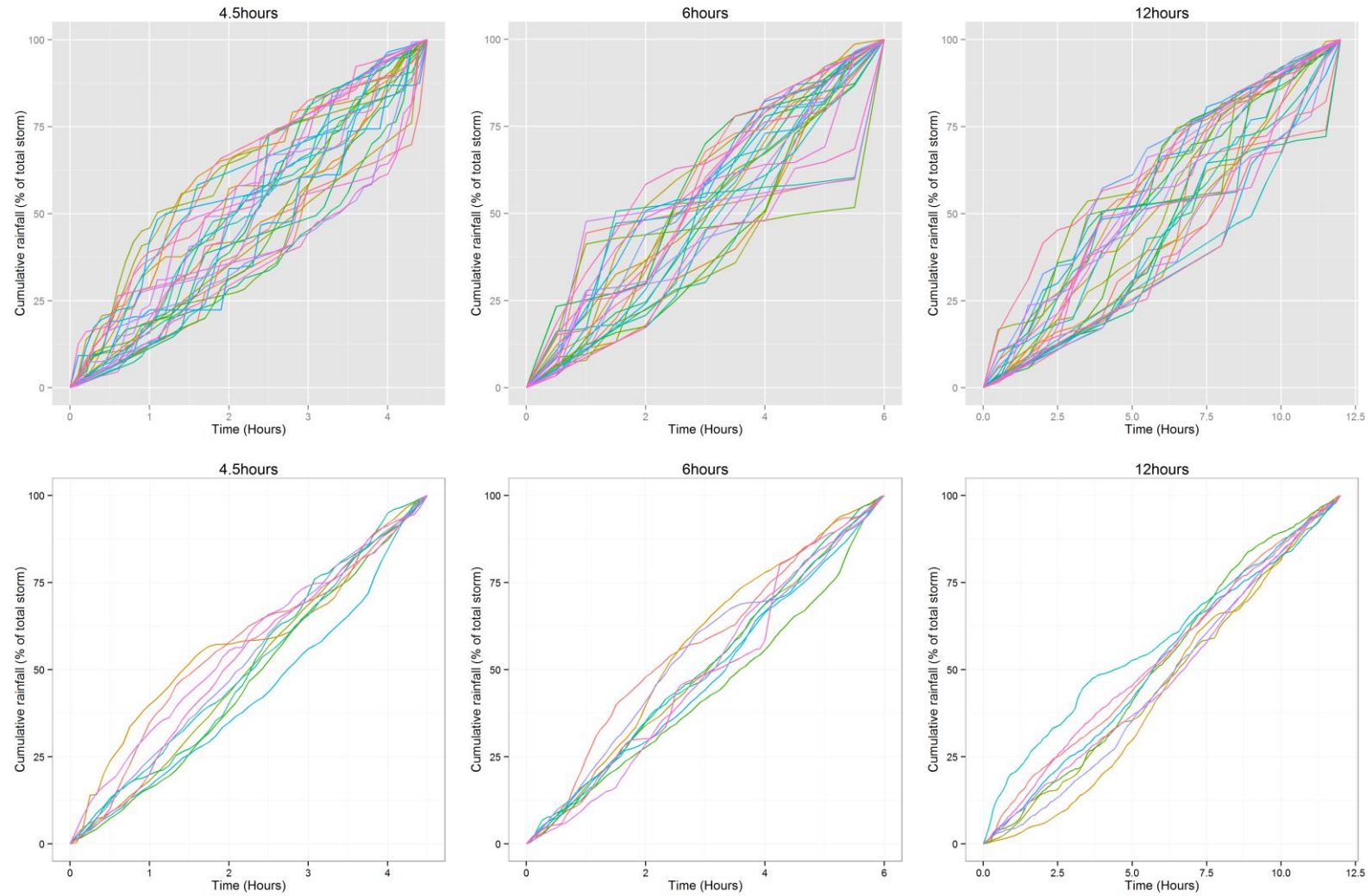


Figure A.9: Temporal Patterns used in Hobart Rivulet models for Monte Carlo (top row) and Design events (bottom row) runs

A1.1.10 Orara River

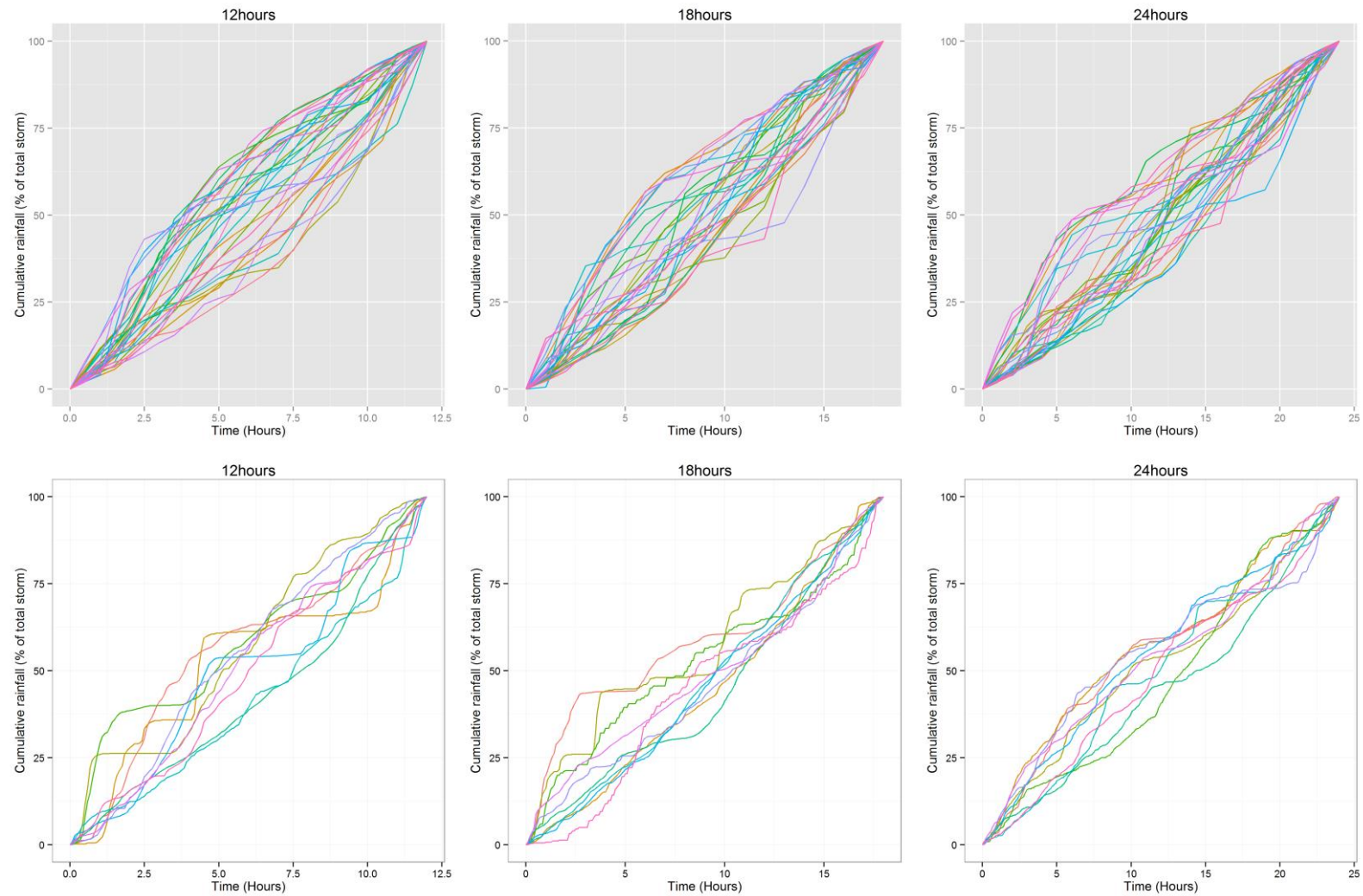


Figure A.10: Temporal Patterns used in Orara River models for Monte Carlo (top row) and Design events (bottom row) runs

## A.2 Design Rainfalls

**Table A.2: Mary River design catchment rainfalls in mm**

AEP	Duration (hours)								
	2	3	4.5	6	12	18	36	48	72
50%	32	39	47	55	79	99	142	161	189
20%	44	54	66	78	117	148	216	247	290
10%	52	64	80	94	144	185	273	313	367
5%	60	74	93	111	172	223	333	383	451
2%	70	88	112	134	212	277	420	485	574
1%	79	99	127	153	244	322	493	572	680
0.1%	108	138	180	220	364	489	774	907	1090

**Table A.3: Hann River design catchment rainfalls in mm**

AEP	Duration (hours)								
	2	3	4.5	6	12	18	36	48	72
50%	24	30	37	42	57	68	87	97	113
20%	32	40	50	57	79	95	124	138	162
10%	36	47	58	67	94	114	150	168	197
5%	41	53	66	77	109	133	176	197	232
2%	47	61	76	89	128	158	212	239	280
1%	51	66	84	99	143	178	240	271	319
0.1%	65	86	110	131	195	247	342	389	457

**Table A.4: Yates Flat Creek design catchment rainfalls in mm**

AEP	Duration (hours)								
	2	3	4.5	6	12	18	36	48	72
50%	15	18	21	23	31	36	46	50	57
20%	20	24	28	31	41	49	63	69	78
10%	24	28	33	37	50	59	77	85	95
5%	28	33	39	43	59	71	93	102	114
2%	34	39	46	53	72	88	117	129	144
1%	38	44	53	60	84	103	138	153	170
0.1%	54	63	75	87	127	160	221	245	272

**Table A.5: Manton River design catchment rainfalls in mm**

AEP	Duration (hours)								
	2	3	4.5	6	12	18	36	48	72
50%	55	61	67	71	84	94	121	137	164
20%	70	78	87	94	114	130	171	193	230
10%	79	89	101	109	136	157	209	236	280
5%	87	100	113	124	158	185	250	284	335
2%	98	112	130	144	189	225	312	354	416
1%	105	122	142	159	215	260	363	412	482
0.1%	127	152	184	212	310	388	557	631	728



**Table A.6: Sixth Creek design catchment rainfalls in mm**

AEP	Duration (hours)								
	2	3	4.5	6	12	18	36	48	72
50%	18	22	26	30	41	50	67	75	87
20%	24	28	34	39	54	65	86	96	111
10%	28	33	40	46	63	75	100	111	127
5%	32	39	46	53	72	86	113	125	142
2%	39	46	56	63	85	102	132	145	162
1%	45	53	63	72	97	114	146	160	178
0.1%	65	77	91	103	136	158	195	210	229

**Table A.7: Lerderderg design catchment rainfalls in mm**

AEP	Duration (hours)								
	2	3	4.5	6	12	18	36	48	72
50%	16	19	23	26	37	44	61	68	77
20%	22	26	31	35	50	60	84	94	107
10%	27	31	37	42	59	72	101	113	128
5%	32	37	44	50	69	84	117	131	148
2%	39	45	53	60	83	100	140	156	176
1%	45	52	61	69	95	114	158	176	198
0.1%	67	77	89	100	136	162	221	245	274

**Table A.8: Florentine River design catchment rainfalls in mm**

AEP	Duration (hours)								
	3	6	9	12	18	24	36	48	72
50%	15	23	29	34	43	50	61	70	84
20%	20	30	38	45	56	64	78	89	107
10%	23	35	44	52	64	75	91	104	124
5%	26	39	50	59	73	85	103	118	140
2%	30	45	57	68	84	98	120	137	163
1%	33	49	63	75	93	109	134	153	181
0.1%	44	64	82	99	123	146	182	208	243

**Table A.9: Tyenna River design catchment rainfalls in mm**

AEP	Duration (hours)								
	3	6	9	12	18	24	36	48	72
50%	16	23	29	33	42	47	57	65	78
20%	21	30	38	44	55	62	75	85	101
10%	25	35	44	51	64	72	87	99	117
5%	28	40	50	58	73	82	100	113	134
2%	32	46	57	67	85	96	117	133	157
1%	35	50	62	74	94	107	131	149	176
0.1%	45	64	81	97	125	144	179	206	243

**Table A.10: Hobart Rivulet design** catchment rainfalls in mm

AEP	Duration (hours)								
	2	3	4.5	6	12	18	36	48	72
50%	14	20	25	29	42	51	57	65	70
20%	19	28	35	41	60	72	81	93	100
10%	23	33	42	49	72	87	98	113	122
5%	27	38	48	57	84	102	116	133	144
2%	31	45	56	66	99	122	139	162	175
1%	35	50	62	74	111	137	157	184	200
0.1%	49	67	84	99	152	191	222	265	290

**Table A.11: Orara River design** catchment rainfalls in mm

AEP	Duration (hours)								
	4.5	6	9	12	18	24	36	48	72
50%	62	73	92	110	141	168	211	243	287
20%	88	104	133	158	204	243	304	351	413
10%	108	128	164	196	250	297	371	425	499
5%	130	154	197	235	300	354	438	500	583
2%	163	194	247	293	370	434	530	600	694
1%	192	228	290	343	429	499	604	678	780
0.1%	300	358	453	530	648	739	867	957	1079

## Appendix B Catchment models

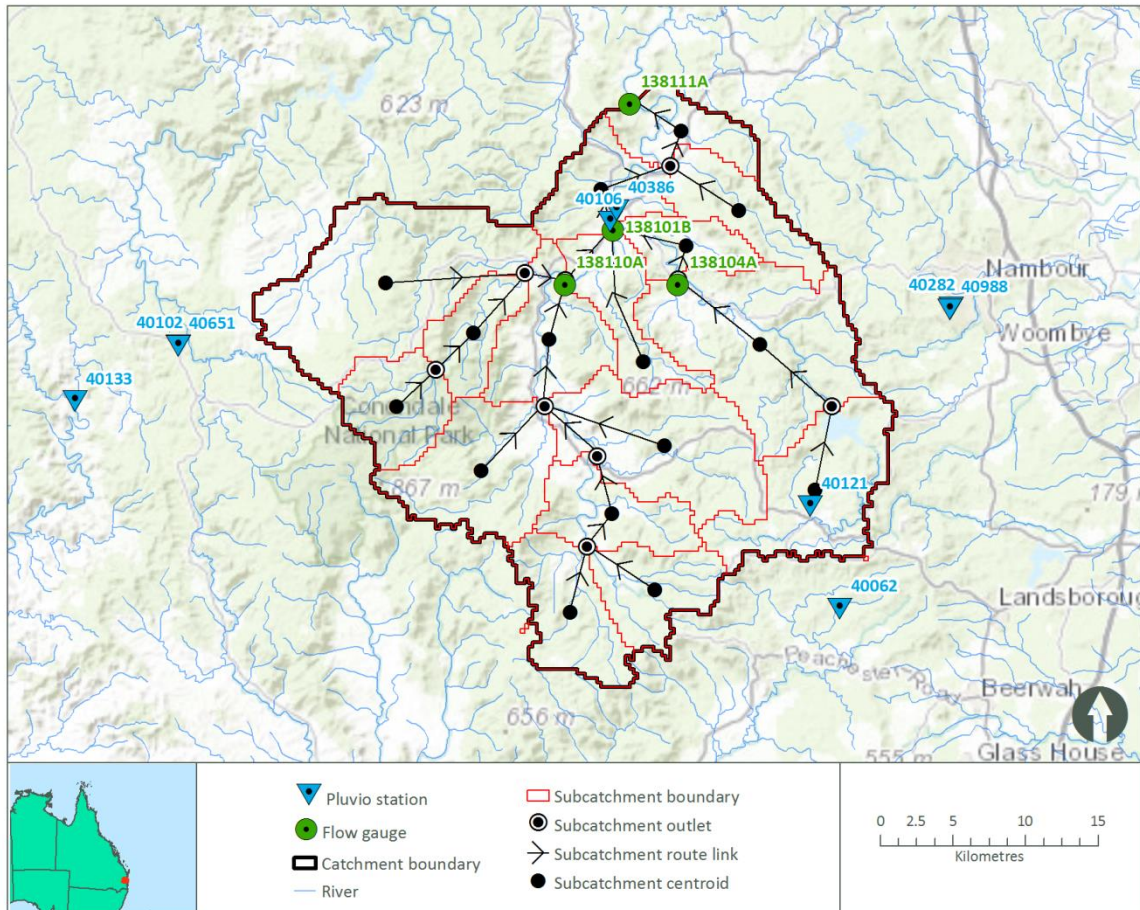


Figure B.1: Subcatchment breakup and routing links for distributed model of Mary River catchment

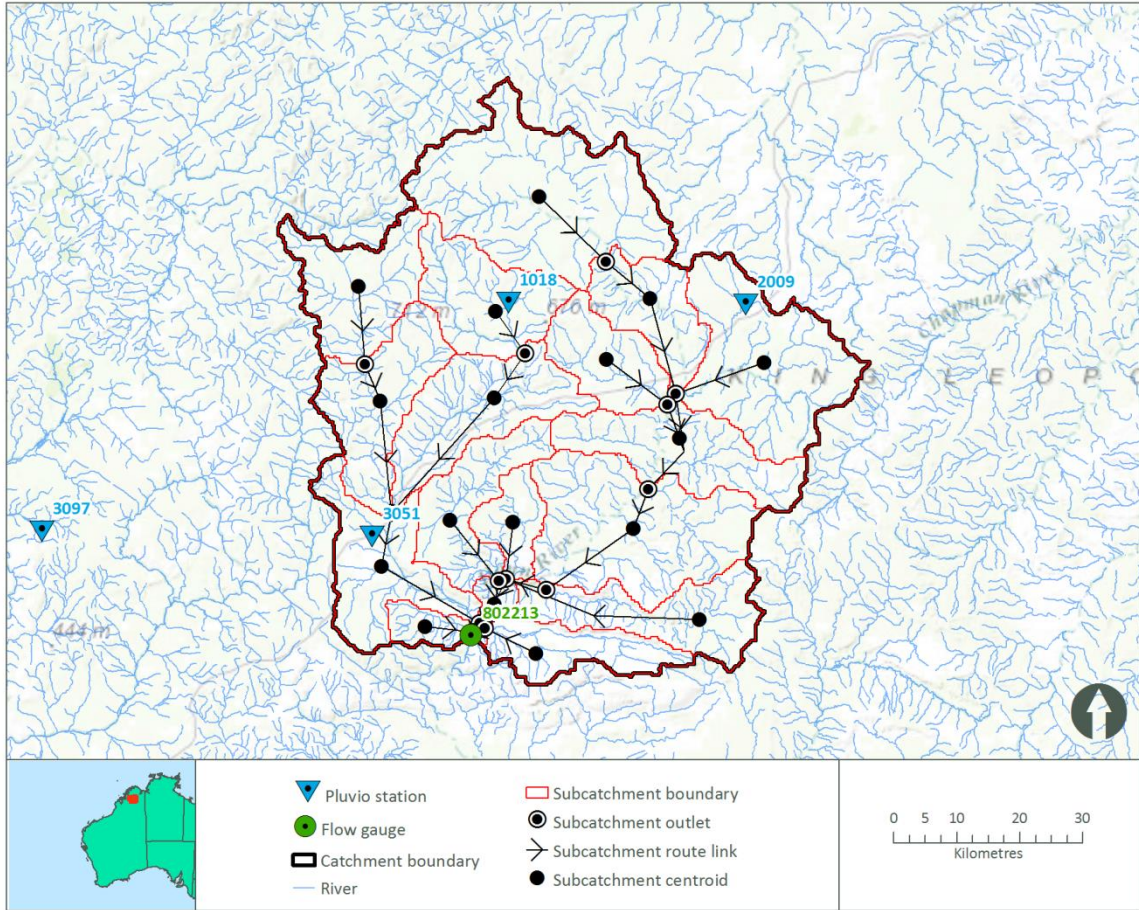


Figure B.13-1: Subcatchment breakup and routing links for distributed model of Hann River catchment

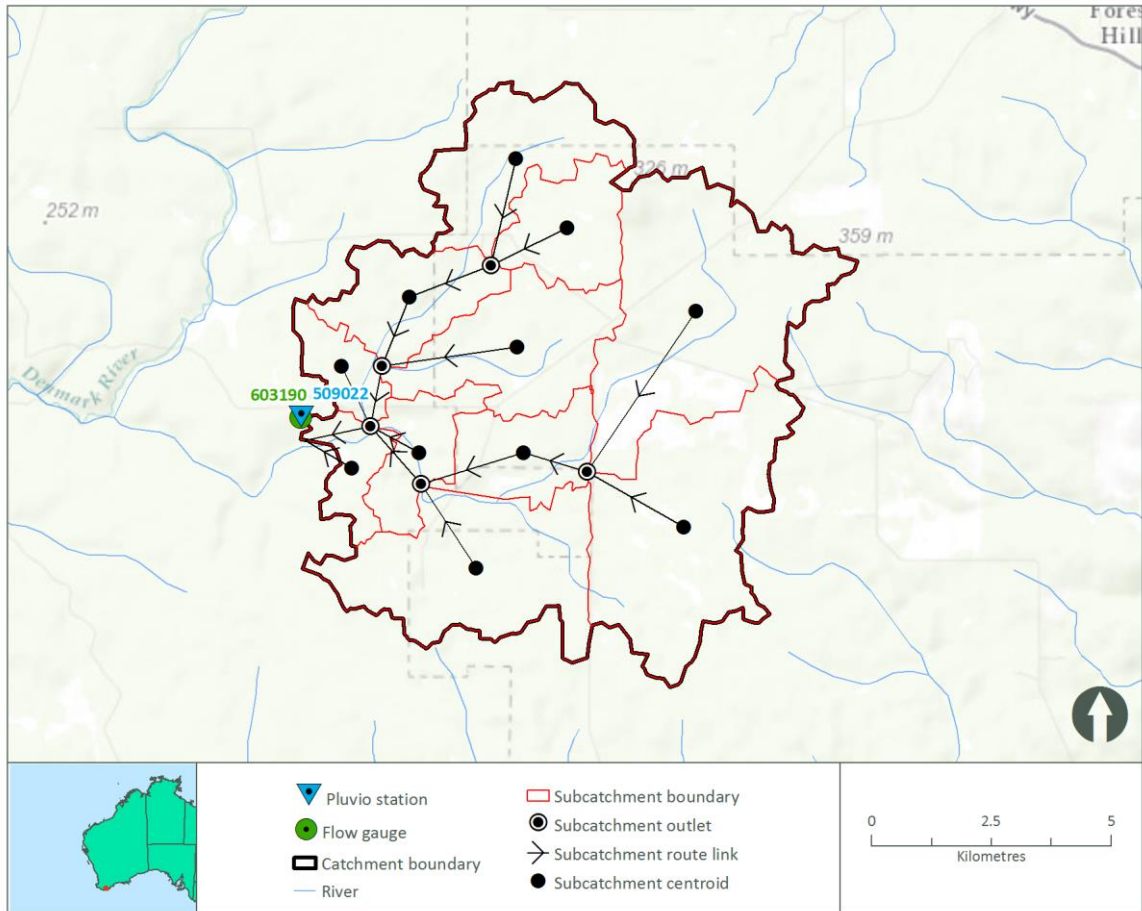


Figure B.13-2: Subcatchment breakup and routing links for distributed model of Yates Flat Creek catchment

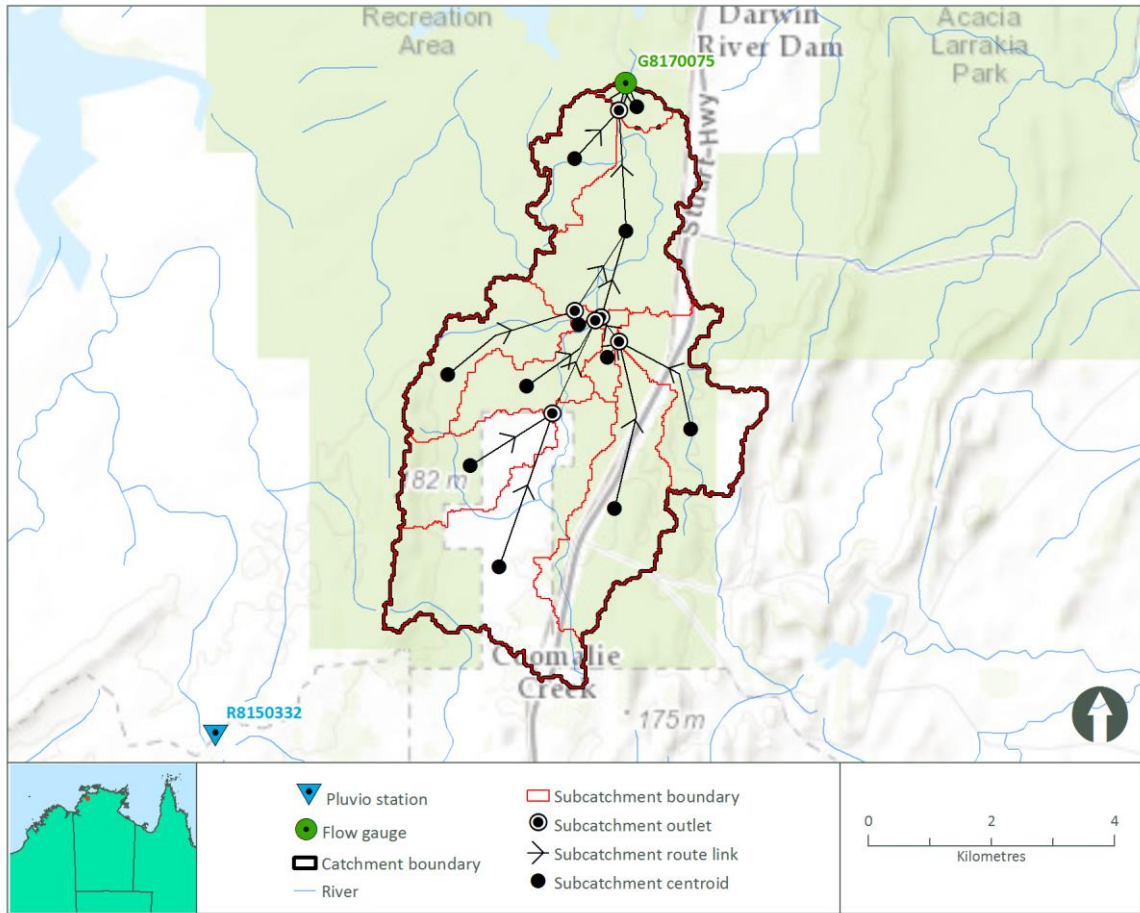


Figure B.13-3: Subcatchment breakup and routing links for distributed model of Manton River catchment

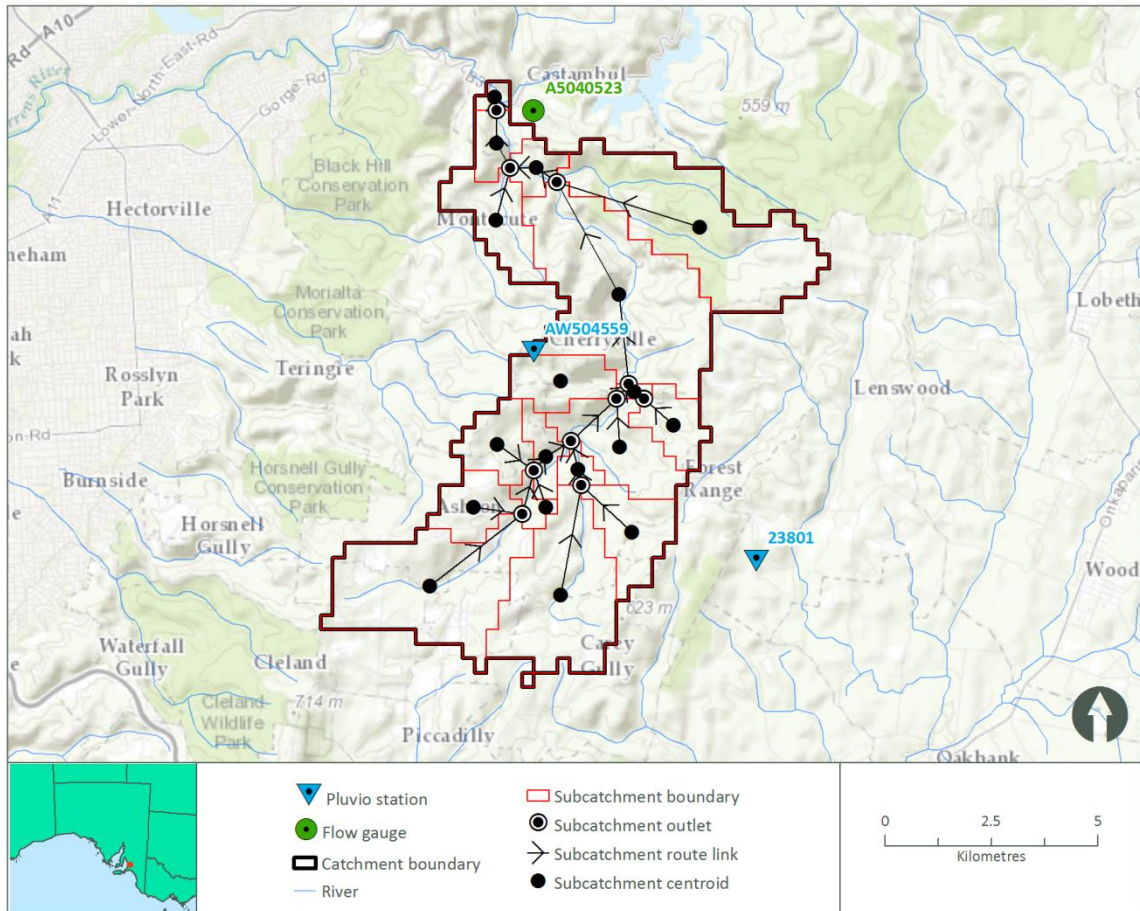


Figure B.13-4 Subcatchment breakup and routing links for distributed model of Sixth Creek catchment



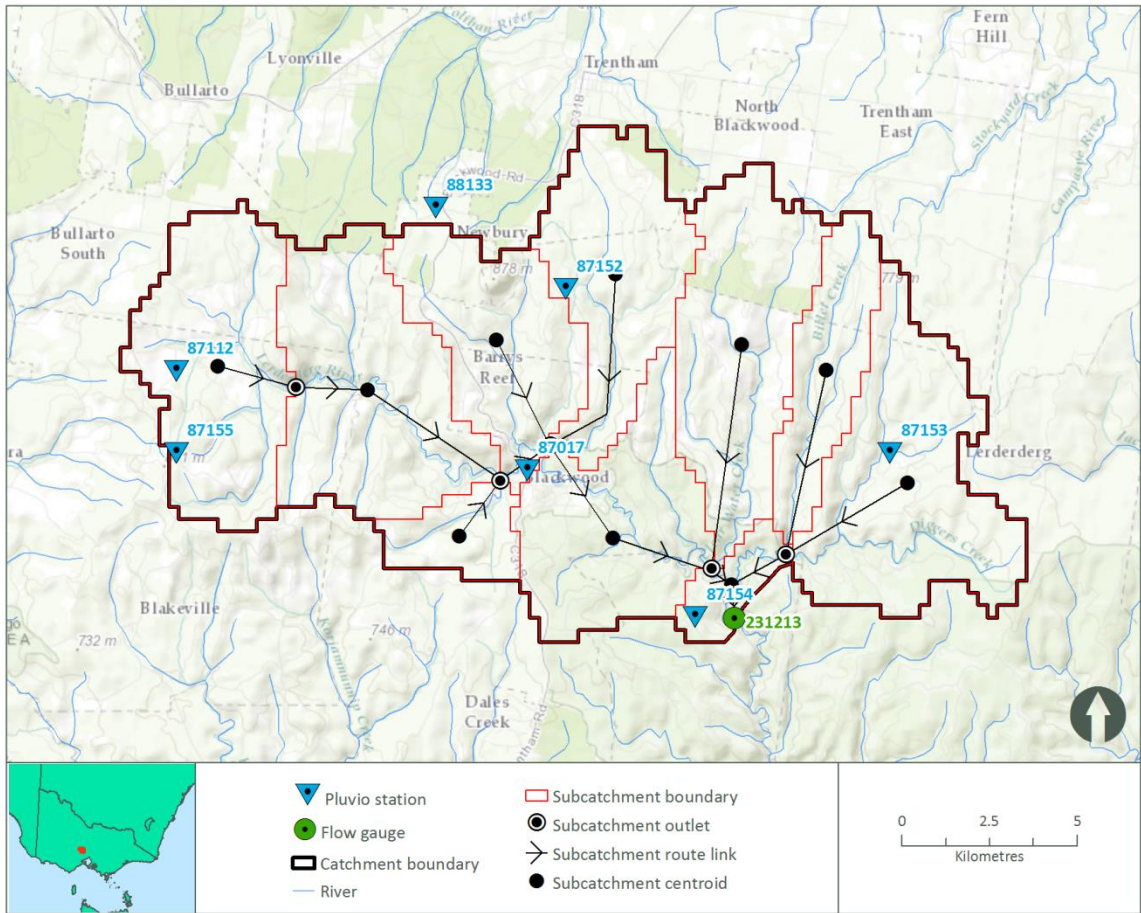


Figure B.13-5: Subcatchment breakup and routing links for distributed model of Lerderberg River catchment

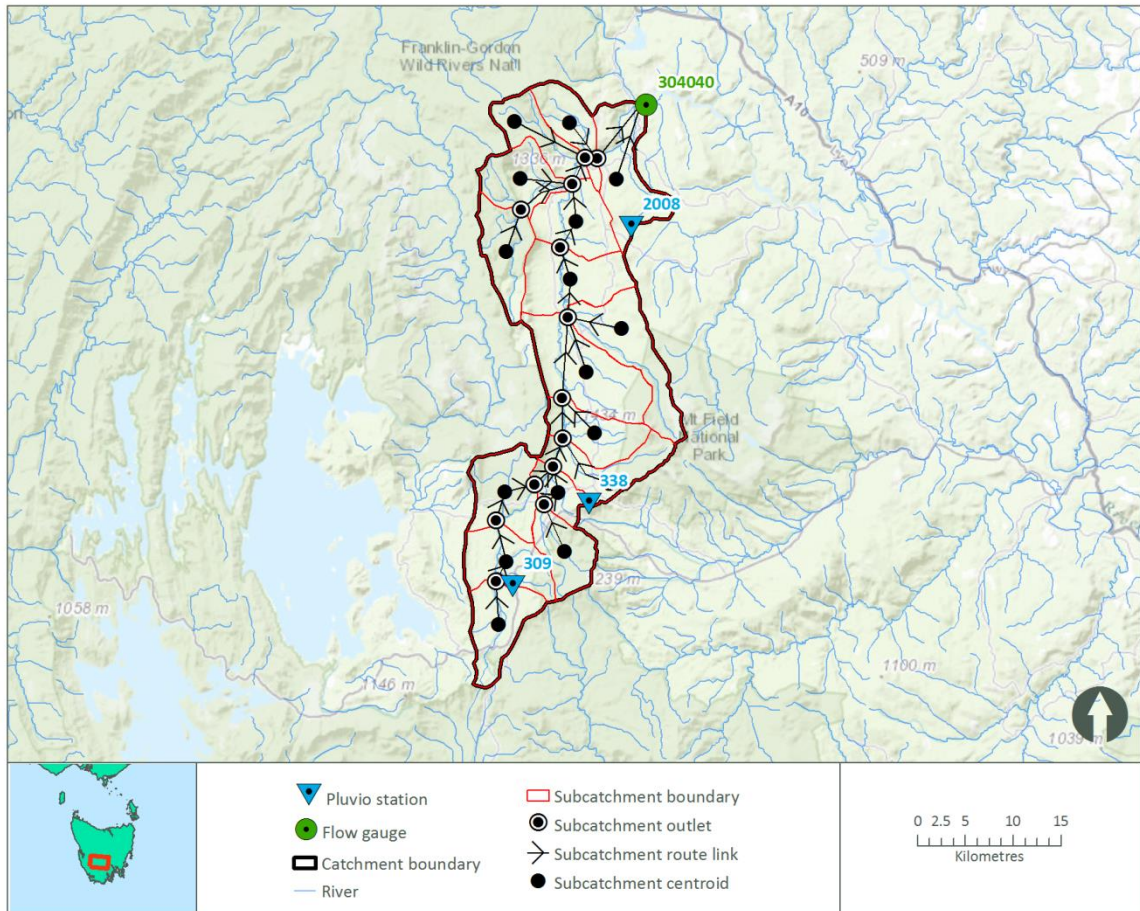


Figure B.13-6: Subcatchment breakup and routing links for distributed model of Florentine River catchment

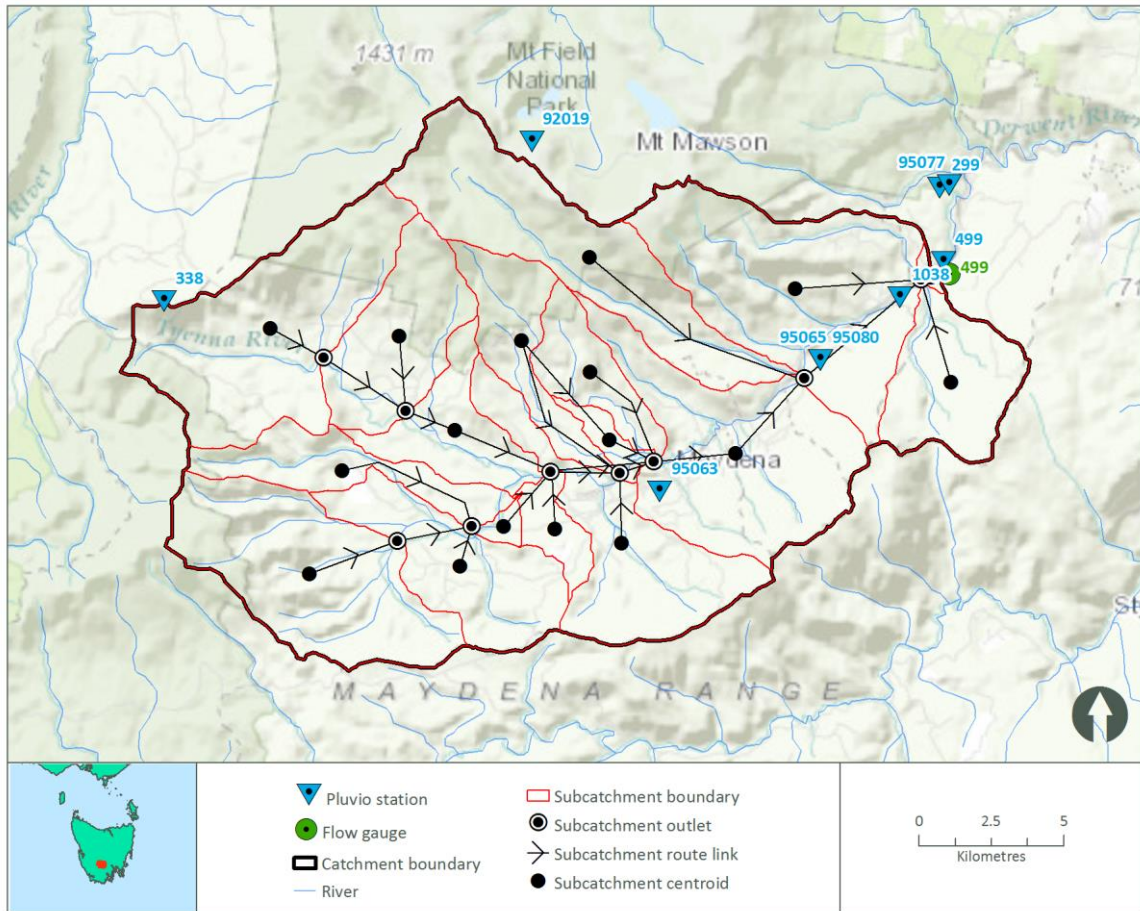


Figure B.13-7: Subcatchment breakup and routing links for distributed model of Tyenna River catchment

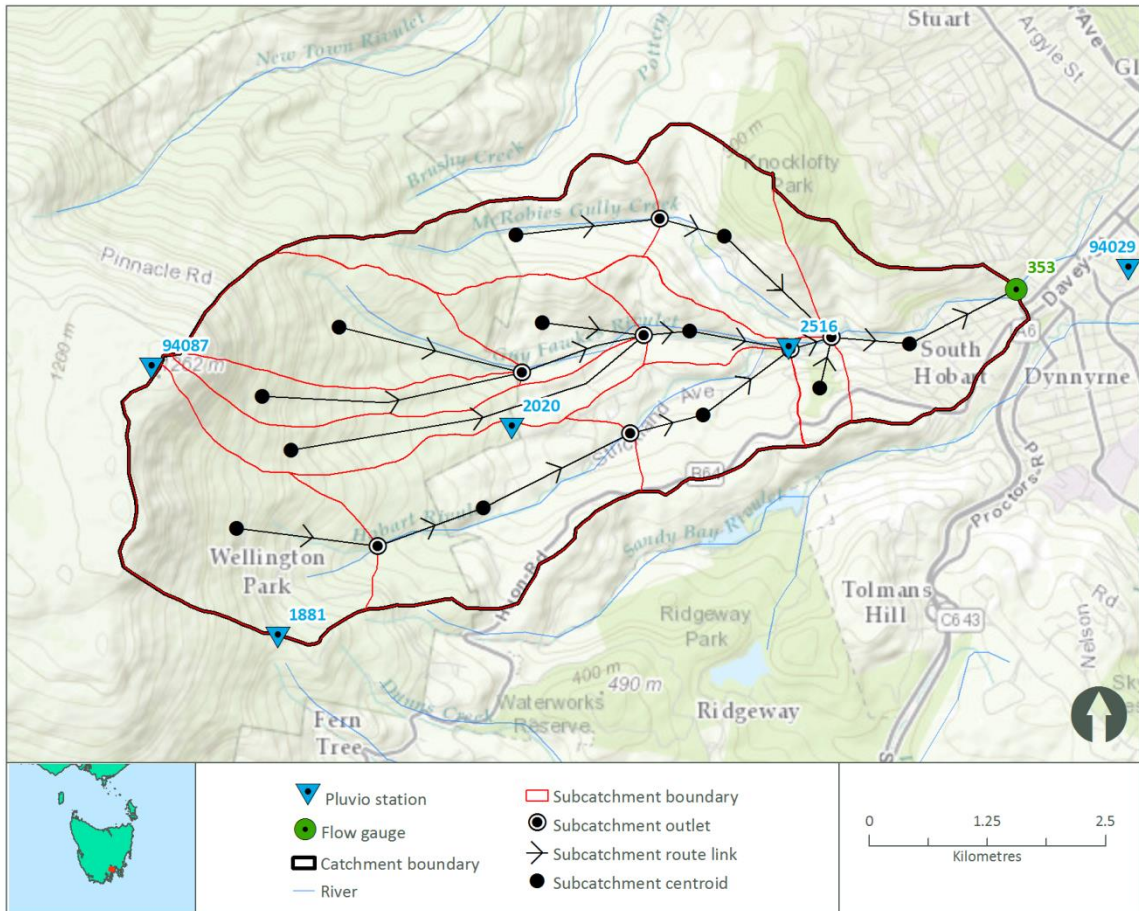


Figure B.13-8: Subcatchment breakup and routing links for distributed model of Hobart Rivulet catchment

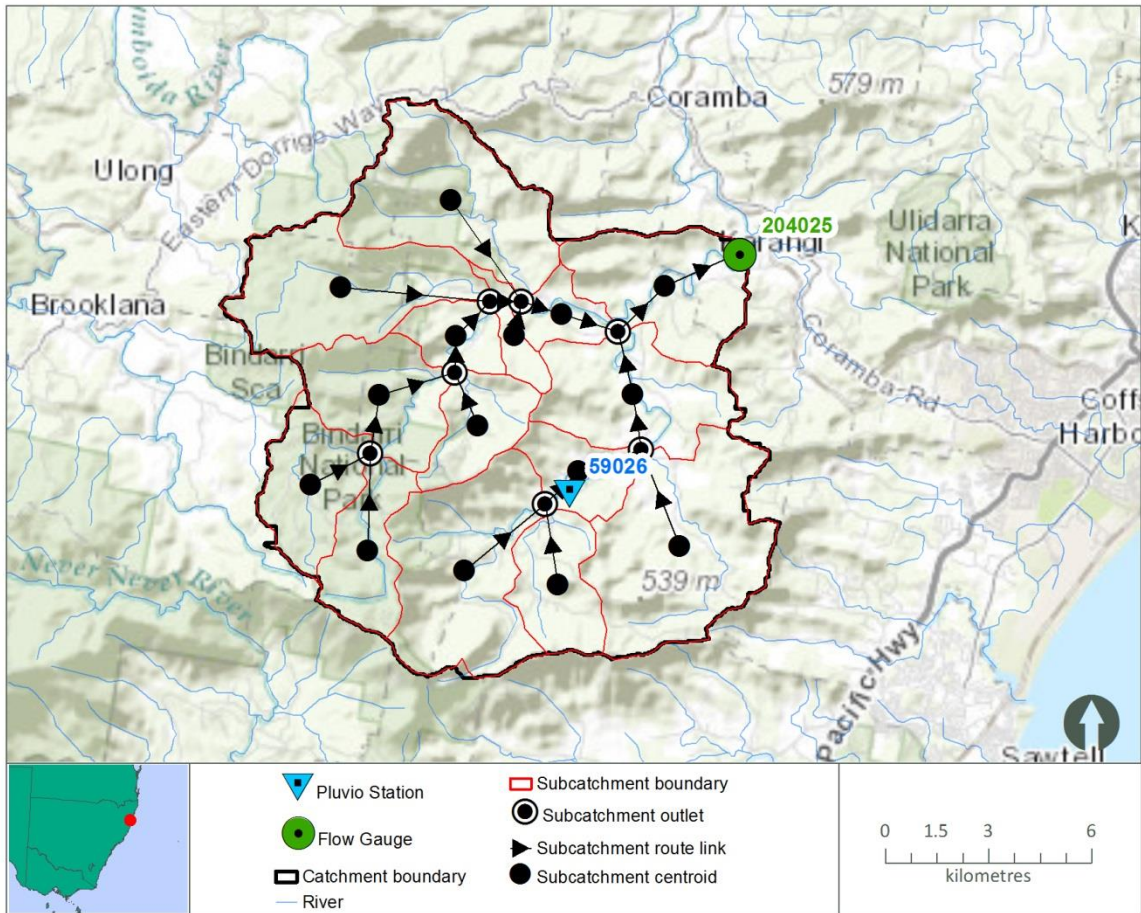


Figure B.13-9: Subcatchment breakup and routing links for distributed model of Orara River catchment

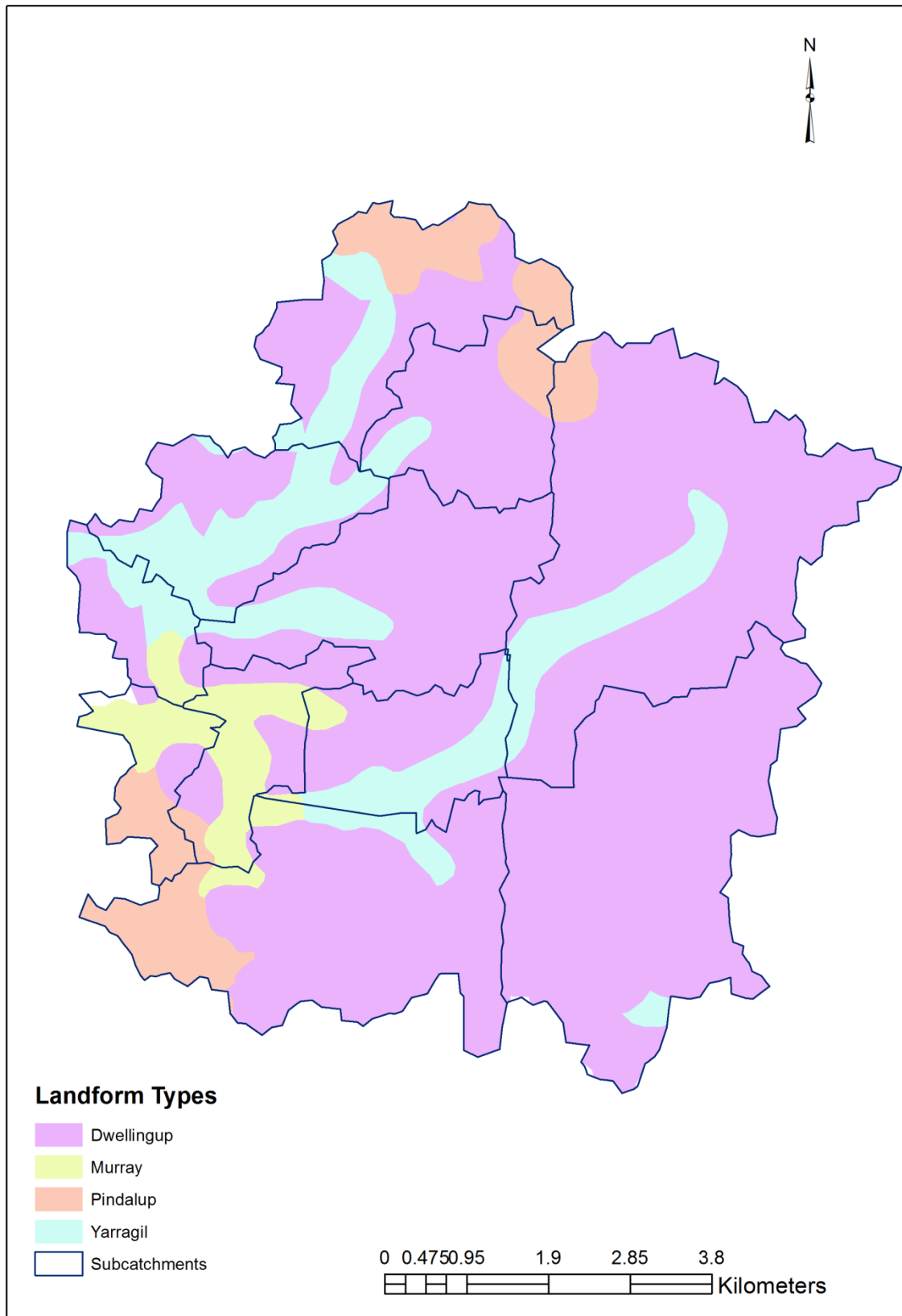


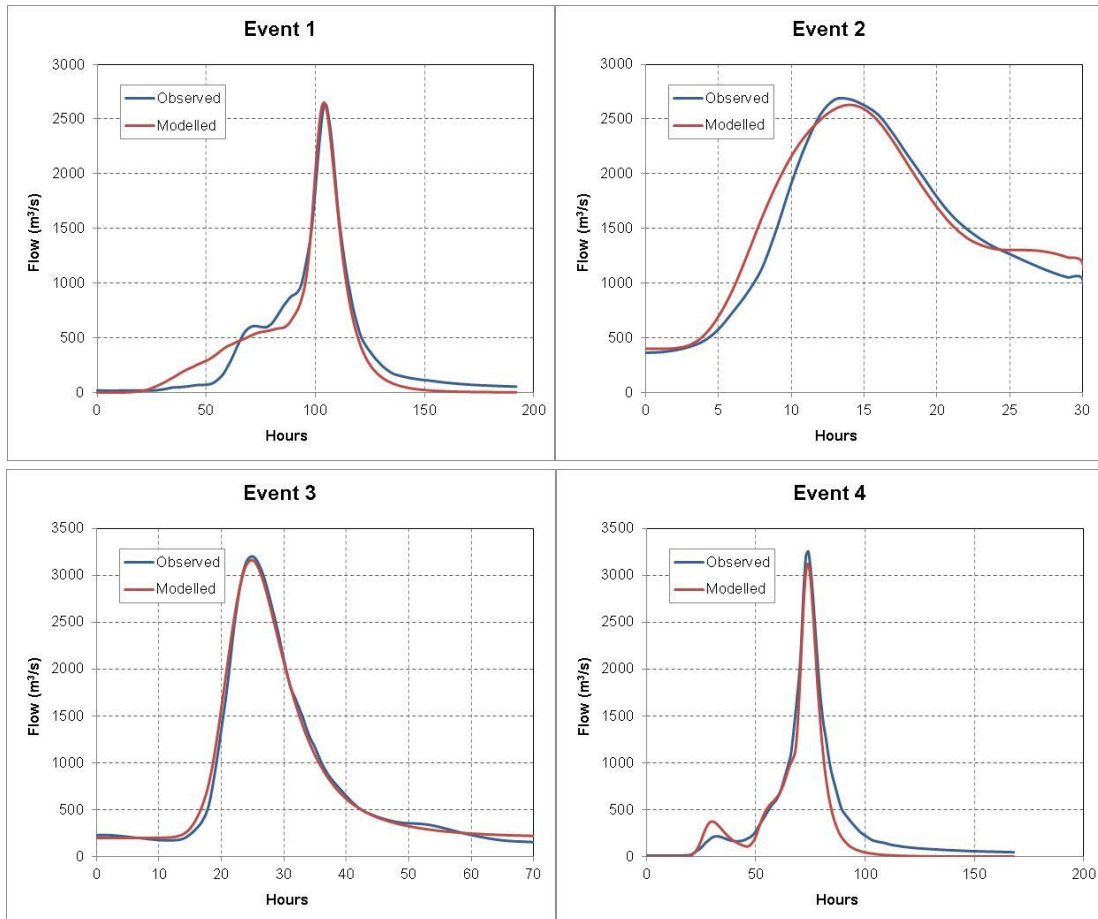
Figure B 13.10: Distribution of the soil – landform types in Yates Flat Creek

**Appendix C Event calibration**

**C.1 Mary River**

**Table C.1: Events used for Mary River model calibration**

Event	Start Date
1	08/02/1972
2	26/01/1974
3	02/04/1989
4	23/04/1989
5	07/02/1999
6	09/01/2011
7	26/01/2013



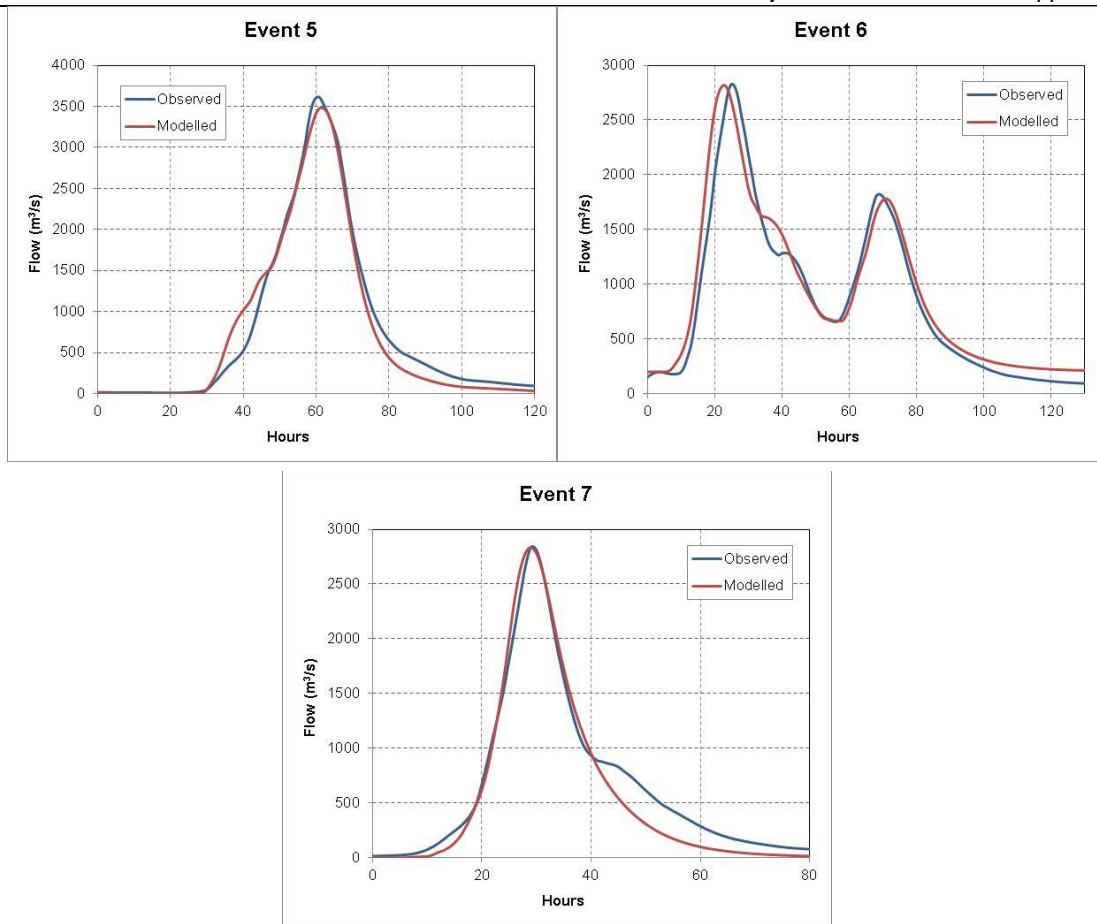


Figure C.1: Mary River model event calibration

Table C.2: Mary River event calibration results

Statistic	Event						
	1	2	3	4	5	6	7
obs_avg	337.92	746.70	593.23	588.74	906.71	1067.36	637.98
mod_avg	360.33	774.86	621.54	506.06	877.34	1124.54	558.48
Bias	1.07	1.04	1.05	0.86	0.97	1.05	0.88
r-sq	0.91	0.98	0.99	0.95	0.98	0.93	0.97
obs_peak	1868.82	2681.33	3201.22	3253.30	3606.53	2828.18	2836.57
mod_peak	2029.72	2629.80	3161.59	3123.88	3479.18	2816.56	2833.27
% diff peak	-8.61	1.92	1.24	3.98	3.53	0.41	0.12

Table C.3: Mary River event calibration model parameters

Event	Alpha	IL (mm)	CL (mm/hr)	Baseflow (m <sup>3</sup> /s)
1	1.2	0	0	0
2	0.7	0	0	400
3	1.1	1	3	200
4	0.8	40	0	0
5	1.0	40	0	0
6	1.2	20	1	200

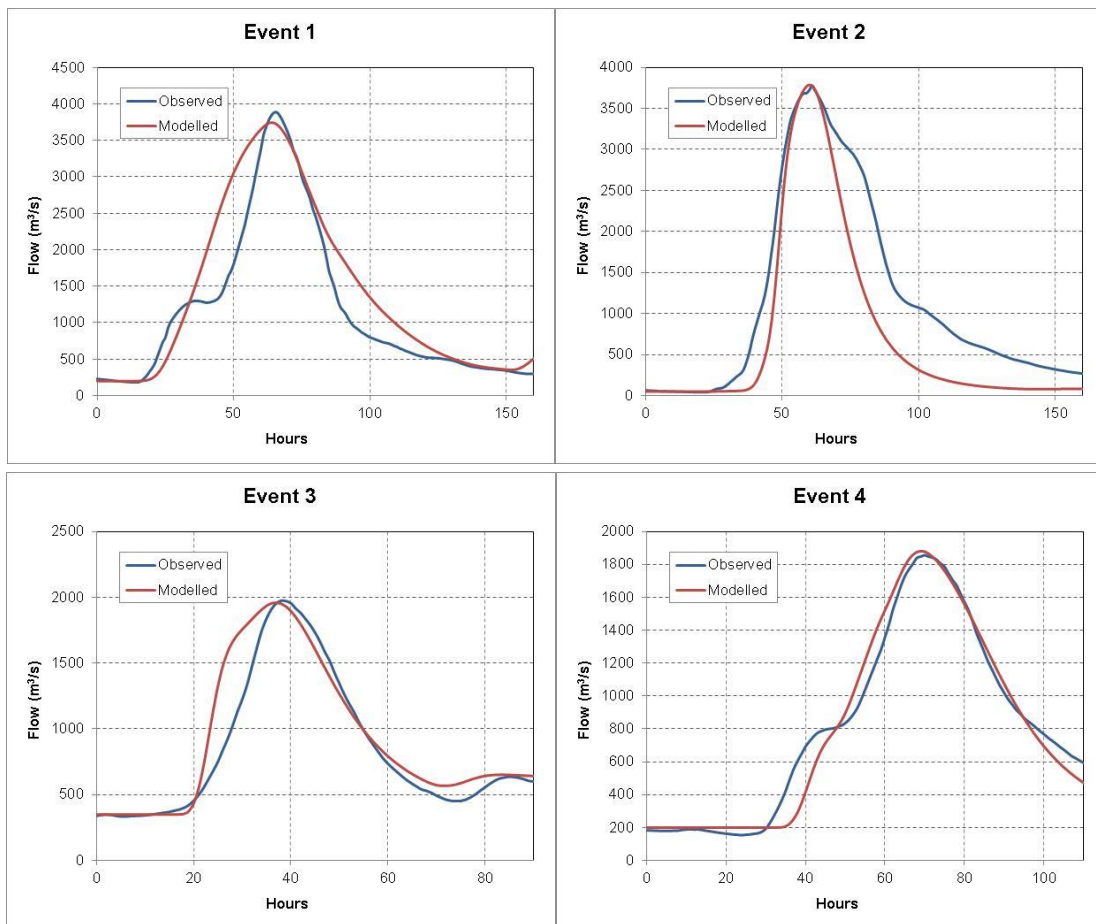


7	1.0	60	6	0
---	-----	----	---	---

## C.2 Hann River

**Table C.4: Events used for Hann River model calibration**

Event	Start Date
1	05/03/1969
2	19/01/1986
3	24/02/1997
4	02/03/2000
5	20/02/2002
6	25/03/2007
7	10/03/2011



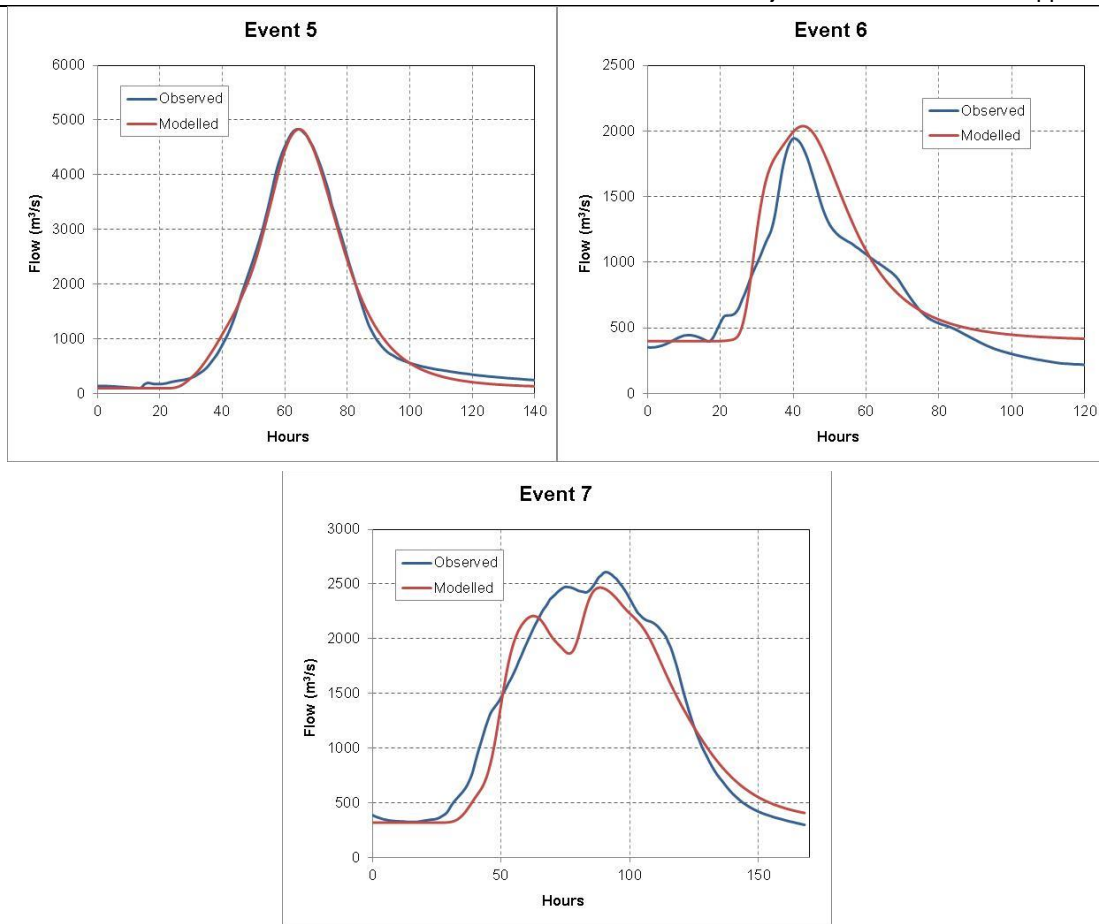


Figure C.2: Hann River model event calibration

Table C.5: Hann River event calibration results

Statistic	Event						
	1	2	3	4	5	6	7
obs_avg	1584	1514	828	835	1650	818	1424
mod_avg	1868	1088	903	839	1646	893	1289
Bias	1.18	0.72	1.09	1.01	1.00	1.09	0.91
r-sq	0.78	0.79	0.87	0.97	1.00	0.89	0.92
obs_peak	3883	3777	1974	1855	4832	1943	2608
mod_peak	3743	3786	1958	1880	4829	2037	2467
% diff peak	3.60	-0.24	0.78	-1.33	0.07	-4.85	5.42

Table C.6: Hann River event calibration model parameters

Event	Alpha	IL (mm)	CL (mm/hr)	Baseflow (m <sup>3</sup> /s)
1	0.8	3	0.2	200
2	0.75	0	0	50
3	0.7	30	4	350
4	0.8	0	2.3	200
5	0.7	10	1.9	100
6	0.7	10	16	400
7	0.8	10	0	320

### C.3 Yates Flat Creek

**Table C.7: Events used for Yates Flat Creek model calibration**

Event	Start Date
1	28/06/1978
2	16/07/1984
3	24/06/1988
4	21/07/1991
5	22/08/2003
6	01/04/2005

#### C.3.1 Calibration of IL-CL model

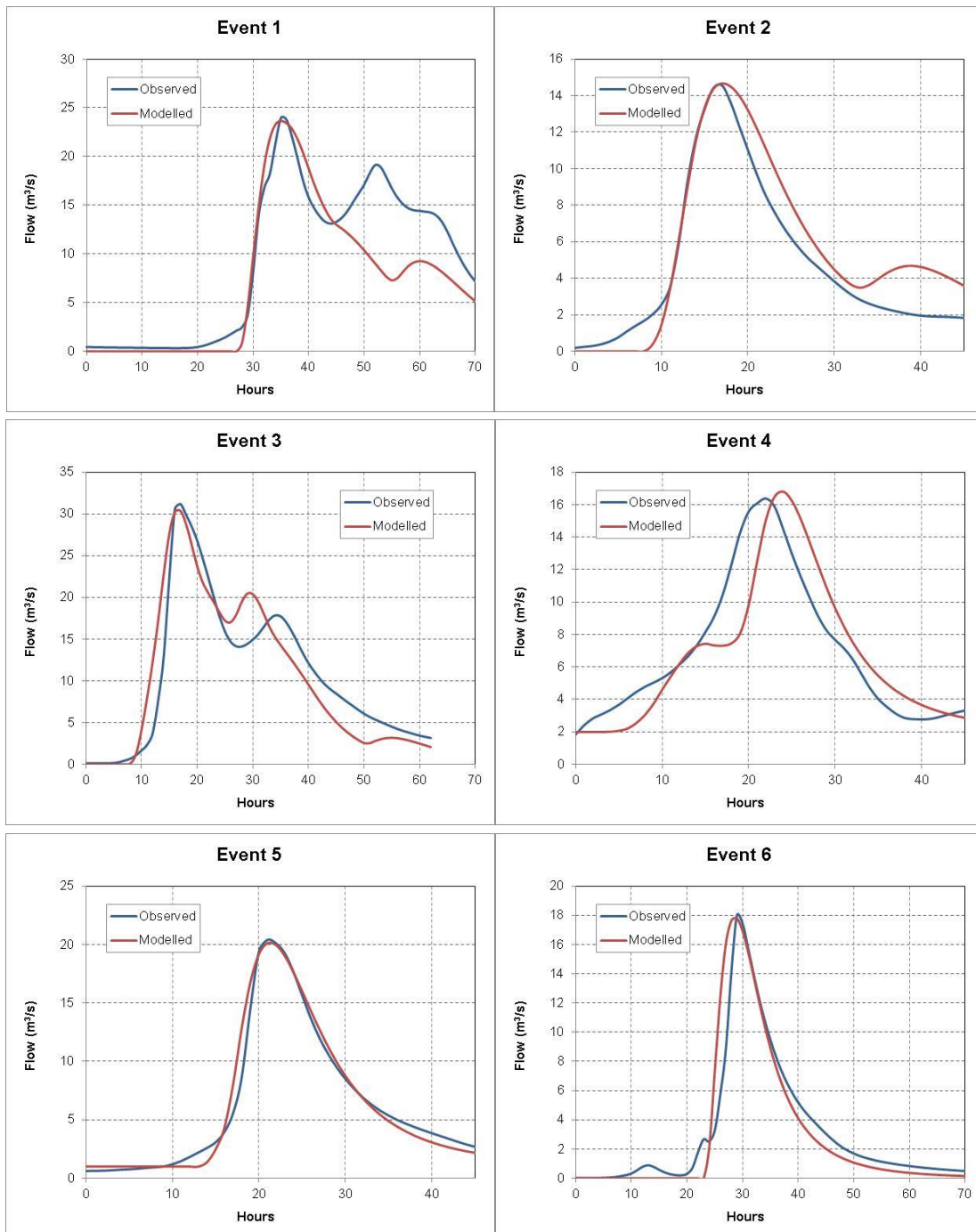


Figure C.3.1: Yates Flat Creek model event calibration

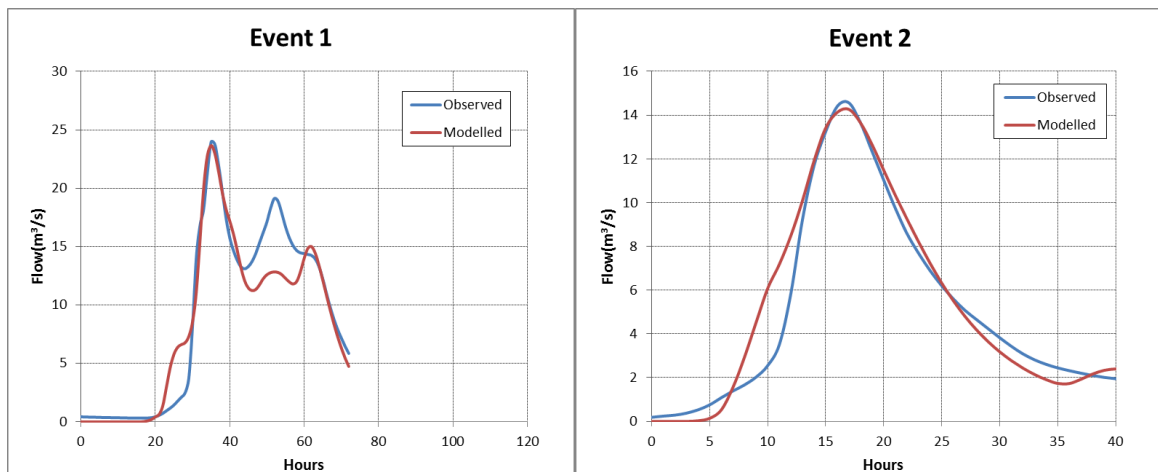
Table C.8.1: Yates Flat Creek event calibration results

Statistic	Event					
	1	2	3	4	5	6
obs_avg	9.03	4.55	10.58	6.69	6.04	3.08
mod_avg	7.17	5.43	10.32	6.52	6.04	2.86
Bias	0.79	1.19	0.98	0.97	1.00	0.93
r-sq	0.76	0.86	0.85	0.75	0.98	0.89
obs_peak	23.95	14.56	31.18	16.37	20.40	18.00
mod_peak	23.65	14.67	30.36	16.79	20.11	17.78
% diff peak	1.29	-0.73	2.63	-2.56	1.41	1.23

Table C.9.1: Yates Flat Creek event calibration model parameters

Event	Alpha	IL (mm)	CL (mm/hr)	Baseflow (m <sup>3</sup> /s)
1	2.5	35	1.9	0
2	2.2	15	0	0
3	1.7	32	0.25	0
4	1.6	10	0.4	2
5	2	25	2.6	1
6	1.75	30	11	0

C3.2 Calibration of SWMOD model



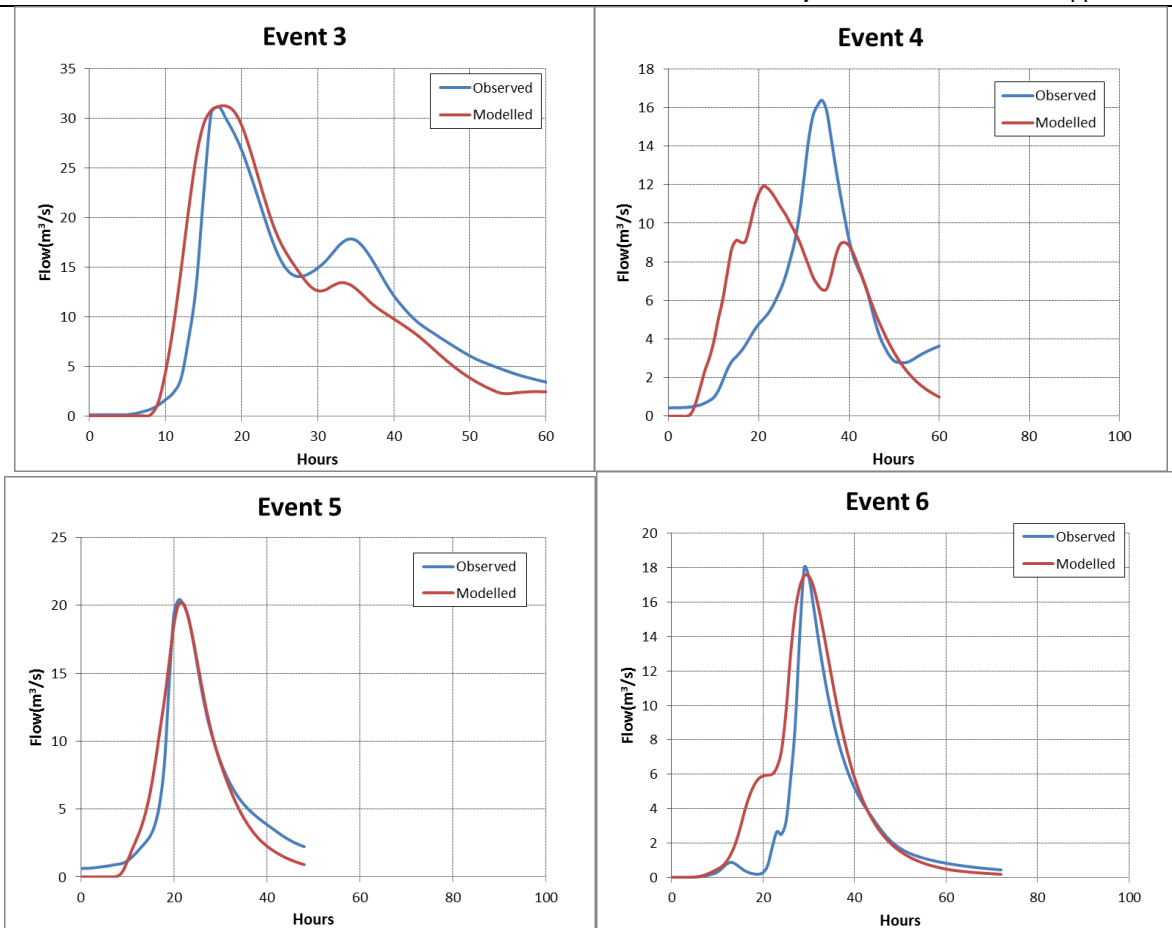


Figure C 3.2 Yates Flat Creek Event calibration parameters for SWMOD

Table C.8.2: Yates Flat Creek (SWMOD) event calibration results

Statistic	Event					
	1	2	3	4	5	6
obs_avg	9.03	4.55	9.21	N/A	6.04	3.08
mod_avg	8.49	4.21	9.01	N/A	5.94	4.15
Bias	0.94	0.93	0.98	N/A	0.98	1.35
r-sq	0.91	0.85	0.85	N/A	0.92	0.73
obs_peak	23.95	14.56	31.18	N/A	20.40	18.00
mod_peak	23.65	14.26	31.24	N/A	20.14	17.54
% diff peak	1.25	2.04	-0.21	N/A	1.29	2.60

Table C.9.2: Yates Flat Creek event calibration model parameters

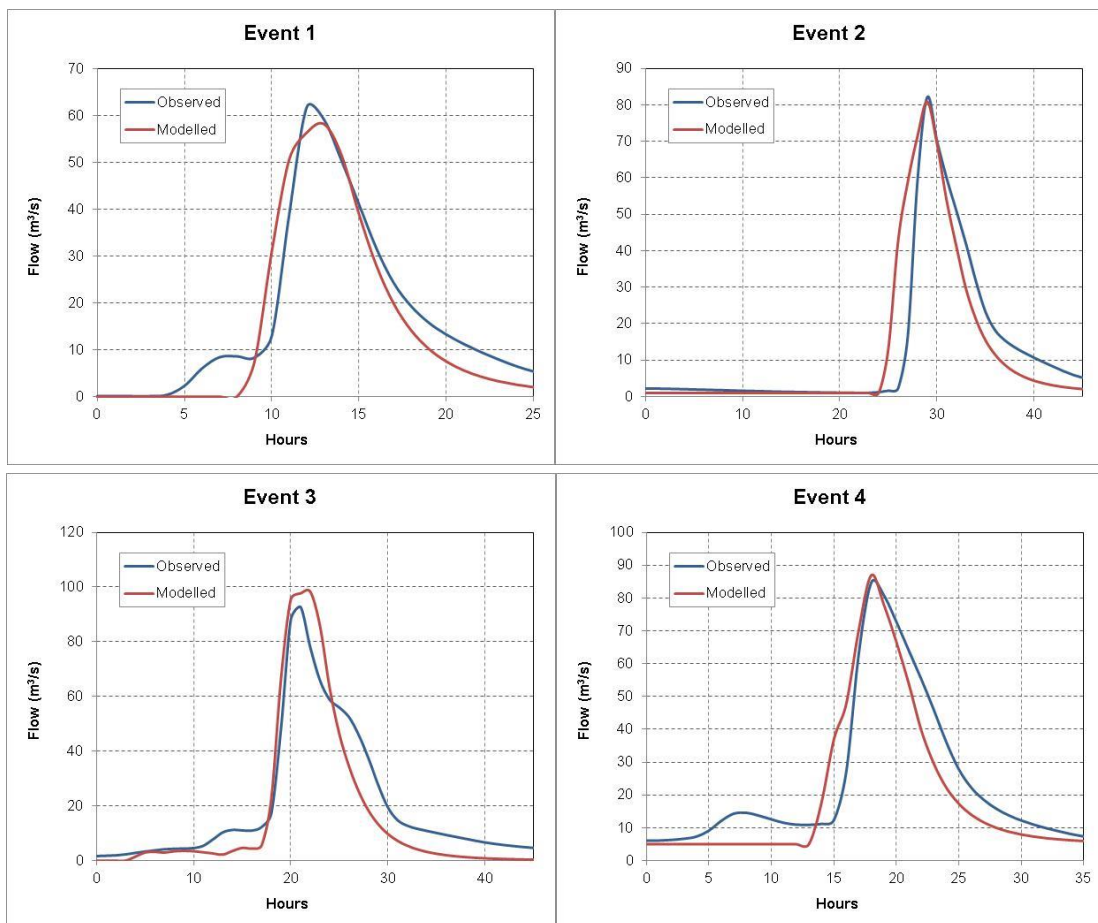
Event	Alpha	Ci Dwellingup (mm)	Ci Yarragil (mm)	Ci Pindalup (mm)	Ci Murray (mm)	Delay (hrs)
1	1.75	210	540	434	275	5
2	1.75	260	1000	1400	1020	5
3	1.75	416	540	434	275	5
4	N/A	N/A	N/A	N/A	N/A	N/A
5	1.75	220	650	87	500	5

6	1.75	110	153	84	100	5
---	------	-----	-----	----	-----	---

### C.4 Manton River

**Table C.10: Events used for Manton River model calibration**

Event	Start Date
1	09/04/1996
2	01/03/1997
3	27/01/1998
4	13/02/2001
5	25/04/2006



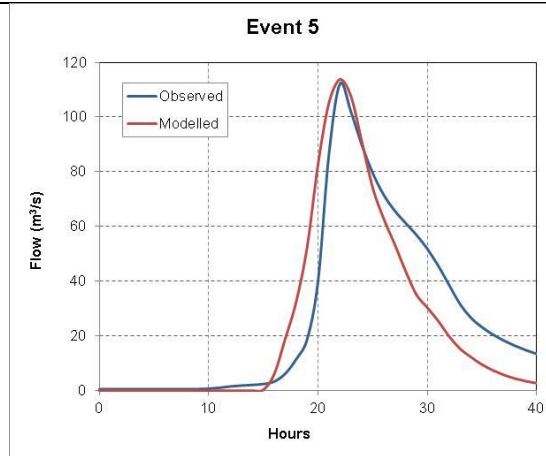


Figure C.4: Manton River model event calibration

Table C.11: Manton River event calibration results

Statistic	Event				
	1	2	3	4	5
obs_avg	15.67	12.20	19.03	23.21	24.29
mod_avg	13.60	11.85	15.45	19.68	20.95
Bias	0.87	0.97	0.81	0.85	0.86
r-sq	0.90	0.76	0.86	0.85	0.82
obs_peak	61.69	82.07	92.74	84.73	112.05
mod_peak	58.10	80.84	98.33	86.94	113.75
% diff peak	5.83	1.49	-6.02	-2.61	-1.51

Table C.12: Manton River event calibration model parameters

Event	Alpha	IL (mm)	CL (mm/hr)	Baseflow (m <sup>3</sup> /s)
1	1.2	5	12	0
2	1.2	0	7	1
3	1.2	3	11	0
4	1.2	2	9	5
5	1.2	10	2.75	0

C.5 Sixth Creek

Table C.13: Events used for Sixth Creek model calibration

Event	Start Date
1	23/6/1987
2	17/9/1991
3	30/8/1992
4	21/07/1995
5	07/11/2005
6	26/06/1981

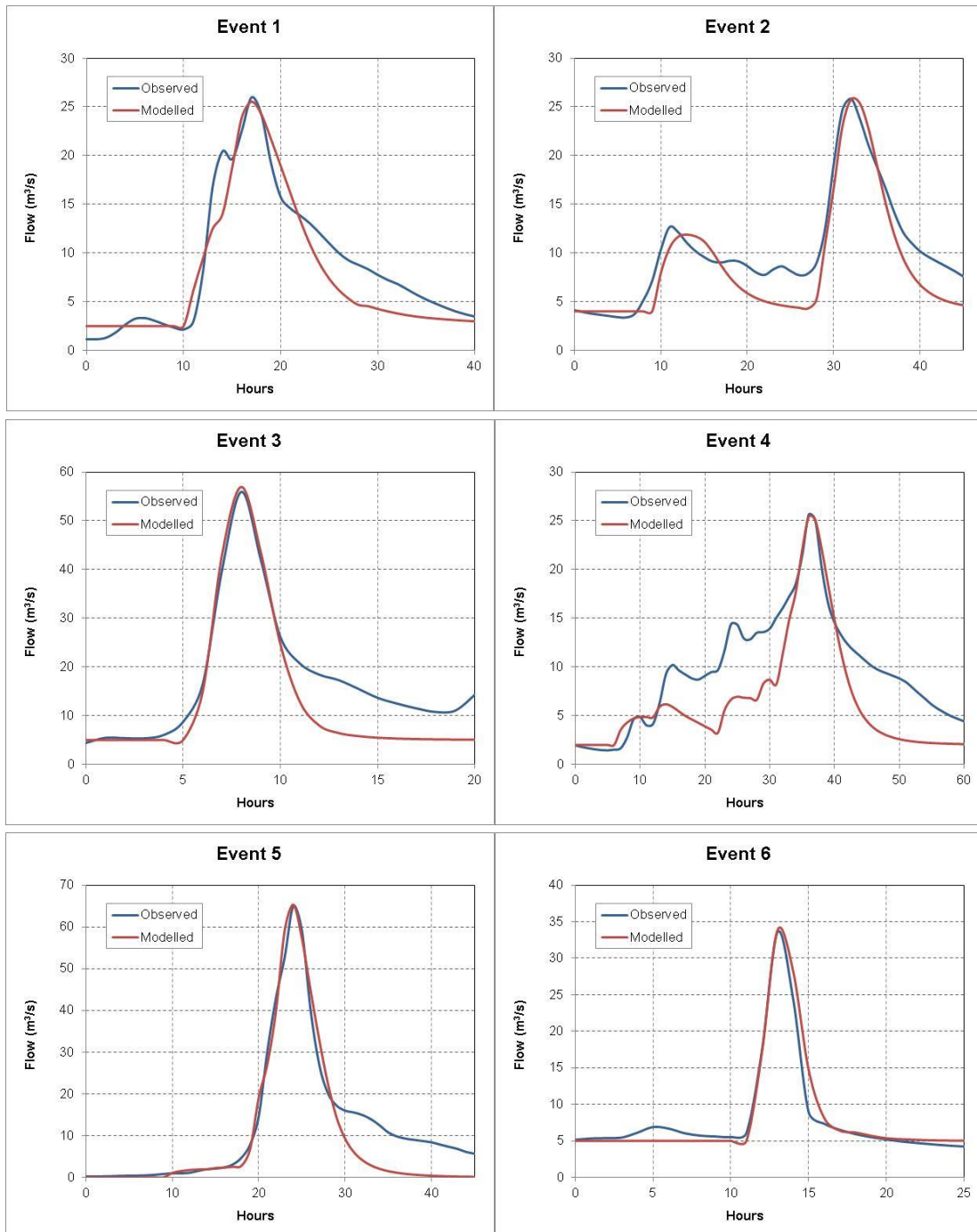


Figure C.5: Sixth Creek model event calibration



**Table C.14: Sixth Creek event calibration results**

Statistic	Event					
	1	2	3	4	5	6
obs_avg	7.72	10.03	17.20	9.64	11.77	6.63
mod_avg	6.87	8.48	13.20	6.55	8.94	7.14
Bias	0.89	0.85	0.77	0.68	0.76	1.08
r-sq	0.89	0.82	0.80	0.45	0.88	0.94
obs_peak	25.98	25.84	55.97	25.62	65.01	33.56
mod_peak	25.53	25.75	56.96	25.40	65.32	33.84
% diff peak	1.72	0.36	-1.77	0.86	-0.46	-0.81

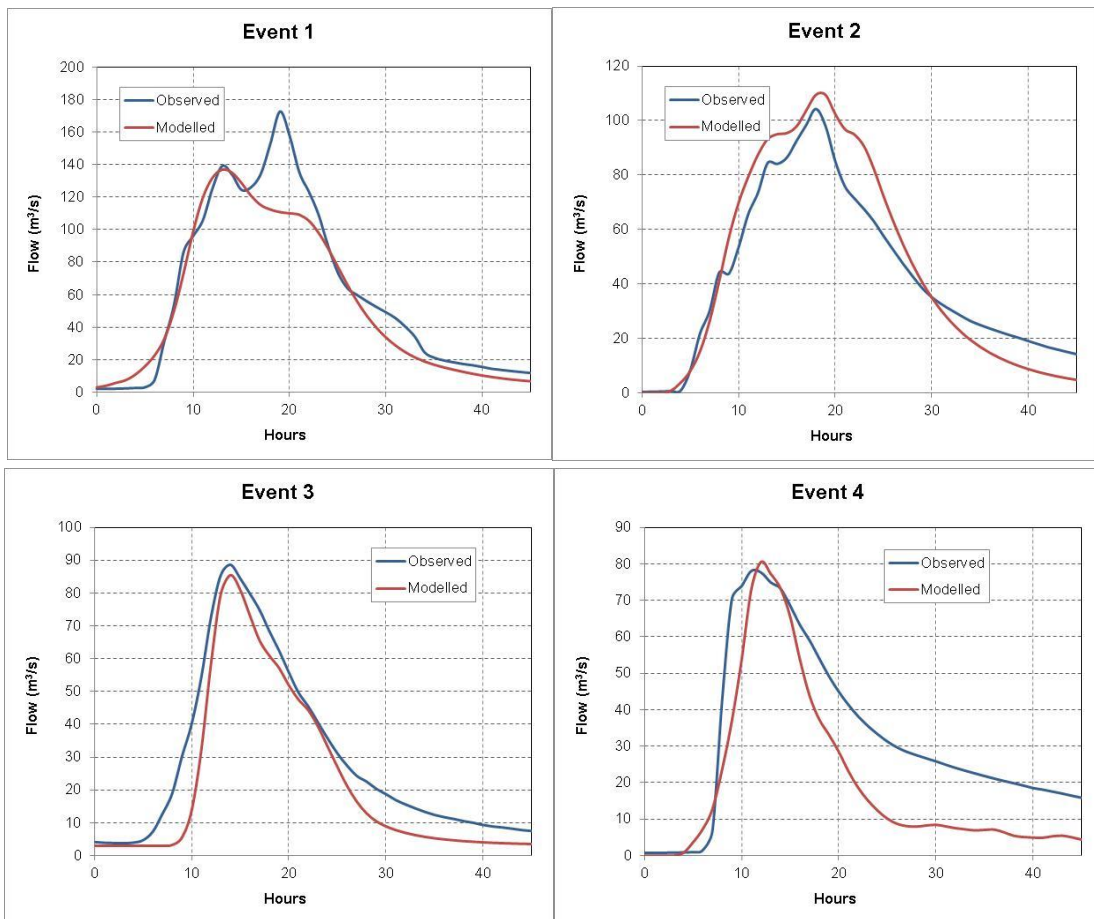
**Table C.15: Sixth Creek event calibration model parameters**

Event	Alpha	IL (mm)	CL (mm/hr)	Baseflow (m <sup>3</sup> /s)
1	1	0	4.1	2.5
2	0.8	9	2.0	4
3	0.4	19.5	3.6	5
4	0.8	2	3	2
5	0.8	10	6	0
6	0.25	22	8	5

**C.6 Lerderberg River**

**Table C.16: Events used for Lerderberg River model calibration**

Event	Start Date
1	15/05/1974
2	23/10/1985
3	22/09/1976
4	07/08/1978
5	05/11/1995
6	23/10/2000
7	27/11/2010



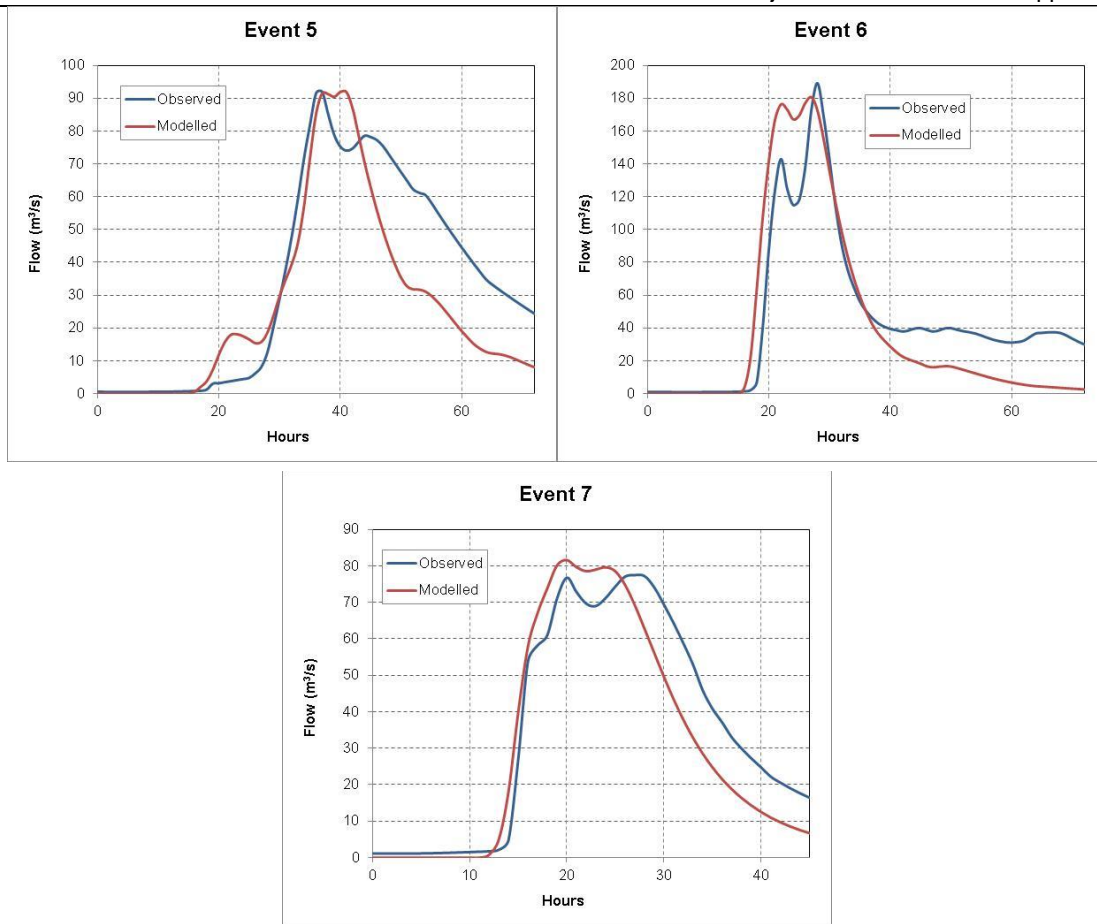


Figure C.6: Lerderderg River model event calibration

Table C.17: Lerderderg River event calibration results

Statistic	Event						
	1	2	3	4	5	6	7
obs_avg	57.61	34.60	27.86	30.75	34.53	39.11	33.82
mod_avg	50.95	34.60	21.17	18.95	26.66	30.97	29.42
Bias	0.88	1.00	0.76	0.62	0.77	0.79	0.87
r-sq	0.91	0.89	0.89	0.60	0.71	0.81	0.88
obs_peak	172.53	104.26	88.61	78.06	91.93	189.11	77.46
mod_peak	136.81	109.44	85.45	80.55	91.87	180.56	81.57
% diff peak	20.70	-4.97	3.56	-3.19	0.07	4.52	-5.31

Table C.18: Lerderderg River event calibration model parameters

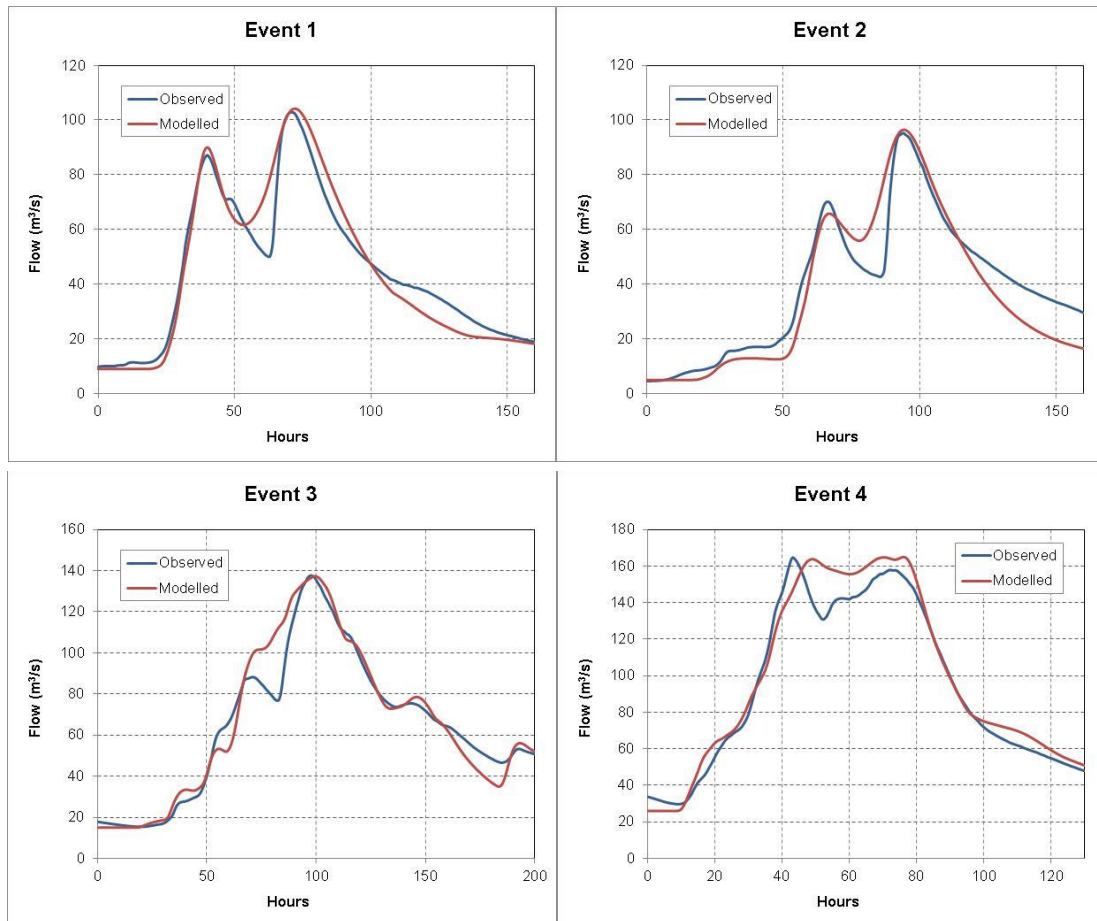
Event	Alpha	IL (mm)	CL (mm/hr)	Baseflow (m <sup>3</sup> /s)
1	1.0	0	0.0	3
2	1.2	17	3.0	0
3	0.3	0	0.0	3
4	0.5	0	0.0	0
5	1.2	5	1.2	0
6	1.2	27	1.5	0
7	1.2	20	1.2	0

### C.7 Florentine River

**Table C.19: Events used for Florentine River model calibration**

Event	Start Date
1	16/08/1995
2	31/03/1996
3	15/09/2003
4	08/08/2007
5	23/08/2009
6	28/07/2014
7	28/06/2004
8	25/05/1994

#### C.7.1 Two sets of routing and loss parameters



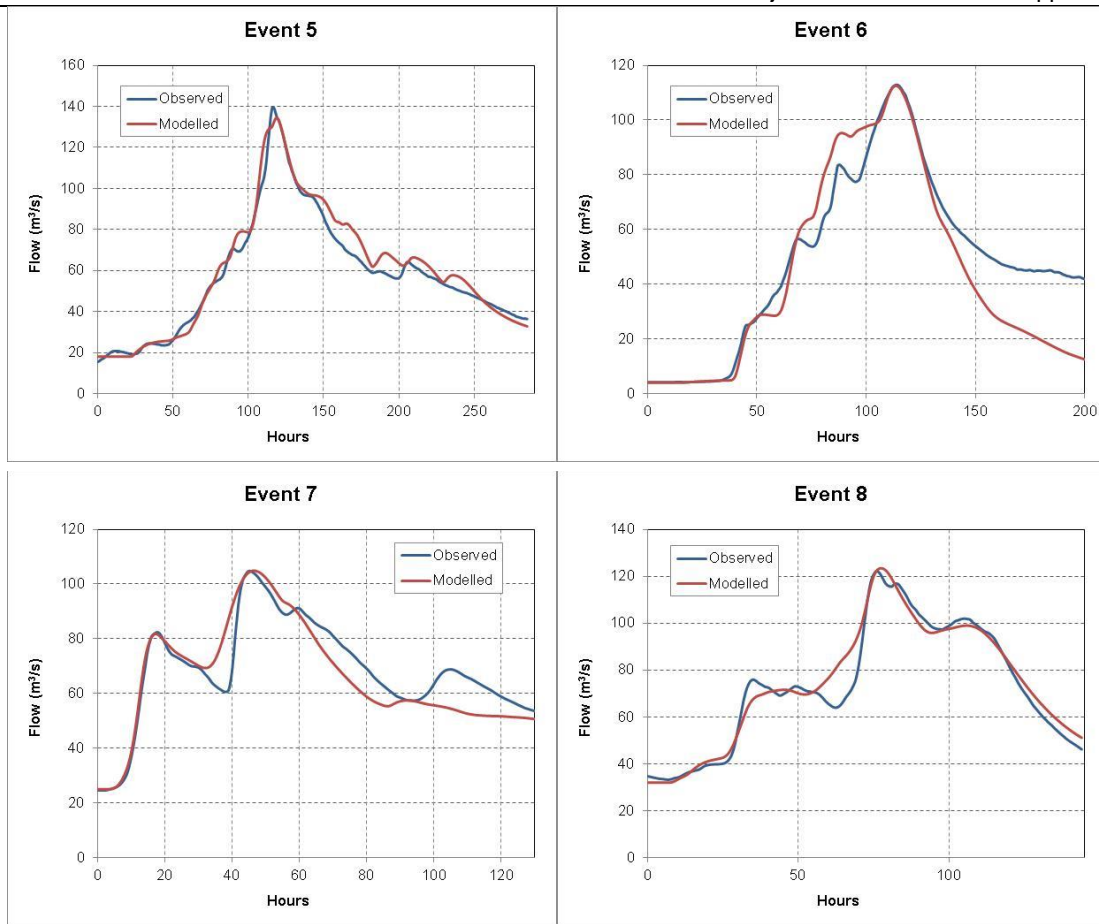


Figure C.7: Florentine River model event calibration

Table C.20: Florentine River event calibration results – two parameter sets

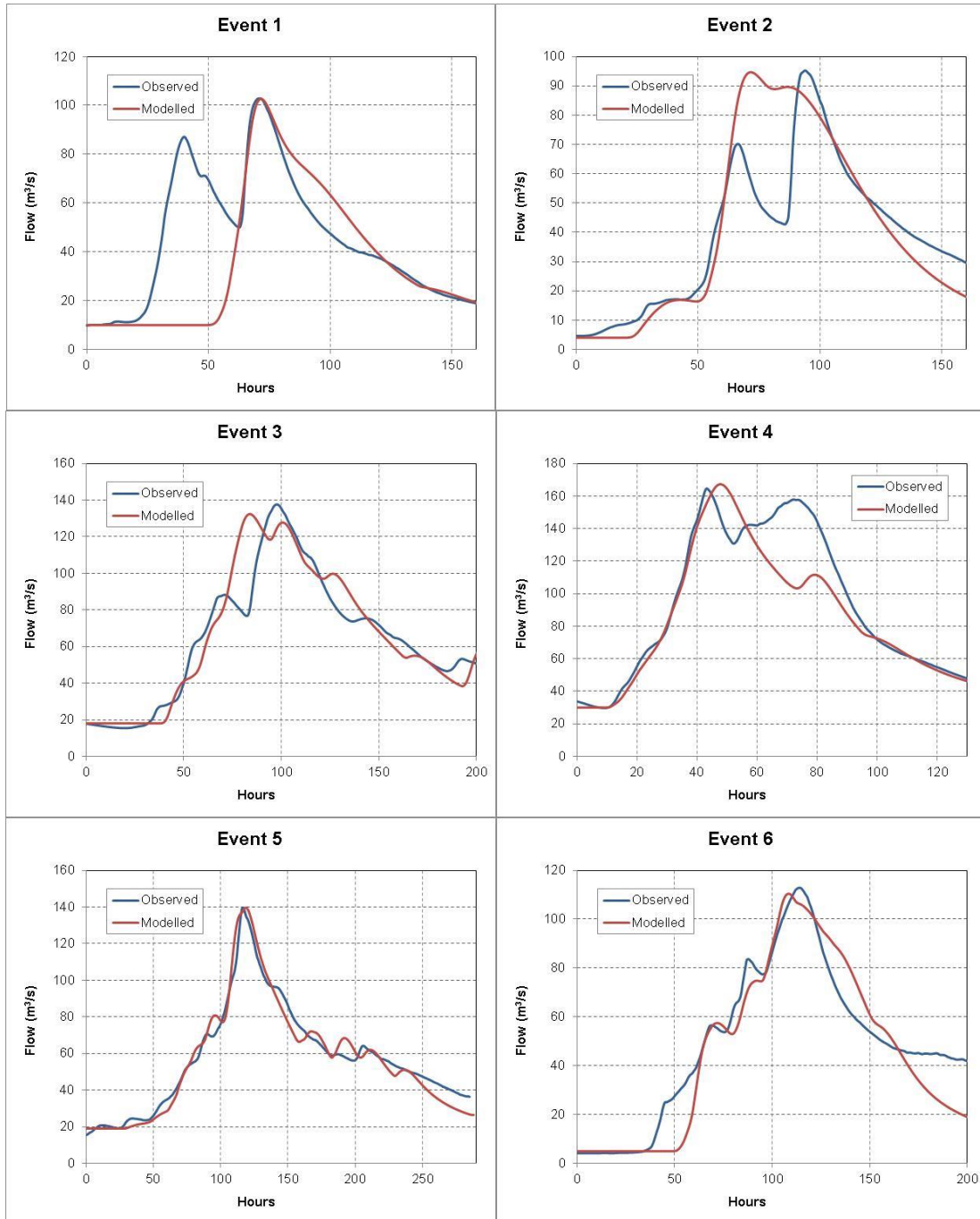
Statistic	Event							
	1	2	3	4	5*	6*	7	8
obs_avg	43.9	36.3	63.3	93.2	57.3	48.5	66.7	73.0
mod_avg	43.7	33.0	64.5	97.5	59.8	41.3	64.2	74.3
Bias	1.00	0.91	1.02	1.05	1.04	0.85	0.96	1.02
r-sq	0.94	0.90	0.93	0.95	0.99	0.95	0.89	0.95
obs_peak	102.9	95.2	137.6	164.4	139.5	112.9	104.7	122.2
mod_peak	104.2	96.4	137.2	164.9	134.4	112.5	104.8	123.3
% diff peak	-1.27	-1.27	0.26	-0.32	3.67	0.37	-0.10	-0.96

Table C.21: Florentine River event calibration model parameters – two parameter sets

Event	Alpha1	IL1 (mm)	CL1 (mm/hr)	Baseflow1 (m <sup>3</sup> /s)	Alpha2	IL2 (mm)	CL2 (mm/hr)	Baseflow2 (m <sup>3</sup> /s)
1	3.2	3	1	2	2	5	1.9	9
2	3	8	1.2	4	2	0	2.1	5
3	2.4	12	0.5	5	2	15	1.1	15
4	2	15	0.65	8	1.6	10	1.55	26
5	2.8	15	0.8	8	2.2	25	0.8	18
6	2.5	20	0.95	1	2.2	25	1	4

7	2.8	0	1.55	11	2	5	2.5	25
8	2.5	10	1.3	3	2.2	3	1.5	32

C.7.2 Single set of routing and loss parameters



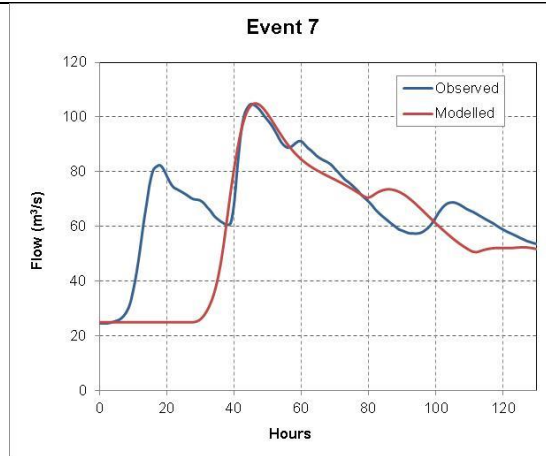


**Table C.22: Florentine River event calibration results – single parameter set**

Statistic	Event						
	1	2	3	4	5	6	7
obs_avg	43.9	36.3	63.3	93.2	57.3	48.5	66.7
mod_avg	35.9	36.8	64.9	85.4	56.2	43.9	57.7
Bias	0.82	1.01	1.03	0.92	0.98	0.91	0.87
r-sq	-0.10	0.52	0.83	0.80	0.98	0.92	0.35
obs_peak	102.9	95.2	137.6	164.4	139.5	112.9	104.7
mod_peak	102.6	94.6	132.4	167.2	139.6	110.4	104.9
% diff peak	0.28	0.63	3.76	-1.72	-0.07	2.26	-0.18

**Table C.23: Florentine River event calibration model parameters – single parameter set**

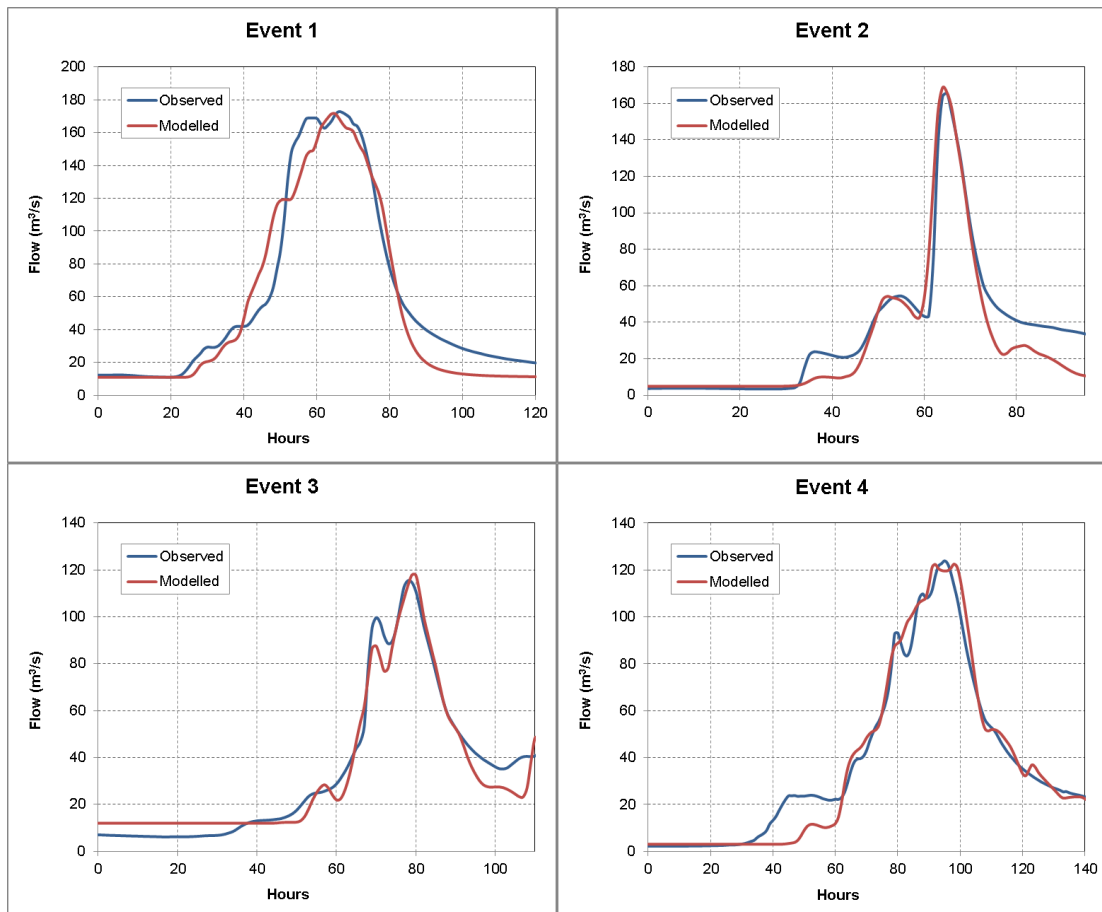
Event	Alpha	IL (mm)	CL (mm/hr)	Baseflow (m <sup>3</sup> /s)
1	2.5	10	1.85	10
2	3.0	8	1.20	4
3	2.5	10	0.80	18
4	2.2	15	1.40	30
5	2.5	15	0.75	19
6	2.5	10	1.00	5
7	2.8	0	1.80	25

## C.8 Tyenna River

**Table C.24: Events used for Tyenna River model calibration**

Event	Start Date
1	08/08/2007
2	23/08/2003
3	15/09/2003
4	28/07/2014
5	09/08/2004
6	14/08/1991
7	06/07/1990

### C.8.1 Single set of routing and loss parameters





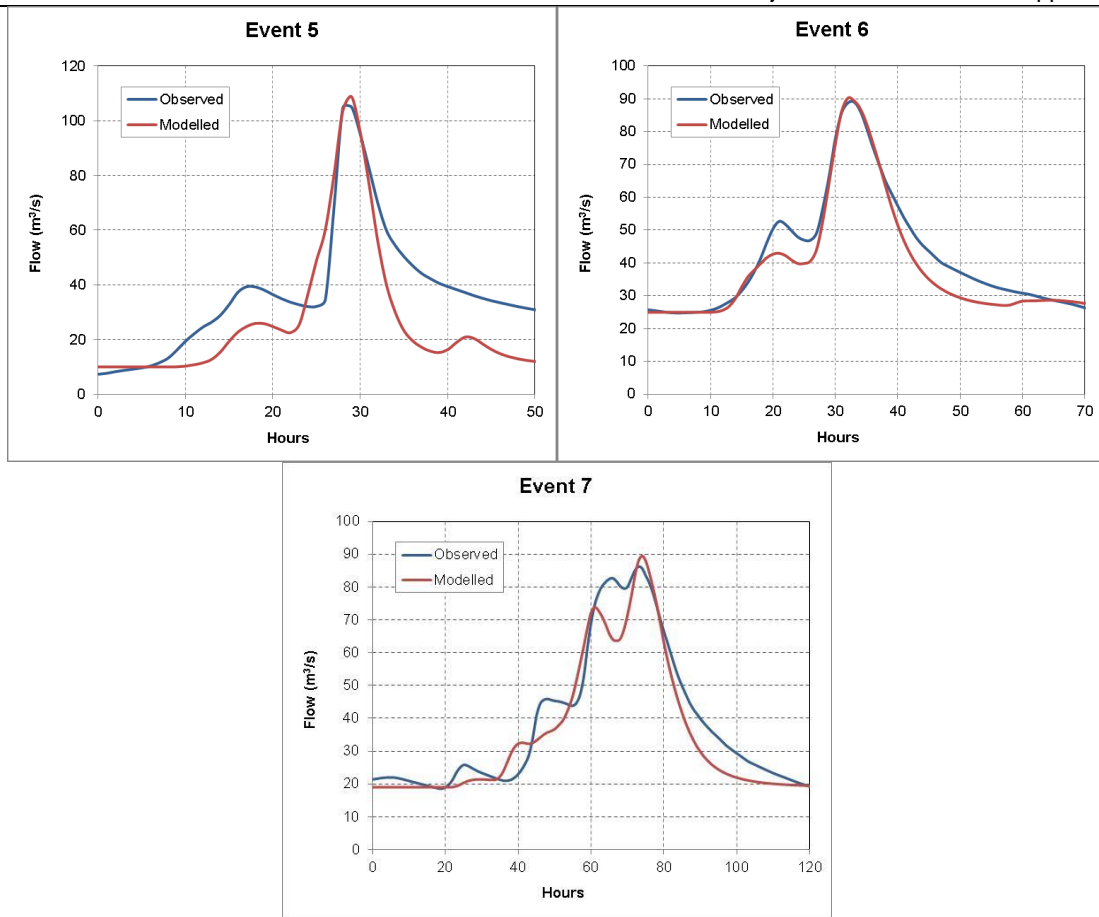


Figure C.8: Tyenna River model event calibration

Table C.25: Tyenna River event calibration results

Statistic	Event						
	1	2	3	4	5	6	7
obs_avg	59.2	35.1	35.4	37.7	37.0	41.6	38.5
mod_avg	54.8	30.1	35.1	36.8	26.8	38.8	35.2
Bias	0.93	0.86	0.99	0.97	0.72	0.93	0.91
r-sq	0.94	0.90	0.97	0.96	0.54	0.93	0.89
obs_peak	172.9	165.5	115.4	123.9	105.0	89.0	86.2
mod_peak	171.5	168.6	117.8	122.5	108.8	90.2	89.4
% diff peak	0.76	-1.85	-2.09	1.13	-3.60	-1.34	-3.79

Table C.26: Tyenna River event calibration model parameters

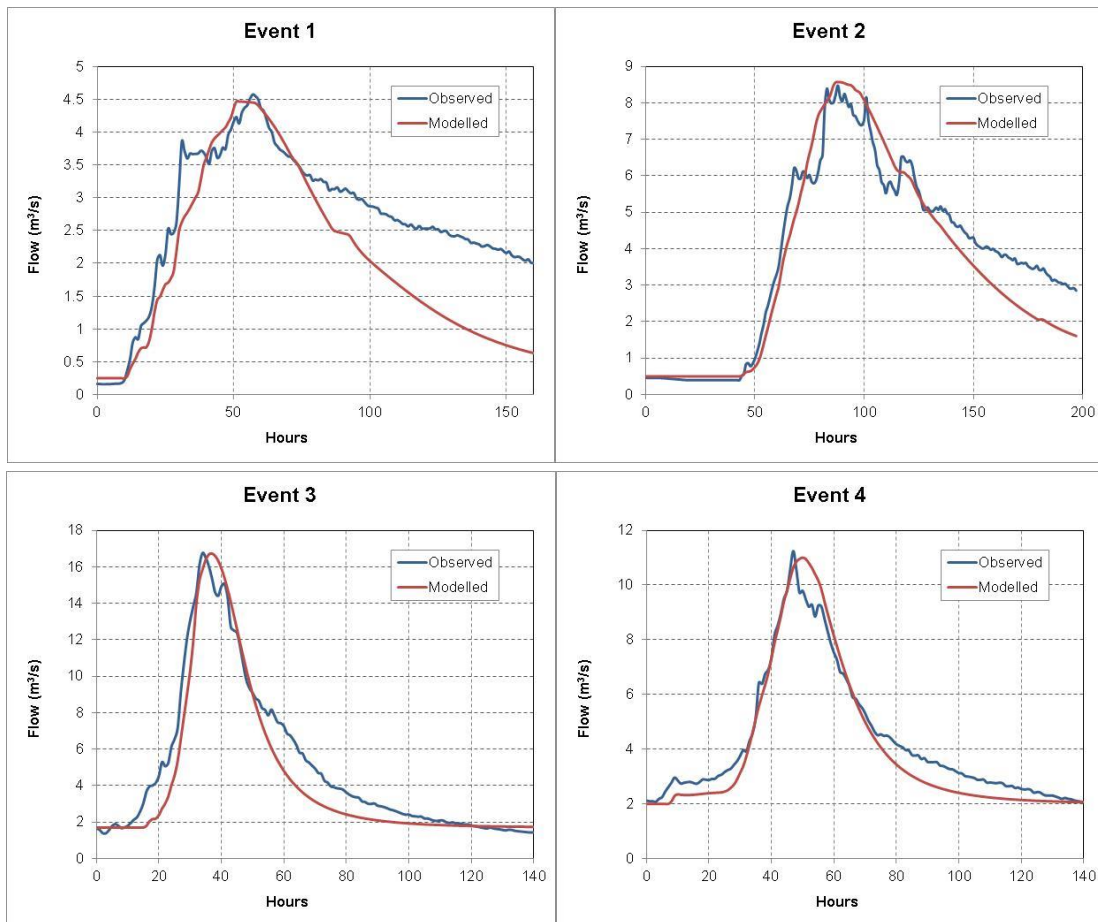
Event	Alpha1	Alpha2	IL (mm)	CL (mm/hr)	Baseflow (m³/s)
1	1	2	25	0.1	11
2	0.7	2.2	0	1.2	5
3	1.2	0.7	35	0.8	12
4	1.5	2.3	41	0.25	3
5	0.5	2	28	2	10

6	1	2	0	2.45	25
7	1.2	2	35	1.4	19

### C.9 Hobart Rivulet

**Table C.27: Events used for Hobart Rivulet model calibration**

Event	Start Date
1	05/08/2011
2	26/09/2009
3	11/08/2010
4	29/11/2009
5	12/04/2011



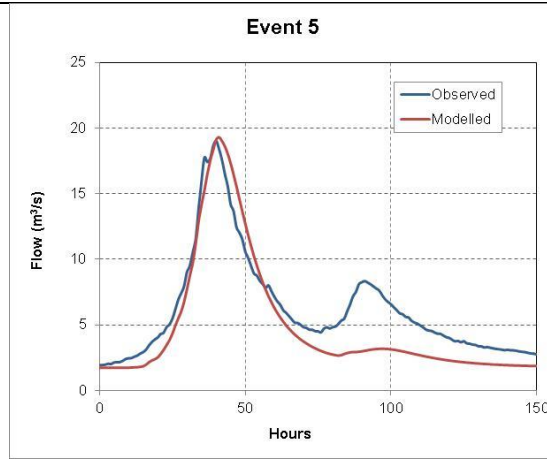


Figure C.9: Hobart Rivulet model event calibration

Table C.28: Hobart Rivulet event calibration results

Statistic	Event				
	1	2	3	4	5
obs_avg	2.85	3.12	6.33	5.02	7.32
mod_avg	2.61	3.17	5.38	4.75	6.16
Bias	0.92	1.01	0.85	0.95	0.84
r-sq	0.89	0.97	0.89	0.93	0.75
obs_peak	4.57	8.47	16.76	11.24	19.01
mod_peak	4.47	8.57	16.73	11.00	19.30
% diff peak	2.32	-1.13	0.19	2.16	-1.50

Table C.29: Hobart Rivulet event calibration model parameters

Event	Alpha	IL (mm)	CL (mm/hr)	Baseflow (m <sup>3</sup> /s)
1	2.5	2.5	0.9	0.25
2	3.5	0	1	0.5
3	1.25	8	7	1.7
4	1.25	4	2	2
5	1.25	5	4.25	1.75

**C.10 Orara River**

**Table C.30: Events used for Orara River model calibration**

Event	Start Date
1	10/03/1974
2	18/05/1977
3	08/07/1985
4	01/04/1989
5	02/05/1996

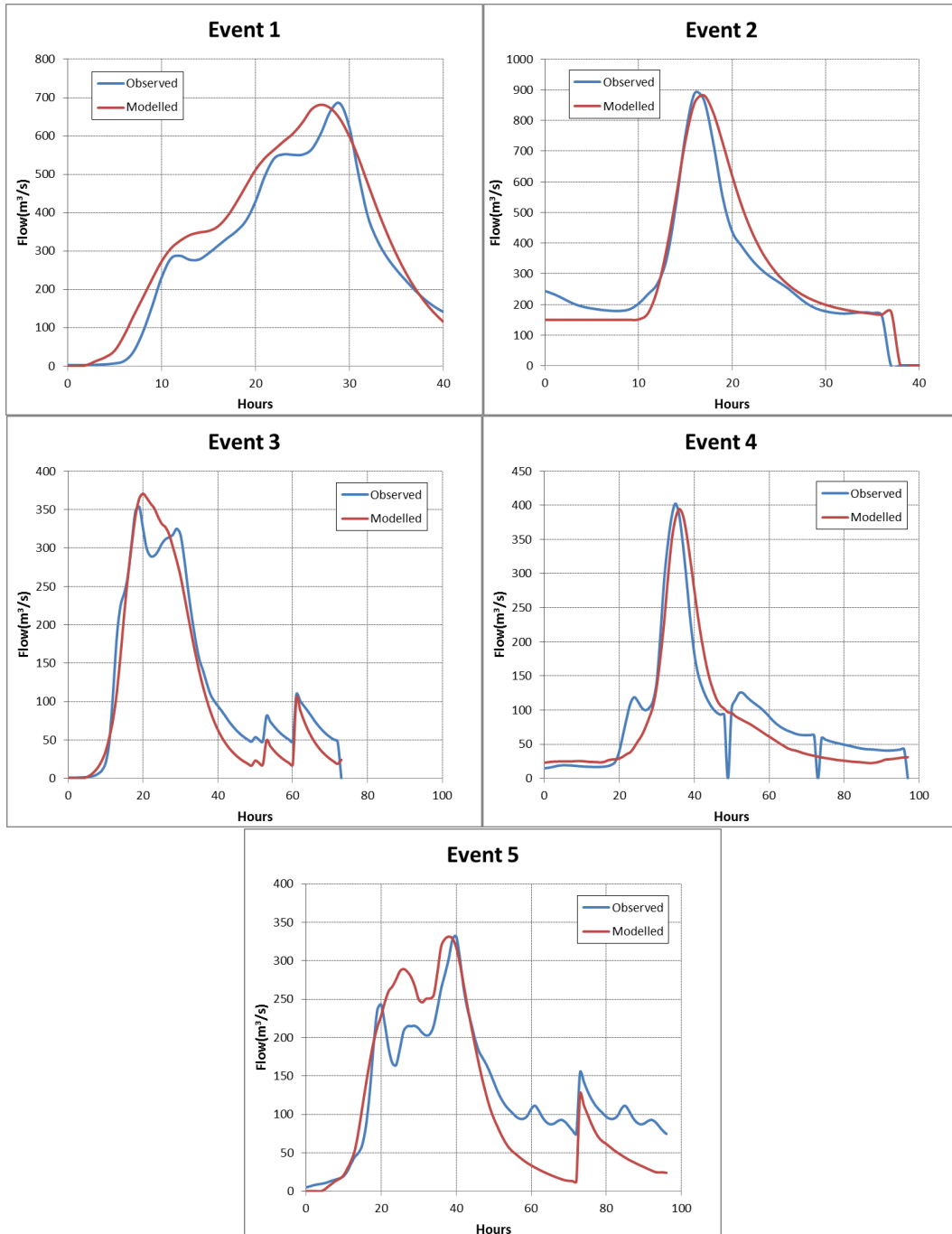


**Table C.31: Orara River event calibration model parameters**

Event	Alpha	IL (mm)	CL (mm/hr)	Baseflow (m <sup>3</sup> /s)
1	1.75	15	2	0
2	1.5	7	12	150
3	1.75	22	4.25	0
4	1.75	0	0	8
5	1.75	7	3	0

## Appendix D Loss calibration

### D.1 Mary River

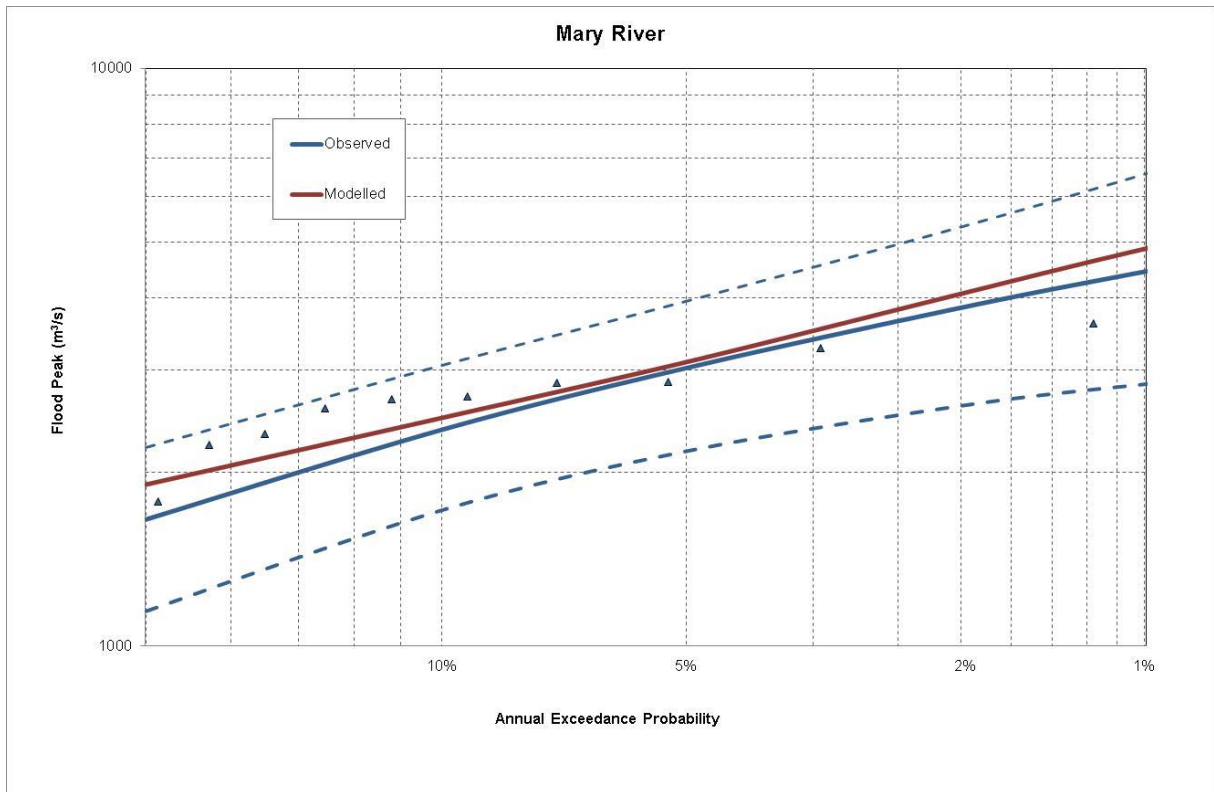


Figure D.1: Mary River Monte Carlo model loss calibration

## D.2 Hann River

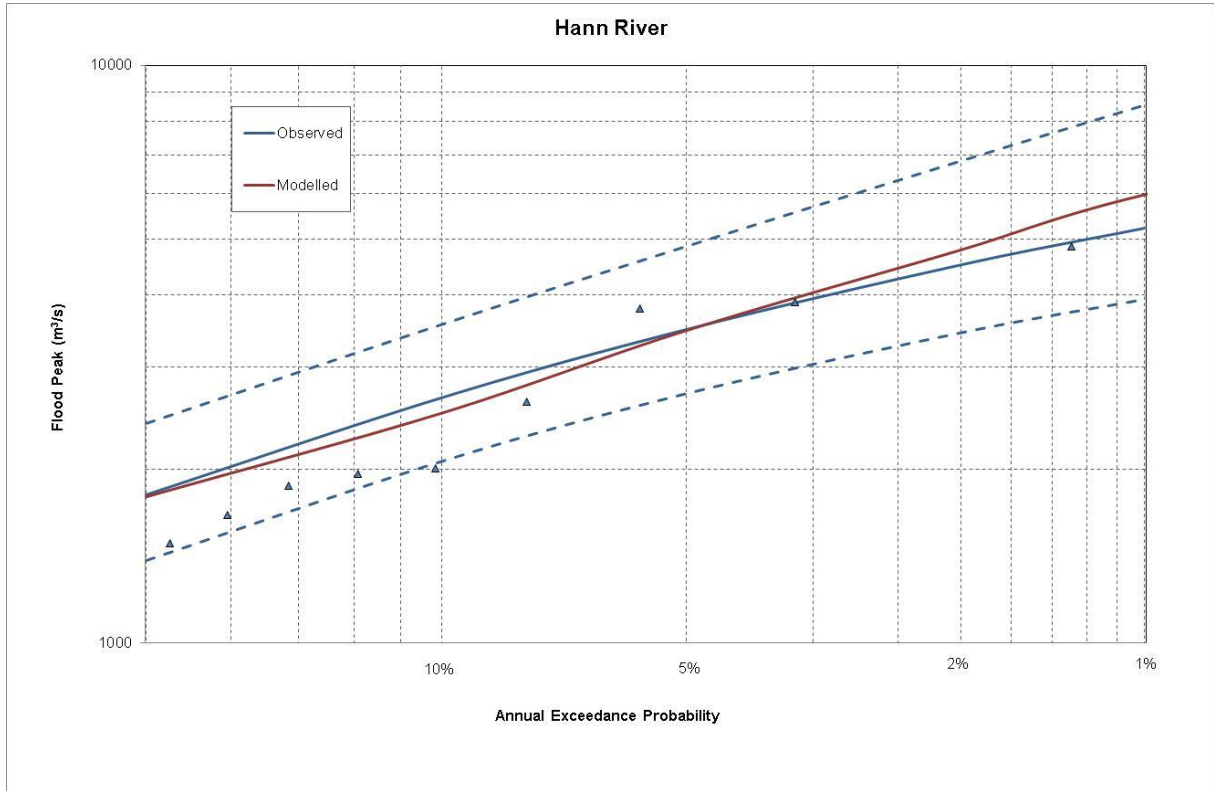


Figure D.2: Hann River Monte Carlo model loss calibration

### D.3 Yates Flat Creek

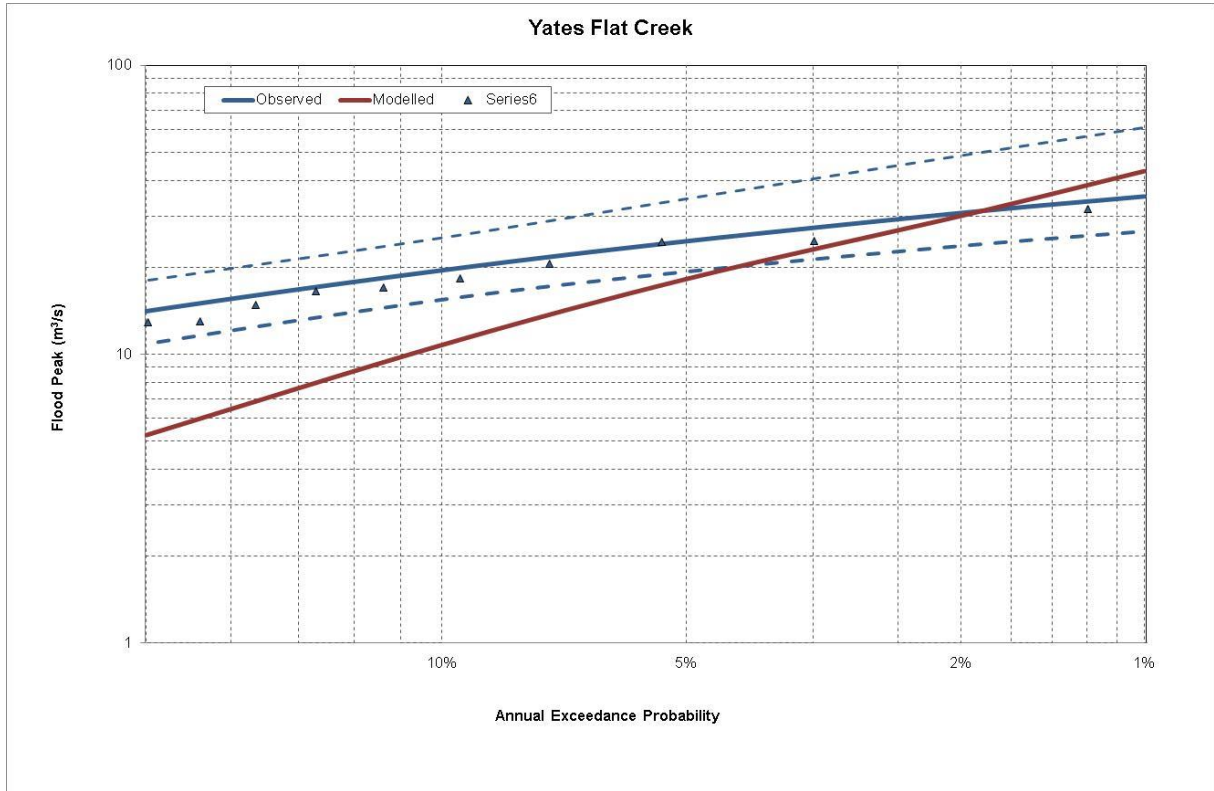


Figure D.3: Yates Flat Creek Monte Carlo model loss calibration

## D.4 Manton River

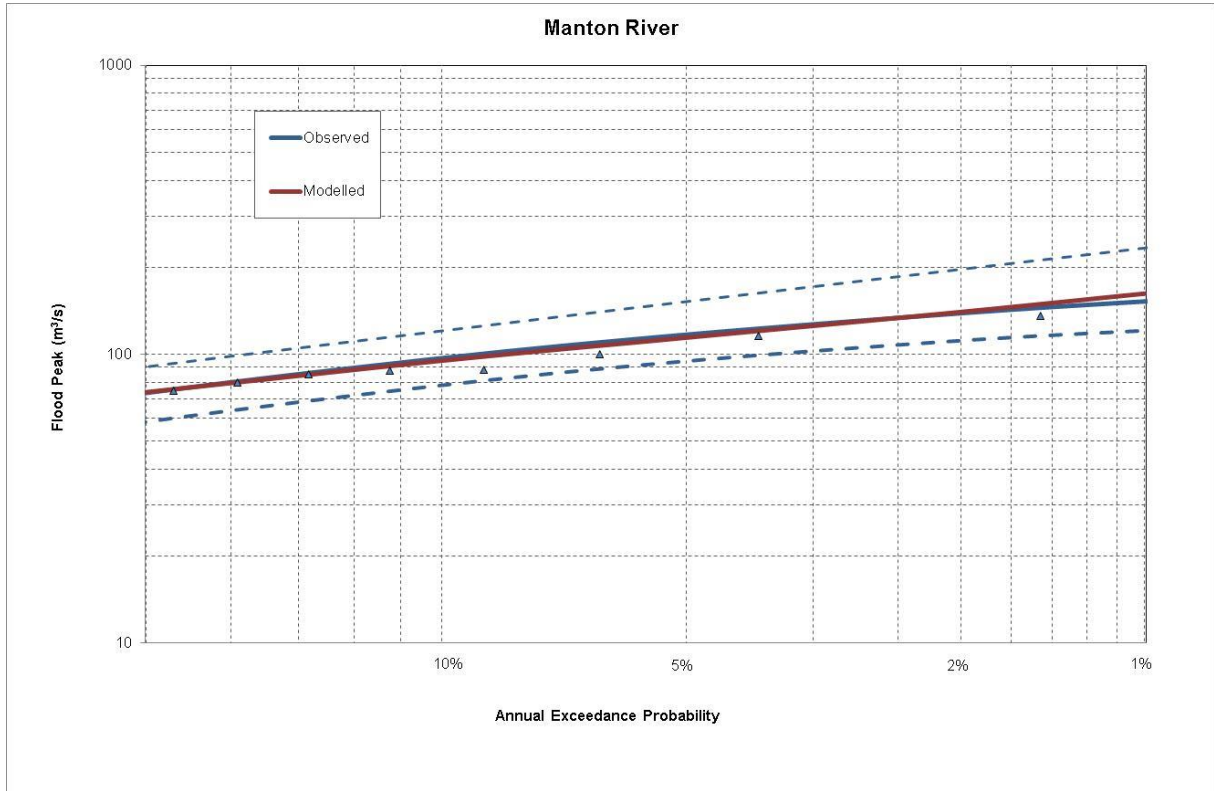


Figure D.4: Manton River Monte Carlo model loss calibration



### D.5 Sixth Creek

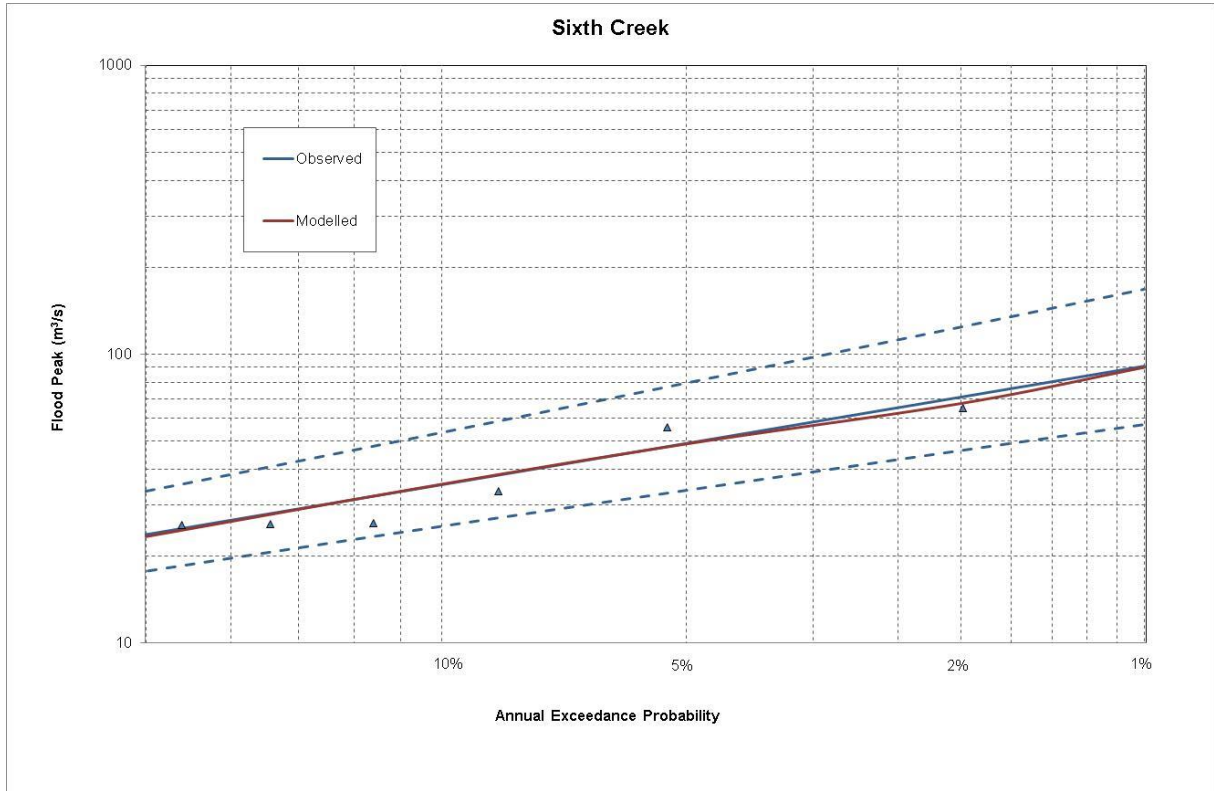


Figure D.5: Sixth Creek Monte Carlo model loss calibration

## D.6 Lerderderg River

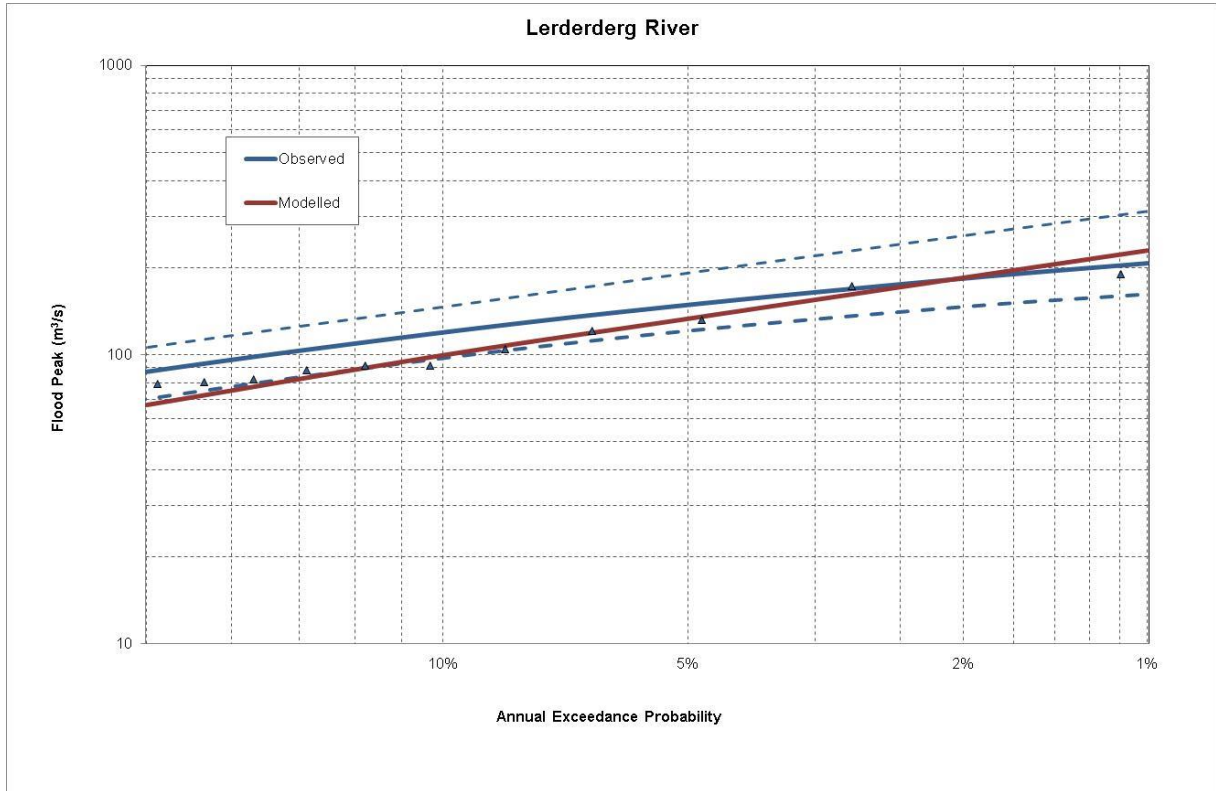


Figure D.6: Lerderderg River Monte Carlo model loss calibration

## D.7 Florentine River

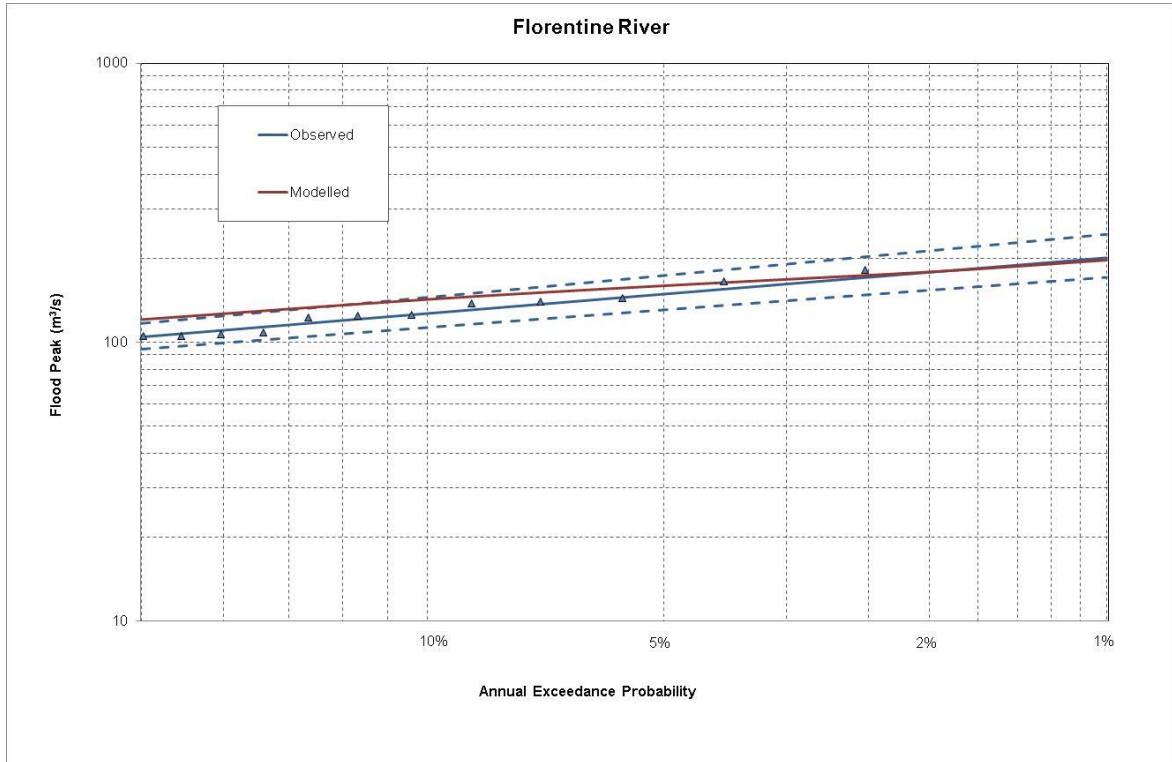


Figure D.7: Florentine River Monte Carlo model loss calibration (single parameter set)

## D.8 Tyenna River

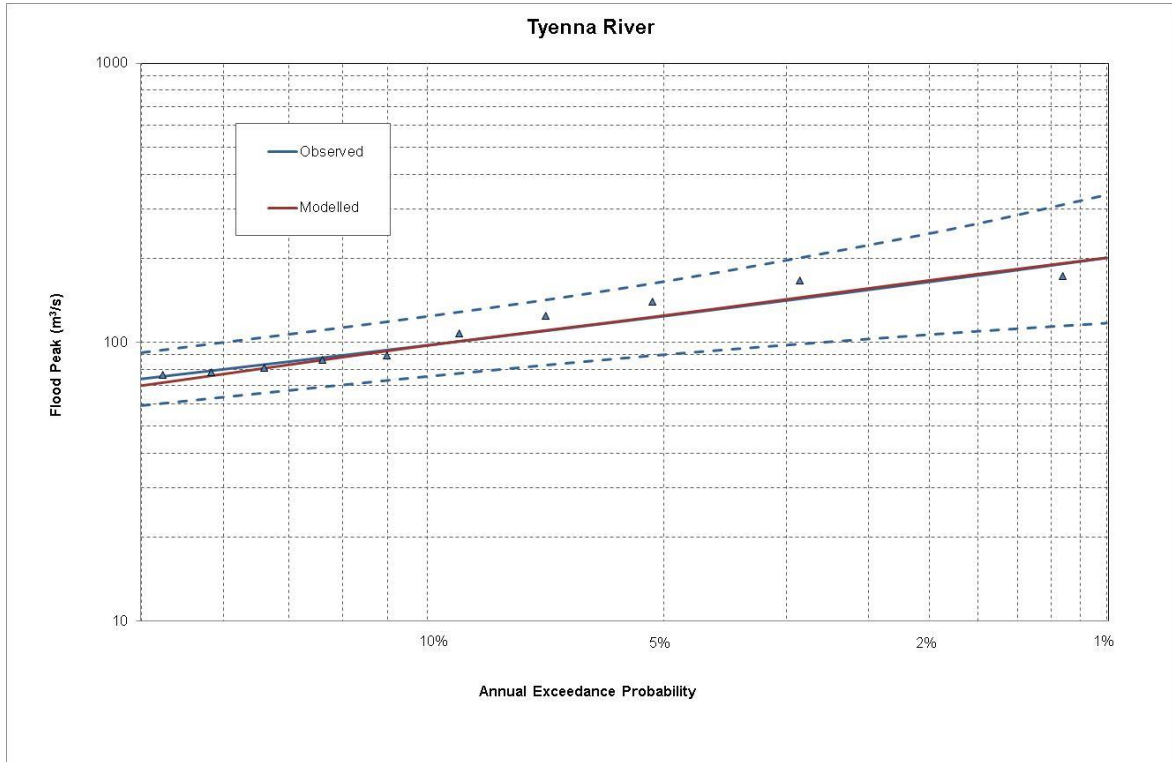


Figure D.8: Tyenna River Monte Carlo model loss calibration

### D.9 Hobart Rivulet

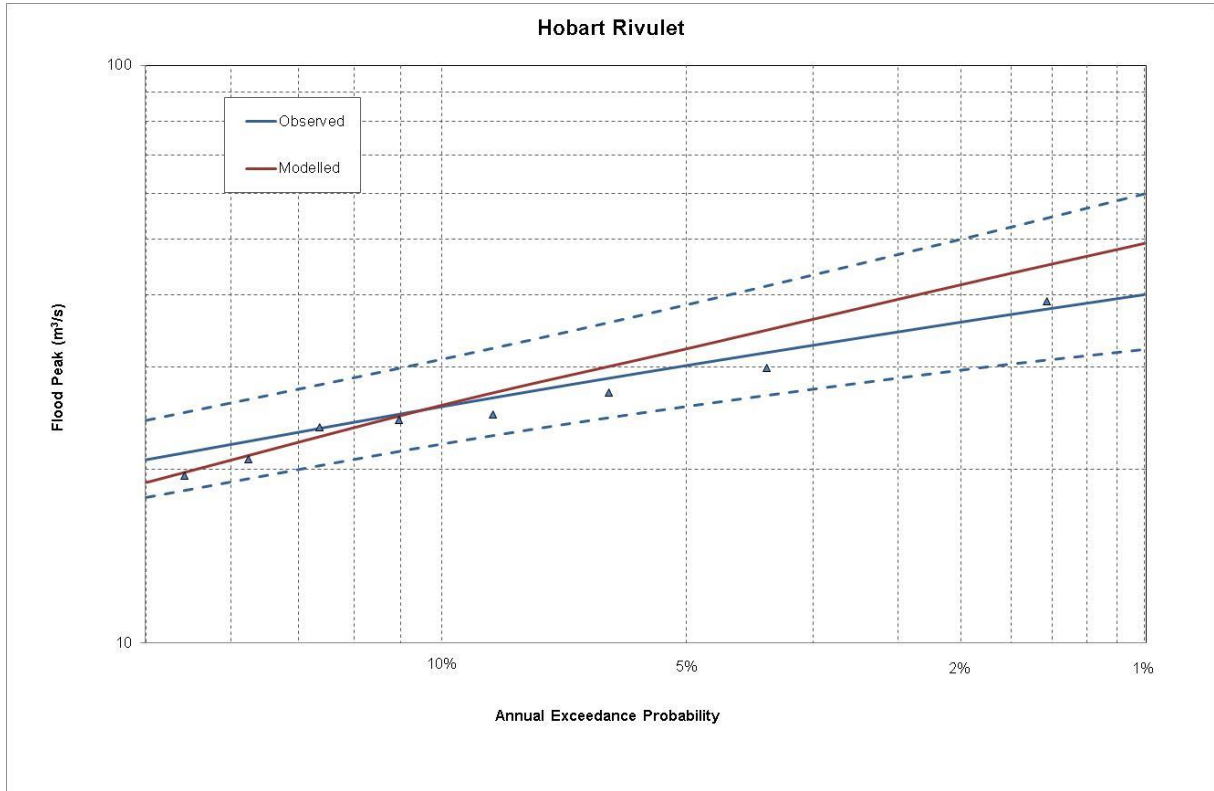


Figure D.9: Hobart Rivulet Monte Carlo model loss calibration

## D.10 Orara River

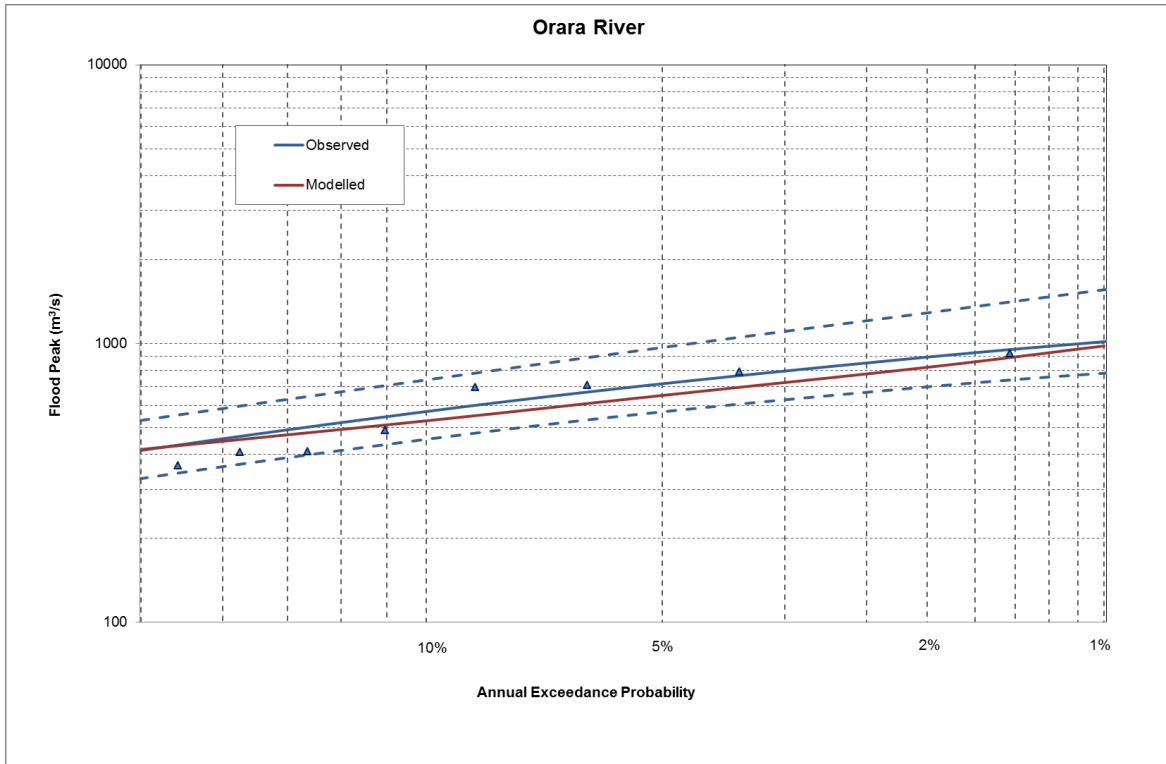


Figure D.10: Orara River Monte Carlo model loss calibration

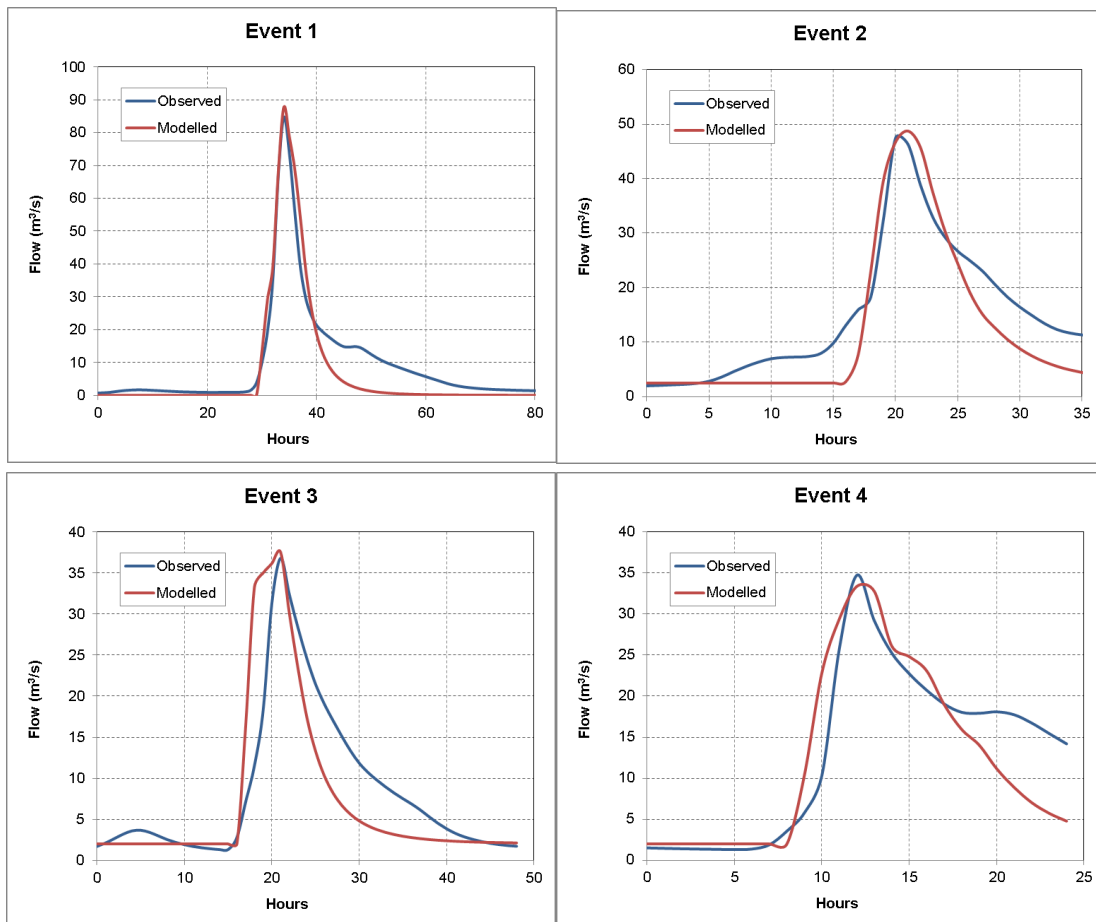
**Appendix E Calibration to subset of data**

**E.1 Manton River**

**Period 1: 1965-1987**

**Table E.1: Events used for Manton River model calibration for Period 1**

Event	Start Date
1	11/03/1981
2	20/03/1977
3	03/03/1974
4	18/03/1974
5	13/02/1975



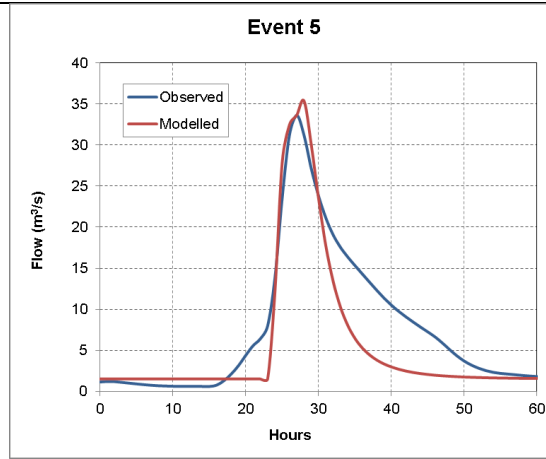


Figure E.1: Manton River model event calibration for Period 1

Table E.2: Manton River event calibration results for Period 1

Statistic	Event				
	1	2	3	4	5
obs_avg	8.31	15.11	8.54	13.08	7.72
mod_avg	5.99	12.02	7.35	12.29	5.63
Bias	0.72	0.80	0.86	0.94	0.73
r-sq	0.88	0.80	0.62	0.75	0.78
obs_peak	84.70	47.47	36.81	34.74	33.63
mod_peak	87.73	48.76	37.54	33.38	35.37
% diff peak	-3.58	-2.72	-1.96	3.90	-5.19

**Period 2: 1990-2012**

All events selected from full record were in period 2, therefore event calibration remains the same as for the full record.

**E.2 Mary River**

**Period 1: 1965-1988**

Table E.3: Events used for Mary River model calibration for Period 1

Event	Start Date
1	08/02/1972
2	26/01/1974
3	08/01/1968
4	05/07/1973
5	02/04/1972



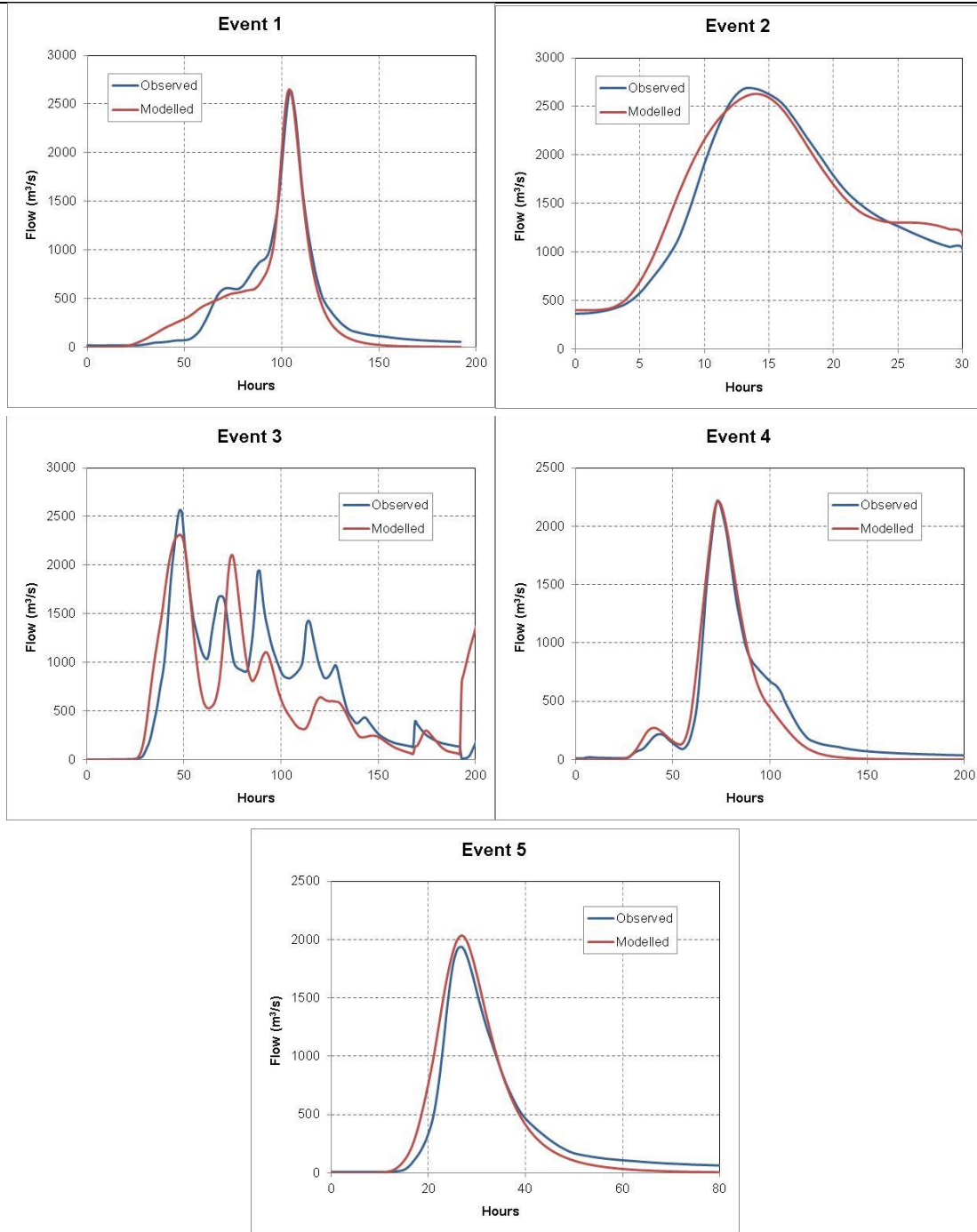


Figure E.2: Mary River model event calibration for Period 1

Table E.4: Mary River event calibration results for Period 1

Statistic	Event				
	1	2	3	4	5
obs_avg	337.92	746.70	912.48	545.14	308.22
mod_avg	360.33	774.86	879.95	575.15	307.60
Bias	1.07	1.04	0.96	1.06	1.00
r-sq	0.91	0.98	0.64	0.98	0.94
obs_peak	1868.82	2681.33	2568.64	2219.98	1934.93
mod_peak	2029.72	2629.80	2312.98	2212.31	2034.21

<b>% diff peak</b>	-8.61	1.92	9.95	0.35	-5.13
--------------------	-------	------	------	------	-------

**Period 2: 1988-2013**

**Table E.1: Events used for Mary River model calibration for Period 2**

<b>Event</b>	<b>Start Date</b>
1	02/04/1989
2	23/04/1989
3	7/02/1999
4	9/01/2011
5	26/01/2013

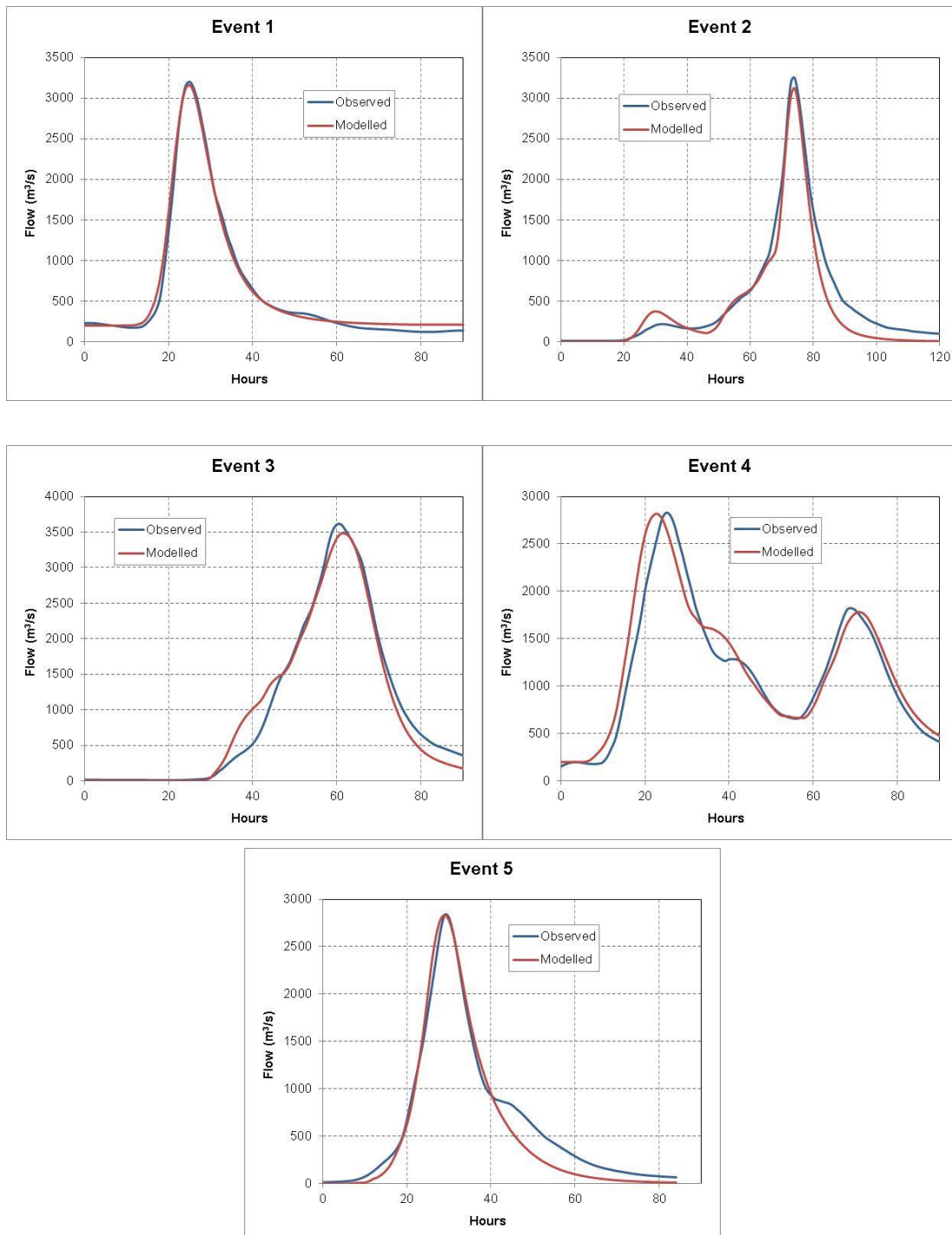


Figure E.3: Mary River model event calibration for Period 2

**Table E.5: Mary River event calibration results for Period 2**

Statistic	Event				
	1	2	3	4	5
<b>obs_avg</b>	912.48	545.14	308.22	1067.36	637.98
<b>mod_avg</b>	879.95	575.15	307.60	1124.54	558.48
<b>Bias</b>	0.96	1.06	1.00	1.05	0.88
<b>r-sq</b>	0.64	0.98	0.94	0.93	0.97
<b>obs_peak</b>	2568.64	2219.98	1934.93	2828.18	2836.57
<b>mod_peak</b>	2312.98	2212.31	2034.21	2816.56	2833.27
<b>% diff peak</b>	9.95	0.35	-5.13	0.41	0.12

## Appendix F Flood frequency curves

### F.1 Mary River

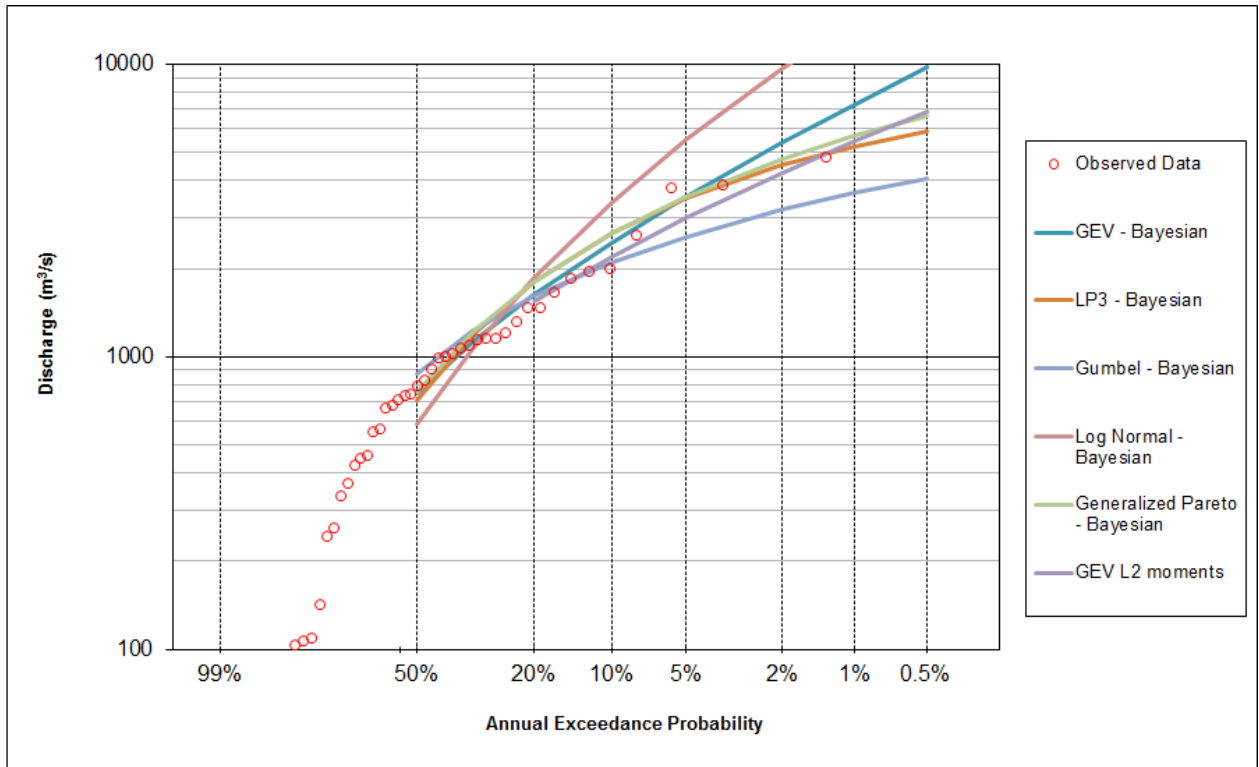


Figure F.1: Mary River flood FLIKE frequency curve fitting results

### F.2 Hann River

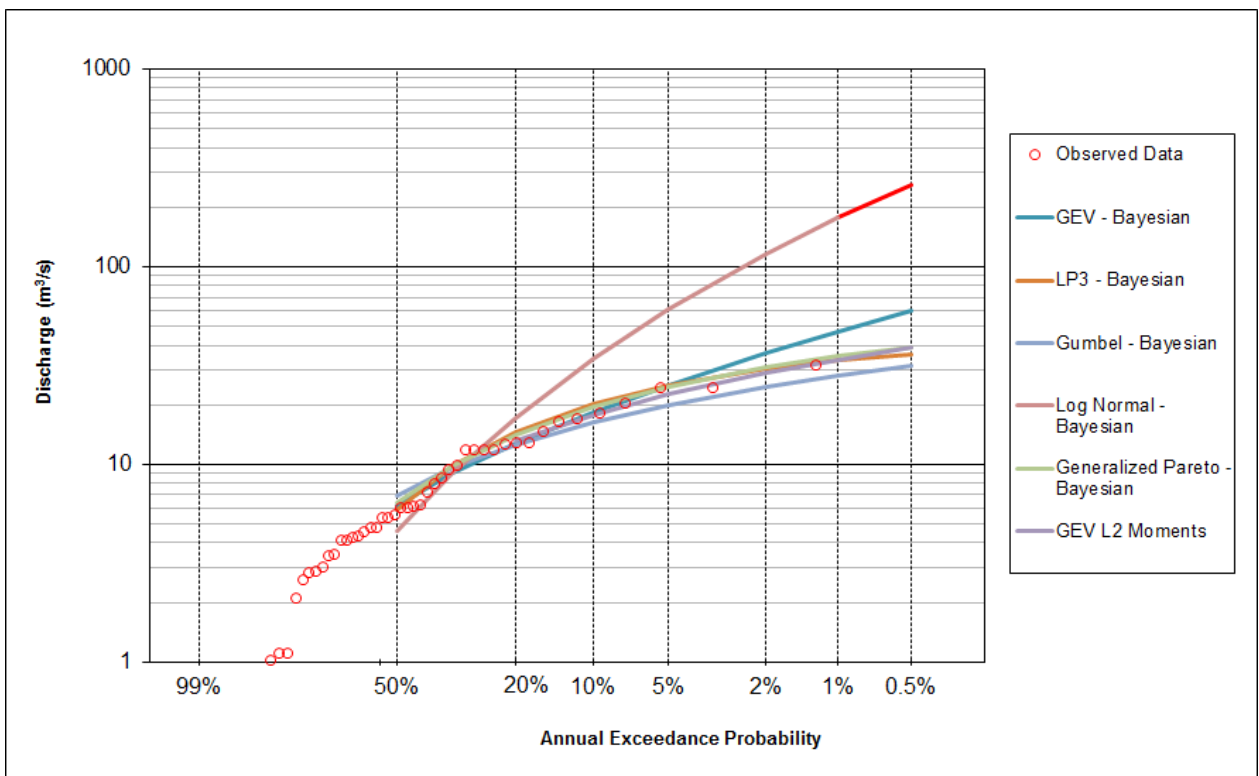


Figure F.2: Hann River flood FLIKE frequency curve fitting results

### F.3 Yates Flat Creek

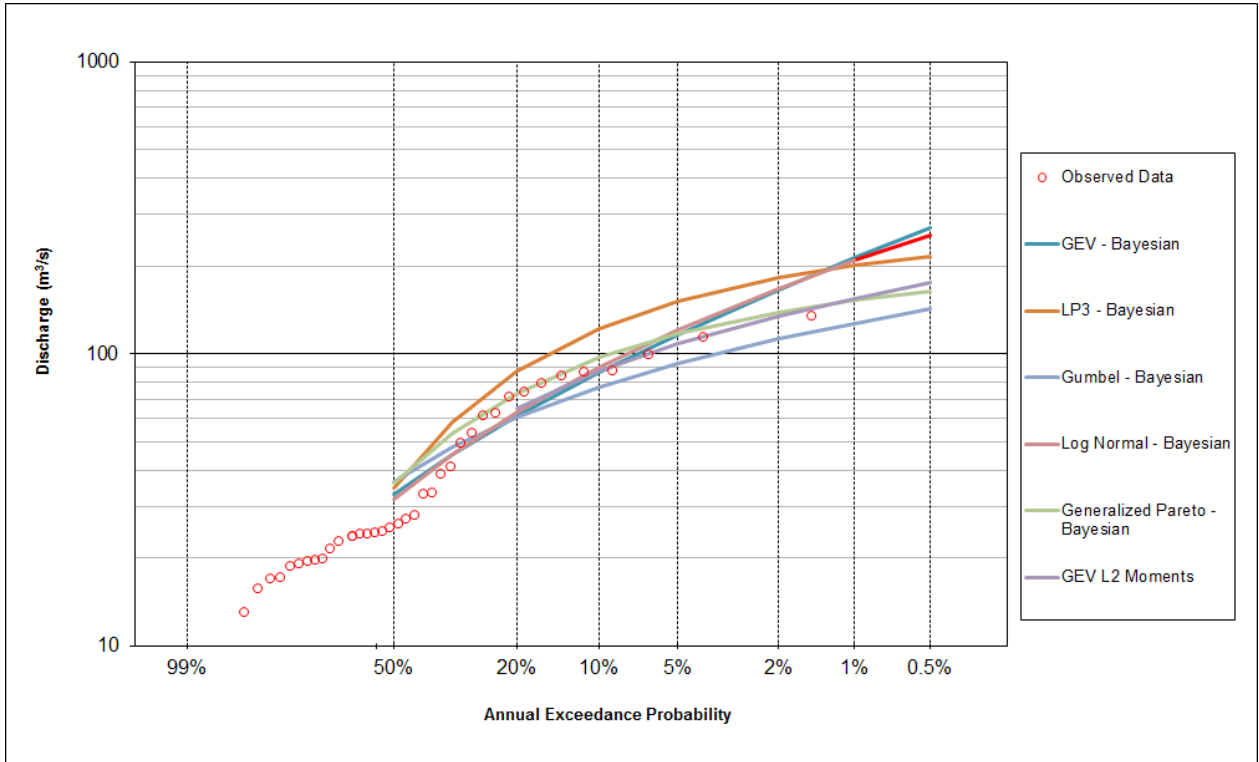


Figure F.3: Yates Flat Creek flood FLIKE frequency curve fitting results

### F.4 Manton River

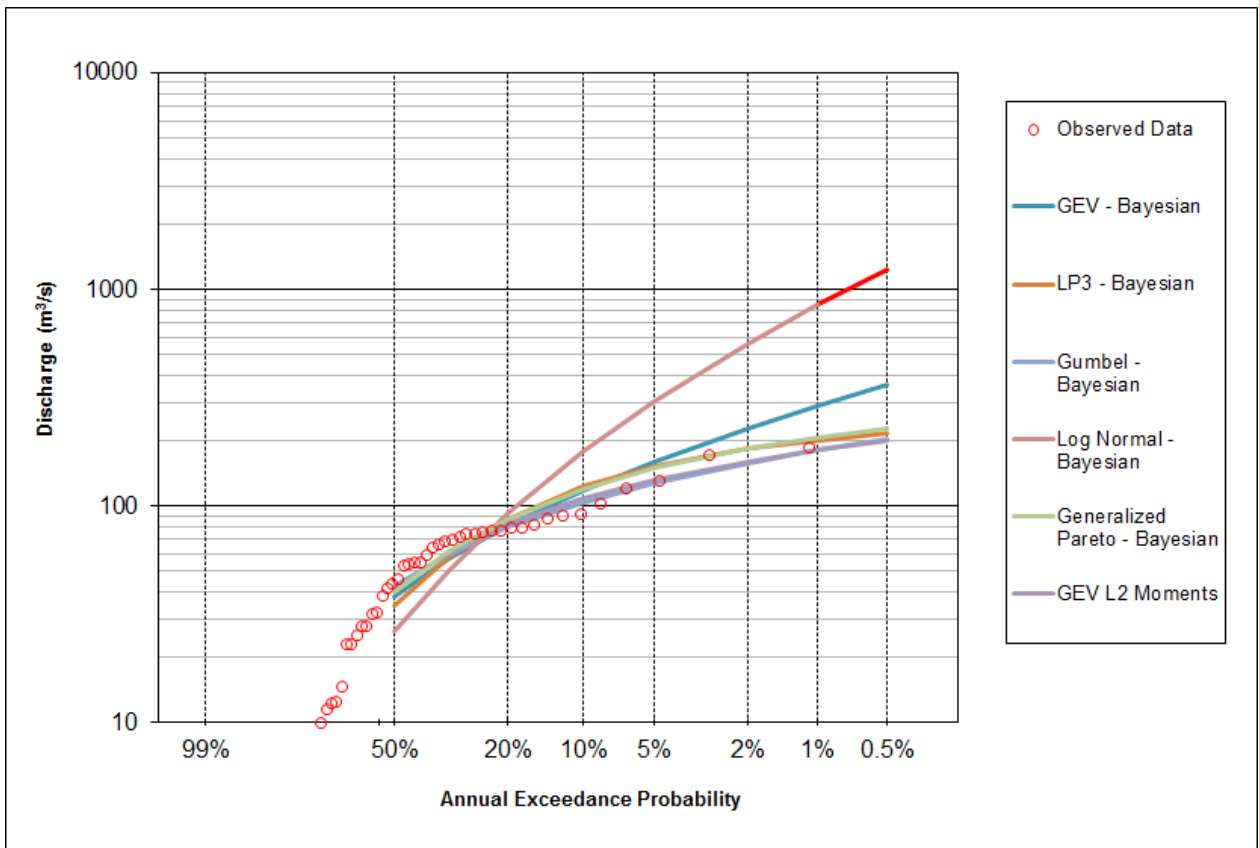


Figure F.4: Manton River flood FLIKE frequency curve fitting results

### F.5 Sixth Creek

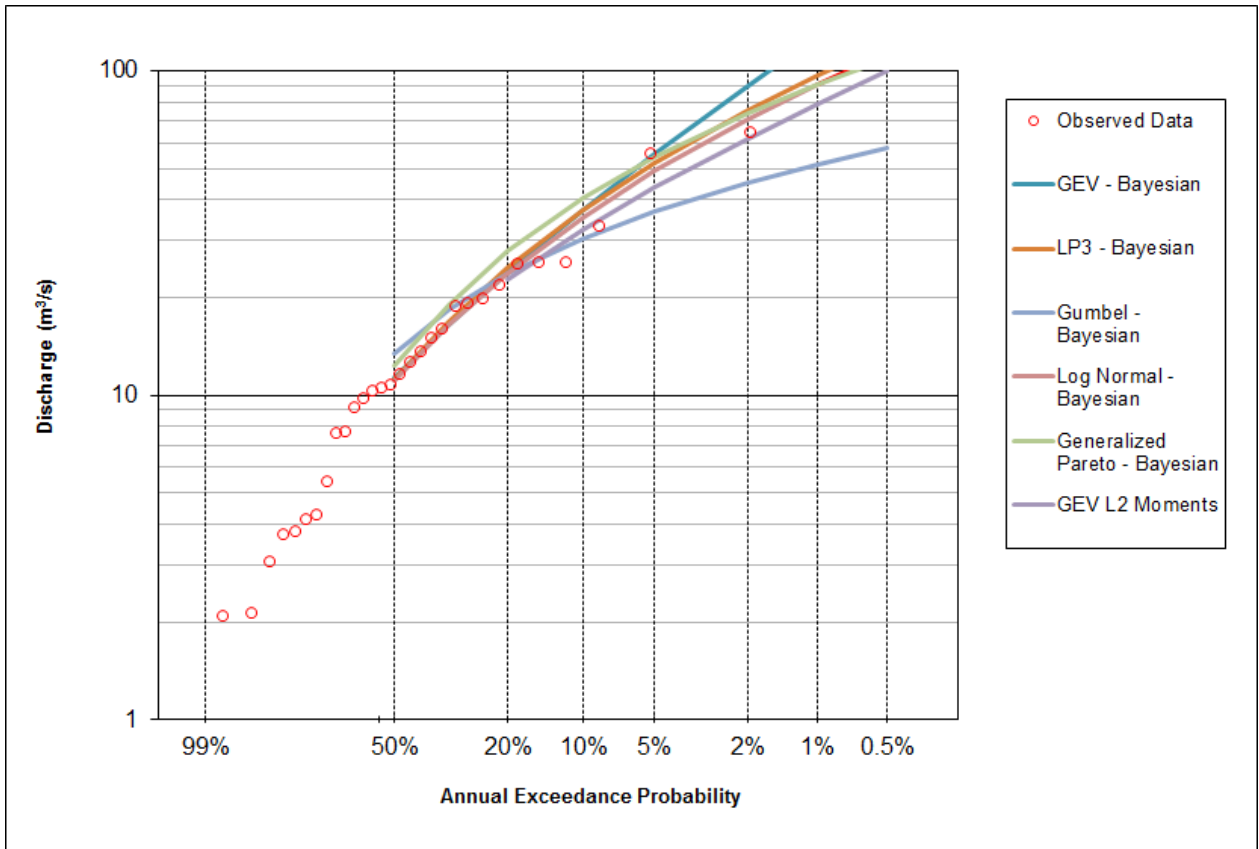


Figure F.5: Sixth Creek flood FLIKE frequency curve fitting results

### F.6 Lerderderg River

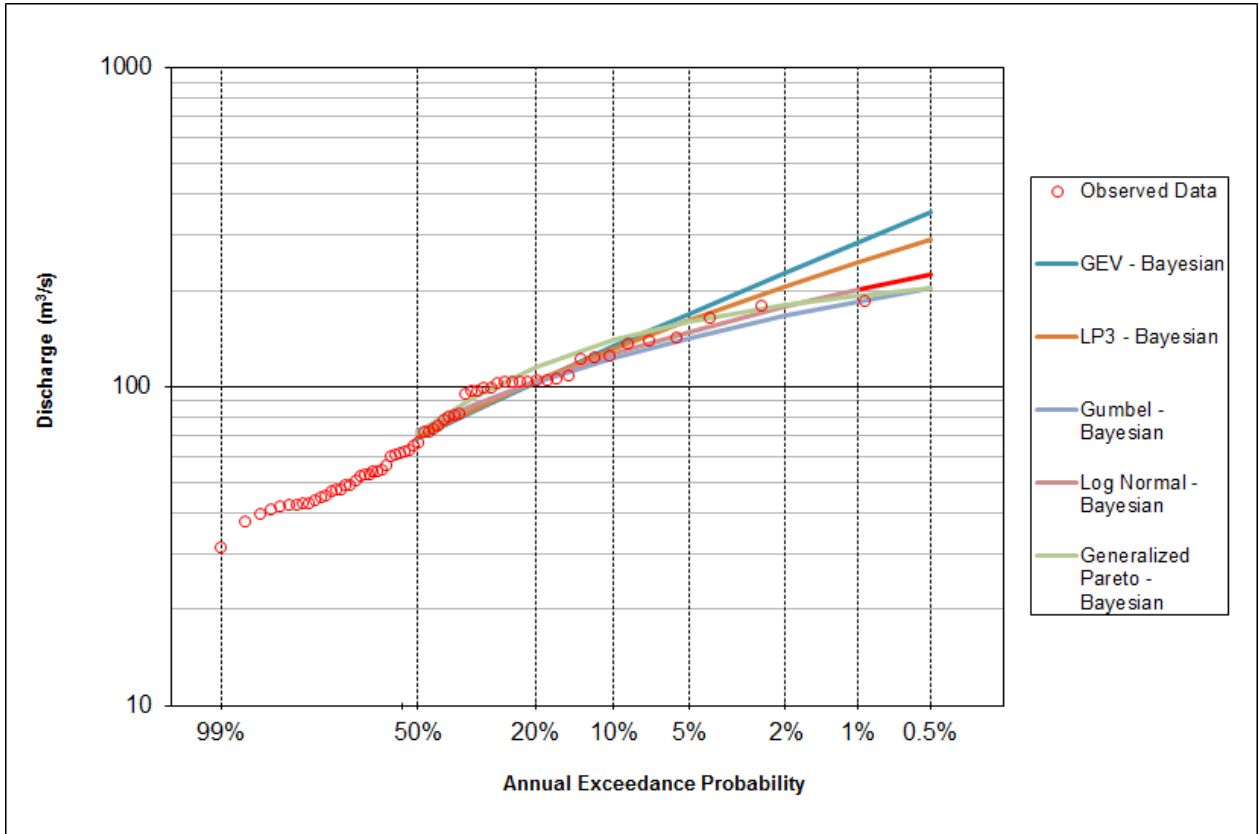


Figure F.6: Lerderderg River flood FLIKE frequency curve fitting results

### F.7 Florentine River

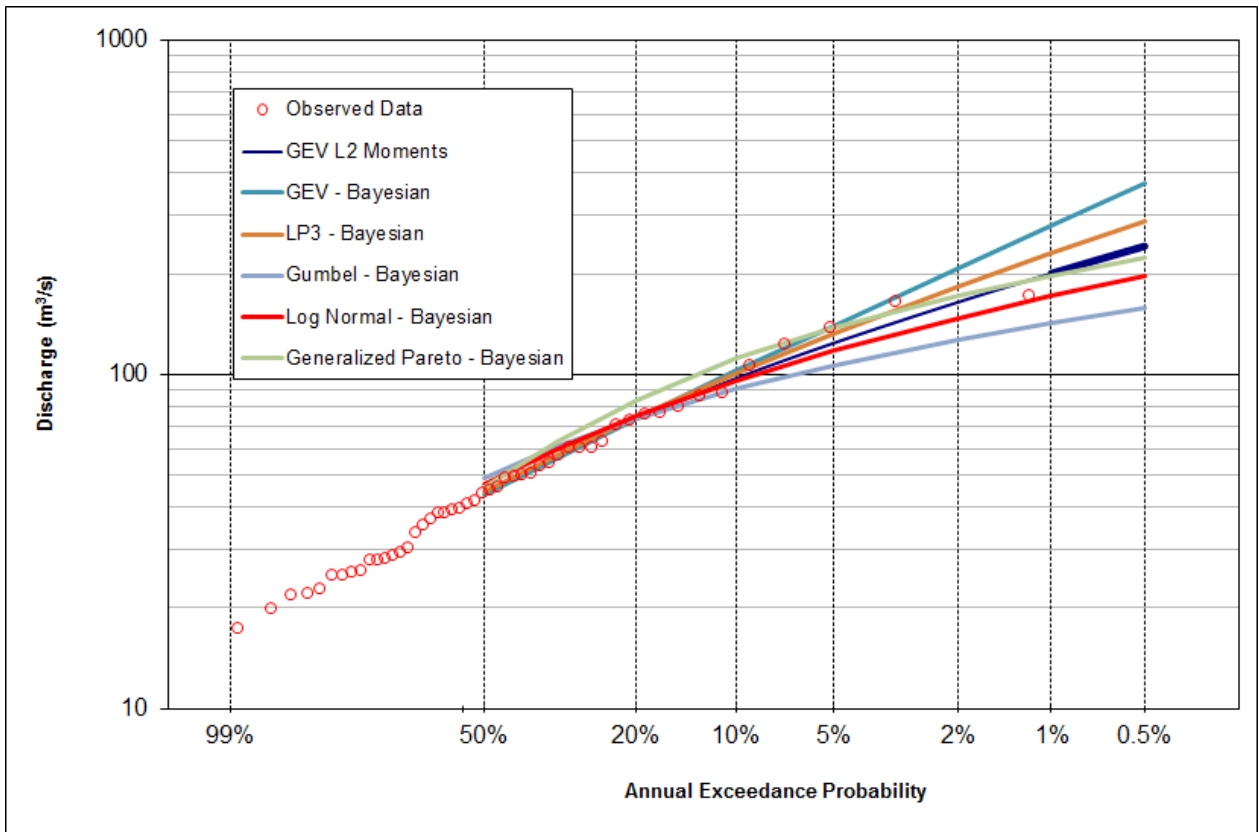


Figure F.7: Florentine River flood FLIKE frequency curve fitting results

### F.8 Tyenna River

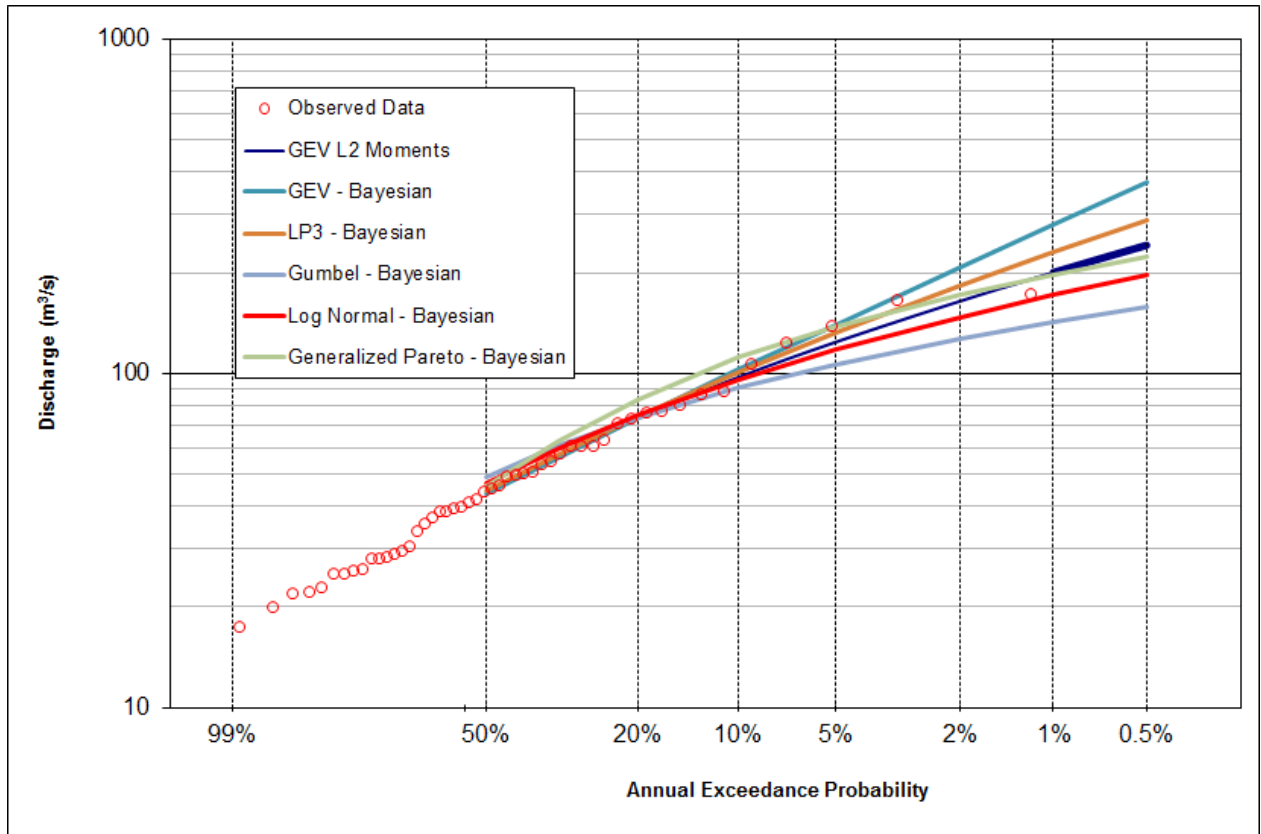


Figure F.8: Manton River flood FLIKE frequency curve fitting results



### F.9 Hobart Rivulet

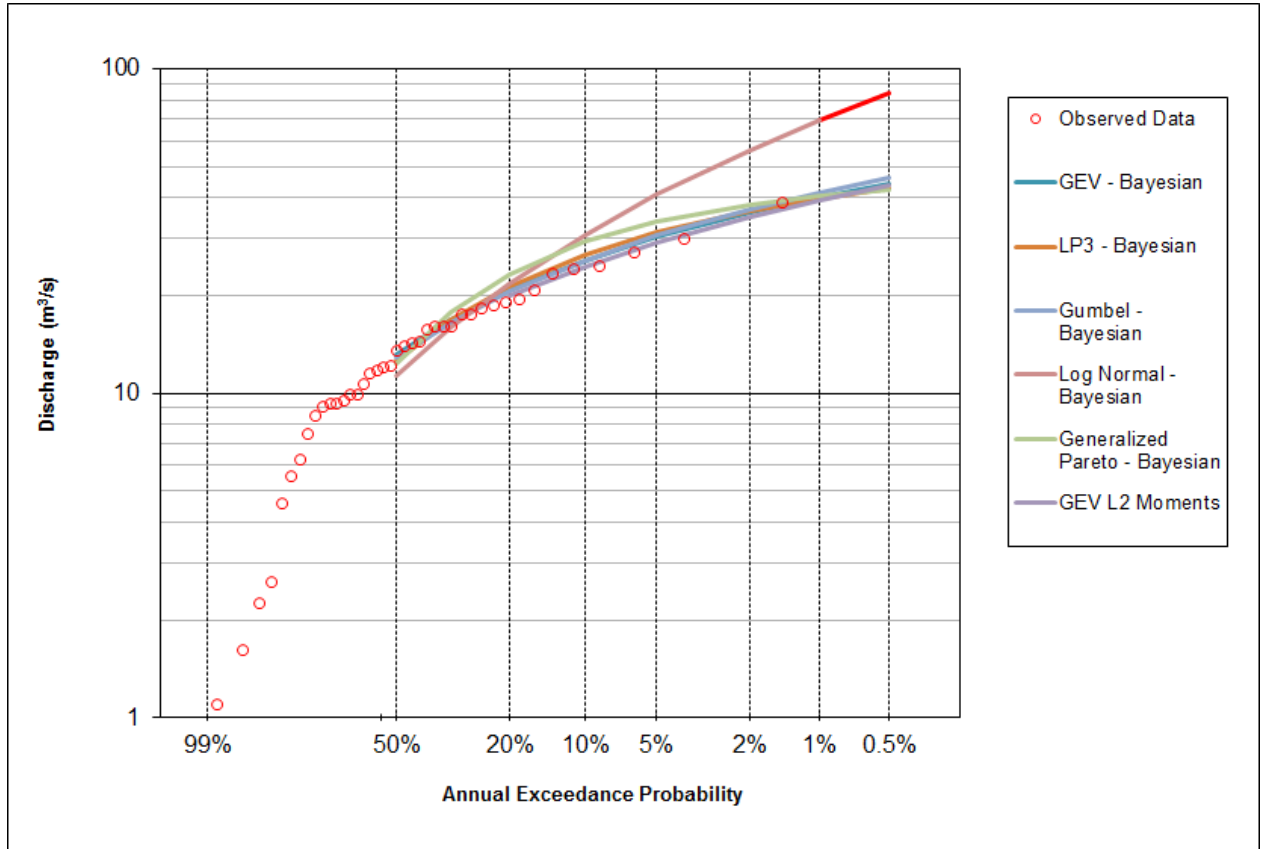


Figure F.9: Hobart Rivulet flood FLIKE frequency curve fitting results

### F.10 Orara River

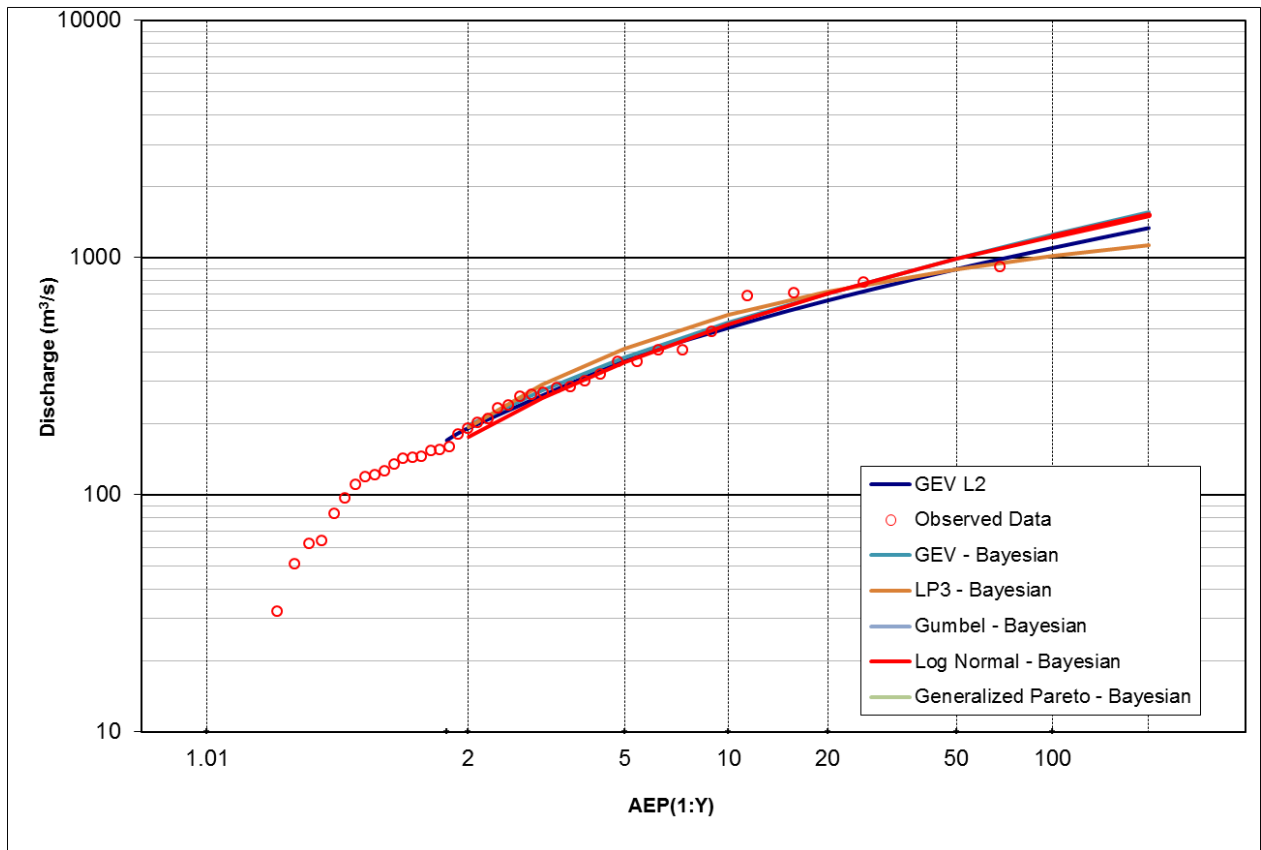


Figure F. 10 Orara River flood FLIKE frequency curve fitting results

## Appendix G Additional model results

### G.1 Florentine River - Derived IFDs from at-site rainfalls and two parameter sets

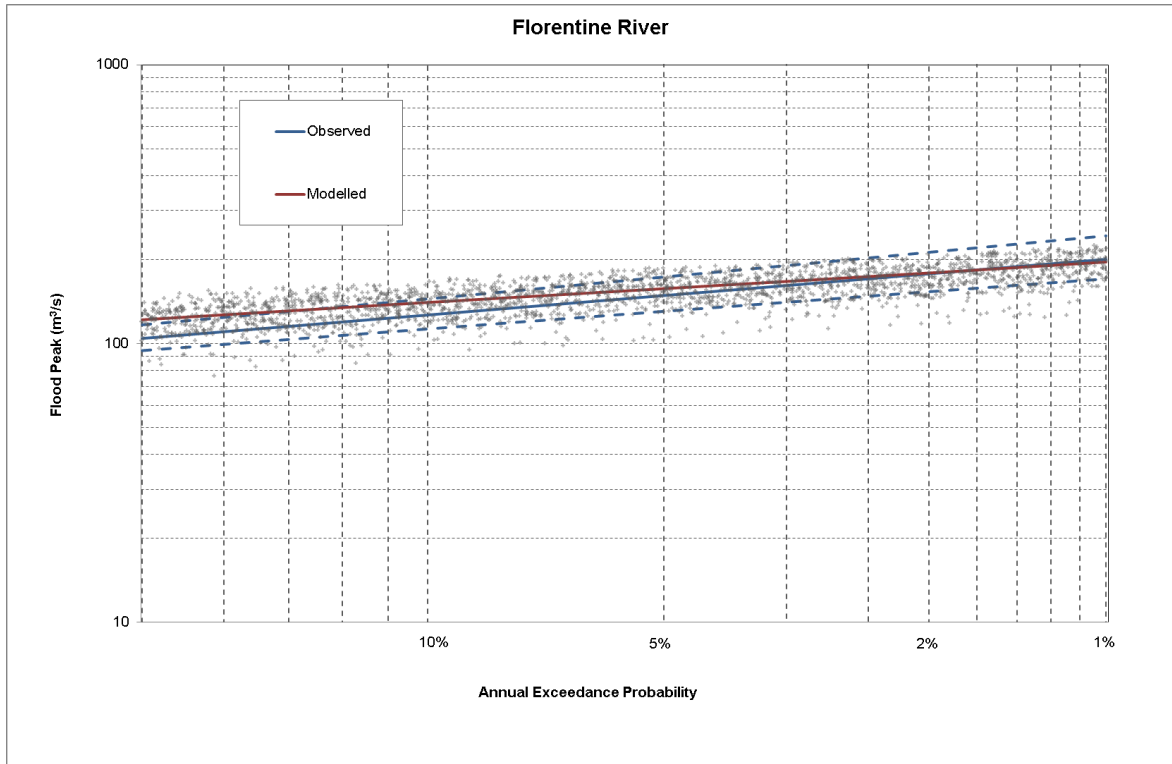


Figure G.1: Florentine River model Monte Carlo results using at-site IFDs and two parameter sets

## **Appendix H**

## **Continuous Simulation model structures**

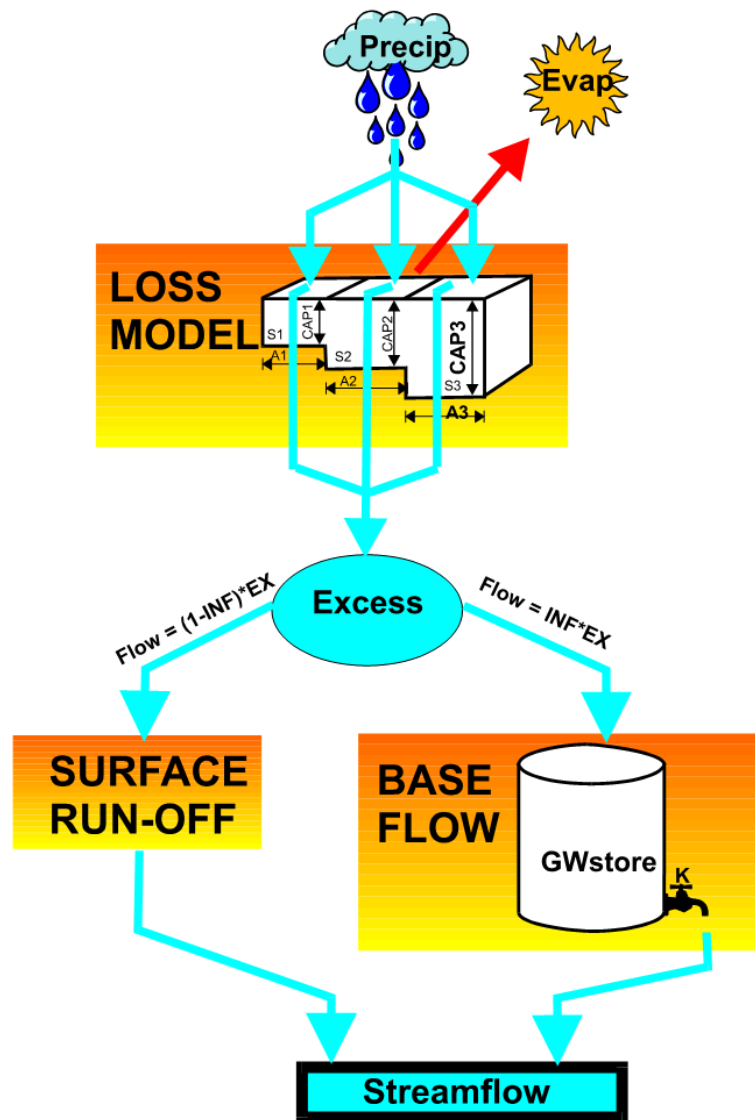


Figure H. 1: Structure of the AWBM model

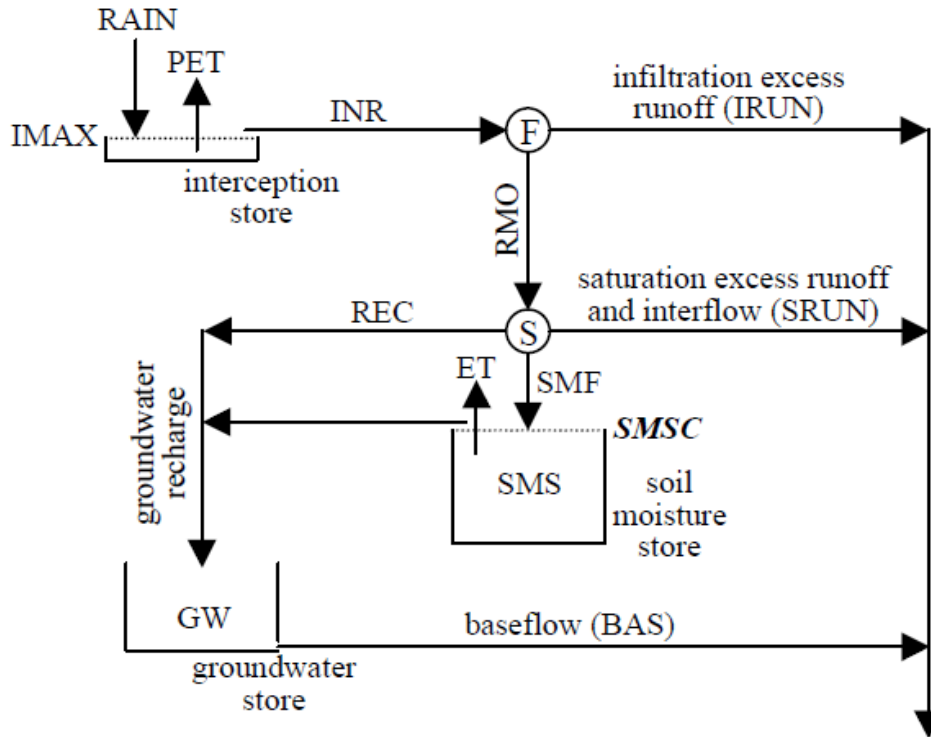


Figure H. 2: Structure of SIMHYD model adapted from (Chiew, et al. 2002)

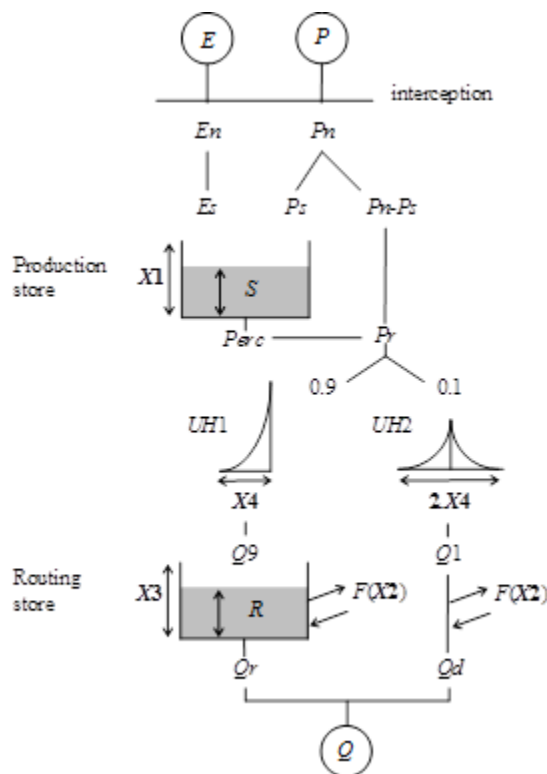


Figure H. 3 : Structure of the GR4H model, directly adapted from (Bennett et al., 2014)

## **Appendix I**

## **Data used for calibration**

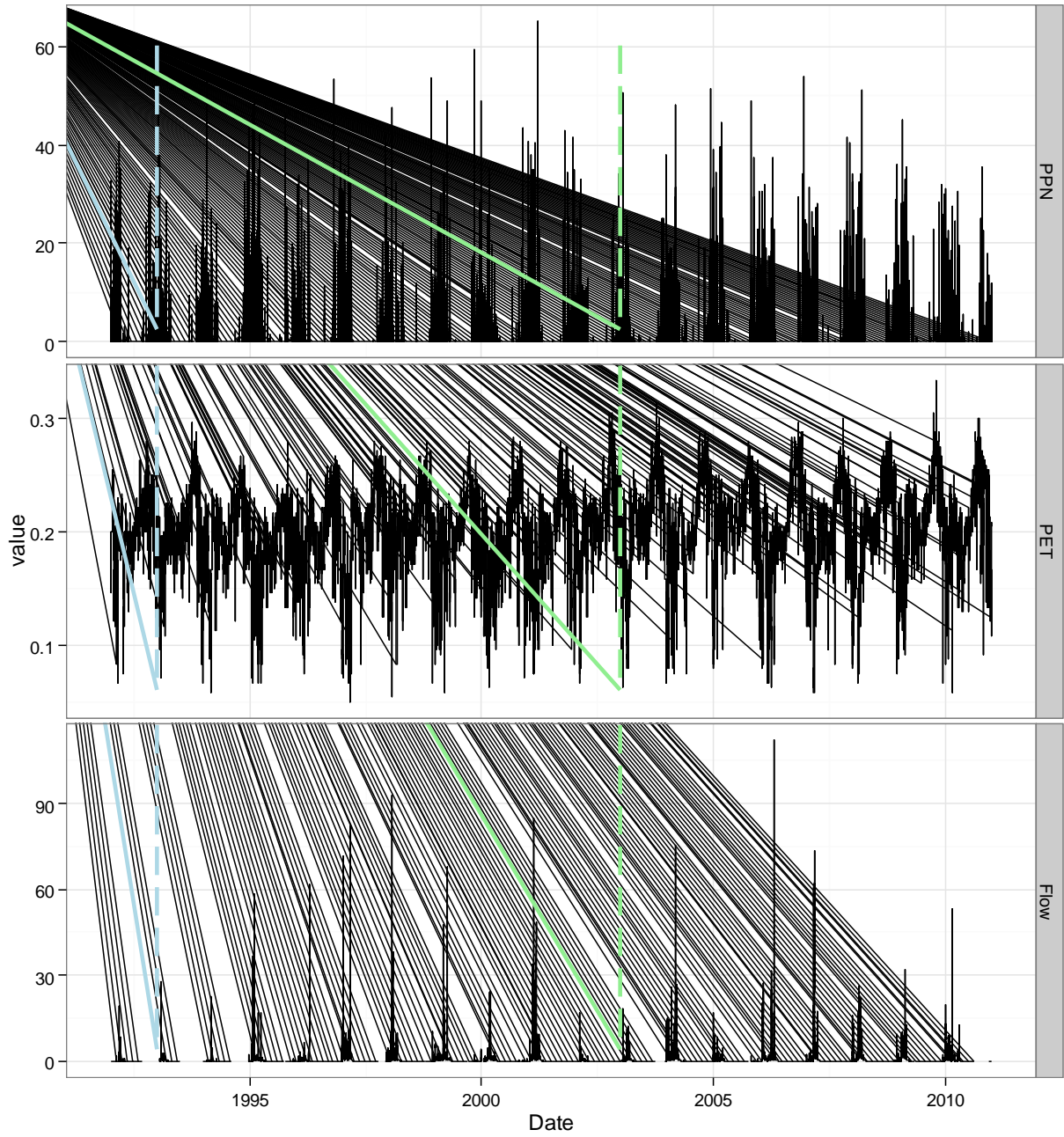


Figure I. 1 : Data used for the calibration of Manton River [Flow in cumecs, precipitation (PPN) and potential evapotranspiration (PET) in mm]



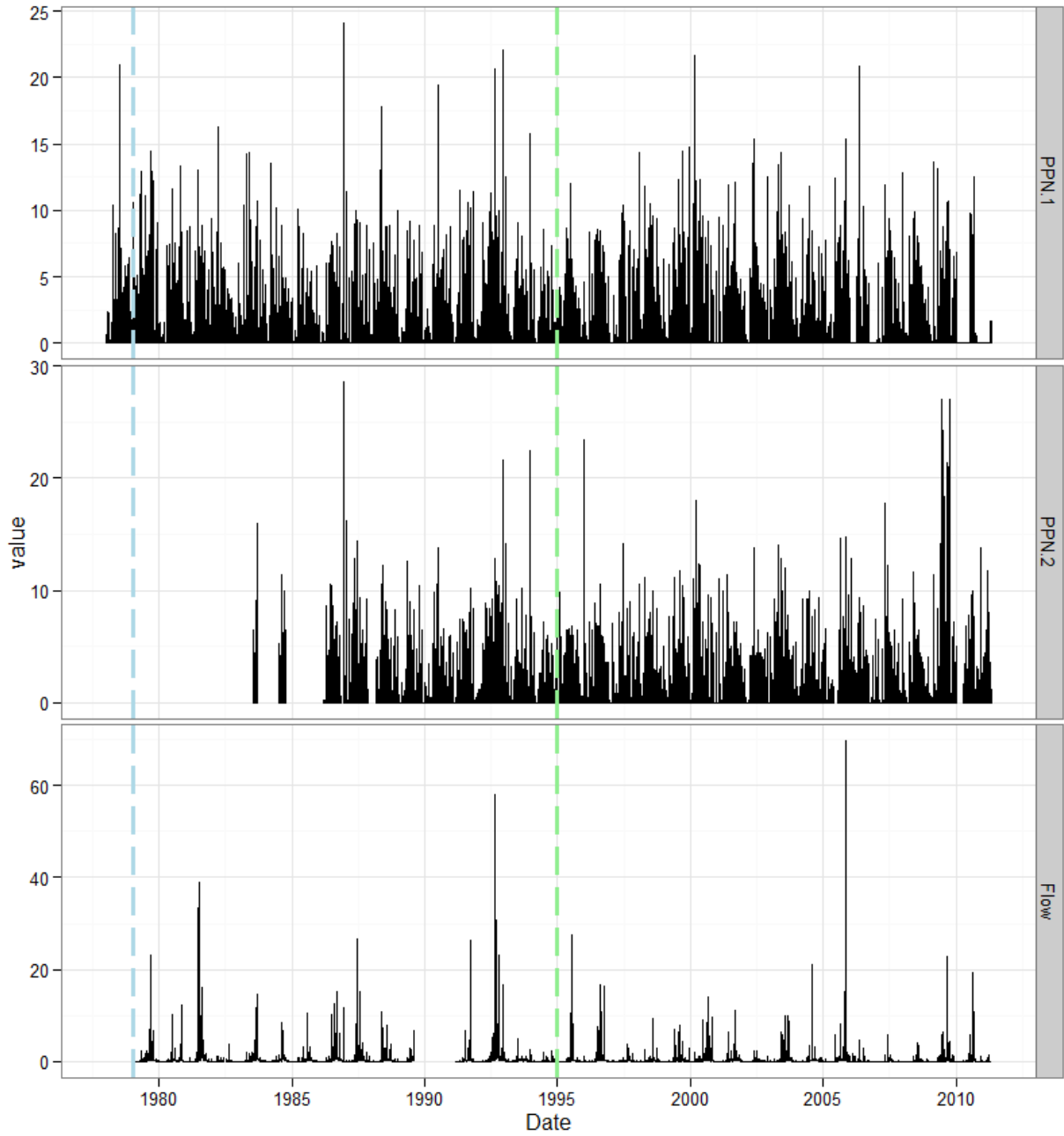


Figure I. 2: Data used for the calibration of Sixth Creek [ *PPN.1* = precipitation in mm from pluviograph station 23801 located in Lenswood Research Centre, *PPN.2* = precipitation in mm from pluvio station AW504559 located in Cherryville, *Flow* in cumecs]

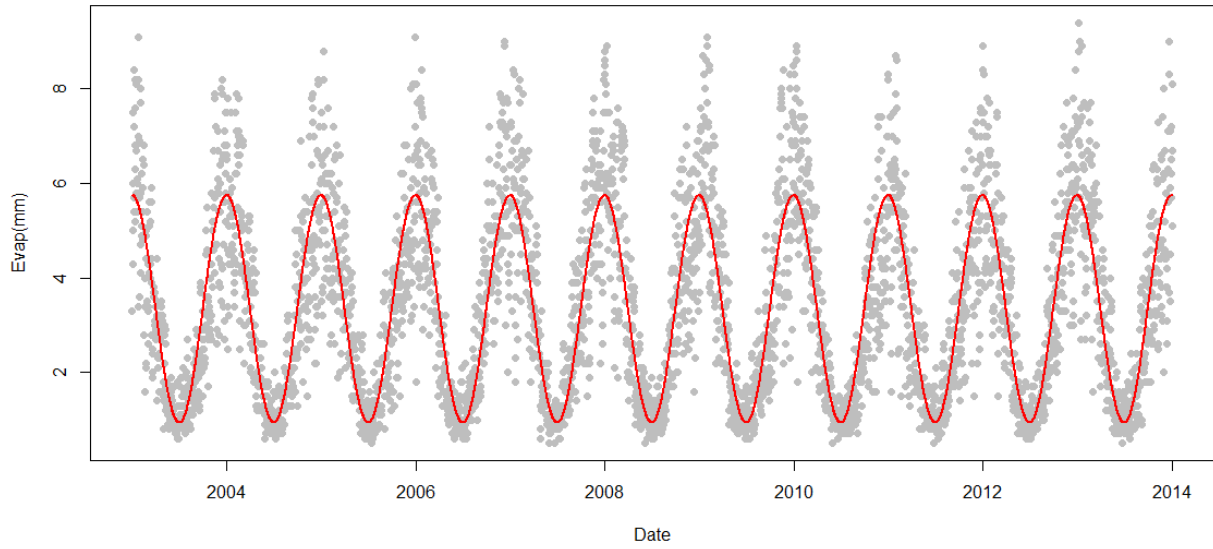


Figure I. 3: Cosine curve fitted to daily PET data in Sixth Creek

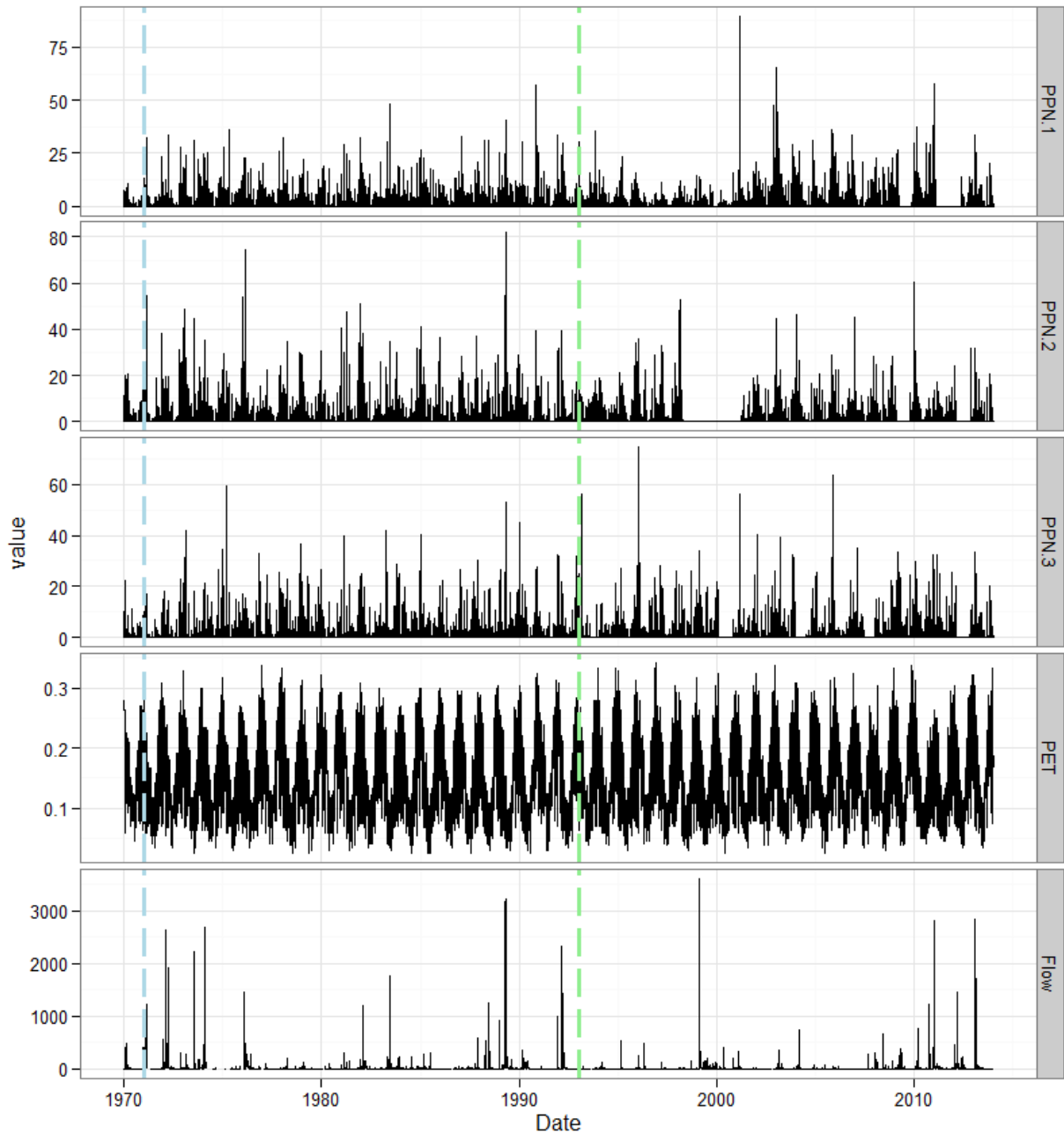


Figure I. 4: Data used for the calibration of Mary River [PPN.1 = precipitation in mm from pluviograph station at Jimna Composite, PPN.2 = precipitation in mm from pluvio station at Maleny Tamarind street, PPN.3 = precipitation in mm from Kenilworth Township, PET in mm and Flow in cumecs]

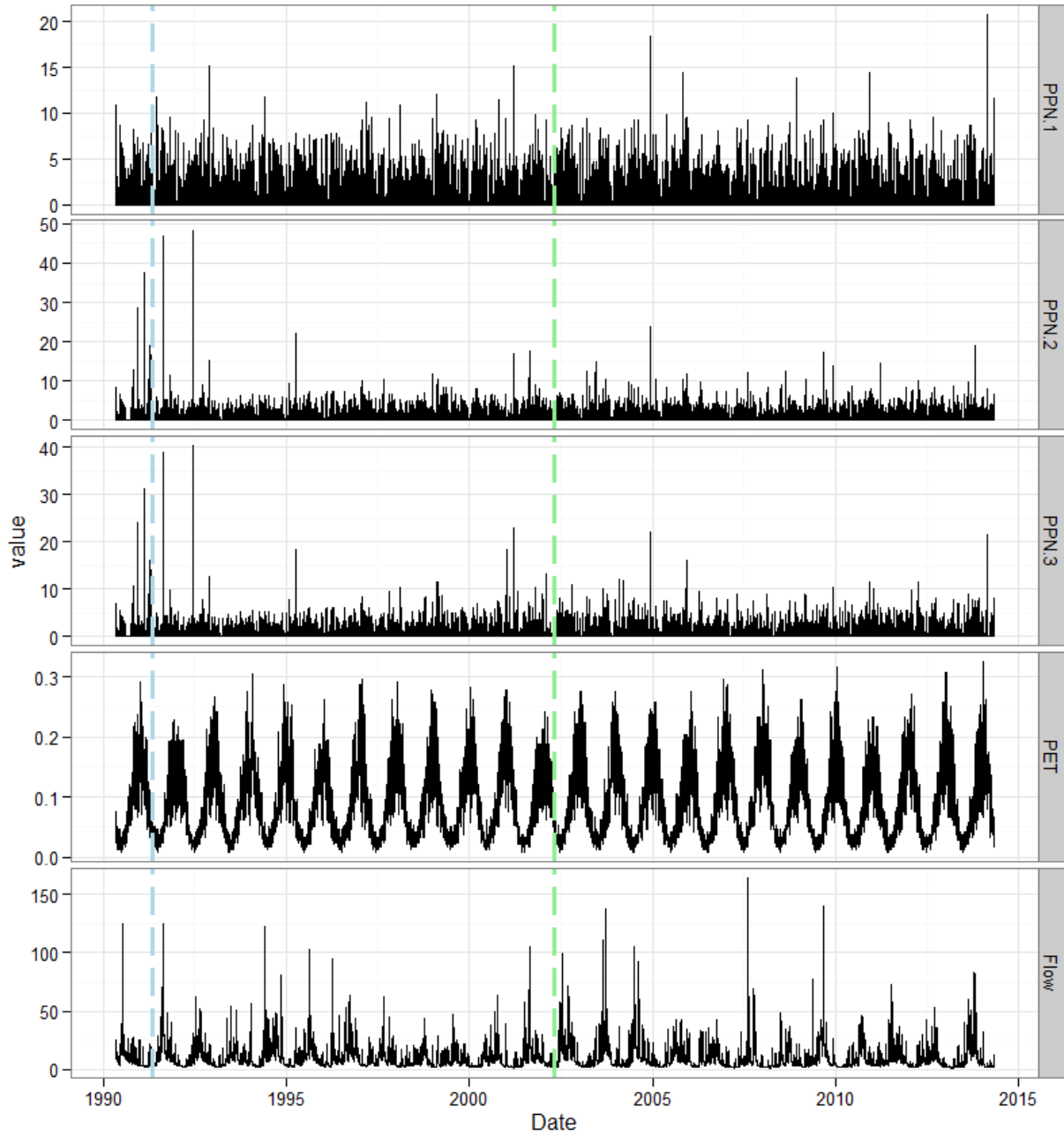


Figure I. 5: Data used for the calibration of Florentine River [PPN.1 = precipitation in mm from pluviograph station at Salvation Creek (309), PPN.2 = precipitation in mm from pluvio station at Tim Shea (338), PPN.3 = precipitation in mm from Misery Plateau (2008), PET in mm and Flow in cumecs]

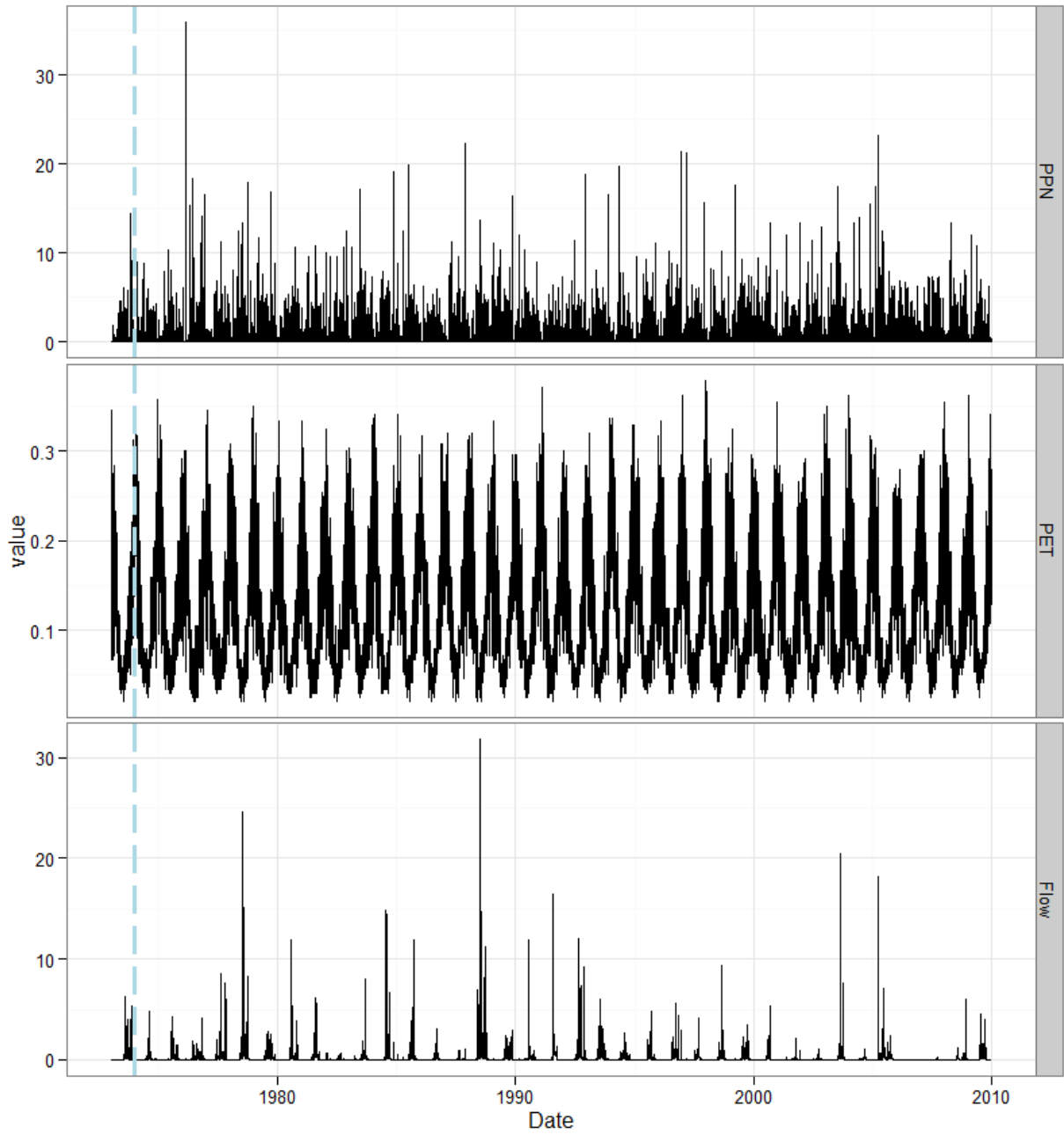


Figure I. 6 : Data used for the calibration of Yates Flat Creek [*PPN = precipitation in mm from pluviograph station at Woonanup, PET in mm and Flow in cumecs*]

## **Appendix J**

## **Results Scenario 1**

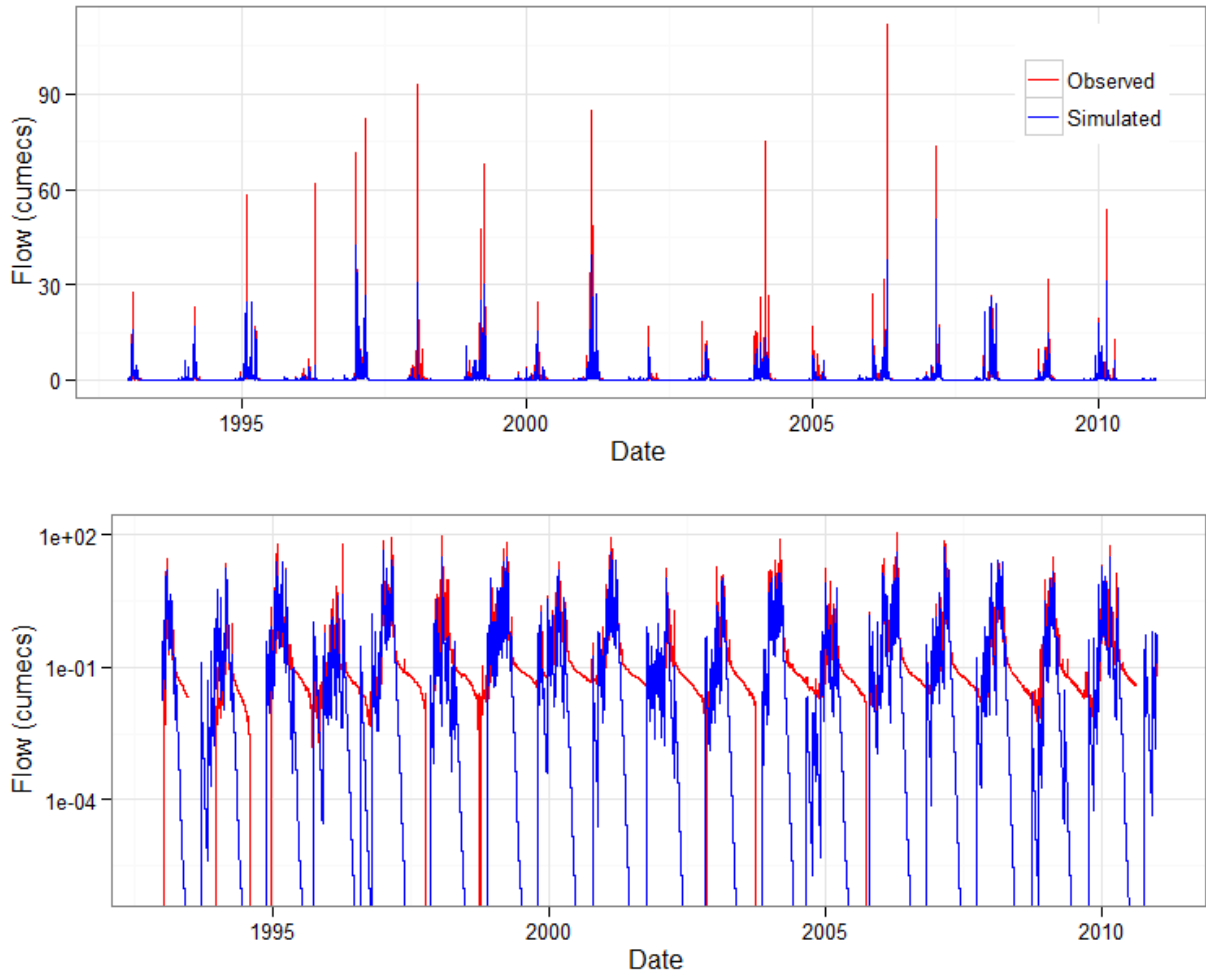


Figure J. 1: Comparison between the observed and simulated hydrographs (Manton River, scenario 1, AWBM) [The Y-axis in the lower plot is in log scale]

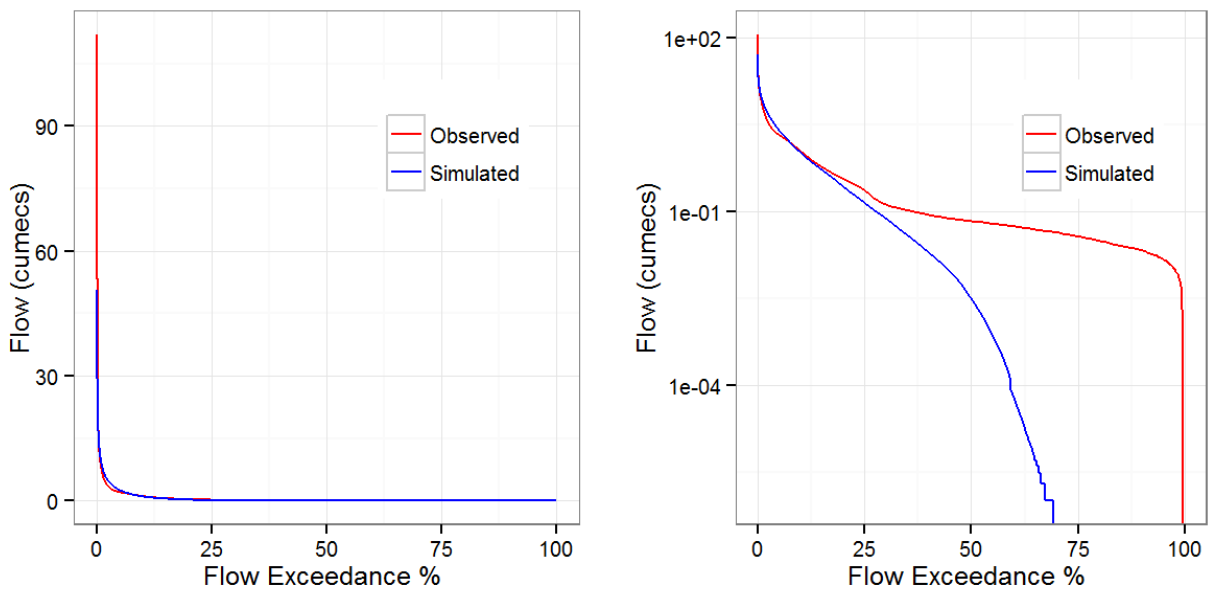


Figure J. 2: Flow duration curves in Manton River for scenario 1, AWBM [right plot Y-axis in log scale]

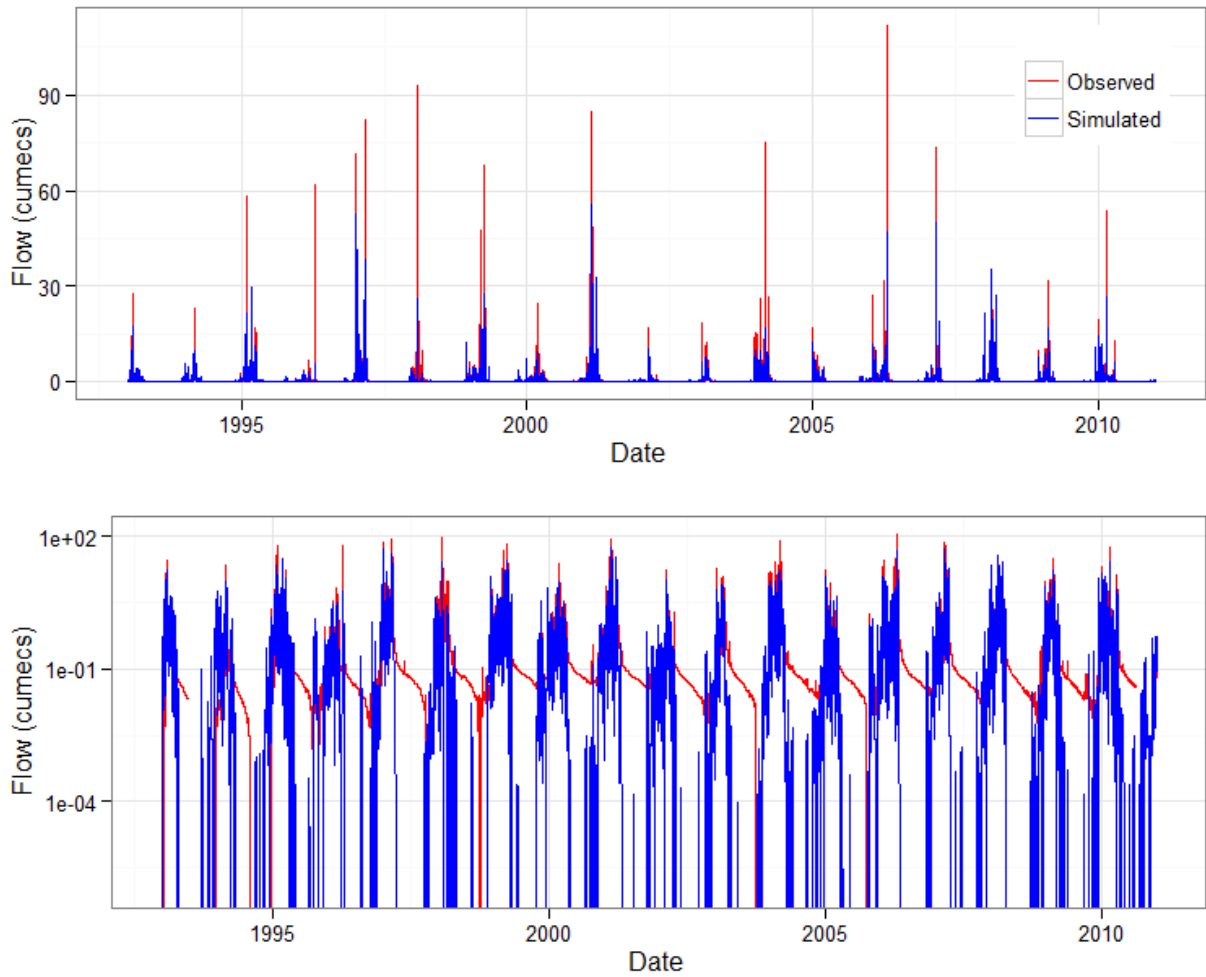


Figure J. 3: Comparison between the observed and simulated hydrographs (Manton River, scenario 1, SIMHYD) [The Y-axis in the lower plot is in log scale]

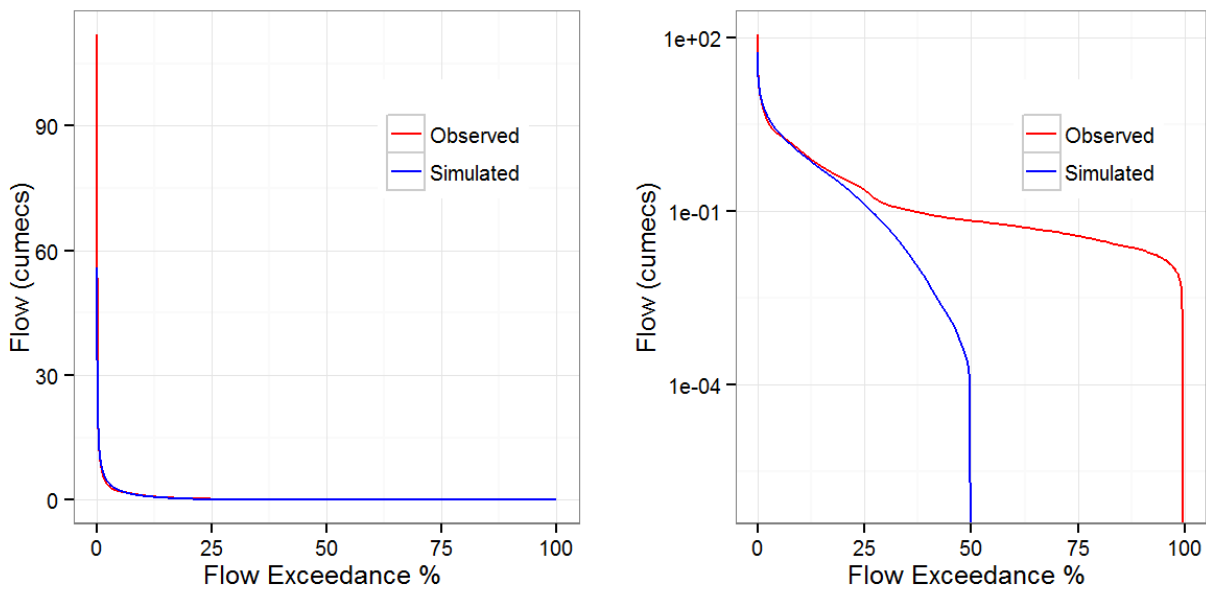


Figure J. 4 : Flow duration curves in Manton River for scenario 1, SIMHYD [right plot Y-axis in log scale]



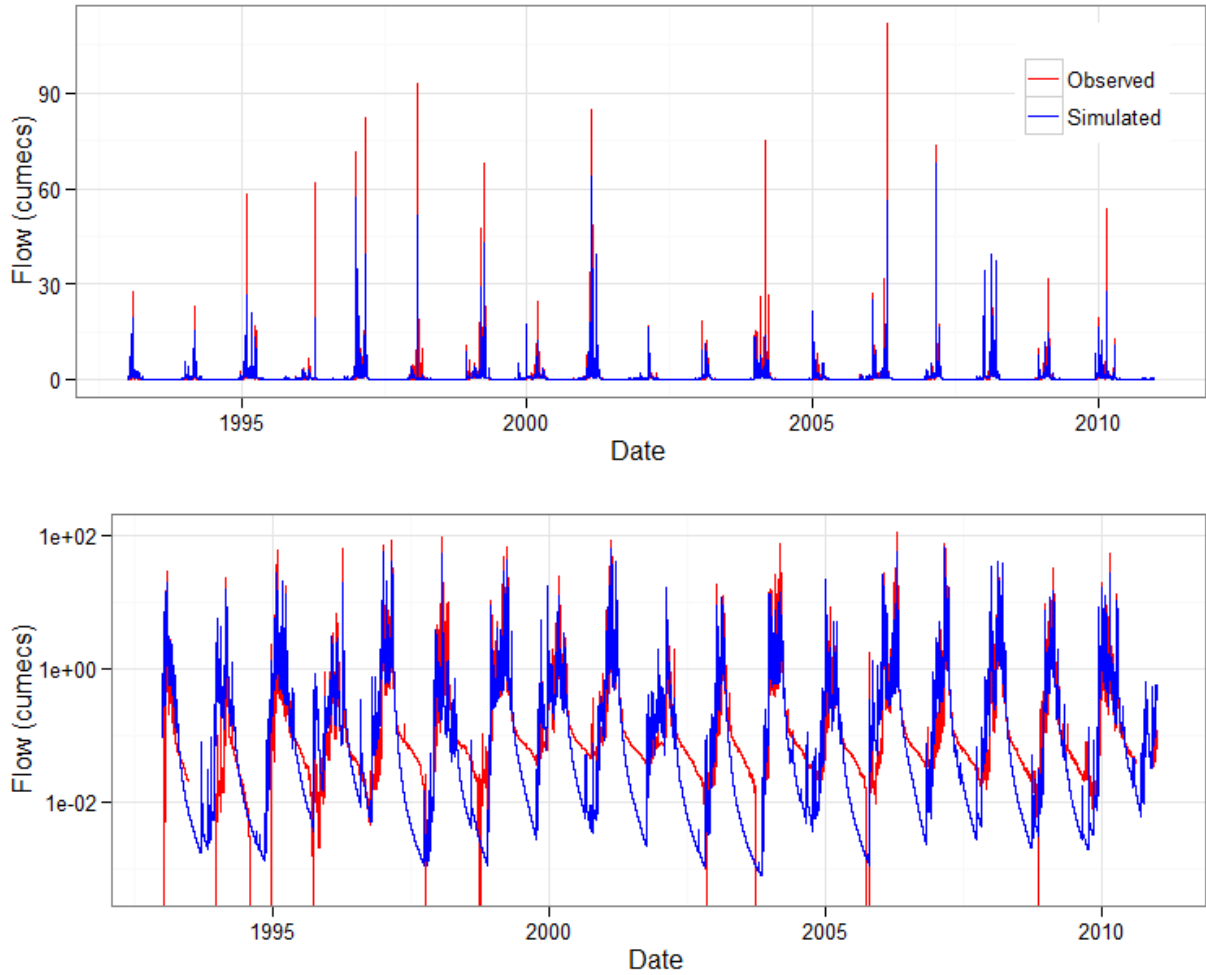


Figure J.5 : Comparison between the observed and simulated hydrographs (Manton River, scenario 1, GR4H) [The Y-axis in the lower plot is in log scale]

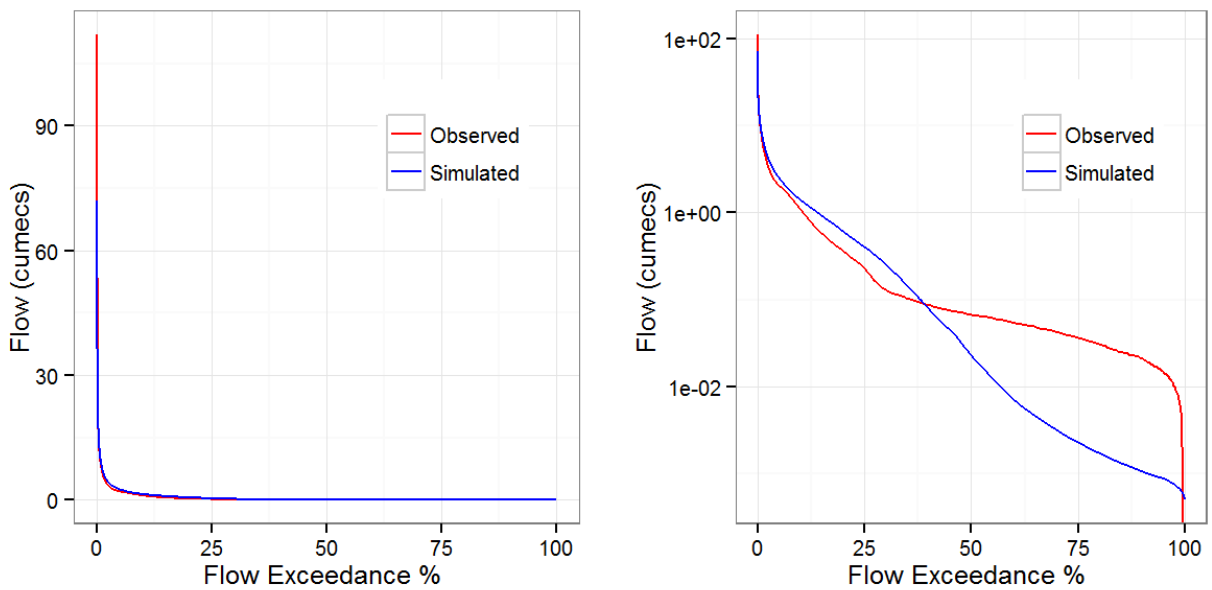


Figure J. 6: Flow duration curves in Manton River for scenario 1, GR4H [right plot Y-axis in log scale]

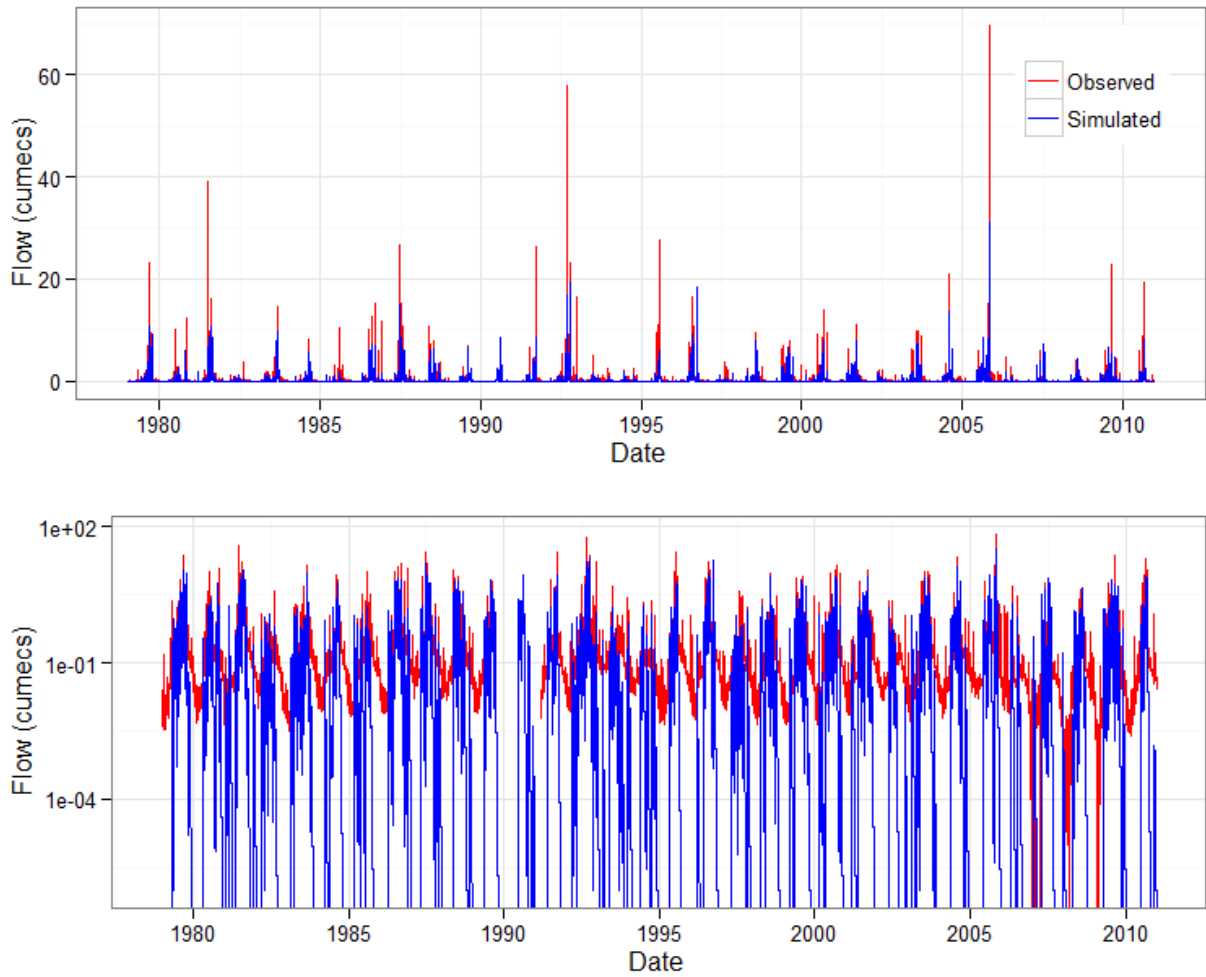


Figure J.7: Comparison between the observed and simulated hydrographs (Sixth Creek, scenario 1, AWBM) [The Y-axis in the lower plot is in log scale]

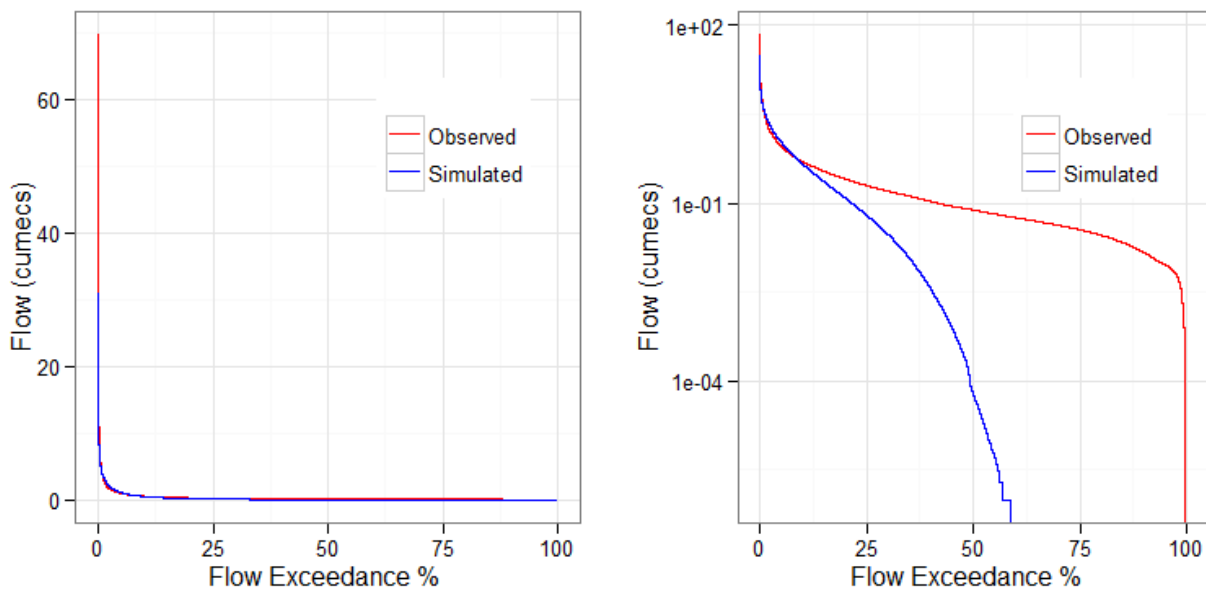


Figure J. 8: Flow duration curves in Sixth Creek for scenario 1, AWBM [right plot Y-axis in log scale]

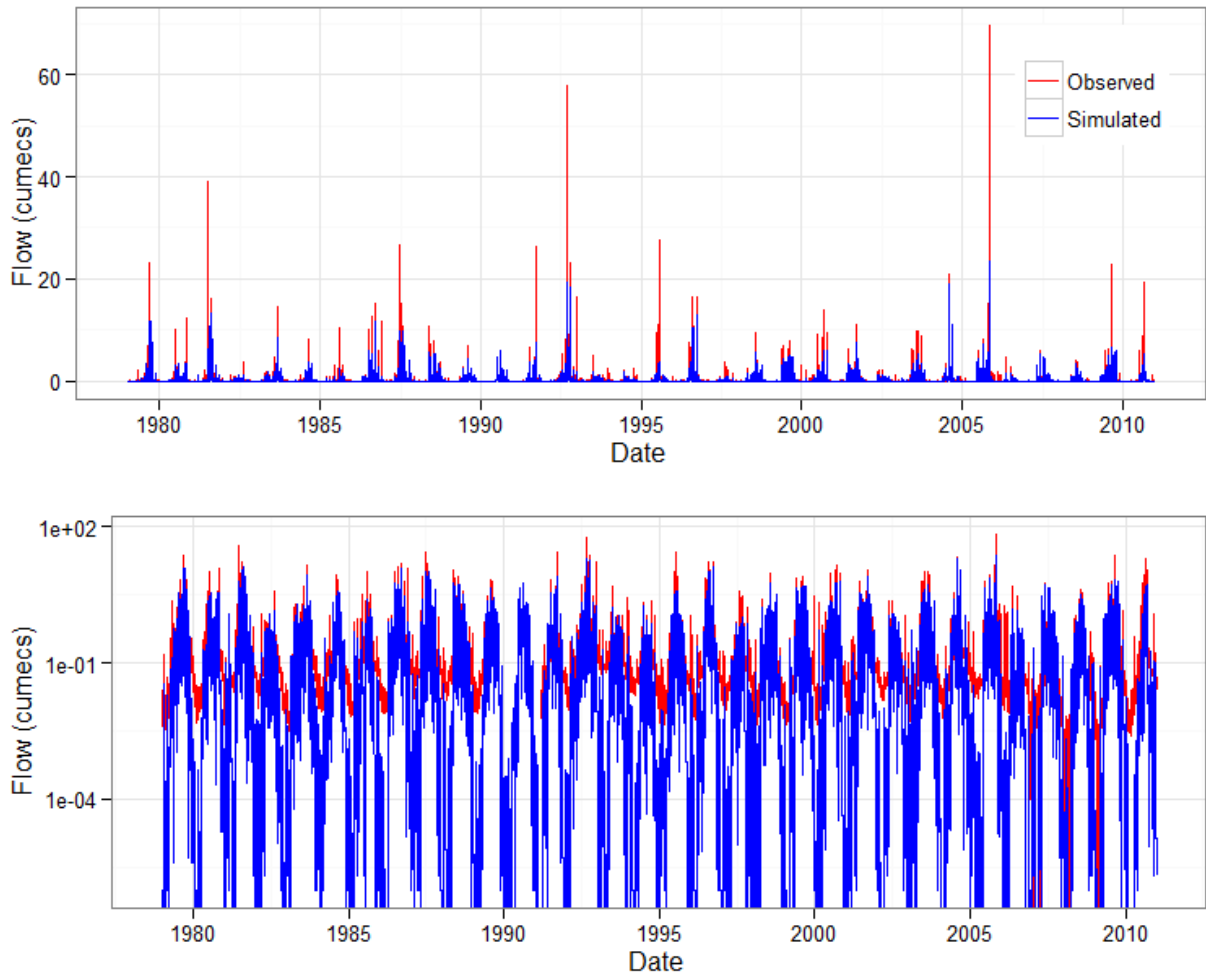


Figure J.9: Comparison between the observed and simulated hydrographs (Sixth Creek, scenario 1, SIMHYD) [The Y-axis in the lower plot is in log scale]

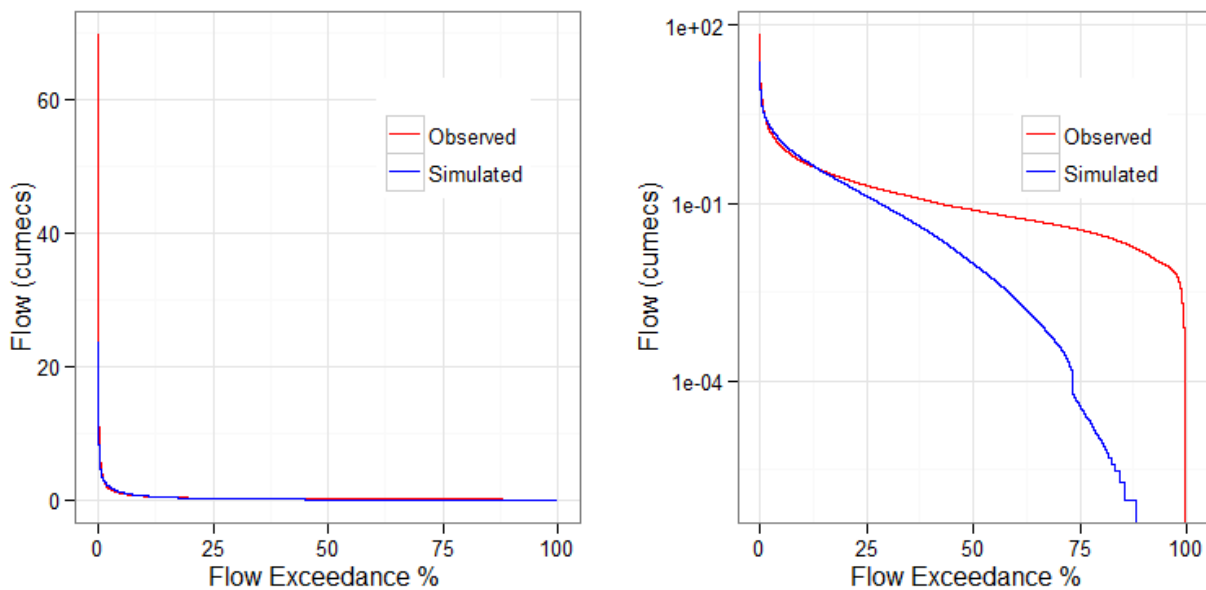


Figure J. 10: Flow duration curves in Sixth Creek for scenario 1, SIMHYD [right plot Y-axis in log scale]

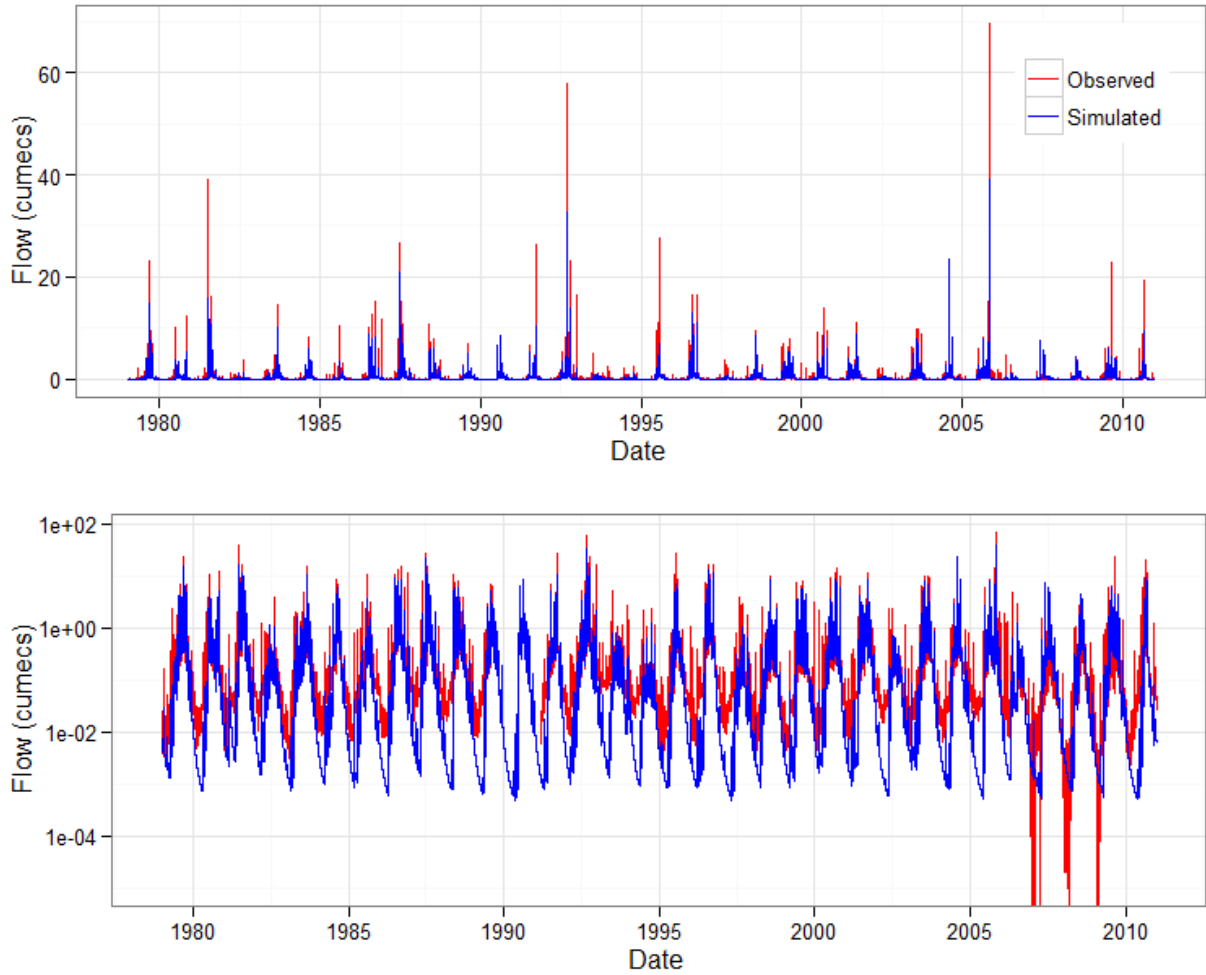


Figure J.11: Comparison between the observed and simulated hydrographs (Sixth Creek, scenario 1, GR4H) [The Y-axis in the lower plot is in log scale]

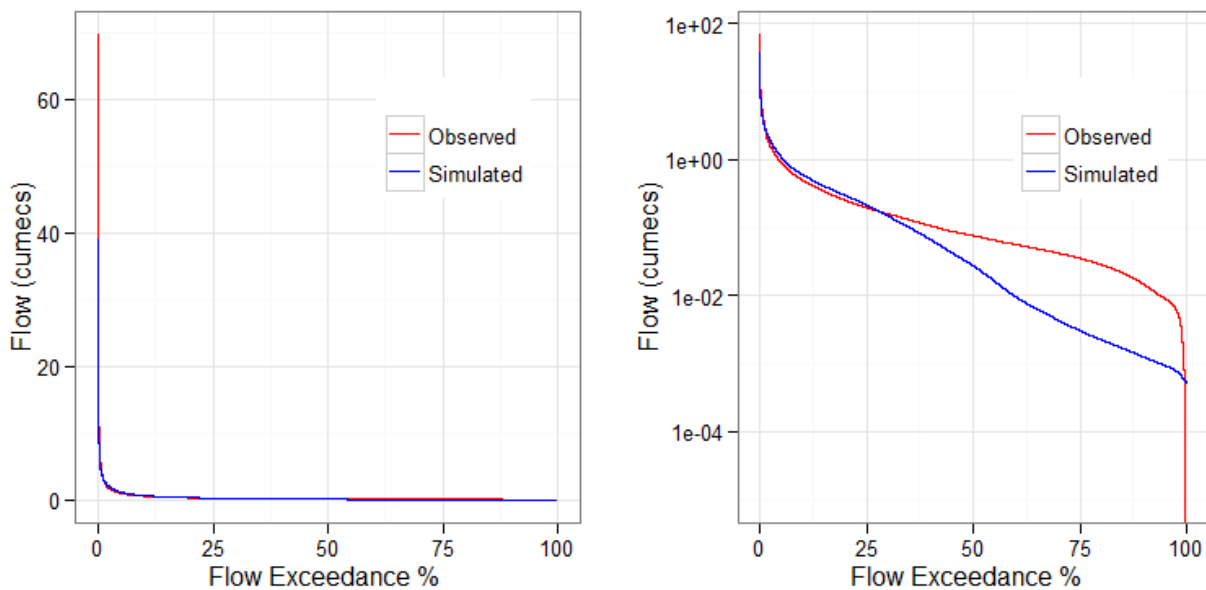


Figure J. 12: Flow duration curves in Sixth Creek for scenario 1, GR4H [right plot Y-axis in log scale]

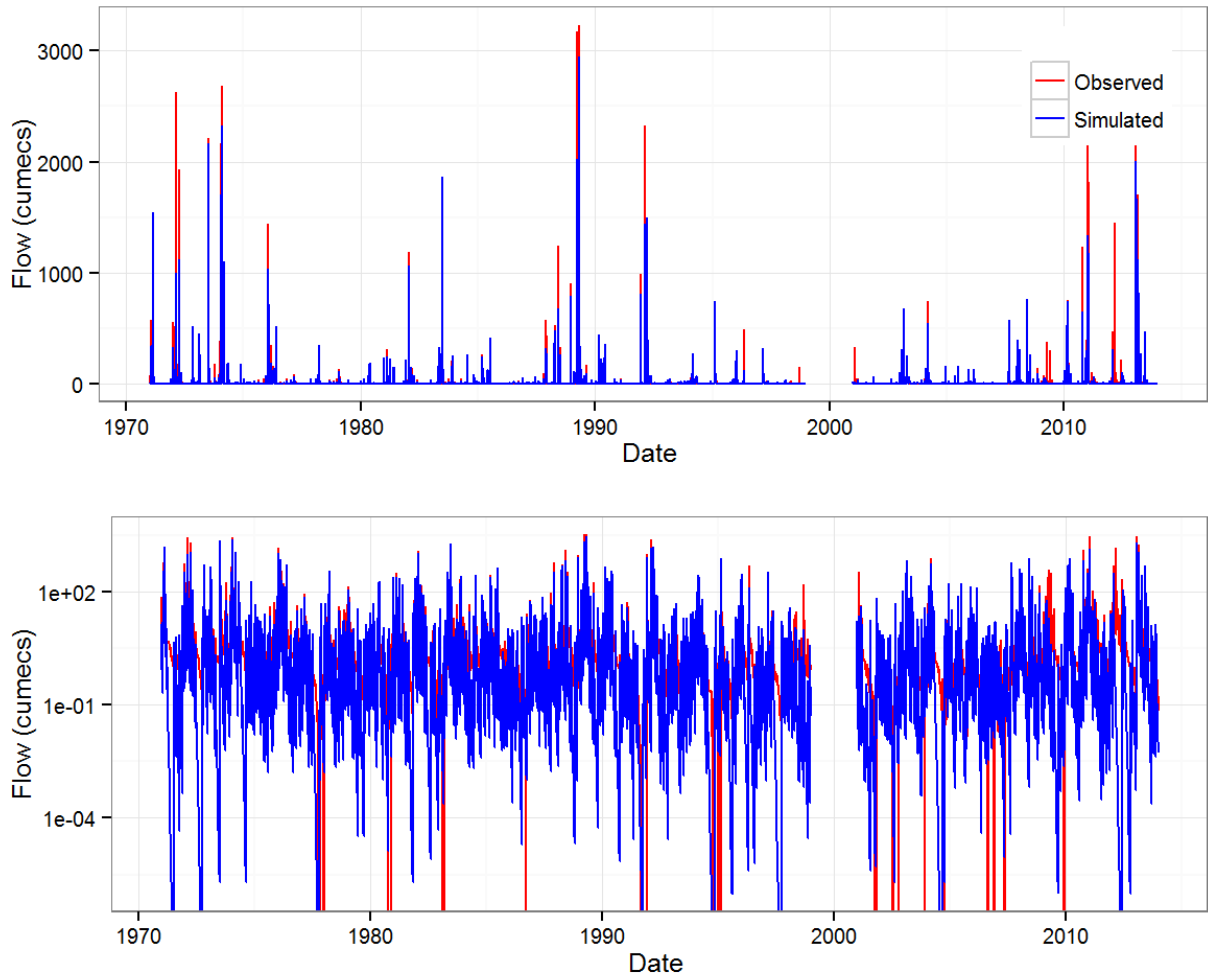


Figure J.13: Comparison between the observed and simulated hydrographs (Mary River, scenario 1, AWBM) [The Y-axis in the lower plot is in log scale]

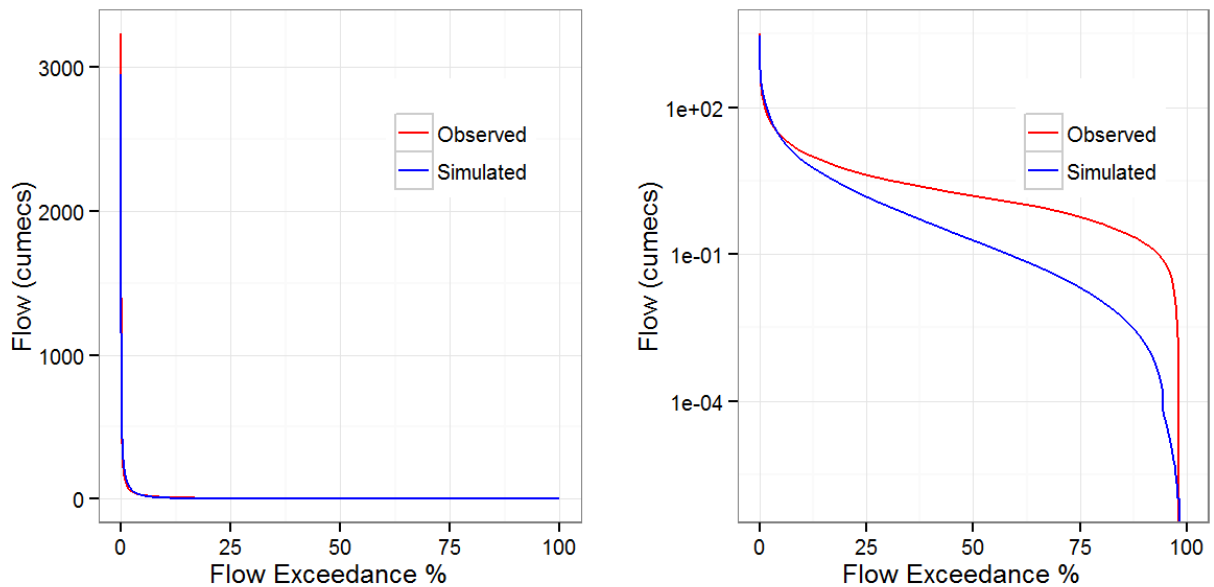


Figure J. 14: Flow duration curves in Mary for scenario 1, AWBM [right plot Y-axis in log scale]

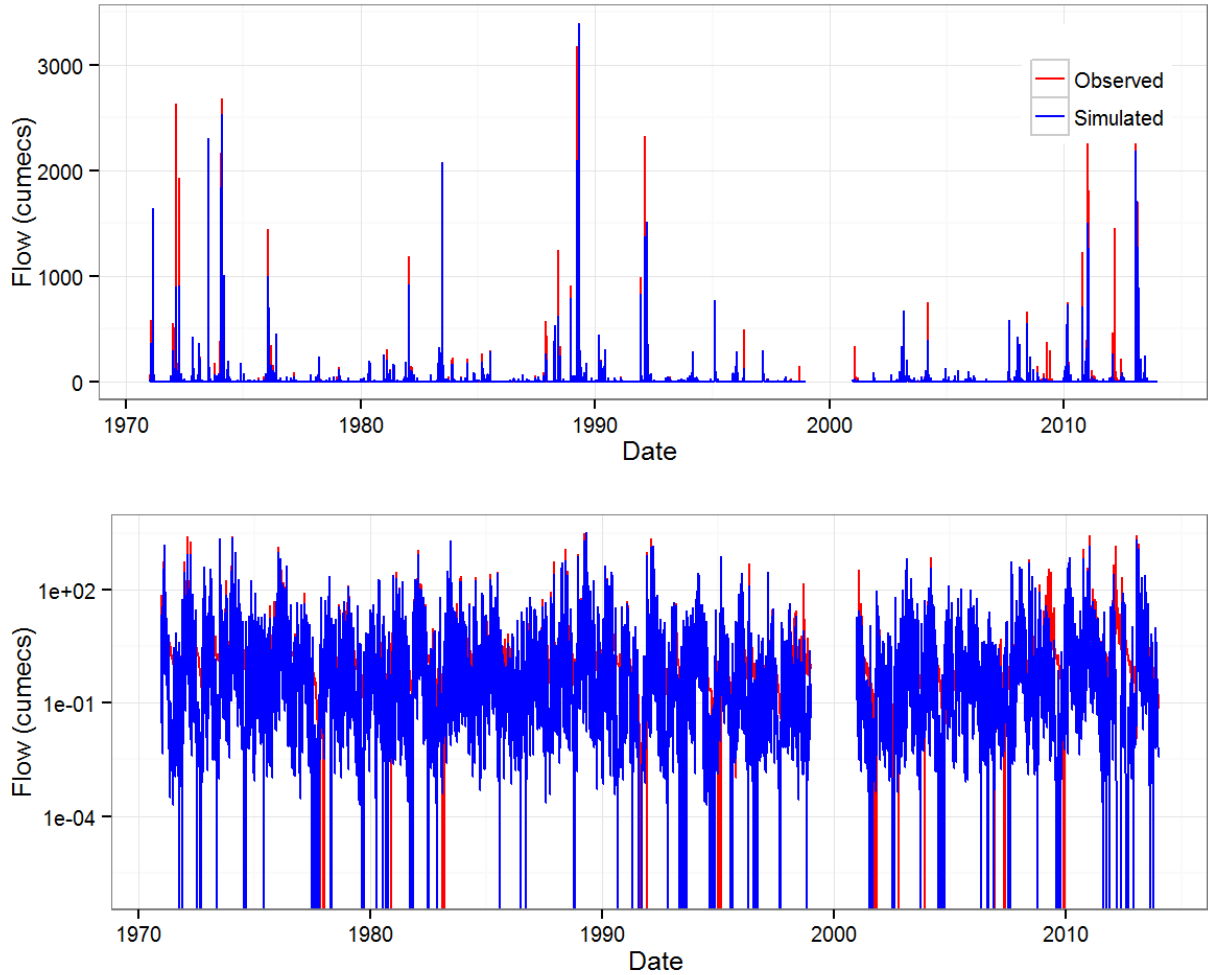


Figure J.15: Comparison between the observed and simulated hydrographs (Mary River, scenario 1, SIMHYD) [The Y-axis in the lower plot is in log scale]

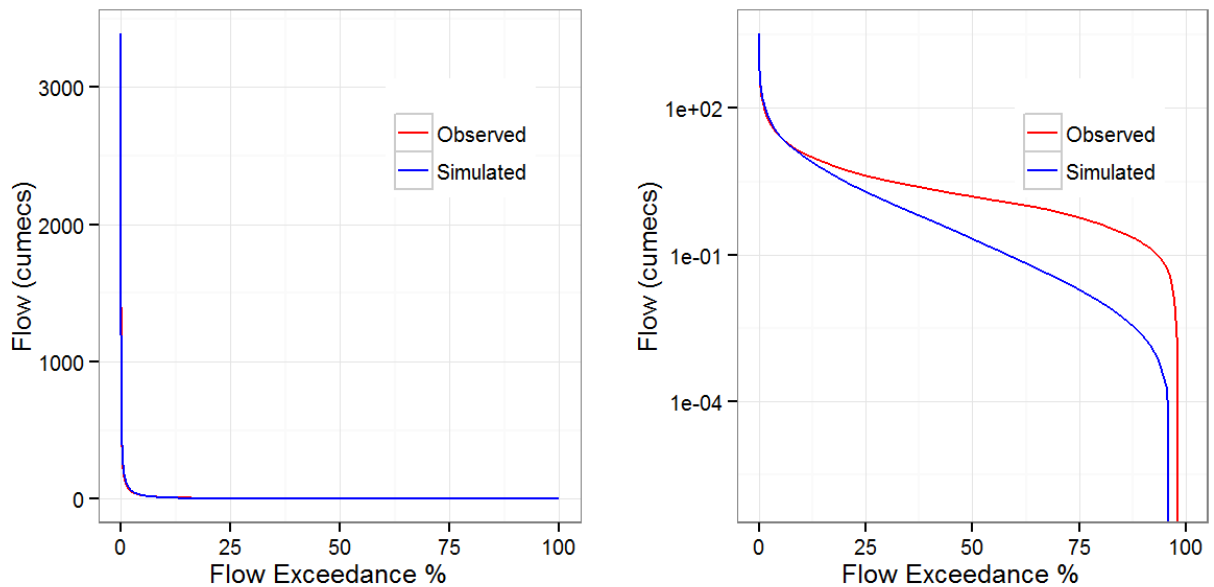


Figure J. 16: Flow duration curves in Mary for scenario 1, SIMHYD [right plot Y-axis in log scale]

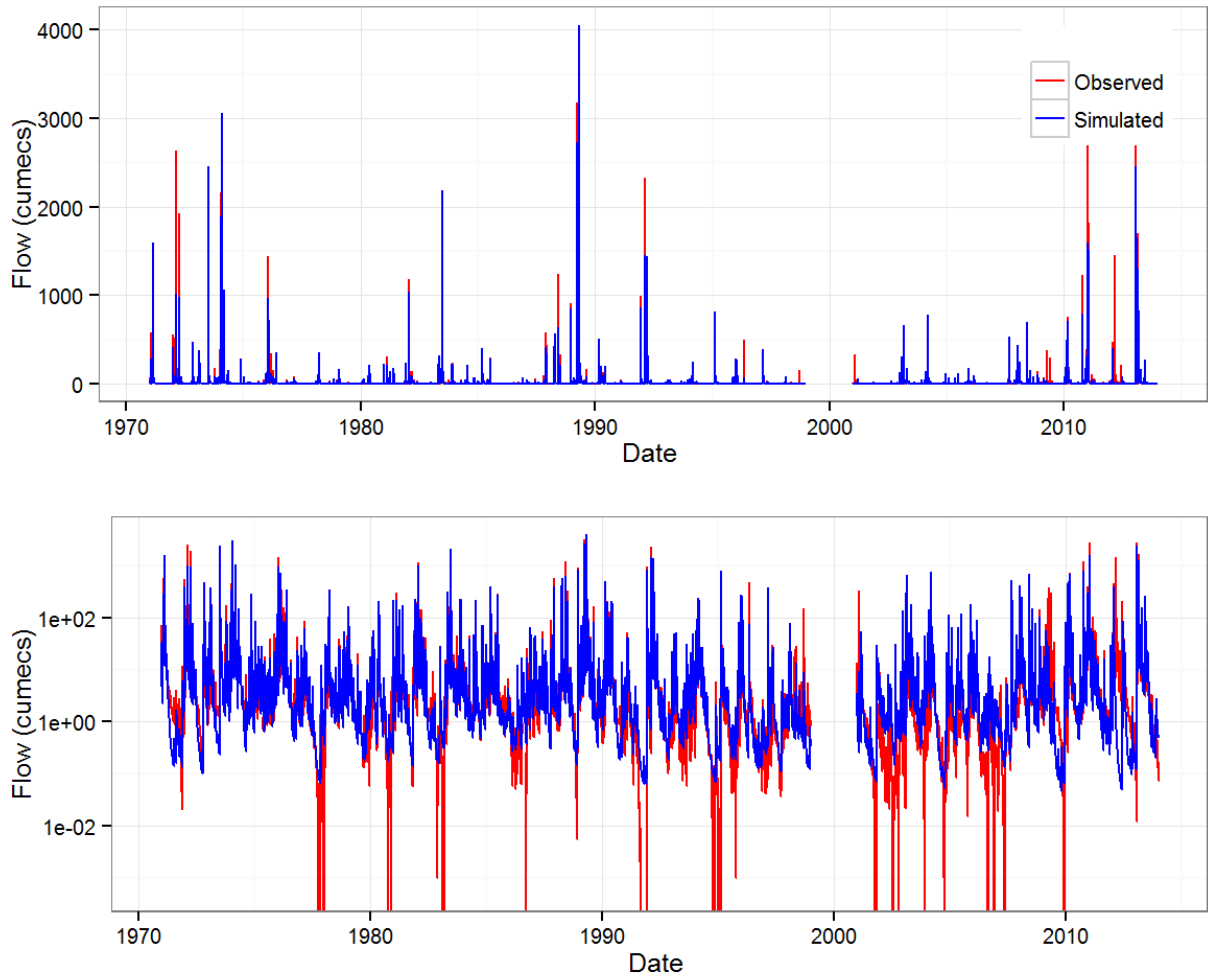


Figure J.17: Comparison between the observed and simulated hydrographs (Mary River, scenario 1, GR4H) [The Y-axis in the lower plot is in log scale]

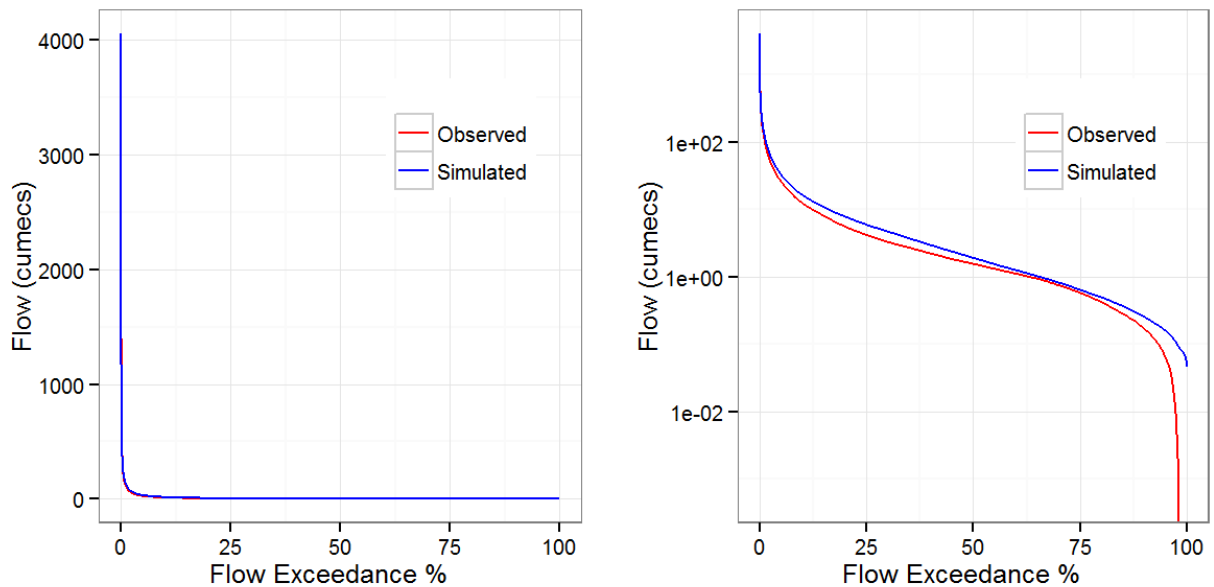


Figure J. 18: Flow duration curves in Mary for scenario 1, GR4H [right plot Y-axis in log scale]

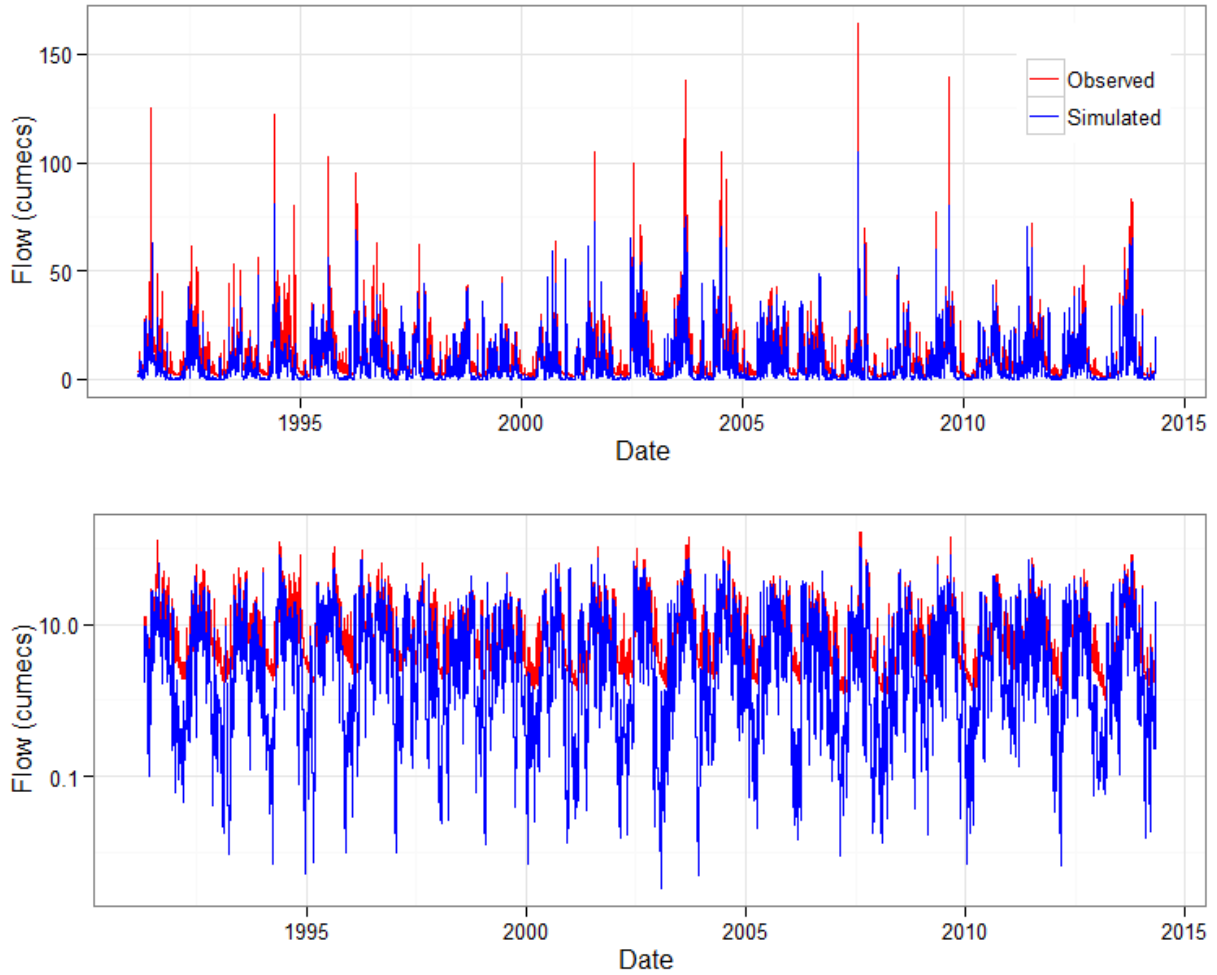


Figure J.19: Comparison between the observed and simulated hydrographs (Florentine River, scenario 1, AWBM) [The Y-axis in the lower plot is in log scale]

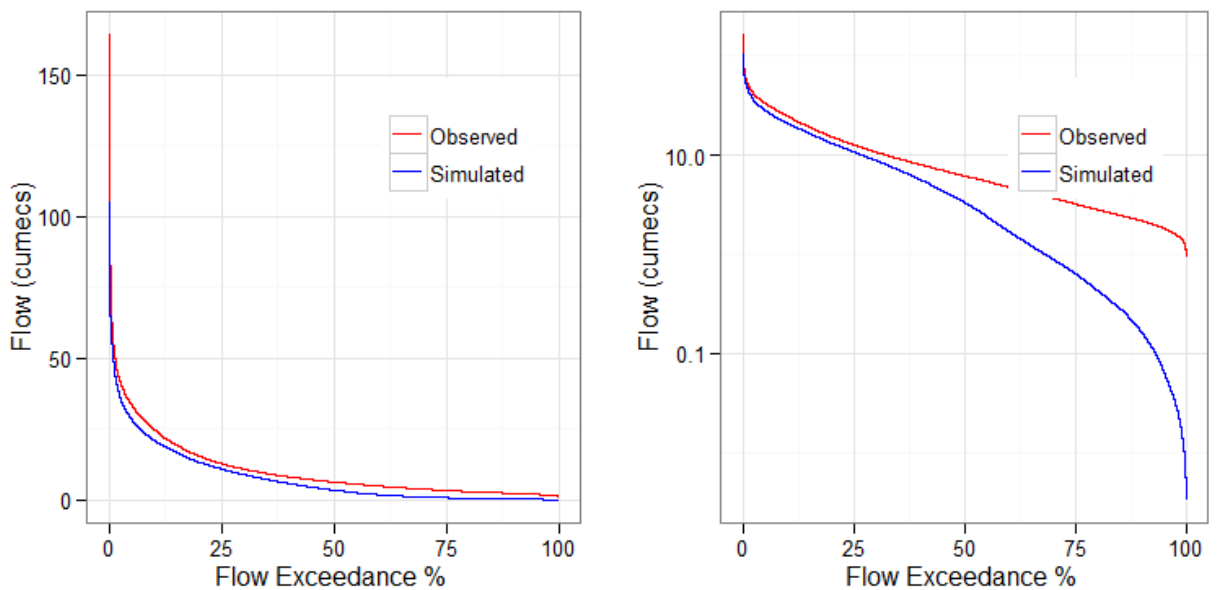


Figure J. 20: Flow duration curves in Florentine for scenario 1, AWBM [right plot Y-axis in log scale]



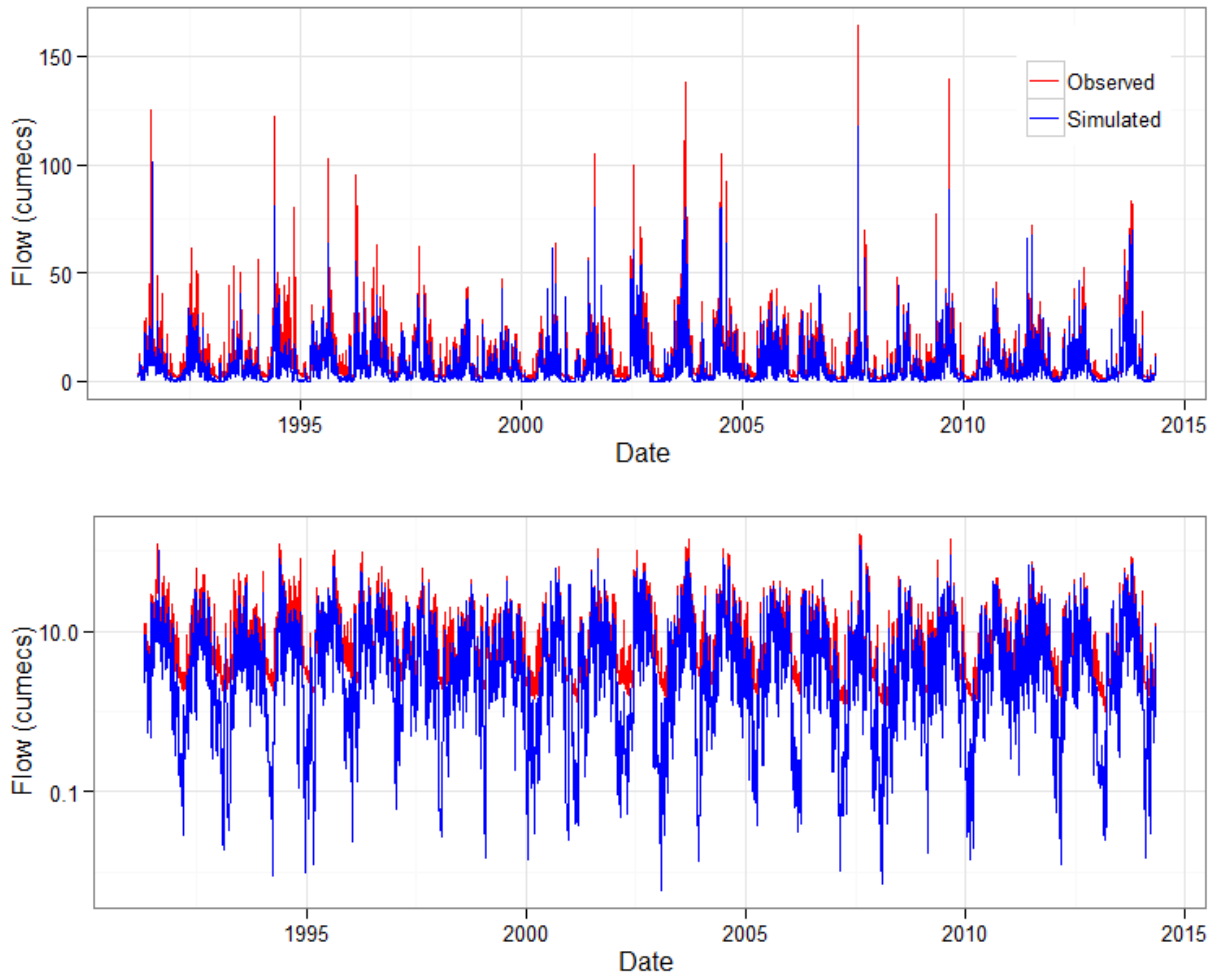


Figure J.21: Comparison between the observed and simulated hydrographs (Florentine River, scenario 1, SIMHYD) [The Y-axis in the lower plot is in log scale]

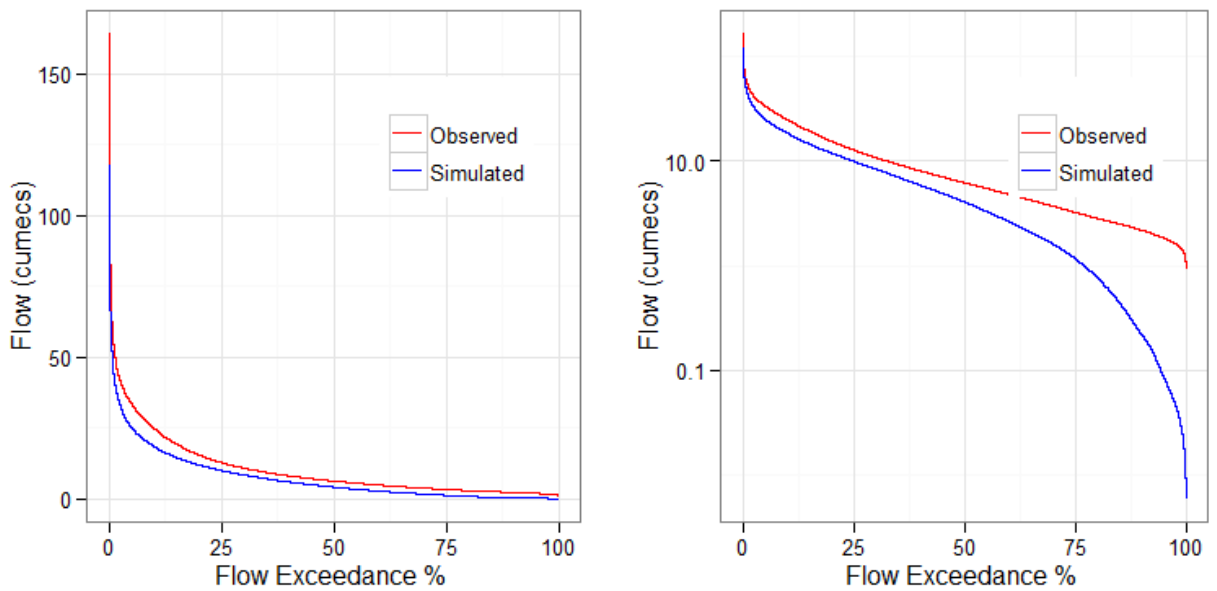


Figure J. 22: Flow duration curves in Mary for scenario 1, SIMHYD [right plot Y-axis in log scale]

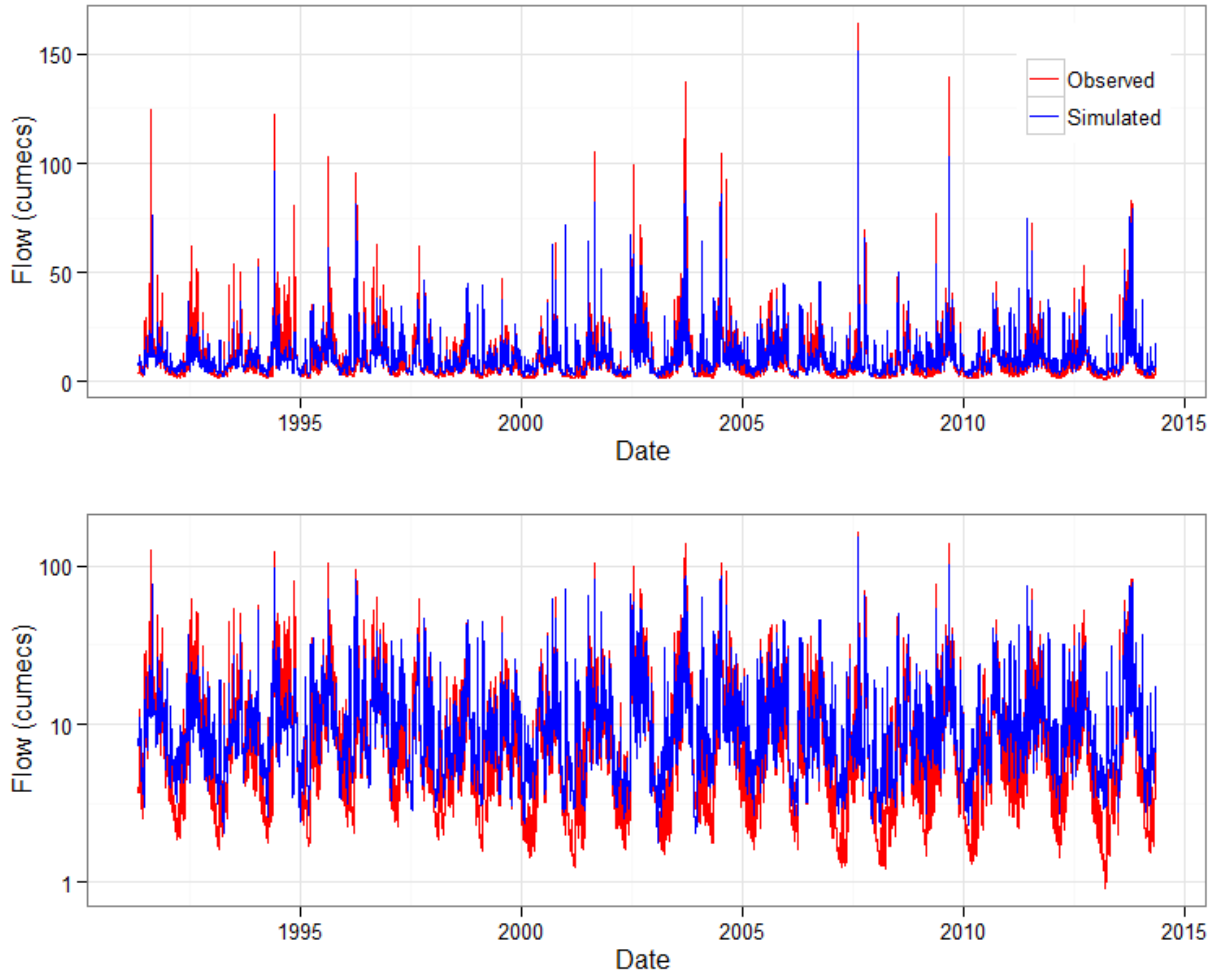


Figure J.23: Comparison between the observed and simulated hydrographs (Florentine River, scenario 1, GR4H) [The Y-axis in the lower plot is in log scale]

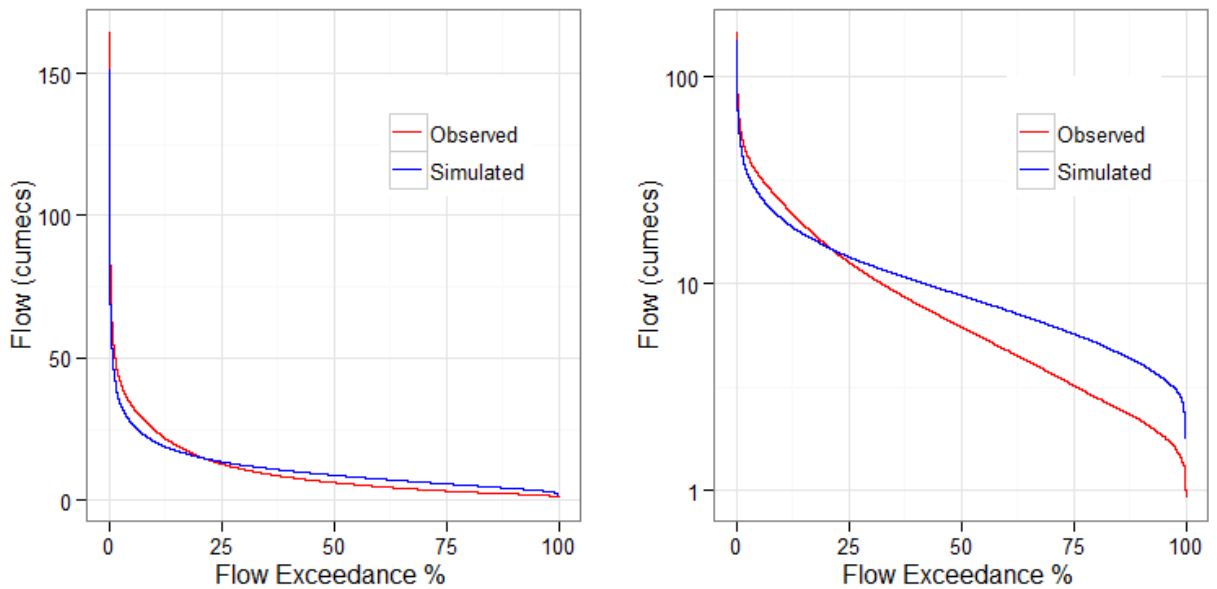


Figure J. 24: Flow duration curves in Mary for scenario 1, GR4H [right plot Y-axis in log scale]

## **Appendix K**

## **Results : Scenario 2**

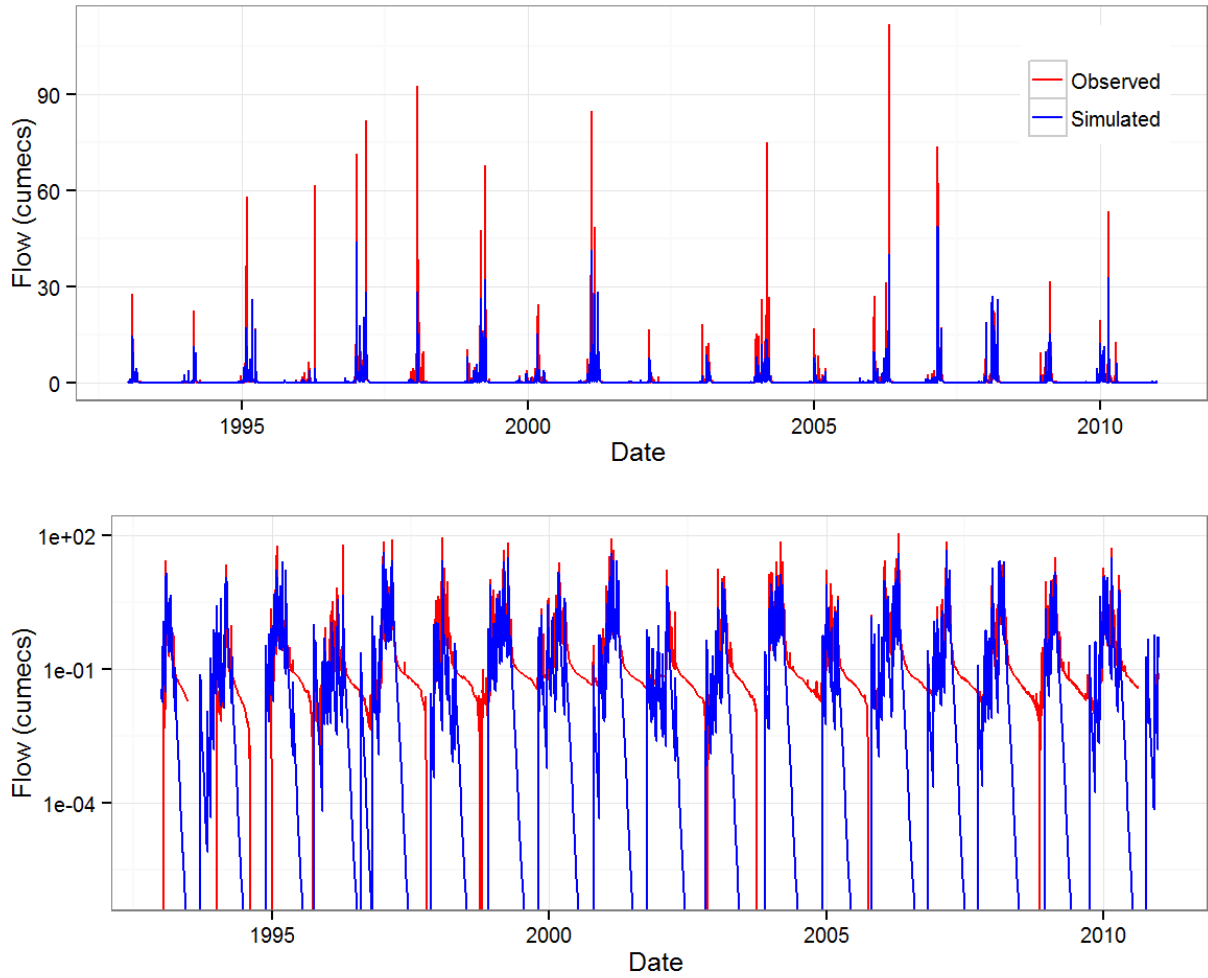


Figure K. 1 : Comparison between the observed and simulated hydrographs (Manton River, scenario 2, AWBM) [The Y-axis in the lower plot is in log scale]

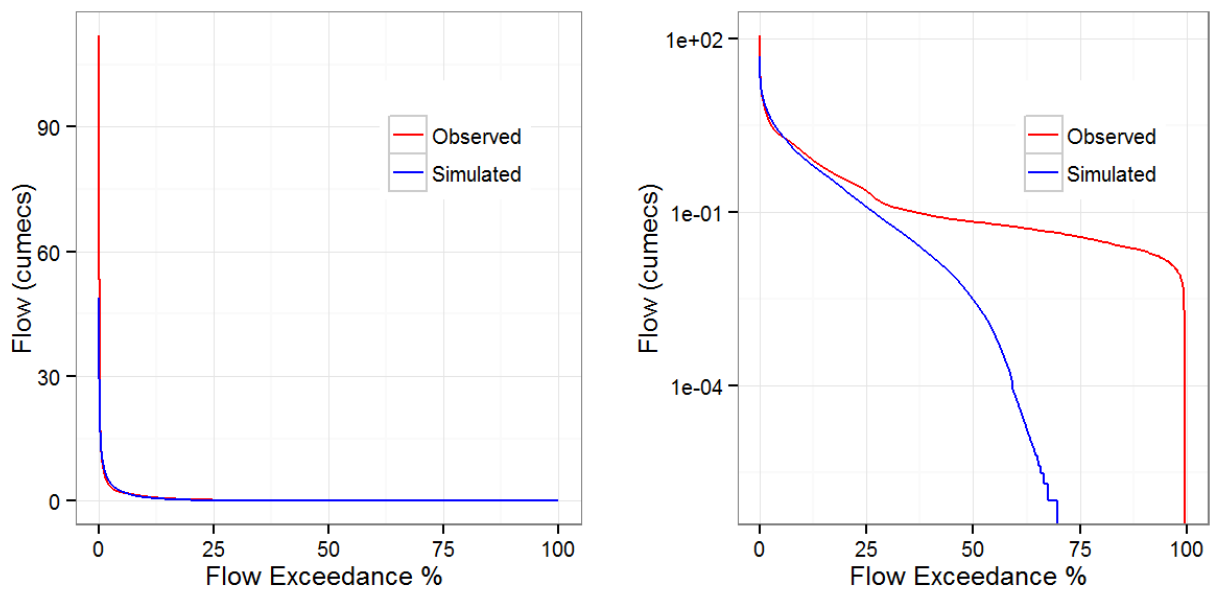


Figure K. 2: Flow duration curves in Manton River for scenario 2, AWBM [right plot Y-axis in log scale]

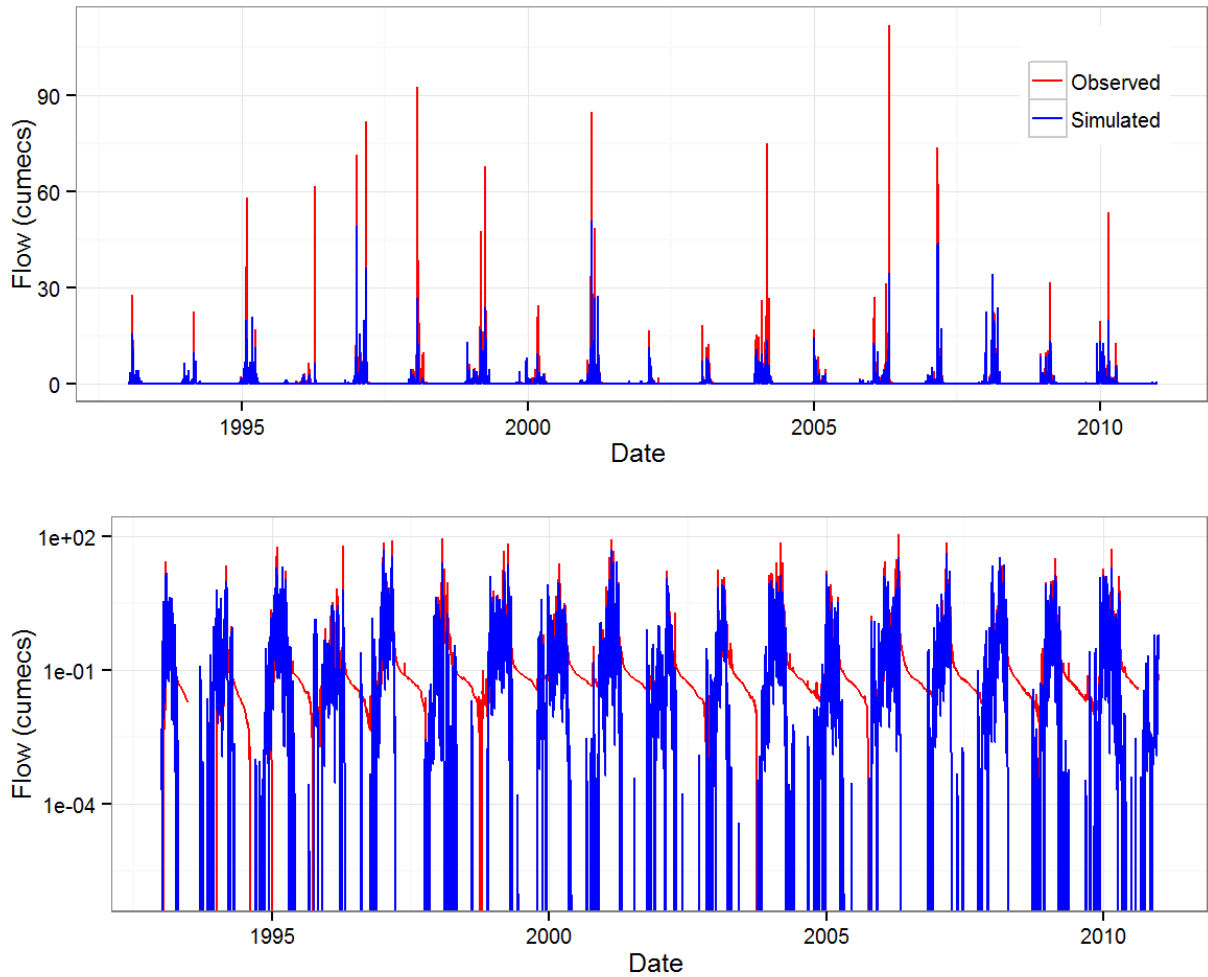


Figure K. 3: Comparison between the observed and simulated hydrographs (Manton River, scenario 2, SIMHYD) [The Y-axis in the lower plot is in log scale]

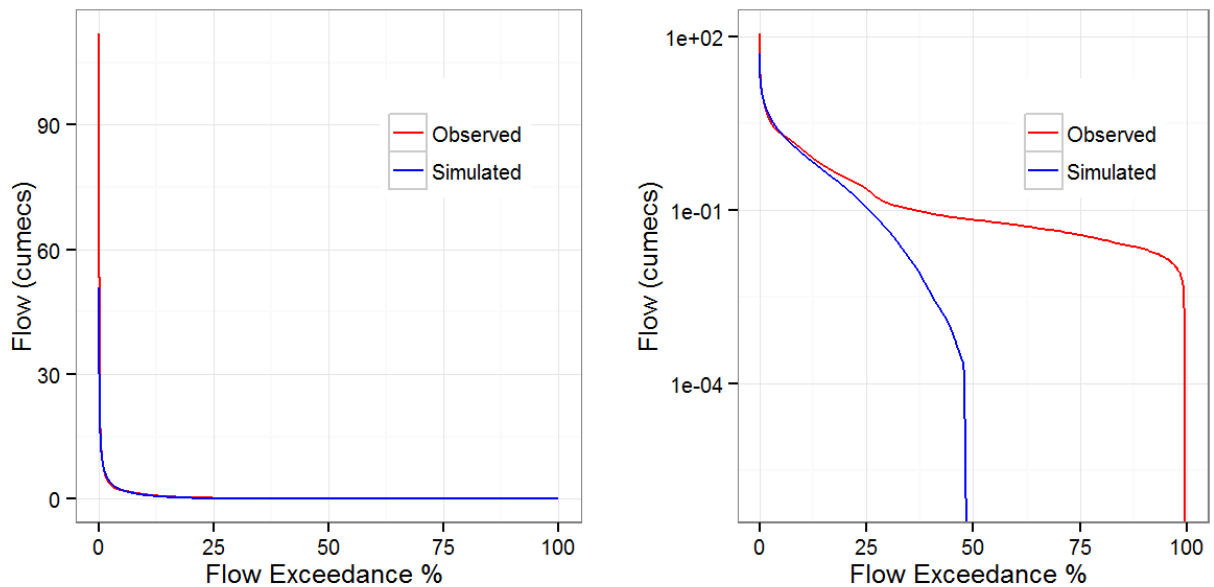


Figure K. 4: Flow duration curves in Manton for scenario 2, SIMHYD [right plot Y-axis in log scale]

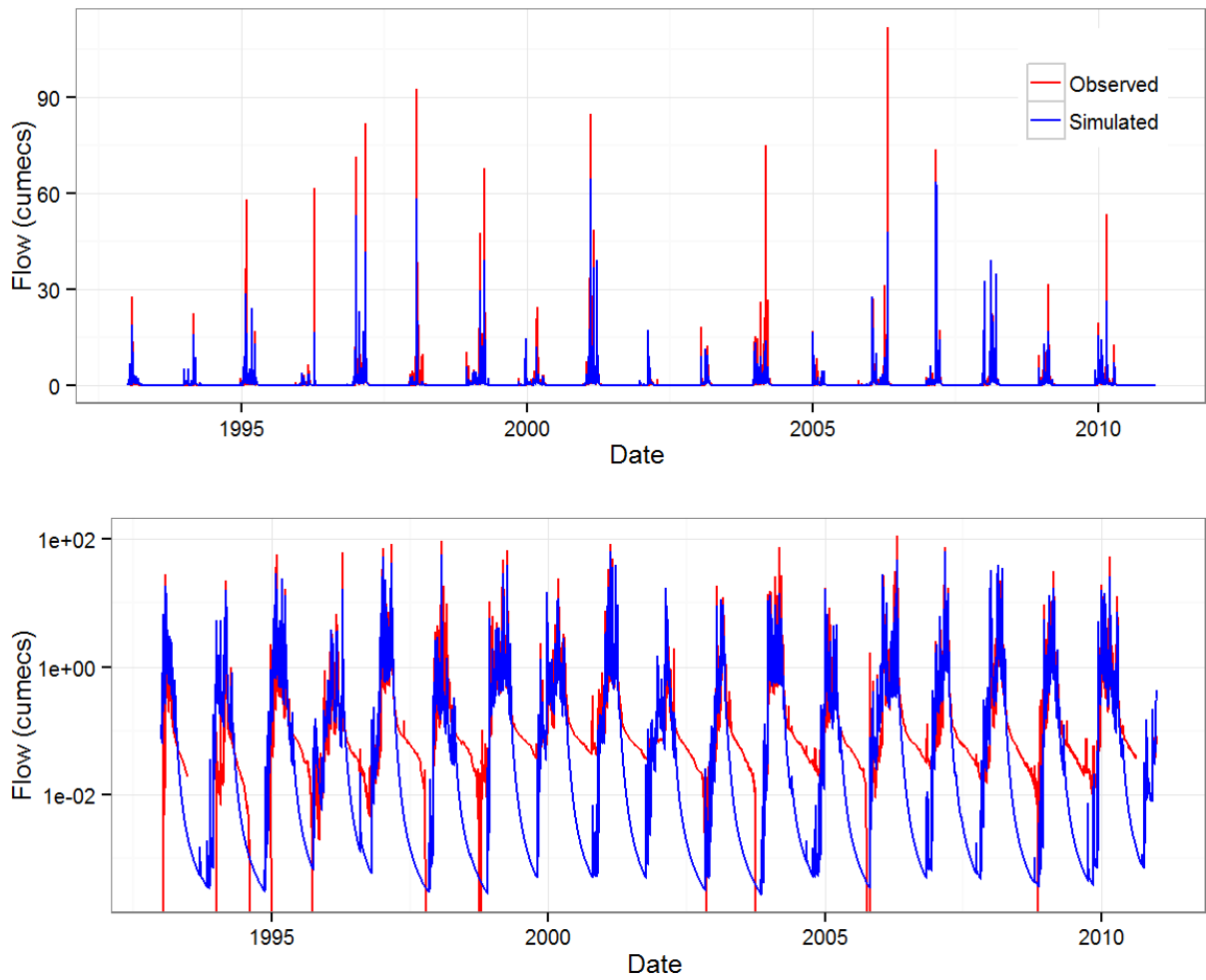


Figure K. 5: Comparison between the observed and simulated hydrographs (Manton River, scenario 2, GR4H) [The Y-axis in the lower plot is in log scale]

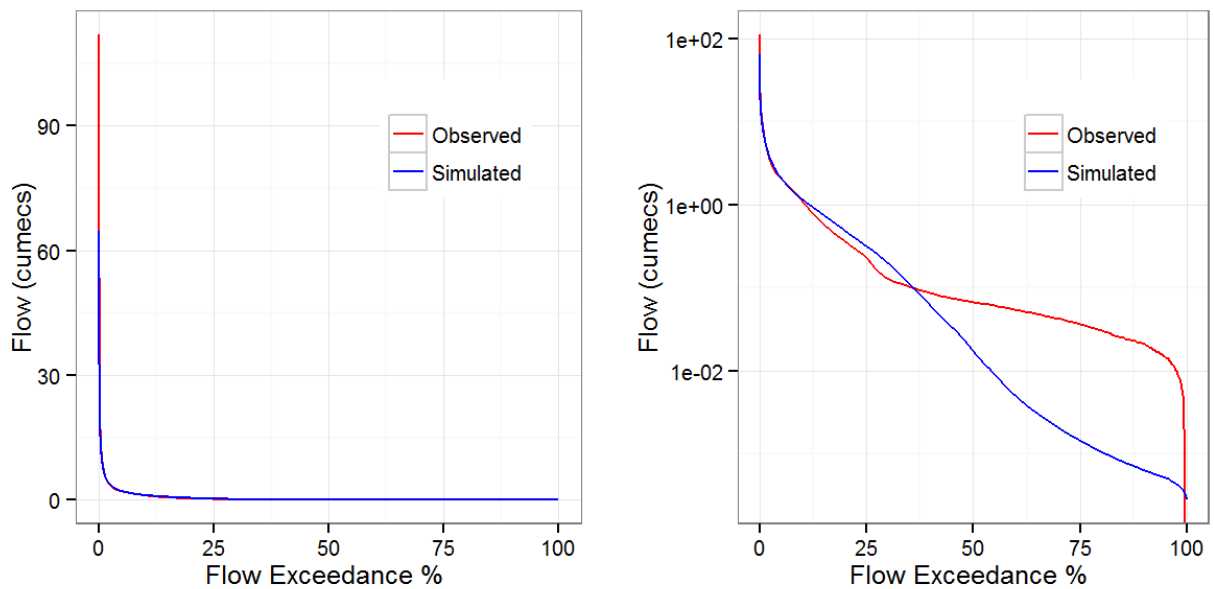


Figure K. 6: Flow duration curves in Manton River for scenario 2, GR4H [right plot Y-axis in log scale]

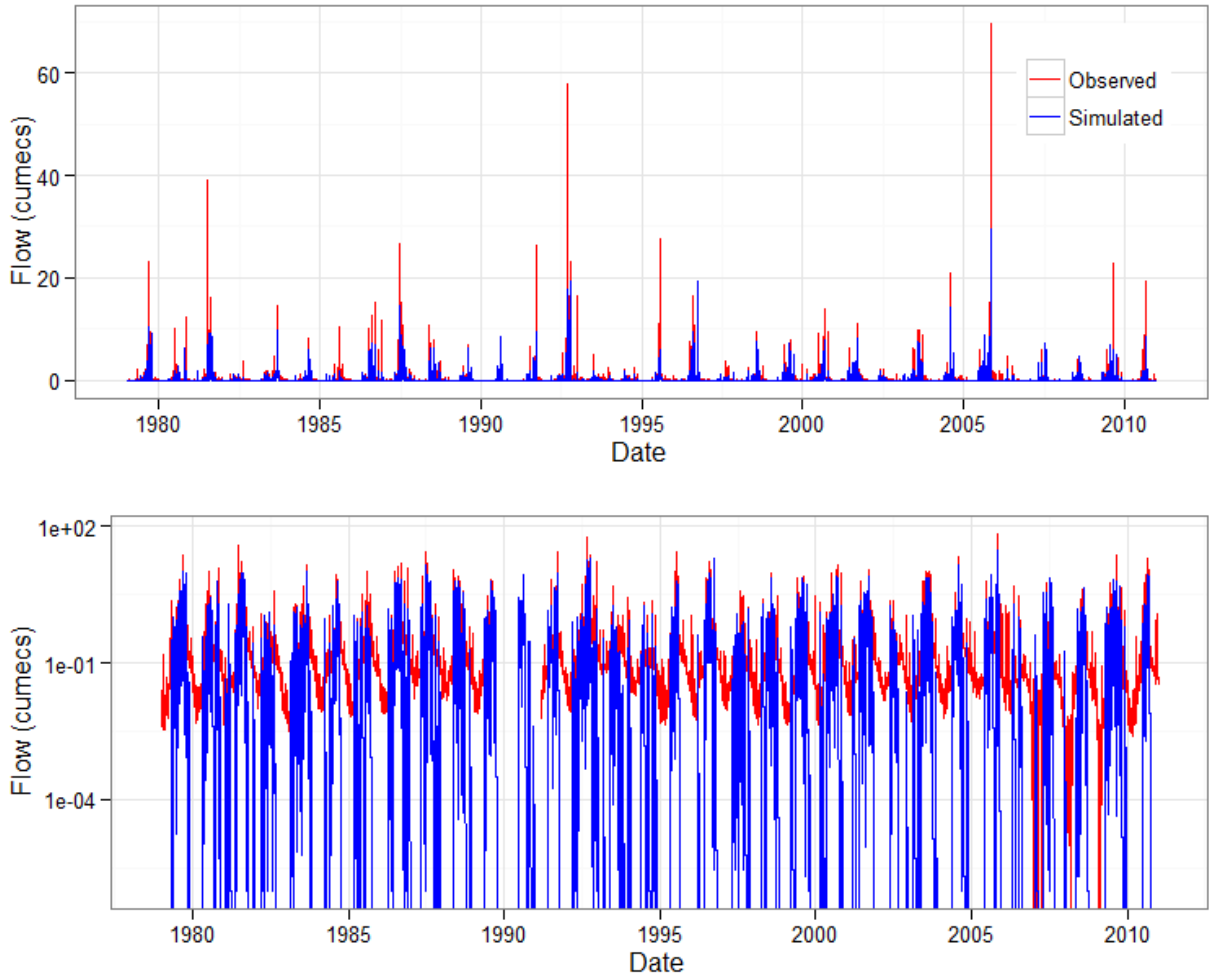


Figure K. 7: Comparison between the observed and simulated hydrographs (Sixth Creek, scenario 2, AWBM) [The Y-axis in the lower plot is in log scale]

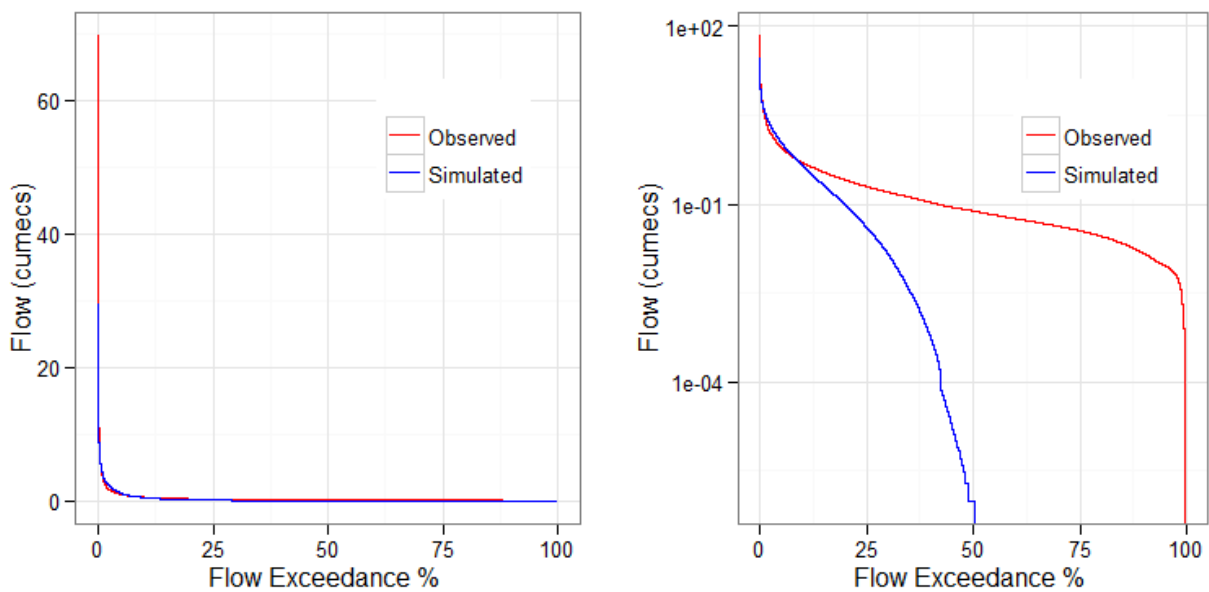


Figure K. 8: Flow duration curves in Sixth Creek for scenario 2, AWBM [right plot Y-axis in log scale]

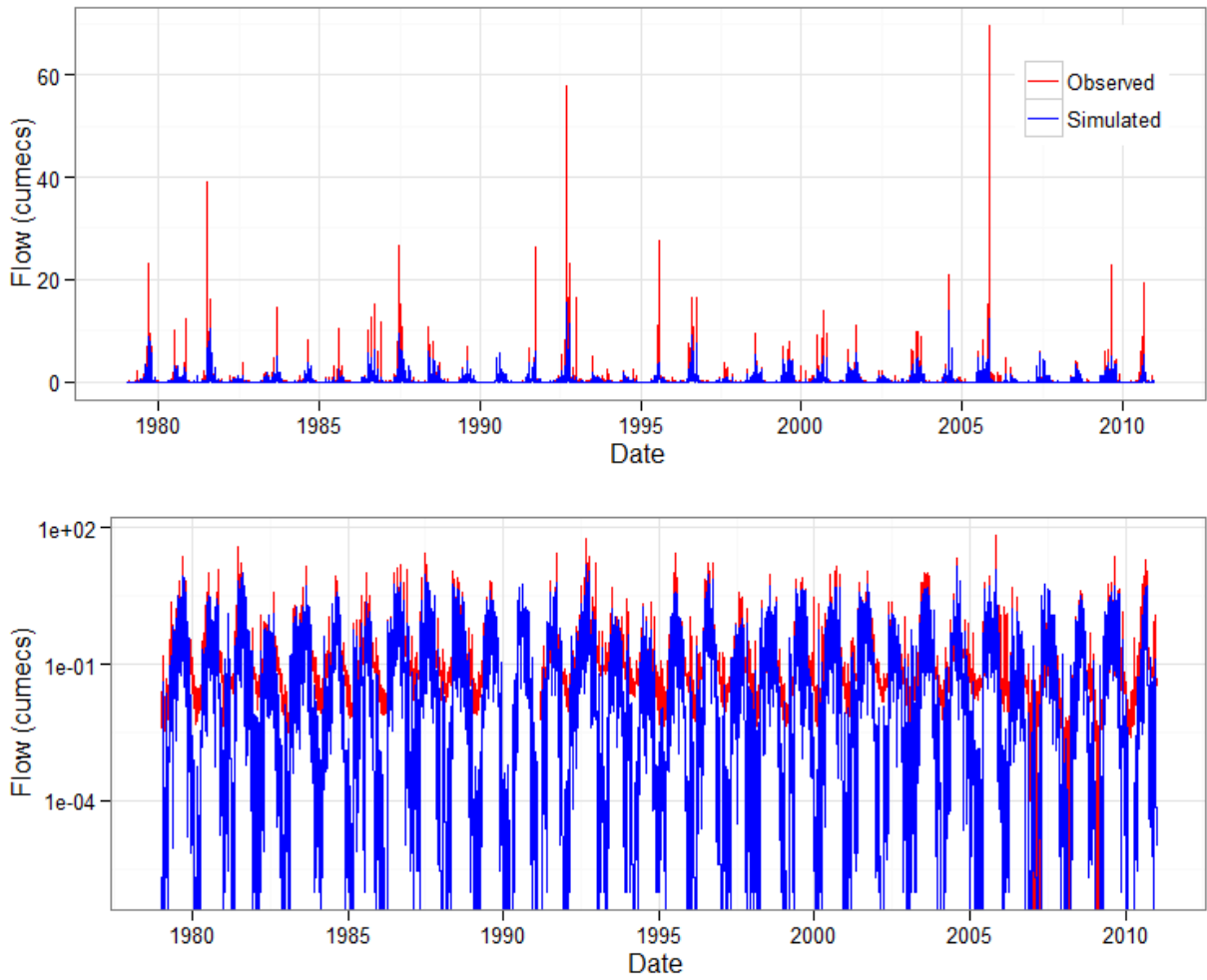


Figure K. 9: Comparison between the observed and simulated hydrographs (Sixth Creek River, scenario 2, SIMHYD) [The Y-axis in the lower plot is in log scale]

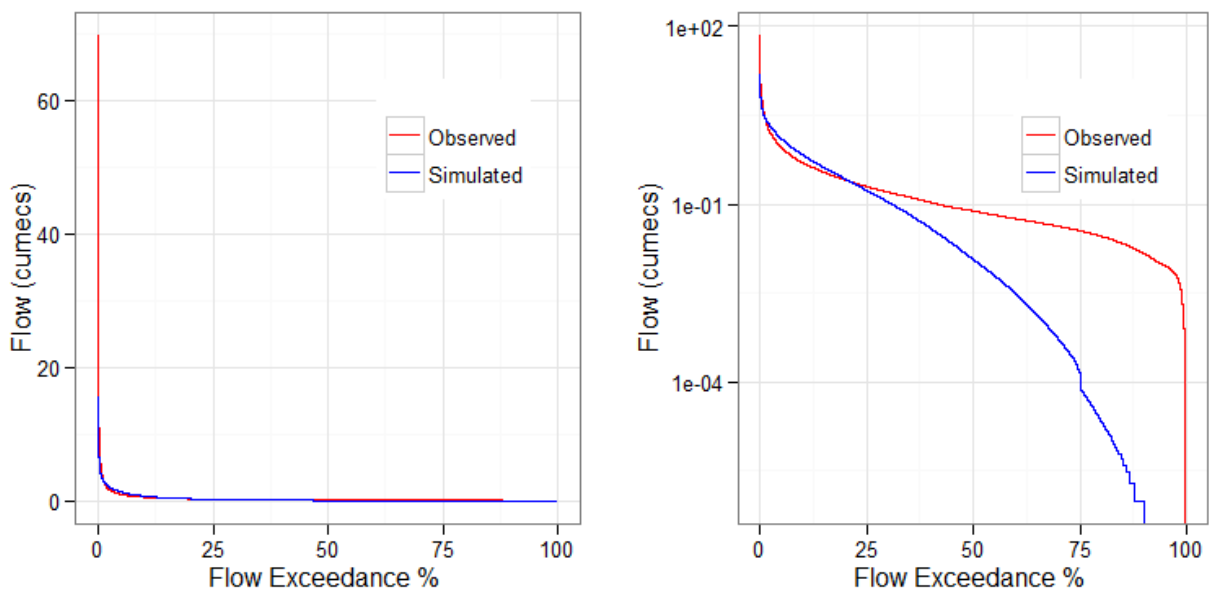


Figure K. 10: Flow duration curves in Sixth Creek for scenario 2, SIMHYD [right plot Y-axis in log scale]



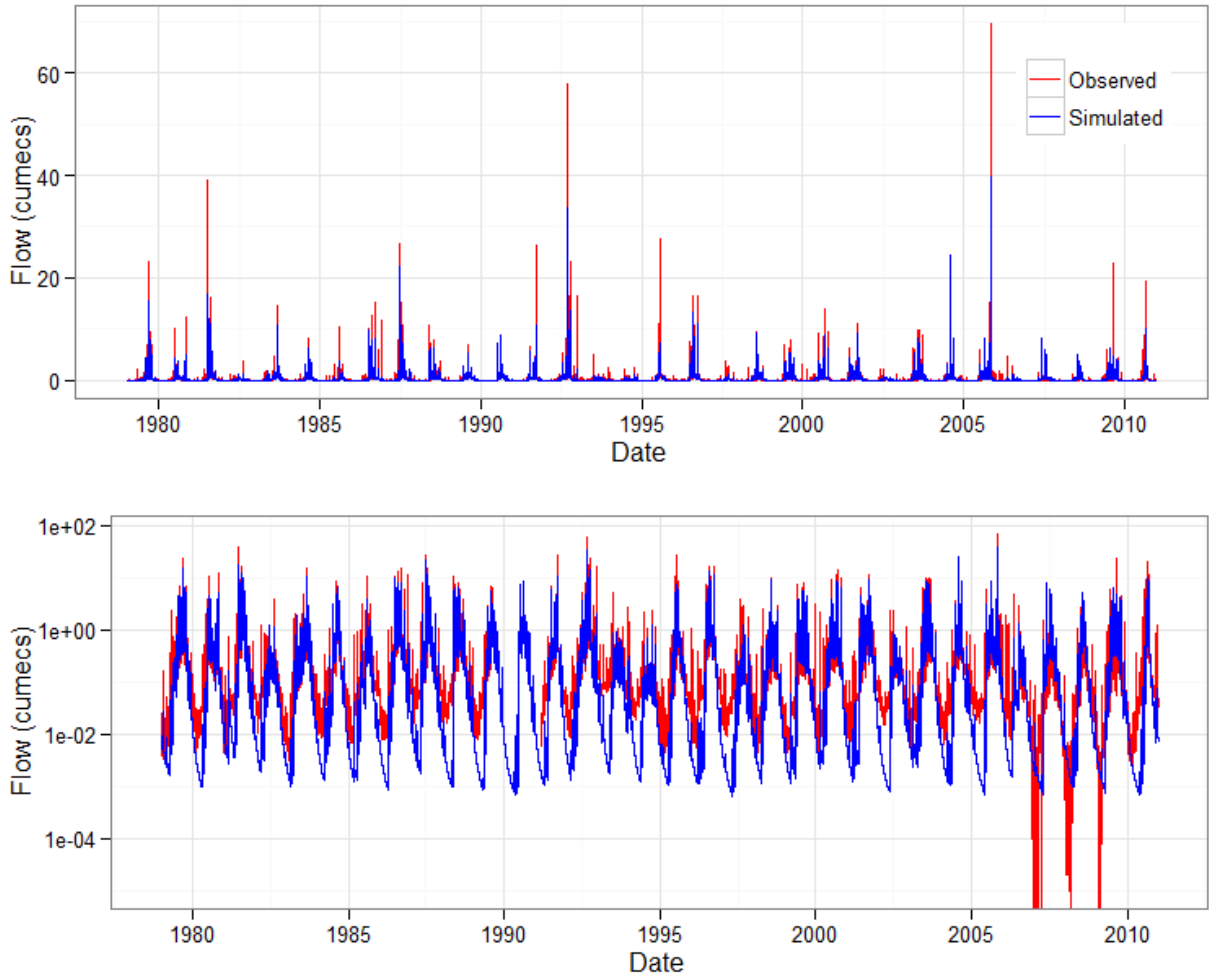


Figure K. 11: Comparison between the observed and simulated hydrographs (Sixth Creek, scenario 2, GR4H) [The Y-axis in the lower plot is in log scale]

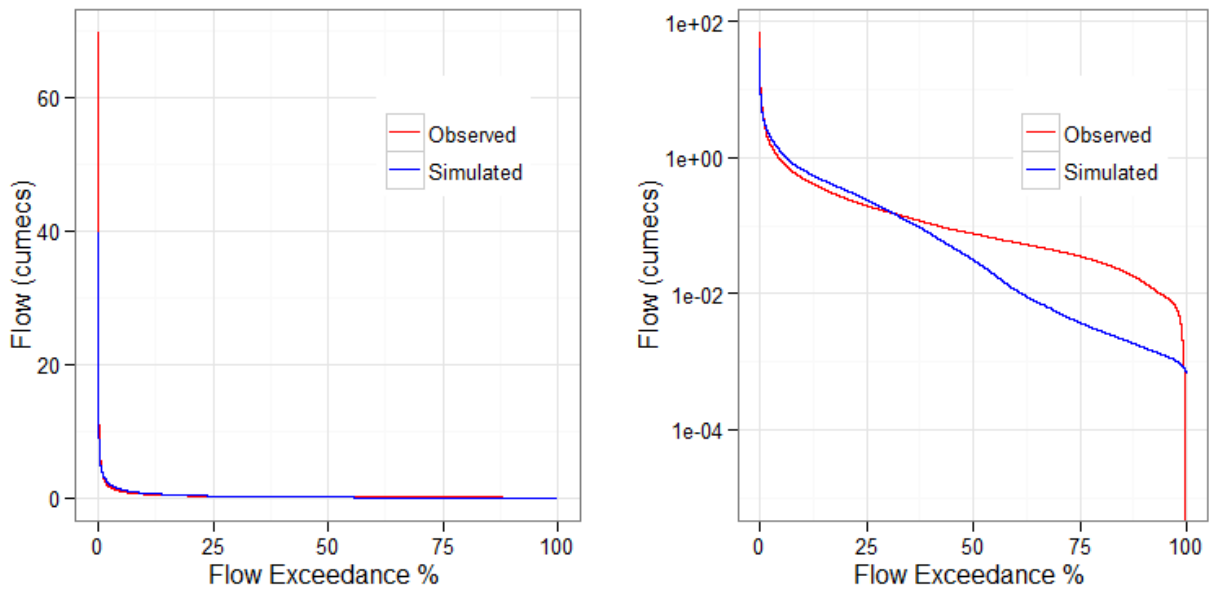


Figure K. 12: Flow duration curves in Sixth Creek for scenario 2, GR4H [right plot Y-axis in log scale]

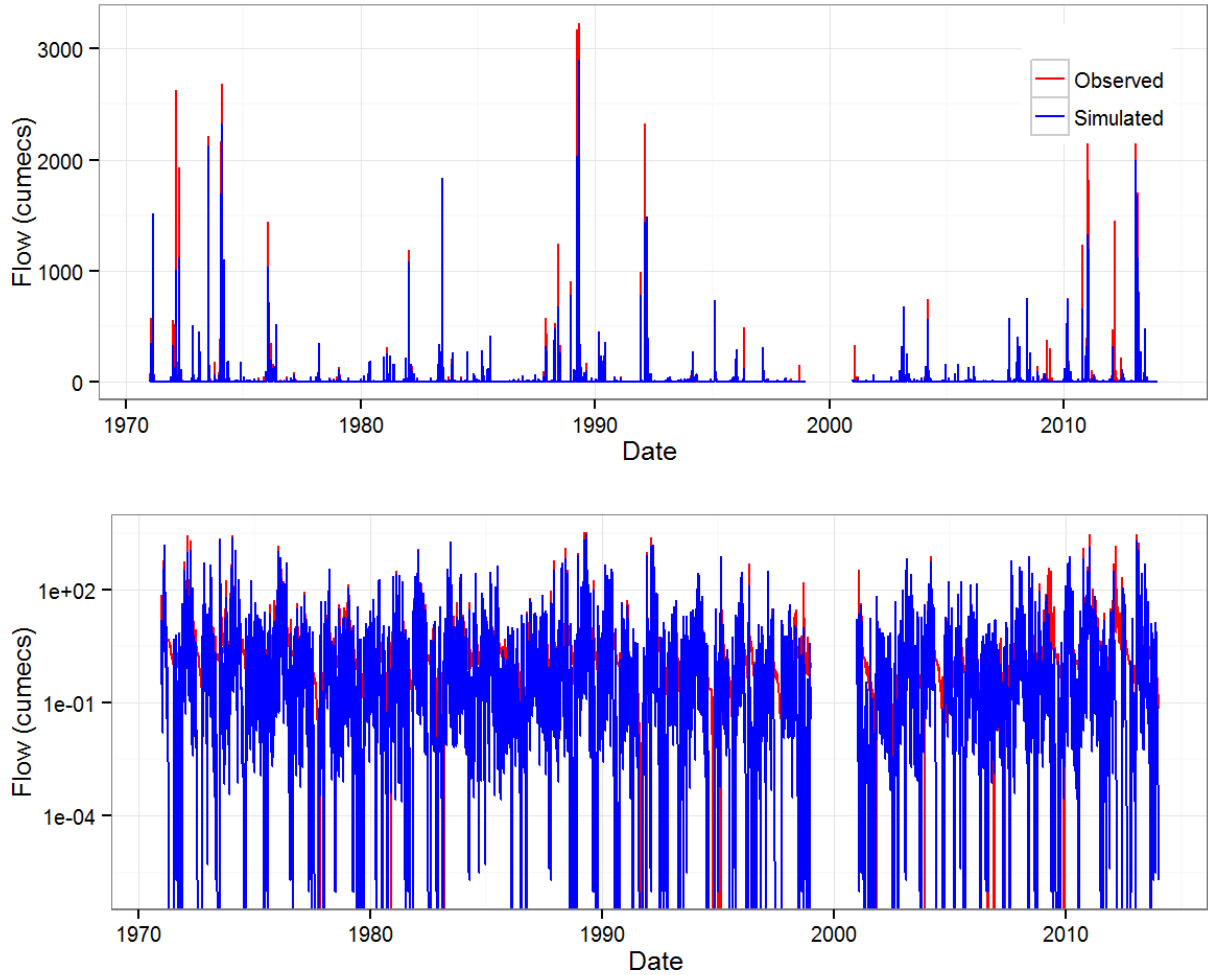


Figure K. 13: Comparison between the observed and simulated hydrographs (Mary River, scenario 2, AWBM) [The Y-axis in the lower plot is in log scale]

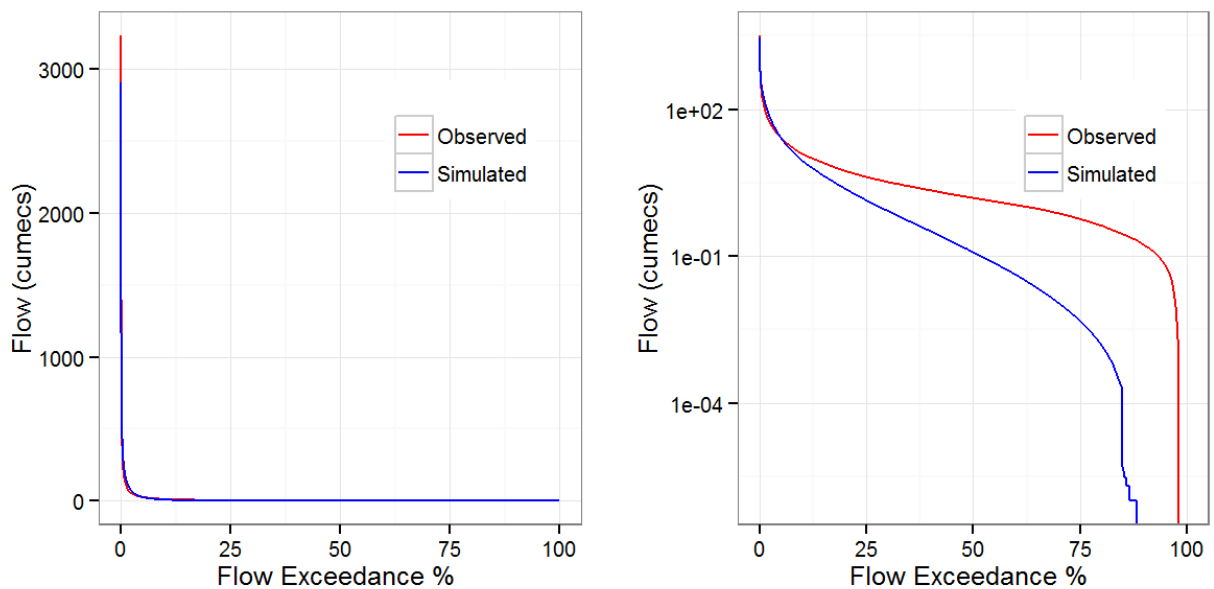


Figure K. 14: Flow duration curves in Mary for scenario 2, AWBM [right plot Y-axis in log scale]

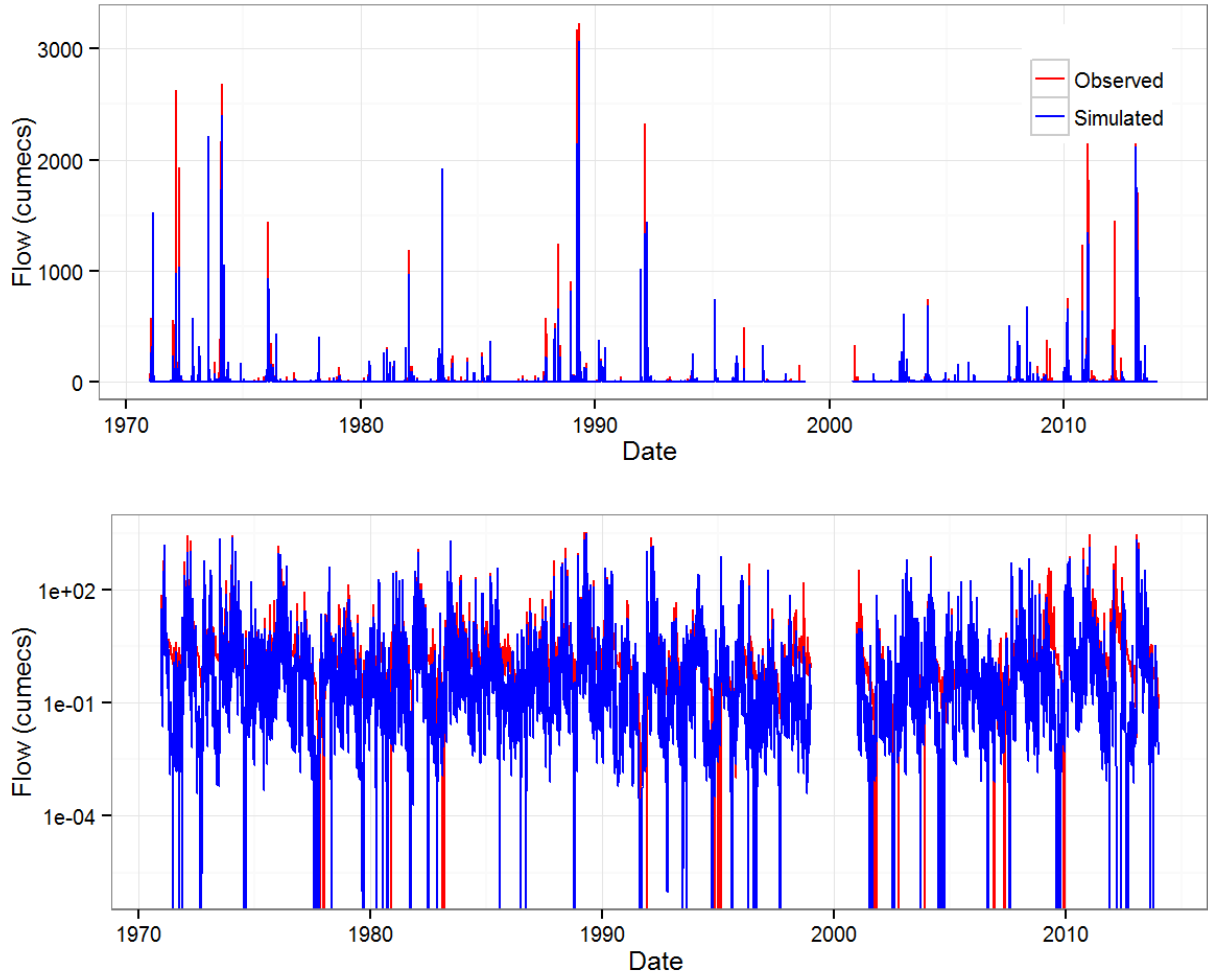


Figure K. 15: Comparison between the observed and simulated hydrographs (Mary River, scenario 2, SIMHYD) [The Y-axis in the lower plot is in log scale]

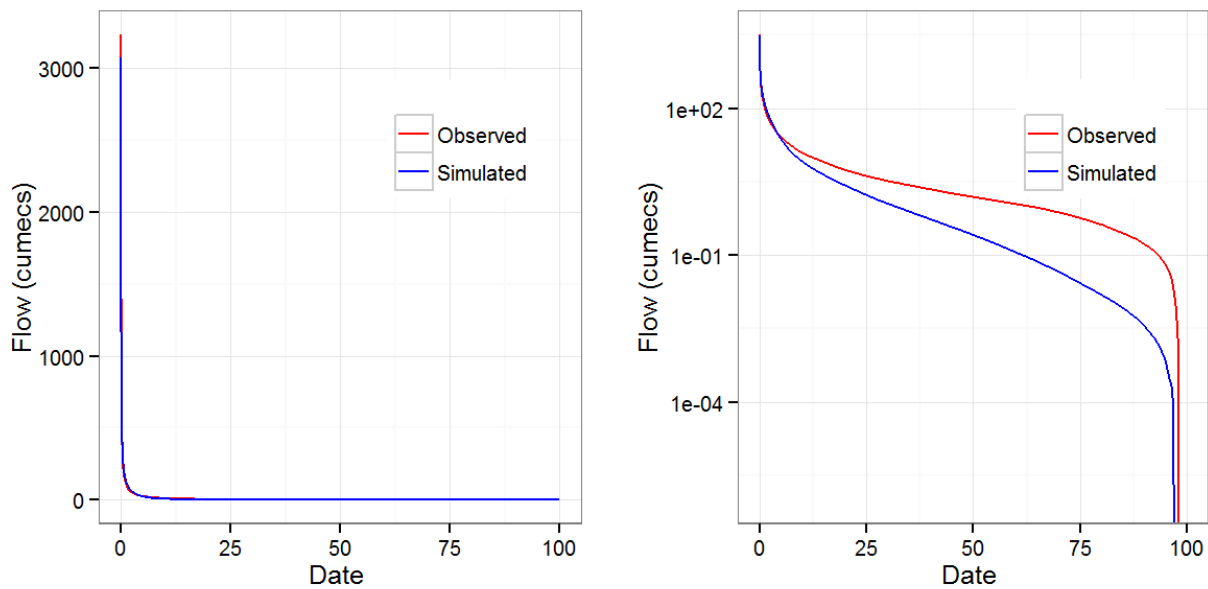


Figure K. 16: Flow duration curves in Mary for scenario 2, SIMHYD [right plot Y-axis in log scale]

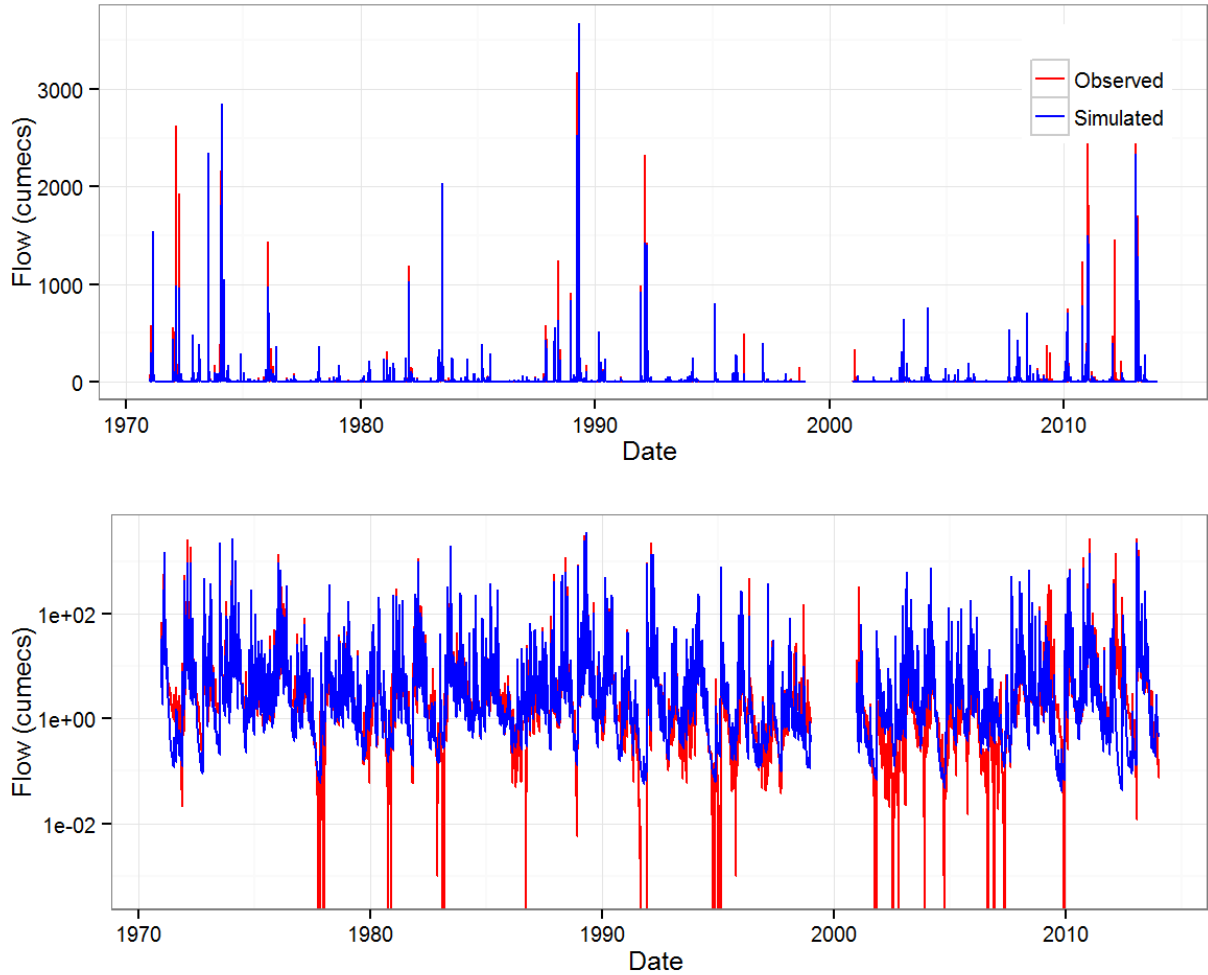


Figure K. 17: Comparison between the observed and simulated hydrographs (Mary River, scenario 2, GR4H) [The Y-axis in the lower plot is in log scale]

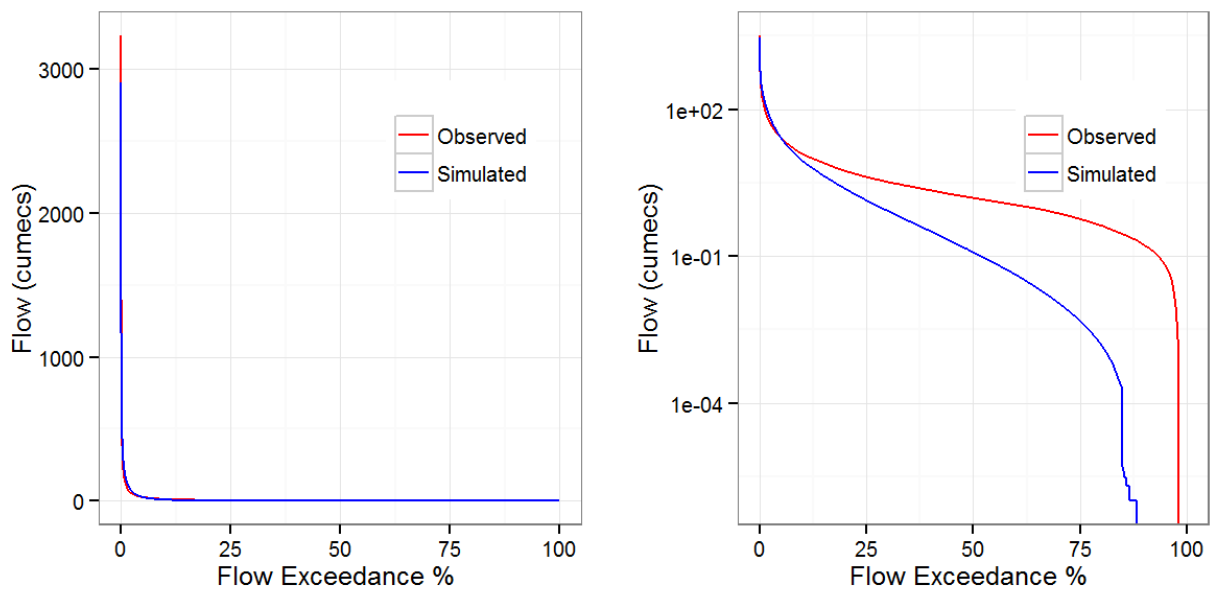


Figure K. 18: Flow duration curves in Mary for scenario 2, GR4H [right plot Y-axis in log scale]

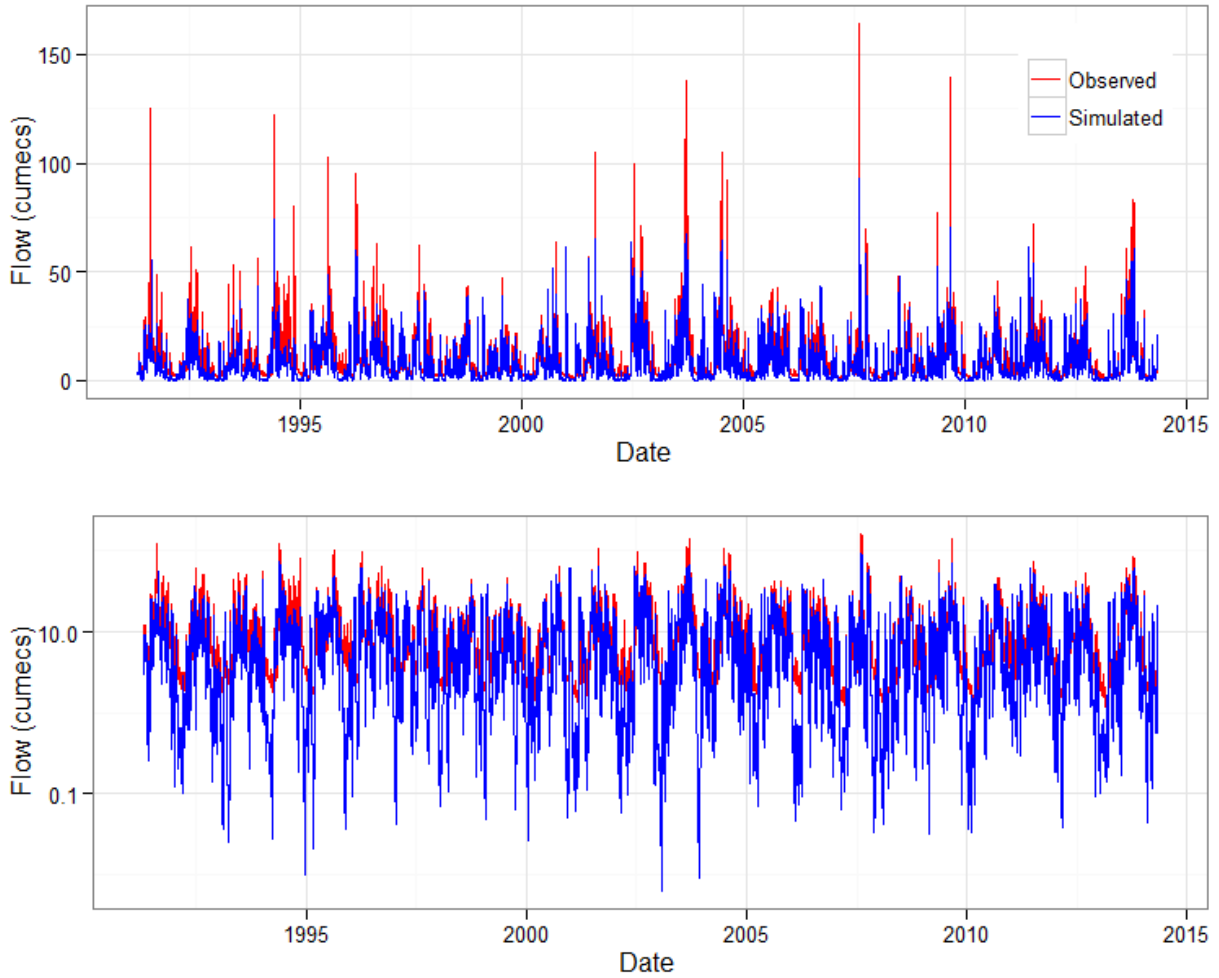


Figure K. 19: Comparison between the observed and simulated hydrographs (Florentine River, scenario 2, AWBM) [The Y-axis in the lower plot is in log scale]

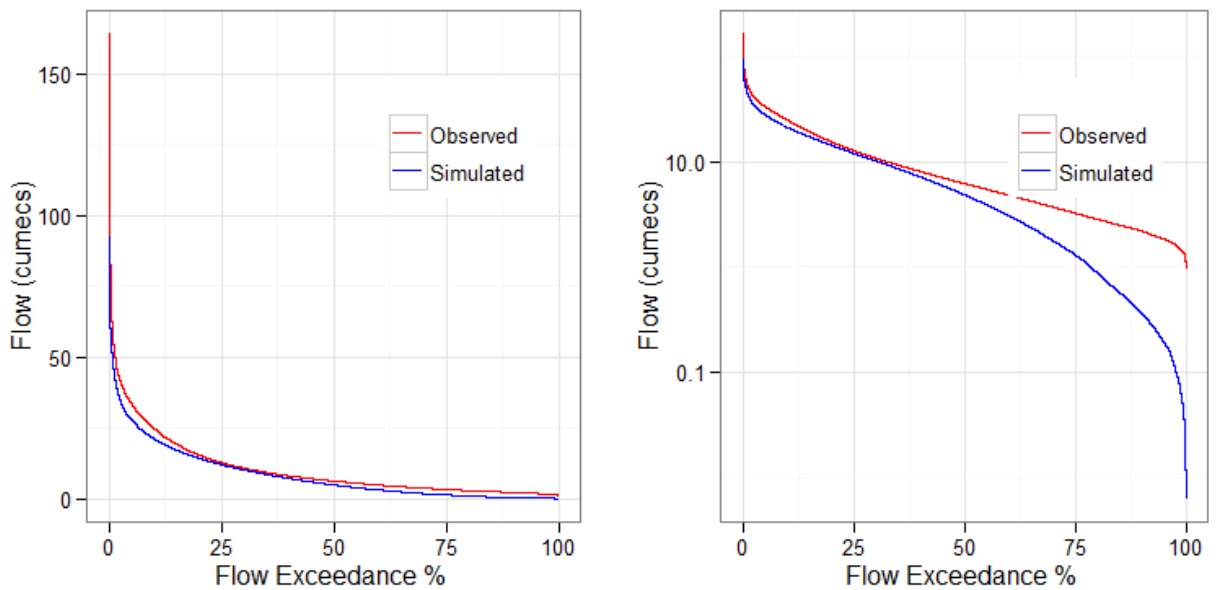


Figure K. 20: Flow duration curves in Florentine for scenario 2, AWBM [right plot Y-axis in log scale]

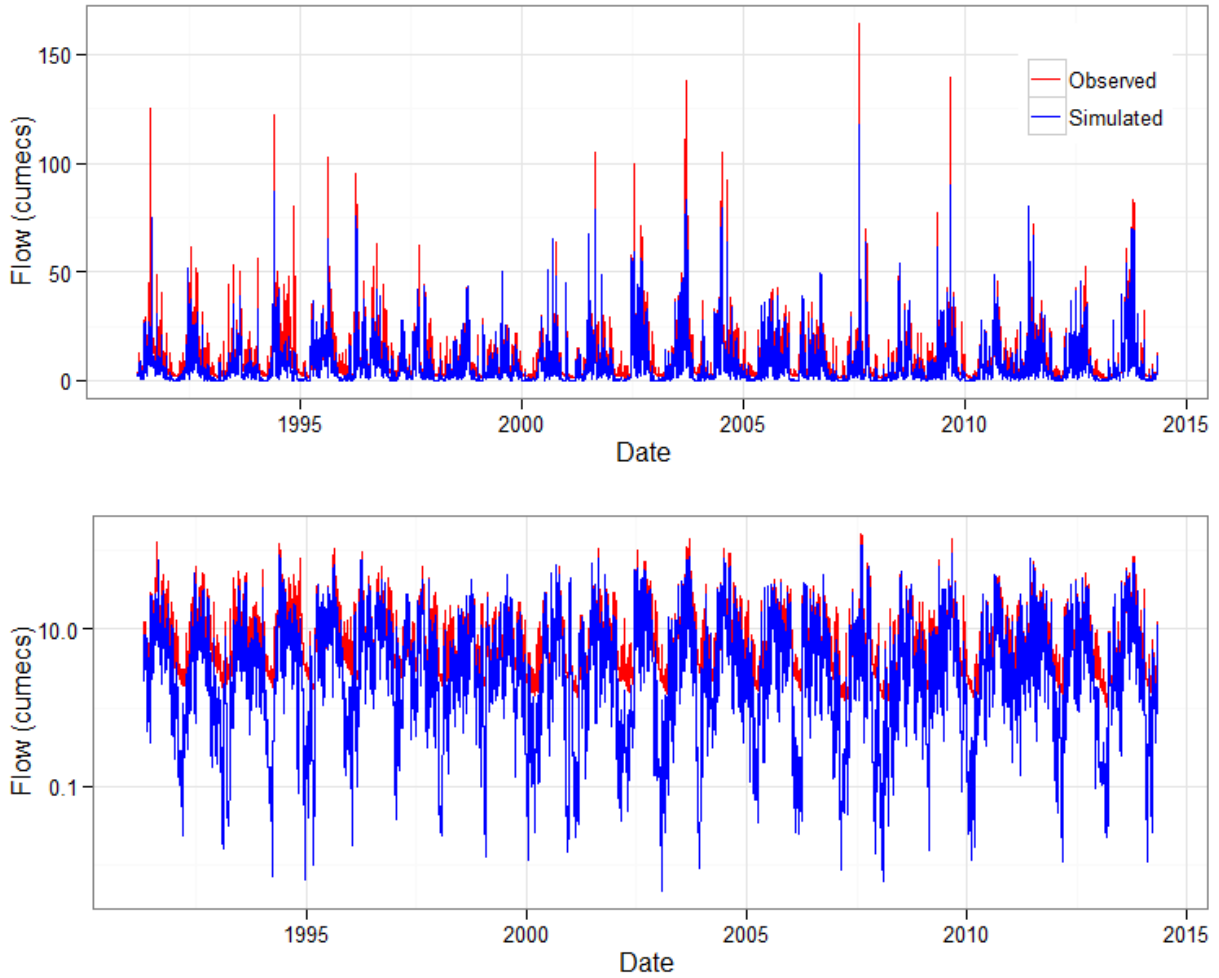


Figure K. 21: Comparison between the observed and simulated hydrographs (Mary River, scenario 2, SIMHYD) [The Y-axis in the lower plot is in log scale]

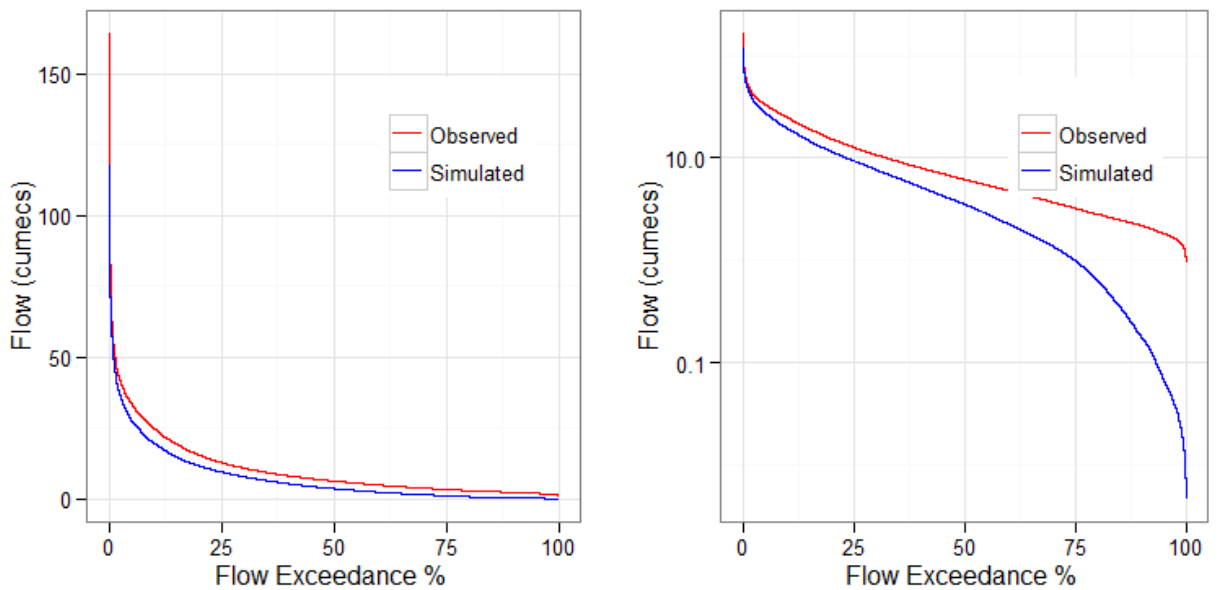


Figure K. 22: Flow duration curves in Florentine for scenario 2, SIMHYD [right plot Y-axis in log scale]

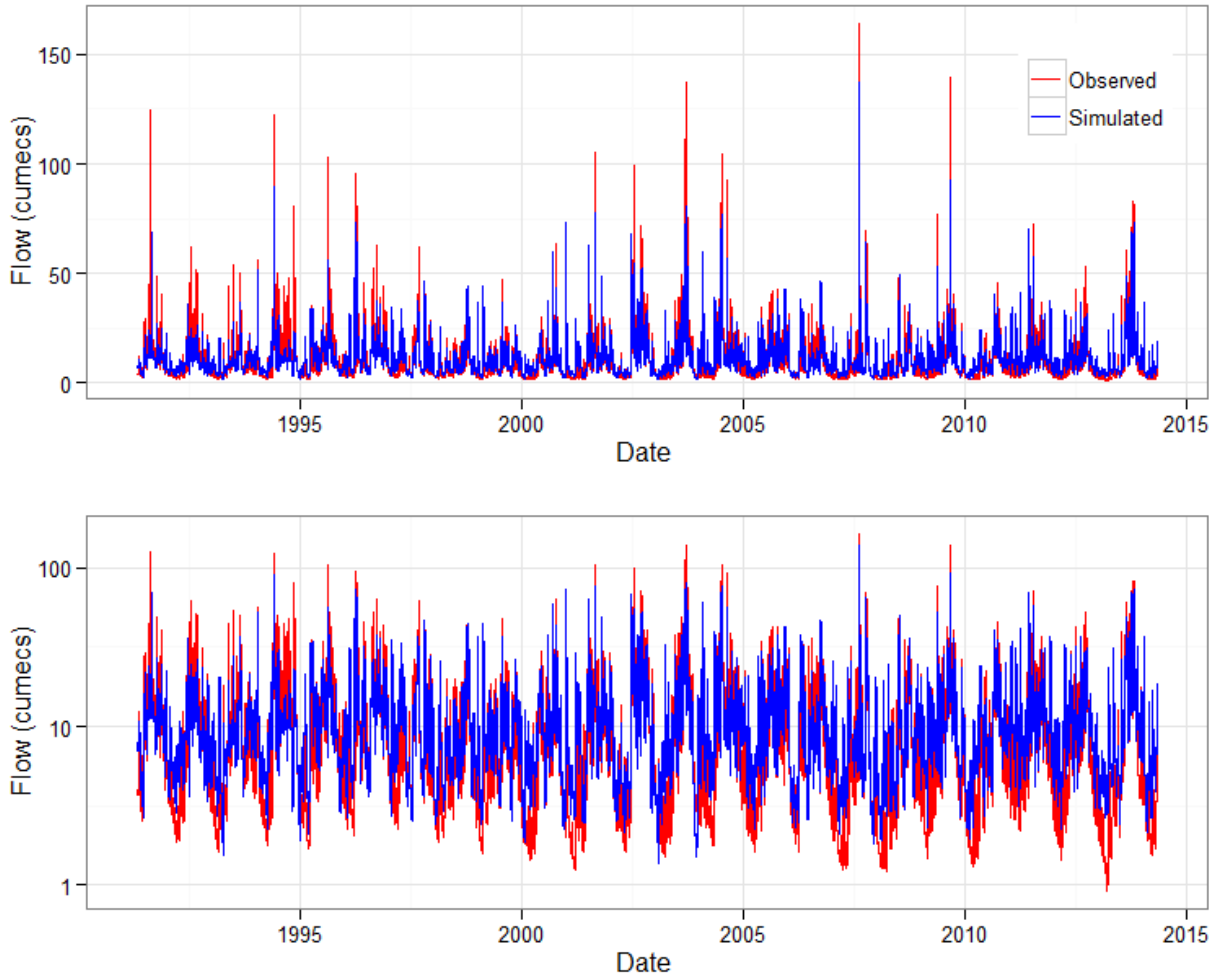


Figure K. 23: Comparison between the observed and simulated hydrographs (Florentine River, scenario 2, GR4H) [The Y-axis in the lower plot is in log scale]

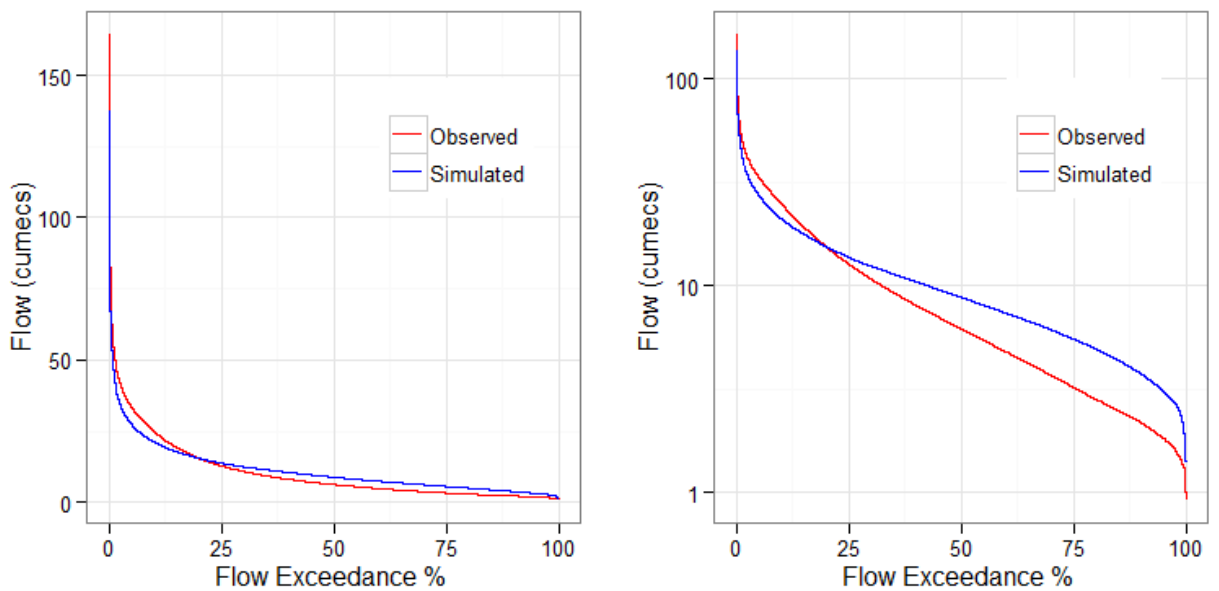


Figure K. 24: Flow duration curves in Florentine for scenario 2, GR4H [right plot Y-axis in log scale]

## **Appendix L**

## **Results: Scenario 3**



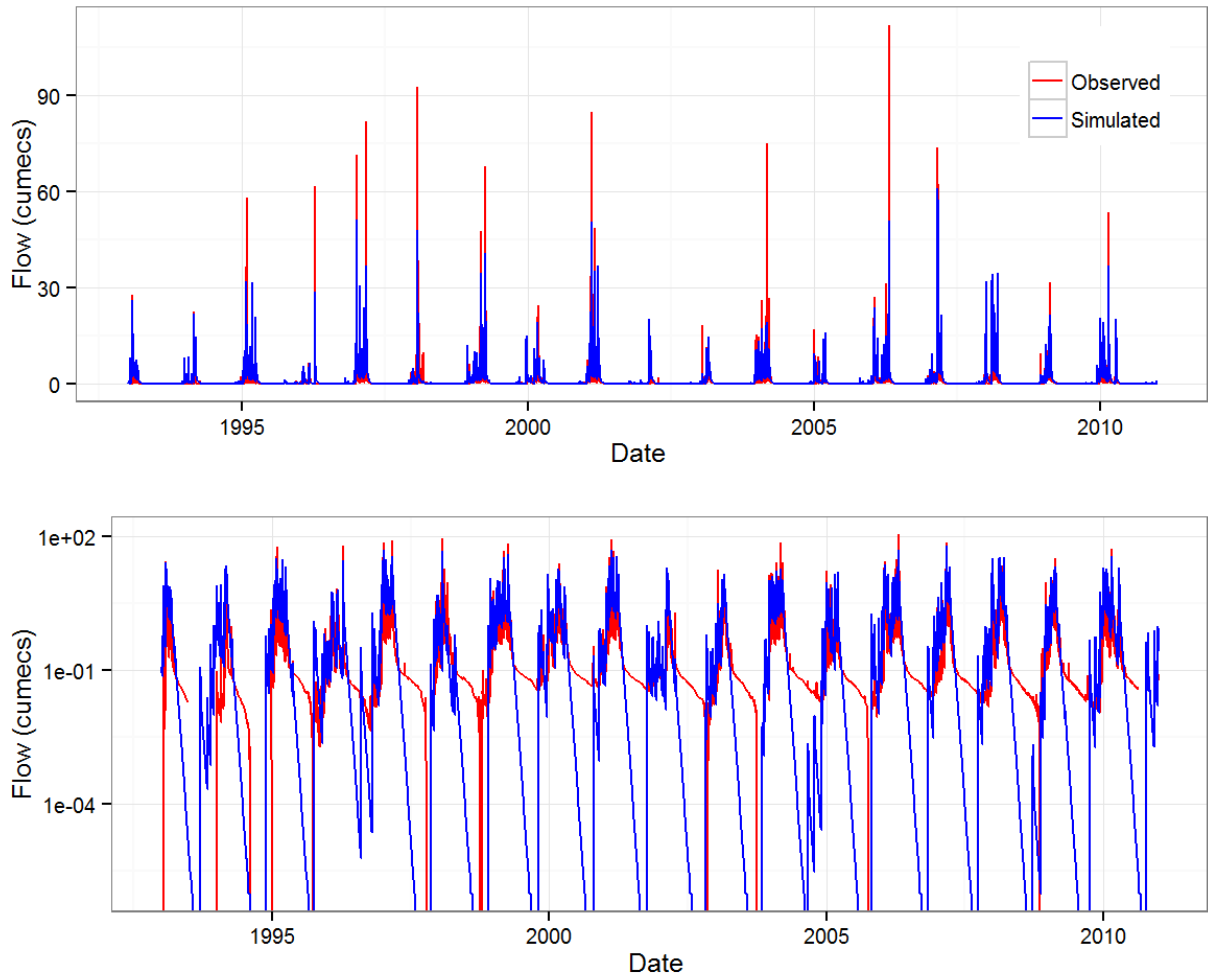


Figure L. 2: Comparison between the observed and simulated hydrographs (Manton River, scenario 3, AWBM) [The Y-axis in the lower plot is in log scale]

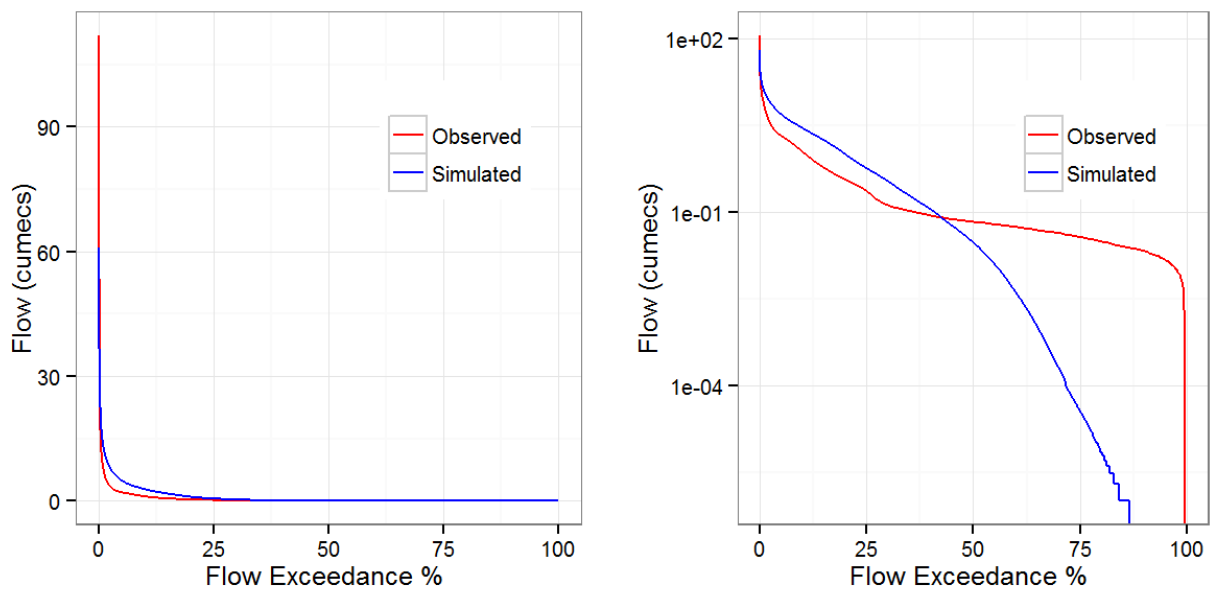


Figure L. 3: Flow duration curves in Manton for scenario 3, AWBM [right plot Y-axis in log scale]

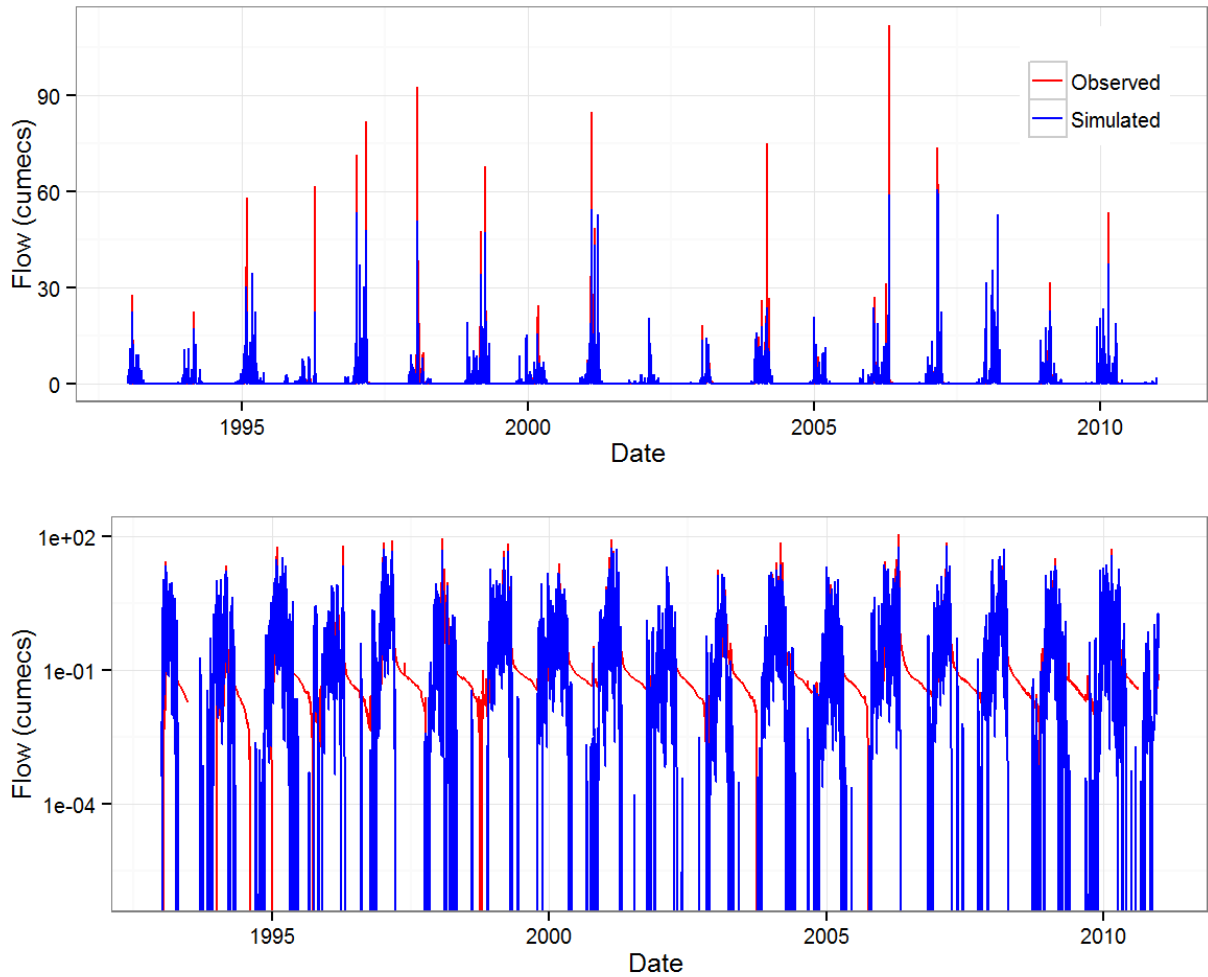


Figure L. 4: Comparison between the observed and simulated hydrographs (Manton River, scenario 3, SIMHYD) [The Y-axis in the lower plot is in log scale]

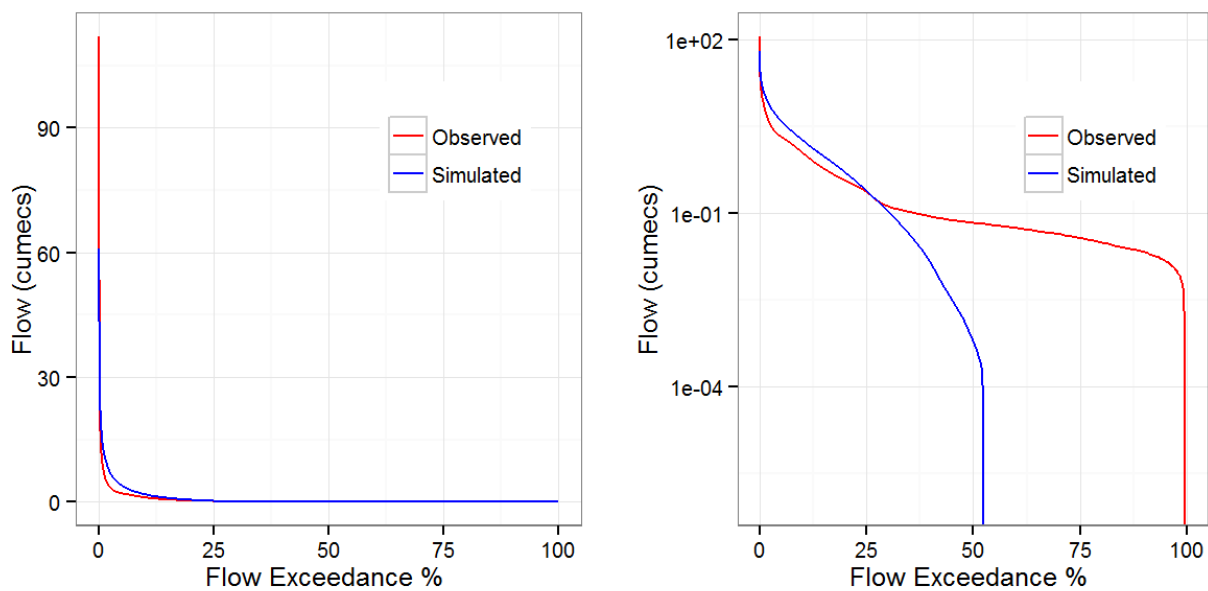


Figure L. 5: Flow duration curves in Manton for scenario 3, SIMHYD [right plot Y-axis in log scale]

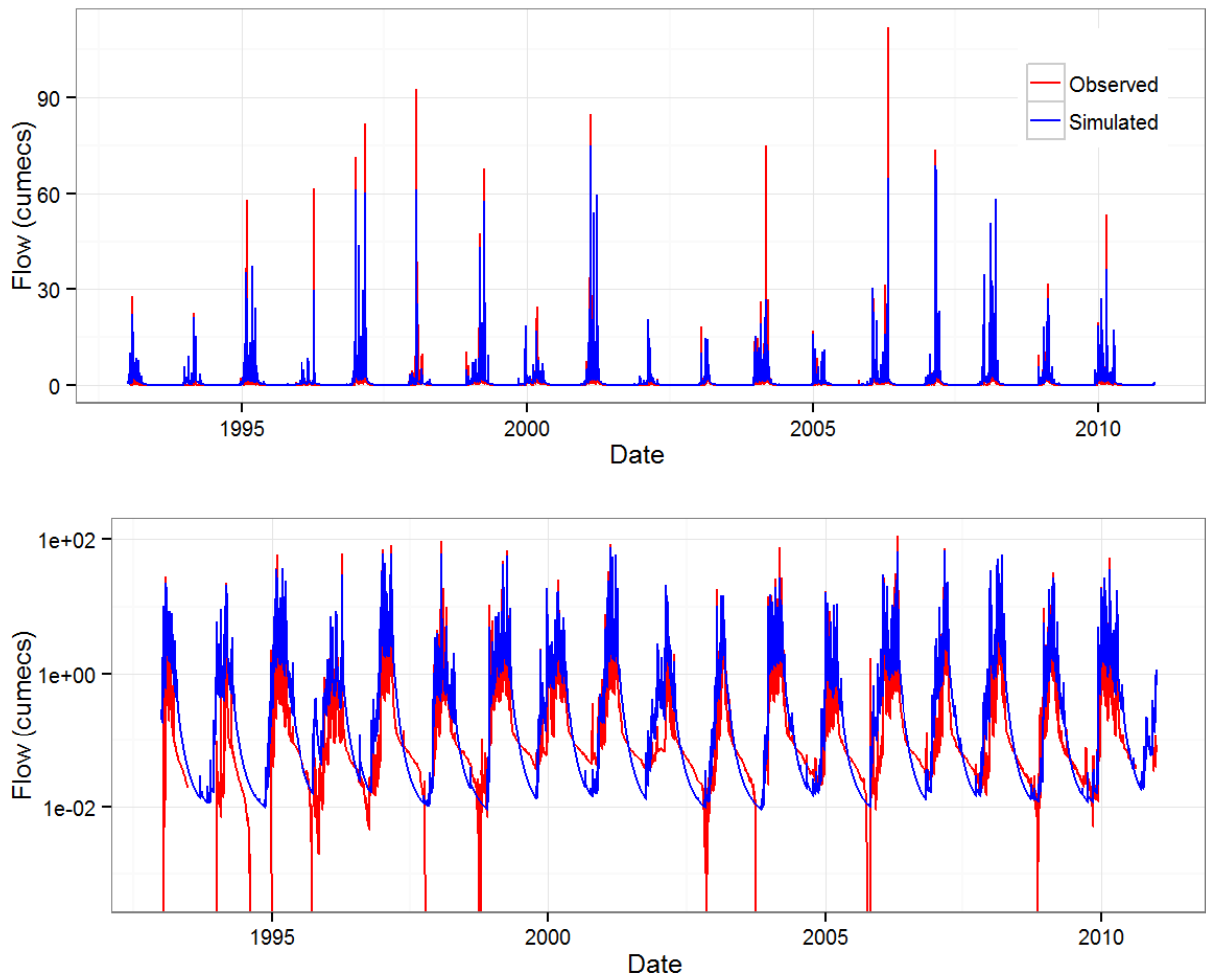


Figure L. 6: Comparison between the observed and simulated hydrographs (Manton River, scenario 3, GR4H) [The Y-axis in the lower plot is in log scale]

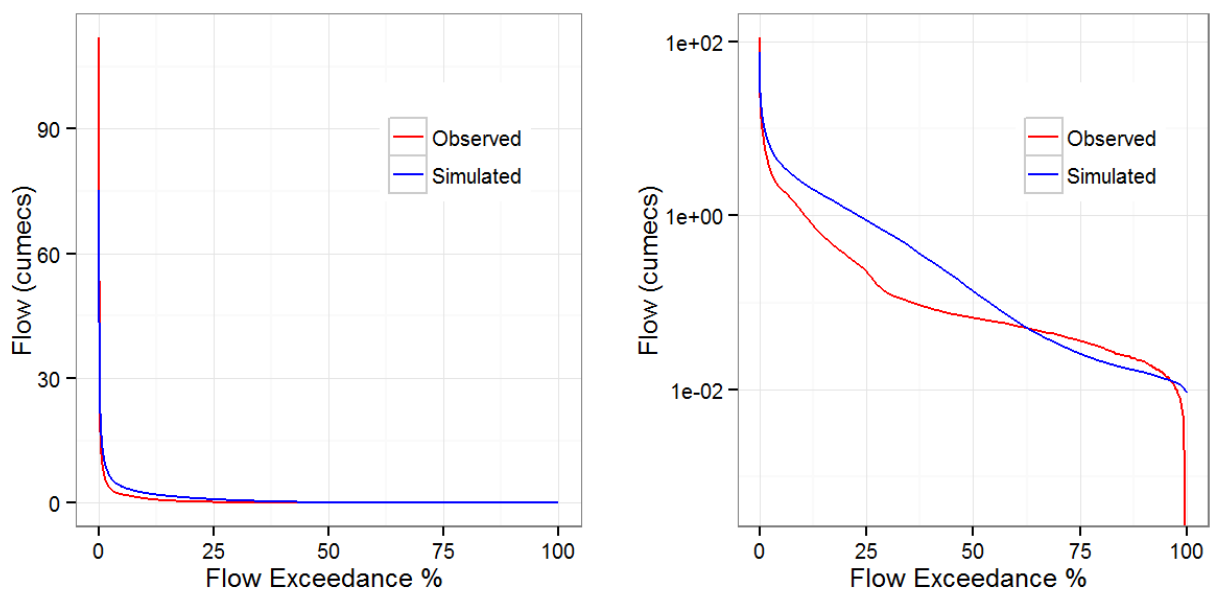


Figure L. 7: Flow duration curves in Manton for scenario 3, GR4H [right plot Y-axis in log scale]

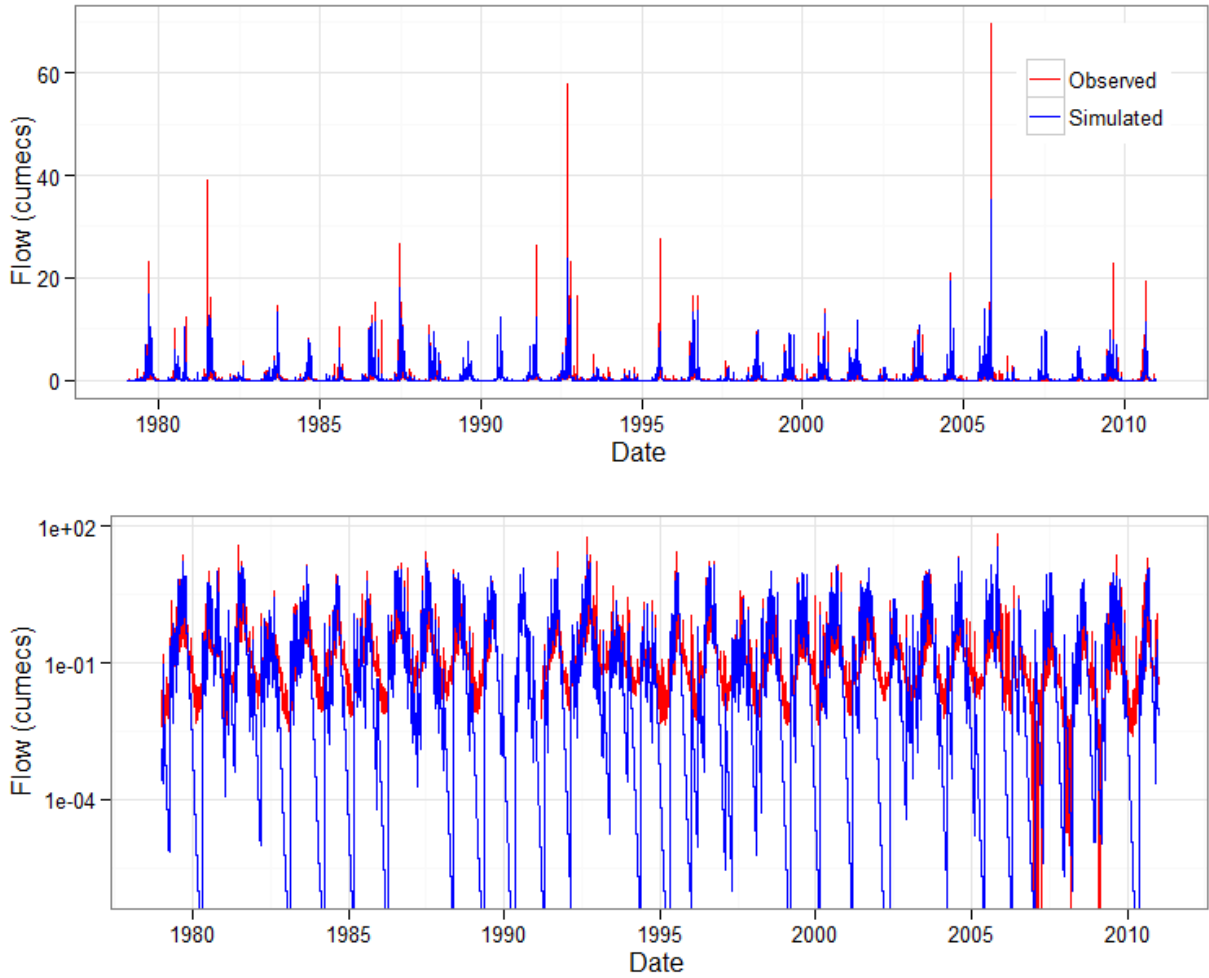


Figure L. 8: Comparison between the observed and simulated hydrographs (Sixth Creek River, scenario 3, AWBM) [The Y-axis in the lower plot is in log scale]

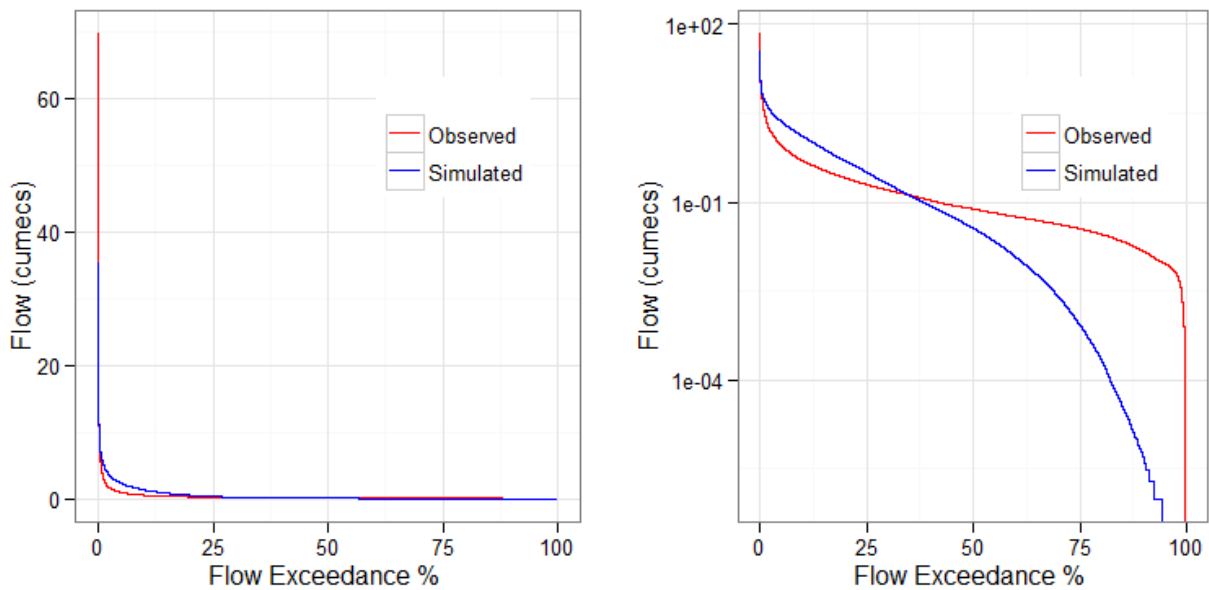


Figure L. 9: Flow duration curves in Sixth Creek for scenario 3, AWBM [right plot Y-axis in log scale]

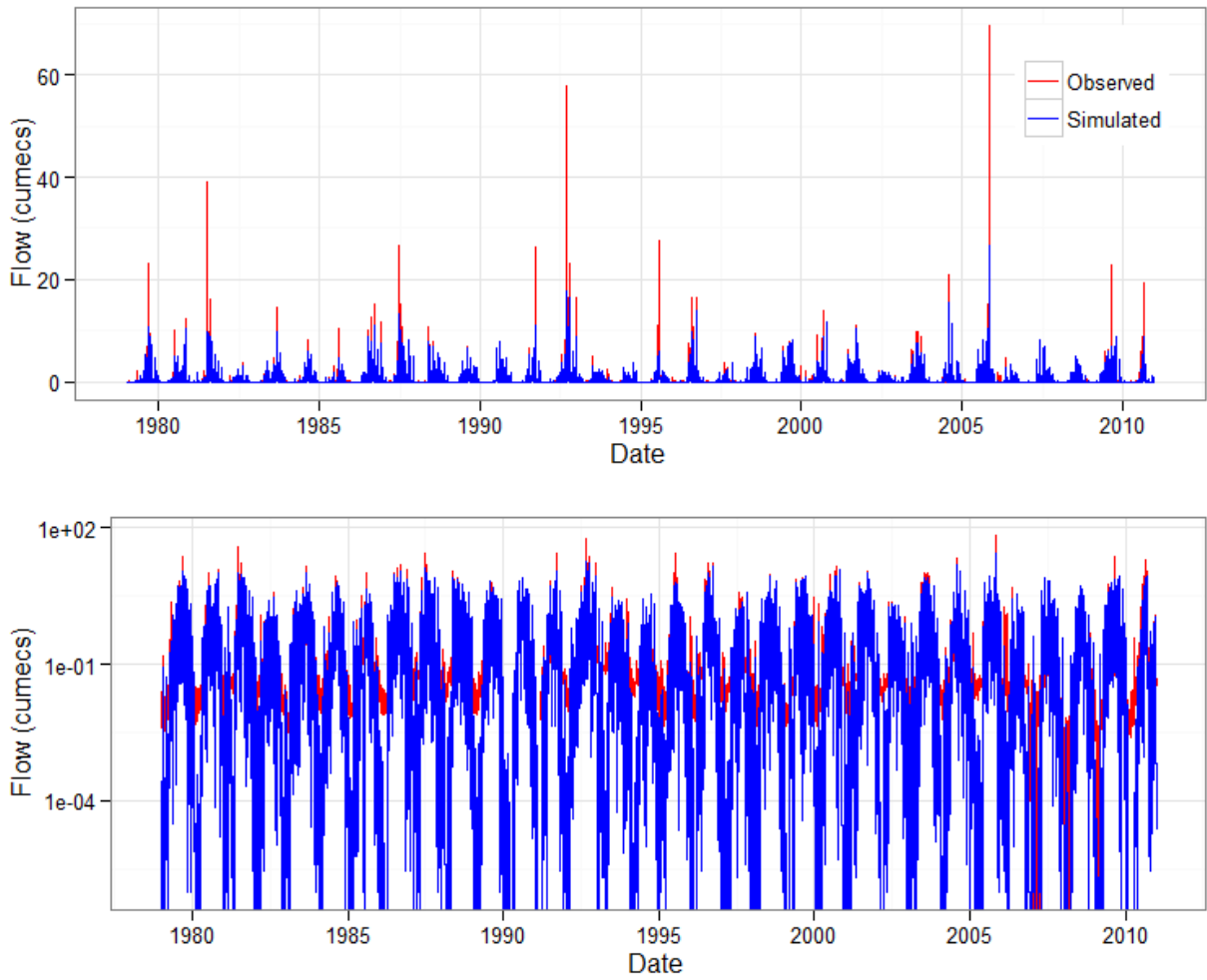


Figure L. 10 : Comparison between the observed and simulated hydrographs (Sixth Creek, scenario 3, SIMHYD) [The Y-axis in the lower plot is in log scale]

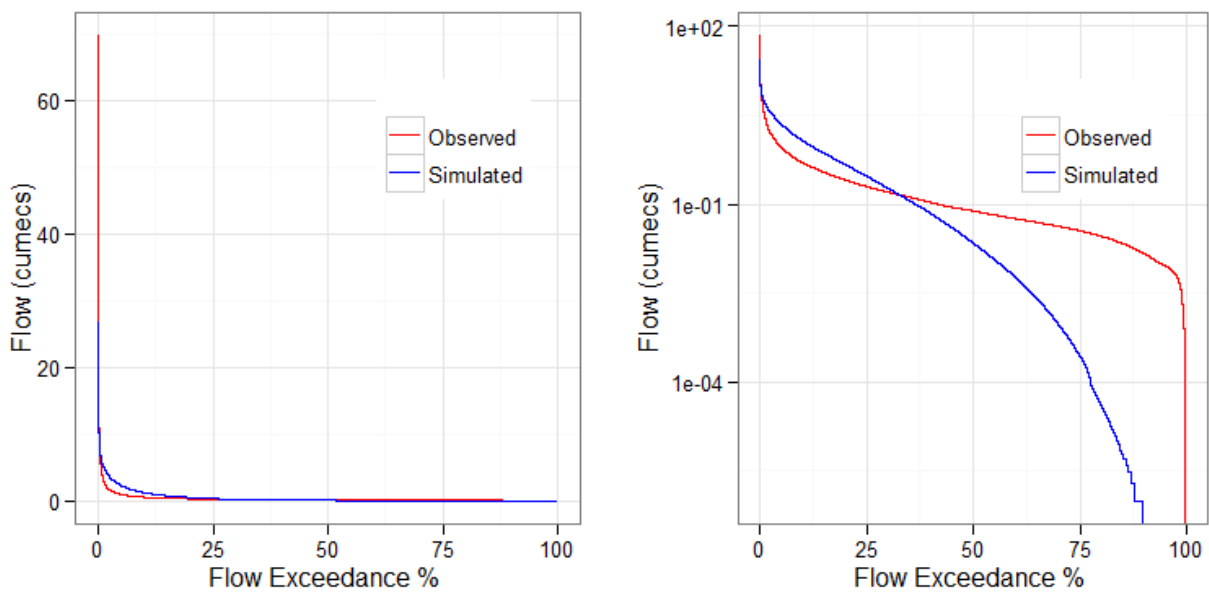


Figure L. 11: Flow duration curves in Sixth Creek for scenario 3, SIMHYD [right plot Y-axis in log scale]

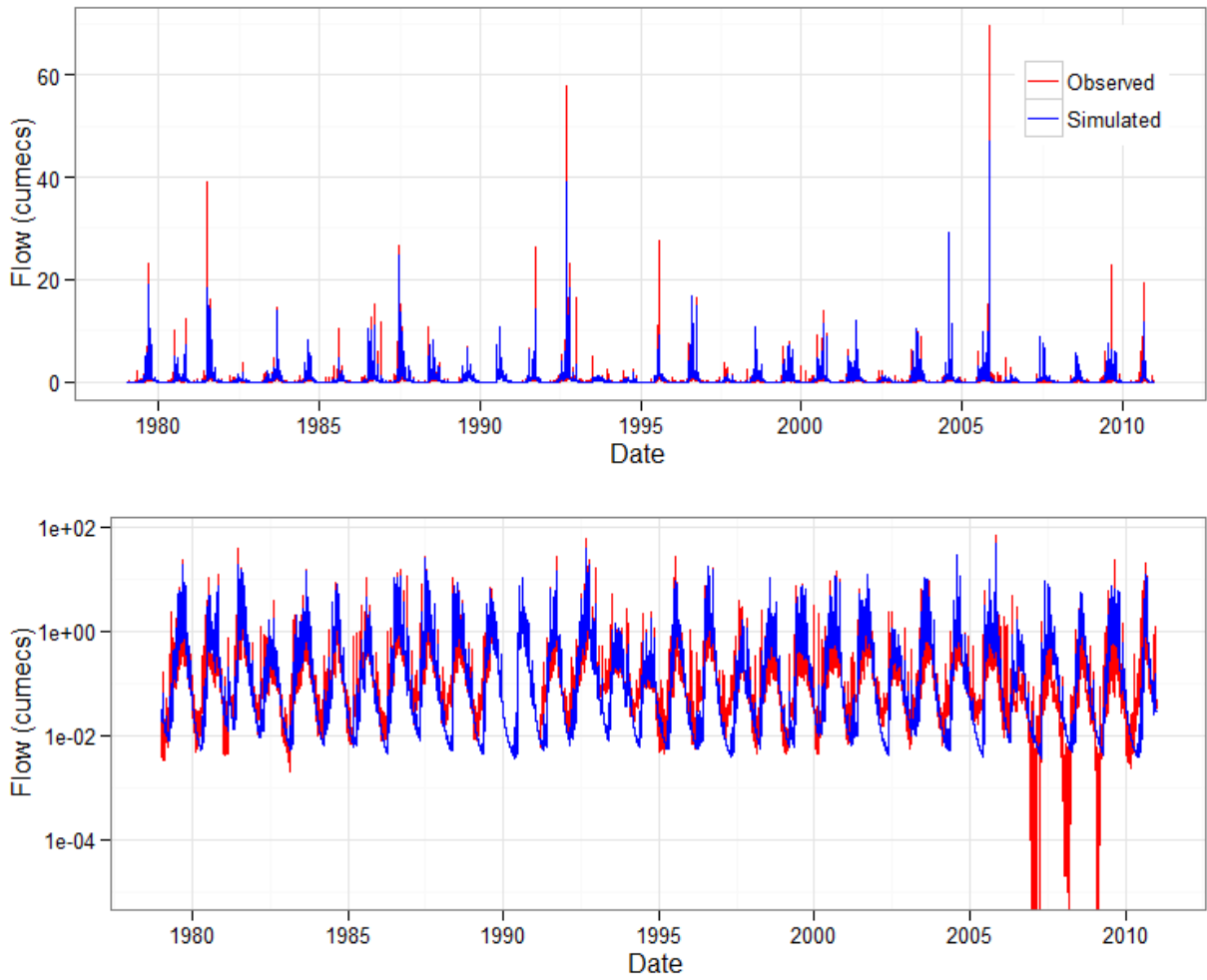


Figure L. 12: Comparison between the observed and simulated hydrographs (Sixth Creek, scenario 3, GR4H) [The Y-axis in the lower plot is in log scale]

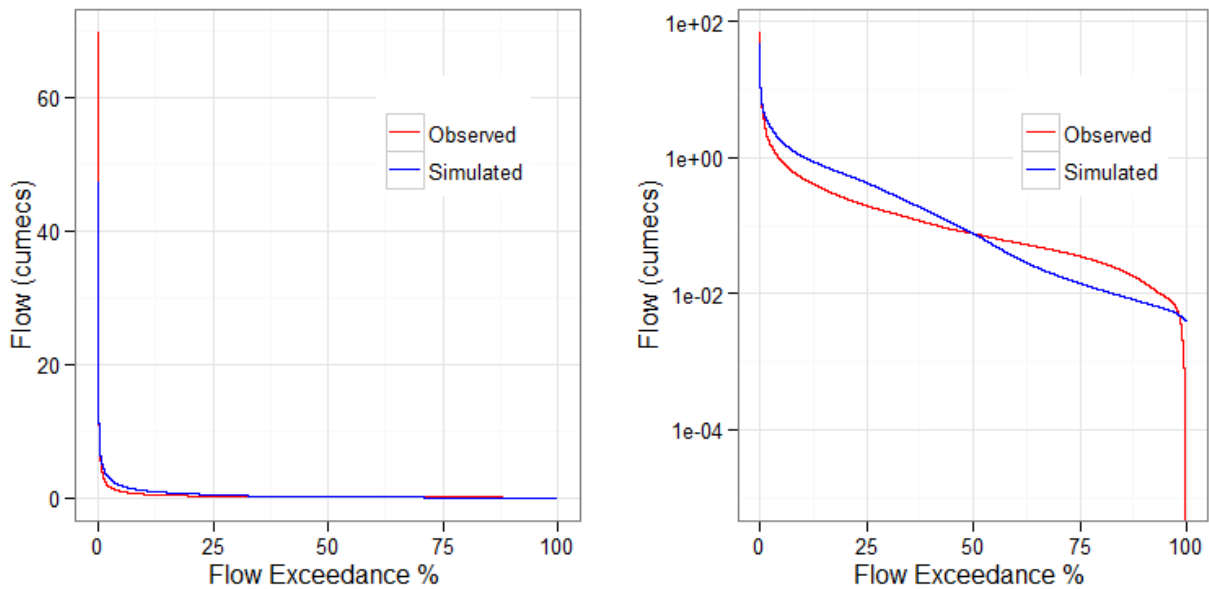


Figure L. 13: Flow duration curves in Sixth Creek for scenario 3, GR4H [right plot Y-axis in log scale]

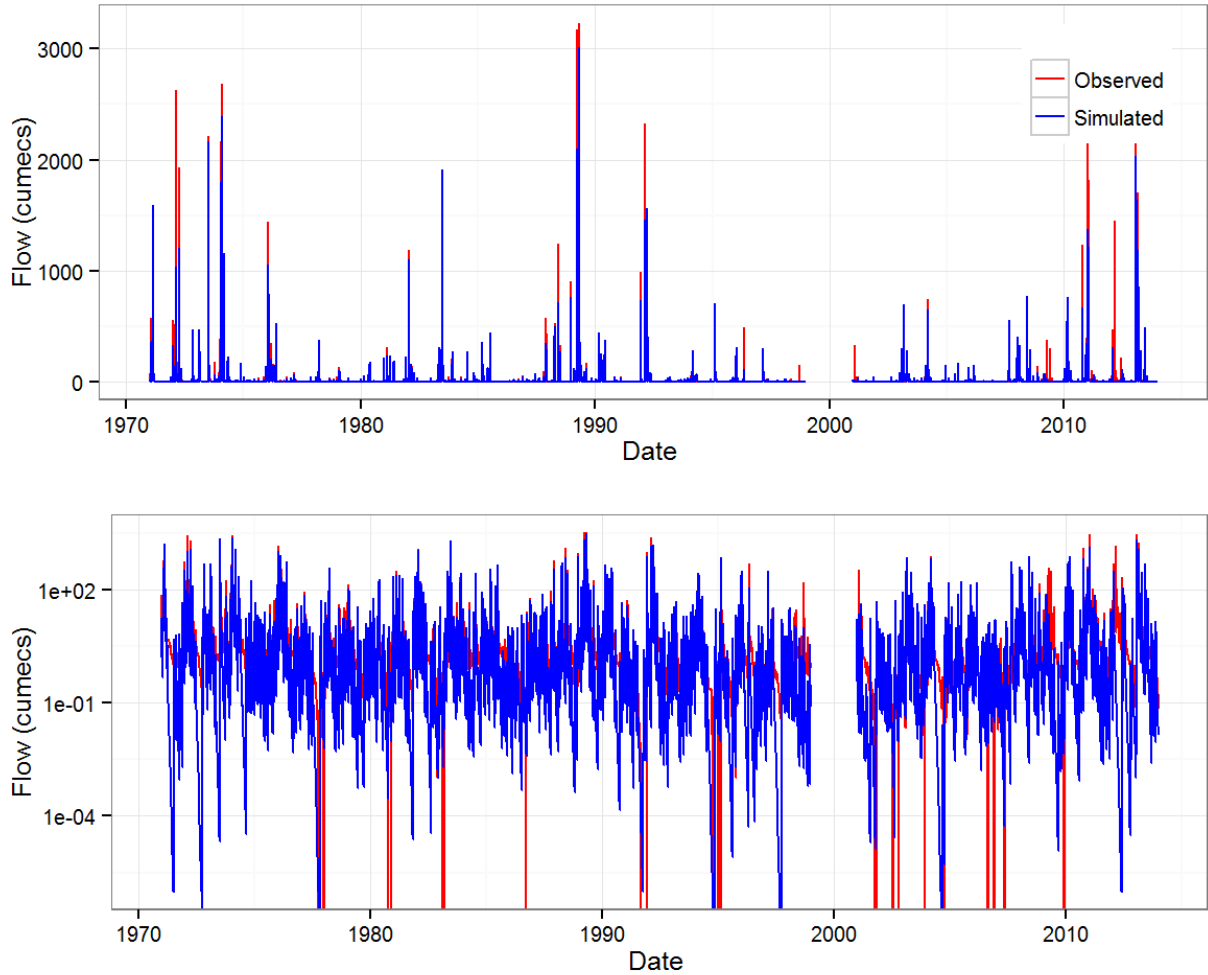


Figure L. 14: Comparison between the observed and simulated hydrographs (Mary River, scenario 3, AWBM) [The Y-axis in the lower plot is in log scale]

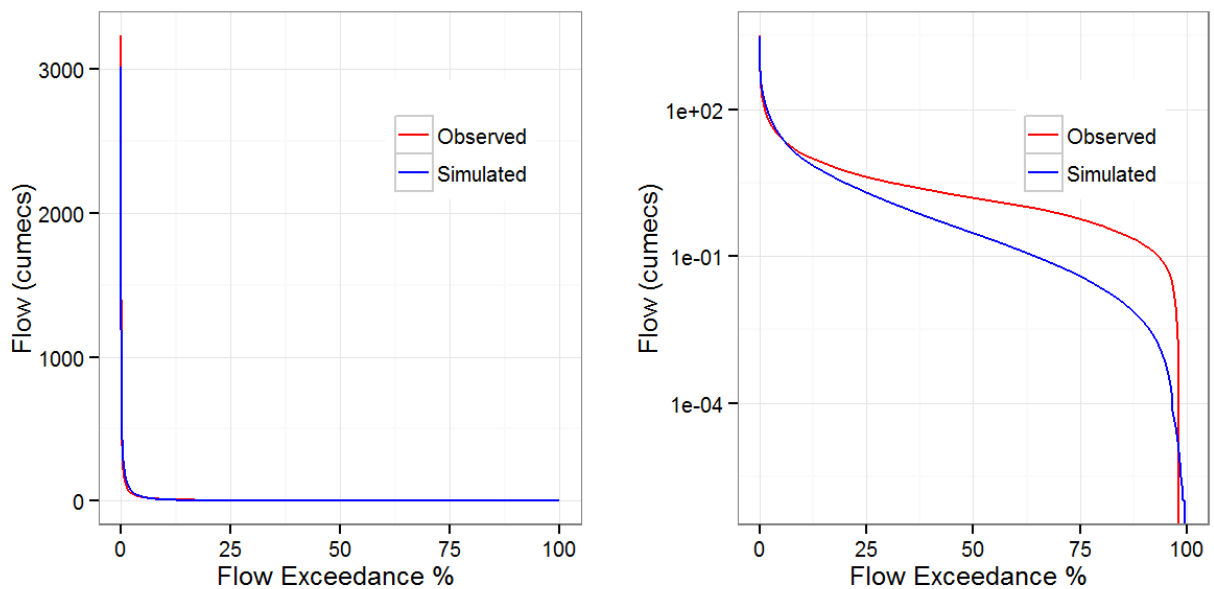


Figure L. 15: Flow duration curves in Mary River for scenario 3, AWBM [right plot Y-axis in log scale]

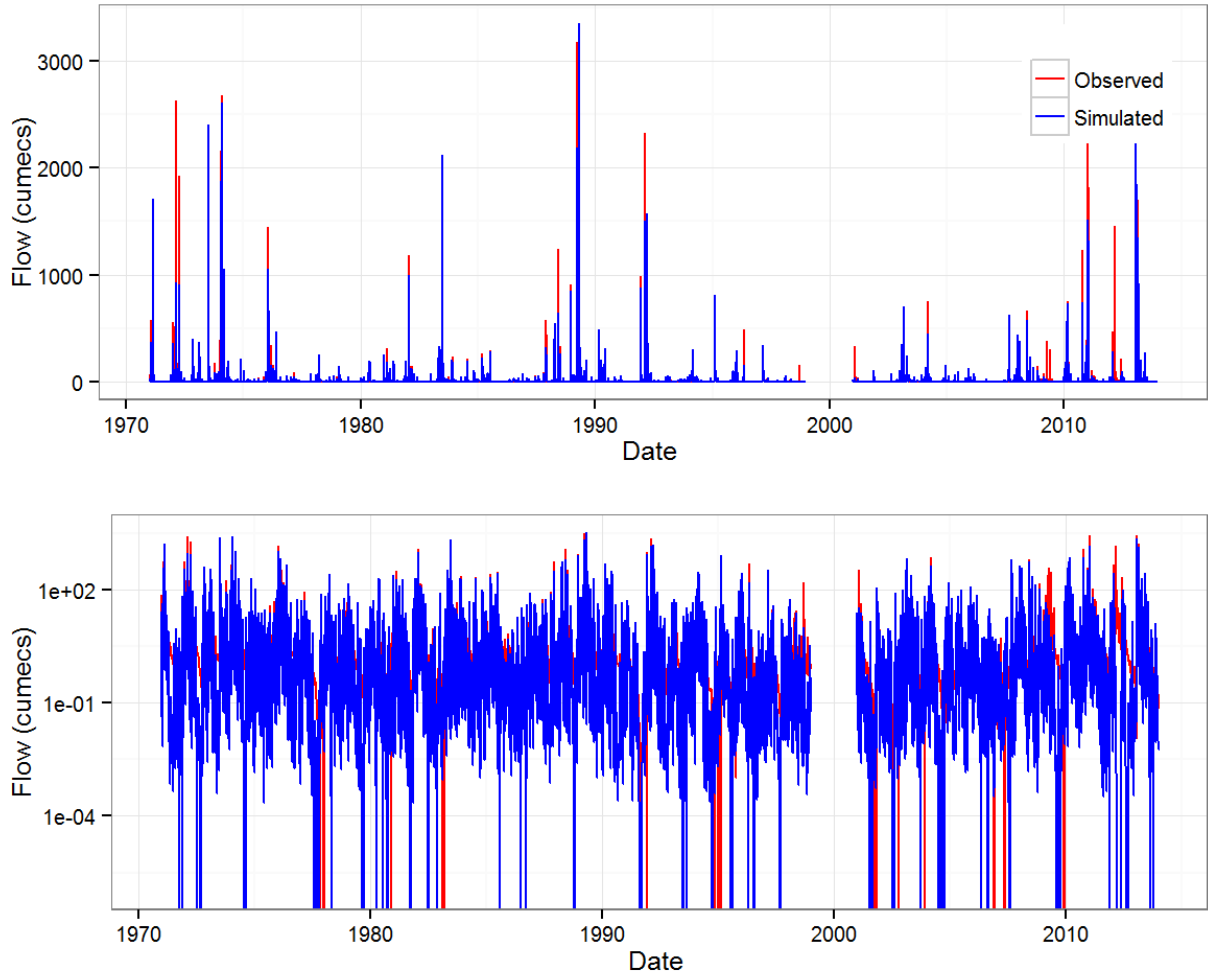


Figure L. 16: Comparison between the observed and simulated hydrographs (Mary River, scenario 3, SIMHYD) [The Y-axis in the lower plot is in log scale]

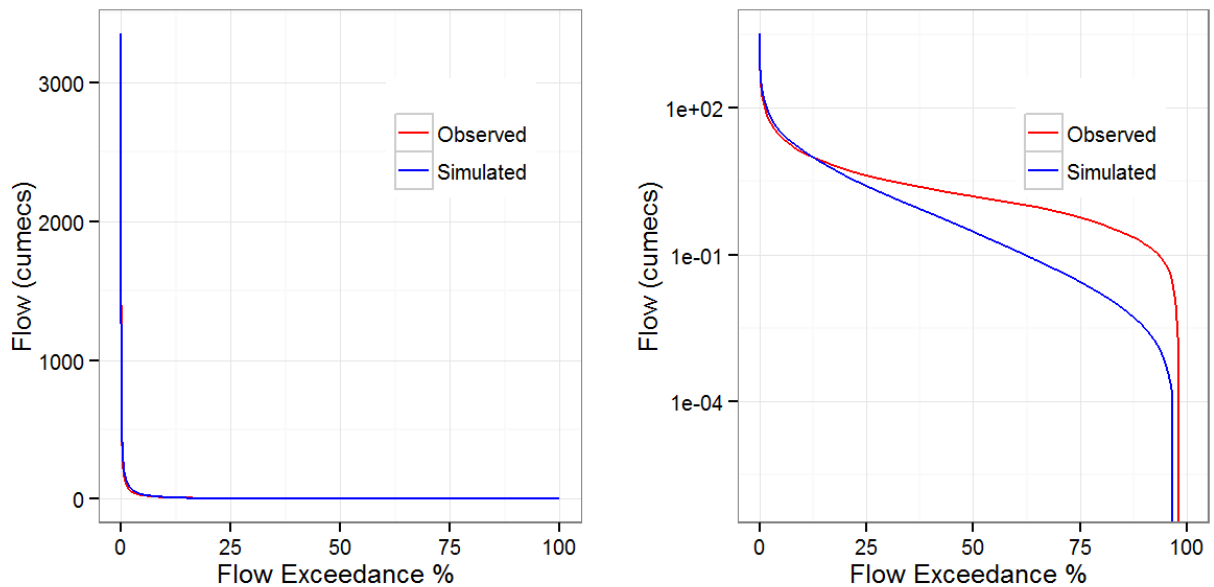


Figure L. 17: Flow duration curves in Mary River for scenario 3, SIMHYD [right plot Y-axis in log scale]



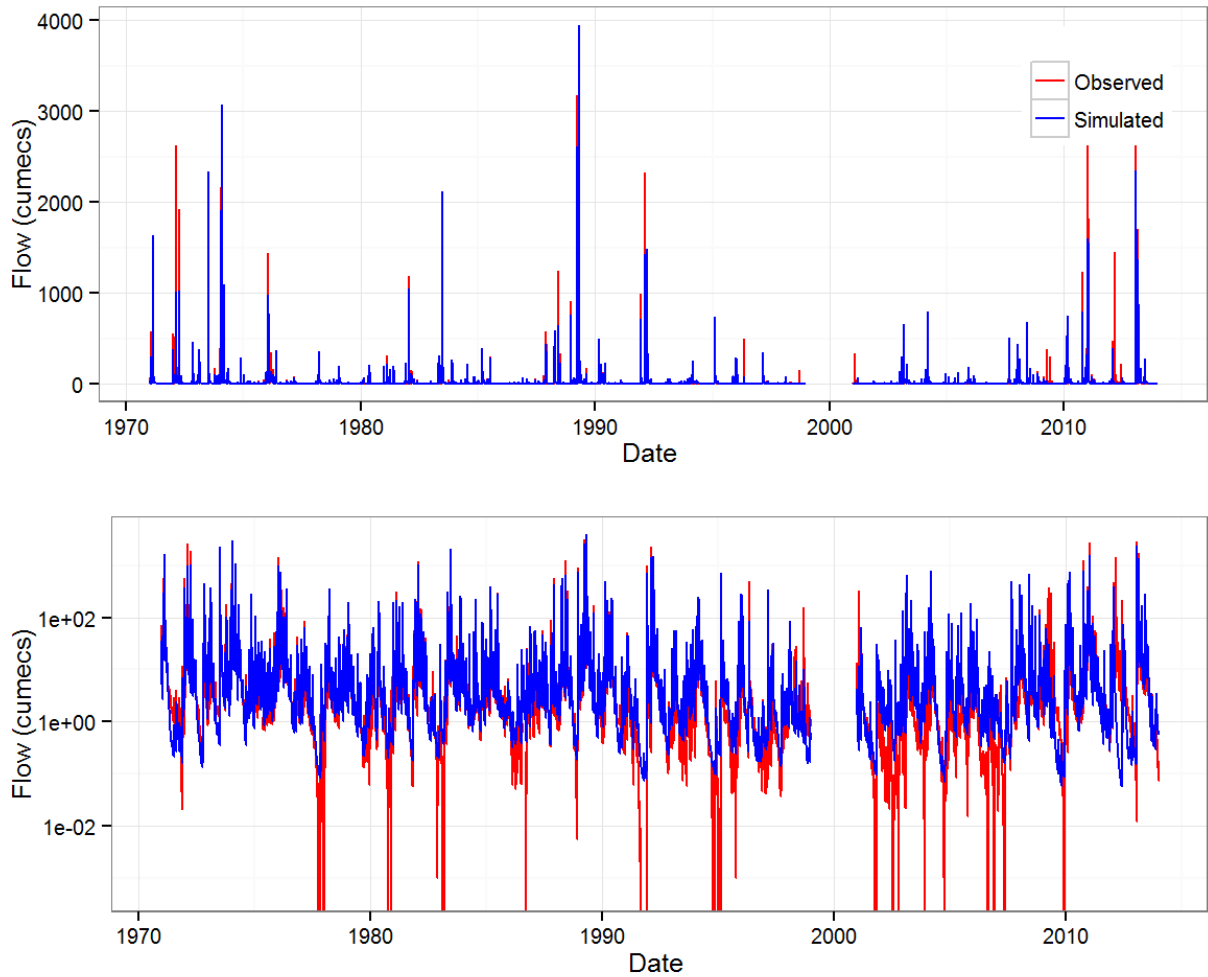


Figure L. 18: Comparison between the observed and simulated hydrographs (Mary River, scenario 3, GR4H) [The Y-axis in the lower plot is in log scale]

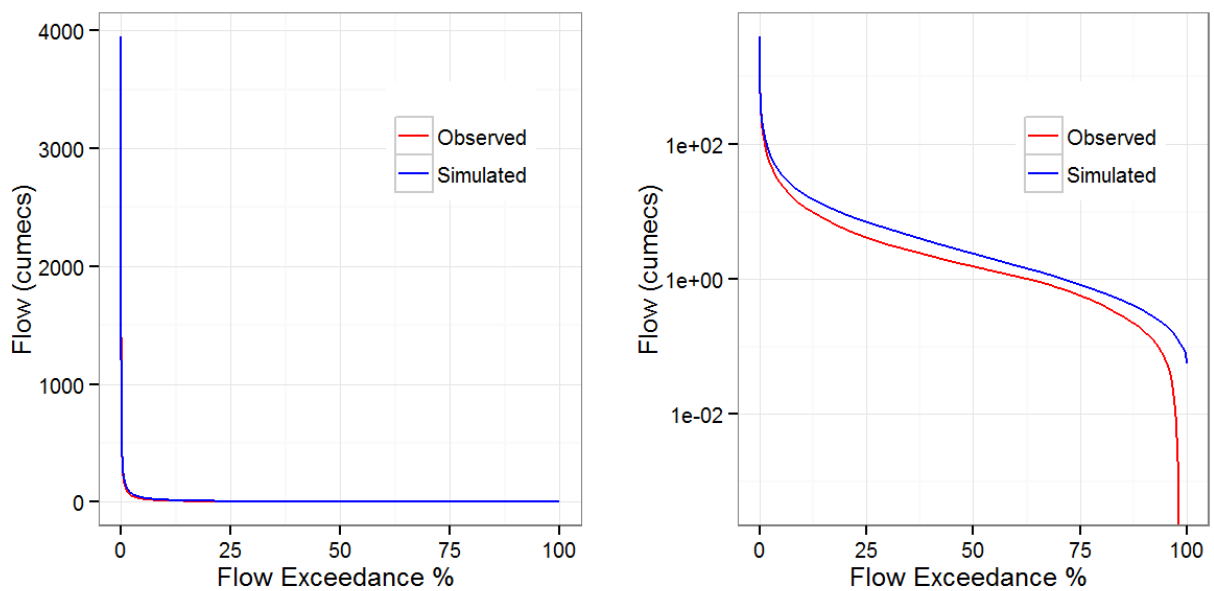


Figure L. 19: Flow duration curves in Mary River for scenario 3, GR4H [right plot Y-axis in log scale]

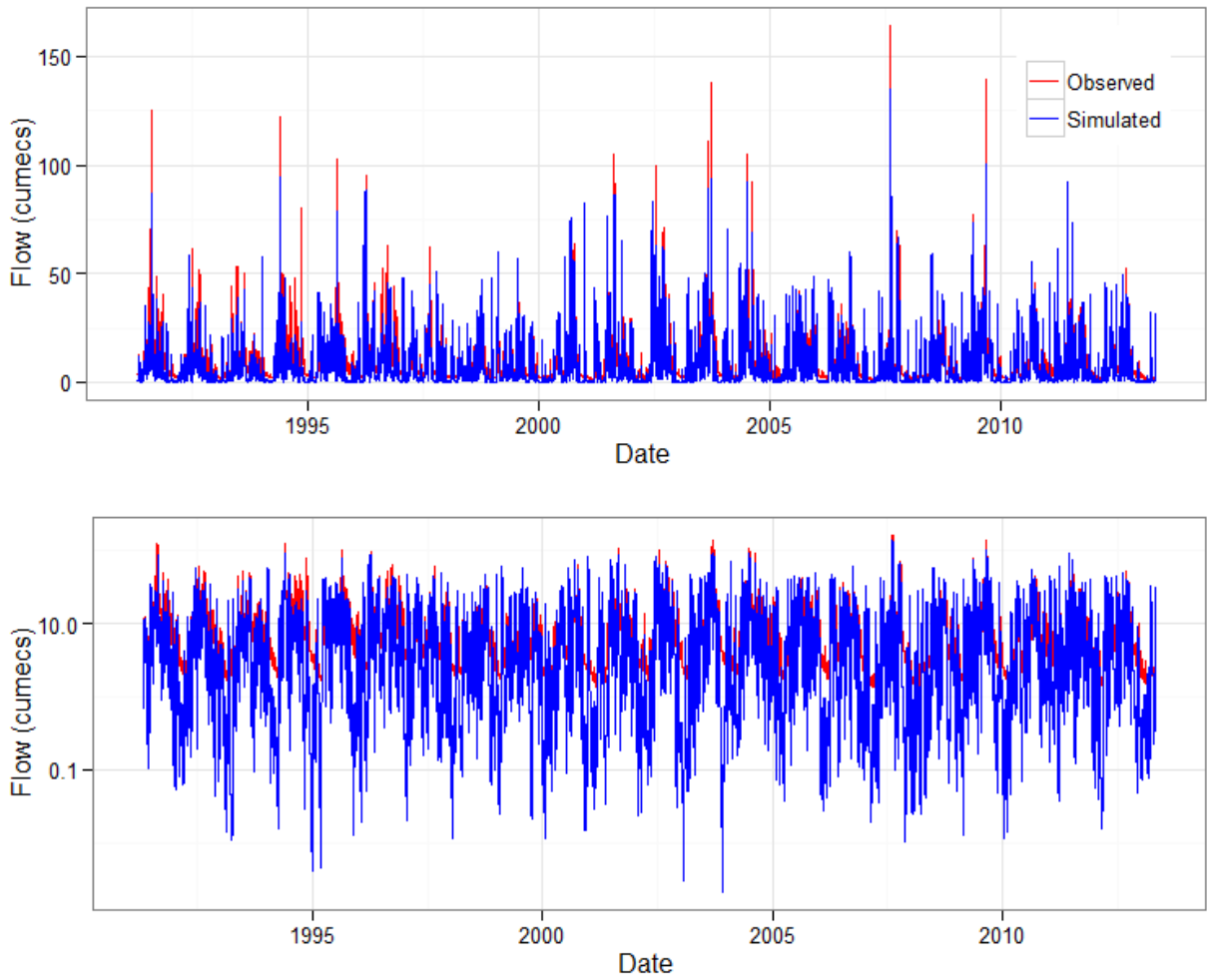


Figure L. 20: Comparison between the observed and simulated hydrographs (Florentine River, scenario 3, AWBM) [The Y-axis in the lower plot is in log scale]

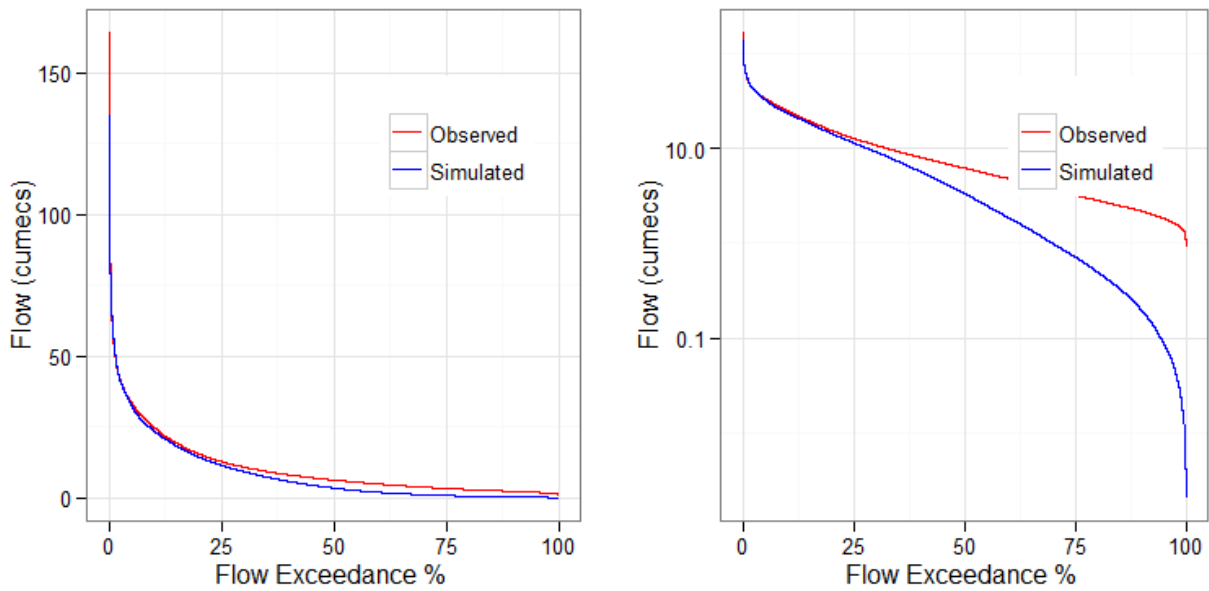


Figure L. 21: Flow duration curves in Florentine River for scenario 3, AWBM [right plot Y-axis in log scale]

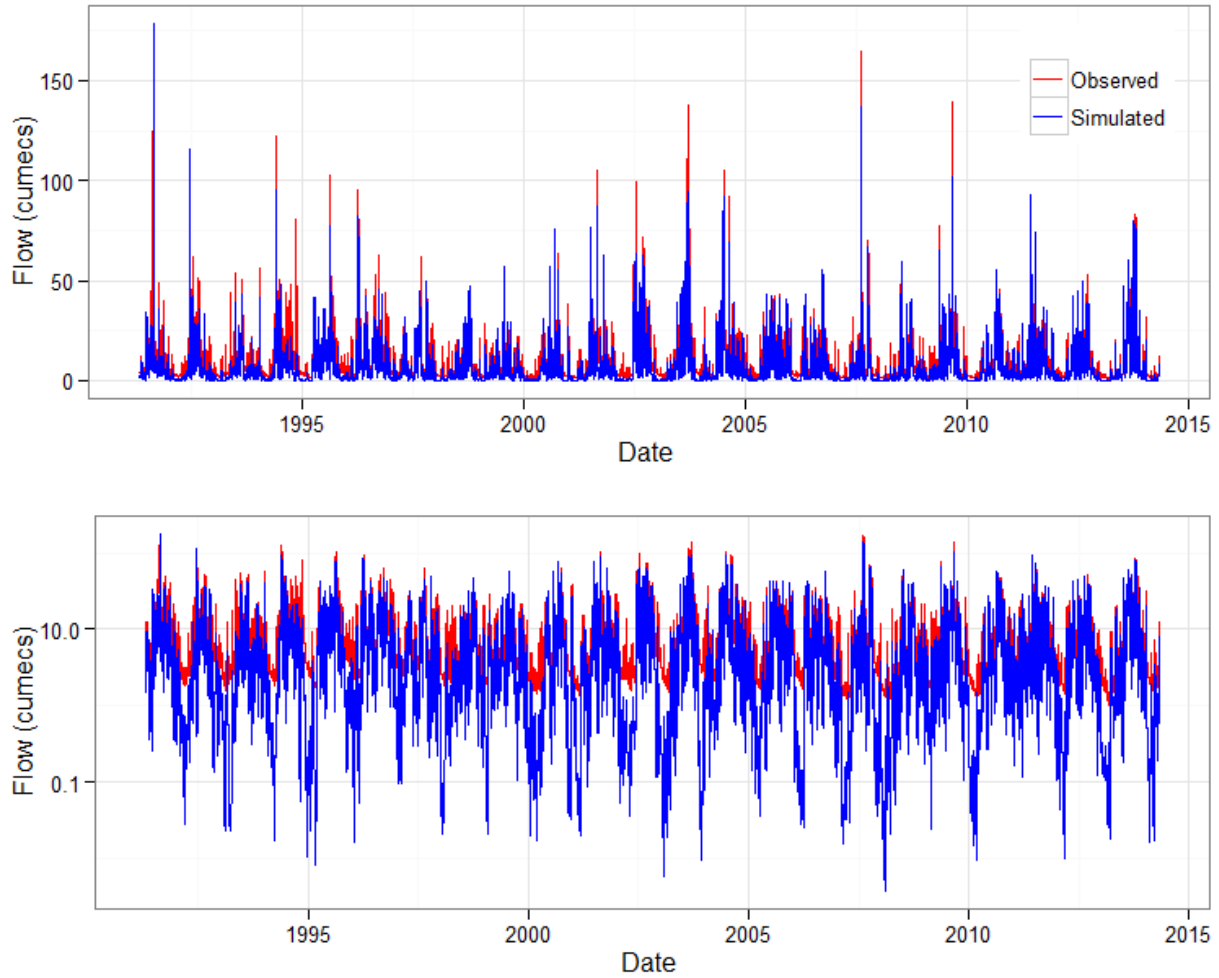


Figure L. 22 : Comparison between the observed and simulated hydrographs (Florentine River, scenario 3, SIMHYD) [The Y-axis in the lower plot is in log scale]

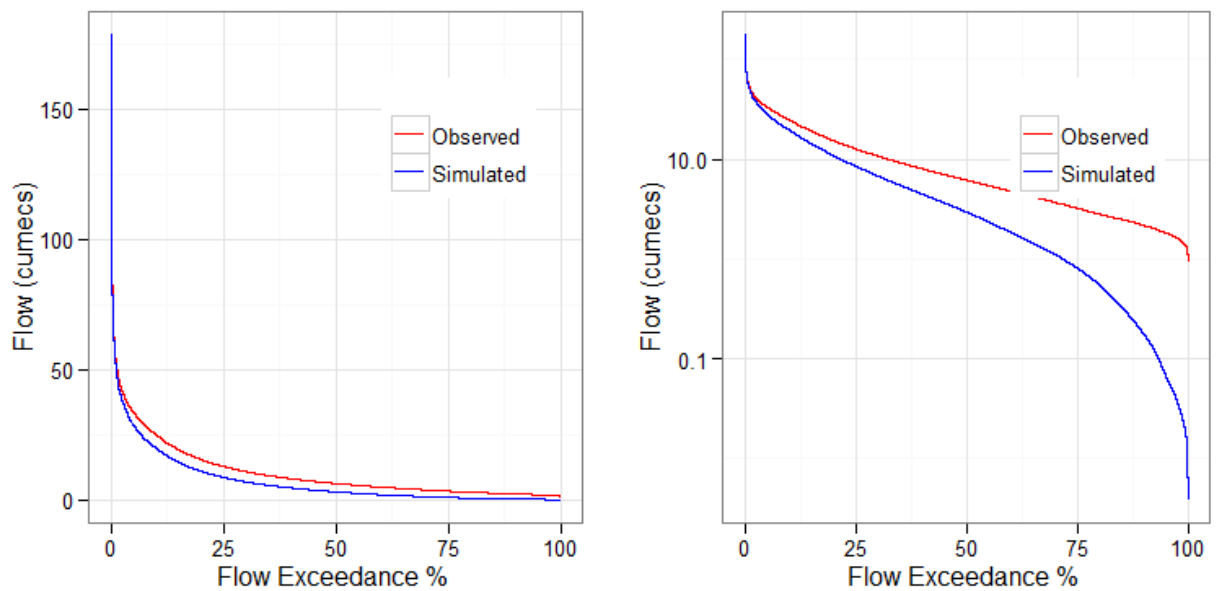


Figure L. 23: Flow duration curves in Florentine River for scenario 3, SIMHYD [right plot Y-axis in log scale]

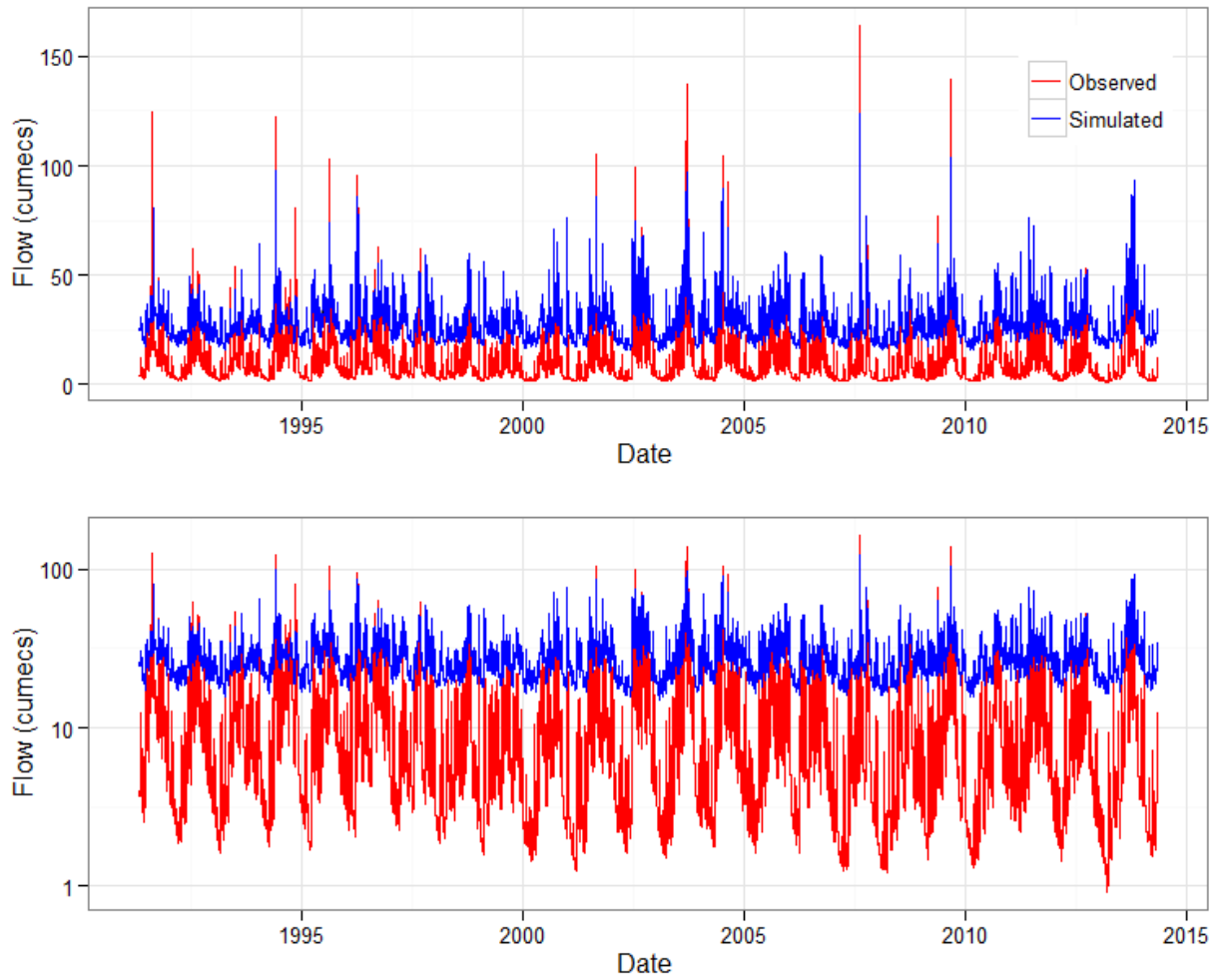


Figure L. 24: Comparison between the observed and simulated hydrographs (Florentine River, scenario 3, GR4H) [The Y-axis in the lower plot is in log scale]

Figure L. 25: Flow duration curves in Florentine River for scenario 3, GR4H [right plot Y-axis in log scale]

## **Appendix M**

## **Results Scenario 4**

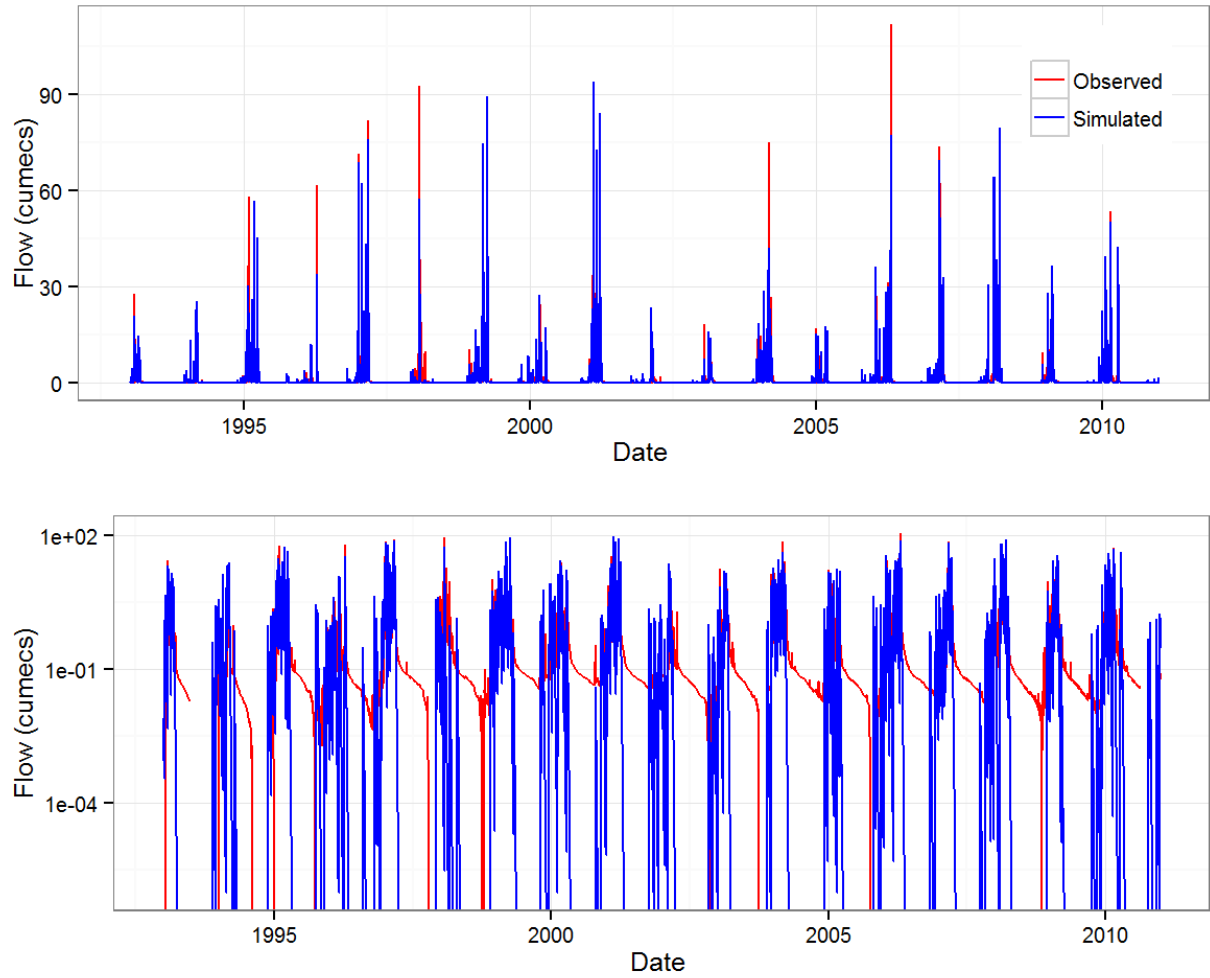


Figure N. 1: Comparison between the observed and simulated hydrographs (Manton River, scenario 4, AWBM) [The Y-axis in the lower plot is in log scale]

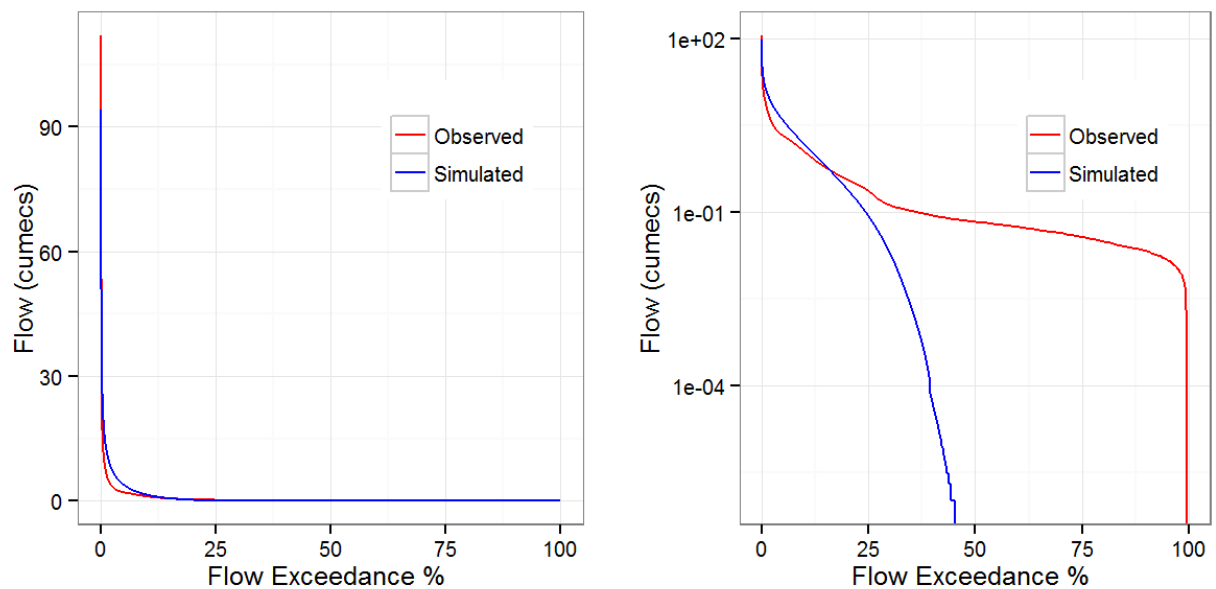


Figure N. 2: Flow duration curves in Manton River for scenario 4, AWBM [right plot Y-axis in log scale]

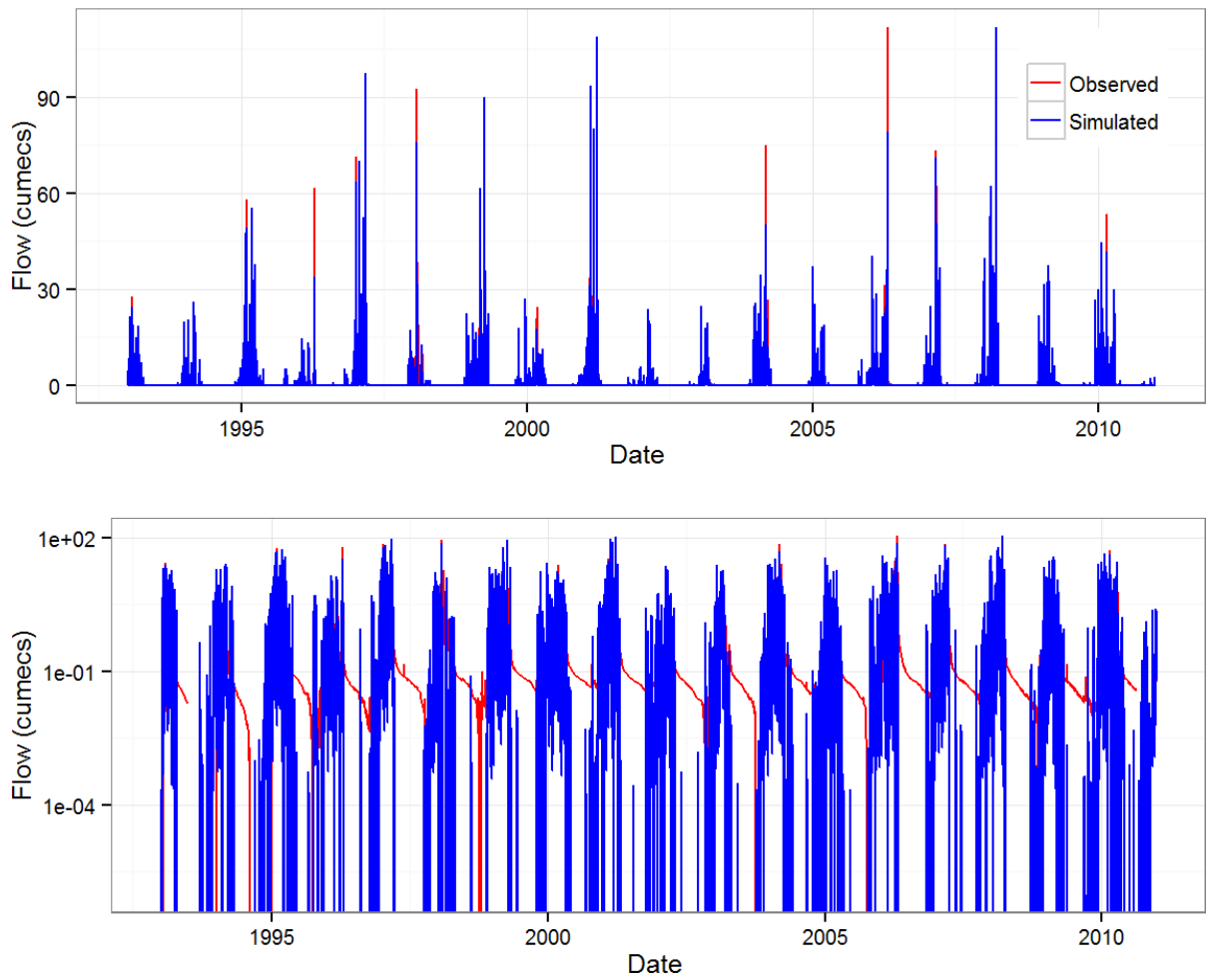


Figure N. 3: Comparison between the observed and simulated hydrographs (Manton River, scenario 4, SIMHYD) [The Y-axis in the lower plot is in log scale]

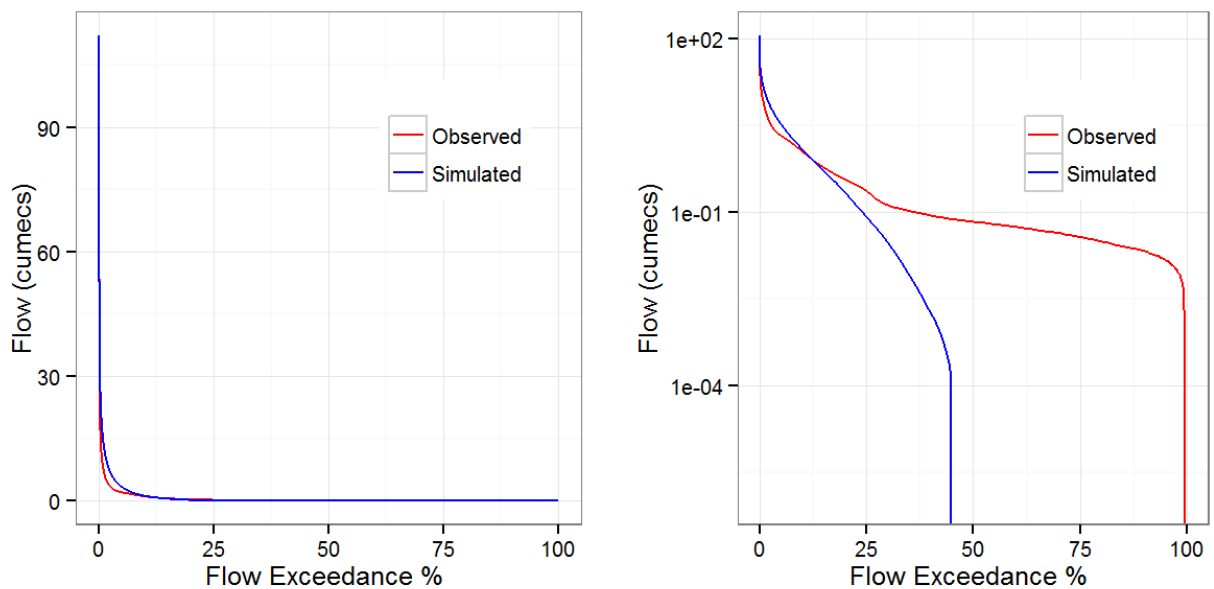


Figure N. 4: Flow duration curves in Manton River for scenario 4, SIMHYD [right plot Y-axis in log scale]

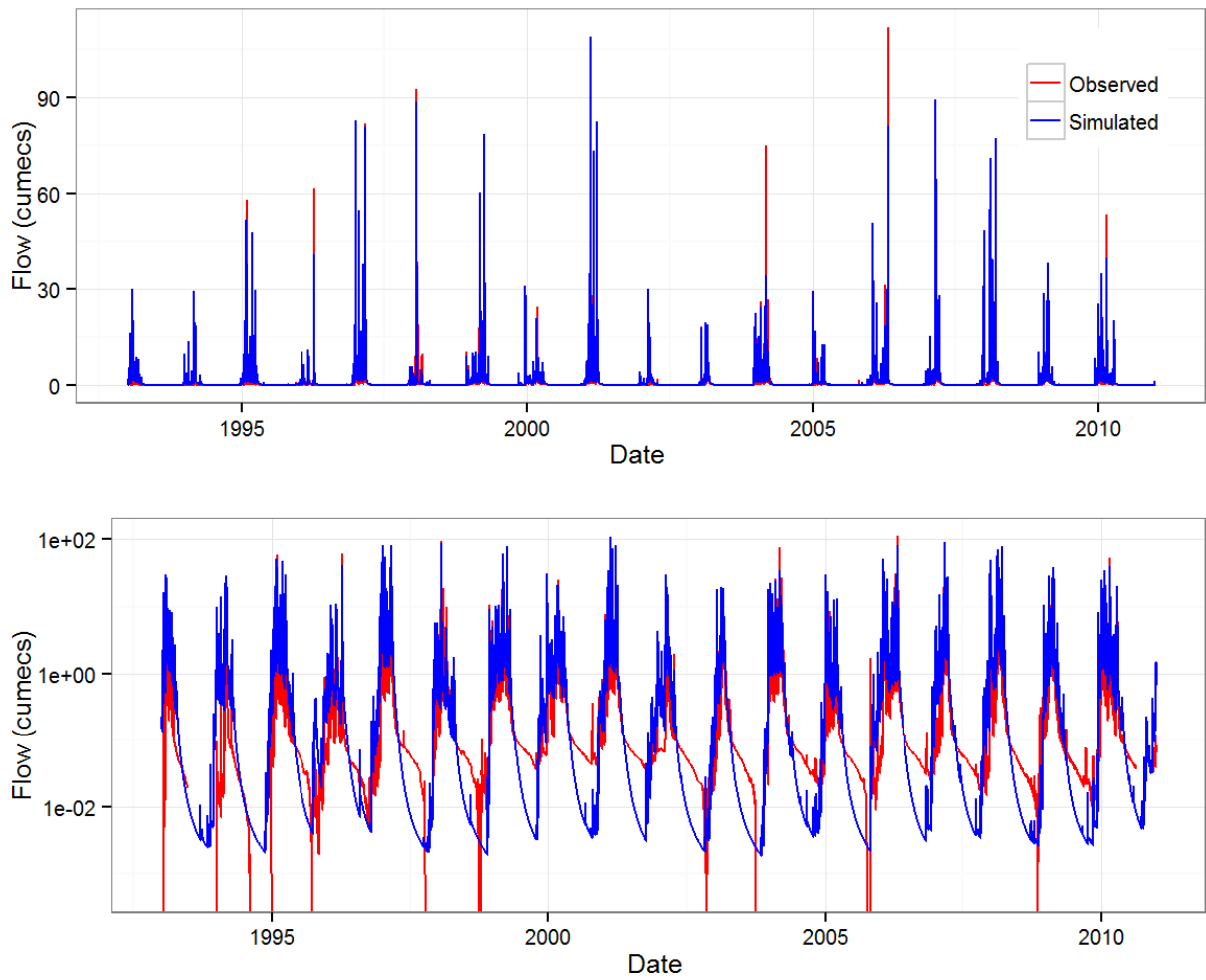


Figure N. 5: Comparison between the observed and simulated hydrographs (Manton River, scenario 4, GR4H) [The Y-axis in the lower plot is in log scale]

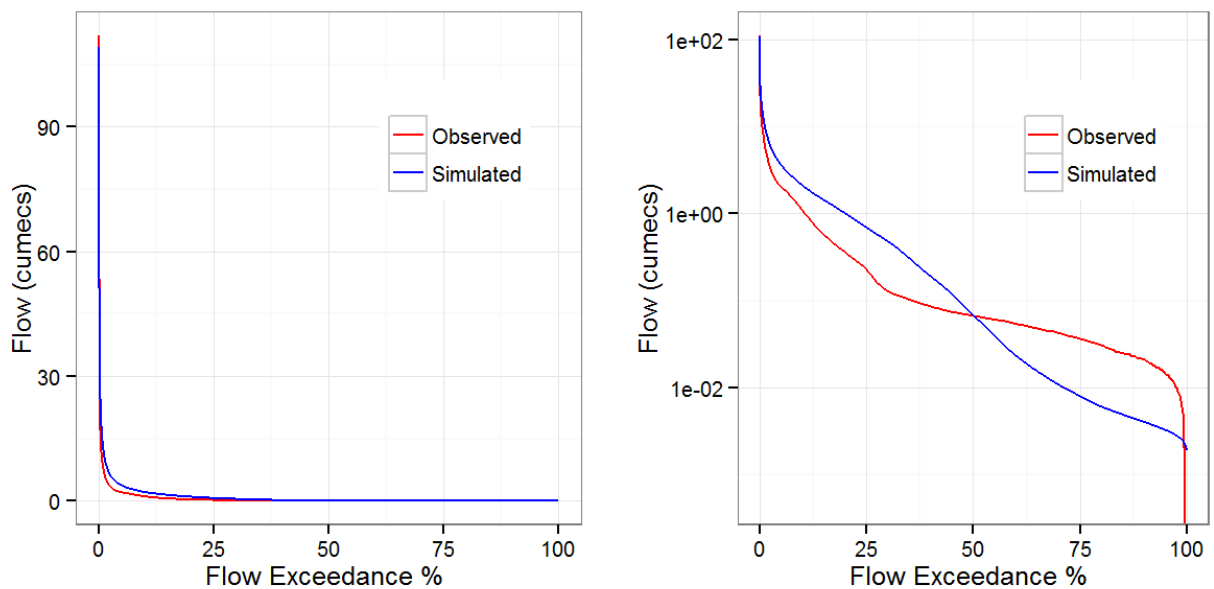


Figure N. 6: Flow duration curves in Manton River for scenario 4, GR4H [right plot Y-axis in log scale]



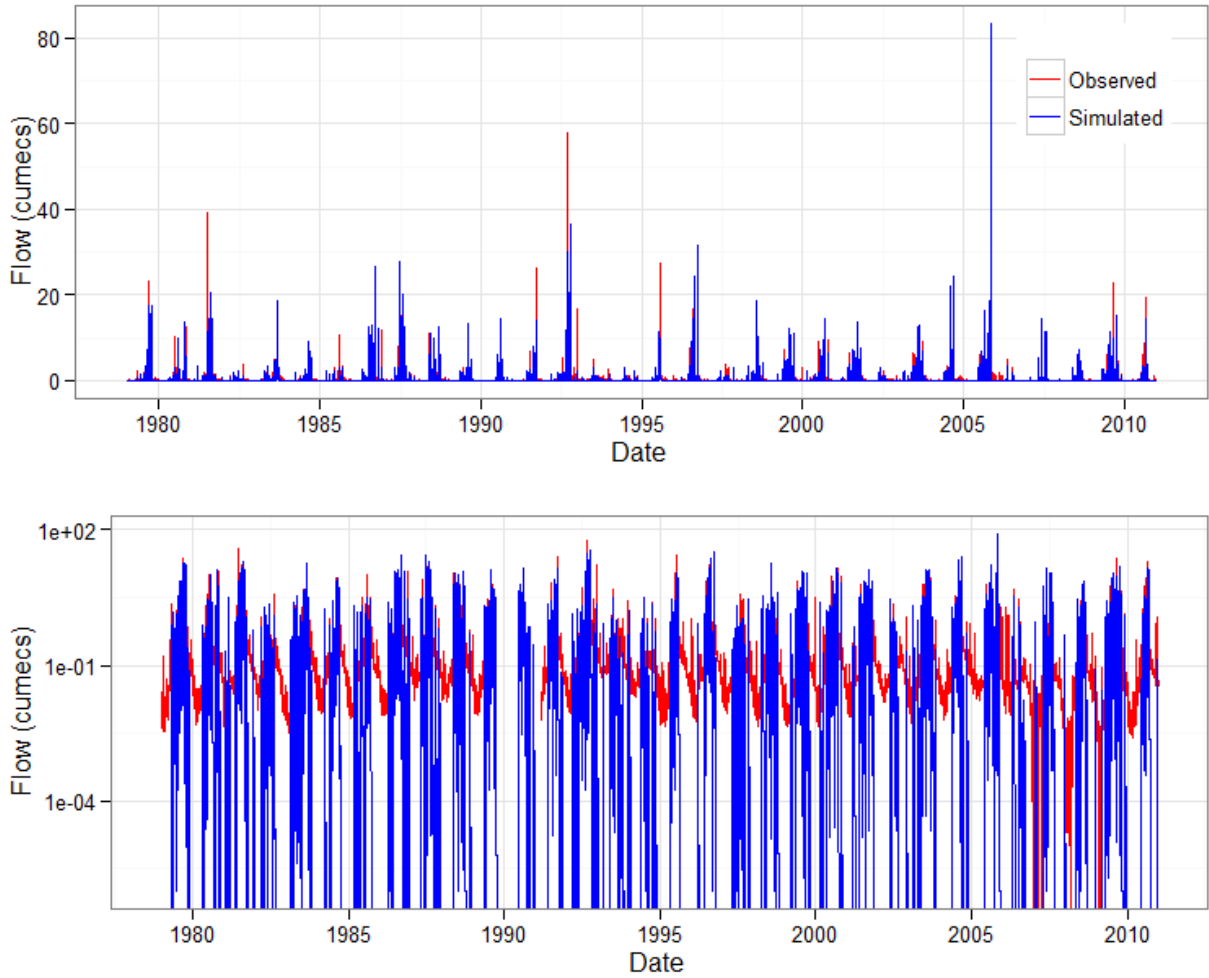


Figure N. 7: Comparison between the observed and simulated hydrographs (Sixth Creek, scenario 4, AWBM) [The Y-axis in the lower plot is in log scale]

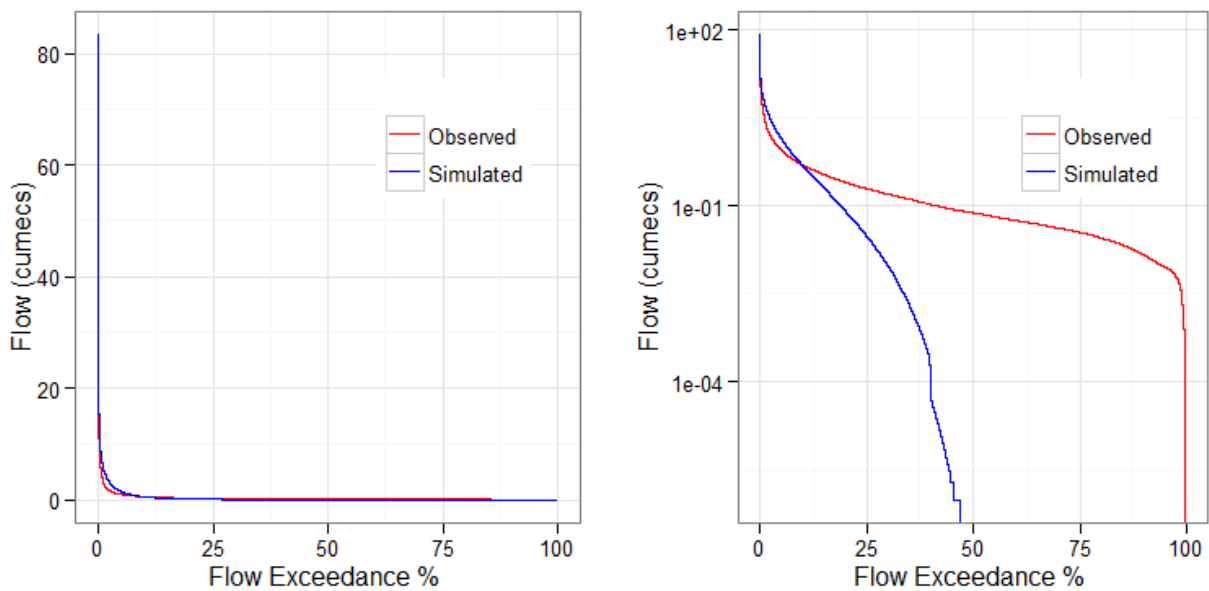


Figure N. 8: Flow duration curves in Sixth Creek for scenario 4, AWBM [right plot Y-axis in log scale]

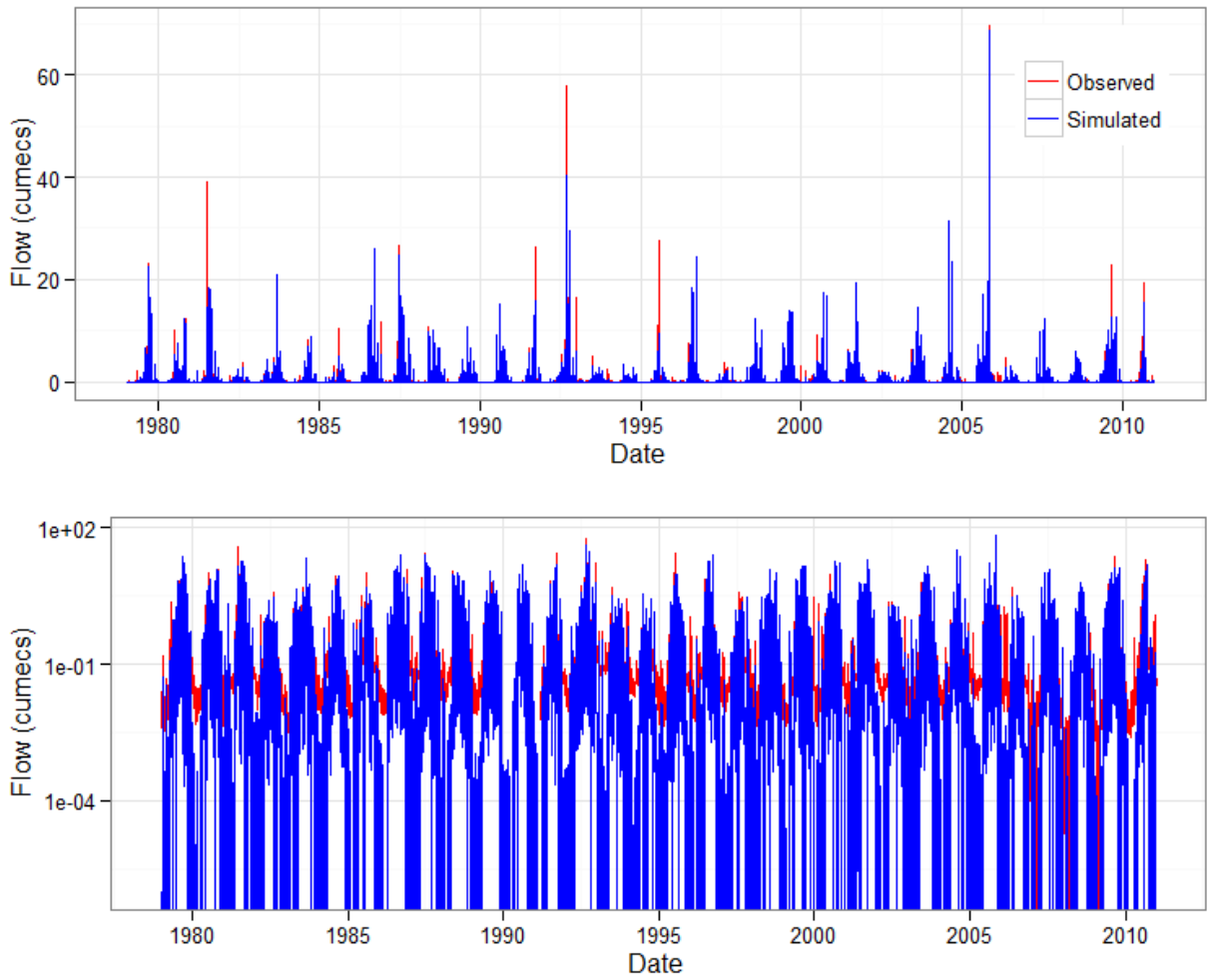


Figure N. 9: Comparison between the observed and simulated hydrographs (Sixth Creek, scenario 4, SIMHYD) [The Y-axis in the lower plot is in log scale]

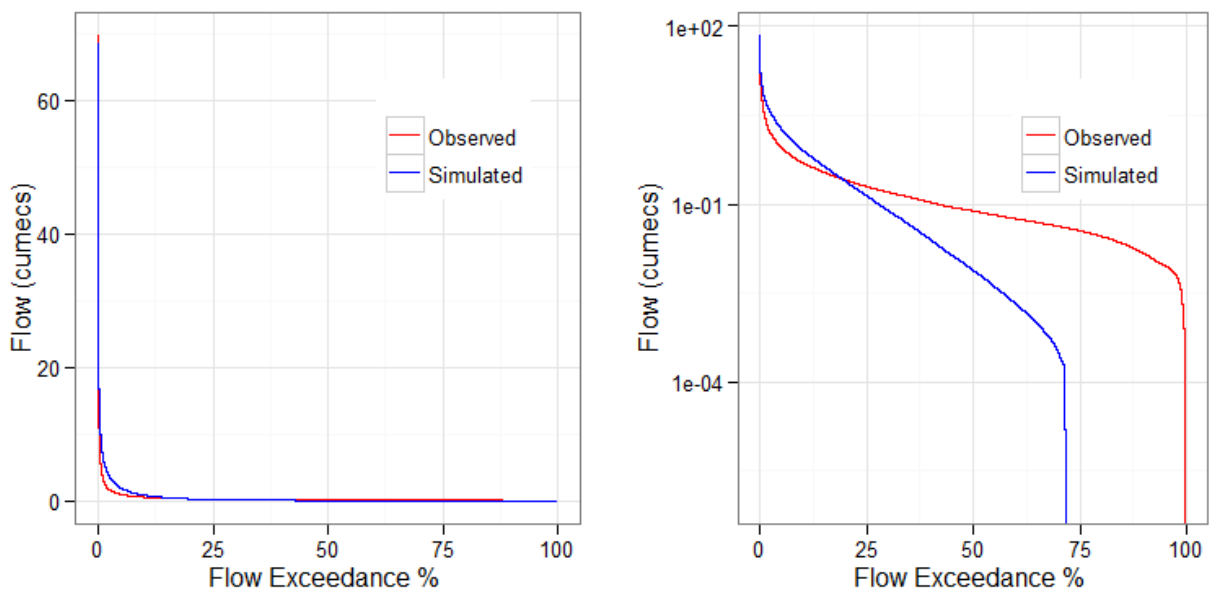


Figure N. 10: Flow duration curves in Sixth Creek for scenario 4, SIMHYD [right plot Y-axis in log scale]

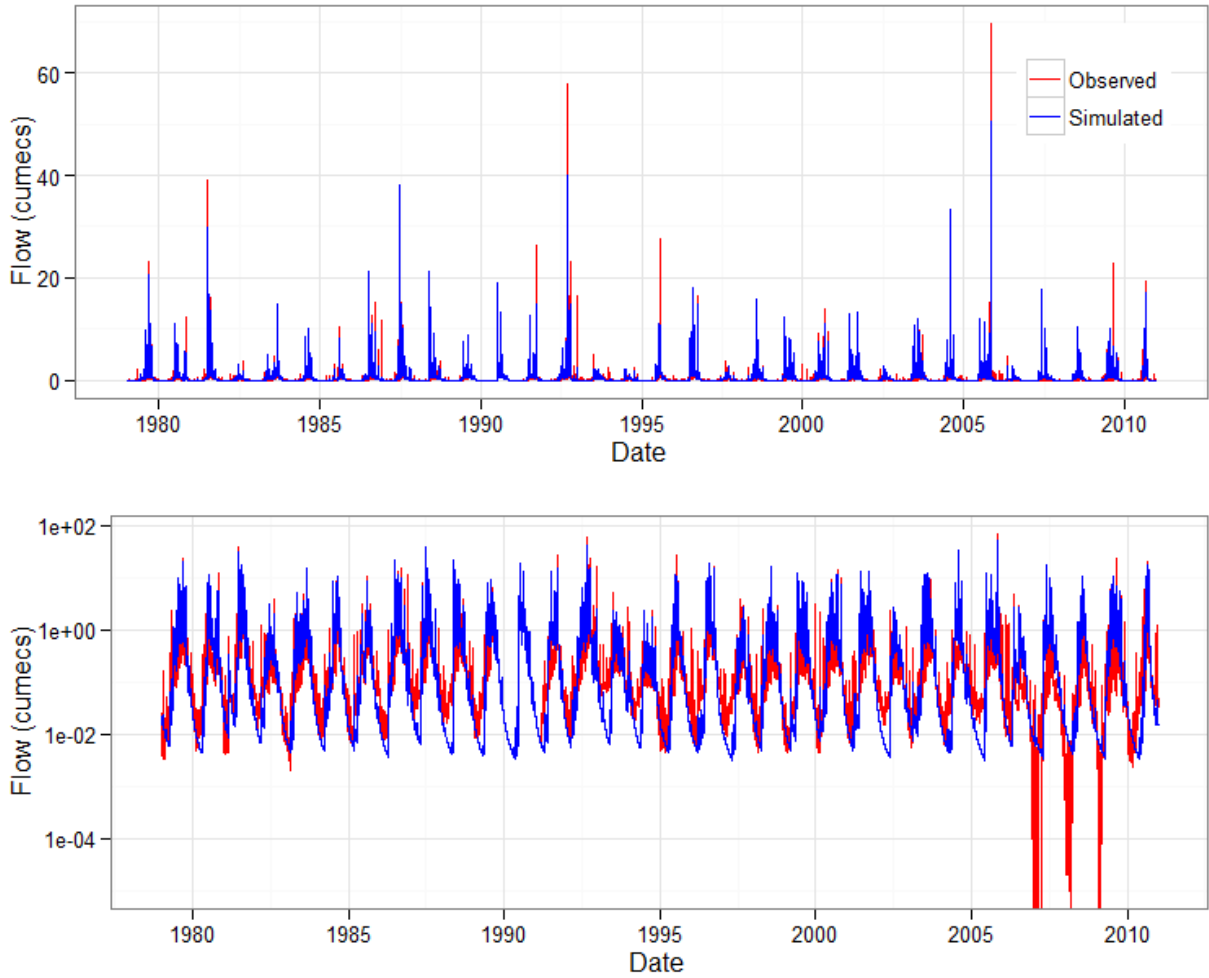


Figure N. 11: Comparison between the observed and simulated hydrographs (Sixth Creek, scenario 4, GR4H) [The Y-axis in the lower plot is in log scale]

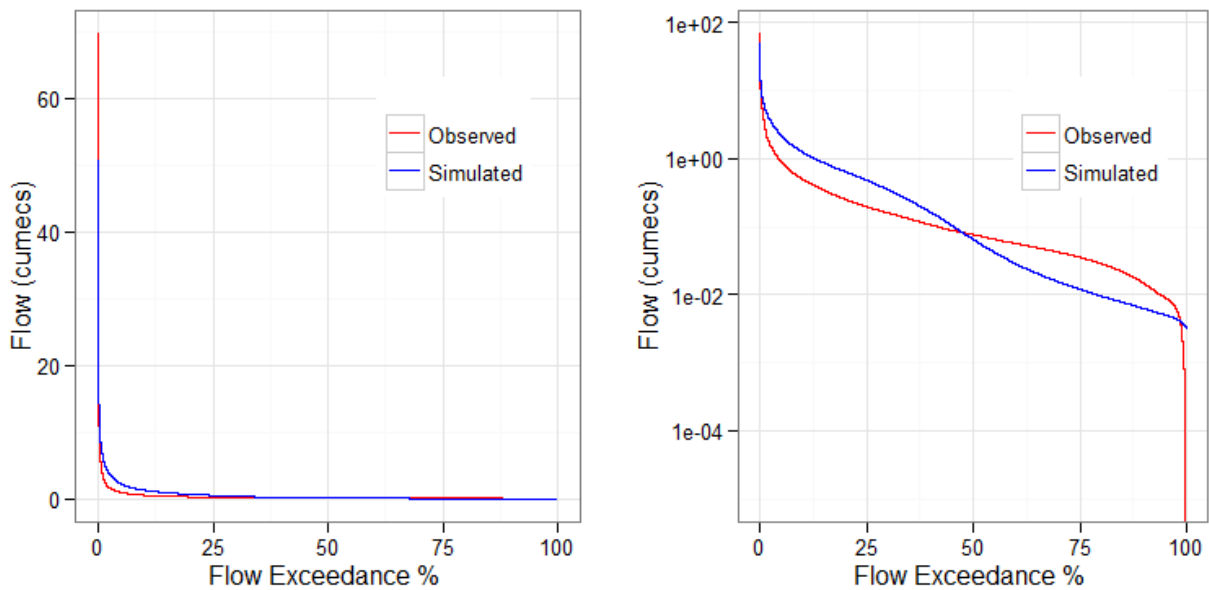


Figure N. 12: Flow duration curves in Sixth Creek for scenario 4, GR4H [right plot Y-axis in log scale]

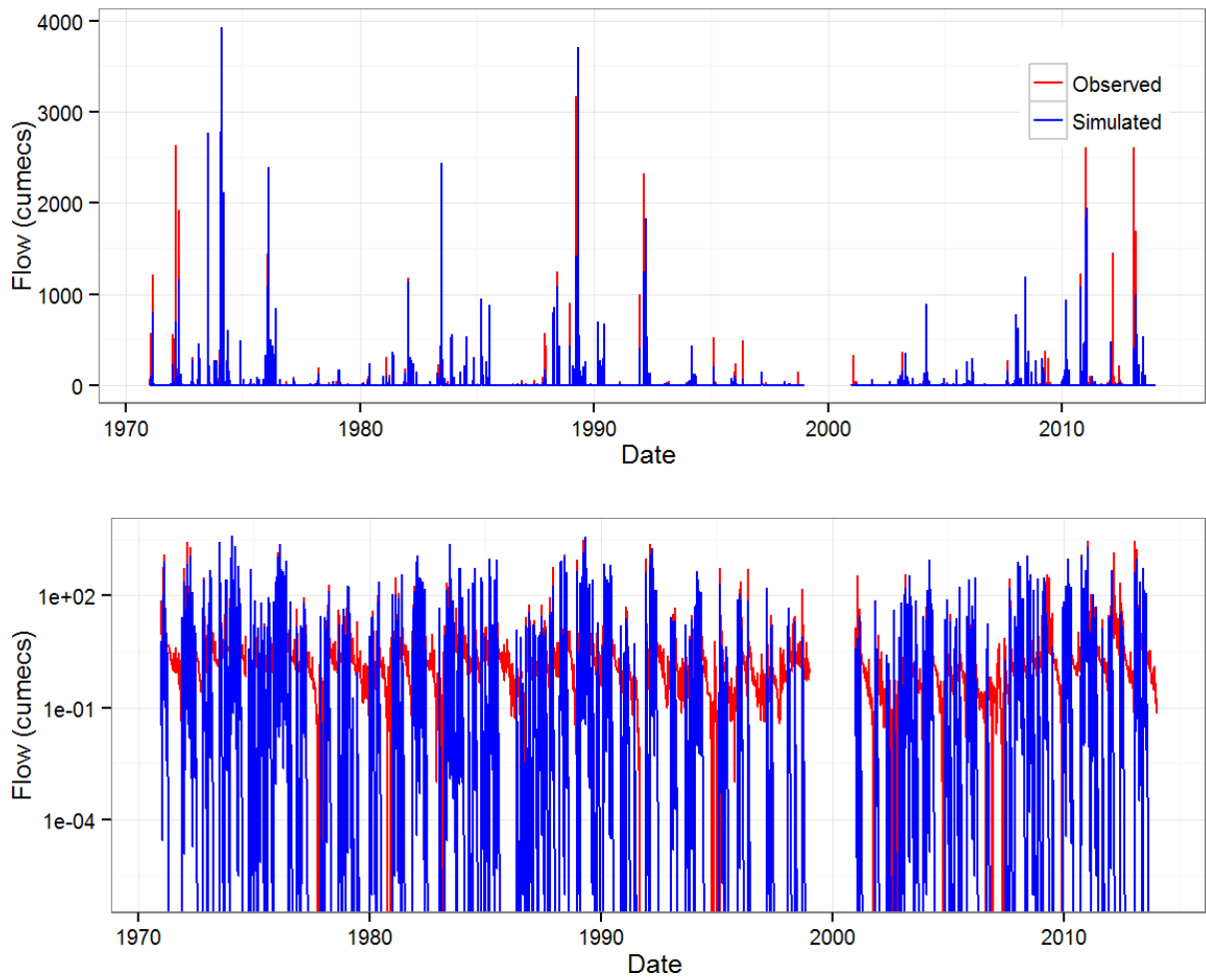


Figure N. 13: Comparison between the observed and simulated hydrographs (Mary River, scenario 4, AWBM) [The Y-axis in the lower plot is in log scale]

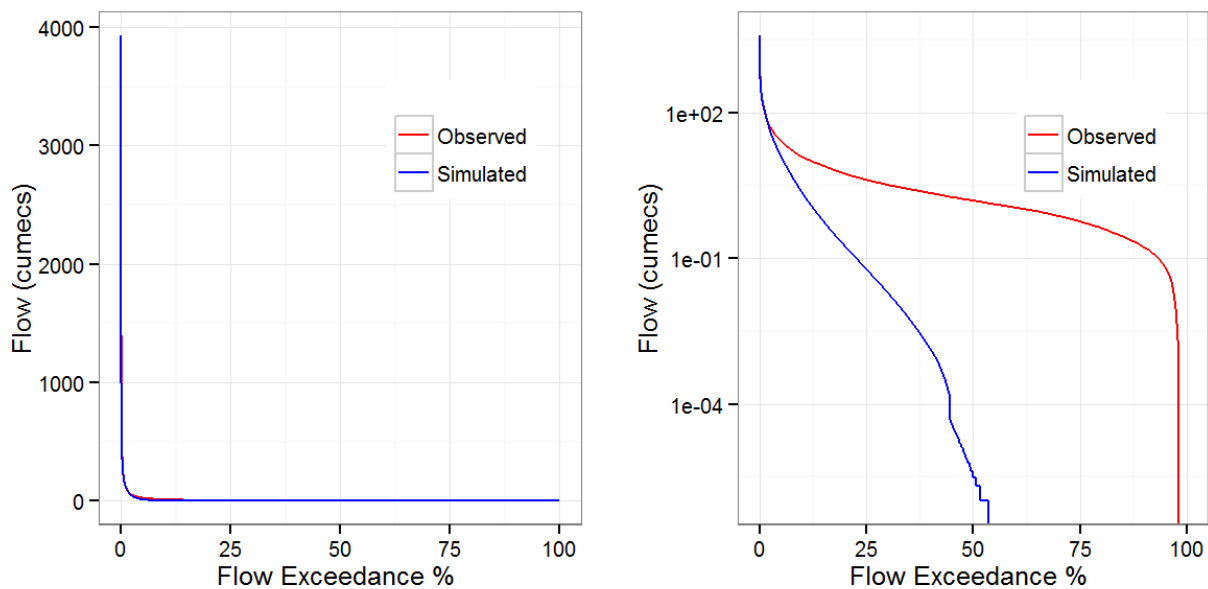


Figure N. 14: Flow duration curves in Mary River for scenario 4, AWBM [right plot Y-axis in log scale]

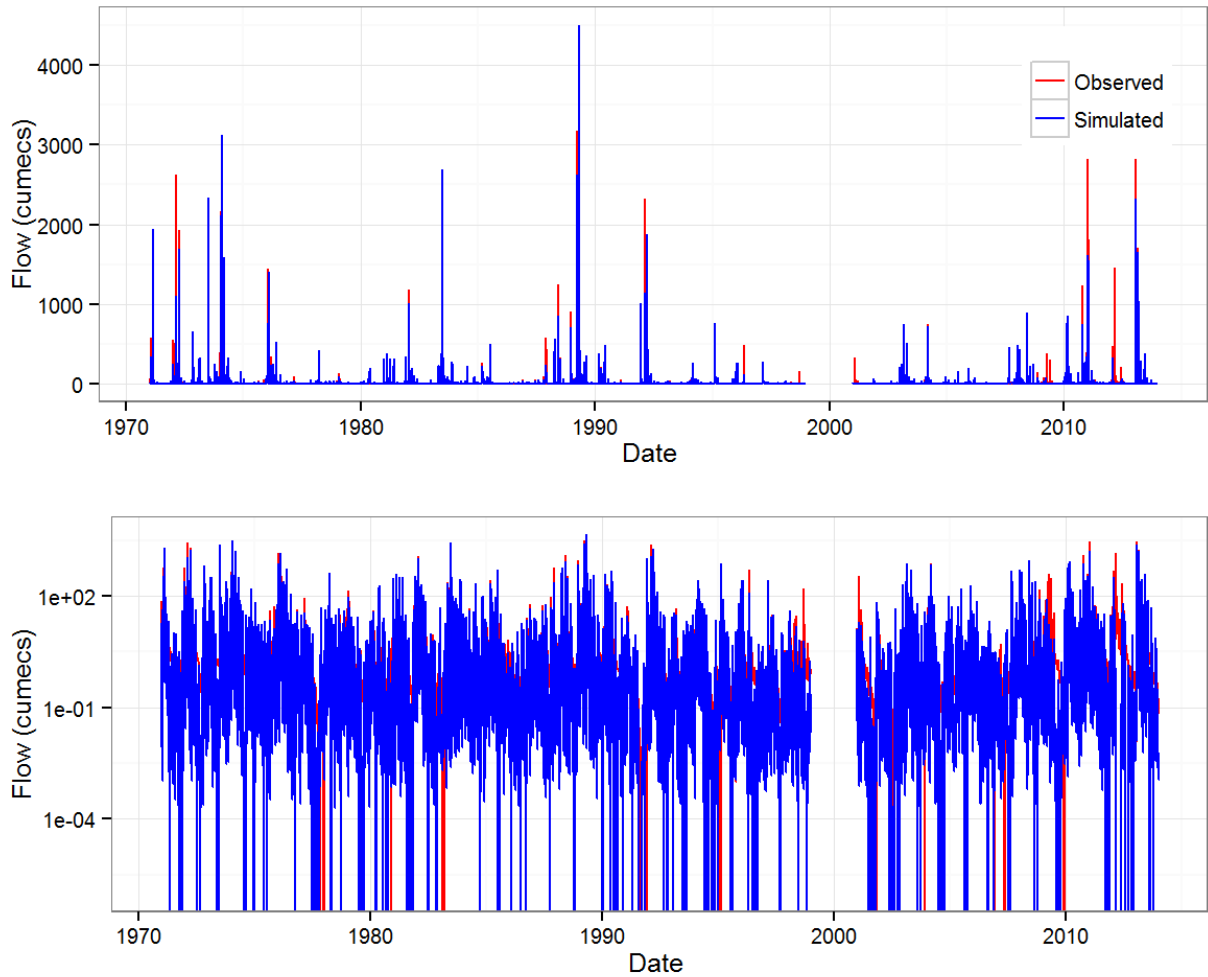


Figure N. 15: Comparison between the observed and simulated hydrographs (Mary River, scenario 4, SIMHYD) [The Y-axis in the lower plot is in log scale]

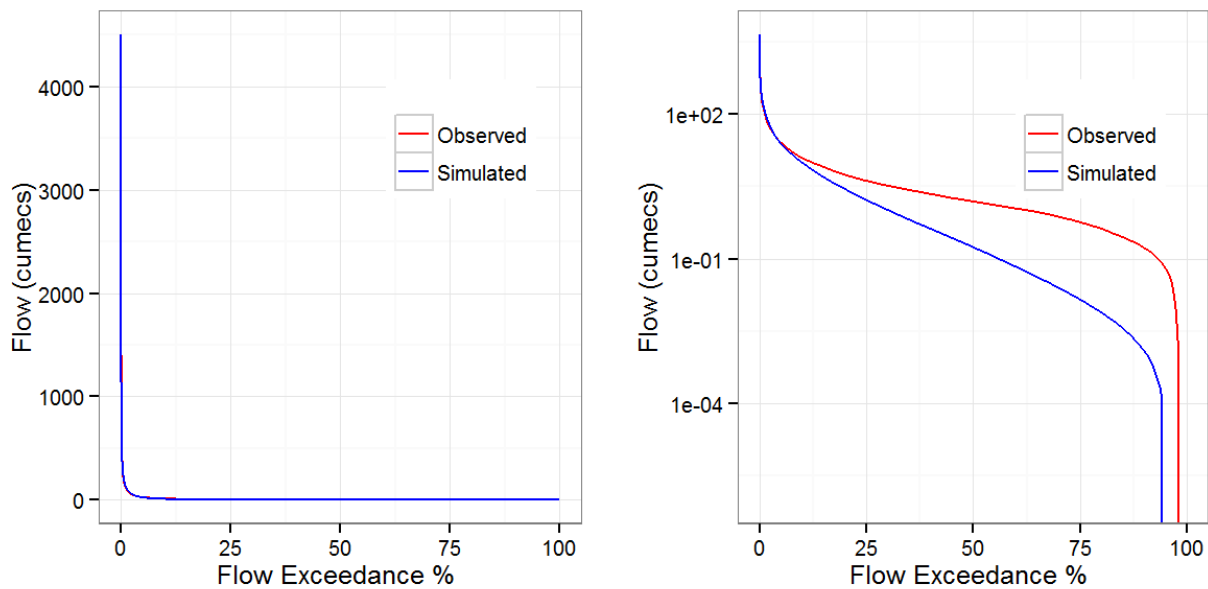


Figure N. 16: Flow duration curves in Mary River for scenario 4, SIMHYD [right plot Y-axis in log scale]

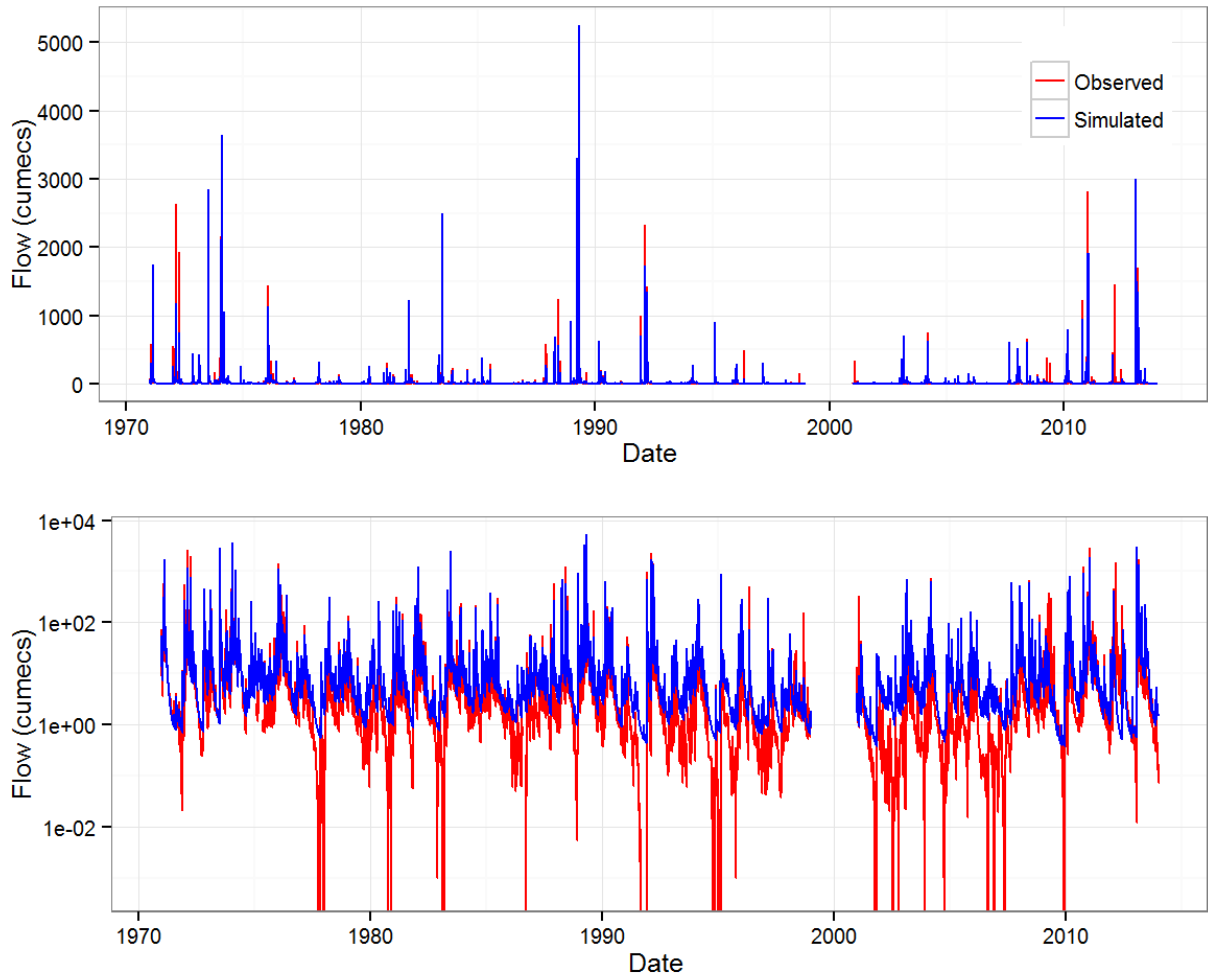


Figure N. 17: Comparison between the observed and simulated hydrographs (Mary River, scenario 4, GR4H) [The Y-axis in the lower plot is in log scale]

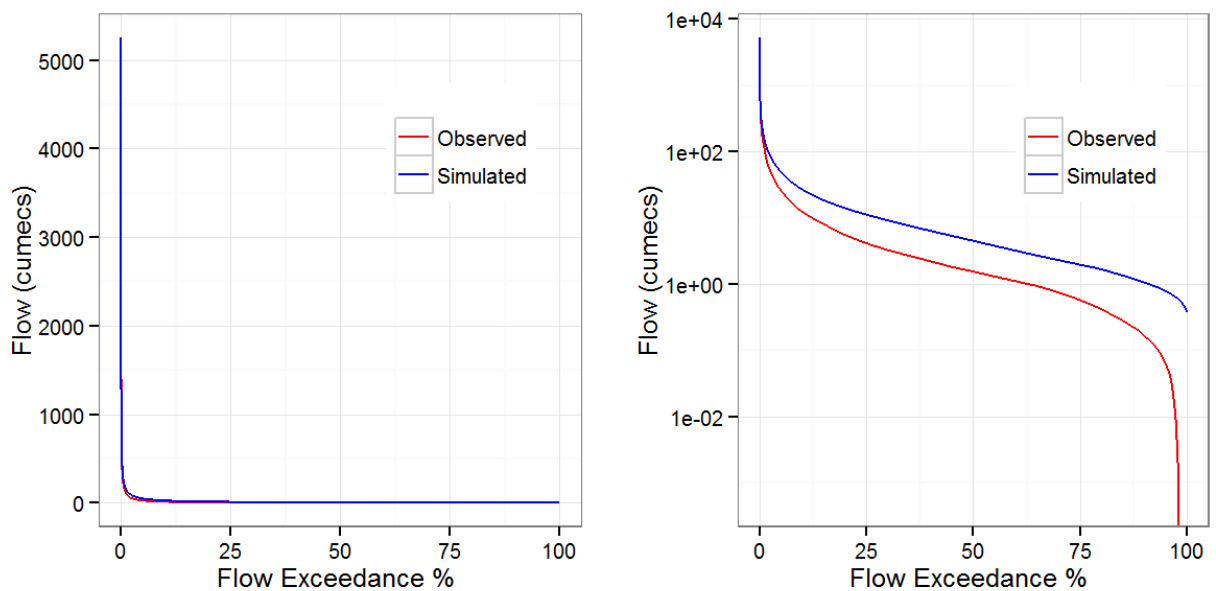


Figure N. 18: Flow duration curves in Mary River for scenario 4, GR4H [right plot Y-axis in log scale]

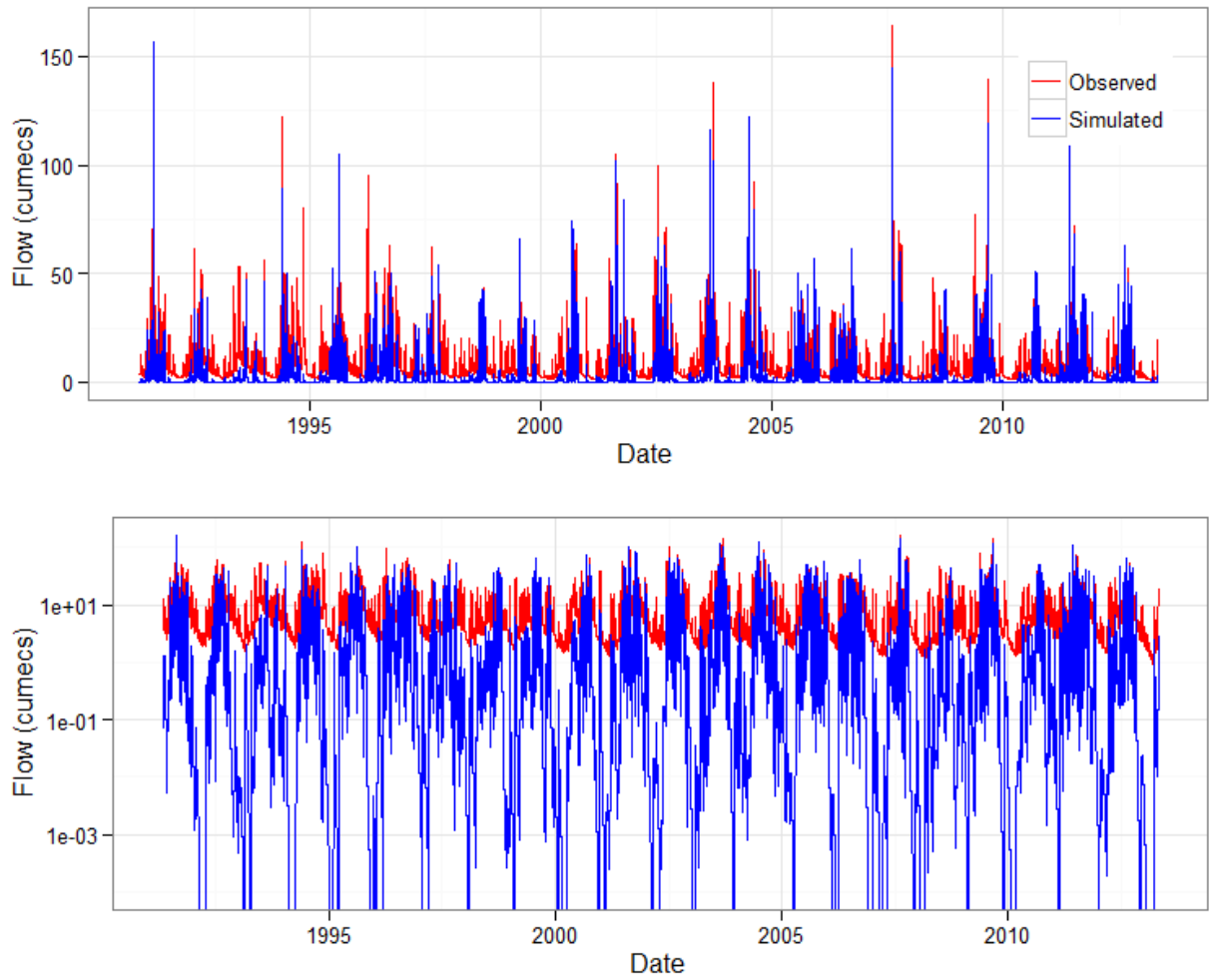


Figure N. 19: Comparison between the observed and simulated hydrographs (Florentine River, scenario 4, AWBM) [The Y-axis in the lower plot is in log scale]

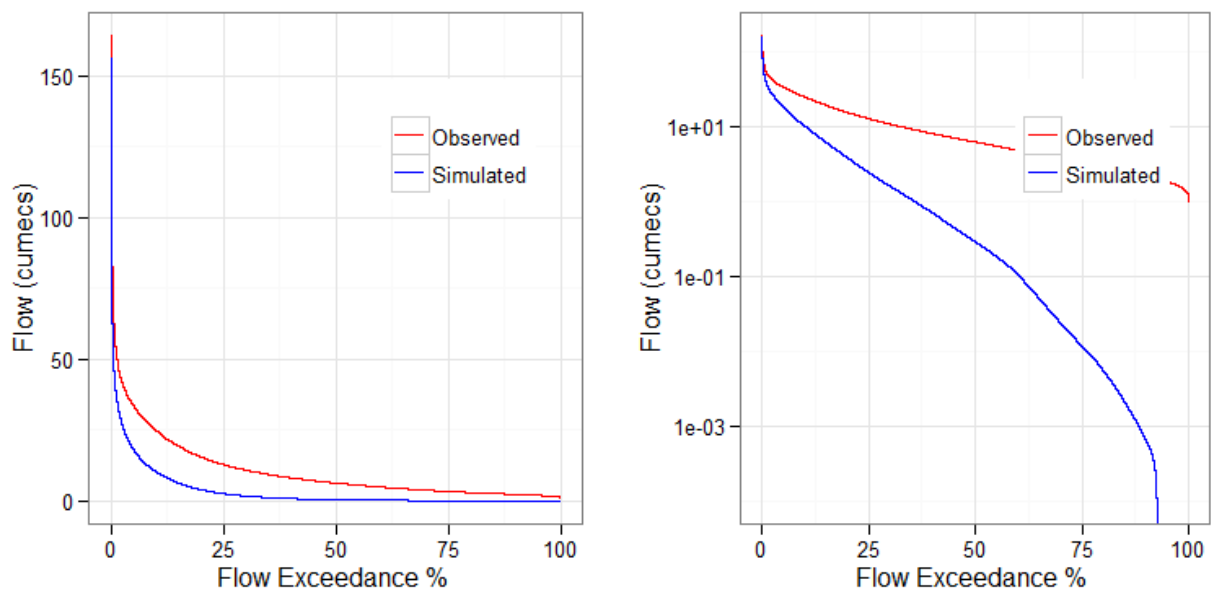


Figure N. 20: Flow duration curves in Florentine River for scenario 4, AWBM [right plot Y-axis in log scale]

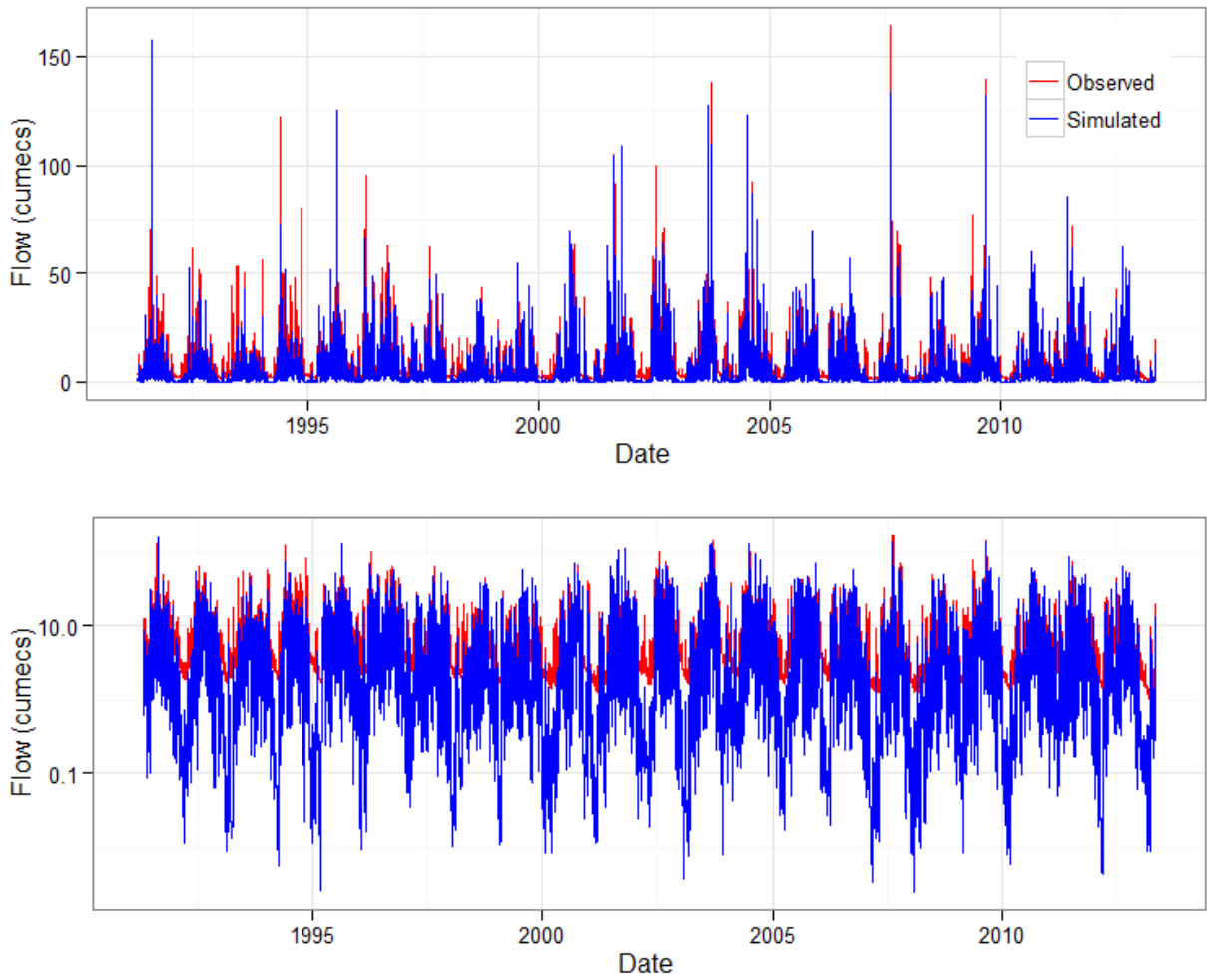


Figure N. 21: Comparison between the observed and simulated hydrographs (Mary River, scenario 4, SIMHYD) [The Y-axis in the lower plot is in log scale]

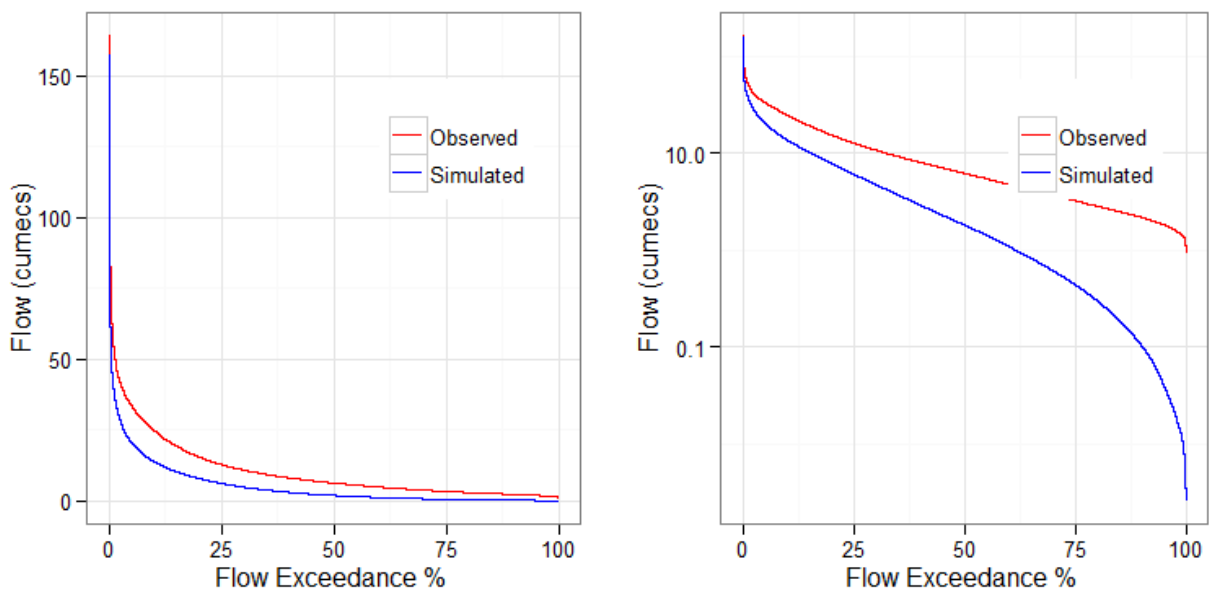


Figure N. 22: Flow duration curves in Florentine River for scenario 4, SIMHYD [right plot Y-axis in log scale]



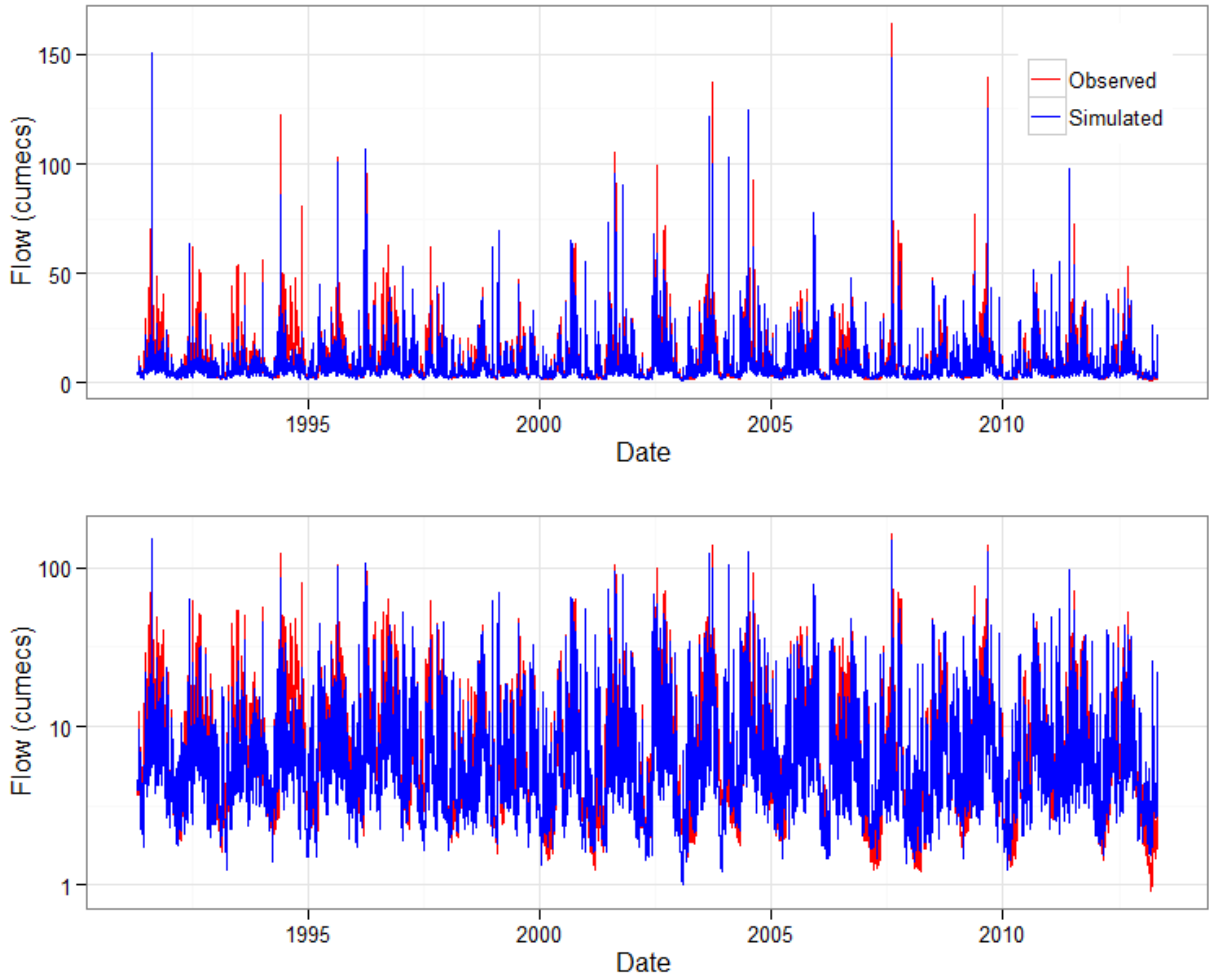


Figure N. 23: Comparison between the observed and simulated hydrographs (Mary River, scenario 4, GR4H) [The Y-axis in the lower plot is in log scale]

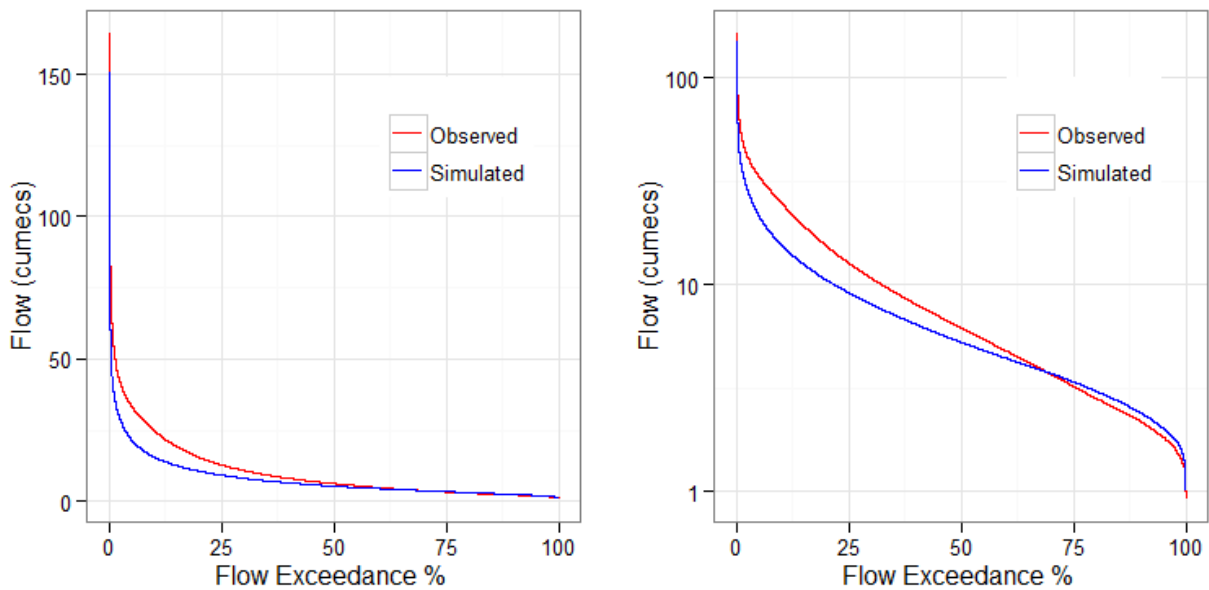


Figure N. 24: Flow duration curves in Florentine River for scenario 4, GR4H [right plot Y-axis in log scale]

## Appendix N Rainfall data

State	Catchment	Station ID	Station Name	Data Source*	Time step	Start	End
QLD	Mary	40059	Cooroy Composite	BOM	6 min	01/11/1971	01/03/2012
QLD	Mary	40062	Crohamhurst	BOM	6 min	01/02/1960	01/02/2001
QLD	Mary	40102	Jimna Composite	BOM	6 min	01/02/1972	01/02/2000
QLD	Mary	40106	Kenilworth Township	BOM	6 min	01/07/1981	01/04/2010
QLD	Mary	40121	Maleny Tamarind St	BOM	6 min	01/08/2002	01/05/2014
QLD	Mary	40133	Monsildale	BOM	6 min	01/08/1963	01/02/1978
QLD	Mary	40282	Nambour Dpi	BOM	6 min	01/01/1954	01/12/2008
QLD	Mary	40386	Kenilworth Bridge	BOM	6 min	01/06/1963	01/08/1981
QLD	Mary	40651	Jimna Forestry	BOM	6 min	01/04/2001	01/02/2014
QLD	Mary	40988	Nambour Daff – Hillside	BOM	6 min	01/12/2007	01/02/2014
NT	Manton	14272	Batchelor Airport	BOM	6 min	01/03/2001	01/03/2013
NT	Manton	R8150332	Darwin R At West Track	DLRM	Hourly	18/01/1963	10/02/2011
SA	Sixth Creek	AW504559	Cherryville		6 min	20/07/1983	22/08/2011
SA	Sixth Creek	23801	Lenswood Research Centre	BOM	6 min	01/10/1972	01/08/2011
TAS	Florentine	2008	Misery Plateau	HT	5 min	09/05/1997	13/10/2014
TAS	Florentine	881	Butlers Gorge	HT	5 min	13/05/1992	23/06/2012
TAS	Florentine	886	Florentine Crossing	HT	6 min	17/06/1960	03/01/1989
TAS	Florentine	309	Salvation Creek	HT	5 min	17/08/1989	30/09/2014
WA	Yates Flat Creek	509022	Woonanup	DOW	6 min	25/05/1972	11/06/2012

\*BOM – Bureau of Meteorology

HCC – Hobart City Council

DPIPWE – Department of Primary Industries Water and Environment

HT – Hydro Tasmania

DLRM – Department of Land and Resource Management

DOW - Department of Water

## **Appendix O**

## **Calibrated parameters**

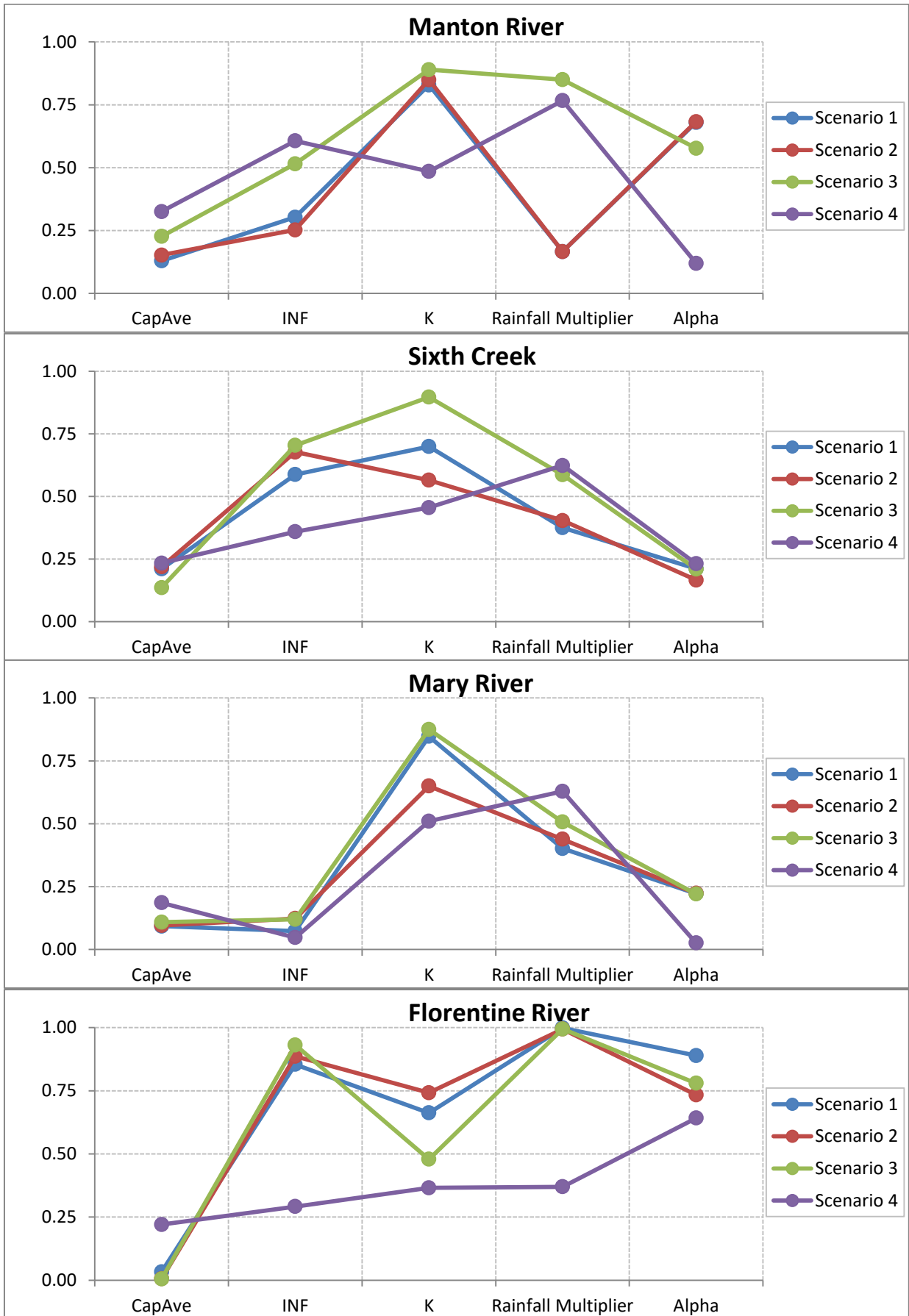


Figure O. 1 : Normalized calibrated parameter values for the AWBM model [parameters are normalized such that they vary between 0 to 1 with 0 representing the lower parameter bound and 1 representing the higher bound]

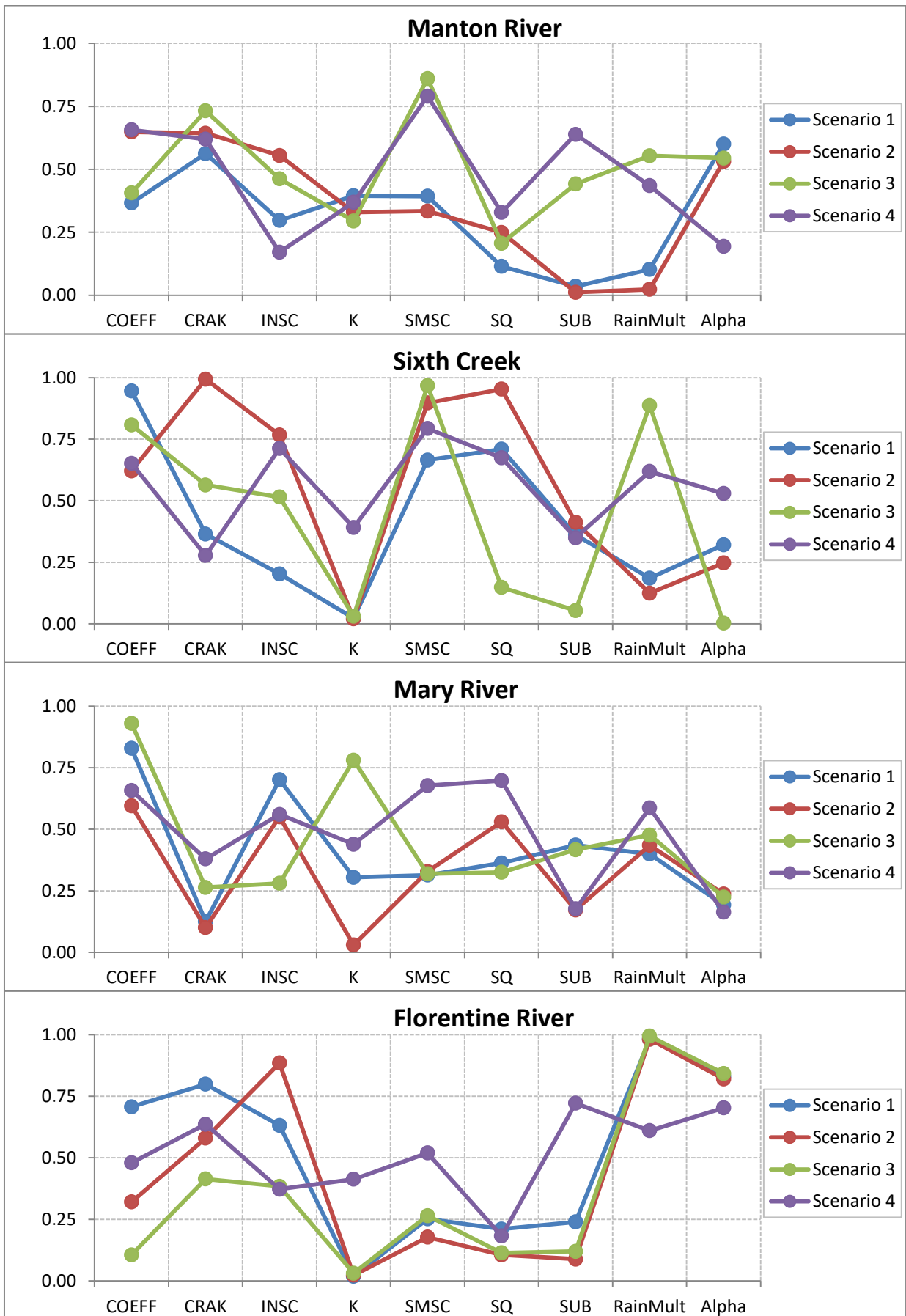


Figure O. 2: Normalized calibrated parameter values for the SIMHYD model [parameters are normalized so that they vary between 0 to 1; 0 = minimum parameter bound, 1 = maximum parameter bound]

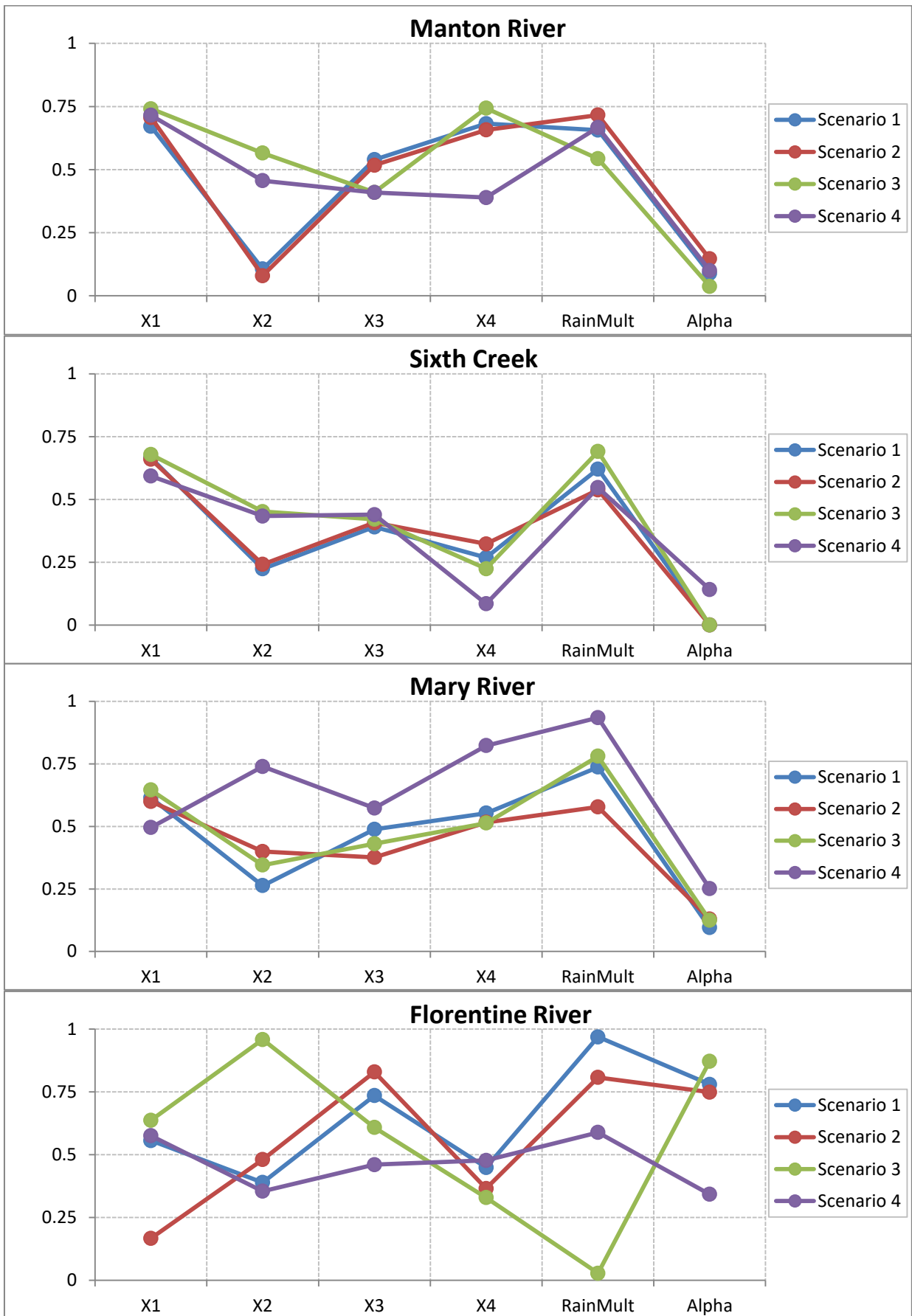


Figure O. 3: Normalized calibrated parameter values for the GR4H model [parameters are normalized so that they vary between 0 to 1; 0 = minimum parameter bound, 1 = maximum parameter bound]

**Appendix P Events selected for volume comparison**

**Table P. 1: Details of the 10 largest independent flood events in each catchment**

Catchments	Events	Event Start	Event End	Observed Volume [Mm <sup>3</sup> ]	Observed Peak Flow [M <sup>3</sup> /s]
Manton River	1	01/02/1995 21:00	04/02/1995 21:00	1.3	58.3
	2	09/04/1996 8:00	12/04/1996 8:00	1.8	61.7
	3	01/03/1997 17:00	04/03/1997 5:00	3.3	82.1
	4	26/01/1998 21:00	28/01/1998 21:00	3.3	92.7
	5	04/04/1999 0:00	07/04/1999 0:00	2.5	67.9
	6	12/02/2001 18:00	15/02/2001 18:00	3.7	84.7
	7	04/03/2004 12:00	08/03/2004 0:00	2.9	75.2
	8	24/04/2006 22:00	27/04/2006 22:00	4.9	112.1
	9	02/03/2007 17:00	04/03/2007 5:00	5.5	73.6
	10	25/02/2010 3:00	28/02/2010 3:00	4.5	53.5
Sixth Creek	1	05/09/1979 10:00	08/09/1979 10:00	1.1	23.2
	2	25/06/1981 13:00	28/06/1981 13:00	1.4	39.0
	3	23/06/1987 17:00	26/06/1987 5:00	1.6	26.5
	4	17/09/1991 7:00	19/09/1991 7:00	1.8	26.3
	5	29/08/1992 7:00	01/09/1992 7:00	3.4	57.9
	6	22/07/1995 0:00	25/07/1995 0:00	2.2	27.5
	7	31/07/2004 22:00	04/08/2004 10:00	1.6	21.0
	8	07/11/2005 0:00	10/11/2005 0:00	2.4	69.7
	9	24/08/2009 7:00	25/08/2009 19:00	0.5	22.8
	10	24/08/2010 7:00	27/08/2010 7:00	1.3	19.4
Mary River	1	10/02/1972 9:00	14/02/1972 21:00	263.0	2629.4
	2	07/07/1973 2:00	10/07/1973 14:00	222.4	2209.9
	3	25/01/1974 8:00	18/02/1974 8:00	305.0	2679.8
	4	18/01/1976 0:00	22/01/1976 0:00	138.8	1442.0
	5	21/06/1983 16:00	24/06/1983 16:00	151.1	1760.4
	6	03/06/1988 12:00	07/06/1988 12:00	93.3	1245.8
	7	23/04/1989 14:00	28/04/1989 14:00	227.8	3231.6
	8	21/02/1992 3:00	24/02/1992 3:00	249.2	2323.3
	9	10/10/2010 5:00	14/10/2010 5:00	98.8	1231.0
	10	08/01/2011 2:00	13/01/2011 14:00	414.4	2815.0
Florentine River	1	09/08/1991 22:00	19/08/1991 22:00	53.7	124.9
	2	25/05/1994 16:00	30/05/1994 16:00	34.7	122.2
	3	16/08/1995 23:00	21/08/1995 11:00	22.8	102.9
	4	01/04/1996 22:00	05/04/1996 22:00	18.9	95.2
	5	17/08/2001 5:00	22/08/2001 5:00	29.9	105.0
	6	08/07/2002 5:00	11/07/2002 5:00	19.8	99.3
	7	16/09/2003 14:00	21/09/2003 14:00	36.4	137.6
	8	27/06/2004 9:00	03/07/2004 9:00	33.4	104.7
	9	08/08/2007 7:00	13/08/2007 19:00	44.4	164.4
	10	25/08/2009 20:00	31/08/2009 8:00	38.1	139.5



Yates Flat Creek	1	28/06/1978 23:00	01/07/1978 23:00	2.7	24.6
	2	11/07/1980 2:00	15/07/1980 2:00	0.7	11.9
	3	15/07/1984 16:00	18/07/1984 16:00	0.9	14.8
	4	16/09/1985 23:00	19/09/1985 23:00	0.8	11.9
	5	24/06/1988 2:00	27/06/1988 2:00	2.4	31.8
	6	22/07/1990 6:00	27/07/1990 6:00	1.9	11.9
	7	19/07/1991 10:00	22/07/1991 22:00	1.2	16.5
	8	27/08/1992 14:00	30/08/1992 14:00	1.0	12.0
	9	21/08/2003 20:00	23/08/2003 20:00	1.0	20.5
	10	31/03/2005 5:00	03/04/2005 5:00	0.8	18.2

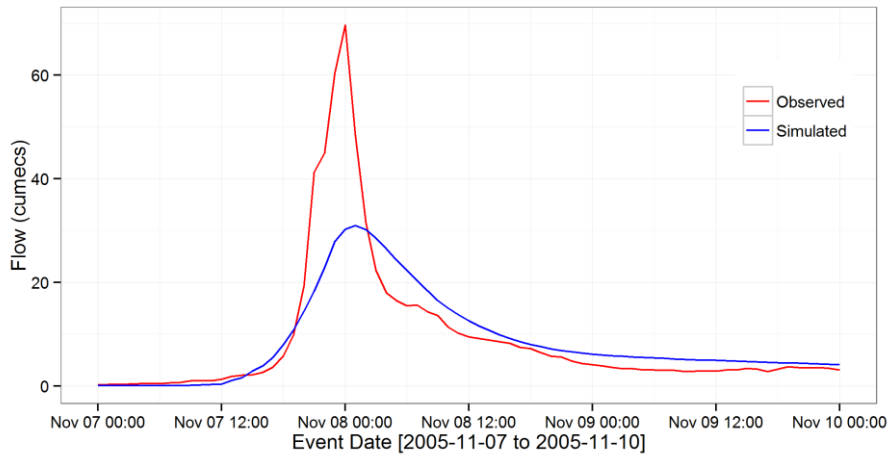
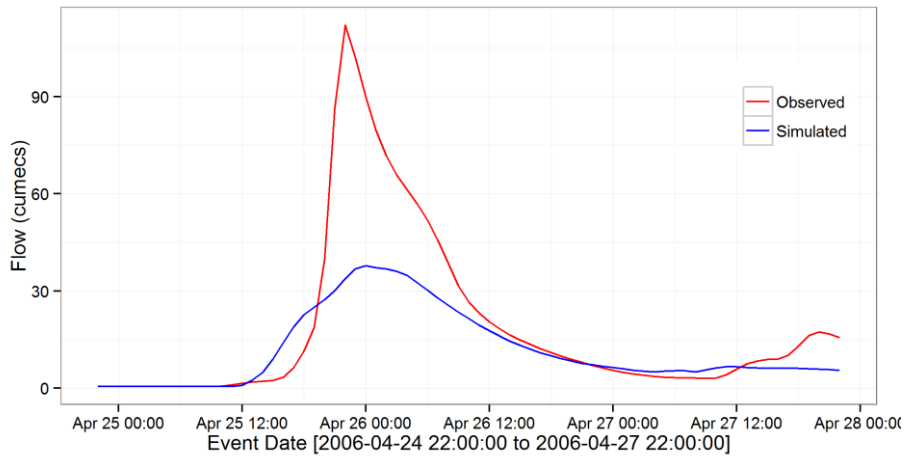


Figure P. 1: Observed and simulated hydrographs, produced by AWBM for scenario 1, for the largest flood events in Manton (left) and Sixth Creek (right)

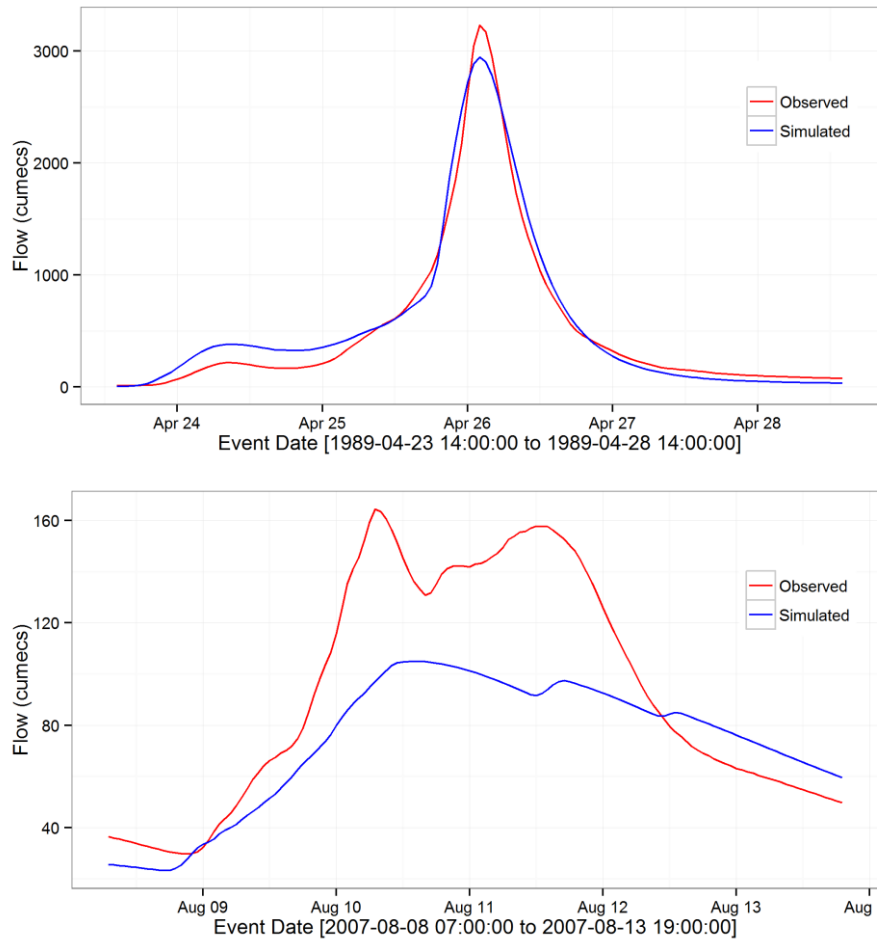


Figure P. 2: Observed and simulated hydrographs produced by AWBM for scenario 1, for the largest flood events in Mary (left) and Florentine (right)

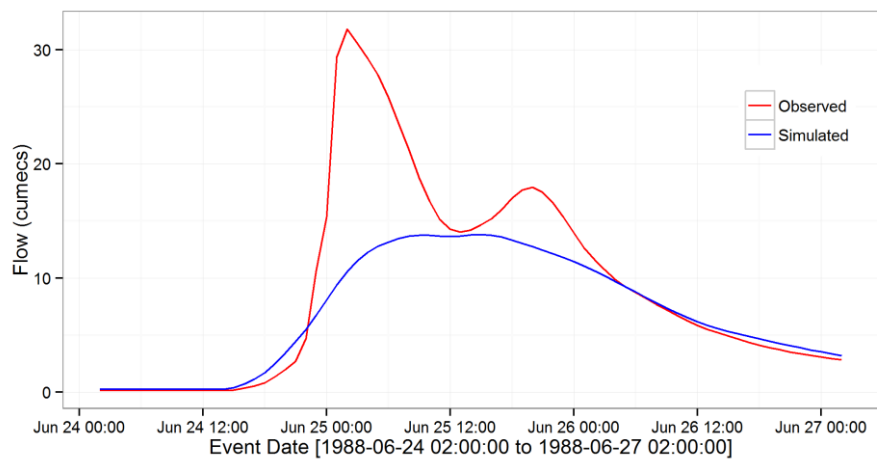


Figure P. 3: Observed and simulated hydrographs, produced by AWBM model for scenario 1, for the largest flood event in Yates Flat Creek

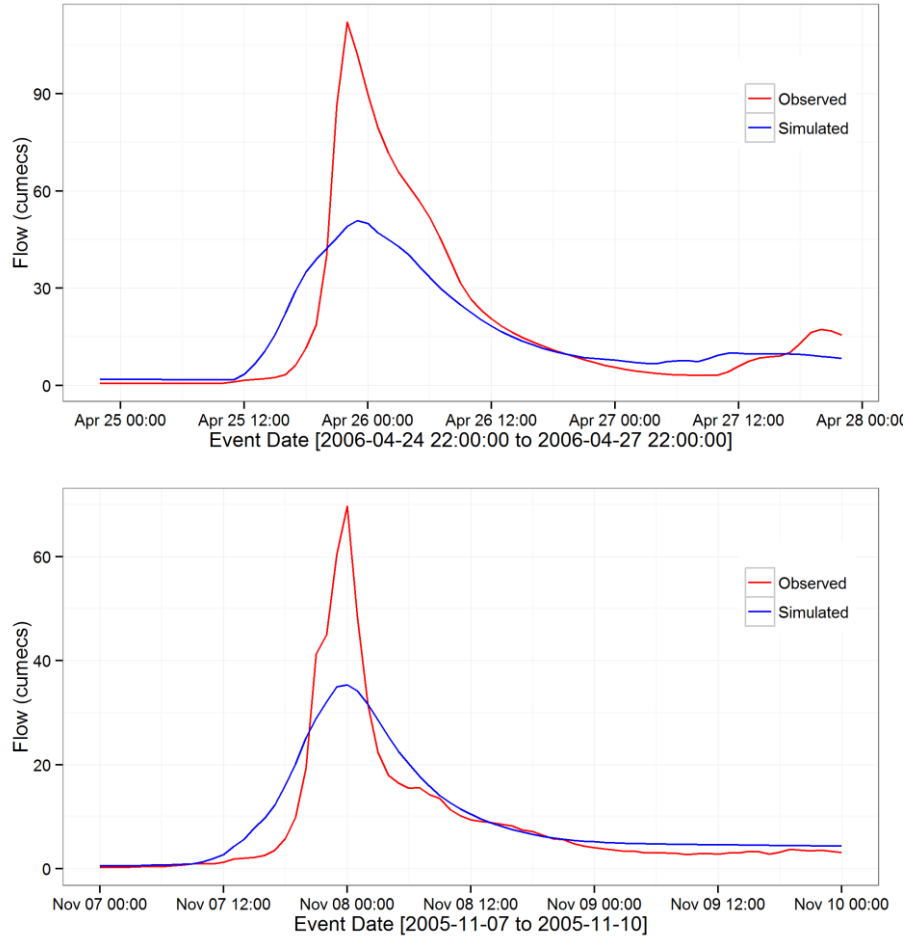
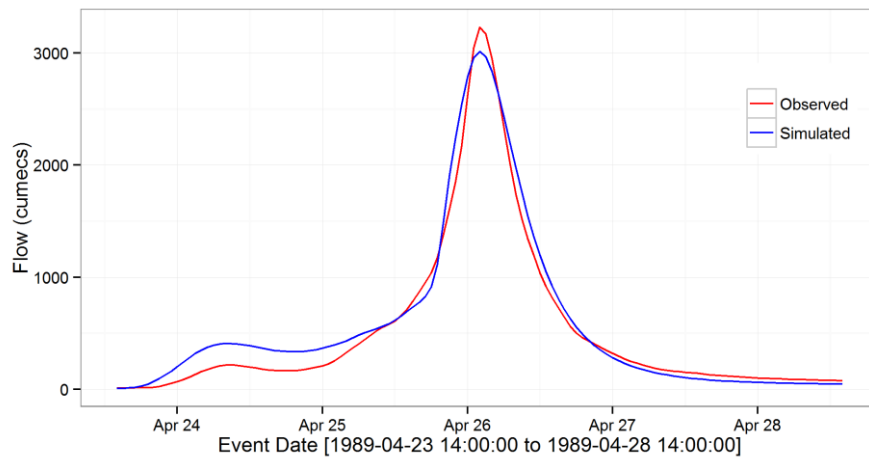


Figure P. 4: Observed and simulated hydrographs, produced by AWBM for scenario 3, for the largest flood events in Manton (left), Sixth Creek (right)



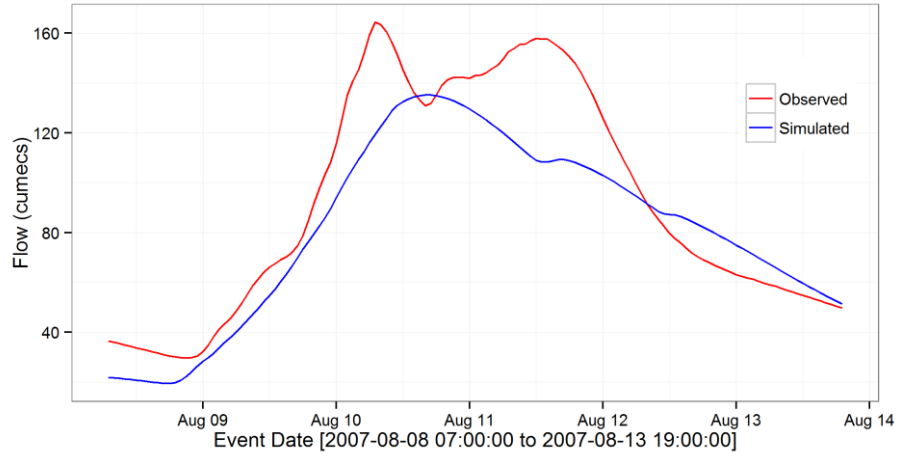


Figure P. 5: Observed and simulated hydrographs, produced by AWBM for scenario 3, for the largest flood events in Mary (left) and Florentine (right)

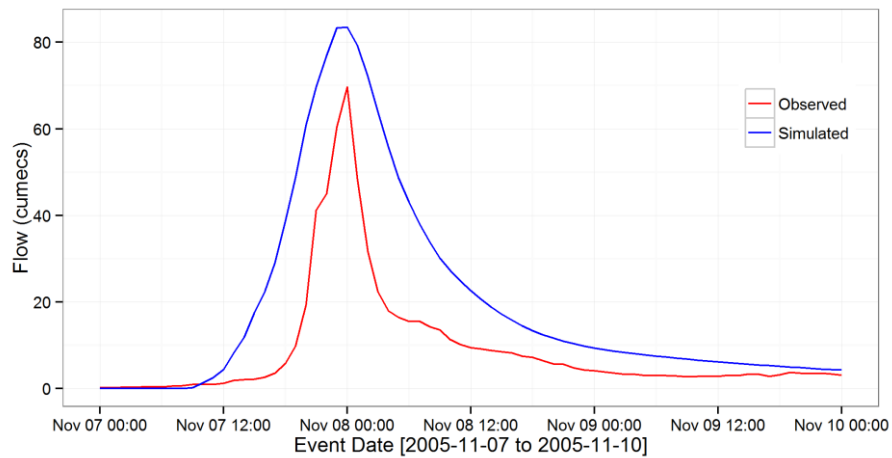
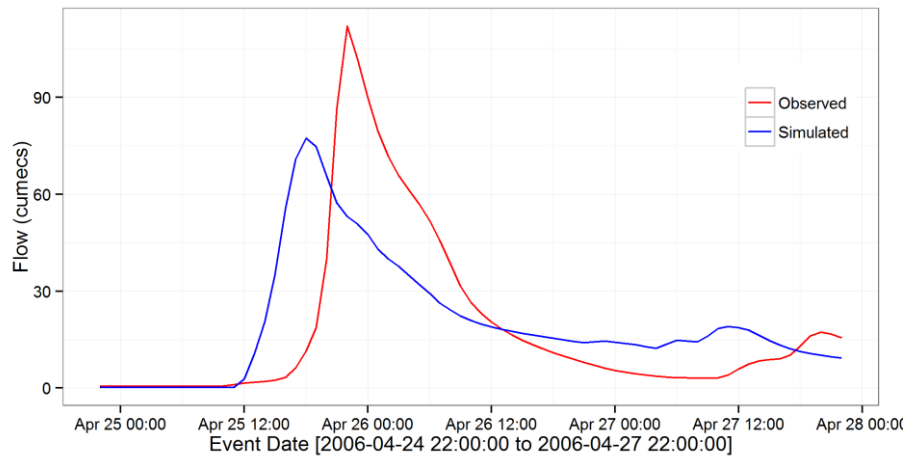


Figure P. 6: Observed and simulated hydrographs, produced by **AWBM** for scenario 4, for the largest flood events in Manton (left), Sixth Creek(right)

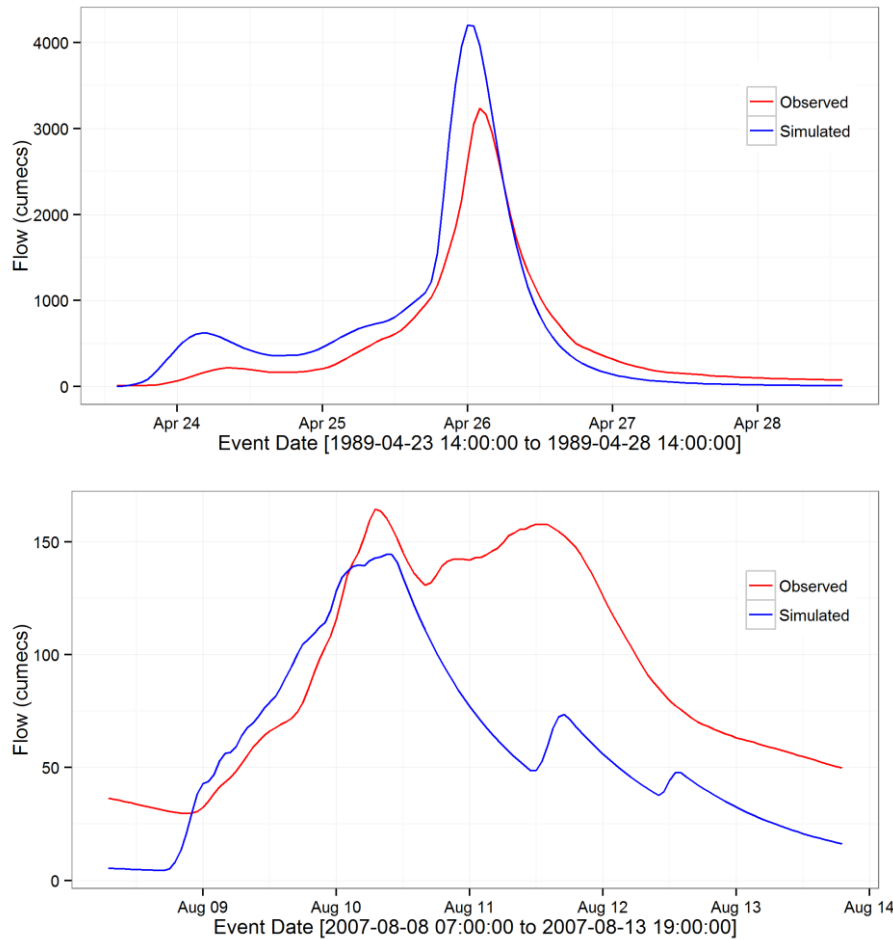


Figure P. 7: Observed and simulated hydrographs, produced by **AWBM** for scenario **4**, for the largest flood events in Mary (left) and Florentine (right)

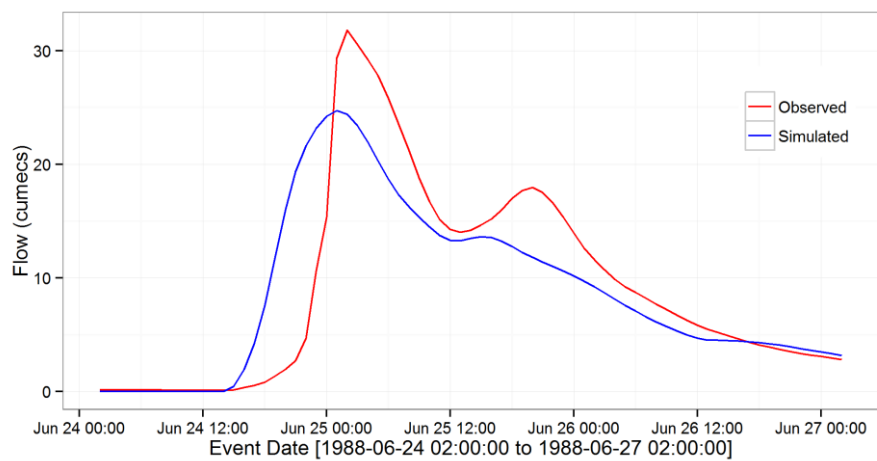


Figure P. 8: Observed and simulated hydrographs, produced by AWBM model for scenario 4, for the largest flood event in Yates Flat Creek

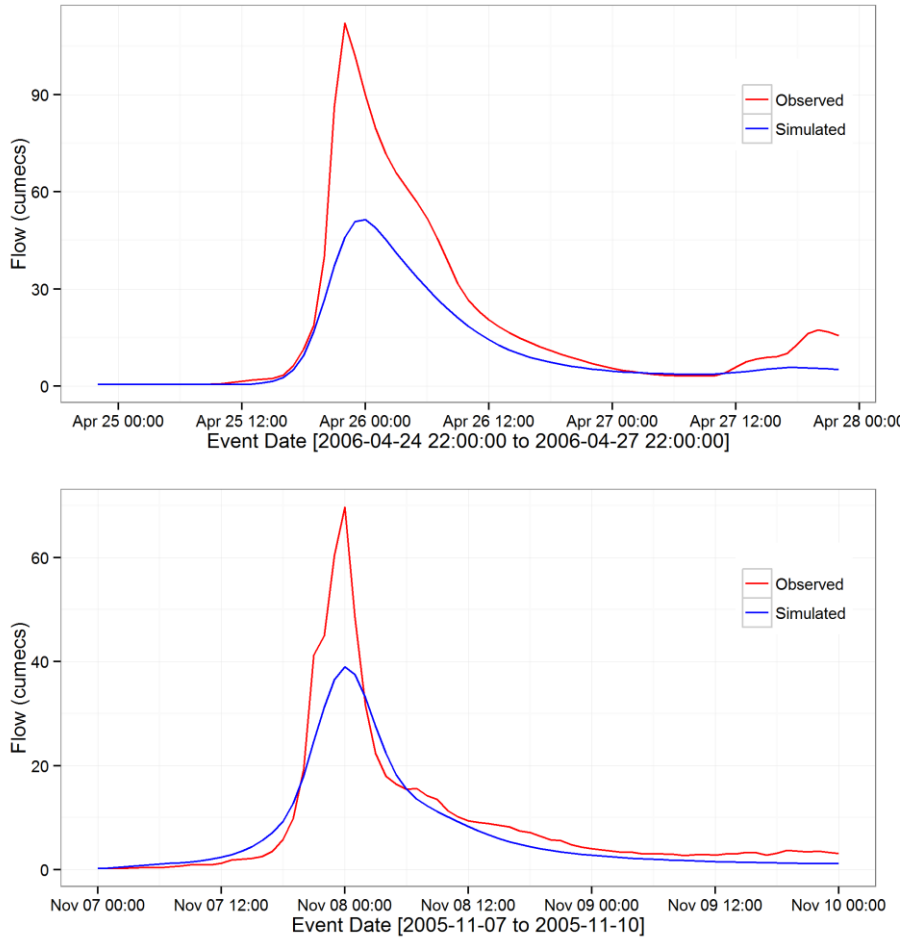
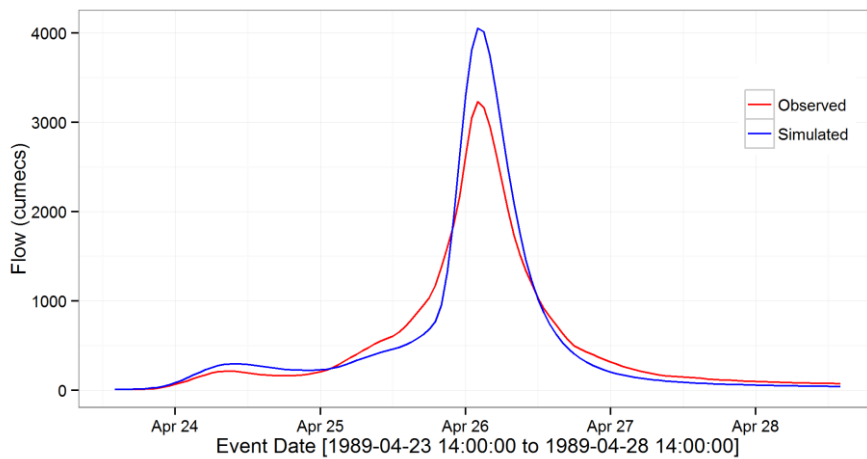


Figure P. 9: Observed and simulated hydrographs produced by GR4H for scenario 1, for the largest flood events in Manton (left) and Sixth Creek (right)



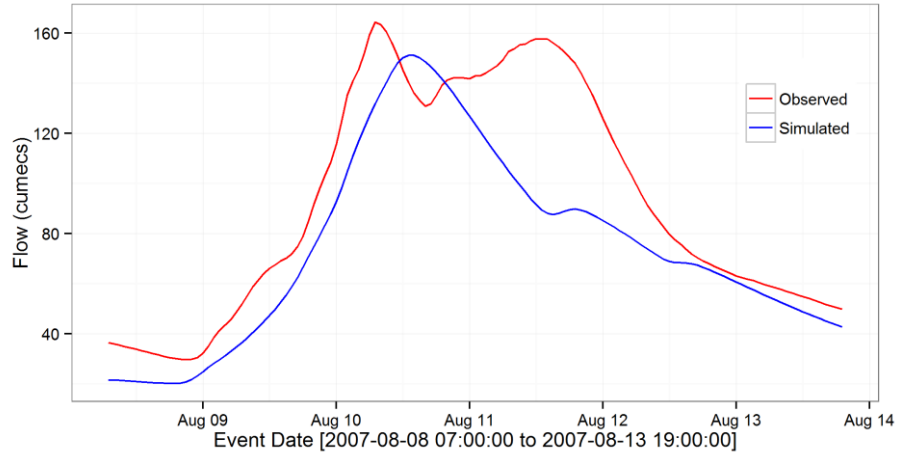


Figure P. 10: Observed and simulated hydrographs produced by GR4H for scenario 1, for the largest flood events in Mary (left) and Florentine (right)

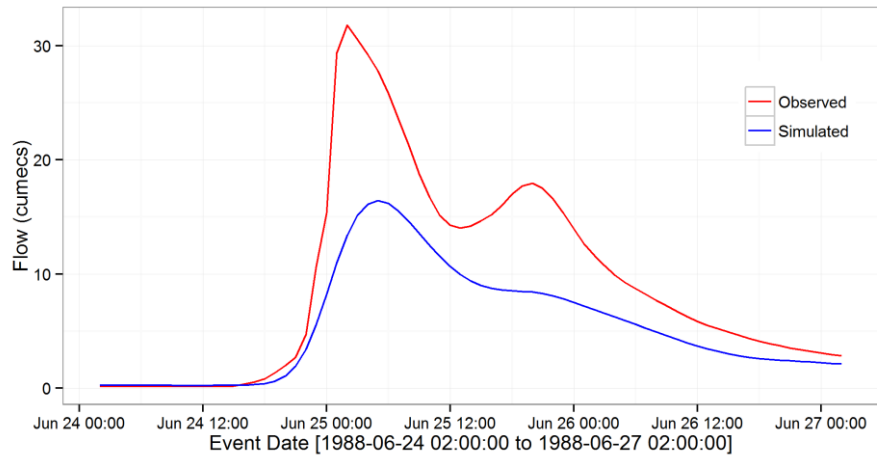


Figure P. 11: Observed and simulated hydrographs, produced by GR4H model for scenario 1, for the largest flood event in Yates Flat Creek

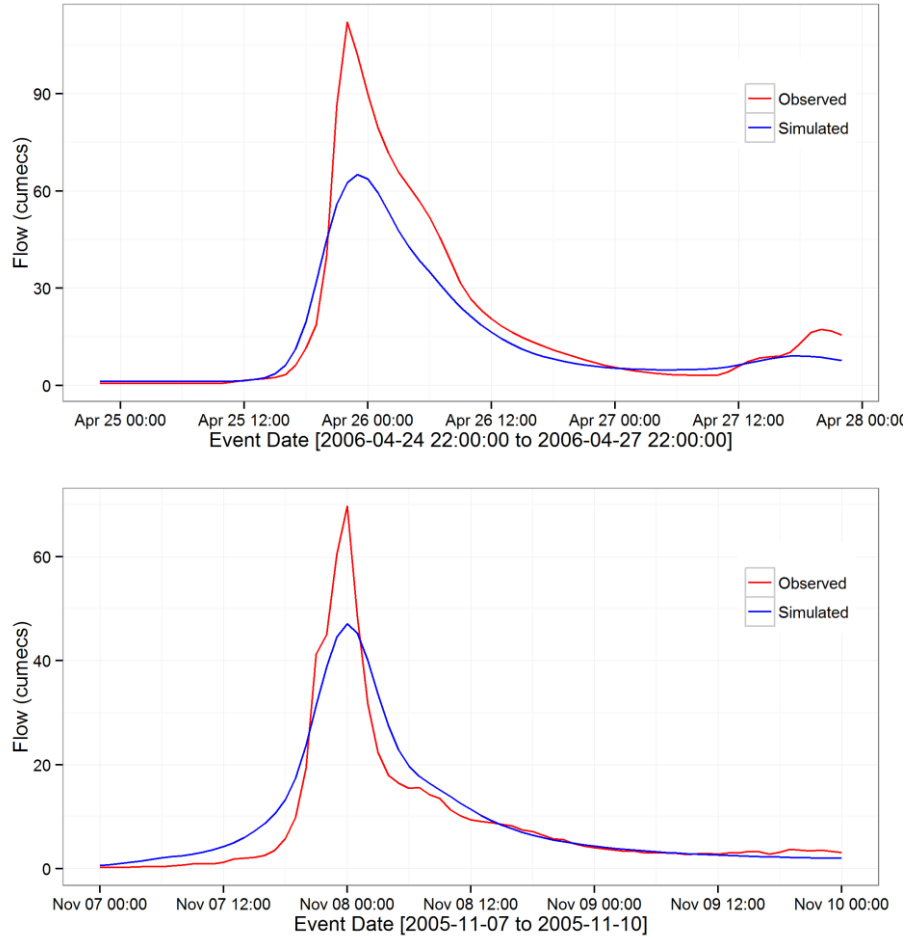


Figure P. 12: Observed and simulated hydrographs, produced by GR4H for scenario 3, for the largest flood events in Manton (left), Sixth Creek(right)

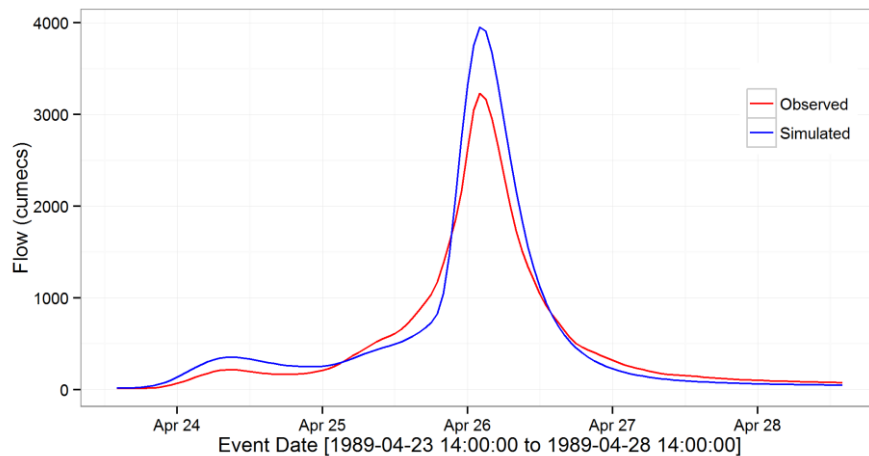


Figure P. 13: Observed and simulated hydrographs, produced by GR4H model for scenario 3, for the largest flood events in, Mary (left) [GR4H model simulation for Scenario 3, has not been included]



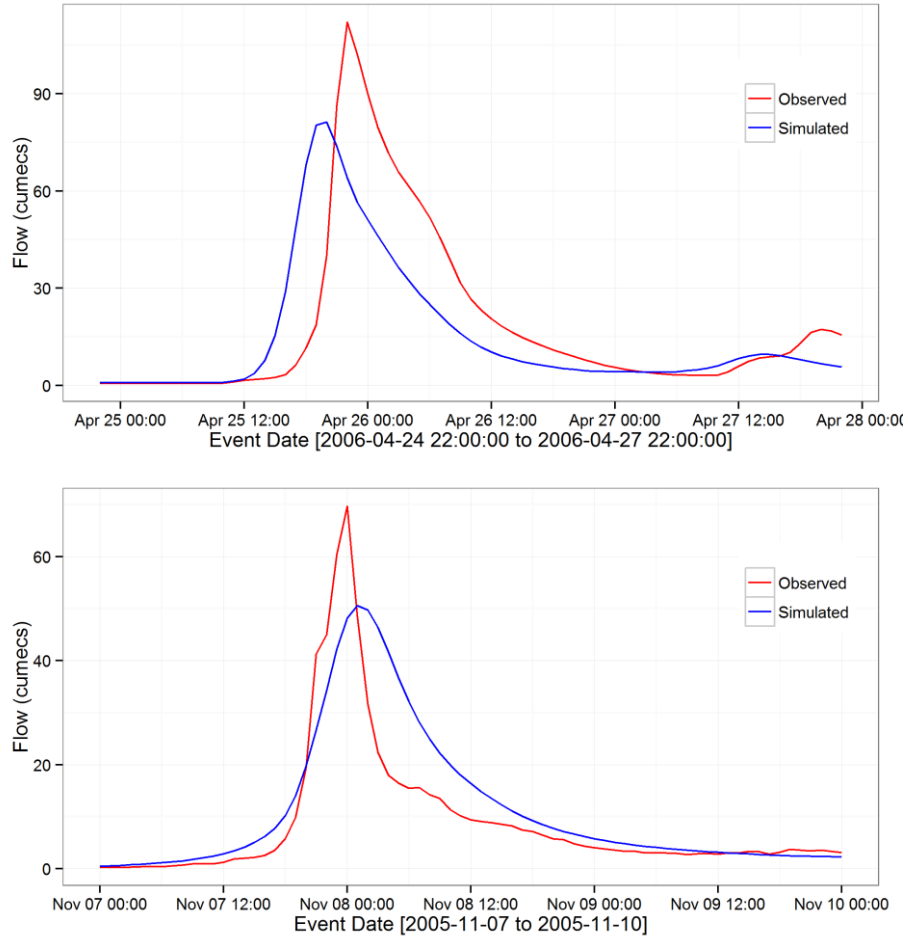
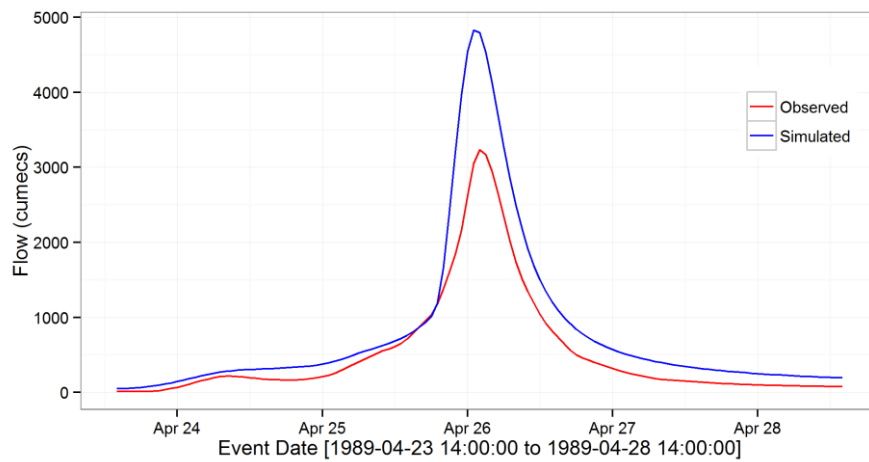


Figure P. 14: Observed and simulated hydrographs, produced by GR4H for scenario 4, for the largest flood events in Manton (left), Sixth Creek(right)



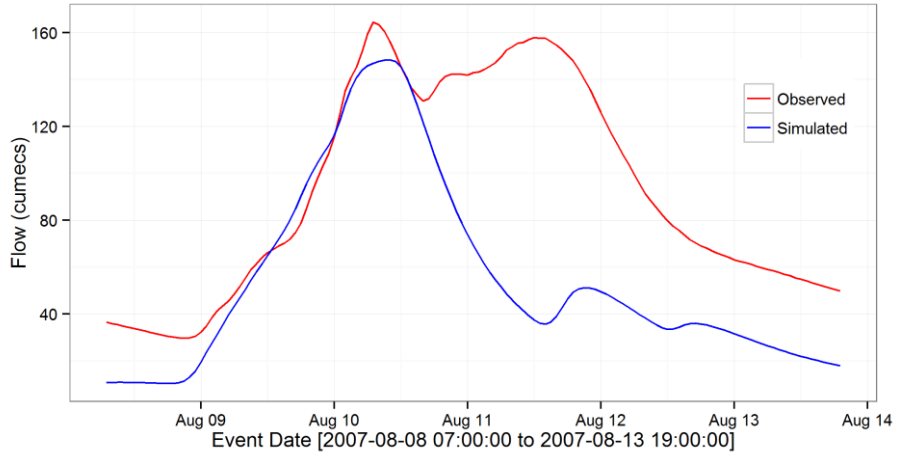


Figure P. 15: Observed and simulated hydrographs, produced by GR4H for scenario 4, for the largest flood events in Mary (left) and Florentine (right)

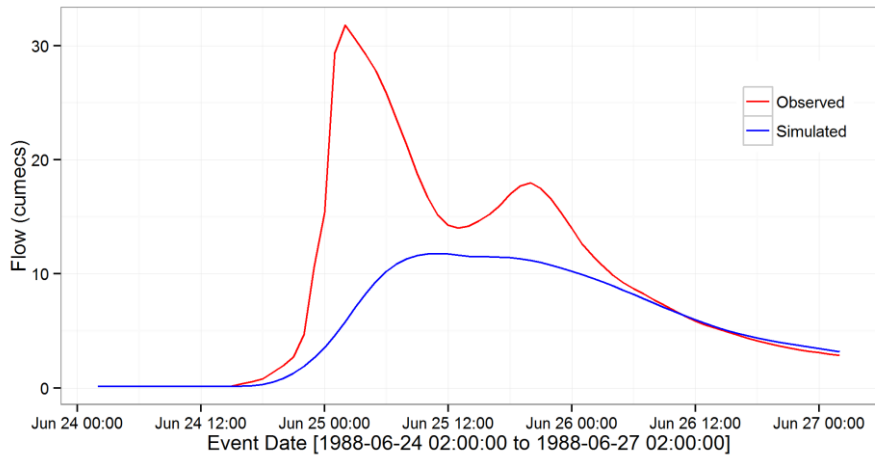


Figure P. 16: Observed and simulated hydrographs, produced by GR4H for scenario 4, for the largest flood event in Yates Flat Creek

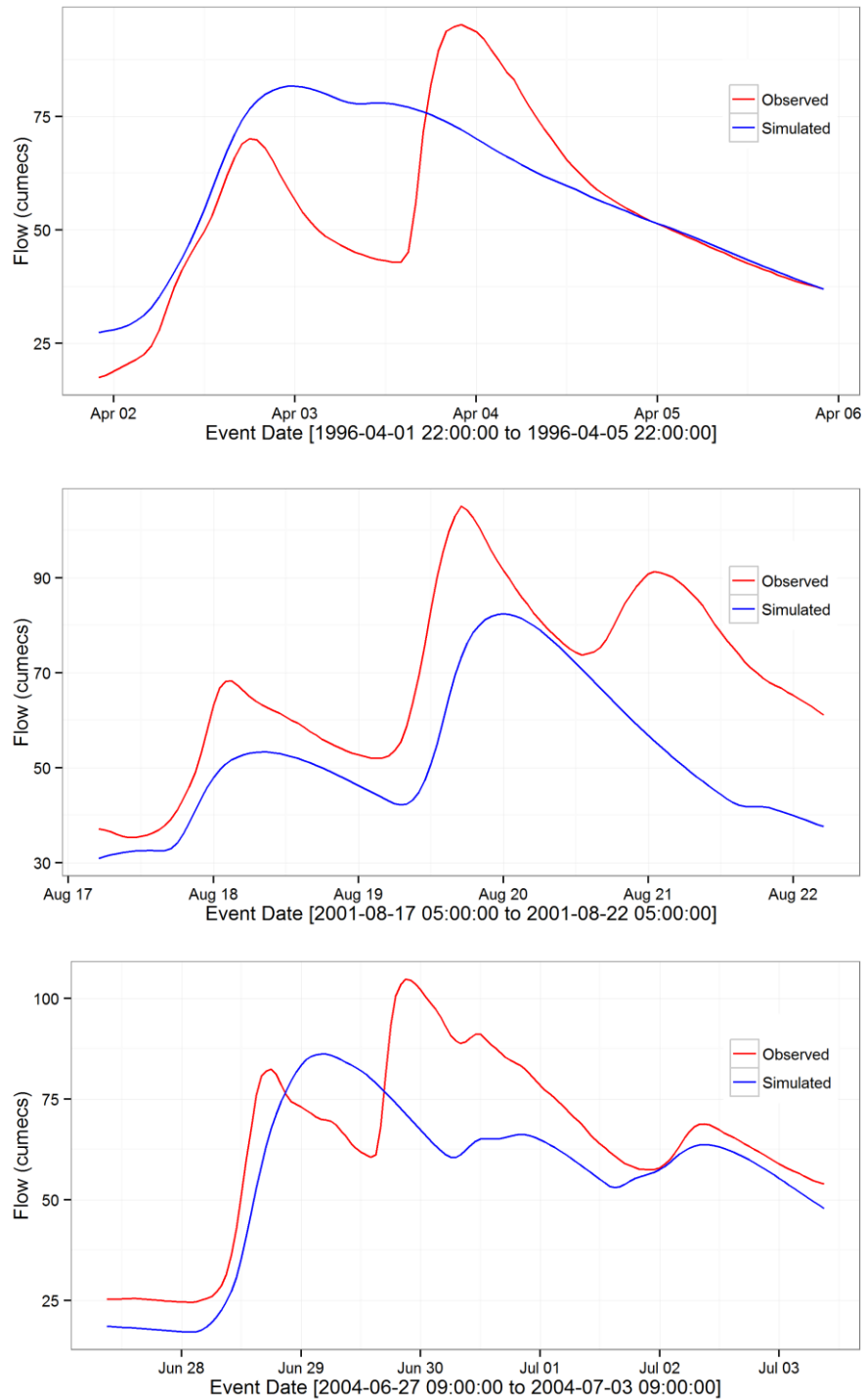


Figure P. 17: Inability of the models to represent the multi-peaked nature of the flood events

**Appendix Q Temporal pattern selection and filtering for Design Event approach**

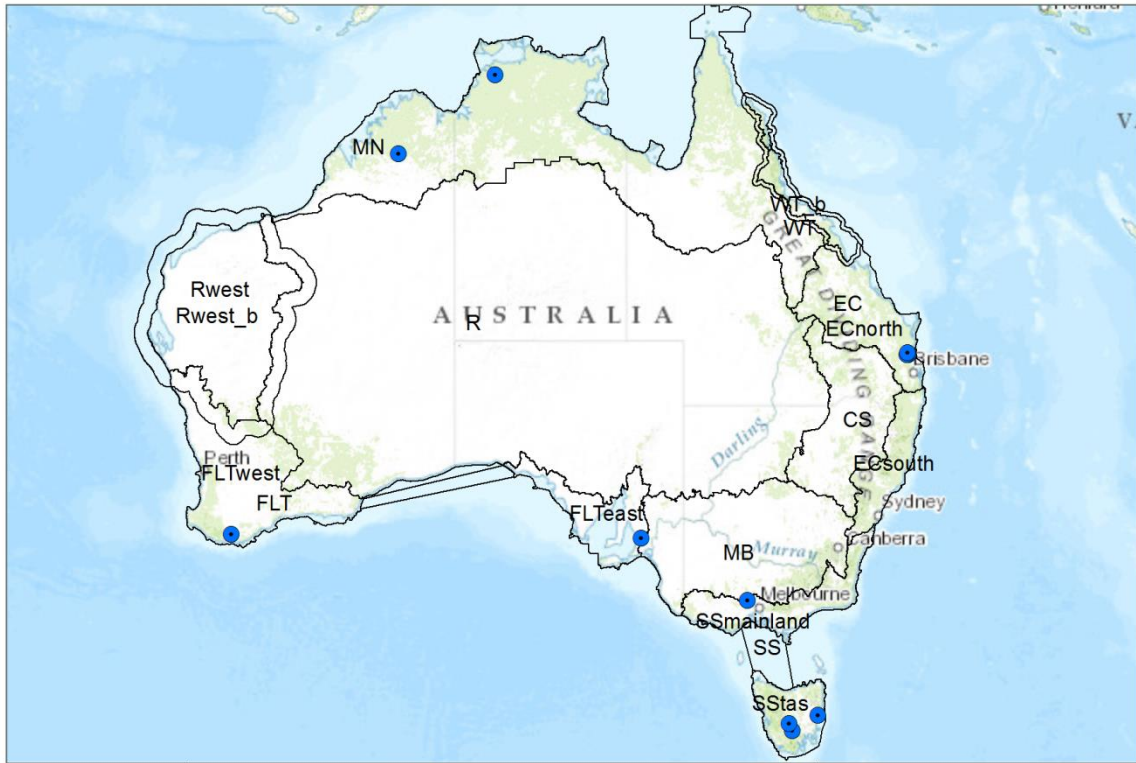


Figure Q. 1: Location of the catchment in relation to the homogenous regions used for temporal pattern extraction

Table Q. 1: Temporal pattern region and names of the catchment located with the region

SN	Code	Temporal Pattern Region	Catchment
1	MN	Monsoonal North	Hann
2	MN	Monsoonal North	Manton
3	FLTwest	Southern and South Western Flatlands (West)	Yates Flat
4	SSmainland	Southern Slopes (Vic/NSW)	Lerderderg
5	FLTeast	Southern and South Western Flatlands (East)	Sixth Creek
6	SStas	Southern Slopes (Tas)	Florentine
7	SStas	Southern Slopes (Tas)	Tyenna
8	SStas	Southern Slopes (Tas)	Hobart
9	ECsouth	East Coast South	Orara
10	ECnorth	East Coast North	Mary

## Temporal pattern filtering approach

The temporal patterns were first checked for presence of embedded storms. The patterns that contained embedded storms were divided into “affected” and “non-affected” region. The affected region of the raw pattern contained embedded storm. The surplus from the affected region was re-distributed to the non – affected region of the temporal pattern using three approaches: Method 1 - using multiplying factor, Method 2 - using addition and Method 3 - combination of both. The filtering approach that resulted in least difference between the raw and filtered patterns, in terms of three measuring criteria (shown below) and upon visual inspection, were used for further analysis.

### Method 1 (Multiplying factor)

The percentage rainfall values in the affected region were progressively reduced by a factor ( $\alpha$ ), and the values non affected region was increased by a multiplier  $\beta$ . The value of  $\alpha$  was progressively reduced till and corresponding values of  $\beta$  were calculated (see below) until all the embedded storms were smoothed.

$$\alpha \sum_{j=1}^K R_j^{affected} + \beta \sum_{m=1}^{N-K} R_m^{non\ affected} = 100$$

$$\beta = \frac{100 - \alpha \sum_{j=1}^K R_j^{affected}}{100 - \sum_{j=1}^K R_j^{affected}}$$

### Method 2 (Addition)

The percentage rainfall values in the affected regions were progressively subtracted by an amount  $\gamma$  from the affected region and  $S$  was uniformly distributed to non-affected areas with values greater than 0 (to preserve no rainfall time steps) until all the embedded patterns were smoothed.

$$S = \sum_{j=1}^K R_j^{affected} - \sum_{j=1}^K \text{MAX} \left[ \left( R_j^{affected} - \gamma \right), 0 \right]$$

### Method 3 (Combination of addition and multiplying factor)

Use of addition or multiplier each changes the shape of the raw temporal pattern in different ways (for example using a multiplier changes a small value by less and large value by larger amount, thus affecting the slope of the relation between the raw and the filtered pattern, while addition results in the constant shift in the values), and each method has its own advantages and disadvantages. Combination of the two provides the advantages of both methods and provides added degrees of freedom in modifying the temporal pattern. The combination method is implemented in following ways

$$F_j = \alpha R_j^{affected} - \gamma$$

$$F_m = \beta R_m^{non\ affected} + \varphi$$

$$F = [F_j, F_m]$$

F is renormalized such that the total is 100 %.

The values of parameters ( $\alpha$ ,  $\beta$ ,  $\gamma$  and  $\varphi$ ) are obtained by maximizing the multicriteria objective function OB.

Maximize ( $OB = w_1 \times OB_1 + w_2 \times OB_2 + w_3 \times OB_3$ )

Subject to constraint

$$\sum_{MvWindow} [F] < \left( \frac{RF_{short}}{RF_{Long}} \right) \times 100$$

Where,  $F$  is the filtered pattern,  $j$  and  $m$  are the time indexes for affected and non-affected regions of the temporal pattern,  $RF_{short}$  is the rainfall depth of the short duration storm, and  $RF_{Long}$  is the rainfall depth of the long duration storm, on which presence of short duration embedded storm is to be checked and filtered.  $MvWindow$  is the moving window of length equal to the duration of the  $RF_{short}$  and is moved over the duration of the temporal pattern.  $w_1, w_2$  and  $w_3$  are the weight allotted for each criteria (in this study  $w_1$  and  $w_2$  were taken as 0.25 each and  $w_3$  was assigned 0.5)

In general the values of the parameters are changed such that shape of the filtered pattern is as close as possible to the raw pattern, while the embedded storm is filtered.

The three criteria used for the maximization of the function F are:

- 1) Weighted rank (OB1) correlation (Costa, 2015) measures the discrepancies in rank ordering between the filtered and the raw patterns. The measure is a modification of Spearman rank correlation and provides higher weight to the differences in the rank of the higher rainfall values at each time step.

$$OB_1 = 1 - \frac{6 \sum_{i=1}^n (R_i - F_i)^2 ((n - R_i + 1) + (n - F_i + 1))}{n^4 + n^3 - n^2 - n}$$

Where,  $i = 1 \dots n$  is the number of time steps in the pattern,  $R$  is the raw pattern and  $F$  is the filtered pattern. The rank ordering is done such that the highest valued rainfall is assigned a rank of 1.

- 2) Normalized difference in the centre of mass (OB2) of the storm pattern. This measures the difference in the centre of mass of the filtered and raw patterns. It is assumed that the shift in the centre of mass of the storm causes the shift in the timing of the flood event.

$$RCM = \frac{\sum_{i=1}^n R_i T_i}{\sum_{i=1}^n R_i}$$

$$FCM = \frac{\sum_{i=1}^n F_i T_i}{\sum_{i=1}^n F_i}$$

$$OB_2 = 1 - \frac{FCM}{RCM}$$

Where  $T$  is the time

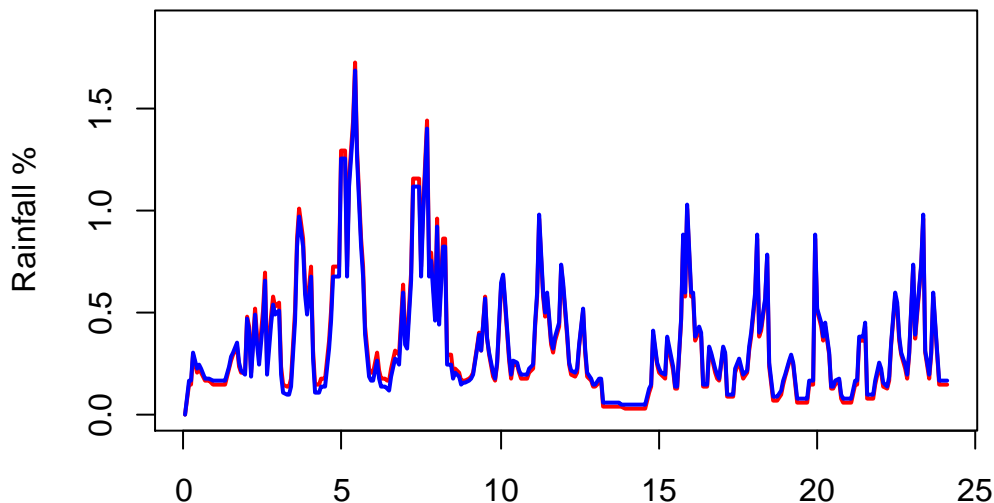
3) Nash Sutcliff Efficiency (NSE) as used in the section 6.

$$OB3 = NSE$$

### Results of the temporal pattern filtering

The temporal pattern filtering was applied to 17 temporal patterns with embedded storm in Mary River catchment for durations 24, 36, 48 and 72 hours and for 36 hours in Florentine. In most cases, the amount of filtering required was small and all the methods provided similar results. As far as practicable, patterns that required least amount of modifications were used in further analysis of the design event approach, but in some cases this resulted in less diversity (more uniform) and patterns with larger diversity were used. In these cases larger amount of filtering was needed, and method 3 provided a much better (in terms of the three criteria used and upon visual inspection) filtering result compared to method 1 and 2.

In general methods 1 and 2 were computationally most efficient and used for temporal patterns that needed small amount of modification. For patterns that required a large amount of modification, Method 3 was used. Figure Q. 1 and show raw and filtered patterns for two cases, one with nominal filtering required, where method 1 provided the best result and the other where method 3 provided the best result.



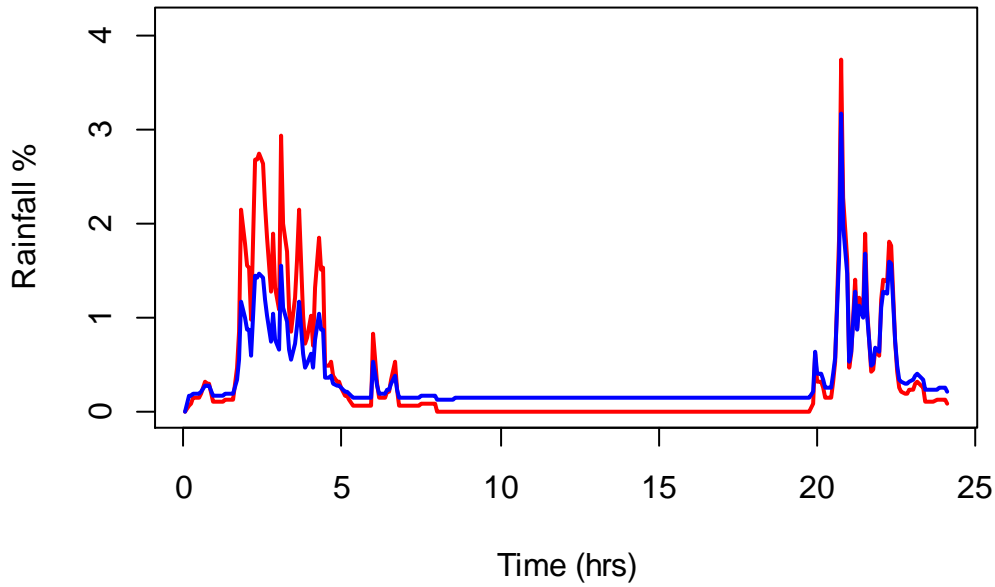


**Figure Q. 1: Filtered (blue) and raw (red) temporal pattern for 25 hour storm, in Mary River**  
[Top plot shows a pattern where minimum amount of filtering was required and method 1 was used and the bottom plot shows large amount of filtering and method 3 provided the best result]

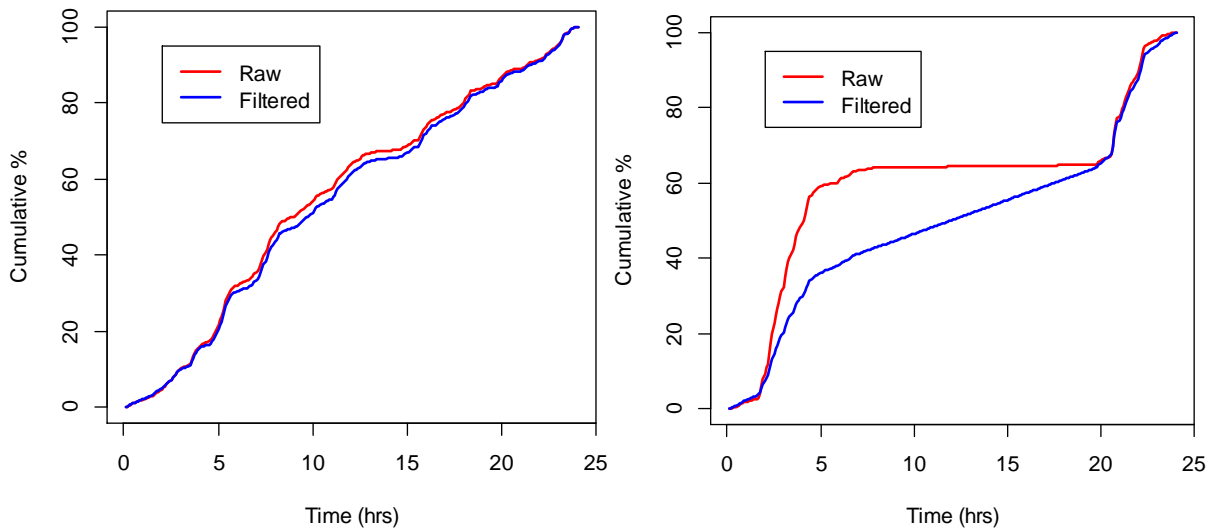


**Figure Q. 2 : Cumulative plots of filtered (blue) and raw (red) temporal pattern for 25 hour storm, in Mary River** [left - pattern where minimum amount of filtering was required and method 1 was used, right - large amount of filtering and method 3 provided the best result]